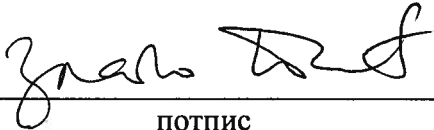


НАУЧНОМ ВЕЋУ ИНСТИТУТА ЗА ФИЗИКУ

Предмет: Захтев за покретање поступка за избор у звање
виши научни сарадник

Молим Научно веће Института за физику да у складу са
Правилником о поступку и начину вредновања и квантитативном
исказивању научноистраживачких резултата истраживача, покрене
поступак за мој избор у звање виши научни сарадник.

У Ватерлоу, Канада 20. 11. 2013. године


ПОТПИС

BIOGRAFSKI PODACI

Zlatko Papić je rođen 25. 10. 1981. godine u Zrenjaninu. Diplomirao je 2006. na Fizičkom fakultetu Univerziteta u Beogradu sa diplomskim radom *Bozonske korelacije u kvantnom Holovom dvosloju na punjenju I*, koji je realizovan pod mentorstvom dr. Milice Milovanović na Institutu za fiziku u Beogradu. Ovaj rad je iste godine osvojio nagradu dr. Ljubomir Ćirković. Nakon diplomskih i master studija, 2007. godine upisuje doktorske studije na Fizičkom fakultetu u Beogradu i Univezitetu Pariz XI u Francuskoj, pod zajedničkim mentorstvom dr. Milice Milovanović, dr. Marka Gerbiga i dr. Nikolasa Rinjoa. Tokom boravka u Francuskoj 2007-2008. godine primao je stipendiju Marija Kiri, a u periodu 2009-2010. bio je zaposlen na Institutu za fiziku u Beogradu u zvanju istraživač-saradnik na projektu 141035 *Modeliranje i numeričke simulacije složenih fizičkih sistema*. Tema doktorske disertacije pod imenom *Frakcioni kvantni Holov efekat u višekomponentnim sistemima* su jako korelisani elektronski sistemi i topološke faze materije, pre svega kao što su kvantne jame i grafen. Ovoj tezi je dodeljena studentska nagrada Instituta za fiziku 2010. godine. Nakon odbrane teze u septembru 2010. godine, prelazi na Univerzitet Princeton (SAD) kao istraživač na postdoktorskim studijama u grupi prof. Ravina Bata i prof. Dankana Holdejna. Od oktobra 2013. godine je na Perimeter institutu u Kanadi kao postdoktorant.

NAUČNA I STRUČNA AKTIVNOST

ELEMENTI ZA KVALITATIVNU ANALIZU RADA KANDIDATA

Uvodna predavanja na konferencijama i druga predavanja po pozivu

Kandidat je održao predavanje po pozivu na **Martovskom skupu Američkog društva fizičara (APS March meeting)** 22. marta 2013. godine u Baltimoru (SAD) pod nazivom *Tunable interactions and ways of engineering fractional quantum Hall states*. Predavanje je bilo deo sesije o novim pravcima u fizici frakcionog kvantnog Holovog efekta (<http://meetings.aps.org/Meeting/MAR13/Event/190149>). Tokom 2013. kandidat je održao predavanje po pozivu i na Purdue univerzitetu (<http://www.physics.purdue.edu/seminar/abstract.php?id=230>), na McGill univerzitetu (http://www.physics.mcgill.ca/events/CPM_papic.html), kao i na Univerzitetu u Tuluzu (<http://www.lpt.ups-tlse.fr/spip.php?article1058&lang=fr>).

Tokom 2011-2012. kandidat je održao predavanja po pozivu u okviru *Conference on Computational Physics CCP2011* (http://ccp2011.ornl.gov/sessions_schedule.shtml) u Getlinburgu (Tenesi, SAD), kao i konferencije *U potrazi za topološkim fazama (In search of topological phases)*, http://pctp.princeton.edu/pctp/lowDsys/lowDsys_SearchTopologicalPoster.pdf na Univerzitetu Princeton (SAD). Pored ovoga, kandidat je održao predavanja po pozivu na Laboratoire de Physique Theorique de la Matiere Condensee – LPTMC u Parizu, Microsoft Station Q <http://research.microsoft.com/en-us/labs/stationq/seminars.aspx> (Santa Barbara, SAD) i Perimeter institutu u Kanadi <http://pirsa.org/12110081/>.

Kandidat je takođe u dva navrata učestvovao na programima Kavli instituta za teorijsku fiziku (KITP) u Santa Barbara: program *Low-dimensional electron systems* 2009. godine, <http://online.itp.ucsb.edu/online/lowdim09/>, kao i *Exotic Phases of Frustrated Magnets* 2012. godine. Pored ovoga, u nekoliko navrata je učestvovao i u programima Nordite u Stokholmu, gde je 2010. održao predavanje (<http://agenda.albanova.se/contributionDisplay.py?contribId=250&confId=1128>).

Dokazni materijal o gorenavedenim predavanjima po pozivu (pozivna pisma na konferencije, najava predavanja i sl.) priložen je na kraju ovog zahteva.

Članstva u uređivačkim odborima časopisa i recenzije naučnih radova

Recenzent je časopisa Science, Physical Review B i Physical Review Letters (40 recenzija).

Kvalitet naučnih rezultata

Zlatko Papić je objavio 22 naučna rada, od čega **20 kategorije M21 (11 u Physical Review B i 7 u Physical Review Letters), 1 kategorije M22 i 1 kategorije M23**.

Uticajnost

Radovi su citirani **153** puta i od toga **123** puta bez autocitata.

U visokocitiranom radu **M21[3]** (citiran 16 (12) puta) dat je teorijski model za tzv. široke kvantne jame na kojima je vršen veći broj transportnih eksperimenata u režimu kvantnog Holovog efekta, što je dovelo do detekcije novih stanja poput onog na punjenju 1/4. Teorijski model ovih eksperimenata je proučavan u okviru obimnih numeričkih simulacija koristeći tehniku egzaktne dijagonalizacije, u potpunosti razvijenu od strane kandidata. Pored objašnjenja novog kvantnog Holovog stanja na punjenju 1/4, ovaj rad je otvorio mogućnosti za proučavanje niza eksperimenata na sličnim sistemima i drugim punjenjima.

U visokocitiranim radovima **M21[7]** (citiran 17 (12) puta) i **M21[10]** (citiran 17 (14) puta) proučavane su jako korelisane faze u grafenu. U radu **M21[7]** dato je prvo teorijsko objašnjenje stanja na punjenju 1/3 koje je nedavno pre toga bilo otkriveno u eksperimentima. Pokazano je da se ovo stanje razlikuje od uobičajenog Laflinovog stanja koje bi se naivno moglo očekivati na punjenju 1/3, usled narušenja SU(4) simetrije koja u grafenu nastaje od kombinacije spinskih i zonskih stepena slobode. Rad **M21[10]** iznosi predlog za eksperimentalnu postavku koja bi omogućila kontrolisano variranje efektivne Kulonove interakcije između elektrona u grafenu pomoću dielektrika ("screening" efekat). Ovaj predlog može dovesti do povećanja stabilnosti određenih jako korelisanih stanja (čak i onih sa tzv. neabelijanskom statistikom), a takođe omogućava proučavanje kvantnih faznih prelaza na kontrolisan način.

Parametri kvaliteta časopisa i pozitivna citiranost kandidatovih radova

Najveći deo publikacija Zlatka Papića je objavljen u vrhunskim međunarodnim časopisima **Physical Review B** i **Physical Review Letters** i citirani su od strane radova objavljenih u istim ili drugim vrhunskim međunarodnim časopisima. Jedan od elemenata za procenu kvaliteta naučnih rezultata kandidata je i kvalitet časopisa u kojima su radovi objavljeni, odnosno njihov impakt faktor (IF). Zlatko Papić je objavio **20 radova kategorije M21**, od kojih

11 u Physical Review B (za poslednjih pet radova: IF=3.364 za 3 rada u 2010, IF=3.405 za 1 rad u 2011, IF=3.603 za 1 rad u 2012. godini, i 2 rada su izašla u 2013. godini)

7 u Physical Review Letters (IF=7.155 za 1 rad, IF=7.013 za 2 rada, IF=7.435 za 2 rada, i dva rada su izašla u 2013. godini)

Efektivni broj radova i broj radova normiran na osnovu broja koautora.

Svi radovi kandidata su sa punom težinom u odnosu na broj koautora.

Stepen samostalnosti i stepen učešća u realizaciji radova

Izrazita je samostalnost ili doprinos osnovne ideje, tj. idejnog rešenja u skoro svim radovima kandidata.

Pregled i analiza naučnih rezultata

Oblasti naučnog rada kandidata su u fizici kondenzovane materije i jako korelisanih sistema: **(1)** frakcioni kvantni Holov efekat, posebno u tzv. višekomponentnim sistemima gde spin ili pseudospin igraju ulogu, **(2)** grafen, **(3)** numeričke simulacije jako korelisanih sistema koje se oslanjaju na koncepte iz polja kvantne informacije, poput entanglement-a i DMRG ("density-matrix renormalization group"), i **(4)** neuređeni višestručni sistemi. Svi navedeni radovi u ovom poglavlju su iz kategorije **M21**.

(1) Frakcioni kvantni Holov efekat:

U radovima **M21[1]**, **M21[2]** proučavan je problem dva kvantna Holova sistema koja su na malom rastojanju jedan od drugog i čine tzv. dvosloj, pri čemu je rastojanje između njih moguće varirati u eksperimentu, dok je totalno punjenje 1. Pri velikim rastojanjima između slojeva, sistem je kompresibilan, dok je za mala rastojanja nekompresibilan fluid koji ispoljava ekscitonsku superfluidnost. Prelaz između ovih, vrlo različitih režima, prilikom promene rastojanja između slojeva predstavlja otvoreni problem. Radovi **M21[1]**, **M21[2]** daju doprinos razumevanju ovog problema sa tačke gledišta varijacionih funkcija koje reprezentuju mešana stanja tzv. kompozitnih fermiona i kompozitnih bozona, koji predstavljaju kvazičestice u limitu velikih, odnosno malih rastojanja, respektivno. Na osnovu varijacionih funkcija za osnovno stanje, konstruisane su i Čern-Sajmons topološke teorije polja na osnovu kojih je računat linearni odgovor sistema, ispitivana topološka svojstva ekscitacija i sl.

U seriji radova **M21[3]**, **M21[5]**, **M21[6]**, **M21[8]** proučavane su tzv. široke kvantne jame gde višekomponentni stepeni slobode predstavljaju elektronske nivoe u kvatnoj jami. U prisustvu jakih interakcija u magnetnom polju, u ovim sistemima nastaju stanja

koja se mogu opisati tzv. Halperinovim funkcijama koje predstavljaju uopštenje Laflinove talasne funkcije. Ono što je posebno zanimljivo sa eksperimentalne tačke gledišta je mogućnost da se, variranjem tuneliranja između elektronskih nivoa, uspostavi prelaz između višekomponentnih i jednokomponentnih (polarizovanih) stanja, koja u određenim slučajevima poseduju neabelijanske ekscitacije. Najvažniji primer ovog scenarija se odnosi na punjenje $1/2$ gde je moguće uspostaviti prelaz između 331 Halperinovog stanja i tzv. Fafijana, koji je reprezentovan čuvenom talasnom funkcijom koju su formulisali Greg Mur i Nikolas Rid. Fafijan je sparno stanje koje se može opisati kao “p-wave” superprovodnik. Njegove kvazičestice su Majorana fermioni koje odlikuje neabelijanska statistika: stanje nakon izmene dveju kvazičestica nije jednako početnom stanju (do na fazu, kao kod fermiona ili bozona). U radu **M21[6]** detaljno je izučavan ovaj prelaz putem BCS modela, kao i egzaktne dijagonalizacije. Istaknuto je da prelaz od 331 stanja ne vodi u sparno stanje, već verovatnije u kompresibilno stanje koje ima svojstva Fermi tečnosti.

(2) Grafen

Rad **M21[7]** pružio je teorijski opis kvantnog Holovog stanja na punjenju $1/3$ u grafenu koje je eksperimentalno uočeno tokom 2009. godine. Iznenadjući aspekt ovog stanja u grafenu je da se razlikuje od Laflinovog stanja koje nastaje pri istom punjenju u galijum arsenidu (GaAs). Razlog za ovo je veća unutrašnja simetrija u slučaju grafena koja potiče od prisustva spina i zonskog pseudospina koji ukupno daju $SU(4)$ simetriju. Posledica ovoga u slučaju $1/3$ je da, iako talasna funkcija osnovnog stanja ima oblik Laflinove funkcije, ekscitacioni spektar je drastično različit: najniža ekscitacija je spinski ili pseudospinski talas, a ne tzv. magneto-roton koji nastaje u slučaju Laflinovog stanja.

U radovima **M21[10]**, **M21[11]**, **M21[12]** ispitivane su praktične mogućnosti grafenskih sistema (jednosloj, dvosloj itd.) za kontrolisano variranje oblika i jačine efektivne Kulonove interakcije između elektrona, u cilju potpunijeg izučavanja jako korelisanih faza i kvantnih faznih prelaza. U radu **M21[10]** pokazano je da se postavljanjem dielektrika u blizini grafenskog sloja može uzrokovati odgovarajući tip “screening”-a koji stabilizuje neabelijanska stanja. U radovima **M21[11]**, **M21[12]** ispitivana je modifikacija interakcije usled promene zonske strukture, na primer dodavanjem masenog člana putem električnog polja u slučaju grafenskog dvosloja. Pokazano je da ovaj metod takođe omogućava proučavanje različitih faznih prelaza između topoloških faza i onih sa narušenom simetrijom.

(3) Numeričke simulacije bazirane na entanglement-u

Poslednjih decenija došlo je do intenzivnog razvoja numeričkih simulacija jako interagujućih sistema u fizici kondenzovane materije. Neki od uticajnih metoda, poput “density-matrix renormalization group” (DRMG), direktno su zasnovani na primeni “entanglement”-a u karakterizaciji kvantnih višestičnih stanja. U slučaju sistema sa topološkim uređenjem, nedavno je pokazano da tzv. entanglement spektar donosi potpunu informaciju o sistemu, uključujući ekscitacije na granici. U radu **M21[9]** proučavan je

entanglement spektar za kvantne Holove sisteme u prisustvu određenog broja kvazičestica. Pokazano je da kod ovih, topoloških uređenih, sistema entanglement spektar daje potpunu informaciju i o eksitacijama, a ne samo o osnovnom stanju. Pored toga, demonstrirano je da entanglement spektar daje jasan uvid u statistiku kvazičestica kada se one premeštaju unutar sistema. U radu **M21[15]** implementiran je DMRG metod za kvantne Holove sisteme i testiran na nekoliko tipova graničnih uslova, kao što su geometrija sfere ili cilindar. Pokazano je da je geometrija cilindra znatno pogodnija sa aspekta numeričke konvergencije, što omogućava DMRG metodu da uspešno simulira znatno veće sisteme od onih koje je moguće egzaktno dijagonalizovati. Razvoj DMRG metoda otvara mogućnosti za proučavanje mnogih fenomena gde egzaktna dijagonalizacija nije uspešla da dostigne odgovarajući broj čestica kod kojih korelaciona dužina postaje znatno manja od dimenzije sistema.

(3) Neuređeni interagujući sistemi i lokalizacija

Još 1958. u svom čuvenom radu, Anderson je pokazao da prisustvo neuređenosti u izolovanim kvantnim sistemima dovodi do lokalizacije i odsustva provodnosti. Međutim, do današnjih dana je ostalo nerazjašnjeno šta se događa kada pored neuređenosti postoji i interakcija među česticama. U radovima **M21[18]** (citiran 5(4) puta) i **M21[20]** (citiran 1(1) put) ispitivana su svojstva nove faze – tzv. višečestične lokalizovane faze – koja je uočena u numeričkim simulacijama modela interagujućih spinova u prisustvu neuređenosti. Pokazano je da se takva faza razlikuje od dobro-poznatog Andersonovog izolatora po vremenskoj evoluciji entanglement entropije sistema. Pored ovoga, pronađeno je da stanja interagujućih neuređenih sistema imaju posebnu strukturu koju odlikuje kratko-dometni entanglement, što sugerise da bi takvi sistemi mogli biti uspešno simularani tehnikama poput DMRG-a. Postojanje višečestične lokalizovane faze je važno za eksperimentalne sisteme poput polarnih molekula ili NV centara u dijamantu koji se koriste za kvantno računanje.

SPISAK NAUČNIH RADOVA RAZVRSTANIH PREMA KATEGORIJAMA NAUČNOG RADA (M KOEFICIJENTI)

RADOVI OBJAVLJENI U NAUČNIM ČASOPISIMA MEĐUNARODNOG ZNAČAJA (M 20)

M21

[1] Z. Papić, M. V. Milovanović
Quantum disordering of the 111 state and the compressible-incompressible transition in quantum Hall bilayer systems,
Phys. Rev. B **75**, 195304 (2007)

Citiran 8 puta (5 bez autocitata)

[2] M. V. Milovanović, Z. Papić
Nonperturbative approach to the quantum Hall bilayer
Phys. Rev. B **79**, 115319 (2009)

Citiran 5 puta (3 bez autocitata)

[3] Z. Papić, G. Moeller, M. V. Milovanović, N. Regnault, M. O. Goerbig
Fractional quantum Hall state at $\nu=1/4$ in a wide quantum well
Phys. Rev. B **79**, 245325 (2009)

Citiran 16 puta (12 bez autocitata)

[4] Z. Papić, N. Regnault, S. Das Sarma
Interaction-tuned compressible-to-incompressible phase transitions in quantum Hall systems
Phys. Rev. B **80**, 201303 (2009)

Citiran 18 puta (14 bez autocitata)

[5] M. V. Milovanović, Z. Papić
Transition from two-component 332 Halperin state to one-component Jain state at filling factor $\nu=2/5$
Phys. Rev. B **82**, 035316 (2010)

Citiran 1 put (1 bez autocitata)

[6] Z. Papić, M. O. Goerbig, N. Regnault, and M. V. Milovanović

Tunneling-driven breakdown of the 331 state and the emergent Pfaffian and composite Fermi liquid phases
Phys. Rev. B **82**, 075302 (2010).

Citiran 3 puta (1 bez autocitata)

[7] Z. Papić, M. O. Goerbig, and N. Regnault
Atypical Fractional Quantum Hall Effect in Graphene at $\nu_G = 1/3$
Phys. Rev. Lett. **105**, 176802 (2010)

Citiran 17 puta (12 bez autocitata)

[8] Michael R. Peterson, Z. Papić, S. Das Sarma
Fractional quantum Hall effects in bilayers in the presence of inter-layer tunneling and charge imbalance
Phys. Rev. B **82**, 235312 (2010)

Citiran 4 puta (4 bez autocitata)

[9] Z. Papić, B. A. Bernevig, N. Regnault
Topological Entanglement in Abelian and Non-Abelian Excitation Eigenstates
Phys. Rev. Lett. **106**, 056801 (2011)

Citiran 13 puta (13 bez autocitata)

[10] Z. Papić, R. Thomale, D. A. Abanin
Tunable Electron Interactions and Fractional Quantum Hall States in Graphene
Phys. Rev. Lett. **107**, 176602 (2011)

Citiran 17 puta (14 bez autocitata)

[11] Z. Papić, D. A. Abanin, Y. Barlas, R. N. Bhatt
Tunable interactions and phase transitions in Dirac materials in a magnetic field
Phys. Rev. B **84**, 241306 (2011)

Citiran 9 puta (7 bez autocitata)

[12] D. A. Abanin, Z. Papić, Y. Barlas, R. N. Bhatt
Stability of the $k = 3$ Read-Rezayi state in chiral two-dimensional systems with tunable interactions
New Journal of Physics **14**, 025009 (2012)

Citiran 1 put (1 bez autocitata)

[13] Bo Yang, Z. Papić, E. H. Rezayi, R. N. Bhatt, F. D. M. Haldane
Band mass anisotropy and the intrinsic metric of fractional quantum Hall systems,

Phys. Rev. B **85**, 165318 (2012)

Citiran 8 puta (7 bez autocitata)

[14] Bo Yang, Z. Hu, Z. Papić, F. D. M. Haldane
Model Wavefunctions for the Collective Modes and the Magneto-roton Theory of the Fractional Quantum Hall Effect
Phys. Rev. Lett. **108**, 256807 (2012)

Citiran 3 puta (3 bez autocitata)

[15] Z. Hu, Z. Papić, S. Johri, R. N. Bhatt, P. Schmitteckert
Comparison of the density-matrix renormalization group method applied to fractional quantum Hall systems in different geometries
Phys. Lett. A **376**, 2157 (2012)

Citiran 3 puta (2 bez autocitata)

[16] Z. Papić, F. D. M. Haldane, E. H. Rezayi
Quantum Phase Transitions and the $\nu=5/2$ Fractional Hall State in Wide Quantum Wells
Phys. Rev. Lett. **109**, 266806 (2012)

Citiran 2 puta (1 bez autocitata)

[17] B. Estienne, Z. Papić, N. Regnault, B. A. Bernevig
Matrix Product States for Trial Quantum Hall States
Phys. Rev. B **87**, 161112(R) (2013)

Citiran 4 puta (4 bez autocitata)

[18] Maksym Serbyn, Z. Papić, Dmitry A. Abanin
Universal slow growth of entanglement in interacting strongly disordered systems
Phys. Rev. Lett. **110**, 260601 (2013)

Citiran 5 puta (4 bez autocitata)

[19] Z. Papić
Fractional quantum Hall effect in a tilted magnetic field
Phys. Rev. B **87**, 245315 (2013)

Citiran 2 puta (2 bez autocitata)

[20] Maksym Serbyn, Z. Papić, Dmitry A. Abanin
Local conservation laws and the structure of the many-body localized states
Phys. Rev. Lett. **111**, 127201 (2013)

Citiran 1 put (1 bez autocitata)

M22

[1] Z. Papić, M. O. Goerbig, N. Regnault
Theoretical expectations for a fractional quantum Hall effect in graphene
Solid State Communications **149**, 1056 (2009)

Citiran 13 puta (12 bez autocitata)

M23

[1] Z. Papić, M. V. Milovanović
Disordering of the correlated state of the quantum Hall bilayer at filling factor $\nu = 1$
Mod. Phys. Lett. B **26**, 1250134 (2012)

ZBORNICI SA MEDJUNARODNIH NAUČNIH SKUPOVA (M 30)

M 31

[1] Z. Papić
Tunable interactions and ways of engineering fractional quantum Hall states
APS March meeting, March 18-22, 2013 Baltimore, USA

M 32

[1] Z. Papić

Numerical studies of the fractional quantum Hall effect in two-dimensional electron systems
Conference on computational physics, October 30-November 3, Gatlinburg, Tennessee, USA

[2] Z. Papić

Designing the non-Abelian states in multicomponent fractional quantum Hall systems
Workshop: Search for topological phases, 21-22 April, Princeton, USA

M 34

[1] Z. Papić, D. A. Abanin, N. Regnault, and M. O. Goerbig
Fractional quantum Hall effect in graphene: multicomponent states and tunable interactions
APS March meeting, March 21-25, 2011 Dallas, USA

[2] Bo Yang, F. D. M. Haldane, Z. Hu, Z. Papić

Model wavefunctions for fractional quantum Hall collective modes
APS March meeting, February 29 – March 2, 2012 Boston, USA

[3] Z. Papić, F. D. M. Haldane, E. H. Rezayi
Finite-size studies of the $\nu=5/2$ quantum Hall state in wide quantum wells: the effect of subband mixing and breaking of particle-hole symmetry
APS March meeting, February 29 – March 2, 2012 Boston, USA

[4] R. N. Bhatt, Z. Papić, D. A. Abanin, Y. Barlas
Phase diagram of massive Dirac fermions with tunable interactions in high magnetic fields
APS March meeting, February 29 – March 2, 2012 Boston, USA

ZBORNICI SKUPOVA NACIONALNOG ZNAČAJA (M 60)

M 62

[1] M. V. Milovanović, Z. Papić
Quantum Disorder of a Quantum Hall Superfluid
XVII National Symposium on Condensed Matter Physics (SFKM - 2007) (2007) **127**,
Vršac – Serbia

M 63

[1] Z. Papić, M. V. Milovanović
Quantum Disorder of the 111 state and the Compressible-Incompressible Transition in Quantum Hall Bilayer Systems
XVII National Symposium on Condensed Matter Physics (SFKM - 2007) (2007) **51**,
Vršac – Serbia

MAGISTARSKE I DOKTORSKE TEZE (M 70)

M 72

Ph. D. thesis: Fractional quantum Hall effect in multicomponent systems
2010, Fizički fakultet, Beograd.

**ELEMENTI ZA KVALITATIVNU OCENU NAUČNOG DOPRINOSA
KANDIDATA I MINIMALNI USLOVI ZA IZBOR U ZVANJE DR ZLATKA
PAPIĆA**

Pošto se kandidat nakon sticanja doktorata bira direktno u zvanje viši naučni saradnik, prikazani su minimalni uslovi za izbor u zvanje naučni saradnik i viši naučni saradnik, kao i zbirni uslov za oba zvanja. Nakon toga su prikazani kvantitativni rezultati kandidata u dosadašnjem naučnom radu i upoređeni sa minimalnim zbirnim uslovima za izbor u zvanje viši naučni saradnik.

Minimalni kvantitativni uslovi za izbor u zvanje

Zvanje	Minimalan broj M bodova	
Naučni saradnik	Ukupno	16
	M10+M20+M31+M32+M33+M41+M42	10
	M11+M12+M21+M22+M23+M24	5
Viši naučni saradnik	Ukupno	48
	M10+M20+M31+M32+M33+M41+M42+M51	40
	M11+M12+M21+M22+M23+M24+M31+M32+M41+M42	28
Zbirno za oba zvanja	Ukupno	64
	M10+M20+M31+M32+M33+M41+M42	50
	M10+M20+M31+M32+M33+M41+M42+M51	50
	M11+M12+M21+M22+M23+M24	33
	M11+M12+M21+M22+M23+M24+M31+M32+M41+M42	33

Ostvareni rezultati kandidata

M kategorija	M bodova po radu	Broj radova	Ukupno M bodova
M21	8	20	160
M22	5	1	5
M23	3	1	3
M31	3	1	3
M32	3	2	3
M34	2	4	2
M61	1	1	1
M62	0,5	1	0,5

Poređenje minimalnih uslova sa ostvarenim rezultatima kandidata

Zbirno za oba zvanja	Uslov	Ostvareni rezultat
Ukupno	64	177,5
M10+M20+M31+M32+M33+M41+M42	50	174
M10+M20+M31+M32+M33+M41+M42+M51	50	174
M11+M12+M21+M22+M23+M24	33	174
M11+M12+M21+M22+M23+M24+M31+M32+M41+M42	33	174

KOPIJE NAUČNIH RADOVA I DOKAZI O CITIRANOSTI

All Databases

<< Return to Web of Science®

Citing Articles Title: **Quantum disordering of the 111 state and the compressible-incompressible transition in quantum Hall bilayer systems**
 Author(s): **Papic, Zlatko ; Milovanovic, Milica V.**
 Source: **PHYSICAL REVIEW B** Volume: **75** Issue: **19** Article Number: **195304** DOI: **10.1103/PhysRevB.75.195304** Published: **MAY 2007**

This item has been cited by items indexed in the databases listed below. [more information]

8 in All Databases

- 8 publication in *Web of Science*
- 0 publication in *BIOSIS Citation Index*
- 0 publication in *SciELO Citation Index*
- 0 publication in *Chinese Science Citation Database*
- 0 data sets in *Data Citation Index*
- 0 publication in *Data Citation Index*

Results: 8 Page 1 of 1 Go Sort by: Publication Date -- newest to oldest

Create Citation Report

Hide Refine

Refine Results

Search within results for Search

Databases

Research Domains Refine

SCIENCE TECHNOLOGY

Research Areas Refine

PHYSICS

Document Types

Authors

Group/Corporate Authors

Editors

Funding Agencies

Source Titles

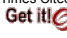
Conference/Meeting Titles

Publication Years

Languages

Countries/Territories

- Select Page | Add to Marked List (0) | Send to:
1. Author(s): Papic, Z.; Milovanovic, M. V.
 Source: MODERN PHYSICS LETTERS B Volume: 26 Issue: 21 Article Number: 1250134 DOI: 10.1142/S0217984912501345
 Published: AUG 20 2012
 Times Cited: 0 (from All Databases)
Get it! [View abstract](#)
 2. Title: TOPOLOGICALLY MASSIVE ELECTROMAGNETIC INTERACTION OF COMPOSITE PARTICLES IN A HIGHER-DERIVATIVE NONRELATIVISTIC GAUGE FIELD MODEL
 Author(s): Manavella, Edmundo C.
 Source: INTERNATIONAL JOURNAL OF MODERN PHYSICS A Volume: 25 Issue: 26 Pages: 4949-4974 DOI: 10.1142/S0217751X10050664 Published: OCT 20 2010
 Times Cited: 2 (from All Databases)
Get it! [View abstract](#)
 3. Title: Quantum Field Formalism for the Electromagnetic Interaction of Composite Particles in a Nonrelativistic Gauge Model III
 Author(s): Manavella, E. C.; Addad, R. R.
 Source: INTERNATIONAL JOURNAL OF THEORETICAL PHYSICS Volume: 48 Issue: 9 Pages: 2473-2485 DOI: 10.1007/s10773-008-9925-5 Published: SEP 2009
 Times Cited: 3 (from All Databases)
Get it! [View abstract](#)
 4. Title: Fractional quantum Hall state at nu=1/4 in a wide quantum well
 Author(s): Papic, Z.; Moeller, G.; Milovanovic, M. V.; et al.
 Source: PHYSICAL REVIEW B Volume: 79 Issue: 24 Article Number: 245325 DOI: 10.1103/PhysRevB.79.245325 Published: JUN 2009
 Times Cited: 16 (from All Databases)
Get it! [View abstract](#)
 5. Title: Nonperturbative approach to the quantum Hall bilayer
 Author(s): Milovanovic, M. V.; Papic, Z.
 Source: PHYSICAL REVIEW B Volume: 79 Issue: 11 Article Number: 115319 DOI: 10.1103/PhysRevB.79.115319 Published: MAR 2009
 Times Cited: 5 (from All Databases)
Get it! [View abstract](#)
 6. Title: Quantum Hall to Insulator Transition in the Bilayer Quantum Hall Ferromagnet
 Author(s): Murthy, Ganpathy; Sachdev, Subir
 Source: PHYSICAL REVIEW LETTERS Volume: 101 Issue: 22 Article Number: 226801 DOI: 10.1103/PhysRevLett.101.226801
 Published: NOV 28 2008
 Times Cited: 6 (from All Databases)
Get it! [View abstract](#)
 7. Title: Entanglement skyrmions in multicomponent quantum Hall systems
 Author(s): Doucot, B.; Goerbig, M. O.; Lederer, P.; et al.
 Source: PHYSICAL REVIEW B Volume: 78 Issue: 19 Article Number: 195327 DOI: 10.1103/PhysRevB.78.195327 Published: NOV 2008
 Times Cited: 7 (from All Databases)
Get it! [View abstract](#)

Title: [Quantum phase transitions in bilayer quantum hall systems at a total filling factor \$\nu\(T\) = 1\$](#)
 8. Author(s): Ye, Jinwu; Jiang, Longhua
 Source: PHYSICAL REVIEW LETTERS Volume: 98 Issue: 23 Article Number: 236802 DOI: 10.1103/PhysRevLett.98.236802
 Published: JUN 8 2007
 Times Cited: 18 (from All Databases)
 Get it!  [View abstract](#)

Select Page |  Add to Marked List (0) |   Send to:

Results: 8 Page 1 of 1 Sort by:

8 records matched your query of the 55,067,330 (contains duplicates) in the data limits you selected.

View in: [简体中文](#) | [繁體中文](#) | [English](#) | [日本語](#) | [한국어](#) | [Português](#) | [Español](#)

© 2013 Thomson Reuters | [Terms of Use](#) | [Privacy Policy](#) | *Please give us your feedback on using Web of Knowledge.*

Quantum disordering of the 111 state and the compressible-incompressible transition in quantum Hall bilayer systems

Zlatko Papić and Milica V. Milovanović

Institute of Physics, P.O. Box 68, 11080 Belgrade, Serbia

(Received 18 December 2006; revised manuscript received 5 February 2007; published 3 May 2007)

We systematically discuss properties of quantum disordered states of the quantum Hall bilayer at $\nu_T=1$. For one of them, the so-called vortex metal state, we find off-diagonal long-range order of *algebraic* kind, and derive its transport properties. It is shown that this state is relevant for the explanation of the “imperfect” superfluid behavior and persistent intercorrelations, for large distances between layers, that were found in experiments.

DOI: [10.1103/PhysRevB.75.195304](https://doi.org/10.1103/PhysRevB.75.195304)

PACS number(s): 73.43.Cd, 73.21.Ac, 73.43.Nq

I. INTRODUCTION

Electrons in quantum Hall bilayer systems at total filling factor $\nu_T=1$ naturally correlate in two different ways due to Pauli principle and Coulomb interaction. If the layers are sufficiently far apart, dominant correlations would be those of intralayer kind because electrons in one layer are unable to sense what is taking place in the opposite layer. This does not hold, however, in the limit of small layer separation. Instead, with decreasing d/l_B , the ratio of the distance between layers to the magnetic length, the correlations between electrons in different layers gain strength and begin to compete with intralayer correlations. It is the interplay of those two kinds of correlations that we focus on in this paper.

For the case of prevalent interlayer correlations, there are already a few theoretical models at hand which provide a satisfactory description: 111 state given by Halperin's¹ 111 wave function $\Psi_{111}=\prod_{i<j}(z_{i\uparrow}-z_{j\uparrow})\prod_{k<l}(z_{k\downarrow}-z_{l\downarrow})\prod_{m,n}(z_{m\uparrow}-z_{n\downarrow})$, quantum Hall ferromagnet,² condensate of excitons,³ or composite bosons.⁴ Nevertheless, both theoretically and experimentally, it is evident that with increasing d/l_B , a quantum disordering of this state is bound to take place. For example, the tunneling peak observed by Spielman *et al.*⁵ is indeed sharp and pronounced, but its nature is more that of a resonance than of the speculated Josephson effect, while the temperature dependences of Hall and longitudinal resistances in experiments of Kellogg *et al.*⁶ and Tutuc *et al.*⁷ do not provide support to the predicted Berezinskii-Kosterlitz-Thouless (BKT) scenario of a bilayer finite temperature phase transition.² Deeper understanding of the regime $d \sim l_B$ is therefore an important, open problem in the physics of quantum Hall bilayers and strongly correlated electron systems in general.

Hereinafter, we present some results which pertain to quantum disordering that is believed to take place in the quantum Hall bilayer at $\nu_T=1$. The ground state at $d=0$ is a Bose condensate well described by 111 wave function due to Halperin, while the low-lying excitations are composite bosons, i.e., electrons dressed with one quantum of magnetic flux.⁴ The idea of disordering that we employ is to allow the formation of composite fermions (i.e., electrons dressed with *two* quanta of magnetic flux) that coexist with composite bosons.⁸ There are two ways to introduce composite fermions into the Bose condensate and this will be explained in

Sec. II. We then pursue a phenomenological Chern-Simons transport theory of Drude in order to examine the elementary predictions of those two model states. In Sec. III, we arrive at an effective gauge theory for both cases. This enables us to calculate the correlation functions, modes of low-lying excitations, and characteristic off-diagonal long-range order (ODLRO). We will be primarily interested in the pseudospin channel of these states. In one of those, the so-called vortex metal state that we believe may appear in the bilayer at larger d/l_B as a manifestation of increasing intracorrelations, we derive an *algebraic* ODLRO. In Sec. IV, we focus on the incompressible region and the crossover around the critical layer separation. We will argue that our field-theoretical, homogeneous picture in fact suggests that vortex metal, if relevant for the strongly coupled, incompressible region, may appear only localized in the form of islands in the background of the superfluid state for smaller d/l_B . In Sec. V, we give a more thorough analysis of the experiments on bilayer, addressing especially the compressible, weakly coupled region, and the question of persistent intercorrelations⁹ in the framework of the vortex metal state. Section VI is devoted to discussion and conclusion. For the sake of clarity and in order to make the text self-contained, some of the known results^{8,10} will be rederived in this paper.

II. TRIAL WAVE FUNCTIONS FOR THE BILAYER

Building on Laughlin's proposal for the wave function of a single quantum Hall layer,¹¹ the construction of Rezayi-Read wave function¹² for $\nu=1/2$ and Halperin's 111 wave function for bilayer,¹ we may formally imagine that there are two species of electrons in each layer (z, w), which are all mutually correlated through intracorrelations (within the same layer) and intercorrelations (between opposite layers) (Fig. 1).

Starting from the 111 function of the Bose condensate, we will minimally deform it in order to include the composite fermions. Given that each particle binds the same number of flux quanta and taking Pauli principle into account, this becomes a combinatorial problem with two solutions. In the first case,

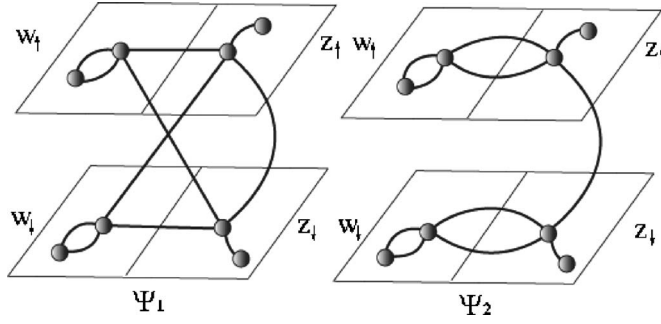


FIG. 1. Correlations between electrons in two layers.

$$\begin{aligned}
 \Psi_1 = \mathcal{P}\mathcal{A} & \left[\prod_{i<j} (z_{i\uparrow} - z_{j\uparrow}) \prod_{k<l} (z_{k\downarrow} - z_{l\downarrow}) \prod_{p,q} (z_{p\uparrow} - z_{q\downarrow}) \right. \\
 & \times \Phi_f(w_{\uparrow}, \bar{w}_{\uparrow}) \prod_{i<j} (w_{i\uparrow} - w_{j\uparrow})^2 \\
 & \times \Phi_f(w_{\downarrow}, \bar{w}_{\downarrow}) \prod_{k<l} (w_{k\downarrow} - w_{l\downarrow})^2 \\
 & \times \prod_{i,j} (z_{i\uparrow} - w_{j\uparrow}) \prod_{k,l} (z_{k\uparrow} - w_{l\downarrow}) \\
 & \left. \times \prod_{p,q} (z_{p,\downarrow} - w_{q,\uparrow}) \prod_{m,n} (z_{m\downarrow} - w_{n\downarrow}) \right]. \quad (1)
 \end{aligned}$$

The first line in this formula can be recognized as 111 function, followed by two $\nu=1/2$ separate layers (Φ_f 's denote the Slater determinants of free composite fermions), while the last two lines stem from the flux-particle constraint (all these correlations are depicted on the left hand side of Fig. 1). \mathcal{P} and \mathcal{A} denote projection to the lowest Landau level (LLL) and fermionic antisymmetrization (independently for each layer), respectively. In the thermodynamic limit, the relation between the number of particles and flux quanta reads¹⁰

$$\begin{aligned}
 N_{\Phi} &= N_{b\uparrow} + N_{b\downarrow} + N_{f\uparrow} + N_{f\downarrow} \\
 &= 2N_{f\uparrow} + N_{b\uparrow} + N_{b\downarrow} = 2N_{f\downarrow} + N_{b\uparrow} + N_{b\downarrow}. \quad (2)
 \end{aligned}$$

N_{Φ} is the number of flux quanta through the system and $N_{b\sigma}$ and $N_{f\sigma}$ are the number of bosons and fermions inside the layer σ , respectively; $\sigma = \uparrow, \downarrow$ is the layer index. Equation (2) enforces an additional constraint $N_{f\uparrow} = N_{f\downarrow}$. Therefore, the number of fermions is balanced in two layers, while the boson numbers are not subject to any such constraint. This fact is important because of the broken symmetry of spontaneous interlayer phase coherence in the 111 state, which demands nonconservation of $N_{b\uparrow} - N_{b\downarrow}$. Although we work in a fixed (relative) number representation (allowed in a broken symmetry case) to account for a broken symmetry situation, we need to have a possibility of unconstrained relative number of bosons. Then, a superposition of the wave functions of the form in Eq. (1) would lead to the usual representation.

In the second case which is expected to describe dominant intracorrelations, fermions bind exclusively within the layer they belong to (right side of Fig. 1) and the corresponding wave function is

$$\begin{aligned}
 \Psi_2 = \mathcal{P}\mathcal{A} & \left[\prod_{i<j} (z_{i\uparrow} - z_{j\uparrow}) \prod_{k<l} (z_{k\downarrow} - z_{l\downarrow}) \prod_{p,q} (z_{p\uparrow} - z_{q\downarrow}) \right. \\
 & \times \Phi_f(w_{\uparrow}, \bar{w}_{\uparrow}) \prod_{i<j} (w_{i\uparrow} - w_{j\uparrow})^2 \\
 & \times \Phi_f(w_{\downarrow}, \bar{w}_{\downarrow}) \prod_{k<l} (w_{k\downarrow} - w_{l\downarrow})^2 \\
 & \left. \times \prod_{i,j} (z_{i\uparrow} - w_{j\uparrow})^2 \prod_{k,l} (z_{k\downarrow} - w_{l\downarrow})^2 \right]. \quad (3)
 \end{aligned}$$

In this case, the flux-particle relation¹⁰ is

$$\begin{aligned}
 N_{\Phi} &= 2N_{f\uparrow} + 2N_{b\uparrow} = 2N_{f\downarrow} + 2N_{b\downarrow} \\
 &= 2N_{f\uparrow} + N_{b\uparrow} + N_{b\downarrow} = 2N_{f\downarrow} + N_{b\uparrow} + N_{b\downarrow}, \quad (4)
 \end{aligned}$$

implying that both fermion and boson numbers must be balanced: $N_{f\uparrow} = N_{f\downarrow}$ and $N_{b\uparrow} = N_{b\downarrow}$.

In Ref. 8, the authors numerically calculated the overlap of Ψ_1 with the exact ground-state wave function for a system of five electrons in each layer with varying d/l_B . Their results seem to demonstrate convincingly that (at least for small systems) the approach with trial wave functions that interpolate between two well-established limits, namely, those of 111 state and decoupled $\nu=1/2$ layers, is not only an artificial mathematical construction but also corresponds to physical reality. Despite the fact that the number of electrons in this simulation is certainly well below the thermodynamic limit, the fact that the overlaps between Ψ_1 and the exact ground state display peaks very close to 1 at small d/l_B provides confidence in the choice of wave function Ψ_1 (at least for small d/l_B).

If there is a phase separation in between the sea of composite bosons and composite fermions, the phase transition will be of the first order. Such a scenario is launched in Ref. 13, where the authors imagine static, isolated regions of incoherent phase inside 111 phase. Although this model correctly explains some of the observed phenomena (e.g., semi-circle law), the persistence of intercorrelations in the weakly coupled, compressible regime⁹ which gradually die out suggests a continuous transition. Such a possibility is naturally present in the picture of composite boson-composite fermion mixture.

A transport theory of Drude kind can be easily formulated⁸ if we consider that composite fermions bind two quanta of magnetic flux, unlike composite bosons which bind only one quantum of magnetic flux. As long as we remain in the random-phase approximation (RPA), they can all be treated as free particles moving in the presence of the effective field which is given by the sum of the external and self-consistently induced electric field. In the first case (Ψ_1), the effective field as seen by particles in the layer σ is

$$\mathcal{E}_f^{\sigma} = \mathbf{E}^{\sigma} - 2\epsilon \mathbf{J}_f^{\sigma} - \epsilon(\mathbf{J}_b^1 + \mathbf{J}_b^2), \quad (5)$$

$$\mathcal{E}_b^{\sigma} = \mathbf{E}^{\sigma} - \epsilon(\mathbf{J}_b^1 + \mathbf{J}_b^2 + \mathbf{J}_f^1 + \mathbf{J}_f^2), \quad (6)$$

where $\mathbf{J}_{f(b)}^{\sigma}$ denote Fermi and Bose currents in the layer σ and

$$\epsilon = \begin{bmatrix} 0 & \delta \\ -\delta & 0 \end{bmatrix},$$

with $\delta = \frac{\hbar}{e^2}$. Transport equations are

$$\mathcal{E}_{f(b)}^\sigma = \rho_{f(b)}^\sigma \mathbf{J}_{f(b)}^\sigma \quad (7)$$

and, as required by symmetry, $\rho_{f(b)}^1 = \rho_{f(b)}^2$, while the total current is given by $\mathbf{J}^\sigma = \mathbf{J}_b^\sigma + \mathbf{J}_f^\sigma$. We define single layer resistance (ρ^{11}) and drag resistance (ρ^D) as follows:

$$\mathbf{E}^1 = \rho^{11} \mathbf{J}^1, \quad (8)$$

$$\mathbf{E}^2 = \rho^D \mathbf{J}^1. \quad (9)$$

When both layers have the same filling, $\nu_1 = \nu_2 = 1/2$, tensors ρ_b and ρ_f are diagonal (because the composite particles are in zero net field): $\rho_b = \text{diag}[\rho_{bxx}, \rho_{bxx}]$ and $\rho_f = \text{diag}[\rho_{fxx}, \rho_{fxx}]$, and in the case of drag, we have in addition $\mathbf{J}^2 = 0$; \mathbf{J}^1 is finite. Then, from Eqs. (5)–(9) via elementary algebraic manipulations, we obtain

$$\rho^{11} = 1/2\{(\rho_b^{-1} + \rho_f^{-1})^{-1} + 2\epsilon + [(\rho_f + 2\epsilon)^{-1} + \rho_b^{-1}]^{-1}\}, \quad (10)$$

$$\rho^D = 1/2\{(\rho_b^{-1} + \rho_f^{-1})^{-1} + 2\epsilon - [(\rho_f + 2\epsilon)^{-1} + \rho_b^{-1}]^{-1}\}, \quad (11)$$

or in terms of matrix elements,

$$\rho_{xx}^D = -\frac{2\rho_{bxx}^2 \delta^2}{(\rho_{bxx} + \rho_{fxx})^3 + 4(\rho_{bxx} + \rho_{fxx}) \delta^2}, \quad (12)$$

$$\rho_{xy}^D = \frac{\delta(2\rho_{bxx}\rho_{fxx} + \rho_{fxx}^2 + 4\delta^2)}{\rho_{bxx}^2 + 2\rho_{bxx}\rho_{fxx} + \rho_{fxx}^2 + 4\delta^2}, \quad (13)$$

$$\rho_{xx}^{11} = \frac{2\rho_{bxx}^2 \delta^2}{(\rho_{bxx} + \rho_{fxx})^3 + 4(\rho_{bxx} + \rho_{fxx}) \delta^2} + \frac{\rho_{bxx}\rho_{fxx}}{(\rho_{bxx} + \rho_{fxx})}. \quad (14)$$

The formulas in Eqs. (12)–(14) include parameters δ , ρ_{bxx} , and ρ_{fxx} , the last two being the free parameters about which nothing can be said *a priori*. This prompted Simon *et al.*⁸ to reason as follows. At large d/l_B , the number of composite bosons is small because the condensate is broken and ρ_{bxx} is large compared to δ , which is the typical Hall resistance. On the other hand, from the experiments,¹⁴ we know that for large d/l_B holds $\rho_{fxx} \ll \delta$. Furthermore, even as d/l_B is decreased, we expect ρ_{fxx} to increase only slightly.⁸ All in all, for large d/l_B , they assume $\rho_{bxx} \gg \delta \gg \rho_{fxx}$, and if in addition we allow $\rho_{bxx}\rho_{fxx} \ll \delta^2$, asymptotically we obtain

$$\rho_{xx}^D \approx -\frac{2\delta^2}{\rho_{bxx}}, \quad (15)$$

$$\rho_{xy}^D \approx 4\delta \left(\frac{\delta}{\rho_{bxx}} \right)^2, \quad (16)$$

$$|\rho_{xx}^{11}| \approx |\rho_{xx}^D|. \quad (17)$$

Semicircle law follows directly from the previous formulas,

$$(\rho_{xx}^D)^2 + \left(\rho_{xy}^D - \frac{\delta}{2} \right)^2 \approx \left(\frac{\delta}{2} \right)^2, \quad (18)$$

in agreement with Ref. 13 (semicircle law is of general validity for two-component systems in two dimensions and it serves us as a crucial test for the line of reasoning quoted above, which may at first sound somewhat naive).

In the opposite limit (when d/l_B is reduced), $\rho_{bxx} \ll \rho_{fxx} \ll \delta$ because ρ_{bxx} drops as a result of Bose condensation.⁸ When $\rho_{bxx} \rightarrow 0$, we obtain the quantization of Coulomb drag,

$$\rho_{xy}^D \approx \delta, \quad (19)$$

$$\rho_{xx}^D \rightarrow 0, \quad (20)$$

as measured by Kellogg *et al.*⁶

Let us return now to the case of dominant intracorrelations, the vortex metal state¹⁰ represented by Eq. (3). From Fig. 1, the formulas for effective fields are modified into

$$\mathcal{E}_f^\sigma = \mathbf{E}^\sigma - 2\epsilon \mathbf{J}_f^\sigma - 2\epsilon \mathbf{J}_b^\sigma, \quad (21)$$

$$\mathcal{E}_b^\sigma = \mathbf{E}^\sigma - \epsilon(\mathbf{J}_b^1 + \mathbf{J}_b^2 + 2\mathbf{J}_f^\sigma), \quad (22)$$

and the analogous calculation yields the resistivity tensors,

$$\rho^{11} = \frac{1}{2}\{(\rho_b^{-1} + \rho_f^{-1})^{-1} + 2\epsilon + [(\rho_b - 2\epsilon)^{-1} + \rho_f^{-1}]^{-1}\} \times [(\rho_b - 2\epsilon)^{-1} \rho_b + 2\rho_f^{-1} \epsilon], \quad (23)$$

$$\rho^D = \frac{1}{2}\{(\rho_b^{-1} + \rho_f^{-1})^{-1} + 2\epsilon - [(\rho_b - 2\epsilon)^{-1} + \rho_f^{-1}]^{-1}\} \times [(\rho_b - 2\epsilon)^{-1} \rho_b + 2\rho_f^{-1} \epsilon]. \quad (24)$$

The matrix elements of these tensors are

$$\rho_{xx}^D = -\frac{2\rho_{fxx}^2 \delta^2}{(\rho_{bxx} + \rho_{fxx})^3 + 4(\rho_{bxx} + \rho_{fxx}) \delta^2}, \quad (25)$$

$$\rho_{xy}^D = \frac{\rho_{fxx}^2 \delta}{(\rho_{fxx} + \rho_{bxx})^2 + 4\delta^2}, \quad (26)$$

$$\rho_{xx}^{11} = \frac{2\rho_{fxx}^2 \delta^2}{(\rho_{bxx} + \rho_{fxx})^3 + 4(\rho_{bxx} + \rho_{fxx}) \delta^2} + \frac{\rho_{bxx}\rho_{fxx}}{(\rho_{bxx} + \rho_{fxx})}. \quad (27)$$

In this case as well, there are two physically significant limits depending on the assumptions for the values of ρ_{bxx} and ρ_{fxx} . In the case when $\rho_{bxx} \ll \rho_{fxx} \ll \delta$,

$$\rho_{xx}^D \approx -\frac{\rho_{fxx}}{2}, \quad (28)$$

$$\rho_{xy}^D \approx \frac{1}{4} \frac{\rho_{fxx}^2}{\delta}, \quad (29)$$

$$\rho_{xx}^{11} \approx \frac{\rho_{fxx}}{2}, \quad (30)$$

and the semicircle law follows [Eq. (18)], whereas $|\rho_{xx}^D| = |\rho_{xx}^{11}|$. Similarly, in the regime $\rho_{bxx} \ll \delta \ll \rho_{fxx}$, we deduce the quantization of Coulomb drag [Eqs. (19) and (20)].

We emphasize that these two limits are different from those in Simon *et al.*⁸ For example, the semicircle law was derived assuming that ρ_{bxx} is small (which is exactly the opposite situation to the one in Ref. 8), while ρ_{fxx} is not necessarily small with respect to δ . As noted in the first case above, the exact values for ρ_{bxx} and ρ_{fxx} are in fact unknown and this prevents us from discriminating between the different proposed limits. In other words, we cannot say which one of the proposed limits is plausible—the analysis above serves us only to conclude that each of the two composite boson-composite fermion mixed states is able (with certain assumptions) to reproduce the phenomenology of drag experiments.

III. CHERN-SIMONS THEORY FOR BILAYER

Encouraged by the preliminary analysis from the previous section, we will pursue the idea of composite boson-composite fermion mixture further by formulating an example of Chern-Simons (CS) field theory which can contain wave functions Ψ_1 , and Ψ_2 as ground states. We do not embark on such a task only for the sake of completeness, but also because such a theory would enable efficient calculation of response functions and provide insight into the long-range order of the system and the nature of low-lying excitations. A general drawback of CS theories is the inability to include the projection to LLL which is the arena where all the physics must be taking place. Nevertheless, we will use these theories established in the works of Zhang *et al.*¹⁵ for composite bosons and Halperin *et al.*¹⁶ for composite fermions because even projected to the LLL type of theories, of Murthy and Shankar,¹⁷ came to the conclusion that in order to get, in the most efficient way, to the qualitative picture of the physics of response, the usual CS theories are quite enough and accurate. In addition to this simplification, in constructing the CS theories, we will neglect the antisymmetrization requirement implied by Eqs. (1) and (3). The reason for this is that just like in hierarchical constructions, composite fermions represent meron excitations (see Ref. 10) that quantum disorder the 111 state, and, as it is usual when we discuss the dual picture of the fractional quantum Hall effect,¹⁸ we do not extend the antisymmetrization requirement to the quasiparticle part of the electron fluid.

Therefore, we start from the Lagrangian given by¹⁰

$$\begin{aligned} \mathcal{L} = \sum_{\sigma} \left[\Psi_{\sigma}^{\dagger} (i\partial_0 - a_0^{F\sigma} + A_0 + \sigma B_0) \Psi_{\sigma} \right. \\ \left. - \frac{1}{2m} |(-i\nabla + \mathbf{a}^{F\sigma} - \mathbf{A} - \sigma \mathbf{B}) \Psi_{\sigma}|^2 \right] \\ + \sum_{\sigma} \left[\Phi_{\sigma}^{\dagger} (i\partial_0 - a_0^{B\sigma} + A_0 + \sigma B_0) \Phi_{\sigma} \right. \end{aligned}$$

$$\begin{aligned} \left. - \frac{1}{2m} |(-i\nabla + \mathbf{a}^{B\sigma} - \mathbf{A} - \sigma \mathbf{B}) \Phi_{\sigma}|^2 \right] + \sum_{\sigma} \sum_{i=F,B} \frac{1}{2\pi} \frac{1}{2} a_0^{i\sigma} \\ \times (\nabla \times \tilde{\mathbf{a}}^{i\sigma}) - \frac{1}{2} \sum_{\sigma, \sigma'} \int d^2\mathbf{r}' \delta\rho_{\sigma}(\mathbf{r}) V_{\sigma\sigma'} \delta\rho_{\sigma'}(\mathbf{r}'), \quad (31) \end{aligned}$$

where σ enumerates the layers, Ψ_{σ} and Φ_{σ} are composite fermion and composite boson fields in the layer σ , $V_{\uparrow\uparrow} = V_{\downarrow\downarrow} \equiv V_a$, $V_{\uparrow\downarrow} = V_{\downarrow\uparrow} \equiv V_e$, and the densities are $\delta\rho_{\sigma} = \delta\rho_{\sigma}^F + \delta\rho_{\sigma}^B$. By \mathbf{A} (and \mathbf{B}) here, we mean external fields in addition to the vector potential of the uniform magnetic field \mathbf{A}_B , which is accounted for and included in gauge fields $\mathbf{a}^{F(B)\sigma}$. Therefore, we have $\mathbf{a}^{F(B)\sigma} = \tilde{\mathbf{a}}^{F(B)\sigma} - \mathbf{A}_B$. External fields \mathbf{A} and \mathbf{B} couple with charge and pseudospin, and in general we must introduce four gauge fields $\mathbf{a}^{F(B)\sigma}$. Fortunately, not all of them are independent. In the first case, the relation analogous to Eq. (2) becomes the following gauge field equation:

$$\frac{1}{2\pi} \nabla \times \mathbf{a}^{F\sigma} = 2\delta\rho^{F\sigma} + \delta\rho^{B\uparrow} + \delta\rho^{B\downarrow},$$

$$\frac{1}{2\pi} \nabla \times \mathbf{a}^{B\sigma} = \delta\rho^{F\uparrow} + \delta\rho^{F\downarrow} + \delta\rho^{B\uparrow} + \delta\rho^{B\downarrow}. \quad (32)$$

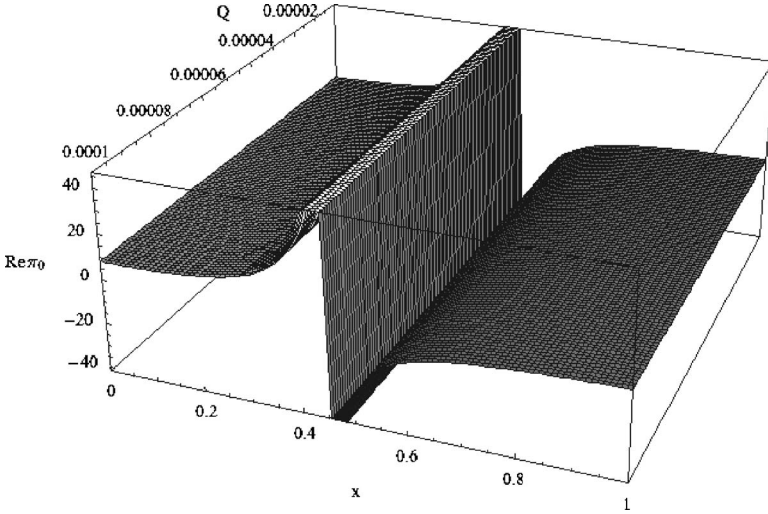
From the equations above, it is obvious that there are only two linearly independent gauge fields: $\mathbf{a}_C = \frac{\mathbf{a}^{F\uparrow} + \mathbf{a}^{F\downarrow}}{2} = \frac{\mathbf{a}^{B\uparrow} + \mathbf{a}^{B\downarrow}}{2}$ and $\mathbf{a}_S = \frac{\mathbf{a}^{F\uparrow} - \mathbf{a}^{F\downarrow}}{2}$, and Eq. (32) expressed in Coulomb gauge reads $\frac{ika_C}{2\pi} = \delta\rho_{\uparrow} + \delta\rho_{\downarrow} \equiv \delta\rho$ and $\frac{ika_S}{2\pi} = \delta\rho^{F\uparrow} - \delta\rho^{F\downarrow} \equiv \delta\rho_S^F$ (a_C and a_S are the transverse components of the gauge fields). These are the constraints we wish to include into the functional integral via Lagrange multipliers a_0^C and a_0^S . The interaction part of the Lagrangian is easily diagonalized by introducing $V_C = \frac{V_a + V_e}{2}$ and $V_S = \frac{V_a - V_e}{2}$.

The strategy for integrating out the bosonic functions is the Madelung ansatz $\phi_{\sigma} = \sqrt{\rho_{\sigma}} + \bar{\rho}_{\sigma} e^{i\theta_{\sigma}}$, which expands the wave function in terms of a product of its amplitude and phase factor, while fermionic functions are treated, as elaborated in Ref. 16. After Fourier transformation, within the quadratic (RPA) approximation, and introducing substitutions $\delta\rho_C^i = \delta\rho_{\uparrow}^i + \delta\rho_{\downarrow}^i$ and $\delta\rho_S^i = \delta\rho_{\uparrow}^i - \delta\rho_{\downarrow}^i$, $i = F, B$ and $\theta_C = \frac{\theta_{\uparrow} + \theta_{\downarrow}}{2}$, $\theta_S = \frac{\theta_{\uparrow} - \theta_{\downarrow}}{2}$, all the terms neatly decouple into a charge and a pseudospin channel,

$$\begin{aligned} \mathcal{L}_C = K_{00}(\delta a_0^C)^2 + K_{11}(\delta a_C)^2 + i\omega\delta\rho_C^B\theta_C - \delta\rho_C^B\delta a_0^C - \frac{\bar{\rho}_b}{m}k^2\theta_C^2 \\ - \frac{\bar{\rho}_b}{m}(\delta a_C)^2 + \frac{1}{2\pi}a_0^C ika_C - \frac{1}{2} \frac{k^2 a_C^2}{(2\pi)^2} V_C, \quad (33) \end{aligned}$$

$$\begin{aligned} \mathcal{L}_{PS} = K_{00}(\delta a_0^S)^2 + K_{11}(\delta a_S)^2 + i\omega\delta\rho_S^B\theta_S - \delta\rho_S^B B_0 - \frac{\bar{\rho}_b}{m}k^2\theta_S^2 \\ - \frac{\bar{\rho}_b}{m}B^2 + \frac{1}{2\pi}a_0^S ika_S - \frac{1}{2} V_S \left(\delta\rho_S^B + \frac{ik}{2\pi} a_S \right)^2, \quad (34) \end{aligned}$$

where $\delta a_0^C \equiv a_0^C - A_0$, $\delta a_C \equiv a_C - A$, $\delta a_0^S \equiv a_0^S - B_0$, $\delta a_S \equiv a_S - B$, and $\bar{\rho}_b$ the mean density of bosons in (each) layer. In writing down Eqs. (33) and (34), we utilize a compact notation suppressing k ($-k$) dependence, where all the quadratic terms of


 FIG. 2. $\text{Re } \pi_{00}(k)$ and the Goldstone mode in the case of Ψ_1 .

the type $(X+Y)^2$ stand for $[X(-k)+Y(-k)][X(k)+Y(k)]$. $K_{00}(k)$ and $K_{11}(k)$ are the free fermion (RPA) density-density and current-current correlation functions.¹⁶ In the long-wavelength limit ($k/k_f \ll 1$), they can be explicitly evaluated from the general expressions,¹⁶

$$K_{00}(k, \omega) = \frac{m}{2\pi} \left[1 - \Theta(x^2 - 1) \frac{|x|}{\sqrt{x^2 - 1}} + i\Theta(1 - x^2) \frac{|x|}{\sqrt{1 - x^2}} \right], \quad (35)$$

$$K_{11}(k, \omega) = \frac{2n_f}{m} \left[-x^2 - \frac{k^2}{24\pi n_f} + \Theta(x^2 - 1)|x|\sqrt{x^2 - 1} + i\Theta(1 - x^2)|x|\sqrt{1 - x^2} \right], \quad (36)$$

where $x = \frac{m\omega}{k k_f}$, k_f the Fermi wave vector, n_f the fermion density, and Θ the Heaviside step function. The mass appearing in expressions for K_{00} and K_{11} is equal to the bare electron mass only in the RPA approximation (in which we work here).

Focusing on the charge channel only [Eq. (33)] and integrating out first $\delta\rho_C^B$, then a_0^C and δa_C , we arrive at the density-density correlator,

$$\pi_{00}(k) = \frac{\left(\frac{k}{2\pi}\right)^2}{\frac{2\bar{\rho}_b}{m} - 2K_{11} + V_C \left(\frac{k}{2\pi}\right)^2 - \frac{\left(\frac{k}{2\pi}\right)^2}{\frac{2\bar{\rho}_b k^2}{m\omega^2} - 2K_{00}}}. \quad (37)$$

In the limiting case $x \ll 1$: $K_{00} \approx \frac{m}{2\pi}(1+ix)$ and $K_{11} \approx -\frac{k^2}{12\pi m} + i\frac{2n_f}{m}x$, and we conclude that as $\omega \rightarrow 0$ (and then $k \rightarrow 0$), the system is incompressible in the charge channel, so long as there is a thermodynamically significant density of bosons $\bar{\rho}_b$.

In the pseudospin channel, we are primarily looking for the signature of a Bose condensate, i.e., whether there exists a Goldstone mode of broken symmetry and what is the long-

range order of the state. Therefore, in Eq. (34) we set $A_\mu = B_\mu = 0$ and integrate over a_0^S , a_S , and $\delta\rho_S^B$,

$$\langle \theta_S(-k) \theta_S(k) \rangle = \frac{V_S}{\omega^2 \frac{1}{2} V_S + \alpha - \frac{2\bar{\rho}_b V_S}{m} k^2}, \quad (38)$$

where $\alpha = \frac{1}{4} K_{00}^{-1} - K_{11} \left(\frac{2\pi}{k}\right)^2$ (in Appendix, we give the full linear response in the pseudospin channel). Indeed, there exists a Goldstone mode, albeit with a small dissipative term (which, if desired, can be removed by pairing construction¹⁰),

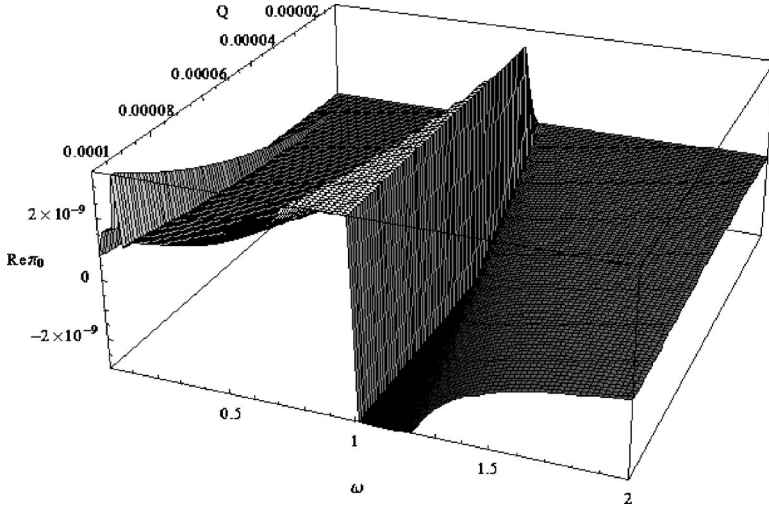
$$\omega^0(k) = \sqrt{\frac{2\bar{\rho}_b V_S}{m}} k - i \frac{V_S}{16\pi^{3/2} \sqrt{n_f}} k^3. \quad (39)$$

Even for large x , it is easy to check that the pole remains at the same value if we assume $\bar{\rho}_b \gg n_f$ (which is, in fact, the most appropriate assumption in this case). Also, the imaginary term disappears in this case. Such robust Goldstone mode implies the existence of a true ODLRO and the genuine Bose condensate. Goldstone mode $\omega^0(k)$ [Eq. (39)] is easily observed in Fig. 2, where we plotted the real part of density-density correlation function $\pi_{00}(k)$ [Eq. (A1)] in terms of parameters $Q \equiv k/k_f$ and $x \equiv \omega/(k k_f)$. Other (fixed) parameters are $m = l_B = 1$, $d = 0.5$, $\epsilon = 12.6$, $V_S = \pi d / \epsilon$, $\bar{\rho}_b + n_f = 1/(4\pi)$, and $\eta = n_f / \bar{\rho}_b = 1/10$.

Let us return to the second case, that of Eq. (3) and dominant intracorrelations. According to Fig. 1, relations [Eq. (32)] are modified to become

$$\begin{aligned} \frac{1}{2\pi} \nabla \times \mathbf{a}^{F\sigma} &= 2\delta\rho^{F\sigma} + 2\delta\rho^{B\sigma}, \\ \frac{1}{2\pi} \nabla \times \mathbf{a}^{B\sigma} &= 2\delta\rho^{F\sigma} + \delta\rho^{B\uparrow} + \delta\rho^{B\downarrow}. \end{aligned} \quad (40)$$

It is obvious that in this case we have only three linearly independent gauge fields, namely, $a_C = \frac{a^{F\uparrow} + a^{F\downarrow}}{2} = \frac{a^{B\uparrow} + a^{B\downarrow}}{2}$, $a_S = \frac{a^{F\uparrow} - a^{F\downarrow}}{2}$, and $a_{FS} = \frac{a^{B\uparrow} - a^{B\downarrow}}{2}$. Introducing the same substitutions


 FIG. 3. $\text{Re } \pi_0(k)$ in the case of Ψ_2 .

as before, the Lagrangian again decouples into a charge channel,

$$\begin{aligned} \mathcal{L}_C = & K_{00}(\delta a_0^C)^2 + K_{11}(\delta a_C)^2 + i\omega\delta\rho_C^B\theta_C - \delta\rho_C^B\delta a_0^C - \frac{\bar{\rho}_b}{m}k^2\theta_C^2 \\ & - \frac{\bar{\rho}_b}{m}(\delta a_C)^2 + \frac{ik}{2\pi}a_0^C a_C - \frac{1}{2}V_C\left(\frac{k}{2\pi}\right)^2 a_C^2, \end{aligned} \quad (41)$$

and a pseudospin channel,

$$\begin{aligned} \mathcal{L}_{PS} = & K_{00}(\delta a_0^S)^2 + K_{11}(\delta a_S)^2 + i\omega\delta\rho_S^B\theta_S - \delta\rho_S^B\delta a_0^{FS} - \frac{\bar{\rho}_b}{m}k^2\theta_S^2 \\ & - \frac{\bar{\rho}_b}{m}(\delta a_{FS})^2 + \frac{ik}{2\pi}a_0^S a_{FS} + \frac{ik}{2\pi}a_0^{FS}(a_S - a_{FS}) \\ & - \frac{1}{2}V_S\left(\frac{k}{2\pi}\right)^2 a_S^2, \end{aligned} \quad (42)$$

where $\delta a_0^{FS} \equiv a_0^{FS} - B_0$ and $\delta a_{FS} = a_{FS} - B$; all the other symbols have retained their meanings.

This time we will not analyze the charge channel in detail. To this end, we note that the system in incompressible in this sector, the fact which is easily established by integrating out all the gauge fields, densities, and boson phase in Eq. (41).

In the pseudospin channel, a calculation of the density-density correlator leads to the conclusion that in this channel, the system is compressible (see also Fig. 3). The θ - θ correlator is

$$\langle \theta_S(-k)\theta_S(k) \rangle = \frac{\frac{1}{k^2}\beta\gamma}{\left(\frac{\omega}{2\pi}\right)^2(\beta + \gamma) - \frac{2\bar{\rho}_b}{m}\beta\gamma}, \quad (43)$$

where $\beta = \frac{1}{2K_{00}}\left(\frac{k}{2\pi}\right)^2 + \frac{2\bar{\rho}_b}{m}$ and $\gamma = V_S\left(\frac{k}{2\pi}\right)^2 - 2K_{11}$. For small k/k_f and x , the correlator diverges for $\omega^0 = \frac{4\pi\bar{\rho}_b}{m} = \text{const}$, which obviously contradicts the original assumption for the range of x and hence we reject this pole. For $x \gg 1$ (and still $k \ll k_f$), the relations [Eqs. (35) and (36)] are approximately $K_{00} \approx -\frac{1}{4\pi x^2}$ and $K_{11} \approx -\frac{n_f}{m}$, and we obtain two poles,

$$\omega^0(k) = \frac{4\pi n_f}{m} \sqrt{\frac{1}{2} + \eta - \frac{1}{2}\sqrt{1+4\eta}}, \quad (44)$$

$$\Omega^0(k) = \frac{4\pi n_f}{m} \sqrt{\frac{1}{2} + \eta + \frac{1}{2}\sqrt{1+4\eta}}, \quad (45)$$

where $\eta = \bar{\rho}_b/n_f$ is the ratio of boson to fermion density [Eqs. (44) and (45) hold for any η , although in the physical limit that we are presently interested, η may be regarded as small]. In Fig. 3 we plotted the real part of the density-density correlation function in the case of Ψ_2 [Eq. (A4)]. In contrast to Fig. 2, here we opt for ω and Q as free parameters and set $d=1.5$ and $\eta = \bar{\rho}_b/n_f = 1/10$ as the more likely values in this case. Distinctive feature of Fig. 3 at $\omega \approx 1$ is the plasma frequency Ω^0 and the smaller singularity at $\omega \approx 1/10$ corresponds to ω^0 . There is also a striking absence of Goldstone mode in this case.

We now proceed to calculate ODLRO in the pseudospin channel of Ψ_2 . As it turns out, ODLRO will be nontrivially modified and assume algebraic form. We know that interaction does not affect the value of characteristic exponent¹⁹ and therefore set $V_S \equiv 0$. Bearing in mind that we work in the long-wavelength limit, we arrive at the following expression for the correlator:

$$\langle \theta_S(-k)\theta_S(k) \rangle = \frac{(2\pi\omega_p/k^2)(\omega^2 - \omega_p^2\eta)}{\{\omega^2 - [\omega^0(k)]^2\}\{\omega^2 - [\Omega^0(k)]^2\}}, \quad (46)$$

where we introduced $\omega_p = \frac{4\pi n_f}{m}$. After contour integration over ω ,¹⁹

$$\langle \theta_S(-k)\theta_S(k) \rangle = -\frac{2\pi}{k^2}f(\eta),$$

where $f(\eta) = \frac{1}{\sqrt{1+4\eta}}$, which leads to the algebraic ODLRO,

$$\langle e^{i\theta_S(\mathbf{r})}e^{-i\theta_S(\mathbf{r}')} \rangle \propto \frac{1}{|\mathbf{r} - \mathbf{r}'|^{f(\eta)}} \approx |\mathbf{r} - \mathbf{r}'|^{-[1-2\eta+o(\eta^2)]}. \quad (47)$$

This algebraic ODLRO persists as long as $\eta > 0$ (function f is positive everywhere in this domain). The expression Eq. (47) is formally reminiscent of BKT XY ordering; only the

role of the temperature is overtaken by the parameter η (the analysis of this paper assumes temperature $T=0$). Pursuing this analogy further, we conclude that the relative fluctuations of composite boson and composite fermion densities represent the mechanism which may lead to the ultimate breakdown of the 111 condensate.

IV. EVOLUTION OF THE GROUND STATE WITH d

In order to investigate the transition from the incompressible, 111-like state at lower d/l_B , to the compressible, possibly vortex metal-like state at higher d/l_B , we are motivated to introduce what we call *generalized vortex metal*. In addition to the ordinary vortex metal (Ψ_2), we include (in each layer) another kind of composite fermions that connect to the composite boson sea as in the case of Ψ_1 . The generalized vortex metal is clearly the only additional option left of connecting electrons divided in composite bosons and composite fermions beside the two extreme cases, Ψ_1 and Ψ_2 . Again, in this state some of composite fermions connect in the manner of 111 state to the composite bosons and the rest of composite fermions connect exclusively to the composite bosons of the same layer in the manner of the Rezayi-Read state. This is succinctly represented by the following gauge field constraints:

$$\frac{1}{2\pi} \nabla \times a^{B\sigma} = \delta\rho_{B\uparrow} + \delta\rho_{B\downarrow} + \delta\rho_{F\uparrow}^{(1)} + \delta\rho_{F\downarrow}^{(1)} + 2\delta\rho_{F\sigma}^{(2)}, \quad (48)$$

$$\frac{1}{2\pi} \nabla \times a_1^{F\sigma} = \delta\rho_{B\uparrow} + \delta\rho_{B\downarrow} + 2\delta\rho_{F\sigma}^{(1)} + 2\delta\rho_{F\sigma}^{(2)}, \quad (49)$$

$$\frac{1}{2\pi} \nabla \times a_2^{F\sigma} = 2\delta\rho_{B\sigma} + 2\delta\rho_{F\sigma}^{(1)} + 2\delta\rho_{F\sigma}^{(2)}, \quad (50)$$

where the superscripts (1) and (2) indicate composite fermion species in each layer. Chern-Simons theory easily follows from the above gauge field equations and yields incompressible behavior in the charge channel. In the pseudospin channel,

$$\begin{aligned} \mathcal{L}_{PS} = & K_{00}^{(1)}(\delta a_{0,1}^{FS})^2 + K_{00}^{(2)}(\delta a_{0,2}^{FS})^2 + K_{11}^{(1)}(\delta a_1^{FS})^2 + K_{11}^{(2)}(\delta a_2^{FS})^2 \\ & + i\omega\delta\rho_S^B\theta_S - \delta\rho_S^B\delta a_0^S - \frac{\bar{\rho}_b}{m}k^2\theta_S^2 - \frac{\bar{\rho}_b}{m}(\delta a_S)^2 \\ & + \frac{ik}{2\pi}a_{0,1}^{FS}(a_1^{FS} - a_S) + \frac{ik}{2\pi}a_0^S(a_2^{FS} - a_1^{FS}) + \frac{ik}{2\pi}a_{0,2}^{FS}a_S \\ & - \frac{1}{2}V_S\left(\frac{k}{2\pi}\right)^2|a_2^{FS}|^2 - \frac{1}{2}V_{hc}\left(\frac{k}{2\pi}\right)^2a_S(a_1^{FS} - a_S), \end{aligned} \quad (51)$$

where the linearly independent fields are given by $a_S = \frac{a^{B\downarrow} - a^{B\uparrow}}{2}$, $a_1^{FS} = \frac{a_1^{F\downarrow} - a_1^{F\uparrow}}{2}$, and $a_2^{FS} = \frac{a_2^{F\downarrow} - a_2^{F\uparrow}}{2}$, subscripts 1 and 2 distinguish between composite fermion species and S denotes antisymmetric combination of the densities in two layers (like in Sec. III). A noteworthy feature of the Lagrangian [Eq. (51)] is the existence of V_{hc} , the hard-core repulsion

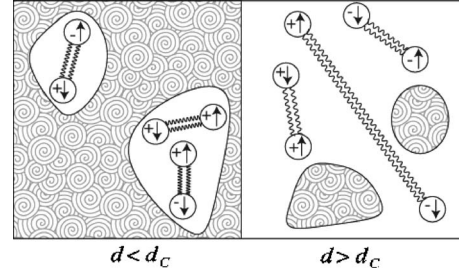


FIG. 4. Evolution of the ground state with varying d , before and after the transition at $d=d_c$. The regions with meron pairs represent the vortex metal (Ψ_2) phase. The background represents the superfluid (Ψ_1) phase.

term between the two species of composite fermions inside each layer. The presence of such a term (added by hand) is natural if we imagine composite fermions residing in two separate Fermi spheres. However, the danger of blindly introducing this term is that it may incidentally bring about the incompressible behavior (otherwise not present) in the system. We have verified that this is *not* the case here; i.e., the system remains incompressible whether or not we choose to introduce V_{hc} . It therefore appears more intuitive to keep V_{hc} , taking the limit $V_{hc} \rightarrow \infty$ in the end. Step by step, eliminating all the gauge fields, we are led to the following correlation function:

$$\langle \theta_S(-k)\theta_S(k) \rangle = \frac{V_S + \frac{2n_{f2}}{m}\left(\frac{2\pi}{k}\right)^2}{\omega^2 - \left[\frac{2\bar{\rho}_b V_S}{m}k^2 + \left(\frac{4\pi}{m}\right)^2 \bar{\rho}_b n_{f2}\right]}, \quad (52)$$

and the low-energy spectrum is dominated by the plasma frequency,

$$\omega^0(k) = \frac{4\pi}{m}\sqrt{\bar{\rho}_b n_{f2}}, \quad (53)$$

where n_{f2} is the density of the composite fermions which bind exclusively within the layer they belong. Generalized vortex metal therefore is a state that only supports gapped collective excitations, despite the presence of composite bosons and the kind of composite fermions which enforce interlayer correlation. If it is pertinent to the region of the tunneling experiments of Spielman *et al.*⁵ and counterflow experiments of Kellogg *et al.*,⁶ we believe that our homogeneous theory of Secs. III and IV then suggests that (generalized) vortex metal can appear only as localized islands (due to presence of disorder at low temperatures) amidst the background of Ψ_1 phase (Fig. 4). In Fig. 4 weakly coupled vortex-antivortex pairs are depicted, i.e., meron-antimeron pairs (due to the charge degree of freedom, there are four kinds of merons²) inside the vortex metal phase. They are expected to exist in the vortex-metal phase on the grounds of disordering of the correlated phase. As argued in Ref. 10, the inclusion of composite fermions into the 111 state (Ψ_1 and Ψ_2) corresponds to the creation of meron-antimeron pairs. There are more pairs and more of larger size as d increases

consistently with the BKT picture of the phase that supports algebraic ODLRO [Eq. (47)].

V. FURTHER COMPARISON WITH EXPERIMENTS

In this section, we wish to address in depth the potential of the model states, Ψ_1 and Ψ_2 , in explaining the phenomenology of experiments on bilayer. The key question in this analysis is: what is the nature of the compressible phase corresponding to higher d/l_B that still harbors some of the intercorrelation present at lower d/l_B ?⁹

The answer to this question cannot be given by looking at simple transport properties. In Sec. II, it was shown that both Ψ_1 and Ψ_2 in certain regimes can recover the two main experimental findings of Kellogg *et al.* in drag experiments: the semicircle law⁹ and the quantization of Hall drag resistance.²⁰ On the other hand, our Chern-Simons RPA approach at $T=0$ stresses that all that states considered in this paper are incompressible. However, at finite T , a finite energy¹⁰ is needed to excite a meron in Ψ_2 and therefore Ψ_2 seems like a better candidate for exhibiting compressible behavior at any finite T or, at least, a very small gap. Furthermore, within the vortex metal picture, Ψ_2 allows the following simple scenario. For $\rho_{bxx} \ll \rho_{fxx} \ll \delta$, one gets the semicircle law derived in Sec. II. As d/l_B increases, the density of bosons decreases and one enters the regime $\rho_{fxx} \ll \rho_{bxx} \ll \delta$, where $|\rho_{xx}^D| \gg \rho_{xy}^D$ (as witnessed in the experiments⁹). The persistence of enhanced longitudinal drag resistance⁹ up to very high d/l_B provides additional support to our choice of Ψ_2 which can explain the remaining intercorrelation (drag) in the case where explicit tunneling is absent. Finally, as $\rho_{bxx} \rightarrow \infty$, both resistances go to zero, the bilayer decouples, and bosons vanish from the system.

Our picture is certainly incomplete because it does not explicitly include the effects of disorder (which must be very relevant for the physics of bilayer in the regimes $d \sim l_B$ —a simple way to see this is to look at the behavior of measured counterflow resistances^{6,7} ρ_{xx}^{CF} and ρ_{xy}^{CF} that enter the insulating regime very quickly after passing through $\nu_T=1$). Fertig and Murthy²¹ provided a realistic model for the effects of disorder and in their disorder-induced coherence network in the incompressible phase of the bilayer, merons are able to sweep by hopping across the system, causing the activated behavior of resistance (dissipation) in counterflow. This finding is consistent with our own.

At the end our picture is in the spirit of the Stern and Halperin proposal¹³ but instead of the 1/2 compressible phase coexisting in a phase separated picture with the superfluid phase (Ψ_1), we assume the existence of the vortex metal phase (Ψ_2). This coincides with the proposal of Fertig and Murthy²¹ for the incompressible region that explains the “imperfect” superfluid behavior. It is the continuous extrapolation of this phase separated picture that brings and favors Ψ_2 for larger d/l_B (instead of Ψ_1). There Ψ_2 is able to explain the persistence of intercorrelations through enhanced longitudinal drag accompanied by the absence of tunneling and phase coherence.²⁰

Finally, we are able to account for the effects of the layer density imbalance in tunneling, drag,²² and counterflow²³ ex-

periments. Spielman *et al.*²² observed that small density imbalance stabilizes the resonant tunneling peak—a simple reason for this is that Ψ_1 can easily accommodate the fluctuations in density [see comment after Eq. (2)]. Because of the same reason, Hall drag resistance remains quantized up to larger d/l_B in the presence of density imbalance. On the other hand, the enhancement of longitudinal drag resistance at large d/l_B was also reported⁹ to be insensitive to density imbalance. While the reason for this cannot be seen only from looking at the form of Ψ_2 [this state constrains both fermion and boson numbers in two layers, see comment after Eq. (4)], we believe that meron excitations are responsible for absorbing the density fluctuations, especially at finite T .

Recently, the quantum Hall bilayer was probed using resonant Rayleigh scattering²⁴ for samples with different tunneling amplitudes and when the in-plane magnetic field is present. They detected a nonuniform spatial structure in the vicinity of the transition, suggesting a phase-separated version of the ground state. Our results (for zero tunneling limit and excluding disorder) hint that such phase separation may indeed be necessary to invoke in order to achieve a full description of the strongly coupled, incompressible phase and the transition in a bilayer.

VI. DISCUSSION AND CONCLUSION

In conclusion, we showed how two model states, Ψ_1 and Ψ_2 , can account for the basic phenomenology of the bilayer that came up from various experiments.

A very interesting question pertains to the model state Ψ_2 . Effectively the state represents a collection of meron excitations interacting through topological interactions. A question comes when they are in a confined (dipole) phase and when in a metallic (plasma) phase. So in principle we can expect that the static correlator in Eq. (47) can be reproduced by considering a two-dimensional (2D) bosonic model with meron excitations interacting via 2D Coulomb plasma interaction.²⁵ Therefore we believe that the Laughlin ansatz²⁶ of considering (static) ground-state correlators as statistical models in 2D can also be applied here. We expect that the ground-state correlators in a dual approach, in which we switch from composite fermion to meron coordinates, can be mapped to a partition function of a 2D Coulomb plasma.²⁷ The 2D Coulomb plasma has two different phases. For large β (inverse T), the charges form dipoles and the system is with long-range correlations (no mass gap). At some critical β , dissociation of dipoles occurs and we have a plasma phase with a Debye screening, and therefore a mass gap. Thus, calculations that will capture more of the meron contribution than our RPA approach in the Chern-Simons theory may find a transition and exponential decay of the correlator [Eq. (47)] before reaching the $\bar{\rho}_b=0$ limit. Indeed, our ODLRO exponent in Eq. (47) at $\bar{\rho}_b=0$ is 1 which is well above the exponent of the BKT transition or critical exponent 1/4. At that point our system may develop a gap in the pseudospin channel and completely lose interlayer coherence (exponential decay of correlators). Furthermore, we expect that the superfluid portion of the composite boson density will disappear leading to compressible behavior in the charge channel.¹⁹

This is all consistent with experiments^{9,20} which find that, at $d/l_B \approx 1.84$, the vanishing of the conventional quantum Hall effect and the system's Josephson-like tunneling characteristics occur simultaneously. Intercorrelated bosons continue to exist without a superfluid property and lead to enhanced $\nu = 1$ drag at large d/l_B . They disappear from the system around $d/l_B \approx 2.6$.⁹

ACKNOWLEDGMENT

The work was supported by Grant No. 141035 of the Ministry of Science of the Republic of Serbia.

APPENDIX

In order to extract the response functions in functional integral formalism, one needs to integrate over all degrees of freedom except those of the external fields. The integration of these fields in the RPA proverbially reduces to the Gaussian integral,

$$\int d(z, z^*) \exp(-z^* w z + u^* z + v z^*) = \frac{\pi}{w} \exp\left(\frac{u^* v}{w}\right), \quad \text{Re } w > 0.$$

For the pseudospin channel in the case of Ψ_1 [Eq. (1)], we therefore obtain the following linear response:

$$\pi_{00}(k) = \frac{1}{\Xi} [\Omega(3V_S + 2\alpha) + 1], \quad (\text{A1})$$

$$\pi_{01}(k) = \pi_{10}(k) = \frac{1 - i\pi}{\Xi} \frac{\pi}{k} K_{11} (1 + \Omega V_S), \quad (\text{A2})$$

$$\pi_{11}(k) = \frac{1}{\Xi} \left[2V_S(1 - \Omega V_S) \left(K_{11} - \frac{\bar{\rho}_b}{m} \right) + K_{11}/K_{00} - 4\alpha \frac{\bar{\rho}_b}{m} \right], \quad (\text{A3})$$

where $\alpha \equiv \frac{1}{4} K_{00}^{-1} - K_{11} \left(\frac{2\pi}{k} \right)^2$, $\Omega \equiv \left[V_S - \frac{m\omega^2}{2\bar{\rho}_b k^2} \right]^{-1}$, and $\Xi = V_S(1 - \Omega V_S) + 2\alpha$.

The response functions in the case of the pseudospin channel of Ψ_2 [Eq. (3)] are

$$\pi_{00} = \frac{1}{\Delta} \left(\frac{k}{2\pi} \right)^2, \quad (\text{A4})$$

$$\pi_{01} = \pi_{10} = \frac{1}{\Delta} \frac{ik}{2\pi} \Lambda, \quad (\text{A5})$$

$$\pi_{11} = \frac{1}{\Delta} \left\{ \Lambda^2 + \Delta \left[2K_{11} - \frac{2\bar{\rho}_b}{m} - 16W^4 \left(\frac{2\pi\bar{\rho}_b}{m\omega} \right)^4 \right] \right\}, \quad (\text{A6})$$

where $W^4 \equiv -\frac{\left(\frac{m\omega^2}{2\bar{\rho}_b(2\pi)^2} \right)^2}{\frac{1}{2K_{00}} \left(\frac{k}{2\pi} \right)^2 - \frac{m\omega^2}{2\bar{\rho}_b(2\pi)^2} + \frac{2\bar{\rho}_b}{m}}$, $\Delta \equiv W^4 - \frac{m\omega^2}{2\bar{\rho}_b(2\pi)^2} - 2K_{11} + V_S \left(\frac{k}{2\pi} \right)^2$, and $\Lambda \equiv 4W^4 \left(\frac{2\pi\bar{\rho}_b}{m\omega} \right)^2 - 2K_{11}$.

-
- ¹B. I. Halperin, *Helv. Phys. Acta* **56**, 75 (1983).
²K. Moon, H. Mori, K. Yang, S. M. Girvin, A. H. MacDonald, L. Zheng, D. Yoshioka, and S.-C. Zhang, *Phys. Rev. B* **51**, 5138 (1995).
³H. A. Fertig, *Phys. Rev. B* **40**, 1087 (1989).
⁴I. Stanić and M. V. Milovanović, *Phys. Rev. B* **71**, 035329 (2005).
⁵I. B. Spielman, J. P. Eisenstein, L. N. Pfeiffer, and K. W. West, *Phys. Rev. Lett.* **84**, 5808 (2000); **87**, 036803 (2001).
⁶M. Kellogg, J. P. Eisenstein, L. N. Pfeiffer, and K. W. West, *Phys. Rev. Lett.* **93**, 036801 (2004).
⁷E. Tutuc, M. Shayegan, and D. A. Huse, *Phys. Rev. Lett.* **93**, 036802 (2004).
⁸S. H. Simon, E. H. Rezayi, and M. V. Milovanović, *Phys. Rev. Lett.* **91**, 046803 (2003).
⁹M. Kellogg, J. P. Eisenstein, L. N. Pfeiffer, and K. W. West, *Phys. Rev. Lett.* **90**, 246801 (2003).
¹⁰M. V. Milovanović, *Phys. Rev. B* **75**, 035314 (2007).
¹¹R. B. Laughlin, *Phys. Rev. Lett.* **50**, 1395 (1983).
¹²E. H. Rezayi and N. Read, *Phys. Rev. Lett.* **72**, 900 (1994).
¹³A. Stern and B. I. Halperin, *Phys. Rev. Lett.* **88**, 106801 (2002).
¹⁴R. L. Willett, *Adv. Phys.* **46**, 447 (1997).
¹⁵S. C. Zhang, T. H. Hansson, and S. Kivelson, *Phys. Rev. Lett.* **62**, 980 (1989).
¹⁶B. I. Halperin, P. A. Lee, and N. Read, *Phys. Rev. B* **47**, 7312 (1993).
¹⁷G. Murthy and R. Shankar, *Rev. Mod. Phys.* **75**, 1101 (2003).
¹⁸B. Blok and X.-G. Wen, *Phys. Rev. B* **42**, 8145 (1990); **43**, 8337 (1991).
¹⁹S.-C. Zhang, *Int. J. Mod. Phys. B* **6**, 25 (1992).
²⁰M. Kellogg, I. B. Spielman, J. P. Eisenstein, L. N. Pfeiffer, and K. W. West, *Phys. Rev. Lett.* **88**, 126804 (2002).
²¹H. A. Fertig and G. Murthy, *Phys. Rev. Lett.* **95**, 156802 (2005).
²²I. B. Spielman, M. Kellogg, J. P. Eisenstein, L. N. Pfeiffer, and K. W. West, *Phys. Rev. B* **70**, 081303(R), (2004).
²³E. Tutuc and M. Shayegan, *Phys. Rev. B* **72**, 081307(R) (2005).
²⁴S. Luin, V. Pellegrini, A. Pinczuk, B. S. Dennis, L. N. Pfeiffer, and K. W. West, *Phys. Rev. Lett.* **97**, 216802 (2006).
²⁵A. O. Gogolin, A. A. Nersisyan, and A. M. Tsvelik, *Bosonization and Strongly Correlated Systems* (Cambridge University Press, Cambridge, 1998).
²⁶R. B. Laughlin, in *The Quantum Hall Effect*, 2nd ed., edited by R. E. Prange and S. M. Girvin (Springer, New York, 1990).
²⁷A. M. Polyakov, *Gauge Fields and Strings* (Harwood Academic, Chur, 1989).

All Databases

<< Return to Web of Science®

Citing Articles Title: **Nonperturbative approach to the quantum Hall bilayer**
 Author(s): **Milovanovic, M. V. ; Papic, Z.**
 Source: **PHYSICAL REVIEW B** Volume: 79 Issue: 11 Article Number: 115319 DOI: 10.1103/PhysRevB.79.115319 Published: MAR 2009

This item has been cited by items indexed in the databases listed below. [more information]

5 in All Databases

- 5 publication in Web of Science
- 0 publication in BIOSIS Citation Index
- 0 publication in SciELO Citation Index
- 0 publication in Chinese Science Citation Database
- 0 data sets in Data Citation Index
- 0 publication in Data Citation Index

Results: 5 Page 1 of 1 Go Sort by: Publication Date -- newest to oldest

Create Citation Report

Hide Refine

Refine Results

Search within results for Search

Databases

Research Domains Refine

SCIENCE TECHNOLOGY

Research Areas Refine

PHYSICS

Document Types

Authors

Group/Corporate Authors

Editors

Funding Agencies

Source Titles

Conference/Meeting Titles

Publication Years

Languages

Countries/Territories

- Select Page | Add to Marked List (0) | Send to:
1. Title: **DISORDERING OF THE CORRELATED STATE OF THE QUANTUM HALL BILAYER AT FILLING FACTOR $\nu=1$**
 Author(s): Papic, Z.; Milovanovic, M. V.
 Source: MODERN PHYSICS LETTERS B Volume: 26 Issue: 21 Article Number: 1250134 DOI: 10.1142/S0217984912501345
 Published: AUG 20 2012
 Times Cited: 0 (from All Databases)
 Get it! [View abstract](#)
 2. Title: **Electromagnetic Interaction of Composite Particles in a Higher-Derivative Nonrelativistic Gauge Field Model**
 Author(s): Manavella, Edmundo C.; Repetto, Carlos E.
 Source: INTERNATIONAL JOURNAL OF THEORETICAL PHYSICS Volume: 51 Issue: 8 Pages: 2564-2584 DOI: 10.1007/s10773-012-1137-3 Published: AUG 20 2012
 Times Cited: 1 (from All Databases)
 Get it! [View abstract](#)
 3. Title: **p-Wave Pairing in Quantum Hall Bilayers**
 Author(s): Papic, Z.; Milovanovic, M. V.
 Source: ADVANCES IN CONDENSED MATTER PHYSICS Article Number: 614173 DOI: 10.1155/2011/614173 Published: 2011
 Times Cited: 2 (from All Databases)
 Get it! [View abstract](#)
 4. Title: **TOPOLOGICALLY MASSIVE ELECTROMAGNETIC INTERACTION OF COMPOSITE PARTICLES IN A HIGHER-DERIVATIVE NONRELATIVISTIC GAUGE FIELD MODEL**
 Author(s): Manavella, Edmundo C.
 Source: INTERNATIONAL JOURNAL OF MODERN PHYSICS A Volume: 25 Issue: 26 Pages: 4949-4974 DOI: 10.1142/S0217751X10050664 Published: OCT 20 2010
 Times Cited: 2 (from All Databases)
 Get it! [View abstract](#)
 5. Title: **Clausius-Clapeyron relations for first-order phase transitions in bilayer quantum Hall systems**
 Author(s): Zou, Yue; Refael, Gil; Stern, Ady; et al.
 Source: PHYSICAL REVIEW B Volume: 81 Issue: 20 Article Number: 205313 DOI: 10.1103/PhysRevB.81.205313 Published: MAY 15 2010
 Times Cited: 1 (from All Databases)
 Get it! [View abstract](#)
- Select Page | Add to Marked List (0) | Send to:

Results: 5 Show 10 per page Page 1 of 1 Go Sort by: Publication Date -- newest to oldest

5 records matched your query of the 55,067,330 (contains duplicates) in the data limits you selected.

View in: [简体中文](#) | [繁體中文](#) | [English](#) | [日本語](#) | [한국어](#) | [Português](#) | [Español](#)

Nonperturbative approach to the quantum Hall bilayer

M. V. Milovanović¹ and Z. Papić²

¹*Institute of Physics, P.O. Box 68, 11080 Belgrade, Serbia*

²*Laboratoire de Physique des Solides, Université Paris-Sud 11, 91405 Orsay, France*

(Received 3 November 2008; published 26 March 2009)

We develop a nonperturbative approach to the quantum Hall bilayer (QHB) at $\nu=1$ using trial wave functions. We predict phases of the QHB for arbitrary distance d and, our approach, in a dual picture, naturally introduces a new kind of quasiparticles—neutral fermions. Neutral fermion is a composite of two merons of the same vorticity and opposite charge. For small d (i.e., in the superfluid phase), neutral fermions appear as dipoles. At larger d dipoles dissociate into the phase of the two decoupled Fermi-liquid-like states. This scenario is relevant for the experimental situation where impurities lock charged merons. In a translation invariant (clean) system, continuous creation and annihilation of meron-antimeron pairs evolves the QHB toward a paired phase. The quantum fluctuations fix the form of the pairing function to $g(z)=1/z^*$. A part of the description of the paired phase is the two-dimensional superconductor i.e., BF Chern-Simons theory. The paired phase is not very distinct from the superfluid phase.

DOI: [10.1103/PhysRevB.79.115319](https://doi.org/10.1103/PhysRevB.79.115319)

PACS number(s): 73.43.Nq, 03.65.Vf

I. INTRODUCTION

The quantum Hall bilayer at $\nu=1$ consists of two layers of two-dimensional (2D) electron gases that are brought close to one another in the quantum Hall regime of strong magnetic fields. When the distance between the layers is much smaller than the average distance between electrons inside each layer, inter- and intra-Coulomb interactions are about the same. Then the expected $\nu=1$ state is the state of a single layer filled lowest Landau level (LLL) generalized to two species. There is obvious degeneracy in dividing electrons into two groups which leads to the phenomenon of spontaneous symmetry breaking¹ and the existence of a Goldstone mode.² The expected superfluid behavior was verified also by very large zero-bias voltage peak in tunneling conductance,³ but no clear evidence was found for finite temperature Berezinskii-Kosterlitz-Thouless (BKT) transition⁴ in transport experiments.⁵

Therefore there is a need to systematically address the question of superfluid disordering in the quantum Hall bilayer (QHB). In particular there is a need to understand the role of quantum disordering in this system that becomes important as the distance between the layers is increased. In most of the previous work the starting point for the discussion of the physics of the bilayer was the ground state (GS) for very small distance between the layers as a mean-field solution to which none or some corrections were developed.^{4,6} We will take a nonperturbative approach inspired by the Laughlin solution of the $\nu=1/3$ problem in which we will uniquely determine possible wave functions (WFs) for the GSs of the bilayer at an arbitrary distance.

There are two basic paradigms of superfluid disordering that are known: (1) BKT (2D XY model) for which the transition proceeds via unbinding of dipoles of vortex-antivortex pairs, and (2) λ transition type [three-dimensional (3D) XY model] for which the transition is characterized by a condensation of vortex-antivortex loops.⁷

On the other hand, in this paper, through an analysis of the allowed possibilities for homogeneous WFs as the dis-

tance is varied, we will identify two families of WFs and relate them to the two ways of disordering the QHB superfluid mentioned previously. The families will be introduced in Sec. II.

One family, as it will turn out does not include elementary vortices—merons of QHB, in its description of superfluid disordering. Merons are part of the description of the QHB superfluid for small distances as is well known and well established in Ref. 4. Therefore this family of (homogeneous) WFs can be relevant only for dirty systems—systems with impurities, which can lock merons due to merons being charged quasiparticles. Then the only vortices that may participate in superfluid disordering and on which description of this family of WFs is based are neutral composites of two merons of opposite charges—neutral vortices, and as we will find fermionic quasiparticles that carry only layer degree of freedom. We will show that the superfluid disordering of this family can be understood through a Coulomb (fermionic) plasma picture of dipoles of these neutral fermions. Therefore this family we can consider as the one that exemplifies the BKT way of superfluid disordering, our first paradigm. This whole picture will be corroborated by the fact that the WFs of this family do not incorporate quantum fluctuations (Sec. IV) and, therefore, do not incorporate quantum disordering that is based on merons. The family from the viewpoint of a dual description (i.e., in terms of quasiparticles—neutral fermions) will be analyzed in Sec. III.

The other family incorporates weak pairing among neutral fermions and, as we will show, by assuming a special kind of pairing agrees and correlates with the description of quantum fluctuations of the usual superfluid disordering in a translatory invariant system that one finds in other approaches (field-theoretical). It is expected that this kind of disordering and pairing would lead to a charge-density wave (CDW) solution.⁸ Still our general considerations open possibilities for other kinds of weak pairing that can be present in this quantum Hall system. The most likely candidate is the one with pairing function $g(z) \sim \frac{1}{z^*}$ that results in nontrivial corrections (from quantum fluctuations and disordering) to the

ground-state wave function as the distance is varied. In general we expect that a weak pairing scenario will correspond to the superfluid disordering of the usual superfluid in 2+1 dimension and therefore to the class of 3D XY , our second paradigm. The family with weak pairing ansatz will be analyzed in Sec. IV.

With respect to the experiments, where impurities are necessarily present and we can expect also inhomogeneous ground-state solutions, our homogeneous candidates of the first family (without neutral fermion weak pairing) are still possible solutions for which transitions may proceed via dissociation of dipoles—pairs of opposite vorticity neutral fermions. In this sense and as will be more clear later, the quantum phase transitions with respect to changing the distance in Refs. 9–11 correspond to this dissociation. On the other hand, an analysis will show that in a translatory invariant system meron excitations via their loop condensation may produce an intercorrelated paired liquid state for the neutral sector, if a transition to a CDW does not occur.

II. UNIVERSALITY CLASSES OF GROUND STATES

A. Introduction

A great deal is known from the experimental and theoretical point of view of the QHB in the two extremes when the distance between layers, d , is (1) much smaller or (2) much larger than the magnetic length, $l_B = (\hbar/eB)^{1/2}$, where B is the magnetic field, the characteristic distance between the electrons inside any of the layers. When $d \ll l_B$, i.e., inter and intra Coulomb interactions are about the same, the good starting point and description is so-called (111) state,¹²

$$\Psi_{111}(z_{\uparrow}, z_{\downarrow}) = \prod_{i < j} (z_{i\uparrow} - z_{j\uparrow}) \prod_{k < l} (z_{k\downarrow} - z_{l\downarrow}) \prod_{p,q} (z_{p\uparrow} - z_{q\downarrow}), \quad (1)$$

where $z_{i\uparrow}$ and $z_{i\downarrow}$ are two-dimensional complex coordinates of electrons in upper and lower layer, respectively, and we omitted the Gaussian factors. This is suggestive of the exciton binding;¹³ any electron coordinate is also zero of the WF for any other electron coordinate—the correlation hole is just opposite to electron. This exciton description can be a viewpoint of the phenomenon of superfluidity found in these systems^{2,3} and is closely connected to the concept of composite bosons (CBs) (Ref. 14) that can be used as natural quantum Hall quasiparticles in this system. When $d \gg l_B$ we have the case of the decoupled layers and the GS is a product of single-layer filling factor 1/2 WFs; each describes a Fermi-liquid-like state,¹⁵

$$\Psi_{1/2}(w) = \mathcal{P} \left\{ \mathcal{F}_s(w, \bar{w}) \prod_{i < j} (w_{i\uparrow} - w_{j\uparrow})^2 \right\}, \quad (2)$$

where \mathcal{F}_s is the Slater determinant of free waves of noninteracting particles in zero magnetic field and \mathcal{P} represents projection to LLL. Underlying quasiparticles are composite fermions (CFs), the usual quasiparticles of the single layer quantum Hall physics.

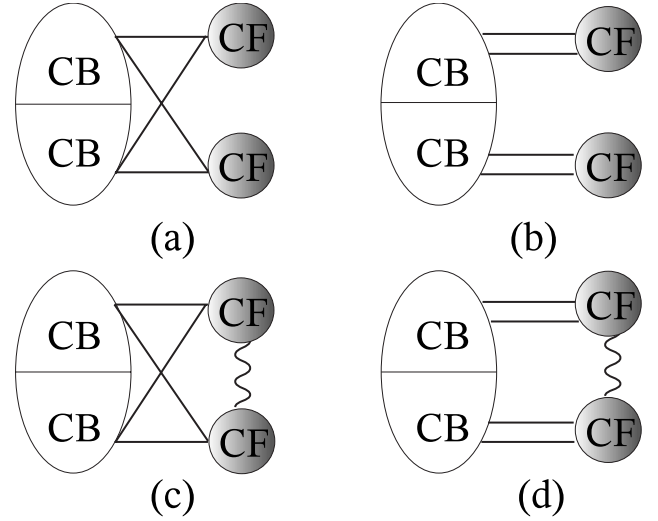


FIG. 1. Universality classes of wave functions.

B. Two families—universality classes of wave functions

To answer the question of intermediate distances we may try to, classically speaking, divide electrons into two groups, one in which electrons correlate as CBs and the other as CFs.¹⁶ The ratio between the numbers of CBs and CFs would be determined by the distance between layers. The WF constructed in this way would need an overall antisymmetrization in the end, but also intercorrelations among the groups as each electron of the system sees the same number of flux quanta through the system (equal to the number of electrons). This requires that the highest power of any electron coordinate is the same as the number of electrons in the thermodynamic limit. If we denote by a line the Laughlin-Jastrow factor $\prod_{A,B} (z_A - z_B)$ between two groups of electrons, A and B ($A, B = CB, CF$), the possibilities for the QHB GSWFs can be summarized as in Fig. 1.

If we ignore the possibility of pairing between CFs (Ref. 17) denoted by wiggly lines in Figs. 1(c) and 1(d) we have two basic families of the GSWFs depicted in Figs. 1(a) and 1(b). The requirement that each electron sees the same number of flux quanta through the system equal to the number of electrons (we are at $\nu=1$) very much reduces the number of possible states—wave functions in the mixed CB-CF approach. We can consider, for example, the possibility (a) depicted in Fig. 1 which stands for the following wave function in the LLL:

$$\begin{aligned} \Psi_1 = \mathcal{P} \mathcal{A}_{\uparrow} \mathcal{A}_{\downarrow} & \left\{ \prod_{i < j} (z_{i\uparrow} - z_{j\uparrow}) \prod_{k < l} (z_{k\downarrow} - z_{l\downarrow}) \prod_{p,q} (z_{p\uparrow} - z_{q\downarrow}) \right. \\ & \times \mathcal{F}_s(w_{\uparrow}, \bar{w}_{\uparrow}) \prod_{i < j} (w_{i\uparrow} - w_{j\uparrow})^2 \\ & \times \mathcal{F}_s(w_{\downarrow}, \bar{w}_{\downarrow}) \prod_{k < l} (w_{k\downarrow} - w_{l\downarrow})^2 \\ & \times \prod_{i,j} (z_{i\uparrow} - w_{j\uparrow}) \prod_{k,l} (z_{k\downarrow} - w_{l\downarrow}) \\ & \left. \times \prod_{p,q} (z_{p,\downarrow} - w_{q,\uparrow}) \prod_{m,n} (z_{m,\downarrow} - w_{n,\downarrow}) \right\}, \quad (3) \end{aligned}$$

where \mathcal{A}_\uparrow and \mathcal{A}_\downarrow denote the overall antisymmetrizations. In the thermodynamic limit, the relation between the number of particles and flux quanta reads

$$\begin{aligned} N_\phi^b &= N_{b\uparrow} + N_{b\downarrow} + N_{f\uparrow} + N_{f\downarrow}, \\ N_\phi^{f\uparrow} &= 2N_{f\uparrow} + N_{b\uparrow} + N_{b\downarrow}, \\ N_\phi^{f\downarrow} &= 2N_{f\downarrow} + N_{b\uparrow} + N_{b\downarrow}, \end{aligned} \quad (4)$$

where we denoted by N_ϕ^b and $N_\phi^{f\sigma}$ separately the number of flux quanta that electrons that correlate as CBs and CFs see, respectively, and $N_{b\sigma}$ and $N_{f\sigma}$ are the number of CBs and CFs inside the layer σ , respectively ($\sigma = \uparrow, \downarrow$ is the layer index). The requirement constrains $N_\phi = N_\phi^b = N_\phi^{f\sigma}$, where N_ϕ is the number of flux quanta through the system. (This leads to the additional requirement $N_{f\uparrow} = N_{f\downarrow}$ which leaves $N_{b\uparrow} - N_{b\downarrow}$ unconstrained, connected with the Bose condensation phenomenon that the wave function should be part of.^{4,13,18})

The only additional way to count the flux quanta that electrons see, with the (symmetric under $\uparrow \leftrightarrow \downarrow$ reversal) application of the Jastrow-Laughlin factors that we need to have, is

$$\begin{aligned} N_\phi^{b\uparrow} &= N_{b\uparrow} + N_{b\downarrow} + 2N_{f\uparrow}, \\ N_\phi^{b\downarrow} &= N_{b\uparrow} + N_{b\downarrow} + 2N_{f\downarrow}, \\ N_\phi^{f\uparrow} &= 2N_{f\uparrow} + 2N_{b\uparrow}, \\ N_\phi^{f\downarrow} &= 2N_{f\downarrow} + 2N_{b\downarrow}, \end{aligned} \quad (5)$$

which leads to the possibility (b) (with constraints $N_{b\uparrow} = N_{b\downarrow}$ and $N_{f\uparrow} = N_{f\downarrow}$). The intercorrelations in the first family in Fig. 1(a) are in the spirit of Ψ_{111} correlations, and those in the second family in Fig. 1(b) are in the spirit of the decoupled state, $\Psi_{1/2} \times \Psi_{1/2}$, where we correlate exclusively inside each layer.

C. Discussion

We can imagine a mixture of both intercorrelations [of Fig. 1(a) and Fig. 1(b)] in a single wave function but these mixed states, by their basic response,¹⁸ fall into one of the universality classes depicted in Fig. 1. In Ref. 18 explicitly such a mixture and possibility under name ‘‘generalized vortex metal’’ was considered, in the scope of a Chern-Simons (CS) theory, and it was proved that it does not support a Goldstone (gapless) mode which was found to exist for the state depicted in Fig. 1(a). These generalized states belong to the universality class of the state depicted in Fig. 1(b) for which in the scope of the same theory we find in the low-energy spectrum only a gapped collective mode.¹⁸

The Chern-Simons theory we mentioned neglects the overall antisymmetrization built in the classes of Fig. 1. We can justify this neglect (1) by taking a point of view that stems from similar situations with quantum Hall states like hierarchy and Jain’s constructions that in the low-energy sector can be considered as multicomponent systems¹⁹ [we will argue later that the state of Eq. (3) can be mapped to a

hierarchy construction], or (2) *a posteriori* because the results of the effective description of the classes in Fig. 1 are quite sensible and are expected for the states we are familiar with from numerics [the state in our Fig. 1(a) as analyzed in Ref. 16]. (We do not ask this type of theory for detailed answers anyway.) In this way it was found by us (Refs. 18 and 20), examining the basic response in the pseudospin channel in the random-phase approximation (RPA) of these Chern-Simons theories that the states in Figs. 1(a) and 1(c) represent superfluids, and the states in Figs. 1(b) and 1(d) represent disordered superfluids, compressible and incompressible, respectively. [Later, in a more complete study, we will find that the states of Fig. 1(d) are also compressible in the neutral channel.]

The two basic possibilities of connecting two extremes as depicted in Fig. 1, i.e., without and with pairing of CFs, must correspond to the two possible ways or paradigms that we know of disordering a superfluid. We will substantiate this claim further by examining the two superfluid constructions [Figs. 1(a) and 1(c)] in more detail.

III. NEUTRAL FERMIONS AND BKT DISORDERING

A. Dual picture of the first family of wave functions with neutral fermions

Let us write out the unprojected in the LLL version of the construction in Fig. 1(a) [Eq. (3)] in the following way:

$$\begin{aligned} \Psi_1 &= \mathcal{A}_\uparrow \mathcal{A}_\downarrow \left\{ \Psi_{111}(z_\uparrow, z_\downarrow) \Psi_{1/2}(w_\uparrow) \Psi_{1/2}(w_\downarrow) \right. \\ &\quad \times \prod_{i,j} (z_{i\uparrow} - w_{j\uparrow}) \prod_{k,l} (z_{k\downarrow} - w_{l\downarrow}) \\ &\quad \left. \times \prod_{p,q} (z_{i\downarrow} - w_{q\uparrow}) \prod_{m,n} (z_{m\downarrow} - w_{n\downarrow}) \right\}, \end{aligned} \quad (6)$$

where, as before, z_σ ’s and w_σ ’s denote coordinates of electrons belonging to the layer with index σ and \mathcal{A}_\uparrow and \mathcal{A}_\downarrow , as before, stand for the antisymmetrizations. Using \mathcal{S}_\uparrow and \mathcal{S}_\downarrow symmetrizers inside each layer, the same function, Ψ_1 , can be written as

$$\begin{aligned} \Psi_1 &= \mathcal{S}_\uparrow \mathcal{S}_\downarrow \left\{ \frac{\prod_{k<l} (w_{k\uparrow} - w_{l\uparrow}) \prod_{p<q} (w_{p\downarrow} - w_{q\downarrow})}{\prod_{i,j} (w_{i\uparrow} - w_{j\downarrow})} \right. \\ &\quad \left. \times \mathcal{F}_s(w_\uparrow) \mathcal{F}_s(w_\downarrow) \right\} \Psi_{111}, \end{aligned} \quad (7)$$

where Ψ_{111} denotes the Vandermonde determinant (Slater determinant in the LLL) of all coordinates in which all groups equally participate.

By using the expressions for the densities of electrons in each layer, $\rho^\sigma(\eta) = \sum_i \delta^2(\eta - z_i^\sigma)$, here now z_σ ’s denote all electrons of the layer σ , we can rewrite the wave function in the following way:

$$\begin{aligned} \Psi_1 = & \int d^2\eta_{1\uparrow} \cdots \int d^2\eta_{n\downarrow} \\ & \times \frac{\prod_{k<l}(\eta_{k\uparrow} - \eta_{l\uparrow}) \prod_{p<q}(\eta_{p\downarrow} - \eta_{q\downarrow})}{\prod_{i,j}(\eta_{i\uparrow} - \eta_{j\downarrow})} \mathcal{F}_s(\boldsymbol{\eta}_{\uparrow}) \\ & \times \mathcal{F}_s(\boldsymbol{\eta}_{\downarrow}) \rho^{\uparrow}(\boldsymbol{\eta}_{1\uparrow}) \cdots \rho^{\downarrow}(\boldsymbol{\eta}_{n\downarrow}) \Psi_{111}(z_{\uparrow}, z_{\downarrow}), \end{aligned} \quad (8)$$

where n is the total number of electrons that correlate as CFs. The equality is exact; any time we have in the product of ρ 's the same layer electron coordinate more than once, the Laughlin-Jastrow factors of $\boldsymbol{\eta}$'s in the same layer force the wave function to become zero. The expression in Eq. (8) reminds us of a dual picture in terms of some quasiparticles with $\boldsymbol{\eta}$ coordinates as in Ref. 21. Certainly we are not describing the incompressible physics of a Laughlin state where quasihole operators of coherent states span the basis of low-energy physics and allow the description in terms of wave functions of quasiholes (dual picture).²¹ Nevertheless we will argue that we can delineate a sector (find a subspace) to which constructions [Eq. (8) where n is arbitrary] belong, which is spanned by a quasiparticle basis of some neutral fermionic quasiparticles.

To find those quasiparticles we will rewrite Eq. (8) as

$$\begin{aligned} \Psi_1 = & \int d^2\eta_{1\uparrow} \cdots \int d^2\eta_{n\downarrow} \\ & \times \frac{\prod_{k<l}|\eta_{k\uparrow} - \eta_{l\uparrow}| \prod_{p<q}|\eta_{p\downarrow} - \eta_{q\downarrow}|}{\prod_{i,j}|\eta_{i\uparrow} - \eta_{j\downarrow}|} \mathcal{F}_s(\boldsymbol{\eta}_{\uparrow}) \mathcal{F}_s(\boldsymbol{\eta}_{\downarrow}) \\ & \times \{\exp\{i\phi(\boldsymbol{\eta}_{1\uparrow} \cdots \boldsymbol{\eta}_{n\downarrow})\} \rho^{\uparrow}(\boldsymbol{\eta}_{1\uparrow}) \cdots \rho^{\downarrow}(\boldsymbol{\eta}_{n\downarrow}) \Psi_{111}(z_{\uparrow}, z_{\downarrow})\}, \end{aligned} \quad (9)$$

where $\exp\{i\phi(\boldsymbol{\eta})\}$ factor denotes the phase part of the Laughlin-Jastrow factors in front of the Fermi seas in Eq. (8). With respect to Eq. (8) we are allowed to take for definiteness that the phase factor always vanishes when any of two $\boldsymbol{\eta}$'s (or more) from the same layer coincide.

Our first question may be why states as

$$\rho^{\uparrow}(\boldsymbol{\eta}_{1\uparrow}) \cdots \rho^{\downarrow}(\boldsymbol{\eta}_{n\downarrow}) \Psi_{111} \sim \Psi_b(\boldsymbol{\eta}_{1\uparrow}, \dots, \boldsymbol{\eta}_{n\downarrow}) \quad (10)$$

would not make a bosonic basis. We look for the following overlap:

$$\int dz_{1\uparrow} \cdots \int dz_{N\downarrow} \Psi_b(\boldsymbol{\eta}'_{1\uparrow}, \dots, \boldsymbol{\eta}'_{n\downarrow}) \Psi_b(\boldsymbol{\eta}_{1\uparrow}, \dots, \boldsymbol{\eta}_{n\downarrow}). \quad (11)$$

In the expansion of the density sums we may get

$$\delta^2(\boldsymbol{\eta}'_1 - z_1^{\uparrow}) \delta^2(\boldsymbol{\eta}'_2 - z_1^{\uparrow}) \delta^2(\boldsymbol{\eta}_1 - z_1^{\uparrow}) \delta^2(\boldsymbol{\eta}_2 - z_2^{\downarrow}) \cdots, \quad (12)$$

which would lead to the following contribution after z integration:

$$\begin{aligned} & \delta^2(\boldsymbol{\eta}'_1 - \boldsymbol{\eta}'_2) \delta^2(\boldsymbol{\eta}_1 - \boldsymbol{\eta}'_1) |\boldsymbol{\eta}_1 - \boldsymbol{\eta}_2|^2 \exp\left\{-\frac{1}{2}(|\boldsymbol{\eta}_1|^2 + |\boldsymbol{\eta}_2|^2)\right\} \\ & \times \frac{1}{|\boldsymbol{\eta}_1 - \boldsymbol{\eta}_2|^2} \exp\left\{\frac{1}{2}(|\boldsymbol{\eta}_1|^2 + |\boldsymbol{\eta}_2|^2)\right\} \cdots. \end{aligned} \quad (13)$$

The last term, before the dots, comes after the integration over z 's that do not participate in the delta functions. As usual²¹ the term is the result of the screening of plasma which we find in the plasma analogy of Ψ_{111} state in its charge channel. The term exactly cancels the preceding one (it is equal to its inverse) and the same cancellation will happen for any pair of $\boldsymbol{\eta}$'s (in the place of ...) that in remaining z integration have the role of impurities (of charge one) in the plasma of remaining z 's. This is very good because of our goal to find basis states and leaves us to consider only delta functions in the contribution. But we can see immediately in Eq. (13) that $\delta(\boldsymbol{\eta}'_1 - \boldsymbol{\eta}'_2)$ spoils our goal that the states mimic a Fock basis of bosonic particles. Therefore as candidates for basis states we should consider fermionic states,

$$\begin{aligned} |\boldsymbol{\eta}_{1\uparrow} \cdots \boldsymbol{\eta}_{n\downarrow}\rangle = & \frac{1}{\sqrt{n! \binom{N}{n}}} \exp\{i\phi(\boldsymbol{\eta}_{1\uparrow} \cdots \boldsymbol{\eta}_{n\downarrow})\} \\ & \times \rho^{\uparrow}(\boldsymbol{\eta}_{1\uparrow}) \cdots \rho^{\downarrow}(\boldsymbol{\eta}_{n\downarrow}) |\Psi_{111}\rangle \end{aligned} \quad (14)$$

for which we cannot get contributions of the type in Eq. (13) because the phase part does not allow two (or more) quasiparticles to coincide. [Eq. (14) represents a fermionic state for $\boldsymbol{\eta}$ quasiparticles because of the phase part introduced in Eq. (9) which is antisymmetric under the exchange of $\boldsymbol{\eta}$'s.] Therefore we should consider fermionic states in Eq. (14) because of the previously found nondesirable terms in the bosonic case (we are looking for quasiparticles and their basis states that would have features of the Fock space basis): the terms like the one with $\delta(\boldsymbol{\eta}'_1 - \boldsymbol{\eta}'_2)$ in Eq. (13) lead to the absence of orthogonality of these states, which we would like to represent coordinate basis states in the bosonic case and that can be mended by taking fermions—then these terms are absent. By a similar analysis which lead to Eq. (13), considering various possibilities for delta function contributions of density operators we can find that the leading most singular and coherent behavior of the states defined in Eq. (14) is

$$\begin{aligned} \langle \boldsymbol{\eta}'_{1\uparrow}, \boldsymbol{\eta}'_{2\uparrow} \cdots \boldsymbol{\eta}'_{n\downarrow} | \boldsymbol{\eta}_{1\uparrow}, \boldsymbol{\eta}_{2\uparrow} \cdots \boldsymbol{\eta}_{n\downarrow} \rangle \rightarrow & \delta^2(\boldsymbol{\eta}'_{1\uparrow} - \boldsymbol{\eta}_{1\uparrow}) \\ & \times \delta^2(\boldsymbol{\eta}'_{2\uparrow} - \boldsymbol{\eta}_{2\uparrow}) \cdots \delta^2(\boldsymbol{\eta}'_{n\downarrow} - \boldsymbol{\eta}_{n\downarrow}) - \delta^2(\boldsymbol{\eta}'_{1\uparrow} - \boldsymbol{\eta}_{2\uparrow}) \\ & \times \delta^2(\boldsymbol{\eta}'_{2\uparrow} - \boldsymbol{\eta}_{1\uparrow}) \cdots \delta^2(\boldsymbol{\eta}'_{n\downarrow} - \boldsymbol{\eta}_{n\downarrow}) + \cdots. \end{aligned} \quad (15)$$

The rest of contribution constitute incoherent phase factors with fewer number ($<n$) of delta functions but of the same kind as in the leading behavior. We cannot prove that the states make exactly a Fock space of neutral fermionic quasiparticles, i.e., we do not have an exact equality in Eq. (15), but they stand fairly close to that status. In other words we do not have the exact equality in Eq. (15), i.e., equality to delta functions only (appropriately antisymmetrized), but we have in addition some finite contributions which cannot change the fact that the overlap is singular—at its maximum

when η' 's and η 's coincide. Therefore quasiparticles are not pointlike fermionic quasiparticles (one certainly cannot expect that from quasiparticles in a strongly correlated system); they are extended, but clearly the overlap has the singular contribution of antisymmetrized delta functions which points out that we are fairly (to a good extent) close to the fermionic Fock basis description. Even in the Laughlin case we cannot prove the exact LLL delta function overlaps of coherent states of quasiholes. The quasiparticles are neutral because in the construction of the states there is no net magnetic flux through the system. See Eq. (14) and the definition of the phase factor in Eq. (9) with Eq. (8).

Now that we know basis states just by looking at Eq. (9) we can read out the GSWF in the dual picture in terms of neutral fermions,

$$\Psi_{\text{dual}}(\eta) = \frac{\prod_{k<l} |\eta_{k\uparrow} - \eta_{l\uparrow}| \prod_{p<q} |\eta_{p\downarrow} - \eta_{q\downarrow}|}{\prod_{i,j} |\eta_{i\uparrow} - \eta_{j\downarrow}|} \mathcal{F}_s(\eta_{\uparrow}) \mathcal{F}_s(\eta_{\downarrow}). \quad (16)$$

This is a wave function of a 2D Coulomb fermionic plasma. In the literature 2D Coulomb fermionic plasma with same charge particles is fairly known and explored.^{22,23} It is a dynamical system of fermionic particles in 2D that interact with the long-range ($\sim -\ln\{r\}$) interaction. As shown in Ref. 22 the Jastrow factor of the type $\prod_{i<j} |z_i - z_j|^\gamma$ (γ proportional to the interaction coupling constant), together with multiplying Slater determinant of free waves, describes the ground-state function in the long-distance limit. In our case we have a generalization of such a system to the one with opposite charges. Assuming that the concentration of particles is not large, which is the case of interest to us, we then expect the dipole configurations of particles that the wave function in Eq. (16) describes.

B. Discussion

Merons are true elementary vorticity quasiparticles of the translatory invariant QHB system at least for small distances between layers as shown in Ref. 4 and carry both charge and vorticity. Therefore the neutral fermion basis that we described can be a complete basis for the ground-state evolution of the QHB in the nontranslatory invariant case in which merons by their charges are bound to impurities.

The wave function in Eq. (16) describes the superfluid state in Fig. 1(a). It encodes dipole positioning of opposite vorticity (layer index) neutral fermions. With increasing distance there are more dipoles of neutral fermions and they are expected to be less tightly bound as in the description of a BKT disordering of a 2D system with increasing temperature. Therefore we do not find quantum fluctuations in this case. This will be explicitly shown by calculations in the following section (see also Appendix A).

In the superfluid phase, with respect to merons, a neutral fermion dipole should be in essence a superposition of quadrupolar combinations of merons—two dipoles which come in pairs but at arbitrary distance as illustrated in Fig. 2. In this way, as special configurations of dipoles, neutral fermi-

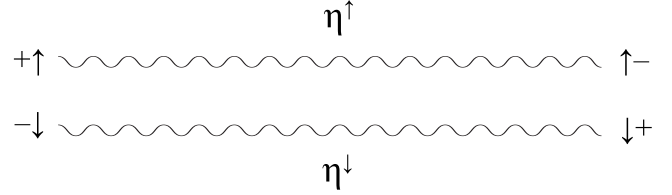


FIG. 2. The quadrupolar configurations of merons that make neutral fermion pair. Compare the same configuration of Laughlin quasiparticles as a description of “magnetophonon” branch in the Laughlin case in Ref. 14.

ons, we expect, constitute the lowest lying states of the QHB—(pseudo)spin or phonon waves.^{2,14}

If neutral fermions may be considered as eigenstates they must lie very high in spectrum; like electrons in fractional quantum Hall states they constitute the physics of Ψ_1 but their wave function Eq. (16) describes a highly correlated state.

The dual expression of Eq. (16) was derived under assumption of the screening properties in the charge channel of the particles participating in the plasma analogy based on Ψ_{111} state. As the distance is increased there are less of them and the breakdown of the description in terms of dipoles of neutral fermions at smaller distances becomes a possibility. We expect that due to impurities there will be patches (islands) of dissociated neutral fermions.²⁴

IV. QUANTUM FLUCTUATIONS AND QUANTUM DISORDERING

A. Introduction

The two paradigms-models of superfluid disordering as applied to our 2+1 dimensional system mean that the time evolution is such that (1) meron-antimeron pairs are locked on impurities or (2) created and annihilated at some later time and therefore making a loop in time. The loops in time signify the presence of quantum disordering.⁷ We will discuss and detect the presence of quantum disordering in the WFs of class (c) in Fig. 1 by examining how they relate to and incorporate ordinary (not quantum disordering that involves merons-vortices) quantum fluctuation phonon contribution in this case.^{6,8} We will find that the WFs of class (a) in Fig. 1 do not have this contribution.

B. Quantum fluctuations due to phonons and quantum disordering

The usual¹⁴ CS field theory approach⁸ in the RPA to the bilayer problem at $\nu=1$ (which in the neutral channel reduces just to the problem of ordinary superfluid with only phonon description and contribution) finds the following correction to the Ψ_{111} state:

$$\Psi_{\text{PH}} = \exp \left\{ -\frac{1}{2} \sum_k \frac{\sqrt{V_-(k)}}{k} \rho_k^- \rho_{-k}^- \right\} \Psi_{111}, \quad (17)$$

where $\rho_k^- = \rho_k^\uparrow - \rho_k^\downarrow$, $V_-(k) = \frac{V_{11}(k) - V_{11}(k)}{2}$, $V_{\uparrow\uparrow} = \frac{2\pi}{k}$, $V_{\uparrow\downarrow} = \frac{2\pi}{k} \exp\{-kd\}$, i.e., $V_-(k)$ is the interaction in the neutral channel, ρ_E

$= \frac{\bar{\rho}}{m}$, where m is the electron mass and $\bar{\rho}$ is the uniform total density. In the small d limit $V_-(k) = \pi d$ and we can expand the expression Ψ_{PH} as

$$\Psi_{\text{PH}} = \Psi_{111} - \left(\sum_k \frac{c\sqrt{d}}{k} \rho_{-k}^- \rho_k^- \right) \Psi_{111} + \dots, \quad (18)$$

where c is a positive constant. The terms after the first one represent corrections, in the order of importance, to the Ψ_{111} ansatz as d increases.

On the other hand the WFs of Fig. 1(c) are more general as they suggest the form of the correction terms of wider class than the one used in the expansion [Eq. (18)] with only exception that the class demands equal number of ρ_k^\uparrow 's and ρ_k^\downarrow 's because in writing down the classes of Fig. 1 we explicitly distinguished \uparrow 's from \downarrow 's and fixed the number of \uparrow 's and \downarrow 's.

We can start comparing and relating the first phonon correction, i.e.,

$$\sim \sum_k \frac{1}{k} \rho_{-k}^\uparrow \rho_k^\downarrow \quad (19)$$

to a wave function of two neutral fermions (\uparrow from \downarrow), i.e., density operators as in Eq. (8) but with a pairing between them as in class Fig. 1(c).

Without pairing we would have

$$\int d^2 \eta_{1\uparrow} \int d^2 \eta_{2\downarrow} \frac{1}{(\eta_{1\uparrow} - \eta_{2\downarrow})} \rho^\uparrow(\eta_{1\uparrow}) \rho^\downarrow(\eta_{2\downarrow}), \quad (20)$$

which is identical to zero (no correction) as can be found out in Appendix A. This is an important result and shows that there are no quantum fluctuations in the first family of WFs discussed in Sec. III. Besides this analytical proof, our statement is further corroborated by the fact that the computer-generated two neutral fermion state also does not exist—see Ref. 16.

Therefore we continue by considering

$$\int d^2 \eta_{1\uparrow} \int d^2 \eta_{2\downarrow} \frac{1}{|\eta_{1\uparrow} - \eta_{2\downarrow}|^\alpha} \rho^\uparrow(\eta_{1\uparrow}) \rho^\downarrow(\eta_{2\downarrow}), \quad (21)$$

where $\alpha=1$ if we take $g(z) = \sqrt{\frac{z}{z^*}}$ for the pairing function or $\alpha=2$ if $g(z) = \frac{1}{z}$. For $\alpha=1$ the expression in Eq. (20) reduces to the form of the first phonon contribution in the long-distance limit with the $\frac{1}{k}$ singularity (see Appendix A) and for $\alpha=2$ this singularity softens to $\sim -\ln\{kl_B\}$ where l_B is the magnetic length (see Appendix A). We will consider only these most weakly pairing cases; the case $g(z) = \frac{1}{z}$ does not produce correction as can be seen in Appendix A.

Next we consider more than two density operator constructions, i.e., more than two neutral fermions constructions as in Eq. (8) but instead of the two decoupled Fermi seas we have a pairing between neutral fermions,

$$\begin{aligned} \Psi_2^n &= \int d^2 \eta_{1\uparrow} \dots \int d^2 \eta_{n\downarrow} \\ &\times \frac{\prod_{k<l} (\eta_{k\uparrow} - \eta_{l\uparrow}) \prod_{p<q} (\eta_{p\downarrow} - \eta_{q\downarrow})}{\prod_{i,j} (\eta_{i\uparrow} - \eta_{j\downarrow})} \\ &\times \text{Det}\{g(\eta_{i\uparrow} - \eta_{j\downarrow})\} \rho^\uparrow(\eta_{1\uparrow}) \dots \rho^\downarrow(\eta_{n\downarrow}) \Psi_{111}(z_\uparrow, z_\downarrow), \\ &= \int d^2 \eta_{1\uparrow} \dots \int d^2 \eta_{n\downarrow} \text{Det}\left\{ \frac{1}{\eta_{i\uparrow} - \eta_{j\downarrow}} \right\} \\ &\times \text{Det}\left\{ \sqrt{\frac{\eta_{i\uparrow} - \eta_{j\downarrow}}{\eta_{i\uparrow}^* - \eta_{j\downarrow}^*}} \right\} \times \rho^\uparrow(\eta_{1\uparrow}) \dots \rho^\downarrow(\eta_{n\downarrow}) \Psi_{111}(z_\uparrow, z_\downarrow), \end{aligned} \quad (22)$$

where in the second expression we used the Cauchy determinant identity, i.e.,

$$\frac{\prod_{k<l} (\eta_{k\uparrow} - \eta_{l\uparrow}) \prod_{p<q} (\eta_{p\downarrow} - \eta_{q\downarrow})}{\prod_{i,j} (\eta_{i\uparrow} - \eta_{j\downarrow})} = \text{Det}\left\{ \frac{1}{\eta_{i\uparrow} - \eta_{j\downarrow}} \right\} \quad (23)$$

and substituted the pairing function that has lead us to the first phonon correction for two paired neutral fermions. Immediately we can see that the diagonal terms in which pairs of the two determinants are the same would make further phononlike corrections, i.e., their superposition with appropriate coefficients would lead to

$$\exp\left\{ - \sum_k \frac{c_d}{k} \rho_{-k}^\uparrow \rho_k^\downarrow \right\} \Psi_{111}. \quad (24)$$

The other nondiagonal terms would lead to more complicated constructions of four and more neutral fermions that should participate in the description of quantum disordering, i.e., describe the physics beyond phonon contribution (24). Although in some sense we are talking just about a class (a pool) of wave functions that should describe quantum disordering we can fix general form, at least for small d , of the superposition that should completely model the ground state at fixed d

$$\Psi_0 = \sum_{n=0,2,\dots} \Psi_2^n c_n. \quad (25)$$

In the long-distance limit (25) should tend to Eq. (24). In other words nondiagonal terms in Eq. (22) should be subleading to the leading behavior in Eq. (24). That this is true from the physical point of view we expect that it is enough to prove the subleading behavior in the case of four neutral fermions (Ψ_2^4) and that can be found in Appendix B. The proof is based on the smallness of higher-order terms that may appear inside the brackets in Eq. (24). This is assumed in the RPA approach and expected in the small d limit.

Therefore the quantum Hall physics besides $g(z) = \sqrt{\frac{z}{z^*}}$ pairing possibility brings or allows the possibility of $g(z) = \frac{1}{z}$ pairing that introduces nontrivial quantum corrections, i.e., brings another kind of quantum disordering. The $g(z)$

$= \sqrt{\frac{z}{z^*}}$ accommodates the usual (on the level of RPA) superfluid description in which we may expect that the disordered phase will break translation symmetry. Indeed, the bosonic CS field theories that are not based on quantum Hall WFs give this scenario of the disordered phase as a charge-density wave.⁸ It seems, therefore, there are two possible scenarios for superfluid disordering not in the BKT class for the bilayer in the translation symmetry invariant case (without impurities). In the following we will discuss the second possibility with $g(z) = \frac{1}{z^*}$ kind of pairing.

C. Weak pairing $g(z) \sim \frac{1}{z^*}$ case and conformal field theory considerations

We expect, if the translational symmetry of the ground state remains unbroken, that also in the case of pairing $g(z) = \frac{1}{z^*}$ the translatory invariant system smoothly evolves with the increase in d into the class of wave functions in Fig. 1(d). We would like to know more about this class—whether it represents a distinct phase. If we take the choice $g(z) = \frac{1}{z^*}$ and examine the final form of the state of Fig. 1(d) when there are no CBs, we are lead to its following forms:

$$\begin{aligned} \Psi_2 &= \text{Det} \left\{ \frac{1}{z_{i\uparrow}^* - z_{j\downarrow}^*} \right\} \prod_{i < j} (z_{i\uparrow} - z_{j\downarrow})^2 \prod_{k < l} (z_{k\downarrow} - z_{l\downarrow})^2 \\ &= \text{Det} \left\{ \frac{1}{z_{i\uparrow}^* - z_{j\downarrow}^*} \right\} \text{Det} \left\{ \frac{1}{z_{k\uparrow} - z_{l\downarrow}} \right\} \Psi_{111}, \end{aligned} \quad (26)$$

where to get the last line we used the Cauchy determinant identity. The neutral part of Ψ_2 (not carrying a net flux through the system as Ψ_{111} does) that consists of the two determinants can be viewed as a correlator of vertex operators of a single *nonchiral* bosonic field. According to²⁵ conformal field theory (CFT) correlators not only describe quantum Hall system WFs but also can be used to find out about excitation spectrum and connect to its edge and bulk theories. In this way motivated neutral excitations are vertex operators that correspond to single-valued WF expressions that multiply Ψ_2 ,

$$\exp\{i\delta_1\phi(w, w^*)\} \rightarrow \frac{\prod_i |z_{i\uparrow} - w|^{2\delta_1}}{\prod_i |z_{i\downarrow} - w|^{2\delta_1}}, \quad (27)$$

$$\exp\{i\delta_2\theta(w, w^*)\} \rightarrow \frac{\prod_i (z_{i\uparrow} - w)^{\delta_2} \prod_i (z_{i\downarrow}^* - w^*)^{\delta_2}}{\prod_i (z_{i\uparrow}^* - w^*)^{\delta_2} \prod_i (z_{i\downarrow} - w)^{\delta_2}}, \quad (28)$$

where $\phi(w, w^*) = \phi(w) + \phi(w^*)$, $\theta(w, w^*) = \phi(w) - \phi(w^*)$, and $\phi(w)$ and $\phi(w^*)$ are holomorphic and antiholomorphic parts of the bosonic field, respectively. δ_2 must be $\frac{1}{2}$ because of the requirement of single-valuedness. For detailed explanations of the bosonic CFT analogies see Appendix C.

If the low-lying spectrum were consisting only of $\delta_1 = \frac{1}{2}$ and $\delta_2 = \frac{1}{2}$ quasiparticle excitations our system would be described by so-called BF Chern-Simons theory or the theory of 2D superconductor.²⁶ The mutual statistics of

quasiparticles-quasiparticles and vortices in this theory is semionic (due to the fact that vortices carry half-flux ($\frac{h}{(2e)c}$) quantum) and that this is also the case with our excitations can be easily checked via CFT correlators—see Appendix C. Combining the analysis with the charge part (Ψ_{111}) in which only charge 1 excitations are allowed (half-flux quantum excitations are strongly confined²⁷) we may come to the conclusion that the degeneracy of the system GSs on the torus must be 4 (Refs. 26 and 28) But the expression for the first kind of excitations [Eq. (27)] allows a real continuum for the value of δ_1 exponent including $\delta_1 = 0$, and therefore we expect a compressible (gapless) behavior of the system despite the incompressibility of the charge channel and seemingly topological phase behavior in the neutral sector. Nevertheless we expect that in our case BF CS theory is a part of the description of the pairing phase in a Lagrangian in which there is a quadratic nonderivative term in one of the two gauge fields; this allows a branch of gapless excitations—see Appendix C for details.

The question may come why we did not do an analysis with the projection to the LLL. Certainly the analysis is more involved where “reversed flux part,” i.e., complex conjugated determinant becomes an operator that acts on the rest of wave function. Nevertheless, an analysis of the edge excitation spectrum²⁹ suggests that it cannot conform to any description of simple free CFT theories, i.e., cannot belong to a totally incompressible class, and it is very likely that the system is, as it follows from our unprojected analysis, compressible in the neutral channel. Therefore it is very hard to distinguish the physics of the states in Figs. 1(c) and 1(d) in the translatory invariant system that involve pairing of the type $g(z) = \frac{1}{z^*}$.

While we were finishing the writing a numerical study (of homogenous WFs in the translatory invariant case) appeared³⁰ that agrees with and complements our conclusions on the nature of pairing.

V. CONCLUSIONS

In conclusion, we presented two families of wave functions that describe two possible ways of homogeneous disordering of the quantum Hall superfluid with their detailed description on the basis of the dual (quasiparticle) picture of the quantum Hall effect. We also presented detailed analysis of the disordering in the translation invariant system on the basis of insights into the pairing function of quasiparticles-neutral fermions. A class of candidate wave functions was clearly connected with the formalism that we find in other (Chern-Simons) theories, and the pairing function $g(z) \sim \frac{1}{z^*}$ was extracted as a clear choice that incorporates quantum disordering and that will describe the system if it does not transform into a CDW (charge-density wave) inhomogeneous solution.

ACKNOWLEDGMENTS

We thank A. Auerbach, G. Möller, E. H. Rezayi, S. H. Simon, Z. Tešanović, and especially N. Read for discussions. M.V.M. gratefully acknowledges the hospitality of the Aspen

Center for Physics. The work was supported by Grant No. 141035 of the Serbian Ministry of Science.

APPENDIX A

We want to prove

$$\int d^2\eta_{1\uparrow} \int d^2\eta_{2\downarrow} \frac{1}{(\eta_{1\uparrow} - \eta_{2\downarrow})} \rho^\dagger(\eta_{1\uparrow}) \rho^\downarrow(\eta_{2\downarrow}) = 0. \quad (\text{A1})$$

After switching to the Fourier space, $\rho^\sigma(\eta) = \sum_k \rho_k^\sigma \exp\{i\vec{k}\vec{\eta}\}$, the left-hand side (l.h.s.) becomes

$$2\pi \sum_k \int d^2\eta \frac{1}{\eta} \exp\{i\vec{k}\vec{\eta}\} \rho_k^\dagger \rho_{-k}^\downarrow. \quad (\text{A2})$$

The angle part of the integration with the help of the table integral³¹

$$\int_0^\pi \exp\{i\beta \cos x\} \cos\{nx\} = i^n \pi J_n(\beta) \quad (\text{A3})$$

yields

$$\begin{aligned} \int d^2\eta \frac{1}{\eta} \exp\{i\vec{k}\vec{\eta}\} &= \int_0^\infty dr [i\pi J_1(kr) - i\pi J_1(-kr)] \\ &= (-) \frac{i\pi}{k} \int_0^\infty dr \left[\frac{dJ_0(kr)}{dr} + \frac{dJ_0(-kr)}{dr} \right] \\ &= i \frac{2\pi}{k}, \end{aligned} \quad (\text{A4})$$

where we used notation $|\vec{k}|=k$ and in the last line the identity for the Bessel functions: $J'_0 = -J_1$. On the other hand

$$\int d^2\eta \frac{1}{\eta} \exp\{-i\vec{k}\vec{\eta}\} = -i \frac{2\pi}{k}, \quad (\text{A5})$$

and therefore Eq. (A2) can be written as

$$\begin{aligned} \pi \sum_k \left[\int d^2\eta \frac{1}{\eta} \exp\{i\vec{k}\vec{\eta}\} \rho_k^\dagger \rho_{-k}^\downarrow + \int d^2\eta \frac{1}{\eta} \exp\{-i\vec{k}\vec{\eta}\} \rho_{-k}^\dagger \rho_k^\downarrow \right] \\ = i2\pi^2 \sum_k \frac{1}{|\vec{k}|} (\rho_k^\dagger \rho_{-k}^\downarrow - \rho_{-k}^\dagger \rho_k^\downarrow) = 0 \quad \text{QED.} \end{aligned} \quad (\text{A6})$$

Next we want to evaluate

$$\int d^2\eta_{1\uparrow} \int d^2\eta_{2\downarrow} \frac{1}{|\eta_{1\uparrow} - \eta_{2\downarrow}|^\alpha} \rho^\dagger(\eta_{1\uparrow}) \rho^\downarrow(\eta_{2\downarrow}). \quad (\text{A7})$$

Again this reduces in the Fourier space to

$$2\pi \sum_k \int d^2\eta \frac{1}{|\eta|^\alpha} \exp\{i\vec{k}\vec{\eta}\} \rho_k^\dagger \rho_{-k}^\downarrow. \quad (\text{A8})$$

In the case of $\alpha=1$ as usual for the real Coulomb interaction in 2D the integral is

$$\int d^2\eta \frac{1}{|\eta|} \exp\{i\vec{k}\vec{\eta}\} = 2\pi \int_0^\infty dr J_0(kr) = \frac{2\pi}{k}. \quad (\text{A9})$$

In the case of $\alpha=2$ we have

$$\int d^2\eta \frac{1}{|\eta|^2} \exp\{i\vec{k}\vec{\eta}\} = 2\pi \int_0^\infty dr \frac{J_0(kr)}{r}. \quad (\text{A10})$$

The integral needs a cutoff at small distances (otherwise diverges) which should be included in our effective description and as usual can be taken to be l_B (magnetic length distance). Therefore, instead of Eq. (A10) we have

$$2\pi \int_0^\infty dr \frac{r J_0(kr)}{r^2 + l_B^2} = 2\pi K_0(l_B k). \quad (\text{A11})$$

In the small momentum limit we can approximate

$$K_0(z) \approx -\ln\left\{\frac{z}{2}\right\} + o(z) \quad (\text{A12})$$

and therefore our first phononlike correction in this case of pairing is

$$\sum_k (-) \ln\{kl_B\} \rho_k^\dagger \rho_{-k}^\downarrow. \quad (\text{A13})$$

For the case of pairing $g(z) = \frac{1}{z}$ we have

$$\int d^2\eta_{1\uparrow} \int d^2\eta_{2\downarrow} \frac{1}{(\eta_{1\uparrow} - \eta_{2\downarrow})^2} \rho^\dagger(\eta_{1\uparrow}) \rho^\downarrow(\eta_{2\downarrow}), \quad (\text{A14})$$

which reduces to the solving of the following Fourier transform

$$\int d^2\eta \frac{1}{\eta^2} \exp\{i\vec{k}\vec{\eta}\}. \quad (\text{A15})$$

With the help of Eq. (A3) we have for the value of the integral

$$\int_0^\infty dr \frac{1}{r} \{-\pi J_2(kr) - \pi J_2(-kr)\}. \quad (\text{A16})$$

We may use the table integral³¹

$$\int_0^\infty \frac{J_\nu(ax)}{x^{\nu-q}} dx = \frac{\Gamma(\frac{1}{2}q + \frac{1}{2})}{2^{\nu-q} a^{q-\nu+1} \Gamma(\nu - \frac{1}{2}q + \frac{1}{2})} \quad (\text{A17})$$

for $-1 < Re q < Re \nu - \frac{1}{2}$ to find out that the value of the integral does not depend on k , i.e.,

$$\int d^2\eta \frac{1}{\eta^2} \exp\{i\vec{k}\vec{\eta}\} = -\pi. \quad (\text{A18})$$

Therefore the phononlike correction in this case is proportional to

$$\left(\sum_k \rho_k^\dagger \rho_k^\downarrow \right) \Psi_{111} \quad (\text{A19})$$

and in the real (coordinate) space this becomes

$$\begin{aligned} \int d^2\eta \rho^\dagger(\eta) \rho^\downarrow(\eta) \Psi_{111} &= \sum_{i,j} \int d^2\eta \delta^2(\eta - z_{i\uparrow}) \delta^2(\eta - z_{j\downarrow}) \Psi_{111} \\ &= \sum_{i,j} \delta^2(z_{i\uparrow} - z_{j\downarrow}) \Psi_{111} = 0, \end{aligned} \quad (\text{A20})$$

i.e., no correction at all.

APPENDIX B

We consider nondiagonal (nonphononlike) corrections that come from the description of quantum disordering by the class of WFs in Fig. 1(c) when the pairing is fixed to be $g(z) = \sqrt{\frac{z}{z^*}}$, i.e., nondiagonal terms of Eq. (22) with $n=4$. We want to prove the subleading behavior with respect to the diagonal terms as the one with $\eta_{1\uparrow} \equiv \eta_1$, $\eta_{3\uparrow} \equiv \eta_3$, $\eta_{2\downarrow} \equiv \eta_2$, and $\eta_{4\uparrow} \equiv \eta_4$ in

$$\int d^2\eta_1 \int d^2\eta_3 \int d^2\eta_2 \int d^2\eta_4 \frac{1}{|\eta_1 - \eta_2|} \frac{1}{|\eta_3 - \eta_4|} \times \rho^\dagger(\eta_1) \rho^\dagger(\eta_3) \rho^\dagger(\eta_2) \rho^\dagger(\eta_4) = \left[\sum_k \frac{(2\pi)^2}{k} \rho_k^\dagger \rho_{-k}^\dagger \right]^2 \quad (\text{B1})$$

of the following nondiagonal term

$$\int d^2\eta_1 \int d^2\eta_3 \int d^2\eta_2 \int d^2\eta_4 \frac{1}{(\eta_1 - \eta_2)} \frac{1}{(\eta_3 - \eta_4)} \times \sqrt{\frac{(\eta_1 - \eta_4)(\eta_3 - \eta_2)}{(\eta_1^* - \eta_4^*)(\eta_3^* - \eta_2^*)}} \rho^\dagger(\eta_1) \rho^\dagger(\eta_3) \rho^\dagger(\eta_2) \rho^\dagger(\eta_4). \quad (\text{B2})$$

The nondiagonal terms by their forms should describe different processes from the phonon contributions, i.e., from those as $(\rho_{k_1}^\dagger \rho_{-k_1}^\dagger) \cdots (\rho_{k_{n/2}}^\dagger \rho_{-k_{n/2}}^\dagger)$ for arbitrary k 's. In the long-distance approximation we will argue that the nondiagonal term [Eq. (B2)] carry less importance than the phonon contribution with the same number of density operators.

Introducing $\eta = \eta_1 - \eta_4$, $\tilde{\eta} = \eta_3 - \eta_2$, $\eta_- = \eta_1 - \eta_3$ and $\eta_+ = \eta_1 + \eta_3$ we can rewrite Eq. (B2) as

$$\sum_{k_1, k_3, \tilde{k}, k} \int d^2\eta \int d^2\tilde{\eta} \int d^2\eta_- \int d^2\eta_+ \frac{1}{(\eta_- + \tilde{\eta})} \frac{1}{(\eta - \eta_-)} \times \sqrt{\frac{\eta\tilde{\eta}}{\eta^*\tilde{\eta}^*}} \exp\{i\eta_1\tilde{k}_1\} \exp\{i\eta_3\tilde{k}_3\} \times \exp\left\{i\left(\frac{1}{2}\tilde{\eta}_+ - \frac{1}{2}\tilde{\eta}_- - \tilde{\eta}\right)\tilde{k}\right\} \times \exp\left\{i\left(\frac{1}{2}\tilde{\eta}_+ + \frac{1}{2}\tilde{\eta}_- - \tilde{\eta}\right)\tilde{k}\right\} \rho_{k_1}^\dagger \rho_{k_3}^\dagger \rho_{\tilde{k}}^\dagger \rho_{-k}^\dagger. \quad (\text{B3})$$

The η_+ integration brings the constraint $\tilde{k} + \tilde{k}_1 + \tilde{k}_3 = 0$. Then the remaining η_- integration gives the following contribution:

$$\int d^2\eta_- \frac{1}{(\eta_- + \tilde{\eta})} \frac{1}{(\eta - \eta_-)} \exp\left\{i\frac{\tilde{\eta}_-}{2}(\tilde{k}_1 - \tilde{k}_3 - \tilde{k} + \tilde{k})\right\} = -i\frac{2\pi}{|\tilde{k} + \tilde{k}_3|} \frac{1}{\eta + \tilde{\eta}} [\exp\{i\tilde{\eta}(\tilde{k}_3 + \tilde{k})\} - \exp\{-i\tilde{\eta}(\tilde{k}_3 + \tilde{k})\}], \quad (\text{B4})$$

where we used the constraint. Therefore the contribution is proportional to

$$\sum_{k_3, \tilde{k}, k} \frac{1}{|\tilde{k} + \tilde{k}_3|} \int d^2\eta \int d^2\tilde{\eta} \frac{1}{(\eta + \tilde{\eta})} \sqrt{\frac{\eta\tilde{\eta}}{\eta^*\tilde{\eta}^*}} \times [\exp\{i\tilde{\eta}(\tilde{k}_3 + \tilde{k})\} - \exp\{-i\tilde{\eta}(\tilde{k}_3 + \tilde{k})\}] \times \exp\{-i\tilde{\eta}\tilde{k}\} \exp\{-i\eta k\} \rho_{-k-k_3}^\dagger \rho_{k_3}^\dagger \rho_{\tilde{k}}^\dagger \rho_{-k}^\dagger. \quad (\text{B5})$$

In the long-distance limit $|\tilde{k} + \tilde{k}_3| \rightarrow 0$ but that does not cancel the part of the 2D volume in the integration measure like in the phonon contribution (that would damp the contribution) but is canceled by the difference of the exponentials in the same limit in Eq. (B5). There is only one more factor, i.e., $\frac{1}{\eta + \tilde{\eta}}$ that can bring the momentum inverse contribution but this only enforces $k \approx \tilde{k}$, i.e., $(\rho_k^\dagger \rho_{-k}^\dagger)^2$ without a significant coefficient. This will only give the next order contribution inside the brackets in Eq. (24) which for small d , and as usual in the RPA approach, we can neglect.

APPENDIX C

We will give a more general view of the CFT analogies of so-called³² doubled CS theories to which BF CS theory belongs. In the work of Freedman *et al.*³² BF CS theory was classified as the low-energy theory of the deconfined phase of \mathbb{Z}_2 gauge theory. There also $SU(2)_1 \times \overline{SU(2)}_1$ doubled CS theory was considered. For the detailed description of these theories the reader should consult Refs. 26 and 32. Here we will, by writing down relevant CFT correlators, demonstrate the analogies between nonchiral-complete CFTs and these doubled CS theories.

First we will consider $SU(2)_1 \times \overline{SU(2)}_1$ case. The possible wave function with coordinates of two species $z_{1\uparrow}, \dots, z_{N\downarrow}$, for which there are equal number of \uparrow 's and \downarrow 's: $N_\uparrow = N_\downarrow$ and $N_\uparrow + N_\downarrow = N$, is

$$\Psi = \frac{\prod_{k<l} |z_{k\uparrow} - z_{l\uparrow}| \prod_{p<q} |z_{p\downarrow} - z_{q\downarrow}|}{\prod_{i,j} |z_{i\uparrow} - z_{j\downarrow}|} = \frac{\prod_{k<l} \sqrt{|z_{k\uparrow} - z_{l\uparrow}|} \prod_{p<q} \sqrt{|z_{p\downarrow} - z_{q\downarrow}|}}{\prod_{i,j} \sqrt{|z_{i\uparrow} - z_{j\downarrow}|}} \times \frac{\prod_{k<l} \sqrt{|z_{k\uparrow}^* - z_{l\uparrow}^*}| \prod_{p<q} \sqrt{|z_{p\downarrow}^* - z_{q\downarrow}^*}|}{\prod_{i,j} \sqrt{|z_{i\uparrow}^* - z_{j\downarrow}^*}|}. \quad (\text{C1})$$

We use the following correlator of vertex operators of a bosonic field ϕ :

$$\langle \exp\{i\beta\phi(z_1, z_1^*)\} \exp\{-i\beta\phi(z_2, z_2^*)\} \rangle = \frac{1}{|z_1 - z_2|^{2\beta^2}}. \quad (\text{C2})$$

If $\alpha = \frac{1}{2}$ we can rewrite our wave function as

$$\Psi = \langle \exp\{i\alpha\phi(z_1, z_1^*)\} \exp\{i\alpha\phi(z_2, z_2^*)\} \dots \exp\{-i\alpha\phi(z_N, z_N^*)\} \rangle, \quad (\text{C3})$$

and define

$$\phi(z, z^*) = \phi(z) + \phi(z^*), \quad (\text{C4})$$

$$\theta(z, z^*) = \phi(z) - \phi(z^*). \quad (\text{C5})$$

Inserting a neutral pair (w_1 and w_2) of $\exp\{i\delta_1\phi(w, w^*)\}$ vertex operators or $\exp\{i\delta_2\phi(w, w^*)\}$ vertex operators we can conclude that these insertions correspond to multiplying the wave function Ψ [Eq. (C1)] by

$$\exp\{i\delta_1\phi(w, w^*)\} \rightarrow \frac{\prod_i |z_{i\uparrow} - w|^{2\delta_1\alpha}}{\prod_i |z_{i\downarrow} - w|^{2\delta_1\alpha}}, \quad (\text{C6})$$

$$\exp\{i\delta_2\theta(w, w^*)\} \rightarrow \frac{\prod_i (z_{i\uparrow} - w)^{\delta_2\alpha} \prod_i (z_{i\downarrow}^* - w^*)^{\delta_2\alpha}}{\prod_i (z_{i\downarrow}^* - w^*)^{\delta_2\alpha} \prod_i (z_{i\uparrow} - w)^{\delta_2\alpha}}. \quad (\text{C7})$$

(The general formula for the many vertex correlator can be found, for example, in Ref. 33.) The single-valuedness of the WFs demands $\delta_2 = \frac{1}{\sqrt{2}}$. If we take also $\delta_1 = \frac{1}{\sqrt{2}} = \delta_2 = \delta$ then

$$\begin{aligned} & \langle \exp\{i\delta\phi(w_1, w_1^*)\} \exp\{-i\delta\phi(w_2, w_2^*)\} \\ & \quad \times \exp\{i\delta\theta(w_3, w_3^*)\} \exp\{-i\delta\theta(w_4, w_4^*)\} \rangle \\ & = \frac{1}{|w_1 - w_2|^{2\delta^2}} \frac{1}{|w_3 - w_4|^{2\delta^2}} \\ & \quad \times \frac{(w_1 - w_3)^{\delta^2} (w_2 - w_4)^{\delta^2} (w_1^* - w_4^*)^{\delta^2} (w_2^* - w_3^*)^{\delta^2}}{(w_1^* - w_3^*)^{\delta^2} (w_2^* - w_4^*)^{\delta^2} (w_1 - w_4)^{\delta^2} (w_2 - w_3)^{\delta^2}}, \end{aligned} \quad (\text{C8})$$

and the mutual statistics between any of two particles of different kinds [Eq. (13), (14), (23), and (24)] is fermionic. To see that, for example, for Eq. (13) pair we send 2 toward 4 and switch w_1 and w_3 coordinates.

In our case of the quantum Hall bilayer,

$$\begin{aligned} \Psi' & = \frac{\prod_{k<l} |z_{k\uparrow} - z_{l\uparrow}|^2 \prod_{p<q} |z_{p\downarrow} - z_{q\downarrow}|^2}{\prod_{i,j} |z_{i\uparrow} - z_{j\downarrow}|^2} \\ & = \text{Det} \left\{ \frac{1}{z_{i\uparrow}^* - z_{j\downarrow}^*} \right\} \text{Det} \left\{ \frac{1}{z_{k\uparrow} - z_{l\downarrow}} \right\}, \end{aligned} \quad (\text{C9})$$

The same analysis as above will fix $\alpha=1$ and $\delta=\frac{1}{2}$ so that in this case the mutual statistics is semionic just as it should be in the BF CS field theory.

The BF CS theory of a 2D superconductor is²⁶

$$\frac{1}{\pi} \epsilon^{\mu\nu\lambda} b_\mu \partial_\nu a_\lambda - a_\mu j^\mu - b_\mu \tilde{j}^\mu, \quad (\text{C10})$$

where a^μ and b^μ , $\mu=0, 1, 2$ are gauge fields; the first term is the CS term and j^μ and \tilde{j}^μ , $\mu=0, 1, 2$ represent quasiparticle and vortex density currents. The Lagrangian encodes in the $\frac{1}{\pi}$ coefficient mutual semionic statistics between the two excitations in 2D superconductor—any time quasiparticle encircles vortex it gets the Bohm-Aharonov phase π because vortex corresponds to the half-flux quantum excitation in the paired system. Higher order in derivatives, i.e., Maxwell terms $\sim(\partial \times a)^2$ and $\sim(\partial \times b)^2$ are present in the description of the ordinary (s wave) gapped 2D superconductor and can describe the plasmon modes that are gapped—see Ref. 26. In our case, because from CFT analogies [Eqs. (C6) and (C7)] we find that δ_1 can be continuous and correspond to a branch of gapless excitations, we expect a quadratic in one of the gauge fields, without derivatives, term to describe such a behavior. For example, if we add a term quadratic in b [$b_\mu b^\mu$ with the $(\partial \times a)^2$ Maxwell term present] our classical equations of motion will be: $\Delta a = 0$ and $\partial \times b = 0$. They describe gapless behavior (Goldstone mode) in one gauge field and associated quasiparticle description, and incompressible behavior in the other.

[The $SU(2)_1 \times SU(2)_1$ theory can be described by the following Lagrangian

$$\frac{1}{2\pi} \epsilon^{\mu\nu\lambda} b_\mu \partial_\nu a_\lambda - a_\mu j^\mu - b_\mu \tilde{j}^\mu, \quad (\text{C11})$$

and we see explicitly mutual fermionic statistics.]

¹X.-G. Wen and A. Zee, Phys. Rev. Lett. **69**, 1811 (1992).

²I. B. Spielman, J. P. Eisenstein, L. N. Pfeiffer, and K. W. West, Phys. Rev. Lett. **84**, 5808 (2000).

³I. B. Spielman, J. P. Eisenstein, L. N. Pfeiffer, and K. W. West, Phys. Rev. Lett. **87**, 036803 (2001).

⁴K. Moon, H. Mori, K. Yang, S. M. Girvin, A. H. MacDonald, L. Zheng, D. Yoshioka, and S. C. Zhang, Phys. Rev. B **51**, 5138 (1995); K. Moon, H. Mori, K. Yang, S. M. Girvin, A. H. MacDonald, L. Zheng, D. Yoshioka, and S. C. Zhang, *ibid.* **51**, 5138 (1995).

⁵M. Kellogg, J. P. Eisenstein, L. N. Pfeiffer, and K. W. West, Phys. Rev. Lett. **93**, 036801 (2004).

⁶A. Lopez and E. Fradkin, Phys. Rev. B **51**, 4347 (1995).

⁷L. Onsager, Nuovo Cim. **6**, 249 (1949); R. P. Feynman, in *Progress in Low Temperature Physics*, edited by C. J. Gorter (North-Holland, Amsterdam, 1955); G. A. Williams, Phys. Rev. Lett. **59**, 1926 (1987); B. Chattopadhyay and S. R. Shenoy, *ibid.* **72**, 400 (1994); W. Janke and T. Matsui, Phys. Rev. B **42**, 10673 (1990); A. K. Nguyen and A. Sudbo, *ibid.* **57**, 3123 (1998).

⁸L. Jiang and J. Ye, Phys. Rev. B **74**, 245311 (2006); J. Ye and L. Jiang, Phys. Rev. Lett. **98**, 236802 (2007).

⁹A. R. Champagne, J. P. Eisenstein, L. N. Pfeiffer, and K. W. West, Phys. Rev. Lett. **100**, 096801 (2008).

¹⁰M. Kellogg, J. P. Eisenstein, L. N. Pfeiffer, and K. W. West, Phys. Rev. Lett. **90**, 246801 (2003).

- ¹¹B. Karmakar, V. Pellegrini, A. Pinczuk, L. N. Pfeiffer, and K. W. West, Phys. Rev. Lett. **102**, 036802 (2009).
- ¹²B. I. Halperin, Helv. Phys. Acta **56**, 75 (1983).
- ¹³H. A. Fertig, Phys. Rev. B **40**, 1087 (1989); A. H. MacDonald, Physica B **298**, 129 (2001).
- ¹⁴S.-C. Zhang, Int. J. Mod. Phys. B **6**, 25 (1992).
- ¹⁵E. H. Rezayi and N. Read, Phys. Rev. Lett. **72**, 900 (1994).
- ¹⁶S. H. Simon, E. H. Rezayi, and M. V. Milovanović, Phys. Rev. Lett. **91**, 046803 (2003).
- ¹⁷N. E. Bonesteel, Phys. Rev. B **48**, 11484 (1993).
- ¹⁸Z. Papić and M. V. Milovanović, Phys. Rev. B **75**, 195304 (2007).
- ¹⁹N. Read, Phys. Rev. Lett. **65**, 1502 (1990); N. Regnault, M. O. Goerbig, and T. Jolicoeur, *ibid.* **101**, 066803 (2008); R. de Gail, N. Regnault, and M. O. Goerbig, Phys. Rev. B **77**, 165310 (2008).
- ²⁰M. V. Milovanović, Phys. Rev. B **75**, 035314 (2007).
- ²¹R. B. Laughlin, in *The Quantum Hall Effect*, 2nd ed., edited by R. E. Prange and S. M. Girvin (Springer, New York, 1990).
- ²²P.-A. Bares and X.-G. Wen, Phys. Rev. B **48**, 8636 (1993).
- ²³N. Lindner, A. Auerbach, and D. Arovas, arXiv:cond-mat/0701571 (unpublished).
- ²⁴A. Stern and B. I. Halperin, Phys. Rev. Lett. **88**, 106801 (2002).
- ²⁵G. Moore and N. Read, Nucl. Phys. B **360**, 362 (1991); for the nonchiral arguments see M. Freedman, C. Nayak, K. Shtengel, K. Walker, and Z. Wang, Ann. Phys. (N.Y.) **310**, 428 (2004).
- ²⁶T. H. Hansson, V. Oganesyan, and S. L. Sondhi, Ann. Phys. (N.Y.) **313**, 497 (2004).
- ²⁷J. Ye and G. S. Jeon, Phys. Rev. B **71**, 035348 (2005).
- ²⁸E. Demler, C. Nayak, and S. Das Sarma, Phys. Rev. Lett. **86**, 1853 (2001); Y. B. Kim, C. Nayak, E. Demler, N. Read, and S. Das Sarma, Phys. Rev. B **63**, 205315 (2001).
- ²⁹M. V. Milovanović and Th. Jolicoeur, arXiv:0812.3764 (unpublished).
- ³⁰G. Möller, S. H. Simon, and E. H. Rezayi, Phys. Rev. Lett. **101**, 176803 (2008); G. Möller, S. H. Simon, and E. H. Rezayi, Phys. Rev. B **79**, 125106 (2009).
- ³¹I. S. Gradstein and I. M. Ryzhik, *Tables* (Fizmatgiz, Moscow, 1962).
- ³²M. Freedman, C. Nayak, K. Shtengel, K. Walker, and Z. Wang, Ann. Phys. **310**, 428 (2004).
- ³³C. Itzykson and J.-M. Drouffe, *Statistical Field Theory* (Cambridge University Press, Cambridge, 1991).

All Databases

Select a Database

Web of Science

Additional Resources

Search Search History

All Databases

<< Return to Web of Science®

Citing Articles Title: **Fractional quantum Hall state at $\nu=1/4$ in a wide quantum well**
 Author(s): **Papic, Z. ; Moeller, G. ; Milovanovic, M. V. ; et al.**
 Source: **PHYSICAL REVIEW B** Volume: 79 Issue: 24 Article Number: 245325 DOI: 10.1103/PhysRevB.79.245325 Published: JUN 2009

This item has been cited by items indexed in the databases listed below. [more information]

16 in All Databases

- 16 publication in Web of Science
- 0 publication in BIOSIS Citation Index
- 0 publication in SciELO Citation Index
- 0 publication in Chinese Science Citation Database
- 0 data sets in Data Citation Index
- 0 publication in Data Citation Index ¹

Results: 16

Page 1 of 1 Go

Sort by: Publication Date -- newest to oldest

Create Citation Report

Refine Results

Search within results for

Search

Databases

Research Domains

Refine

 SCIENCE TECHNOLOGY

Research Areas

Refine

 PHYSICS

Document Types

Authors

Group/Corporate Authors

Editors

Funding Agencies

Source Titles

Conference/Meeting Titles

Publication Years

Languages

Countries/Territories

 Select Page Add to Marked List (0) | | | Send to:

1. Title: **Fractional quantum Hall states in charge-imbalanced bilayer systems**
 Author(s): Thiebaut, N.; Regnault, N.; Goerbig, M. O.
 Book Group Author(s): IOP
 Conference: 20th International Conference on the Application of High Magnetic Fields in Semiconductor Physics (HMF) Location: Chamonix, FRANCE Date: JUL 22-27, 2012
 Sponsor(s): Lab Natl Champs Magnetiques Intenses; European High Magnet Field Lab
 Source: 20TH INTERNATIONAL CONFERENCE ON THE APPLICATION OF HIGH MAGNETIC FIELDS IN SEMICONDUCTOR PHYSICS (HMF-20) Book Series: Journal of Physics Conference Series Volume: 456 Article Number: UNSP 012036 DOI: 10.1088/1742-6596/456/1/012036 Published: 2013
 Times Cited: 0 (from All Databases)
 Get it! [View abstract](#)
2. Title: **Quantum Phase Transitions and the $\nu=5/2$ Fractional Hall State in Wide Quantum Wells**
 Author(s): Papic, Z.; Haldane, F. D. M.; Rezayi, E. H.
 Source: PHYSICAL REVIEW LETTERS Volume: 109 Issue: 26 Article Number: 266806 DOI: 10.1103/PhysRevLett.109.266806
 Published: DEC 27 2012
 Times Cited: 2 (from All Databases)
 Get it! [View abstract](#)
3. Title: **Quasi-Particle Localization by Disorder in $\nu=5/2$ Fractional Quantum Hall State and Its Potential Application**
 Author(s): Goswami, P.
 Source: ACTA PHYSICA POLONICA A Volume: 122 Issue: 4 Pages: 741-747 Published: OCT 2012
 Times Cited: 0 (from All Databases)
 Get it! [View abstract](#)
4. Title: **EXPLANATION OF COMPOSITE FERMION STRUCTURE IN FRACTIONAL QUANTUM HALL SYSTEMS**
 Author(s): Jacak, Janusz; Gonczarek, Ryszard; Jacak, Lucjan; et al.
 Source: INTERNATIONAL JOURNAL OF MODERN PHYSICS B Volume: 26 Issue: 23 Article Number: 1230011 DOI: 10.1142/S0217979212300113 Published: SEP 20 2012
 Times Cited: 0 (from All Databases)
 Get it! [View abstract](#)
5. Title: **Decomposition of fractional quantum Hall model states: Product rule symmetries and approximations**
 Author(s): Thomale, Ronny; Estienne, Benoit; Regnault, Nicolas; et al.
 Source: PHYSICAL REVIEW B Volume: 84 Issue: 4 Article Number: 045127 DOI: 10.1103/PhysRevB.84.045127 Published: JUL 19 2011
 Times Cited: 15 (from All Databases)
 Get it! [View abstract](#)
6. Title: **Fractional quantum Hall effects in bilayers in the presence of interlayer tunneling and charge imbalance**
 Author(s): Peterson, Michael R.; Papic, Z.; Das Sarma, S.
 Source: PHYSICAL REVIEW B Volume: 82 Issue: 23 Article Number: 235312 DOI: 10.1103/PhysRevB.82.235312 Published: DEC 9 2010
 Times Cited: 4 (from All Databases)
 Get it! [View abstract](#)
7. Title: **Non-Abelian two-component fractional quantum Hall states**
 Author(s): Barkeshil, Maissam; Wen, Xiao-Gang
 Source: PHYSICAL REVIEW B Volume: 82 Issue: 23 Article Number: 233301 DOI: 10.1103/PhysRevB.82.233301 Published: DEC 2 2010
 Times Cited: 4 (from All Databases)
 Get it! [View abstract](#)

8. Title: [Classification of Abelian and non-Abelian multilayer fractional quantum Hall states through the pattern of zeros](#)
 Author(s): Barkeshli, Maissam; Wen, Xiao-Gang
 Source: PHYSICAL REVIEW B Volume: 82 Issue: 24 Article Number: 245301 DOI: 10.1103/PhysRevB.82.245301 Published: DEC 2 2010
 Times Cited: 9 (from All Databases)
[Get it!](#)  [View abstract](#)
9. Title: [Correlation-Hole Induced Paired Quantum Hall States in the Lowest Landau Level](#)
 Author(s): Lu, Yuan-Ming; Yu, Yue; Wang, Ziqiang
 Source: PHYSICAL REVIEW LETTERS Volume: 105 Issue: 21 Article Number: 216801 DOI: 10.1103/PhysRevLett.105.216801
 Published: NOV 17 2010
 Times Cited: 2 (from All Databases)
[Get it!](#)  [View abstract](#)
10. Title: [TOPOLOGICALLY MASSIVE ELECTROMAGNETIC INTERACTION OF COMPOSITE PARTICLES IN A HIGHER-DERIVATIVE NONRELATIVISTIC GAUGE FIELD MODEL](#)
 Author(s): Manavella, Edmundo C.
 Source: INTERNATIONAL JOURNAL OF MODERN PHYSICS A Volume: 25 Issue: 26 Pages: 4949-4974 DOI: 10.1142/S0217751X10050664 Published: OCT 20 2010
 Times Cited: 2 (from All Databases)
[Get it!](#)  [View abstract](#)
11. Title: [Subband engineering even-denominator quantum Hall states](#)
 Author(s): Scarola, V. W.; May, C.; Peterson, M. R.; et al.
 Source: PHYSICAL REVIEW B Volume: 82 Issue: 12 Article Number: 121304 DOI: 10.1103/PhysRevB.82.121304 Published: SEP 9 2010
 Times Cited: 3 (from All Databases)
[Get it!](#)  [View abstract](#)
12. Title: [Tunneling-driven breakdown of the 331 state and the emergent Pfaffian and composite Fermi liquid phases](#)
 Author(s): Papic, Z.; Goerbig, M. O.; Regnault, N.; et al.
 Source: PHYSICAL REVIEW B Volume: 82 Issue: 7 Article Number: 075302 DOI: 10.1103/PhysRevB.82.075302 Published: AUG 3 2010
 Times Cited: 3 (from All Databases)
[Get it!](#)  [View abstract](#)
13. Title: [Quantum Hall phase diagram of half-filled bilayers in the lowest and the second orbital Landau levels: Abelian versus non-Abelian incompressible fractional quantum Hall states](#)
 Author(s): Peterson, Michael R.; Das Sarma, S.
 Source: PHYSICAL REVIEW B Volume: 81 Issue: 16 Article Number: 165304 DOI: 10.1103/PhysRevB.81.165304 Published: APR 15 2010
 Times Cited: 13 (from All Databases)
[Get it!](#)  [View abstract](#)
14. Title: [Evidence for Developing Fractional Quantum Hall States at Even Denominator 1/2 and 1/4 Fillings in Asymmetric Wide Quantum Wells](#)
 Author(s): Shabani, J.; Gokmen, T.; Chiu, Y. T.; et al.
 Source: PHYSICAL REVIEW LETTERS Volume: 103 Issue: 25 Article Number: 256802 DOI: 10.1103/PhysRevLett.103.256802
 Published: DEC 18 2009
 Times Cited: 11 (from All Databases)
[Get it!](#)  [View abstract](#)
15. Title: [Interaction-tuned compressible-to-incompressible phase transitions in quantum Hall systems](#)
 Author(s): Papic, Z.; Regnault, N.; Das Sarma, S.
 Source: PHYSICAL REVIEW B Volume: 80 Issue: 20 Article Number: 201303 DOI: 10.1103/PhysRevB.80.201303 Published: NOV 20 2009
 Times Cited: 18 (from All Databases)
[Get it!](#)  [View abstract](#)
16. Title: [Correlated States of Electrons in Wide Quantum Wells at Low Fillings: The Role of Charge Distribution Symmetry](#)
 Author(s): Shabani, J.; Gokmen, T.; Shayegan, M.
 Source: PHYSICAL REVIEW LETTERS Volume: 103 Issue: 4 Article Number: 046805 DOI: 10.1103/PhysRevLett.103.046805
 Published: JUL 24 2009
 Times Cited: 14 (from All Databases)
[Get it!](#)  [View abstract](#)
- Select Page  Add to Marked List (0)   Send to:

Results: 16 Show 50 per page

Page 1 of 1 

Sort by: Publication Date -- newest to oldest

16 records matched your query of the 55,067,330 (contains duplicates) in the data limits you selected.

View in: [简体中文](#) | [繁體中文](#) | [English](#) | [日本語](#) | [한국어](#) | [Português](#) | [Español](#)© 2013 Thomson Reuters | [Terms of Use](#) | [Privacy Policy](#) | Please give us your [feedback](#) on using Web of Knowledge.

Fractional quantum Hall state at $\nu=\frac{1}{4}$ in a wide quantum well

Z. Papić,^{1,2} G. Möller,³ M. V. Milovanović,² N. Regnault,⁴ and M. O. Goerbig¹

¹*Laboratoire de Physique des Solides, Université Paris-Sud, CNRS UMR 8502, F-91405 Orsay Cedex, France*

²*Institute of Physics, P.O. Box 68, 11 000 Belgrade, Serbia*

³*Theory of Condensed Matter Group, Cavendish Laboratory, J. J. Thomson Avenue, Cambridge CB3 0HE, United Kingdom*

⁴*Laboratoire Pierre Aigrain, Ecole Normale Supérieure, CNRS, 24 rue Lhomond, F-75005 Paris, France*

(Received 1 April 2009; published 23 June 2009)

We investigate, with the help of Monte Carlo and exact-diagonalization calculations in the spherical geometry, several compressible and incompressible candidate wave functions for the recently observed quantum Hall state at the filling factor $\nu=1/4$ in a wide quantum well. The quantum well is modeled as a two-component system by retaining its two lowest subbands. We make a direct connection with the phenomenological effective-bilayer model, which is commonly used in the description of a wide quantum well and we compare our findings with the established results at $\nu=1/2$ in the lowest Landau level. At $\nu=1/4$, the overlap calculations for the Halperin (5,5,3) and (7,7,1) states, the generalized Haldane-Rezayi state and the Moore-Read Pfaffian, suggest that the incompressible state is likely to be realized in the interplay between the Halperin (5,5,3) state and the Moore-Read Pfaffian. Our numerics show the latter to be very susceptible to changes in the interaction coefficients, thus indicating that the observed state is of multicomponent nature.

DOI: [10.1103/PhysRevB.79.245325](https://doi.org/10.1103/PhysRevB.79.245325)

PACS number(s): 73.43.Cd, 73.21.Fg, 71.10.Pm

I. INTRODUCTION

Advances in fabrication of high-quality GaAs semiconductor systems have led to an ever growing collection of the observed incompressible fractional quantum Hall states in a variety of settings.¹ These states occur at particular ratios between the number of electrons N and the number of magnetic flux quanta N_ϕ that pierce the system in the direction perpendicular to the sample. This commensurability can be expressed as the filling factor $\nu=N/N_\phi=p/q$ in terms of integers p , q , which is the single most important quantity that characterizes the quantum Hall state.

In a thin layer, q usually turns out to be an odd integer, the fact which had its pioneering explanation in terms of the Laughlin wave function² for the case of $p=1$, $q=3,5,7,\dots$ and its subsequent generalizations in terms of composite fermions³ (CFs), applicable to general integers p,q as long as q is odd, and hierarchy theory.⁴ However, a state with an even denominator has also been observed⁵ but in the first excited Landau level (LL). One cannot account for it in the usual Laughlin/composite fermion approach and the idea of pairing has commonly been invoked to explain the origin of this fraction.^{6,7} The simplest realization of pairing between spin-polarized electrons is the so-called Pfaffian defined by the Moore-Read wave function⁷ and supporting excitations with non-Abelian statistics.⁸

The possibility of an extra degree of freedom lifts the requirement of Fermi antisymmetry and hence gives another route toward realizing even denominator fractions. The additional degree of freedom can be the ordinary spin or else a “pseudospin” in case of a wide quantum well, where the two lowest electronic subbands correspond to \uparrow , \downarrow . If the sample is etched in such a way to create a barrier in the middle, thus suppressing tunneling between the two “sides,” one can think of it as a bilayer with \uparrow , \downarrow denoting the left and right layers where electrons can be localized. Incompressible quantum Hall states for such systems have been theoretically predicted

in Ref. 9 and experimentally confirmed for cases of bilayer at filling factor $\nu=1$ and $\nu=1/2$.^{10,11} Later on, essentially the same quantum Hall state at $\nu=1/2$ was observed in a sample which had the geometry of a single wide well.¹² It was argued, on the basis of a self-consistent Hartree-Fock approximation, that in a wide well the electrons (due to their mutual repulsion) reorganize themselves so as to form an effective bilayer distribution of charge. Hence, an equivalence between the two very different samples was claimed and theoretical works set out to analyze the problem from this premise.^{13,14}

On the basis of the quantum mechanical overlap with the ground state obtained in exact diagonalization (ED), including a realistic bilayer confinement potential, Ref. 13 established that the ground state is well described by the so-called (3,3,1) Halperin wave function.¹⁵ This wave function distinguishes between two kinds of electrons and the fact that it describes the system is what we mean by the system being “multicomponent.” Experimental work gave further insight into the nature of the multicomponent state at $\nu=1/2$ and strengthened the belief that the (3,3,1) wave function is a correct physical description.¹² Namely, the behavior of the excitation gap as a function of tunneling amplitude Δ_{SAS} (i.e., the splitting between the two lowest subbands) was found to have upward cusp at the intermediate value of Δ_{SAS} and the state was quickly destroyed by the application of electrostatic bias (charge imbalance).¹² In Ref. 14, a numerical study was able to reproduce the observed upward cusp in the activation gap by diagonalizing the bilayer Hamiltonian with explicit interlayer tunneling.

A recent experimental paper¹⁶ reports the observation of the $\nu=1/4$ quantum Hall state in a wide quantum well. The state is fragile and almost indiscernible when only a perpendicular magnetic field is applied (although one could expect that with yet higher sample qualities, a small plateau would be developed already at that point). However, when the magnetic field is tilted, there is a clear dip in the value of longi-

tudinal resistance R_{xx} , signifying the presence of an incompressible state.

In this paper we analyze the complex interplay between the single- and multicomponent nature of the ground state at $\nu=1/4$ in a wide quantum well, in comparison with the ground state at $\nu=1/2$. Contrary to previous studies,^{13,14} we do not make the *ad hoc* assumption that the wide quantum well may be described as an effective bilayer. Instead, we consider the two lowest electronic subbands of the quantum well, which is modeled by the infinite square well for the sake of convenience but cross-checked with other confinement models. The energy splitting between these two subbands, the associated wave functions of which are symmetric and antisymmetric, respectively, in the z direction is given by Δ_{SAS} (occasionally referred to as the tunneling amplitude). Due to the low filling factor ($\nu=1/4$), the power of the ED method will be rather limited and other complementary approaches may be needed to fully explain the experimental findings.

The paper is organized as follows. Section II is devoted to the single-component candidate for $\nu=1/4$ and we study its overlap with the exact Coulomb ground state within various confinement models. In Sec. III, we define the multicomponent wave functions expected to be relevant at this filling factor. The two likely candidates, the Halperin (5,5,3) and (7,7,1) states, are investigated within a simple bilayer model without tunneling. The two-subband model of the quantum well is introduced and described in Sec. IV. Our main results of ED calculations in the spherical geometry are presented in Sec. V. To extend the reach of our numerics, we furthermore deploy Monte Carlo simulations of the trial wave functions identified beforehand to analyze their energetic competition. We summarize with our view on the nature of the state at $\nu=1/4$ in Sec. VI.

II. ONE COMPONENT STATE

A. Pfaffian at $\nu=1/4$

There is a natural candidate for the fully polarized quantum Hall state at $\nu=1/4$ —it is the generalized Moore-Read Pfaffian,⁸

$$\Psi_{\text{Pf}}(z_1, \dots, z_N) = \text{Pf} \left(\frac{1}{z_i - z_j} \right) \prod_{i < j} (z_i - z_j)^4, \quad (1)$$

expressed in terms of the complex coordinate of the electron in the plane where $z_j = x_j + iy_j$. The object Pf is defined as

$$\text{Pf } M_{ij} = \frac{1}{2^{N/2}(N/2)!} \sum_{\sigma \in S_N} \text{sgn } \sigma \prod_{k=1}^{N/2} M_{\sigma(2k-1)\sigma(2k)},$$

acting upon the antisymmetric $N \times N$ matrix M_{ij} and S_N is a group of permutations of N objects. Pf renders the wave function totally antisymmetric and encodes the same kind of correlations as in the more familiar $\nu=5/2$ case.⁷ In the spherical geometry^{4,17} many-body states are characterized by the number of electrons N , the number of flux quanta N_ϕ generated by a magnetic monopole placed in the center of the sphere and extending radially through its surface, and an

additional topological number which is the shift. For the Pfaffian in Eq. (1), the three numbers are related by the formula $N_\phi = 4N - 5$. Ψ_{Pf} is a zero-energy eigenstate of a certain three-body Hamiltonian⁸ but in our calculations it was generated from its root configuration via the squeezing technique.¹⁸ On the other hand, the Coulomb (two-body) Hamiltonian commutes with the angular momentum operator \mathbf{L} because of rotational invariance and, by Wigner-Eckart theorem, the interaction is parametrized by discrete set of numbers V_L known as the Haldane pseudopotentials.⁴ The motion of electrons is therefore fully described in terms of the in-plane (spherical) coordinates θ , ϕ and the use of different confinement models in the (perpendicular) z direction (neglecting the in-plane magnetic field) will only modify the values of pseudopotentials.

B. Finite thickness models

Most of the candidate wave functions for quantum Hall fractions have been extensively studied via numerical techniques such as ED or Monte Carlo. For the sake of convenience but also due to the intrinsic ambiguity which stems from the fact that in a strongly correlated system many input parameters (e.g., the precise form of the interaction) are unknown, it is natural to start off from the limit of infinitely thin layer of electrons interacting via Coulomb force and hope that the inclusion of, e.g., realistic confinement and sample thickness will have small, perturbative corrections. There have been different proposals to account for the finite thickness of the sample in the perpendicular direction but the one that is straightforward and most natural from the point of view of ED is the Zhang–Das Sarma (ZDS) model¹⁹ which is simply given by substituting the interaction

$$\frac{1}{r} \rightarrow \frac{1}{\sqrt{r^2 + (w/2)^2}} \quad (2)$$

(we will always denote by w the width of the sample and the energy is always expressed in units of $e^2/\epsilon l_B$, where the magnetic length is $l_B = \sqrt{\hbar c/eB}$ is given in terms of the perpendicular magnetic field B). Qualitatively, this substitution softens the interaction¹⁹ and was studied extensively (together with other confinement models, some of which we will introduce below) in Ref. 20, where it was advertised to significantly stabilize the Moore-Read Pfaffian at $\nu=1/2$ (the effect being most pronounced in the second LL) but (in most cases) decrease the overlap somewhat for the Laughlin states at $\nu=1/3$ and $1/5$. In Ref. 21 it was noticed that this kind of interaction can lead to an instability of the composite fermion sea, which is believed to describe the compressible state at $\nu=1/2$ in the lowest LL, toward the paired state described by the Pfaffian. Indeed, the CF Fermi liquid can be regarded as a special member of the general class of paired CF wave functions,²² of which it represents the limit of vanishing gap.

Although the ZDS model (2) has a very simple form, there is no physical wave function that corresponds to this confinement potential in the z direction. Other popular choices for the confinement in the z direction include the infinite square well (ISQW) and Fang-Howard (FH), which

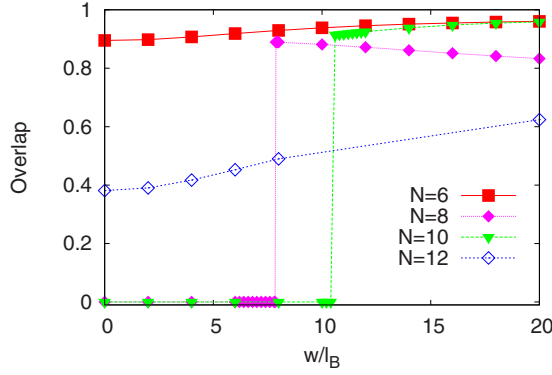


FIG. 1. (Color online) Overlap $|\langle \Psi_{\text{Pf}} | \Psi_{\text{exact}} \rangle|$ between the exact Coulomb state for finite width (ZDS model) and the Pfaffian at $\nu = 1/4$.

are presumably more realistic than ZDS because they are defined by the actual wave functions of simple model potentials for the quantum well, given by

$$\phi_{\text{ISQW}}(z) = \sqrt{\frac{2}{w}} \sin\left(\frac{\pi z}{w}\right), \quad (3)$$

$$\phi_{\text{FH}}(z) = \sqrt{\frac{27}{2w^3}} z e^{-3z/2w}, \quad (4)$$

respectively.

C. Overlaps

We have performed ED calculations for various confinement models [Eqs. (2)–(4)] and all system sizes $N = 6, 8, 10, 12$ accessible at present. In Fig. 1 we present the overlap $|\langle \Psi_{\text{Pf}} | \Psi_{\text{exact}} \rangle|$ between the exact Coulomb ground state at $\nu = 1/4$ and Ψ_{Pf} , finite width being modeled by the ZDS ansatz [Eq. (2)]. The size of the Hilbert space at $N = 12$ is noteworthy: the dimension of the $L_z = 0$ sector is 218 635 791.

It appears that the overlap of the Pfaffian state is rather high for large values of the width (even if it is negligible for small w). These values could likely be increased further by considering general pairing wave functions.²² However, these overlaps alone cannot be taken as solid evidence for a pairing nature of the $\nu = 1/4$ for two reasons. First, for $N = 6$ and 12 there is the aliasing problem with composite fermion states: Jain states with different physical properties (e.g., Abelian instead of non-Abelian statistics) occur at the same values of N and N_ϕ on the sphere (because of finite system size). High overlap for the aliased states may therefore come from other incompressible states different from the Pfaffian. Second, for the nonaliased states at $N = 8$ and 10 , there appears to be a critical value of the width at which the overlap as a function of w suffers a sharp jump. By analyzing the entire low energy spectrum on the sphere as a function of width, we have established that the (neutral) gap collapses at the critical point of w/l_B . Therefore, in order to get to the Pfaffian phase, one must go through a (first-order) phase transition. Before the transition, the ground state is obtained

in the $L > 0$ sector of the Hilbert space and the overlap with the Pfaffian (which resides in $L = 0$ sector) remains zero due to the difference in symmetry.

The lack of adiabatic continuity and the aliasing problem cast some doubt on the Pfaffian state as a good candidate for $\nu = 1/4$ in the lowest LL. We have also checked using other confinement models [Eqs. (3) and (4)] but in these cases for $N = 8$ and 10 the overlap remains zero for any value of w/l_B . Thus our ED results do not yield a definite answer with respect to the relevance of Ψ_{Pf} in the single layer at $\nu = 1/4$.

We would like to stress the qualitative difference in our results obtained by using ZDS versus other confinement models which appears, to the best of our knowledge, to be the first such case in the literature. The smaller overall energy scale (and the smaller gap as well) is very likely to be at the origin of this discrepancy. We note in passing that, contrary to the finite-width models which change *all* pseudopotentials at once, one may start from the pure Coulomb interaction and vary just a few strongest pseudopotentials.²³ We have tried varying both V_1 and V_3 but this procedure does not stabilize the Pfaffian phase in any finite region of the parameter space for $N = 8$.

III. TWO-COMPONENT STATES

Soon after Laughlin’s wave function describing the incompressible state at $\nu = 1/3$ when the electron spins are fully polarized, Halperin¹⁵ proposed a class of generalized wave functions defined as

$$\Psi_{mm'n}(z_1^\uparrow, \dots, z_{N_\uparrow}^\uparrow, z_1^\downarrow, \dots, z_{N_\downarrow}^\downarrow) = \prod_{i < j}^{N_\uparrow} (z_i^\uparrow - z_j^\uparrow)^m \prod_{k < l}^{N_\downarrow} (z_k^\downarrow - z_l^\downarrow)^{m'} \prod_s^{N_\uparrow} \prod_t^{N_\downarrow} (z_s^\uparrow - z_t^\downarrow)^n, \quad (5)$$

where the electrons are distributed over two components (labeled by \uparrow, \downarrow). The exponents m, m' denote the “intracomponent” correlations originating from the basic Laughlin-Jastrow building blocks within each component, whereas n describes “intercomponent” correlations (we have omitted the ubiquitous Gaussian factors and implicitly assume that there is a spinor part to this wave function as well as an overall antisymmetrization between \uparrow and \downarrow). In order for these wave functions to be eligible candidates for the ground state of the system, one must enforce an additional requirement that they be eigenstates of the Casimir operator of the $SU(2)$ group, i.e., the total spin S^2 , as long as the interaction is symmetric with respect to intracomponent and intercomponent (e.g., the usual case of electrons with spin). However, apart from electrons with spin, the wave functions [Eq. (5)] have also been used in bilayer systems where this symmetry is broken as soon as the layer separation is nonzero. In this case, the wave functions [Eq. (5)] need not be eigenstates of the total spin. There have been generalizations of these wave functions in the physics of bilayer systems at total filling factor^{24–26} $\nu = 1$ and to more than two components,²⁷ where further constraints on the possible values of m, m', n were derived within the plasma analogy.²⁸ In a two-component case, these turn out to be the intuitive requirement that intra-

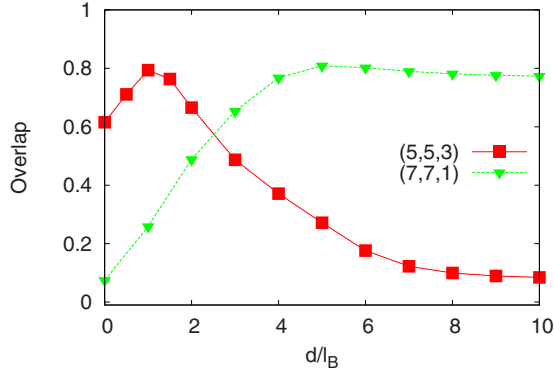


FIG. 2. (Color online) Overlap between the exact bilayer state with the (5,5,3) and (7,7,1) states for $N=8$ particles.

component interactions are stronger than intercomponent interactions: $m, m' \geq n$. For the particular case of two components and $m=m'=n+2$ (which includes Ψ_{331} and Ψ_{553}), the Halperin wave function [Eq. (5)] can be analytically cast into a paired form^{26,29} via Cauchy determinant identity (up to the unimportant phase factor),

$$\frac{\prod_{i<j}^{N_{\uparrow}} (z_i^{\uparrow} - z_j^{\uparrow}) \prod_{k<l}^{N_{\downarrow}} (z_k^{\downarrow} - z_l^{\downarrow})}{\prod_s^{N_s} \prod_t^{N_t} (z_s^{\uparrow} - z_t^{\downarrow})} = \det \left[\frac{1}{z_i^{\uparrow} - z_j^{\downarrow}} \right],$$

where the pairing function is given by $\det[\frac{1}{z_i^{\uparrow} - z_j^{\downarrow}}]$. In the case of the 111 state, this pairing nature was recently exploited to make a connection to paired composite fermion states and to construct wave functions interpolating between these two regimes.²⁶ Halperin wave functions are the exact zero-energy eigenstates of the two-body Hamiltonian

$$H = \sum_{i<j} \left[\sum_{L=0}^{m-1} V_L^{\uparrow\uparrow} P_{ij}^{\uparrow\uparrow} (N_{\phi} - L) + \sum_{L=0}^{m'-1} V_L^{\downarrow\downarrow} P_{ij}^{\downarrow\downarrow} (N_{\phi} - L) \right] + \sum_{i,j} \sum_{L=0}^{n-1} V_L^{\uparrow\downarrow} P_{ij}^{\uparrow\downarrow} (N_{\phi} - L), \quad (6)$$

where $P_{ij}^{\sigma\sigma'}(L)$ projects onto the state with angular momentum L of particles i and j with respective (pseudo)spins σ and σ' . Besides offering great convenience for handling Halperin wave functions [Eq. (5)] in ED, Eq. (6) enabled counting of the number of excited quasihole states and reaffirming the idea that the states described by Eq. (5) possess Abelian statistics.⁸

At the filling factor $\nu=1/4$, there are three wave functions of form (5) that meet the necessary physical requirements, $\Psi_{553} \equiv (5, 5, 3)$, $\Psi_{771} \equiv (7, 7, 1)$, and $\Psi_{5131} \equiv (5, 13, 1)$. None of them is an eigenstate of \mathbf{S}^2 , so they are more adapted to the case of a bilayer than that of real spin. In Fig. 2 we present the basic overlap characterization of the first two wave functions in a simple bilayer model defined by the interaction $V^{\uparrow\uparrow}(r) = V^{\downarrow\downarrow}(r) = 1/r$, $V^{\uparrow\downarrow}(r) = 1/\sqrt{r^2 + d^2}$ (where d being the distance between the layers).³⁰ (5,5,3) displays a familiar maximum in the overlap for small distance between the layers. (7,7,1) was dismissed in Ref. 16 arguing that it would more likely lead to two coupled Wigner crystals than

an incompressible liquid. Our diagonalization scheme is not adapted to address states with broken translation symmetry, so we do not see an *a priori* reason to reject this state. The results in Fig. 2 are for $N=8$ particles, they are fully consistent with those of smaller N but direct comparison between (5,5,3) and (7,7,1) is not possible because they are characterized by different shifts (-5 and -7 , respectively).²⁸ We will address this issue below by extrapolating to the thermodynamic limit the respective trial energies from Monte Carlo simulations for both of these states.

The last possibility, (5,13,1), is a peculiar one because it can only occur in the case of a strong density imbalance. Such an imbalance would lead to an increase in the charging energy but if one of the coupled states is a prominent quantum Hall state, the gain in correlation energy can outweigh the price of charge imbalance, as it has been experimentally verified.³¹ However, in the present case, our numerical calculations confirmed that this candidate can be discarded because it takes unrealistically high values of the sample width for this wave function to have any numerical relevance at all.

Given the low filling factor $\nu=1/4$ we are studying, one must also consider the possibility of nearby compressible states that can intervene for some values of the external parameters. Apart from the obvious metallic state similar to the Fermi-liquidlike state proposed by Rezayi and Read,³² there is in principle also the Haldane-Rezayi (HR) state,^{6,8} which is defined by

$$\Psi_{\text{HR}}(\{z_i^{\uparrow}, z_i^{\downarrow}\}) = \det \left[\frac{1}{(z_i^{\uparrow} - z_j^{\downarrow})^2} \right] \prod_{i<j}^N (z_i - z_j)^4.$$

The last term is a global Laughlin-Jastrow factor for all particles regardless of their spin. Ψ_{HR} is the zero energy eigenstate of the interaction parametrized by the set of pseudopotentials $V_L = \{1, 1, 0, 1, 0, \dots\}$ and occurs at the shift of -6 . It is also a spin singlet⁶ and compressible on the basis of its nonunitary parent conformal field theory.^{8,33} However, its edge theory³³ is closely related to that of the Abelian (5,5,3) state, which suggests that the HR state may be in the vicinity of the incompressible state and nonetheless affect the physical properties of the system. Recently there have been proposals that compressible states can be molded into incompressible ones.³⁴

IV. QUANTUM-WELL MODEL

So far we have discussed the stability of the one-component Pfaffian state in different finite-width models (Sec. II) and two-component states in a bilayer model where each layer is considered as an infinitely narrow quantum well (Sec. III). In this section, we consider an infinite square well of width w in the direction $z \in [0, w]$. The electronic motion in the z direction will then be quantized, yielding an electronic subband structure.

A. Two-subband approximation

Instead of a full description with all the electronic subbands, we only consider the two lowest subbands and iden-

tify them with the two pseudospin states, $\Psi_{\uparrow,\downarrow} = \phi_{\uparrow,\downarrow}(z) Y_{N_\phi/2, N_\phi/2, m}(\theta, \phi)$, where

$$\phi_{\uparrow}(z) = \sqrt{\frac{2}{w}} \sin\left(\frac{\pi z}{w}\right), \quad (7)$$

$$\phi_{\downarrow}(z) = \sqrt{\frac{2}{w}} \sin\left(\frac{2\pi z}{w}\right), \quad (8)$$

and the Y s represent monopole spherical harmonics with $-N_\phi/2 \leq m \leq N_\phi/2$ (we assume that the states are entirely within the lowest LL). We refer to states (7) and (8) as symmetric and antisymmetric, respectively, because of their reflection symmetry with respect to the center of the well. If their energy difference is denoted by Δ_{SAS} , the corresponding second quantized Hamiltonian is given by³⁵

$$H = -\frac{\Delta_{SAS}}{2} \sum_m (c_{m\uparrow}^\dagger c_{m\uparrow} - c_{m\downarrow}^\dagger c_{m\downarrow}) + \frac{1}{2} \sum_{\{m\}} \sum_{\{\sigma\}} V_{m_1, m_2, m_3, m_4}^{\sigma_1, \sigma_2, \sigma_3, \sigma_4} c_{m_1 \sigma_1}^\dagger c_{m_2 \sigma_2}^\dagger c_{m_4 \sigma_4} c_{m_3 \sigma_3}, \quad (9)$$

where $c_{m\sigma}^{(\dagger)}$ annihilates (creates) an electron in the state m with pseudospin σ .

The matrix elements $V_{m_1, m_2, m_3, m_4}^{\sigma_1, \sigma_2, \sigma_3, \sigma_4}$ can be straightforwardly evaluated from the Haldane pseudopotentials for the resulting in-plane interaction

$$V_{2D}^{\sigma_1, \sigma_2, \sigma_3, \sigma_4}(\vec{r}_1 - \vec{r}_2) = \frac{e^2}{\epsilon l_B} \int dz_1 \int dz_2 \frac{\phi_{\sigma_1}^*(z_1) \phi_{\sigma_2}^*(z_2) \phi_{\sigma_3}(z_1) \phi_{\sigma_4}(z_2)}{\sqrt{(\vec{r}_1 - \vec{r}_2)^2 + (z_1 - z_2)^2}}, \quad (10)$$

where the position variables are expressed in units of l_B such that the integral is dimensionless.

In this paper we do not make an attempt to quantitatively model the experiment of Ref. 16 but we are interested in the possible phases that may occur and the transitions between them. Therefore, we expect the model described by Hamiltonian (9) to be qualitatively correct and in agreement with other confinement models that assume the lowest subband to be symmetric and the first excited one to have a node in the center ($z = w/2$). Any difference of the confining potential away from the infinite square well will modify the energy eigenvalues and the associated wave functions $\phi_\sigma(z)$. However, it is expected that the energies are more strongly affected than the wave functions. In particular, the nodal structure of the wave functions is robust, such that the two lowest eigenstates of the infinite well faithfully represent the underlying features. However, we will allow for the general values of the level splitting Δ_{SAS} to account for the variations in the eigenenergies.

B. Connection between the quantum-well model and the bilayer Hamiltonian

From a more general point of view, the quantum-well model exposed above is a two-component model such as the bilayer model, which has been used in the discussion of the

wide quantum well.¹² Indeed, the wide quantum well allows the electrons to reduce their mutual Coulomb repulsion by exploring more efficiently the z direction and it has been argued that due to this effect, a spontaneous bilayer may be formed, under appropriate conditions, in a wide quantum well.^{12,13} Here, a connection is made between both two-component models, on the basis of Hamiltonian (9). The intermediate steps in the derivation of the effective model may be found in the Appendix.

Hamiltonian (9) may be rewritten in terms of the density and spin-density operators projected to a single Landau level. The Fourier components of the projected density operator of pseudospin- σ electrons read

$$\bar{\rho}_\sigma(\mathbf{q}) = \sum_{m, m'} \langle m | e^{-i\mathbf{q}\cdot\mathbf{R}} | m' \rangle c_{m\sigma}^\dagger c_{m'\sigma},$$

in terms of the two-dimensional (2D) wave vector \mathbf{q} and the guiding-center operator \mathbf{R} , the latter acting on the states labeled by the quantum numbers m . It is furthermore useful to define the total (projected) density operator

$$\bar{\rho}(\mathbf{q}) = \bar{\rho}_\uparrow(\mathbf{q}) + \bar{\rho}_\downarrow(\mathbf{q}) \quad (11)$$

and the projected pseudospin density operators,

$$\bar{S}^\mu(\mathbf{q}) = \sum_{m, m'} \langle m | e^{-i\mathbf{q}\cdot\mathbf{R}} | m' \rangle c_{m\sigma}^\dagger \frac{\tau_{\sigma, \sigma'}^\mu}{2} c_{m'\sigma'}, \quad (12)$$

where $\tau_{\sigma, \sigma'}^\mu$ are the usual 2×2 Pauli matrices with $\mu = x, y, z$.

In terms of the projected (pseudospin) density operators, Hamiltonian (9) approximately reads as

$$H \simeq \frac{1}{2} \sum_{\mathbf{q}} V_{\text{SU}(2)}(\mathbf{q}) \bar{\rho}(-\mathbf{q}) \bar{\rho}(\mathbf{q}) + 2 \sum_{\mathbf{q}} V_{\text{sb}}^x(\mathbf{q}) \bar{S}^x(-\mathbf{q}) \bar{S}^x(\mathbf{q}) - \tilde{\Delta}_{SAS} \bar{S}^z(\mathbf{q} = 0), \quad (13)$$

where the SU(2)-symmetric interaction potential $V_{\text{SU}(2)}(\mathbf{q})$ and the symmetry-breaking potential $V_{\text{sb}}^x(\mathbf{q})$ are linear combinations of the Fourier-transformed potentials defined in Eq. (10). Their precise form is given in the Appendix by Eqs. (A2) and (A5), respectively. Hamiltonian (13) neglects a particular term $\propto \bar{S}^z(-\mathbf{q}) \bar{S}^z(\mathbf{q})$, which turns out to constitute the lowest energy scale in the interaction Hamiltonian (9) [see Eq. (A9) in the Appendix].

Furthermore,

$$\tilde{\Delta}_{SAS} = \Delta_{SAS} - \gamma \nu \frac{e^2 w}{\epsilon l_B l_B} \quad (14)$$

is the effective subband gap. The numerical prefactor γ depends on the precise nature of the considered confinement potential and, as shown in the Appendix, expression (14) is derived within a mean-field approximation of a particular term in Hamiltonian (9). Expression (14) is easy to understand; whereas the subband gap Δ_{SAS} tends to polarize the system in the \uparrow state, namely, in narrow samples, the second term in Eq. (14) indicates that the interactions are weaker in the \downarrow subband. From the interaction point of view, it is therefore energetically favorable to populate the first excited sub-

band. This effect becomes more pronounced in larger quantum wells. Notice furthermore that this argument also delimits the regime of validity of the two-subband approximation of the wide quantum well; when the term $\gamma\nu(e^2/\epsilon l_B) \times (w/l_B)$ becomes much larger than the bare subband gap Δ_{SAS} , the electrons may even populate higher subbands, which are neglected in the present model and the system eventually crosses over into a three-dimensional regime.

Notice that Hamiltonian (13) has the same form as the Hamiltonian which describes a bilayer quantum Hall system,³⁶ up to a rotation from the z to x axis. In this rotated reference frame, one may define the intralayer and interlayer interactions as

$$V_A(\mathbf{q}) = V_{SU(2)}(\mathbf{q}) + V_{sb}^x(\mathbf{q}) = \frac{1}{4}[V_{2D}^{\uparrow\uparrow\uparrow\uparrow}(\mathbf{q}) + V_{2D}^{\downarrow\downarrow\downarrow\downarrow}(\mathbf{q}) + 2V_{2D}^{\uparrow\downarrow\uparrow\downarrow}(\mathbf{q})] + V_{2D}^{\uparrow\uparrow\downarrow\downarrow}(\mathbf{q}) \quad (15)$$

and

$$V_E(\mathbf{q}) = V_{SU(2)}(\mathbf{q}) - V_{sb}^x(\mathbf{q}) = \frac{1}{4}[V_{2D}^{\uparrow\uparrow\uparrow\uparrow}(\mathbf{q}) + V_{2D}^{\downarrow\downarrow\downarrow\downarrow}(\mathbf{q}) + 2V_{2D}^{\uparrow\downarrow\uparrow\downarrow}(\mathbf{q})] - V_{2D}^{\uparrow\uparrow\downarrow\downarrow}(\mathbf{q}). \quad (16)$$

As for the case of the true bilayer, the thus defined intralayer interaction is stronger than the interlayer interaction, for all values of \mathbf{q} .

Since our ED calculations employ Hamiltonian (9), in order to compare the numerical results with the Halperin states [Eq. (5)] which are the native eigenstates of true bilayer Hamiltonian (6), we can apply the mapping between the two models described above in a reverse fashion. As Halperin wave functions are commonly labeled by the single particle states $|\uparrow\rangle$, $|\downarrow\rangle$ (which are the eigenstates of S_z) and defined by interaction potentials $\{V_A, V_E\}$, we can imagine a linear transformation (rotation from z to x) that transforms them into (unnormalized) symmetric $|+\rangle = |\uparrow\rangle + |\downarrow\rangle$ and antisymmetric $|-\rangle = |\uparrow\rangle - |\downarrow\rangle$ combinations. Then, by inverting the Eqs. (15) and (16), we obtain the set of interaction potentials that generate Halperin states (m, m', n) in a quantum-well description. In what follows, Halperin states (5) are understood to be indexed by $|+\rangle$, $|-\rangle$ instead of the usual notation $|\uparrow\rangle$, $|\downarrow\rangle$, unless explicitly stated otherwise.

C. Energetics of trial wave functions

To extend the reach of our calculations to system sizes larger than those which can be treated in ED, we set up Monte Carlo simulations of the trial states which have emerged as good candidates for the ground state. The general strategy of this approach is to obtain an estimate of the energy in the thermodynamic limit for the different trial states based on a scaling with system size of their energies.

As detailed in Sec. IV B above, we expect formation of two-component wave functions where S_x is a good quantum number, such that the Halperin wave functions are expressed in terms of the coordinates of electrons in the $|+\rangle$ and $|-\rangle$ states, and lower well, indexed below by σ . We consider

cases with equal population of electrons in these two bands or full population of the lowest subband in the ISQW for the single-component cases.

In order to calculate efficiently the interaction of electrons in a well of finite width using Monte Carlo simulations, we replace the interaction [Eq. (10)] with an effective potential that reproduces all pseudopotential coefficients of the original potential V_{2D} . Many such potentials can be constructed. Here, we use an interaction of the form proposed in Ref. 37, built from simple polynomials³⁸

$$V_{\text{eff}}^{\sigma\sigma'}(r) = \sum_{k=-1}^{N_{\text{max}}^{\sigma\sigma'}} c_k^{\sigma\sigma'} r^k. \quad (17)$$

The pseudopotentials of the monomials r^n can be evaluated analytically (generalizing Ref. 39). Choosing c_k to match the pseudopotential coefficients of the interaction [Eq. (10)] becomes a simple linear problem. Crucially, we allow for the coefficient of the Coulomb term c_{-1} to be varied, also. The number of terms is chosen equal to the minimal number required to match the relevant pseudopotentials (odd pseudopotentials V_{2m+1} for intra(pseudo)spin interactions and all $N_\phi + 1$ terms, otherwise).

It is habitual in the literature to introduce a neutralizing background, in order to highlight the correlation energy associated with a wave function. We use a background $E_{\text{bg}}[\phi]$ that matches the distribution $|\phi(z)|^2$ of electrons in their subbands, in order to study the *correlation* energy of the different states. However, to establish a final comparison between the different wave functions, a unique convention for the background is required and we adopt the background of the single layer configuration as a reference point $E_{\text{ref}} = E_{\text{bg}}[\phi_\uparrow]$.

Extrapolation to the thermodynamic limit is undertaken as two separate steps. The correlation energy is obtained by linear scaling over the inverse system size N^{-1} , using the habitual rescaling of the magnetic length $l'_B = [N/(\nu N_\phi)]^{1/2} l_B$.⁴⁰ For the two-component states, the difference in background energy $E_{\text{ref}} - \sum_\sigma E_{\text{bg}}^\sigma[\phi_{\sigma'}]$ is extrapolated separately and added to the correlation energy.

V. COMPETING PHASES IN THE QUANTUM-WELL MODEL

In order to justify the model of the quantum well, in this section we present the ED study of Hamiltonian (9) and analyze the energetics of the relevant trial wave functions in Monte Carlo simulations. We briefly revisit the problem of $\nu = 1/2$ extending the results of Refs. 12 and 14 (Sec. V A) and then present results pertaining to $\nu = 1/4$ (Sec. V B).

A. $\nu = 1/2$ in a quantum well

At this filling factor the competing phases we consider here are the (3,3,1) Halperin state, the Moore-Read Pfaffian, and the HR state. Reference 14 demonstrated a competition between the multicomponent (3,3,1) state and the fully polarized single-component Moore-Read Pfaffian. In the region of small tunneling, the ground state shows high overlap with the Halperin state; as the tunneling is increased, the Halperin

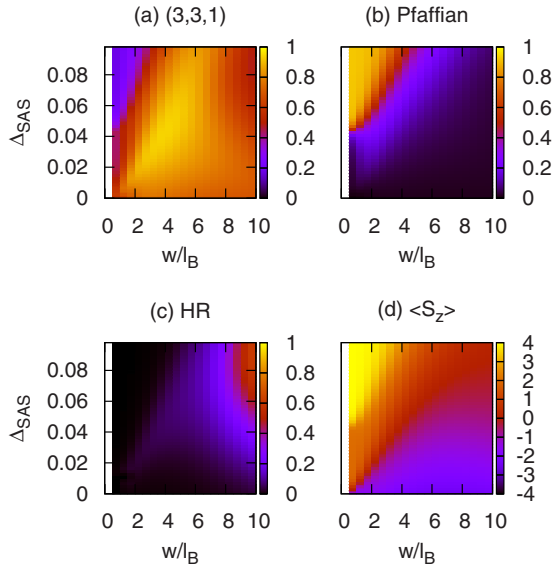


FIG. 3. (Color online) Overlap between the exact Coulomb state of the quantum well for $N=8$ particles at $\nu=1/2$ with (a) the Halperin (3,3,1) state, (b) the Pfaffian, and (c) the HR states. The expectation value of the S_z component of the pseudospin is plotted in (d).

state is destroyed and the Pfaffian takes over. The point of crossover between the two is related to the upward cusp in the activation gap.¹⁴

Figure 3 shows our ED results for eight particles in the quantum well at the filling factor $\nu=1/2$. Figures 3(a)–3(c) represent the overlap between the exact ground state and the (3,3,1), the Pfaffian, and the HR states, respectively, as a function of the well width w/l_B and the bare subband gap Δ_{SAS} . In general, the latter is a monotonically decreasing function of the well width. Again, we choose w and Δ_{SAS} as independent parameters of the model. Furthermore, we plot the quantity denoted by $\langle S_z \rangle$, the expectation value of the $S_z = \bar{S}^z(\mathbf{q}=0)$ component of the pseudospin which has the meaning of the “order parameter” [Fig. 3(d)]. One notices that $\langle S_z \rangle$ continuously crosses over from a full polarization in the \uparrow subband at low values of w/l_B and a large gap Δ_{SAS} to a polarization in the \downarrow subband for larger quantum wells and small gaps Δ_{SAS} . As it is discussed in the previous section, the interactions in a wider quantum well favor a population of the first excited electronic subband \downarrow because of the node in the wave function in the z direction and, therefore, decrease the effective subband gap. Indeed, Eq. (14) indicates that the crossover line from positive to negative $\tilde{\Delta}_{SAS}$ is characterized by a border that is linear in w/l_B . This behavior is also apparent in Fig. 3(d). Notice, however, that for large negative polarizations (large negative $\tilde{\Delta}_{SAS}$), the two-subband approximation is no longer valid and the occupation of even higher electronic subbands must be taken into account, as already mentioned in Sec. IV B.

Note, furthermore, that we have defined our (3,3,1) state to be an eigenstate of the S_x operator in the terminology of the true bilayer and not the usual S_z operator (naively defining the Halperin state to be the eigenstate of S_z does not give any appreciable overlap with the exact ground state). There

is a simple reason why this needs to be done: because the states of the quantum well possess nodal structure [Eq. (7)], the true bilayer states (like the Halperin states) need to be rotated first from the z to x direction, in order to match this symmetric/antisymmetric property, before direct comparison can be made.

With this convention, the (3,3,1) state has its largest overlap (≈ 0.95) with the exact ground state in the vicinity of the crossover line $\langle S_z \rangle = 0$. However, the overlap remains quite large even in regions beyond this line, where the polarization becomes nonzero [Fig. 3(a)], in agreement with Ref. 12. This behavior may have two different origins. First, one notices that S_z is not a good quantum number if the SU(2) symmetry-breaking terms of Hamiltonian (13) in the x direction are taken into account. Especially in the vicinity of the crossover line $\tilde{\Delta}_{SAS} \approx 0$, the symmetry breaking is governed by these terms in the x direction and $\bar{S}^x(\mathbf{q}=0)$, which does not commute with S_z , is expected to be a good quantum number. An alternative origin of the large overlap with the (3,3,1) state even in regions with $\langle S_z \rangle \neq 0$ may be a possible admixture ($\sim 5\%$) of states to the ground state that are orthogonal to the (3,3,1) and possess a finite polarization in the z direction.

The largest values of the overlap between the compressible HR state and the exact ground state are also found in the vicinity of the crossover line from positive to negative $\tilde{\Delta}_{SAS}$, though at extremely large values of w/l_B . Notice that the overlap (0.64 for $w/l_B=10.0$) is generally much lower than for the (3,3,1) state. At large values of the bare subband gap Δ_{SAS} (and narrow quantum wells), the system becomes polarized in the \uparrow subband and the ground state crosses over smoothly from the (3,3,1) state to the spin-polarized Pfaffian (overlap of ≈ 0.92). However, the increase in Δ_{SAS} , somewhat counterintuitively, does not immediately destroy the Halperin state but at first even increases the overlap.

Finally, Fig. 4 shows the results of our Monte Carlo study of the energies of the (3,3,1) and Pfaffian states. The correlation energies of both states were obtained from the finite size scaling of systems with $N=6-18$ electrons as described above in Sec. IV C. All data were obtained in Monte Carlo simulations with 10^7 samples. The uncertainty in the energy of the two-component states was obtained as the difference between linear and quadratic extrapolation of the background energies (Fig. 4), as this was larger than the bare numerical errors of the simulation. The energetic competition of these two phases qualitatively recovers the picture gained from studying the overlaps with the exact ground state. Again, some finite amount of tunneling is required for the single-component-paired state to outcompete the Halperin state. As shown in Fig. 4, the critical tunneling value Δ_{SAS}^c above which the Pfaffian state is energetically favored has a similar upturning shape as the boundary of large overlaps for the Pfaffian state in Fig. 3. However, there are some quantitative differences at small w , where the thermodynamic values indicate that polarization occurs at smaller values of the tunneling.

B. $\nu=1/4$ in a quantum well

We proceed with analyzing the quantum well at $\nu=1/4$ (Figs. 5–8). Because of the rapid increase in size of the Hil-

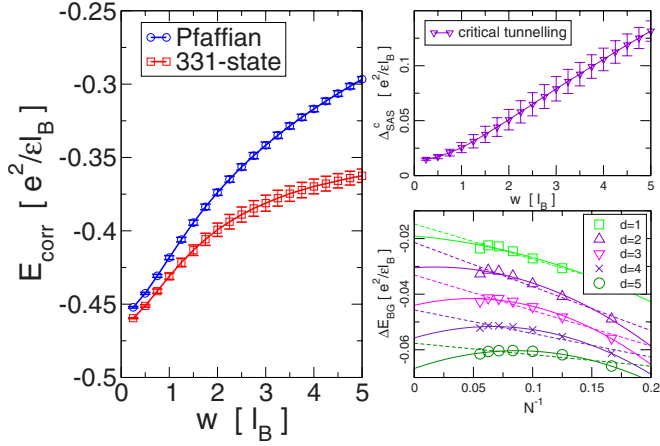


FIG. 4. (Color online) Energies in the thermodynamic limit for the (3,3,1) and Pfaffian states at $\nu=1/2$ (left). Data shown are for the infinite square well as a function of the well width w . The correlation energies are shown with respect to the single-component background. In the absence of tunneling, the (3,3,1) state has lower energy at all w . The critical tunneling strength required to favor the Pfaffian state (top right) and a few typical differences in the extrapolation of the background energies for different values of the well width (bottom right).

bert space, there are only two system sizes accessible in ED at this filling factor: $N=6$ and 8 . The dimension of the $L_z=0$ sector of the Hilbert space of the latter, taking into account discrete $L_z \rightarrow -L_z$ symmetry, is on the order of 13 million, thus making $N=6$ the only case amenable to study in great detail. However, for $N=6$ we also must keep in mind the aliasing problem that occurs for (5,5,3) and the Pfaffian (there is no such problem for the HR state). We will present results for both particle numbers because of the important

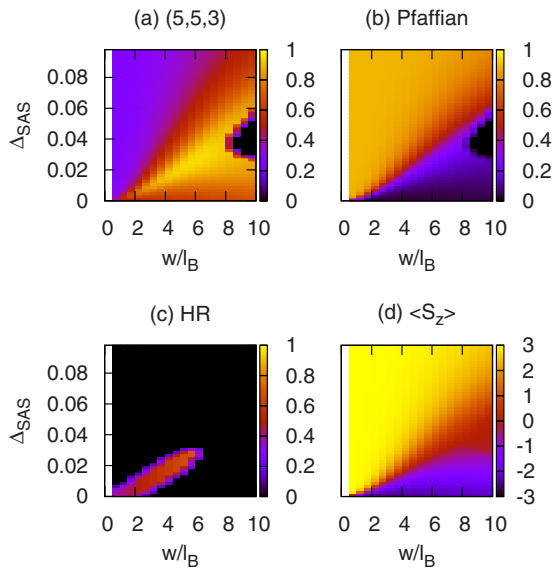


FIG. 5. (Color online) Overlap between the exact Coulomb state of the quantum well for $N=6$ particles at $\nu=1/4$ with (a) the Halperin (5,5,3) state, (b) the Pfaffian, and (c) the HR states. The expectation value of the S_z component of the pseudospin is plotted in (d).

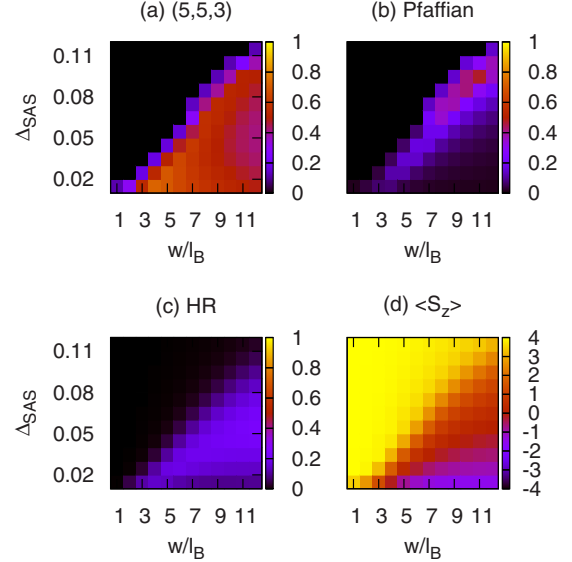


FIG. 6. (Color online) Overlap between the exact Coulomb state of the quantum well for $N=8$ particles at $\nu=1/4$ with (a) the Halperin (5,5,3) state, (b) the Pfaffian, and (c) the HR states. The expectation value of the S_z component of the pseudospin is plotted in (d).

differences between them. In view of the comments in Sec. III, we note that the overlap with the (7,7,1) state is negligible in the range of widths $w/l_B \lesssim 10.0$ and therefore we will exclude it from the present discussion of ED results. Note that, similarly to the (3,3,1) state in Sec. V A, the (5,5,3) state hereinafter is defined as an eigenstate of the S_x operator (if defined as an eigenstate of S_z , the overlap with the exact ground state is negligible).

In Fig. 5 we plot the overlap between the ground state of the quantum well for $N=6$ particles at $\nu=1/4$ and the Halperin (5,5,3) state (a), the Pfaffian (b) and the HR state (c), accompanied by the expectation value of the S_z component of the pseudospin. These results are reminiscent of $\nu=1/2$ (Fig. 3); however, due to the smaller energy scale and the

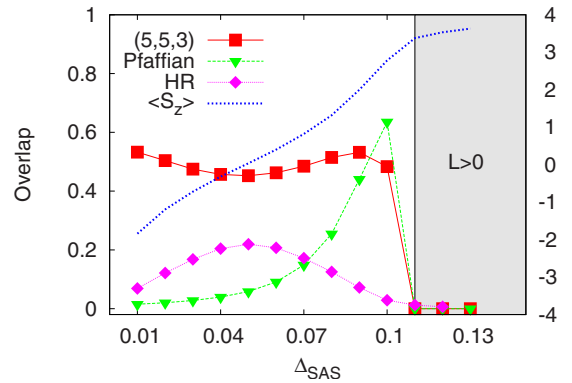


FIG. 7. (Color online) Overlap between the exact Coulomb state of the quantum well for $N=8$ particles at $\nu=1/4$ and $w/l_B=10.5$ with the Halperin (5,5,3) state, the Pfaffian, and the HR states (left axis). The expectation value of the S_z component of the pseudospin is given on the right axis. The shaded region denotes where the ground state is no longer rotationally invariant ($L > 0$).

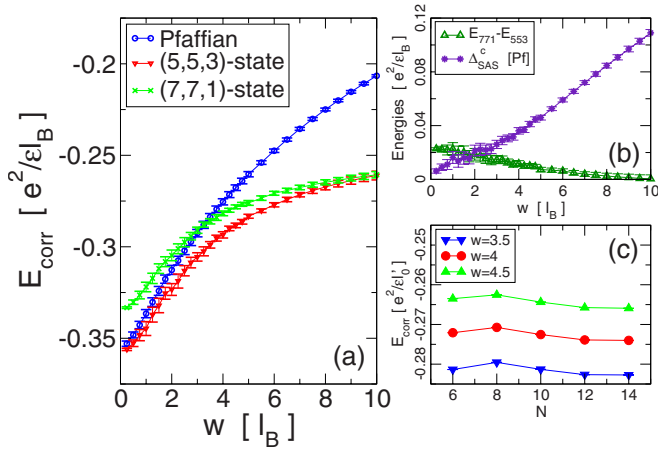


FIG. 8. (Color online) Results from our Monte Carlo study of states at $\nu=1/4$: (a) correlation energies of the Pfaffian, (5,5,3), and (7,7,1) states with respect to the single-component background, as a function of the well width w in the thermodynamic limit; (b) difference in energy between the different Halperin states and, in particular, the tunneling strength Δ_{SAS}^c for the Pfaffian state to be favored over the (5,5,3) state, and (c) correlation energies for the Pfaffian state in units of rescaled magnetic length (Ref. 40) $l_B' = [N/(\nu N \phi)]^{1/2} l_B$ for some values of w : note the particularly high value at $N=8$.

gap, it is much easier to polarize the system at $\nu=1/4$. For intermediate values of the width and small tunneling, the maximum overlap with the Halperin (5,5,3) state is high (0.96) but the region that would correspond to this phase is quite narrow in comparison to that of (3,3,1). On the other hand, the Pfaffian phase is much more extended. Given the intrinsic tunneling¹² of the samples, which is on the order of $\Delta_{SAS}/(e^2/\epsilon l_B) \lesssim 0.1$, it seems more likely that the system will be found in this phase than the (5,5,3).

The small island where the overlap abruptly goes to zero for large w/l_B is due to the ground state belonging to a sector with $L > 0$ —this can be due to the admixture of compressible physics at large widths. The HR state appears to be present in the transition region between one-component and two-component phases, its overlap steadily increasing with w and peaking at 0.7 for $w/l_B=6.0$. Because of the fact that the HR state occurs at a different shift on the sphere, we stress that the overlap presented here does not constitute a proof that it is an intermediary phase (moreover, the overlap drops rapidly when larger systems are considered, see Fig. 7).

In Fig. 6 we plot the same quantities for the system of $N=8$ particles which is expected to display weaker finite-size effects and does not suffer from the aliasing problem. The (5,5,3) state is found in a sizable parameter range but the maximum overlap is moderate compared to the case previously studied (0.74 for $w/l_B=4.5$). While the HR state generally has a small overlap (not exceeding 0.2) and the evolution of $\langle S_z \rangle$ remains smooth, the striking difference in comparison with the $N=6$ results (Fig. 5) is the Pfaffian phase. Although it similarly develops with the increase in Δ_{SAS} , once the system reaches full polarization, the phase is destroyed.

To shed more light on how this occurs, it is useful to look at the “cross section” of Fig. 6 for a fixed value of the width

$w/l_B=10.5$, chosen to represent the region where the Pfaffian phase is most clearly pronounced (Fig. 7). Although the Pfaffian overlap peaks in the region where (5,5,3) starts to drop, very abruptly both overlaps fall to zero, and the ground state is no longer rotationally invariant. The fact that $L > 0$ is a hallmark of compressibility. Precisely at the transition point, a small kink is now visible in $\langle S_z \rangle$. The origin of this kink or the reason why the ground state is obtained in $L > 0$ sector is not entirely clear at present. However, the zero overlap with the Pfaffian beyond $\Delta_{SAS}/(e^2/\epsilon l_B)=0.1$ (where the ground state reduces to a spinless case) agrees with our results of Sec. II. Notice that a compressible ground state with $L > 0$ may also indicate a phase with modulated charge density, such as the Wigner crystal. Indeed, an insulating behavior, as one would expect for an electron crystal, has been found at filling factors slightly above $\nu=1/5$.⁴¹ Such a state is not captured in the present ED calculations on the sphere and the question whether a Wigner crystal is the true ground state at large values of Δ_{SAS} in a wide quantum well is beyond the scope of the present paper.

We refer to Monte Carlo simulations (Fig. 8) to obtain additional information about the candidate incompressible states from larger model systems. We include systems with $N=6-16$ electrons in the finite size scaling for the ground-state energies, again using 10^7 Monte Carlo samples, and taking errors as the difference between linear and quadratic extrapolation of the background energies. The results of this study are summarized in Fig. 8, where we compare the Pfaffian to the (5,5,3) and (7,7,1) Halperin wave functions. Again, a two-component state is always preferred in the absence of tunneling. At the layer separations shown, this is (5,5,3) as shown in Fig. 8(a). These data also confirm that the (7,7,1) state becomes relevant only at large well width $w > 10l_B$. In Fig. 8(b), we display the value of tunneling Δ_{SAS}^c required to polarize the system into the paired Pfaffian phase. This feature of the energetic competition of (5,5,3) and the Pfaffian is very close to the results obtained in ED for $N=6$ both qualitatively and quantitatively: the shape of $\Delta_{SAS}^c(w)$ is nearly linear and reproduces the location where the overlaps with the exact ground state cross over between the two trial states, as was shown in Fig. 5. The splitting Δ_{SAS} required for the Pfaffian to be the ground state is significant and probably larger than the splitting in the experiments of Luhman *et al.*,¹⁶ which can be estimated to about $\Delta_{SAS} \approx 0.069 e^2/\epsilon l_B$ at the sample width $w \approx 10l_B$ and their baseline electron density.

This similarity between the energetics in the thermodynamic limit and the exact spectrum for $N=6$ particles may be circumstantial. However, there is another indication that the very different behavior at $N=8$ might be exceptional. In Fig. 8(c), we show the correlation energies of the Pfaffian state for different system sizes N and well widths w . This representation reveals the case of $N=8$ as having particularly high energy. This may be a finite-size effect that can be explained in the composite fermion picture. The Pfaffian wave function can be expressed as a paired state of ${}^4\text{CF}$ feeling one quantum of negative effective flux.^{22,42} The shell structure of these composite fermions on the sphere yields filled shell states for $N=6$ and 12, whereas for $N=8$ two CFs remain in the highest, partially filled shell. In this configuration, CFs

are susceptible to follow Hund's rule by maximizing their angular momentum and breaking rotational invariance.

For $N=8$ and 10 , Hund's rule predicts an angular momentum of $L=4$, which is indeed found in ED. This gives us confidence that the system is still described by liquidlike composite fermion physics at large Δ_{SAS} . We therefore consider the competition between a Hund's rule state and the paired Pfaffian state. For a similar situation with weak pairing in a $\nu=1/2+1/2$ bilayer system at large layer separation, it was argued²² that for larger systems, the shell-filling effects and Hund's rule should become less important whereas the pairing effects will remain the same strength, as only $\sim\sqrt{N}$ benefit from Hund's rule, whereas all ($\sim N$) particles within some gap energy of the Fermi surface contribute to pairing.

Although the above argument speaks in favor of the possibility for a paired Pfaffian state to be realized at $\nu=1/4$ for large tunneling gap Δ_{SAS} , we insist on the variational character of the Monte Carlo calculations. In these calculations, we have indeed considered several competing candidate wave functions for a liquid ground state at this filling factor. However, this analysis may not eliminate the possibility that a compressible state, such as that seen in ED, or even other incompressible phases may indeed be singled out as a true ground state of the system.

Finally, we would like to point out that in ED it is possible to calculate the quantity that we refer to as the "charge gap,"

$$\Delta E = E_{N,N_\phi+1} + E_{N,N_\phi-1} - 2E_{N,N_\phi}, \quad (18)$$

where E_{N,N_ϕ} is the ground-state energy for a given number of particles N and number of flux quanta N_ϕ . This quantity probes the response of the system to the introduction of quasiparticles/quasiholes on top of the ground state and its dependence on Δ_{SAS} has been used to delineate between the one-component and two-component phases.¹⁴ With the appropriate finite-size corrections, Eq. (18) should correspond to the experimentally measurable "activation" gap¹² that governs the temperature scaling of longitudinal resistance $R_{xx} \sim \exp(-\Delta E/2T)$. For states that undergo a typical one-component to two-component transition, such as the one at $\nu=2/3$ (for small tunneling, it is the state of two-decoupled Laughlin liquids, $\nu=1/3+1/3$, which develops into a single-component $2/3$ state for large tunneling amplitudes⁴³), the charge gap [Eq. (18)] displays a minimum as a function of Δ_{SAS} in the center of the transition region.¹² On the other hand, for $\nu=1/2$ where the tunneling-driven transition connects the (3,3,1) state and the Pfaffian, the charge gap [Eq. (18)] shows an upward cusp. Our calculations of the charge gap [Eq. (18)] in the case of $\nu=1/4$ indicate that this quantity is a less robust way to characterize the nature of the ground state than the calculation of the overlaps with trial wave functions. While for $N=6$ particles at $\nu=1/4$ the charge gap displays a minimum as a function of Δ_{SAS} , there is a very weak dependence of ΔE on Δ_{SAS} when a larger system of $N=8$ particles is considered. Thus finite-size effects are too strong in order to extract useful information from Eq. (18) in small systems that can be treated by ED.

VI. CONCLUSION

In this paper we have presented a systematic study of several candidates for the ground-state wave function at the recently observed¹⁶ fraction $\nu=1/4$. Assuming that the (pseudo)spin plays no role, i.e., in a one-component picture, the generalized Moore-Read Pfaffian state (1) shows high overlap for the values of the sample width which are on the order of those in the experiment of Ref. 16 but only if the confinement in the perpendicular direction is modeled by ZDS model (2). For other confinement models [Eqs. (3) and (4)] it was not possible to reproduce such high values of the overlap. We believe that this inconsistency means that the high overlap must be due to a special softening of the pseudopotentials that occurs as a pathology of ZDS model but does not appear in other (more realistic) confinement models.

Therefore, the existence of a fractional quantum Hall state at $\nu=1/4$ is necessarily linked to the specific features of the quantum well used in Ref. 16 that enable the multicomponent physics to manifest itself. Additional degrees of freedom in our theoretical study are conveniently taken into account within the quantum-well model, which is the simplest model that can naturally interpolate between a single layer and bilayer charge distribution as the parameters w and Δ_{SAS} are varied. This two-parameter model is related to the previous studies¹⁴ of the true bilayer with tunneling at $\nu=1/2$ (which had to assume at least three independent parameters) by reproducing the same physical picture of the crossover between the (3,3,1) state and the Pfaffian.

At the filling factor $\nu=1/4$, we have not been able to produce clear cut evidence for the expected crossover between the (5,5,3) state and the Pfaffian in ED due to the strong finite-size effects in case of the latter. We have shown that the (5,5,3) state is indeed present for a range of widths and small tunneling gaps Δ_{SAS} but its maximum overlap is not as high as that of the (3,3,1) state. ED cannot delimit the range of parameters for the Pfaffian phase due to the difference in the results for the two available system sizes, $N=6$ and 8 , and the effect of compressible physics which is difficult to treat within the spherical geometry. However, our Monte Carlo simulations go some way toward clarifying the situation. The correlation energies of the Pfaffian state reveal $N=8$ as a particularly unfavorable system size. We can explain this from the finite-size effect in terms of filling shells of CF orbitals on the sphere. The competing $L \neq 0$ states at $N=8$, as well as $N=10$, seem to be related to Hund's rule for CFs. However, the competition between Hund's rule and pairing is likely favorable for the paired state in the thermodynamic limit. In addition, projecting from the two-component model onto the fully polarized (spinless) case, on the other hand, can be seen as analogous to the scenario of LL mixing⁴⁴ which may provide another mechanism to stabilize the Pfaffian state via generating three-body terms in the effective interaction. Such effects are beyond the scope of the present paper. By analyzing the competition between the paired single component and the Halperin states from their variational wave functions, we find, in the Monte Carlo simulations, that the tunneling gap Δ_{SAS}^c required to form a single-component state roughly behaves linearly as 1.0

$\times (w/l_B) \times 10^{-2} e^2 / \epsilon l_B$. Although the tunneling splitting indicated for the experiment described in Ref. 16 is not far below the transition between the Pfaffian and (5,5,3), our numerics still show it safely in the two-component regime of the (5,5,3) wave function.

Although we believe that our quantum-well model takes properly into account the effects of finite thickness, we have entirely neglected the effect of the in-plane magnetic field which may nevertheless prove essential in order to stabilize the incompressible state at $\nu=1/4$. The existing experimental work⁴⁵ on the $\nu=2/3$ state witnessed that the introduction of an in-plane magnetic field may lead to a strengthening of the minimum in R_{xx} , thus inducing the same one-component to two-component transition as by varying Δ_{SAS} . Similar strengthening occurs for $\nu=1/2$ if the tilt is not too large.⁴⁵ Therefore, the application of the in-plane field may be a likely reason to further stabilize the (5,5,3) state at $\nu=1/4$ if the symmetric-antisymmetric gap Δ_{SAS} is sufficiently small. However, Ref. 16 also pointed out the difference between $\nu=1/2$ state and $\nu=1/4$ state: when the electron density is increased, the former displays a deeper minimum in R_{xx} while the latter remains largely unaffected. This difference suggests that in the case of $\nu=1/4$ the quantum-well ground state may be effectively fully polarized and in the class of the Pfaffian rather than the two-component (5,5,3) state.

In order to answer without ambiguity which of the two possibilities is actually realized in the quantum well under the experimental conditions of Ref. 16, it would be useful to know the dependence of the activation gap as a function of Δ_{SAS} and also as a function of transferred charge from the front to the back of the quantum well using a gate biasing. These results would help to discriminate between the one-component and two-component nature of the ground state.

ACKNOWLEDGMENTS

This work was funded by the Agence Nationale de la Recherche under Grant No. ANR-JCJC-0003-01. Z.P. was supported by the European Commission through Marie Curie Foundation Contract No. MEST CT 2004-51-4307 and Center of Excellence under Grant No. CX-CMCS. M.V.M. was supported by the Serbian Ministry of Science under Grant No. 141035. G.M. would like to thank Steven Simon for stimulating discussions.

APPENDIX: EFFECTIVE BILAYER DESCRIPTION OF THE WIDE QUANTUM WELL

As in Sec. IV, we consider the quantum well to be symmetric around $w/2$, i.e., the lowest subband (\uparrow) state is symmetric and the first excited one (\downarrow) is antisymmetric. Furthermore, we consider, in this section, the electrons to be in the 2D plane, for illustration reasons, although the conclusions remain valid also in the spherical geometry. In this Appendix, we yield the derivation of the effective bilayer description of the wide quantum well.

The interaction part of Hamiltonian (9) consists of a density-density interaction and terms beyond, which may be described as a spin-spin interaction. Indeed, the density-

density part consists of the effective interactions [Eq. (10)] $V_{2D}^{\uparrow\uparrow\uparrow}$, $V_{2D}^{\downarrow\downarrow\downarrow}$, and $V_{2D}^{\uparrow\downarrow\downarrow} = V_{2D}^{\downarrow\uparrow\uparrow}$. Notice that the interactions in the first excited subband (\downarrow) are generally weaker than in the lowest one (\uparrow) because the wave function [Eq. (8)] $\phi_{\downarrow}(z)$ possesses a node at $w/2$, in the center of the well, i.e., $V_{2D}^{\uparrow\uparrow\uparrow} > V_{2D}^{\downarrow\downarrow\downarrow}$. With the help of the (spin) density operators [Eqs. (11) and (12)], the density-density part of the interaction Hamiltonian reads as

$$H = \frac{1}{2} \sum_{\mathbf{q}} V_{\text{SU}(2)}(\mathbf{q}) \bar{\rho}(-\mathbf{q}) \bar{\rho}(\mathbf{q}) + 2 \sum_{\mathbf{q}} V_{\text{sb}}^z(\mathbf{q}) \bar{S}^z(-\mathbf{q}) \bar{S}^z(\mathbf{q}) + \sum_{\mathbf{q}} V_B^z(\mathbf{q}) \bar{\rho}(-\mathbf{q}) \bar{S}^z(\mathbf{q}) \quad (\text{A1})$$

in terms of the SU(2)-symmetric interaction

$$V_{\text{SU}(2)}(\mathbf{q}) = \frac{1}{4} [V_{2D}^{\uparrow\uparrow\uparrow}(\mathbf{q}) + V_{2D}^{\downarrow\downarrow\downarrow}(\mathbf{q}) + 2V_{2D}^{\uparrow\downarrow\downarrow}(\mathbf{q})] \quad (\text{A2})$$

and the SU(2)-symmetry breaking interaction terms

$$V_{\text{sb}}^z(\mathbf{q}) = \frac{1}{4} [V_{2D}^{\uparrow\uparrow\uparrow}(\mathbf{q}) + V_{2D}^{\downarrow\downarrow\downarrow}(\mathbf{q}) - 2V_{2D}^{\uparrow\downarrow\downarrow}(\mathbf{q})] \quad (\text{A3})$$

and

$$V_B^z(\mathbf{q}) = \frac{1}{2} [V_{2D}^{\uparrow\uparrow\uparrow}(\mathbf{q}) - V_{2D}^{\downarrow\downarrow\downarrow}(\mathbf{q})]. \quad (\text{A4})$$

The remaining 12 interaction terms, which may not be treated as density-density interactions, fall into two different classes; the eight terms with three equal spin orientations σ and one opposite $-\sigma$ are zero due to the antisymmetry of the integrand in Eq. (10). The remaining four interaction terms with two \uparrow spins and two \downarrow spins are all equal due to the symmetry of the quantum well around $w/2$,

$$V_{\text{sb}}^x \equiv V_{2D}^{\uparrow\uparrow\downarrow} = V_{2D}^{\downarrow\downarrow\uparrow} = V_{2D}^{\uparrow\downarrow\uparrow} = V_{2D}^{\downarrow\uparrow\downarrow}. \quad (\text{A5})$$

They yield the term

$$H_{\text{sb}}^z = 2 \sum_{\mathbf{q}} V_{\text{sb}}^x(\mathbf{q}) \bar{S}^x(-\mathbf{q}) \bar{S}^x(\mathbf{q}), \quad (\text{A6})$$

which needs to be added to the interaction Hamiltonian (A1), as well as the term

$$H_{SAS} = -\Delta_{SAS} \bar{S}^z(\mathbf{q}=0), \quad (\text{A7})$$

which accounts for the electronic subband gap between the \uparrow and the \downarrow levels.

Collecting all terms, Hamiltonian (9) thus becomes

$$H = \frac{1}{2} \sum_{\mathbf{q}} V_{\text{SU}(2)}(\mathbf{q}) \bar{\rho}(-\mathbf{q}) \bar{\rho}(\mathbf{q}) + 2 \sum_{\mathbf{q}} V_{\text{sb}}^x(\mathbf{q}) \bar{S}^x(-\mathbf{q}) \bar{S}^x(\mathbf{q}) + 2 \sum_{\mathbf{q}} V_{\text{sb}}^z(\mathbf{q}) \bar{S}^z(-\mathbf{q}) \bar{S}^z(\mathbf{q}) + \sum_{\mathbf{q}} V_B^z(\mathbf{q}) \bar{\rho}(-\mathbf{q}) \bar{S}^z(\mathbf{q}) - \Delta_{SAS} \bar{S}^z(\mathbf{q}=0). \quad (\text{A8})$$

Several comments are to be made with respect to this result. First, we have checked that for the infinite-square-well model as well as for a model with a parabolic confinement

potential there is a natural hierarchy of the energy scales in Hamiltonian (A8),

$$V_{\text{SU}(2)} > V_{\text{sb}}^x \cong V_B^z \cong V_{\text{sb}}^z. \quad (\text{A9})$$

This hierarchy is valid both for the interaction potentials in Fourier space as for the pseudopotentials.

Whereas the first term of the Hamiltonian describes the SU(2)-symmetric interaction, the second and the third one break this SU(2) symmetry. Because $V_{\text{sb}}^x(\mathbf{q}) > V_{\text{sb}}^z(\mathbf{q}) > 0$ for all values of \mathbf{q} , states with no polarization in the x and z directions are favored, with $\langle S^x \rangle = 0$ and $\langle S^z \rangle = 0$, respectively. Due to the hierarchy [Eq. (A9)] of energy scales, a depolarization in the x direction is more relevant than that in the z direction. These terms are similar to those one encounters in the case of a bilayer quantum Hall system, where due to the finite layer separation a polarization of the layer isospin in the z direction costs capacitive energy.³⁶

The fourth term of Hamiltonian (A8) is due to the stronger electron-electron repulsion in the lowest electronic subband as compared to the first excited one, where the wave function possesses a node at $z = w/2$. In order to visualize its effect, one may treat the density, which we consider to be homogeneous in an incompressible state, on the mean-field level, $\langle \bar{\rho}(\mathbf{q}) \rangle = \nu \delta_{\mathbf{q},0}$, in which case the fourth term of Eq. (A8) becomes $\nu V_B^z(\mathbf{q}=0) \bar{S}^z(\mathbf{q}=0)$ and, thus, has the same form as the subband-gap term [Eq. (A7)]. It therefore renormalizes the energy gap between the lowest and the first excited electronic subbands, and it is natural to define the effective subband gap as

$$\Delta_{\text{SAS}} \rightarrow \tilde{\Delta}_{\text{SAS}} = \Delta_{\text{SAS}} - \nu V_B^z(\mathbf{q}=0) = \Delta_{\text{SAS}} - \gamma \nu \frac{e^2 w}{\epsilon l_B l_B}, \quad (\text{A10})$$

where γ is a numerical prefactor that depends on the precise nature of the well model.

-
- ¹W. Pan, J. S. Xia, H. L. Stormer, D. C. Tsui, C. Vicente, E. D. Adams, N. S. Sullivan, L. N. Pfeiffer, K. W. Baldwin, and K. W. West, *Phys. Rev. B* **77**, 075307 (2008).
- ²R. B. Laughlin, *Phys. Rev. Lett.* **50**, 1395 (1983).
- ³J. Jain, *Composite Fermions* (Cambridge University Press, Cambridge, England, 2007).
- ⁴F. D. M. Haldane, *Phys. Rev. Lett.* **51**, 605 (1983).
- ⁵R. Willett, J. P. Eisenstein, H. L. Stormer, D. C. Tsui, A. C. Gossard, and J. H. English, *Phys. Rev. Lett.* **59**, 1776 (1987).
- ⁶F. D. M. Haldane and E. H. Rezayi, *Phys. Rev. Lett.* **60**, 956 (1988).
- ⁷G. Moore and N. Read, *Nucl. Phys. B* **360**, 362 (1991).
- ⁸N. Read and E. Rezayi, *Phys. Rev. B* **54**, 16864 (1996).
- ⁹E. H. Rezayi and F. D. M. Haldane, *Bull. Am. Phys. Soc.* **32**, 892 (1987).
- ¹⁰J. Eisenstein, in *Perspectives in Quantum Hall Effects*, edited by S. Das Sarma and A. Pinczuk (John Wiley & Sons, New York, 1997).
- ¹¹Y. W. Suen, L. W. Engel, M. B. Santos, M. Shayegan, and D. C. Tsui, *Phys. Rev. Lett.* **68**, 1379 (1992).
- ¹²Y. W. Suen, H. C. Manoharan, X. Ying, M. B. Santos, and M. Shayegan, *Phys. Rev. Lett.* **72**, 3405 (1994).
- ¹³S. He, S. Das Sarma, and X. C. Xie, *Phys. Rev. B* **47**, 4394 (1993).
- ¹⁴K. Nomura and D. Yoshioka, *J. Phys. Soc. Jpn.* **73**, 2612 (2004).
- ¹⁵B. I. Halperin, *Helv. Phys. Acta* **56**, 75 (1983).
- ¹⁶D. R. Luhman, W. Pan, D. C. Tsui, L. N. Pfeiffer, K. W. Baldwin, and K. W. West, *Phys. Rev. Lett.* **101**, 266804 (2008).
- ¹⁷F. D. M. Haldane and E. H. Rezayi, *Phys. Rev. Lett.* **54**, 237 (1985).
- ¹⁸B. A. Bernevig and F. D. M. Haldane, *Phys. Rev. Lett.* **100**, 246802 (2008).
- ¹⁹F. C. Zhang and S. Das Sarma, *Phys. Rev. B* **33**, 2903 (1986).
- ²⁰M. R. Peterson, T. Jolicoeur, and S. Das Sarma, *Phys. Rev. B* **78**, 155308 (2008).
- ²¹K. Park, V. Melik-Alaverdian, N. E. Bonesteel, and J. K. Jain, *Phys. Rev. B* **58**, R10167 (1998).
- ²²G. Möller and S. H. Simon, *Phys. Rev. B* **77**, 075319 (2008).
- ²³E. H. Rezayi and F. D. M. Haldane, *Phys. Rev. Lett.* **84**, 4685 (2000).
- ²⁴Z. Papić and M. V. Milovanović, *Phys. Rev. B* **75**, 195304 (2007).
- ²⁵G. Möller, S. H. Simon, and E. H. Rezayi, *Phys. Rev. Lett.* **101**, 176803 (2008).
- ²⁶G. Möller, S. H. Simon, and E. H. Rezayi, *Phys. Rev. B* **79**, 125106 (2009).
- ²⁷M. O. Goerbig and N. Regnault, *Phys. Rev. B* **75**, 241405(R) (2007).
- ²⁸R. de Gail, N. Regnault, and M. O. Goerbig, *Phys. Rev. B* **77**, 165310 (2008).
- ²⁹N. Regnault, M. O. Goerbig, and Th. Jolicoeur, *Phys. Rev. Lett.* **101**, 066803 (2008).
- ³⁰D. Yoshioka, A. H. MacDonald, and S. M. Girvin, *Phys. Rev. B* **39**, 1932 (1989).
- ³¹H. C. Manoharan, Y. W. Suen, T. S. Lay, M. B. Santos, and M. Shayegan, *Phys. Rev. Lett.* **79**, 2722 (1997).
- ³²E. H. Rezayi and N. Read, *Phys. Rev. Lett.* **72**, 900 (1994).
- ³³M. V. Milovanović and N. Read, *Phys. Rev. B* **53**, 13559 (1996).
- ³⁴M. Milovanović, T. Jolicoeur, and I. Vidanović, arXiv:0902.1719 (unpublished).
- ³⁵M. Abolfath, L. Belkhir, and N. Nafari, *Phys. Rev. B* **55**, 10643 (1997).
- ³⁶For a review, see K. Moon, H. Mori, K. Yang, S. M. Girvin, A. H. MacDonald, L. Zheng, D. Yoshioka, and S. C. Zhang, *Phys. Rev. B* **51**, 5138 (1995); S. M. Girvin and A. H. MacDonald, in *Perspectives in Quantum Hall Effects*, edited by S. Das Sarma and A. Pinczuk (John Wiley & Sons, New York, 1997).
- ³⁷C. Töke and J. K. Jain, *Phys. Rev. Lett.* **96**, 246805 (2006).
- ³⁸In practice, the use of the effective potential [Eq. (17)] is limited to moderately large systems with $N_\phi \lesssim 60$. For larger systems, it is more suitable to use effective potentials based explicitly on the asymptotic behavior of the in-plane interaction [Eq. (10)].

- ³⁹G. Fano, F. Ortolani, and E. Colombo, Phys. Rev. B **34**, 2670 (1986).
- ⁴⁰R. Morf, N. d'Ambrumenil, and B. I. Halperin, Phys. Rev. B **34**, 3037 (1986).
- ⁴¹H. W. Jiang, R. L. Willett, H. L. Stormer, D. C. Tsui, L. N. Pfeiffer, and K. W. West, Phys. Rev. Lett. **65**, 633 (1990); H. W. Jiang, H. L. Stormer, D. C. Tsui, L. N. Pfeiffer, and K. W. West, Phys. Rev. B **44**, 8107 (1991).
- ⁴²G. Möller and S. H. Simon, Phys. Rev. B **72**, 045344 (2005).
- ⁴³A single-component $\nu=2/3$ state can be regarded either as the particle-hole conjugate of the $\nu=1/3$ Laughlin state or as composite fermions at negative effective flux filling $p=-2$ CF LLs (Ref. 42).
- ⁴⁴C. Töke, N. Regnault, and J. K. Jain, Solid State Commun. **144**, 504 (2007).
- ⁴⁵T. S. Lay, T. Jungwirth, L. Smrčka, and M. Shayegan, Phys. Rev. B **56**, R7092 (1997).

Search | Search History

All Databases

[<< Return to Web of Science®](#)

Citing Articles Title: **Interaction-tuned compressible-to-incompressible phase transitions in quantum Hall systems**
 Author(s): Papic, Z.; Regnault, N.; Das Sarma, S.
 Source: PHYSICAL REVIEW B Volume: 80 Issue: 20 Article Number: 201303 DOI: 10.1103/PhysRevB.80.201303 Published: NOV 2009

This item has been cited by items indexed in the databases listed below. [\[more information\]](#)

18 in All Databases

- 18 publication in Web of Science
- 0 publication in BIOSIS Citation Index
- 0 publication in ScELO Citation Index
- 0 publication in Chinese Science Citation Database
- 0 data sets in Data Citation Index
- 0 publication in Data Citation Index [\[i\]](#)

Results: 18

Page 1 of 1

Sort by: Publication Date -- newest to oldest

Create Citation Report

Refine Results

Search within results for

Databases

 SCIENCE TECHNOLOGY PHYSICS Select Page Add to Marked List (0) Send to:

Title: **Typology for quantum Hall liquids**
 Author(s): Parameswaran, S. A.; Kivelson, S. A.; Rezayi, E. H.; et al.
 Source: PHYSICAL REVIEW B Volume: 85 Issue: 24 Article Number: 241307 DOI: 10.1103/PhysRevB.85.241307 Published: JUN 20 2012
 Times Cited: 3 (from All Databases)
 Get it! [\[View abstract\]](#)

Title: **Spin polarization of the $\nu=12/5$ fractional quantum Hall state**
 Author(s): Zhang, Chi; Huan, Chao; Xia, J. S.; et al.
 Source: PHYSICAL REVIEW B Volume: 85 Issue: 24 Article Number: 241302 DOI: 10.1103/PhysRevB.85.241302 Published: JUN 7 2012
 Times Cited: 2 (from All Databases)
 Get it! [\[View abstract\]](#)

Title: **Band mass anisotropy and the intrinsic metric of fractional quantum Hall systems**
 Author(s): Yang, Bo; Papic, Z.; Rezayi, E. H.; et al.
 Source: PHYSICAL REVIEW B Volume: 85 Issue: 16 Article Number: 165318 DOI: 10.1103/PhysRevB.85.165318 Published: APR 24 2012
 Times Cited: 8 (from All Databases)
 Get it! [\[View abstract\]](#)

Title: **Stability of the $k=3$ Read-Rezayi state in chiral two-dimensional systems with tunable interactions**
 Author(s): Abanin, D. A.; Papic, Z.; Barlas, Y.; et al.
 Source: NEW JOURNAL OF PHYSICS Volume: 14 Article Number: 025009 DOI: 10.1088/1367-2630/14/2/025009 Published: FEB 28 2012
 Times Cited: 1 (from All Databases)
 Get it! [\[View abstract\]](#)

Title: **Trace index and spectral flow in the entanglement spectrum of topological insulators**
 Author(s): Alexandradinata, A.; Hughes, Taylor L.; Bernevig, B. Andrei
 Source: PHYSICAL REVIEW B Volume: 84 Issue: 19 Article Number: 195103 DOI: 10.1103/PhysRevB.84.195103 Published: NOV 3 2011
 Times Cited: 3 (from All Databases)
 Get it! [\[View abstract\]](#)

Title: **Anomalous Robustness of the $\nu=5/2$ Fractional Quantum Hall State near a Sharp Phase Boundary**
 Author(s): Liu, Yang; Kamburov, D.; Shayegan, M.; et al.
 Source: PHYSICAL REVIEW LETTERS Volume: 107 Issue: 17 Article Number: 176805 DOI: 10.1103/PhysRevLett.107.176805 Published: OCT 17 2011
 Times Cited: 9 (from All Databases)
 Get it! [\[View abstract\]](#)

Title: **The hierarchical structure in the orbital entanglement spectrum of fractional quantum Hall systems**
 Author(s): Sterdyniak, A.; Bernevig, B. A.; Regnault, N.; et al.
 Source: NEW JOURNAL OF PHYSICS Volume: 13 Article Number: 105001 DOI: 10.1088/1367-2630/13/10/105001 Published: OCT 4 2011
 Times Cited: 11 (from All Databases)
 Get it! [\[View abstract\]](#)

Title: **Quantitative analysis of the disorder broadening and the intrinsic gap for the $\nu=5/2$ fractional quantum Hall state**
 Author(s): Samkharadze, N.; Watson, J. D.; Gardner, G.; et al.
 Source: PHYSICAL REVIEW B Volume: 84 Issue: 12 Article Number: 121305 DOI: 10.1103/PhysRevB.84.121305 Published: SEP 19 2011
 Times Cited: 6 (from All Databases)
 Get it! [\[View abstract\]](#)

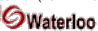

Title: **Decomposition of fractional quantum Hall model states: Product rule symmetries and approximations**
 Author(s): Thomale, Ronny; Estienne, Benoit; Regnault, Nicolas; et al.
 Source: PHYSICAL REVIEW B Volume: 84 Issue: 4 Article Number: 045127 DOI: 10.1103/PhysRevB.84.045127 Published: JUL 19 2011
 Times Cited: 15 (from All Databases)
 Get it! [\[View abstract\]](#)

Title: **Impact of Disorder on the $5/2$ Fractional Quantum Hall State**
 Author(s): Pan, W.; Masuhara, N.; Sullivan, N. S.; et al.
 Source: PHYSICAL REVIEW LETTERS Volume: 106 Issue: 20 Article Number: 206806 DOI: 10.1103/PhysRevLett.106.206806 Published: MAY 18 2011

Times Cited: 14 (from All Databases)

Get it!  [ -View abstract]

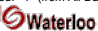

11. Title: [Particle-hole asymmetry of fractional quantum Hall states in the second Landau level of a two-dimensional hole system](#)
 Author(s): Kumar, A.; Samkharadze, N.; Csathy, G. A.; et al.
 Source: PHYSICAL REVIEW B Volume: 83 Issue: 20 Article Number: 201305 DOI: 10.1103/PhysRevB.83.201305 Published: MAY 13 2011
 Times Cited: 3 (from All Databases)

Get it!  [ -View abstract]

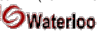

12. Title: [Nonconventional Odd-Denominator Fractional Quantum Hall States in the Second Landau Level](#)
 Author(s): Kumar, A.; Csathy, G. A.; Manfra, M. J.; et al.
 Source: PHYSICAL REVIEW LETTERS Volume: 105 Issue: 24 Article Number: 246808 DOI: 10.1103/PhysRevLett.105.246808 Published: DEC 10 2010
 Times Cited: 30 (from All Databases)

Get it!  [ -View abstract]

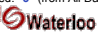

13. Title: [Fractional quantum Hall effects in bilayers in the presence of interlayer tunneling and charge imbalance](#)
 Author(s): Peterson, Michael R.; Pappic, Z.; Das Sarma, S.
 Source: PHYSICAL REVIEW B Volume: 82 Issue: 23 Article Number: 235312 DOI: 10.1103/PhysRevB.82.235312 Published: DEC 9 2010
 Times Cited: 4 (from All Databases)

Get it!  [ -View abstract]

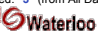

14. Title: [Correlation-Hole Induced Paired Quantum Hall States in the Lowest Landau Level](#)
 Author(s): Lu, Yuan-Ming; Yu, Yue; Wang, Ziqiang
 Source: PHYSICAL REVIEW LETTERS Volume: 105 Issue: 21 Article Number: 216801 DOI: 10.1103/PhysRevLett.105.216801 Published: NOV 17 2010
 Times Cited: 2 (from All Databases)

Get it!  [ -View abstract]



15. Title: [Subband engineering even-denominator quantum Hall states](#)
 Author(s): Scarola, V. W.; May, C.; Peterson, M. R.; et al.
 Source: PHYSICAL REVIEW B Volume: 82 Issue: 12 Article Number: 121304 DOI: 10.1103/PhysRevB.82.121304 Published: SEP 9 2010
 Times Cited: 3 (from All Databases)

Get it!  [ -View abstract]

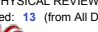
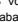
16. Title: [Tunneling-driven breakdown of the 331 state and the emergent Pfaffian and composite Fermi liquid phases](#)
 Author(s): Pappic, Z.; Goerbig, M. O.; Regnault, N.; et al.
 Source: PHYSICAL REVIEW B Volume: 82 Issue: 7 Article Number: 075302 DOI: 10.1103/PhysRevB.82.075302 Published: AUG 3 2010
 Times Cited: 3 (from All Databases)

Get it!  [ -View abstract]

17. Title: [Multiparticle interference in electronic Mach-Zehnder interferometers](#)
 Author(s): Kovrizhin, D. L.; Chalker, J. T.
 Source: PHYSICAL REVIEW B Volume: 81 Issue: 15 Article Number: 155318 DOI: 10.1103/PhysRevB.81.155318 Published: APR 15 2010
 Times Cited: 19 (from All Databases)

Get it!  [ -View abstract]

18. Title: [Quantum Hall phase diagram of half-filled bilayers in the lowest and the second orbital Landau levels: Abelian versus non-Abelian incompressible fractional quantum Hall states](#)
 Author(s): Peterson, Michael R.; Das Sarma, S.
 Source: PHYSICAL REVIEW B Volume: 81 Issue: 16 Article Number: 165304 DOI: 10.1103/PhysRevB.81.165304 Published: APR 15 2010
 Times Cited: 13 (from All Databases)

Get it!  [ -View abstract]

Select Page   Add to Marked List (0) |  |  | Send to:

Results: 18

Page 1 of 1

Sort by:

18 records matched your query of the 55,067,330 (contains duplicates) in the data limits you selected.

View in: [简体中文](#) | [繁體中文](#) | [English](#) | [日本語](#) | [한국어](#) | [Português](#) | [Español](#)

© 2013 Thomson Reuters | [Terms of Use](#) | [Privacy Policy](#) | [Please give us your feedback on using Web of Knowledge.](#)

Interaction-tuned compressible-to-incompressible phase transitions in quantum Hall systems

Z. Papić,^{1,2,3} N. Regnault,¹ and S. Das Sarma⁴

¹Laboratoire Pierre Aigrain, Ecole Normale Supérieure, CNRS, 24 rue Lhomond, F-75005 Paris, France

²Laboratoire de Physique des Solides, Université Paris-Sud, CNRS UMR 8502, F-91405 Orsay Cedex, France

³Institute of Physics, P.O. Box 68, 11 000 Belgrade, Serbia

⁴Condensed Matter Theory Center, Department of Physics, University of Maryland, College Park, Maryland 20742, USA

(Received 1 August 2009; revised manuscript received 22 September 2009; published 2 November 2009)

We analyze transitions between quantum Hall ground states at prominent filling factors ν in the spherical geometry by tuning the width parameter of the Zhang-Das Sarma interaction potential. We find that incompressible ground states evolve adiabatically under this tuning, whereas the compressible ones are driven through a first-order phase transition. Overlap calculations show that the resulting phase is increasingly well described by appropriate analytic model wave functions (Laughlin, Moore-Read, Read-Rezayi). This scenario is shared by both odd ($\nu=1/3, 1/5, 3/5, 7/3, 11/5, 13/5$) and even denominator states ($\nu=1/2, 1/4, 5/2, 9/4$). In particular, the Fermi-liquid-like state at $\nu=1/2$ gives way, at large enough value of the width parameter, to an incompressible state identified as the Moore-Read Pfaffian on the basis of its entanglement spectrum.

DOI: [10.1103/PhysRevB.80.201303](https://doi.org/10.1103/PhysRevB.80.201303)

PACS number(s): 73.43.Cd, 73.21.Fg, 71.10.Pm

We address in this work, via large-scale exact diagonalization (ED) calculations on finite spheres, the important and interesting question of how to tune various fractional quantum Hall (FQH) ground states between ungapped compressible and gapped incompressible phases by continuously varying the effective electron-electron interaction. Such numerical studies have been a standard theoretical tool in FQH physics since the beginning¹ because of the nonperturbative nature of the FQH ground states. In the current work, which is complementary to the pseudopotential description of quantum phase transitions (QPTs) in quantum Hall systems as pioneered by Morf² and Haldane,³ we report that a simple single-parameter parametrization of the effective interaction through the so-called Zhang–Das Sarma (ZDS) model⁴ provides a flexible and powerful method of studying QPTs between compressible and incompressible phases at both even and odd-denominator FQH states. We will show that ZDS interaction possesses a rich structure that can drive the FQH system from parameter regions where it appears to be compressible (manifested by the ground state that breaks rotational invariance, i.e., the value of angular momentum $L \neq 0$) toward the incompressible region where the ground state is rotationally invariant ($L=0$), along with the corresponding overlap with the trial states like Laughlin¹ or paired states (Moore-Read Pfaffian,⁵ Read-Rezayi,⁶ etc.) jumping to a value close to unity and an energy gap opening up in the excitation spectrum. In agreement with the experimental phenomenology, we find that the well-known (small) odd-denominator incompressible FQH states (e.g., $1/3$, $1/5$, $7/3$, and $11/5$) are robust and usually do not manifest any interaction-tuned QPT whereas the more fragile, even denominator (e.g., $1/2$, $1/4$, $5/2$, and $9/4$) FQH states typically exhibit characteristic QPT from a compressible to an incompressible phase as the Coulomb interaction is softened by increasing the ZDS tuning parameter.

Our calculations are performed in the spherical geometry introduced and described in detail by Haldane;³ here, we make only a few essential comments. We consider spin to be fully polarized and use the ZDS model interaction which was

originally proposed to study the finite-thickness effect of the quasi-two-dimensional (2D) layer,⁴ but in our analysis, the thickness parameter w (expressed in units of the rescaled magnetic length, l_B) enters simply as the tuning parameter for the Hamiltonian,

$$V_{\text{ZDS}}(r) = \frac{1}{\sqrt{r^2 + w^2}}. \quad (1)$$

We emphasize that ZDS interaction (1) appears to have the same qualitative pseudopotential decomposition as the realistic models (e.g., the Fang-Howard, infinite square well, etc.), as has recently been shown in details in Ref. 7. However, it was also observed in Ref. 8 that realistic confinement models do not always reproduce the QPTs induced by the ZDS interaction, suggesting there may be subtle quantitative differences between ZDS and alternative confinement models which are important in the vicinity of a QPT. In this Rapid Communication we focus on the ZDS model in carrying out our ED studies since a single parameter enables us to study FQH QPTs in a compact manner. In order to establish the connection with the experiments, we should mention that w in the ZDS model corresponds roughly to the root-mean-square fluctuation in the electron coordinate in the transverse direction.⁷

With this choice of the interaction, we use the overlap between the exact, numerically diagonalized finite system, and a candidate analytical wave function (e.g., the Laughlin or the Moore-Read wave function) to determine the tentative quantum phase of the system, i.e., if the overlap is “large” (“small”), the system is supposed to be in the candidate state (or not). We calculate the overlap as a continuous function of the varying Hamiltonian which is being tuned by w . All the model wave functions studied in this Rapid Communication are Jack polynomials that have squeezable configurations⁹ which can be efficiently generated and compared with the exact ground state. Note that each FQH state on a finite sphere at the filling factor ν is characterized, beside the num-

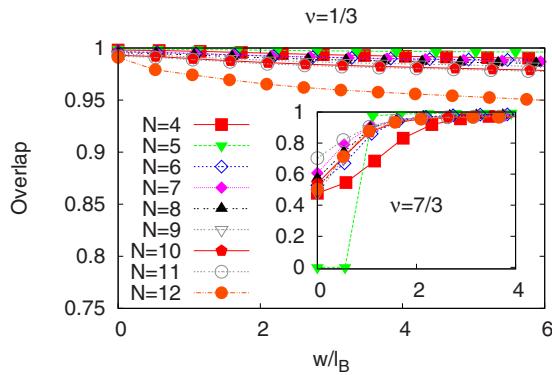


FIG. 1. (Color online) Overlap $|\langle \Psi_L | \Psi_{\text{exact}} \rangle|$ between the exact Coulomb state for finite width (ZDS model) at $\nu=1/3$ and the Laughlin wave-function $N=4-12$ particles. Inset: same quantity but in the first-excited Landau level, i.e., $\nu=7/3$.

ber of electrons N and the number of flux quanta N_ϕ , also by a topological invariant δ called shift, defined by $N_\phi = \nu^{-1}N + \delta$. In the thermodynamic limit of an infinite plane, the shift plays no role, but for a finite *sphere* it is a crucial aspect of the ED technique³ as it can lead to an “aliasing”¹⁰ problem: at a fixed choice of (N_ϕ, N) , more than one quantum Hall state (having different ν , δ and, therefore, different physical properties) may be realized. To avoid such loss of uniqueness for finite sphere ED, we disregard the aliased states from our considerations. Notwithstanding the aliasing problem, the system sizes we analyze are the largest that can be presently handled in ED studies.

We begin with the Laughlin fractions $\nu=1/3$ and $\nu=1/5$ in the lowest Landau level (LLL) and in the first-excited Landau level ($\nu=2+1/3, 2+1/5$) (Figs. 1 and 2). In agreement with previous studies,⁷ in the LLL we find that the ZDS potential leads to the monotonous decrease in the overlap with the Laughlin wave function with increasing the thickness parameter w .

In the second Landau level (SLL) and for zero thickness (Figs. 1 and 2 inset) one first notices that the Laughlin $1/5$ wave function appears to be a better candidate than the one for $1/3$. Furthermore, certain particle numbers yield zero overlap for $\nu=7/3$ (for $N=5$ particles, the ground state is

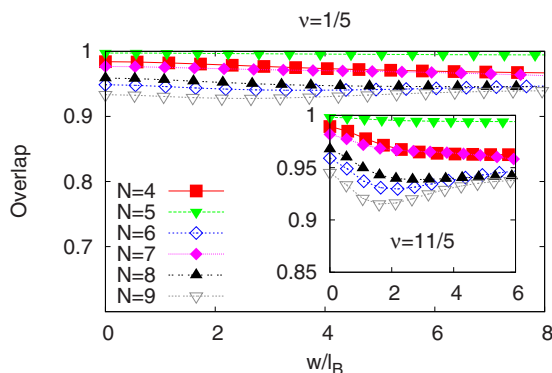


FIG. 2. (Color online) Overlap $|\langle \Psi_L | \Psi_{\text{exact}} \rangle|$ between the exact Coulomb state for finite width (ZDS model) at $\nu=1/5$ and the Laughlin wave function for $N=4-9$ particles. Inset: same quantity but in the first-excited Landau level, i.e., $\nu=11/5$.

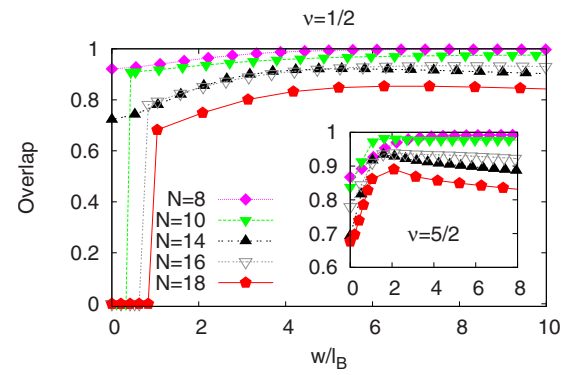


FIG. 3. (Color online) Overlap $|\langle \Psi_{\text{Pf}} | \Psi_{\text{exact}} \rangle|$ between the exact Coulomb state for finite width (ZDS model) at $\nu=1/2$ and the Pfaffian for $N=8-18$ particles. Inset: same quantity but in the first-excited Landau level, i.e., $\nu=5/2$. Only nonaliased states are shown. Note: the critical width of the QPT increases with system size; however, for the three available points and $N \rightarrow \infty$, it extrapolates to a value of $4l_B$.

obtained in $L=2$ sector; therefore, the overlap with the Laughlin wave function is zero due to the difference in symmetry). Things change once the ZDS potential is turned on: the states which are homogeneous ($L=0$) increase their overlap, while the finite-size artifact $N=5$ undergoes a QPT turning into an $L=0$ state just under $w < l_B$.

It will be shown in what follows that the induced QPT for $N=5$, $\nu=7/3$ is not an exceptional case.¹¹ Even denominator fractions, such as $\nu=5/2$ which is believed to be the Moore-Read Pfaffian⁵ or the recently discovered $\nu=1/4$,¹² and various paired states of the Read-Rezayi sequence⁶ such as $\nu=12/5, 13/5$, attract considerable attention because of their unusual ground states and the exotic spectrum of excitations that may be utilized in topological quantum computation.¹³ While their realization in the SLL seems a likely possibility, there has been little expectation to observe them in the conditions of the LLL (see however Ref. 14.). In particular, at the thin single layer $\nu=1/2$ in the LLL only the compressible, Fermi-liquid-like state has been observed. In Fig. 3 we show the overlap results of finite-size calculations on $\nu=1/2$ in the LLL and $\nu=5/2$ in the SLL with ZDS interaction.

At $\nu=1/2$ a QPT is induced by increasing the parameter w . Certain particle numbers yield good overlap already for zero thickness and their overlap will improve as w increases. Other particle numbers produce ground states with well-defined values of $L > 0$ that undergo a QPT at a critical value of the thickness. For $\nu=5/2$, the Coulomb ground state for zero thickness is already reasonably well approximated^{15,16} by the Moore-Read Pfaffian and the effect of ZDS interaction is only to increase the overlap in a smooth way. However, the increase is substantial—up to 20% for the largest system amenable to ED. This adiabatic continuity of the Moore-Read description for the SLL $\nu=5/2$ has been discussed in Ref. 16 and recently at great length by Storni *et al.*¹⁷

The nonzero values of L that appear at $\nu=1/2$ in the LLL can be fully understood from the CF theory.¹⁸ Indeed, former work hinted at the possibility of p -wave paired CF state as a

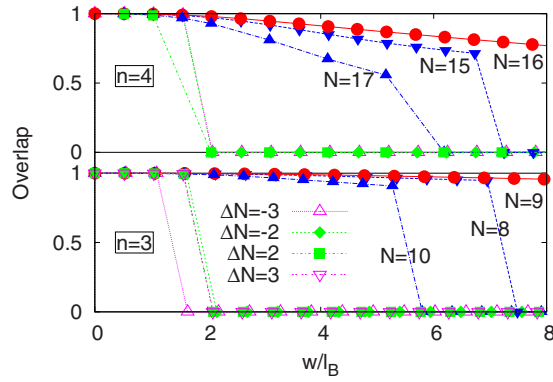


FIG. 4. (Color online) Overlap $|\langle \Psi_{\text{exact}}(w=0) | \Psi_{\text{exact}}(w) \rangle|$ between the exact Coulomb state for finite width (ZDS model) at $\nu=1/2$ and the CF sea state defined to be exact Coulomb ground state for zero thickness. Red circles represent filled CF shells ($N=n^2$, $n=3,4$), blue triangles are the lowest excited states $\Delta N=N-n^2=\pm 1$ and so on.

result of CF sea being perturbed by ZDS interaction.¹⁹ However, in Ref. 19 only the variational energies of trial states were compared. In Fig. 4 we will show that one can establish a connection between the ZDS-induced QPT and the Pfaffian and CF sea states in the LLL at $\nu=1/2$.

Because the CF sea state and the Moore-Read Pfaffian occur at different shifts on the sphere (-2 and -3 , respectively), one cannot simultaneously study their evolution with w . However, by analyzing the excitations of CF sea occurring at the Pfaffian shift, one can show (using Hund's rule) that the L values obtained in ED at the Pfaffian shift (Fig. 3) are indeed those stemming from the CF sea excitations. Moreover, assuming that the Coulomb ground state in the LLL for zero thickness is exceedingly well approximated by Rezayi-Read wave function,²⁰ we define the CF sea state for our purposes as the interacting Coulomb ground state for zero thickness and study its overlap with the $w \geq 0$ ground states (Fig. 4). CF theory tells us that (at the shift of -2) the $L=0$ configurations are obtained when the CF shells are completely filled, i.e., for $N=n^2$, $n=1,2,3,\dots$. These configurations are particularly robust and adding/subtracting electrons from them ($\Delta N=N-n^2=\pm 1, \pm 2, \dots$) creates a configuration that is destroyed at some critical value of the width which depends on how far away the system is from the filled shell. Obviously, there is ambiguity in defining precisely the critical width where the CF sea is destroyed, but this argument nonetheless provides further support for the claim that the ZDS-induced compressible-incompressible transition indeed proceeds via destruction of CF sea toward the Moore-Read Pfaffian. Transition of the same kind can be relevant for the multicomponent candidates²¹ at $\nu=3/8$. We emphasize that the possible finite-width-induced LLL $\nu=1/2$ FQH state that we find arising out of the destabilization of the CF sea, even if it exists, is likely to be extremely fragile with a neutral excitation gap smaller than $0.03e^2/\epsilon l_B$.¹⁷ However, numerically extrapolated gap is generally known to be difficult to relate to the experimental value,²² and in our data we cannot rule out the possibility that it goes to zero in thermodynamic limit.

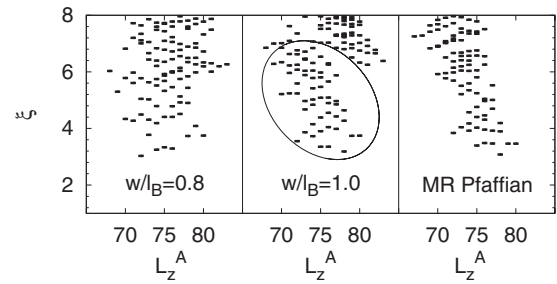


FIG. 5. Entanglement spectrum of the exact ground state for $N=18$ particles at $\nu=1/2$ in the LLL, just before ($w/l_B=0.8$) and after ($w/l_B=1.0$) the QPT, and the spectrum of Moore-Read Pfaffian for comparison. Vertical axes show the quantity $\xi=-\log \lambda_A$, where λ_A are the eigenvalues of the reduced density matrix of the subsystem A which comprises of 8 particles and 15 orbitals, given as a function of angular momentum L_z^A . Data shown is only for the partitioning denoted by $[0|0]$ in Ref. 23; other sectors give a similar result.

Another way to look at the QPT toward the Moore-Read Pfaffian is to analyze the entanglement spectrum proposed in Ref. 23. This is a powerful way to identify topological order in the given ground-state wave function and establish a direct connection with the underlying CFT that produces the given ground state as its correlator and thus offering more information than the simple overlap calculation.²⁴ In Fig. 5 we show the change in the entanglement spectrum for $N=18$ particles at $\nu=1/2$ in the LLL, before and after QPT. For $w < l_B$, there is no visible CFT branch in the entanglement spectrum—the generic Coulomb part dominates—leading to a likely compressible ground state. After the QPT, a CFT branch separates from the Coulomb part of the spectrum and the level counting begins to match the first few Virasoro levels of the Ising CFT. This is additional evidence in favor of the possibility of a finite-width-induced QPT to an incompressible half-filled single-layer LLL FQH state.

We have also examined the effect of ZDS potential on other even denominator and paired states. In the LLL, a QPT is induced for $\nu=1/4$ (Ref. 8) around $w \sim 3-5l_B$ and for Read-Rezayi $\nu=3/5$ state around $w \sim 4l_B$. In the SLL, a $\nu=9/4$ state is similarly stabilized when ZDS parameter is around $w \sim 3l_B$.

Our work establishes that the continuous tuning of the interaction through the ZDS Hamiltonian enables a direct study of FQH quantum phase transitions showing that the usual odd-denominator states are robust in both the LLL and the SLL, whereas the fragile even denominator FQH states are stable only in a regime of the interaction strength where the bare electron-electron interaction is considerably softer than the pure 2D Coulomb interaction. We find that the ZDS interaction allows for the existence of non-Abelian incompressible FQH states even at unusual even fractions such as $1/2$, $1/4$, and $9/4$, raising the intriguing possibility that such exotic non-Abelian states may indeed exist if one can sufficiently soften the interaction along the ZDS prescription. Whether this can be physically achieved in 2D semiconductor systems remains an interesting open question and may require some “reverse engineering” of the quasi-2D samples

to achieve a suitable density profile using the fact that the width parameter in the ZDS model corresponds roughly to the variance of the electron position in the transverse direction.

This work was funded by the Agence Nationale de la Recherche under Grant No. ANR-JCJC-0003-01. We also

thank KITP for support through NSF (Grant No. PHY05-51164). Z.P. was partly supported by the European Commission, through a Marie Curie Foundation contract (Contract No. MEST CT 2004-51-4307) and by the Serbian Ministry of Science under Grant No. 141035. S.D.S. is supported by a Microsoft Q Research Grant.

-
- ¹R. B. Laughlin, Phys. Rev. Lett. **50**, 1395 (1983); Phys. Rev. B **27**, 3383 (1983).
- ²R. H. Morf, Phys. Rev. Lett. **80**, 1505 (1998).
- ³F. D. M. Haldane, Phys. Rev. Lett. **51**, 605 (1983); see also *The Quantum Hall Effect*, 2nd ed., edited by R. E. Prange and S. M. Girvin (Springer-Verlag, New York, 1990).
- ⁴F. C. Zhang and S. Das Sarma, Phys. Rev. B **33**, 2903 (1986).
- ⁵G. Moore and N. Read, Nucl. Phys. B **360**, 362 (1991).
- ⁶N. Read and E. Rezayi, Phys. Rev. B **59**, 8084 (1999).
- ⁷M. R. Peterson, Th. Jolicoeur, and S. Das Sarma, Phys. Rev. B **78**, 155308 (2008); Phys. Rev. Lett. **101**, 016807 (2008).
- ⁸Z. Papić, G. Möller, M. V. Milovanović, N. Regnault, and M. O. Goerbig, Phys. Rev. B **79**, 245325 (2009).
- ⁹B. A. Bernevig and F. D. M. Haldane, Phys. Rev. Lett. **100**, 246802 (2008).
- ¹⁰N. d’Ambrumenil and R. Morf, Phys. Rev. B **40**, 6108 (1989).
- ¹¹Another example where ZDS potential “rectifies” the problem of compressibility is the supposedly interacting composite fermion (CF) state at $\nu=4/11$ where the ground state for $N=8$ electrons is compressible with $L=2$. We have verified that turning on ZDS potential in this case causes a QPT to the $L=0$ state beyond $w \sim 4l_B$.
- ¹²D. R. Luhman, W. Pan, D. C. Tsui, L. N. Pfeiffer, K. W. Baldwin, and K. W. West, Phys. Rev. Lett. **101**, 266804 (2008); J. Shabani, T. Gokmen, and M. Shayegan, *ibid.* **103**, 046805 (2009).
- ¹³C. Nayak, S. H. Simon, A. Stern, M. Freedman, and S. Das Sarma, Rev. Mod. Phys. **80**, 1083 (2008).
- ¹⁴J. Shabani, T. Gokmen, Y. Chiu, and M. Shayegan, arXiv:0909.2262 (unpublished).
- ¹⁵E. H. Rezayi and F. D. M. Haldane, Phys. Rev. Lett. **84**, 4685 (2000).
- ¹⁶G. Möller and S. H. Simon, Phys. Rev. B **77**, 075319 (2008).
- ¹⁷M. Stormi, R. Morf, and S. Das Sarma, arXiv:0812.2691 (unpublished).
- ¹⁸R. Morf and N. d’Ambrumenil, Phys. Rev. Lett. **74**, 5116 (1995).
- ¹⁹K. Park, V. Melik-Alaverdian, N. E. Bonesteel, and J. K. Jain, Phys. Rev. B **58**, R10167 (1998).
- ²⁰E. H. Rezayi and N. Read, Phys. Rev. Lett. **72**, 900 (1994).
- ²¹V. W. Scarola, J. K. Jain, and E. H. Rezayi, Phys. Rev. Lett. **88**, 216804 (2002).
- ²²R. Morf and N. d’Ambrumenil, Phys. Rev. B **68**, 113309 (2003).
- ²³H. Li and F. D. M. Haldane, Phys. Rev. Lett. **101**, 010504 (2008).
- ²⁴O. S. Zozulya, M. Haque, and N. Regnault, Phys. Rev. B **79**, 045409 (2009); N. Regnault, B. A. Bernevig, and F. D. M. Haldane, Phys. Rev. Lett. **103**, 016801 (2009).

Search Search History

All Databases

<< Return to Web of Science®

Citing Articles Title: Transition from two-component 332 Halperin state to one-component Jain state at filling factor 2/5
Author(s): Milovanovic, M. V.; Papic, Z.
Source: PHYSICAL REVIEW B Volume: 82 Issue: 3 Article Number: 035316 DOI: 10.1103/PhysRevB.82.035316 Published: JUL 27 2010

This item has been cited by items indexed in the databases listed below. [more information]

- 1 in All Databases
1 publication in Web of Science
0 publication in BIOSIS Citation Index
0 publication in SciELO Citation Index
0 publication in Chinese Science Citation Database
0 data sets in Data Citation Index
0 publication in Data Citation Index

Results: 1 Page 1 of 1 Go Sort by: Publication Date -- newest to oldest

Create Citation Report

Hide Refine

Refine Results

Search within results for

Search

Databases

Research Domains Refine

SCIENCE TECHNOLOGY

Research Areas Refine

PHYSICS

Document Types

Authors

Group/Corporate Authors

Editors

Funding Agencies

Source Titles

Conference/Meeting Titles

Publication Years

Languages

Countries/Territories

Select Page Add to Marked List (0) Send to: my.endnote.com

Title: Composite fermion states on the torus
Author(s): Hermanns, M.
Source: PHYSICAL REVIEW B Volume: 87 Issue: 23 Article Number: 235128 DOI: 10.1103/PhysRevB.87.235128 Published: JUN 21 2013
Times Cited: 0 (from All Databases)
Get it! Waterloo View abstract

Select Page Add to Marked List (0) Send to: my.endnote.com

Results: 1 Show 50 per page Page 1 of 1 Go Sort by: Publication Date -- newest to oldest

1 records matched your query of the 55,067,330 (contains duplicates) in the data limits you selected.

View in: 简体中文 繁體中文 English 日本語 한국어 Português Español

Transition from two-component 332 Halperin state to one-component Jain state at filling factor $\frac{2}{5}$

M. V. Milovanović¹ and Z. Papić^{1,2}

¹*Scientific Computing Laboratory, Institute of Physics, University of Belgrade, P.O. Box 68, 11 000 Belgrade, Serbia*

²*Laboratoire de Physique des Solides, Université Paris-Sud–CNRS, UMR 8502, F-91405 Orsay Cedex, France*

(Received 18 March 2010; revised manuscript received 27 June 2010; published 27 July 2010)

We study the transition induced by tunneling from the two-component 332 Halperin's state to the one-component Jain's state at the filling factor $\nu=2/5$. In exact diagonalizations of small systems two possibilities for the transition are found: (a) avoided level crossing, and (b) level crossing, i.e., first-order transition in the case of Coulomb interaction and short range interaction, respectively. An effective bosonic model with p -wave pairing for the transition is proposed. The relevance of the Gaffnian state for the transition is discussed as well as possible consequences of our model on the effective description of the Jain's state.

DOI: [10.1103/PhysRevB.82.035316](https://doi.org/10.1103/PhysRevB.82.035316)

PACS number(s): 73.43.Cd, 73.21.Fg, 71.10.Pm

I. INTRODUCTION

Topological phases of matter¹ find their concrete realizations in quantum Hall physics within the systems of two-dimensional (2D) electrons in high-magnetic fields. They are characterized by a gap to all excitations and by degeneracy of the ground state on higher genus surfaces. By changing a parameter of the electronic system, we may induce a quantum phase transition from one topological phase to the other. Due to their nature and discrete characterization, we expect that the system gap closes at the transition between topological phases that differ in the topological invariants, i.e., the numbers that characterize them.

The fractional quantum Hall (FQH) states can be characterized by the filling factor ν i.e. particular ratio between the density of electrons and the strength of the magnetic field at which they appear. In spin-polarized systems, a successful explanation of various FQH states at different filling factors is given by Jain's states.² On the other hand, for the same filling factors we may have states with two or more different species i.e. the Halperin states.³ Usually for a given filling factor described by the Jain's state, the corresponding Halperin state has the same vacuum degeneracy but some other characteristic numbers may differ. By applying tunneling to a two-component Halperin state we may transform this state into the one-component (spin-polarized) Jain's state. Tunneling as a perturbation that drives the transition from the two-component to a one-component FQH system was studied previously by analytical^{4,5} and numerical⁶ means.

In this paper we study the transition from Halperin's two-component 332 state to the one-component Jain state at the filling factor $\nu=2/5$ via tunneling. The interest is threefold: we would like to find out (a) about the nature of quantum phase transitions between topological phases which are similar (332 and Jain's state have the same ground state degeneracy⁷⁻⁹ but different shift^{10,11}), (b) we would like to find if Gaffnian¹² can be characterized as a critical state in these circumstances when the gap closes, and (c) we explore possible consequences for the effective description of the Jain state due to a better understanding of the transition. In Sec. II, we define the electronic system that we consider. Section III contains the results of the exact diagonalization stud-

ies of the transition. In Sec. IV, we introduce an effective bosonic model of the system and the transition induced by tunneling. Section V is devoted to conclusions.

II. SYSTEM UNDER CONSIDERATION

We consider the quantum Hall bilayer in the presence of the vector potential \mathbf{A} that describes a strong magnetic field, $B\hat{z}=\nabla\times\mathbf{A}$, perpendicular to both layers. In the rotationally symmetric gauge, the lowest Landau level (LLL) eigenstates of an electron with the coordinate $z=x+iy$ in the plane and localized in the layer $\sigma\in\{\uparrow,\downarrow\}$ are given by

$$z^m \exp\{-|z|^2/4l_B^2\} \eta_\sigma, \quad m=0, \dots, N_\phi-1, \quad (1)$$

where η_σ is the usual spinor wave function and the unit of length is given by the magnetic length, $l_B=\sqrt{\hbar c/eB}$. The number of flux quanta, N_ϕ , denotes the number of available states in the LLL. In the thermodynamic limit, the ratio of the number of electrons N_e and the number of flux quanta N_ϕ defines the filling factor $\nu=N_e/N_\phi$ and we focus on the particular case $\nu=2/5$.

The many-body interacting system of electrons is defined by the following Lagrangian density in the second quantized formulation:

$$\begin{aligned} \mathcal{L} = \sum_{\sigma} \left\{ \Psi_{\sigma}^{\dagger} \partial_{\tau} \Psi_{\sigma} - \Psi_{\sigma}^{\dagger} \frac{(\partial_{\mathbf{r}} + e\mathbf{A})^2}{2m} \Psi_{\sigma} - \Psi_{\sigma}^{\dagger} \frac{\Delta_{SAS}}{2} \Psi_{-\sigma} \right. \\ \left. + \frac{1}{2} \int d\mathbf{r}' \rho_{\sigma}(\mathbf{r}) V_c^{\text{intra}}(\mathbf{r} - \mathbf{r}') \rho_{\sigma}(\mathbf{r}') \right. \\ \left. + \frac{1}{2} \int d\mathbf{r}' \rho_{\sigma}(\mathbf{r}) V_c^{\text{inter}}(\mathbf{r} - \mathbf{r}') \rho_{-\sigma}(\mathbf{r}') \right\}, \quad (2) \end{aligned}$$

where Ψ_{σ} is the electron field which carries the pseudospin (layer) index and Δ_{SAS} denotes the tunneling term. The interaction is defined by

$$V_c^{\text{intra}}(r) = \frac{e^2}{\epsilon r} \quad (3)$$

and in general V_c^{inter} is different. When we model a quantum Hall bilayer,

$$V_c^{\text{inter}}(r) = \frac{e^2}{\epsilon\sqrt{r^2 + d^2}}, \quad (4)$$

d has the meaning of the distance between two layers of two-dimensional gases and it is of the order of l_B . In the Lagrangian density Eq. (2) and the remainder of this paper we set $\hbar=c=l_B=1$. Significant insight into the physics described by the Lagrangian Eq. (2) can be obtained using first-quantized trial wave functions for its ground states.¹³ In the remainder of this section we list several candidate wave functions that are expected to describe the ground state of Eq. (2) in different limits of Δ_{SAS} and d . Trial wave functions in the LLL are analytic in z variables and we will omit the omnipresent Gaussian factor for each electron as the one in Eq. (1).

In the small tunneling regime, the FQH system at $\nu=2/5$ is two component, described by the 332 Halperin state for two distinguishable species of electrons, $z_{i\sigma}; \sigma=\uparrow, \downarrow; i=1, \dots, N_e/2$

$$\Psi_{332} = \prod_{i<j} (z_{i\uparrow} - z_{j\uparrow})^3 \prod_{k<l} (z_{k\downarrow} - z_{l\downarrow})^3 \prod_{p,q} (z_{p\uparrow} - z_{q\downarrow})^2. \quad (5)$$

Due to the fact that the correlation exponents between electrons of the same layer are bigger than those between electrons of the opposite layers, we expect the wave function Eq. (5) to be more appropriate for non-zero d , e.g., in the range $d \sim l_B$. However, as it possesses the necessary symmetry properties,¹¹ it can be a candidate also for $d=0$. The properties of the wave function Eq. (5) were numerically verified in Ref. 14.

As the tunneling strength Δ_{SAS} is increased, the electrons find it energetically favorable to be in the superposition of two layers, $\uparrow+\downarrow$, and the system loses its two-component character. The effective single-component state is characterized by full polarization in the x -direction. At $\nu=2/5$ in the LLL, a compelling candidate for the polarized state is Jain's composite fermion (CF) state:²

$$\Psi_{\text{Jain}} = \mathcal{P}_{LLL} \left\{ \prod_{i<j} (z_i - z_j)^2 \cdot \chi_2(\{z\}) \right\}, \quad (6)$$

where \mathcal{P}_{LLL} is a projector to the LLL and χ_2 represents the Slater determinant of two filled pseudo-Landau levels of CFs.² Note that a single index suffices to label the electron coordinates as the pseudospin index is implicitly assumed to be $\uparrow+\downarrow$.

Recent work¹² has introduced an alternative candidate for the polarized state at the filling factor $\nu=2/5$, the so-called Gaffnian state:

$$\Psi_{\text{Gaff}} = \mathcal{A} \left[\Psi_{332} \text{perm} \left(\frac{1}{z_{\uparrow} - z_{\downarrow}} \right) \right]. \quad (7)$$

In the notation of Eq. (7) one can think of the Gaffnian originating from the two-component 332 state with the additional pairing represented by the permanent, a determinant with plus signs.^{15,16} The two-component state is made single-component under the action of the antisymmetrizer \mathcal{A} between \uparrow and \downarrow electron coordinates. Gaffnian Eq. (7) has generated a surge of interest because in finite size (spherical)

exact diagonalization it shows high overlaps with the Coulomb ground state, comparable to those of Jain's state, yet the topological properties of the two states are very different.¹² Moreover, the strong evidence for Gaffnian in numerical calculations is puzzling in view of the fact that it is a correlator of a nonunitary conformal field theory and, hence, not expected to describe a stable phase.¹⁷ In the spherical geometry, Jain's state and the Gaffnian can only be distinguished by their excitation spectrum¹⁸ or by using advanced tools such as the entanglement spectrum.¹⁹

Since the antisymmetrizer \mathcal{A} can, to some extent, be mimicked by the tunneling term,²⁰ and since the Gaffnian incorporates the pairing defined by the permanent, there is an additional natural candidate which we refer to as the permanent state,

$$\Psi_{\text{perm}} = \Psi_{332} \text{perm} \left\{ \frac{1}{z_{\uparrow} - z_{\downarrow}} \right\}. \quad (8)$$

This state distinguishes between \uparrow and \downarrow electrons, hence it is expected in the limit of intermediate tunneling Δ_{SAS} before a full x polarization has been achieved. Like the Gaffnian, the state Eq. (8) is related to a nonunitary conformal field theory²¹ and one may expect that it plays a role of the critical state in the transition region before full x polarization.

In the following section, we study numerically the transitions between two-component and one-component states at the filling factor $\nu=2/5$ via tunneling Δ_{SAS} . We use the exact diagonalization in the spherical and torus geometries to gain complete insight into topological properties of the different competing trial states introduced here.

III. EXACT DIAGONALIZATIONS

We consider the transition from the 332 (two-component) Halperin state to the one-component state at $\nu=2/5$ via tunneling. The one-component state is identified below as Jain's (Abelian) state Eq. (6), though it is not at the same shift on the sphere as the 332 state.^{10,11} The shift $\delta=N_e/\nu-N_\phi$ is a topological number^{1,17} and defined through a relation between N_e and N_ϕ that is necessary for the appearance of a particular FQH state on the sphere. For example, in case of the 332 state $\delta=3$, whereas for the states in Eqs. (6)–(8) $\delta=4$. This mismatch is an unfortunate feature of the spherical geometry which prevents the direct study of the transition. However, all of the mentioned states describe the filling $\nu=2/5$ and therefore occur in the same Hilbert space under the periodic boundary conditions where the shift is trivially zero.^{11,22} By that, the phases in the torus geometry do not "loose" the topological number connected with the shift on the sphere, this number that reflects the orbital spin can be characterized by the Hall viscosity of the system.¹⁷ Thus, in the torus geometry we can study the transitions in a direct manner. As we mention below, another advantage of the torus geometry is the specific ground-state degeneracy which can be used as a fingerprint of a phase. The physical results derived from the two geometries, however, ought to agree for large enough systems. Our numerical studies are restricted to a small number of electrons because the tunneling does not conserve particle number in each layer. Since, we anticipate

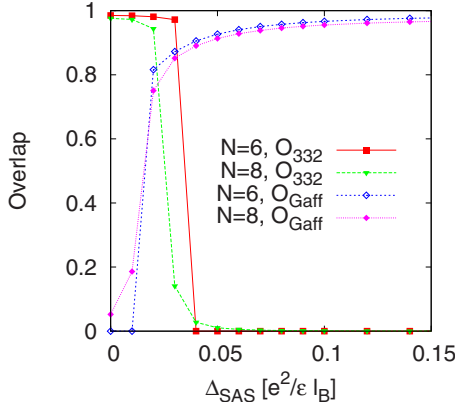


FIG. 1. (Color online) Overlaps between the exact Coulomb bilayer ground state for $d=l_B$ and the 332 (O_{332}) and Gaffnian state (O_{Gaff}), as a function of tunneling Δ_{SAS} . Data shown is for $N_e=6$ and 8 electrons. Note that O_{332} and O_{Gaff} can not be directly compared due to the difference in shift between the 332 state and the Gaffnian.

incompressible states for most of the range of Δ_{SAS} , small system sizes are nonetheless expected to be relevant as usual in the context of quantum Hall effect.¹¹

A. Sphere

In the spherical geometry, Coulomb or any interaction that depends on the distance between two electrons is parameterized by a discrete series of the so-called pseudopotentials in the LLL.¹¹ Each pseudopotential is an eigenvalue of the interaction strength corresponding to the state of definite relative angular momentum (l) of two electrons. Therefore a series of pseudopotentials $\{V_l | l=0, 1, \dots\}$ completely specifies the interaction in the LLL. Model pseudopotentials define an interaction in the LLL for which the analytic functions of some simple fractional quantum Hall states are the densest zero energy eigenstates. This is the case for the 332 state when $V^{\text{intra}}=\{0, V_1^a, 0, 0, \dots\}$ and $V^{\text{inter}}=\{V_0, V_1^b, 0, 0, \dots\}$. There is some freedom in choosing $V_0, V_1^{a,b}$ apart from the requirement that they should all be positive and we set them to unity. Values of $V_0, V_1^{a,b}$ control the gap for the 332 state and thereby affect the critical value for the tunneling Δ_{SAS} in the following discussion, but our main conclusions remain unaffected by this choice. In the case of the Jain state we do not have a pseudopotential formulation (a useful ansatz¹² that does not lead to a unique zero-energy eigenstate is $\{0, V_1, 0, 0, \dots\}$).

In Fig. 1, we present our results for the case of the bilayer Coulomb interaction on the sphere with the bilayer distance d equal to l_B . Overlaps of the exact state with the 332 state and the Gaffnian are calculated as a function of tunneling Δ_{SAS} . Separate diagonalizations have been performed because the two trial states, 332 and Gaffnian, occur in slightly different Hilbert spaces due to the mismatch in shift ($\delta=3$ and $\delta=4$, respectively). Following the rapid destruction of the 332 state with the increase of Δ_{SAS} , the overlap with the Gaffnian state rises to the high value known from earlier studies in a single-layer model.^{12,19} This occurs at the point

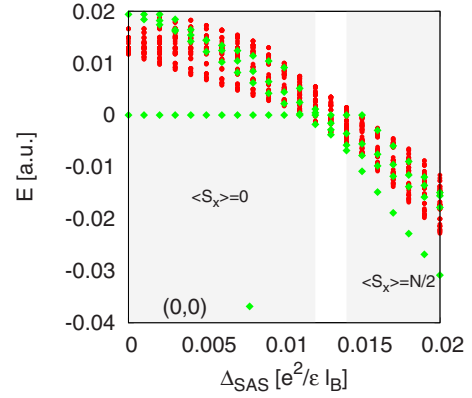


FIG. 2. (Color online) Energy spectrum of the SU(2)-symmetric 332 Hamiltonian on torus (in arbitrary units) for $N_e=8$ and aspect ratio 0.97. The $\mathbf{k}=0$ levels that cross define regions of fully polarized $\langle S_x \rangle = N/2$ and unpolarized $\langle S_x \rangle = 0$ phases.

when the system is almost fully x polarized. Consequently, the overlap with the Jain state for large Δ_{SAS} is also high and virtually indistinguishable from that of the Gaffnian on the scale of this figure.

B. Torus

In the torus geometry, Figs. 2–6, trial states which describe the same filling factor $\nu=p/q$ can be directly compared because the shift is zero. What is then characteristic of the Abelian states such as the 332 and Jain's state, is that on the torus they only possess the ground state degeneracy due to the motion of the center of mass of the system, equal to q .⁷ This is a trivial degeneracy and we will note its presence in the data. In the case of Gaffnian the degeneracy of the ground state is expected^{12,23} to be doubled with respect to the trivial one, i.e., equal to $2 \times 5 = 10$. In the literature there is no consensus that Gaffnian is a gapless state,^{12,18} but if we can establish that the nature of the lowest lying states is as expected for the Gaffnian, we could nonetheless claim its presence at the transition from the 332 to the Jain's state.

In Fig. 2, we plot the low energy spectrum of the 332 short-range Hamiltonian (Sec. III A) on the torus for N

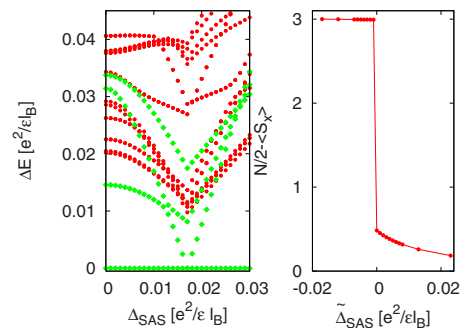


FIG. 3. (Color online) Energy spectrum relative to the ground state of the Coulomb bilayer on torus, for $N_e=6$ electrons, $d=l_B$ and aspect ratio 0.97 (left). We indicate the states characterized by $\mathbf{k}=(0,0)$ Haldane pseudomomenta. Also shown is the polarization $N/2 - \langle S_x \rangle$ as a function of tunneling around the transition point $\Delta_{\text{SAS}}^C \approx 0.017 e^2 / \epsilon l_B$ (right).

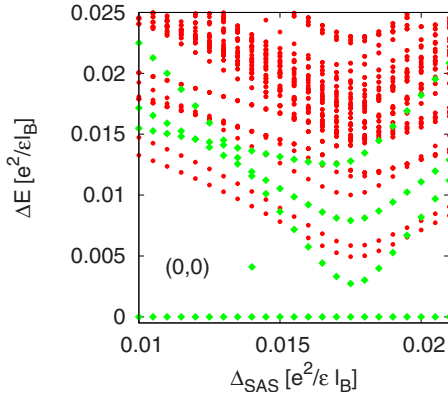


FIG. 4. (Color online) Energy spectrum relative to the ground state of the Coulomb bilayer on torus, for $N_e=8$ electrons, $d=l_B$ and aspect ratio 0.97. An approximate doublet of states with $\mathbf{k}=(0,0)$ Haldane pseudomomenta is formed around the transition point $\Delta_{SAS} \approx 0.018e^2/\epsilon l_B$.

$=8$ electrons and close to the square unit cell (aspect ratio $a/b=0.97$). We observe the 332 state, distinctly marked by its zero energy, which remains unaffected by Δ_{SAS} until level crossing is induced with the excited polarized state. We also calculate the mean value of the S_x projection of pseudo-spin which plays the role of the “order parameter” and has previously been used to detect the transition between quantum Hall phases.^{24–26} The state characterized by $\langle S_x \rangle = N/2$ that becomes the ground state for large tunneling develops into a Jain CF state, Eq. (6). This is expected because the original system defined in terms of $V_c^{intra}(r), V_c^{inter}(r)$ (3, 4), in the limit of very large tunneling becomes an effective one-component model with the modified interaction $[V_c^{intra}(r) + V_c^{inter}(r)]/2$.²⁰ For the short-range 332 Hamiltonian, this is simply a V_1 pseudopotential which yields a good approximation to Jain’s state.¹² Furthermore, as we vary the aspect ratio of the torus, we find the following thin torus configuration...01001..., which is that of the Jain state.²⁷

Coulomb interaction shows stronger finite size effects that we exemplify with the spectra for $N=6$ (Fig. 3) and 8 electrons (Fig. 4). In these calculations, we tune the aspect ratio to the same value of $a/b=0.97$ (slightly away from unity to

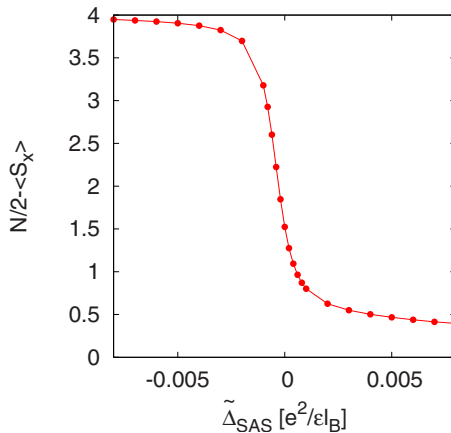


FIG. 5. (Color online) Polarization $N/2 - \langle S_x \rangle$ as a function of tunneling around the transition point for the system of Fig. 4.

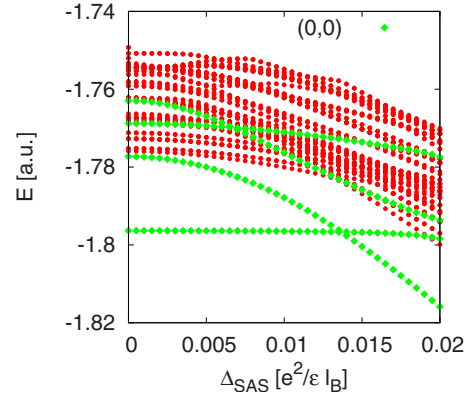


FIG. 6. (Color online) Energy spectrum of the Coulomb bilayer on torus (in arbitrary units) for $N_e=8$ and aspect ratio 0.5.

avoid accidental geometric degeneracy) and distance between layers is set to $d=l_B$. The incompressible states for small and large tunneling in Fig. 3 can be identified as the 332 and the Jain state, with the transition between them occurring for $\Delta_{SAS}^C \approx 0.017e^2/\epsilon l_B$ when the levels cross (Fig. 3, right), suggestive of the first order transition. As a consequence, the polarization (“order parameter”) $N/2 - \langle S_x \rangle$ experiences a sharp discontinuity at the point of transition (Fig. 3, left). We stress that this level crossing occurs for a wide range of aspect ratios of the torus and not only in the vicinity of the square unit cell.

On the other hand, for the larger system of $N_e=8$ electrons interacting with Coulomb interaction, we obtain the transition that proceeds via level repulsion instead of level crossing, Fig. 4. We again identify incompressible states for small and large tunneling as the 332 and the Jain state, with the transition between them occurring for $\Delta_{SAS}^C \approx 0.018e^2/\epsilon l_B$. The states can be identified, e.g., with respect to the Fig. 2 by calculating overlaps. If we denote the ground state of the short-range and Coulomb Hamiltonian for a given tunneling Δ_{SAS} as $\Psi_{short}(\Delta_{SAS})$ and $\Psi_C(\Delta_{SAS})$, respectively, we obtain the following overlap $\langle \Psi_{332} | \Psi_C(\Delta_{SAS}) \rangle \equiv \langle \Psi_{short}(\Delta_{SAS}=0) | \Psi_C(\Delta_{SAS}=0) \rangle \approx 0.95$. This means that the Coulomb bilayer ground state is nearly the same as the 332 state, assuming zero tunneling. Also, in the large tunneling limit, we obtain e.g. $\langle \Psi_{Jain} | \Psi_C(\Delta_{SAS} \rightarrow \infty) \rangle \approx \langle \Psi_{short}(\Delta_{SAS} \rightarrow \infty) | \Psi_C(\Delta_{SAS} \rightarrow \infty) \rangle \approx 0.948$, i.e. Jain’s state. The quantity which describes the density of the odd channel, $N/2 - \langle S_x \rangle$, characterizes the transition by an approximately linear or even steplike discontinuity as a function of $\tilde{\Delta}_{SAS} = \Delta_{SAS} - \Delta_{SAS}^C$, Fig. 5. In the transition region, an approximate doublet of states with $\mathbf{k}=0$ Haldane pseudomomenta is formed (Fig. 4). Although the doublet has the expected quantum numbers of the Gaffnian,²³ the specific root configurations in the thin torus limit²⁷ cannot be unambiguously identified as those of the Gaffnian. Both of the members of the doublet share the following thin torus configuration...01001..., among other spurious patterns, which is that of the Jain state. Moreover, the member of the doublet higher in energy has a lower polarization $\langle S_x \rangle$ than the ground state. These facts suggest that the excited $\mathbf{k}=0$ state in the transition region is a spinful CF state rather than the (polarized) Gaffnian.

For the long-range $N=8$ Coulomb system on the torus and the aspect ratio close to 1, the transition between the Jain and

332 state proceeds as an avoided level crossing or a smooth crossover without an obvious closing of the gap. The gap is expected to close in the thermodynamic limit between the two distinct topological phases, although we are unable to perform a proper finite-size scaling of the gap due to the inaccessibility of the $N=10$ electron system. However, for the short-range interaction that defines the 332 state as the zero-energy ground state and for the identical geometry of the torus ($a/b=0.97$), it appears that the gap indeed closes, Fig. 2. This difference between Figs. 2 and 4 can be attributed to the symmetry of the interaction. For the short range interaction used in Fig. 2, $V_1^{\text{inter}}=V_1^{\text{intra}}$, hence it does not break the SU(2) symmetry. In this case, the tunneling part of the total Hamiltonian, being proportional to S_x component, commutes with the interaction part and we expect level crossing which we indeed observe in Fig. 2. The interaction in the bilayer with $d=l_B$, on the other hand, breaks SU(2) invariance (Fig. 4), but we can nevertheless show that the level crossing persists and can be induced by changing the aspect ratio of the torus away from unity. In Fig. 6, we show one such energy spectrum (without the ground state energy subtraction) when the aspect ratio is equal to 0.5. The level crossing is induced by deforming the system towards the crystalline limit, when the Coulomb interaction is increasingly of short range. Note, however, that the states at $\Delta_{SAS}=0$ and Δ_{SAS} -large are still 332 and Jain's, respectively (verified by the overlaps with the ground state of the short-range interaction and by their thin torus limit).

IV. EFFECTIVE BOSONIC MODEL

A. Introduction

High overlaps with the Gaffnian on the sphere around and after the transition are a motivation for considering the system of Chern-Simons (CS) transformed composite bosons^{28,29} (\uparrow and \downarrow) that pair in the way of p -wave in a picture of the underlying neutral sector physics. This bosonic system is, by its very nature, unstable towards the ordinary Bose condensation, as shown for the first time in Ref. 30, and, as we will elaborate more, the pairing may be realized only in its excited states or at a transition point. As we will discuss in this Section, a simple underlying CS bosonic picture of the 332 and Jain's state will be enlarged by p -wave fluctuations. The fluctuations are expected to play a role near the transition and in the description of the critical and excited states, but not in the well-developed phases—the ground states away from the transition. As we already pointed out in the preceding section, the high Gaffnian overlaps are not to be taken as a proof that we have the Gaffnian phase after the transition, in the thermodynamic limit, but may serve as a motivation for discussing the role for the Gaffnian as a critical state. More generally, as the system is closer to the one-component limit, the theory may inherit the pairing structure built in the Gaffnian state and this is captured in the permanent state, Eq. (8). As we mentioned in Sec. II, the connection between the Gaffnian Eq. (7) and the permanent state (a p -wave state of bosons) Eq. (8) is the antisymmetrization. We assume that the operation of antisymmetrization corre-

sponds, in the language of effective theory, to a tunneling term.²⁰

B. Bosonic model

To begin with, one may perform CS transformations in the field-theoretical description of the system Eq. (2) that would leave, in the mean field, \uparrow and \downarrow bosons that pair in the way of a p -wave. At $\nu=2/5$, for no tunneling, in the presence of Coulomb or suitable short range interaction, we expect that the bilayer (two-component) system is described by 332 state. We know very well how to define the CS transformation to bosons in these circumstances, for the first time it was given in Ref. 29. It entails a transformation from electronic Ψ_σ fields [in Eq. (2) with $\Delta_{SAS}=0$] to bosonic Φ_σ fields:

$$\Psi_\sigma(\mathbf{r}) = U_\sigma(\mathbf{r})\Phi_\sigma(\mathbf{r}), \quad (9)$$

where

$$U_\sigma(\mathbf{r}) = \exp \left\{ -i \int d\mathbf{r}' \arg(\mathbf{r} - \mathbf{r}') [3\rho_\sigma(\mathbf{r}') + 2\rho_{-\sigma}(\mathbf{r}')] \right\}, \quad (10)$$

where $\arg(\mathbf{r} - \mathbf{r}')$ is the angle the vector $\mathbf{r} - \mathbf{r}'$ forms with the x axis. In the mean field (when the fluctuations of gauge fields are neglected) we, in fact, describe a system of \uparrow and \downarrow bosons that interact. Therefore, we have in the first approximation two ordinary Bose condensates. By the virtue of the Anderson-Higgs mechanism i.e. gauge fluctuations, the two Goldstone modes become gapped and the two gapped bosonic systems describe the two-component 332 system.

The complication comes when we consider the tunneling term as an extra perturbation and an extra term in our starting Hamiltonian for the electrons. The tunneling term is

$$H_T = -\lambda [\Psi_\uparrow^\dagger(\mathbf{r})\Psi_\downarrow(\mathbf{r}) + \Psi_\downarrow^\dagger(\mathbf{r})\Psi_\uparrow(\mathbf{r})], \quad (11)$$

where λ denotes the tunneling amplitude in this section. Due to the CS transformation Eq. (9) this can not be translated simply into the hopping of bosons because:

$$\Psi_\sigma^\dagger \Psi_{-\sigma} = \Phi_\sigma^\dagger U_\sigma^\dagger U_{-\sigma} \Phi_{-\sigma} \quad (12)$$

and only in the mean-field approximation for which

$$U_\sigma^\dagger U_{-\sigma} \approx I \quad (13)$$

(where I is the identity) we have a simple tunneling of bosons i.e.

$$H_T \approx -\lambda (\Phi_\uparrow^\dagger(\mathbf{r})\Phi_\downarrow(\mathbf{r}) + \text{H.c.}). \quad (14)$$

The necessary assumption in Eq. (13) is $\rho_s = \rho_\uparrow(\mathbf{r}) - \rho_\downarrow(\mathbf{r}) \approx 0$ i.e. that the fluctuations in density in \uparrow pseudospin parallel the ones in \downarrow or the fluctuations in the pseudospin density are negligible.

Treating the residual interaction in a mean field manner, i.e., taking the Hartree-Fock and BCS decomposition, we come to the following form of the Hamiltonian for the effective description of \uparrow and \downarrow bosons around the $\mathbf{k}=0$ point in the momentum space:

$$H = \sum_{\mathbf{k}} \left(\sum_{\sigma} e \hat{b}_{\mathbf{k}\sigma}^{\dagger} \hat{b}_{\mathbf{k}\sigma} - \lambda (\hat{b}_{\mathbf{k}\uparrow}^{\dagger} \hat{b}_{\mathbf{k}\downarrow} + \hat{b}_{\mathbf{k}\downarrow}^{\dagger} \hat{b}_{\mathbf{k}\uparrow}) + d \hat{b}_{\mathbf{k}\uparrow}^{\dagger} \hat{b}_{-\mathbf{k}\downarrow}^{\dagger} + c \hat{b}_{-\mathbf{k}\downarrow} \hat{b}_{\mathbf{k}\uparrow} \right), \quad (15)$$

where $e = \epsilon_{\mathbf{k}} - \mu$ and $d = c^*$ is the p -wave order parameter function $d \sim k_x - ik_y$. The question of mutual statistics (between \uparrow and \downarrow electrons and the ensuing composite bosons) may be raised but we will assume that it is bosonic.

The Bogoliubov equations, $[\alpha_{\mathbf{k}}, H] = E\alpha_{\mathbf{k}}$, where

$$\alpha_{\mathbf{k}} = u_{\uparrow} \hat{b}_{\mathbf{k}\uparrow} + u_{\downarrow} \hat{b}_{\mathbf{k}\downarrow} + v_{\uparrow} \hat{b}_{-\mathbf{k}\uparrow}^{\dagger} + v_{\downarrow} \hat{b}_{-\mathbf{k}\downarrow}^{\dagger} \quad (16)$$

define the following matrix

$$\begin{bmatrix} e & -\lambda & 0 & -c \\ -\lambda & e & c & 0 \\ 0 & -d & -e & \lambda \\ d & 0 & \lambda & -e \end{bmatrix}$$

for the eigenvalue problem. There are two pairs of eigenvalues:

$$E + \lambda, E - \lambda, \quad \text{and} \quad -E + \lambda, -E - \lambda, \quad (17)$$

where $E = \sqrt{e^2 - \Delta^2}$, $\Delta^2 = dc$, with the corresponding unnormalized eigenvectors:

$$\alpha_{\mathbf{k}}^+ = [a, -a, 1, 1], \quad \beta_{\mathbf{k}}^+ = [a, a, -1, 1], \quad \text{and} \quad (18)$$

$$\alpha_{\mathbf{k}}^- = [b, -b, 1, 1], \quad \beta_{\mathbf{k}}^- = [b, b, -1, 1], \quad (19)$$

where $a = \frac{e+E}{d}$ and $b = \frac{e-E}{d}$.

C. Bose condensate solution

The last two eigenvalues $-E \pm \lambda$ and vectors $\alpha_{\mathbf{k}}^-, \beta_{\mathbf{k}}^-$ Eq. (19) define a pair of solutions in the form of Eq. (16) and represent well-defined excitations of the system. The ground state can be expressed as

$$\exp \left\{ \sum \frac{1}{b} \hat{b}_{\mathbf{k}e}^{\dagger} \hat{b}_{-\mathbf{k}o}^{\dagger} \right\} |0\rangle, \quad (20)$$

where $\hat{b}_{\mathbf{k}e} = \hat{b}_{\mathbf{k}\uparrow} + \hat{b}_{\mathbf{k}\downarrow}$ and $\hat{b}_{\mathbf{k}o} = \hat{b}_{\mathbf{k}\uparrow} - \hat{b}_{\mathbf{k}\downarrow}$. We have for $\mu > 0$:

$$-E \pm \lambda \approx -\mu + \epsilon_{\mathbf{k}} + \frac{\Delta^2}{2\mu} \pm \lambda, \quad (21)$$

i.e., ordinary noninteracting boson description where the tunneling λ defines the transition at $\lambda = \mu$ from the two Bose condensates to a one Bose condensate (one disappears because $\mu^{\text{eff}} = \mu - \lambda < 0$ i.e. we have vacuum for these particles). The mean field ground state in the $\mathbf{k} \rightarrow 0$ limit is approximately constant ($1/b \sim d \rightarrow 0$) as it should be for the effective description of the system with (two-becoming one) Bose condensates.

This simple system in the presence of a short-ranged interaction, in the channel that changes the sign of the effective chemical potential, is described in Chapter 11.3 of Ref. 31. There $d_{\text{spatial}} = 2$ was identified as an upper critical dimension.

Therefore we might expect in that case, with an interaction, that the density of bosons in this channel for $\lambda < \lambda_c = \mu$ vanishes linearly with $\mu - \lambda = \mu^{\text{eff}}$ as $\lambda \rightarrow \lambda_c$.

The quantum Hall system as a whole, together with the CS fluctuations, may experience a transition with the Bose condensates becoming gapped via Anderson-Higgs mechanism(s) away from the transition.

This analogy also motivates to consider that a viable composite boson effective description of the $\nu = 2/5$ Jain's state is with only one composite boson condensate and a Bose vacuum. This comes as a natural consequence from our analysis and the multicomponent approach to Jain's states.¹⁶ From the results of the experiments on the edge of FQH states,³² it is justified to assume an existence of a single charge mode that stems from a single Bose condensate in an effective description.

D. Role of the permanent

The transition may be discussed considering also the other pair of eigenvalues from the eigenvalue problem:

$$E \pm \lambda \quad (22)$$

and the excitations that they define Eq. (18). It is obvious from Eq. (21) that they are unstable and may describe excited states. As particular solutions of the Bogoliubov equations for the Hamiltonian defined in Eq. (15), the solutions described by $E \pm \lambda$ and their corresponding eigenvectors Eq. (18) are nonunitary and nonphysical because they are related to the physical solutions Eq. (19) by the following nonunitary relationships: $(\alpha_{\mathbf{k}}^-)^{\dagger} = i\beta_{\mathbf{k}}^+$ and $(\beta_{\mathbf{k}}^-)^{\dagger} = -i\alpha_{\mathbf{k}}^+$ which imply: $[(\beta_{\mathbf{k}}^+)^{\dagger}, \beta_{\mathbf{k}}^+] = [(\alpha_{\mathbf{k}}^+)^{\dagger}, \alpha_{\mathbf{k}}^+] = 1$. We assume a possibility that the description of the system is given by H and an additional term²⁰ λN , i.e., $H + \lambda N$, where N is the number of particles. This term is of a purely phenomenological origin; it is designed to regularize the behavior at large λ [compare with Eq. (24)]. It can be incorporated in the previous description by a simple redefinition of $e = \epsilon_{\mathbf{k}} - \mu$ into $e = \epsilon_{\mathbf{k}} - \mu + \lambda$. This yields

$$E = \sqrt{(\epsilon_{\mathbf{k}} - \mu + \lambda)^2 - \Delta^2} = |\mu - \lambda| \sqrt{1 - \frac{(\mu - \lambda)}{(\mu - \lambda)^2} 2\epsilon_{\mathbf{k}} - \frac{\Delta^2}{(\mu - \lambda)^2}}, \quad (23)$$

and for large tunneling $\lambda > \mu$ we have

$$E \approx \lambda - \mu + \epsilon_{\mathbf{k}} - \frac{1}{2} \frac{\Delta^2}{(\lambda - \mu)}. \quad (24)$$

The excitations Eq. (22) become $E - \lambda \approx \epsilon_{\mathbf{k}} - \mu$ and $E + \lambda = \epsilon_{\mathbf{k}} + 2\lambda - \mu$, and we obtain Bose condensation in one channel and Bose vacuum in the other, as in the case of Sec. IV C. Here, for $\lambda < \mu$ we allow the possibility that by this formalism we can describe an excited state of the system which is given by the Bogoliubov expression:

$$\exp \left\{ \sum \frac{1}{a} \hat{b}_{\mathbf{k}e}^{\dagger} \hat{b}_{-\mathbf{k}o}^{\dagger} \right\} |0\rangle \quad (25)$$

and because $\frac{1}{a} = \frac{e-E}{c}$, and $\sum \frac{1}{a} \hat{b}_{\mathbf{k}e}^{\dagger} \hat{b}_{-\mathbf{k}o}^{\dagger} \sim \sum \frac{1}{a} \hat{b}_{\uparrow\mathbf{k}}^{\dagger} \hat{b}_{\downarrow-\mathbf{k}}^{\dagger}$ we have a p -wave paired permanent state in the long distance limit.

This must be an excited state because the excitations Eq. (22) are unstable for $\lambda < \mu$

$$E \approx \mu - \lambda - \epsilon_k - \frac{1}{2} \frac{\Delta^2}{(\mu - \lambda)}. \quad (26)$$

At the transition $\lambda = \mu$ we have

$$E \approx \pm i\Delta_0|k|, \quad (27)$$

where Δ_0 is defined by $\Delta^2 = \Delta_0^2 k^2$. This defines a nonunitary system with complex values for the excitations $E \pm \lambda$. If we neglect the presence of λ for a moment, we can describe this system by a 2+1 dimensional theory for bosons β and γ with the following Hamiltonian:

$$H = \gamma \partial_x \beta. \quad (28)$$

We quantize the system in the following manner:

$$\begin{aligned} \gamma &= \sum (\exp\{-ikx\}b_k + \exp\{ikx\}a_k^\dagger) \\ \beta &= \sum (-\exp\{ikx\}b_k^\dagger + \exp\{-ikx\}a_k) \end{aligned} \quad (29)$$

and this reproduces the spectrum we have for $\lambda=0$. This system is closely related to the β - γ ghost system in 1+1 dimension or the CFT connected with permanent state²¹ and more generally Gaffnian¹² in its two-component formulation Eq. (7). The complete spectrum is reproduced by $H = \gamma \partial_x \beta + \lambda(\gamma\beta)$.

Therefore before reaching the strong tunneling limit and the incompressible FQH state connected with the single BCS condensate in this description at $\nu=2/5$ (Jain's state), we may find a state at the transition that evolves from an excited state. The excited state above the 332 ground state Eq. (25) is described in the long-distance limit by a permanent times the Abelian 332 factor, Eq. (8). We note that the permanent state carries the maximum pseudospin [$S=N_e/2$, $S^2=S(S+1)$], because only such states (with also $S_z=0$) can be antisymmetrized completely in the coordinate space and make a polarized electronic wave function just as in the case of the permanent state and the ensuing Gaffnian wave function. The 332 state, on the other hand, cannot be antisymmetrized,¹⁶ because it is a spin-singlet ($S=0$). Depending on the ground state evolution, the polarization of the system ($\langle S_x \rangle$) may either experience a jump across the transition or the ground state may evolve smoothly into a ($\uparrow+\downarrow$) polarized state. The state at the transition in the second case might be Gaffnian—its description in the BCS formulation is that of a state which evolves from the permanent under the effect of tunneling which may mimic the antisymmetrization as in Eq. (7). But our analysis above (Eq. (25) with the redefined e and Eq. (27)) shows that the system at the transition is still unpolarized and cannot describe the Gaffnian.

E. Discussion

According to our numerical results in Figs. 3–5 in the presence of Coulomb interaction a possible scenario is the scenario described in the Sec. IV C with effectively one of the two Bose condensates disappearing with the increase of

tunneling. If we include interactions in the simple bosonic model they can smooth the transition (compare with results in Figs. 4 and 5). In Fig. 5, we see the linear dependence of the number of odd channel electrons on the tunneling strength near the transition. In the $\mathbf{k} \rightarrow 0$ limit the density of the odd channel is equal to the density of the vanishing Bose condensate. Therefore this linear dependence may stem from the critical behavior of dilute bosons as described in Ref. 31. $d_{\text{spatial}}=2$ is the upper critical dimension in this case and we may expect a logarithmic correction to the linear behavior as demonstrated in Ref. 33, in the case of a short range interaction among bosons. In our case Coulomb interaction may be driving the fixed point for the short range interactions into a mean field one with linear behavior. We calculated the density-density correlator in the transition region, but definite conclusion about the power of the decay of the correlations could not be drawn because of the finite size effects. A lower bound for the exponent that governs the decay with the distance is equal to 2, as expected in the mean field.

Thus the bosonic model with interactions may lead to a second-order transition with gradually disappearing bosons. In a more elaborate description one may hope that Gaffnian will appear as a polarized critical state before the polarized Jain state. But if the state at the transition is partially polarized, as we find in exact diagonalizations and effective bosonic model (without repulsive interactions), even in the Coulomb case we may expect a first-order transition or a smooth crossover without Gaffnian.

In the following, we discuss implications of our analysis for the effective bosonic description of the Jain's $\nu=2/5$ state. If, due to tunneling, one Bose condensate indeed vanishes, the effective description would then comprise only one Bose condensate and a Bose vacuum. On the other hand any effective description of quantum Hall states must encompass the edge physics as the low-energy physics of these states happens on the edge. In the effective description based on the usual picture with composite bosons¹ of the $\nu=2/5$ fractional quantum Hall edge, both charge and neutral edge modes of two condensates propagate in the same direction as relativistic particles and the discrepancy with respect to experiments,³² which detect only one (charge) mode, has to be resolved.³⁴ In the effective description based on composite fermions,³⁵ at $\nu=2/5$ edge only the charge mode is propagating, in agreement with the experiment, but the reason why the neutral mode does not propagate is not obvious. Here, we suggest an effective picture of the neutral i.e. multicomponent degrees of freedom of Jain's state at $\nu=2/5$ via a Bose vacuum. An edge excitation of the system that involves also these, multicomponent, degrees of freedom, is accompanied by a bosonic excitation of a vacuum that propagates, not relativistically, but according to Schrödinger equation,³¹ which in an effective description for certain probes can be neglected with respect to the charge wave propagation along the edge.

V. CONCLUSIONS

We studied, by numerical and analytical means, the transition from the two-component to a one-component quantum

Hall state induced by tunneling at the filling factor $\nu=2/5$. The transition is studied in the presence of the Coulomb interactions appropriate for a quantum Hall bilayer and a model short-ranged interaction appropriate for the 332 Halperin's state. In exact diagonalizations of small systems two possibilities for the transition are found: (a) avoided level crossing, and (b) level crossing, i.e., first-order transition in the case of the Coulomb interaction and short range interaction, respectively.

With respect to the appearance of the Gaffnian state in the transition region between 332 and Jain state, we can conclude that in finite systems this is only possible for the interaction that breaks SU(2) invariance, like the Coulomb bilayer interaction. It is an unlikely possibility, however, even for non-SU(2) invariant interaction, because of the difficulty in establishing the thin torus limit for the approximate $\mathbf{k}=0$ doublet found for the torus with aspect ratio close to unity (Fig. 4). In other words, on the thin torus we observe only a "half"¹² of the Gaffnian physics that corresponds to Jain's state. So long as the interaction is nearly SU(2) invariant, the

transition occurs via level crossing (Figs. 2 and 6) and it is a first-order transition between the unpolarized and polarized Abelian states.

Also, to probe the question of p -wave pairing and related Gaffnian correlations at the transition we introduced an effective bosonic model. We find that the transition in the presence of the Coulomb interaction may be viewed as a transition from two Bose condensates to a Bose condensate and a Bose vacuum. The outcome, with the Bose vacuum, can serve as an effective description of the Jain state. In the simple bosonic picture we find that the state at the transition does not correspond to the polarized Gaffnian state, in accordance with the exact diagonalizations.

ACKNOWLEDGMENTS

We thank Mark Goerbig and Nicolas Regnault for discussions. This work was supported by the Serbian Ministry of Science under Grant No. 141035.

-
- ¹X.-G. Wen, *Int. J. Mod. Phys. B* **6**, 1711 (1992).
²J. Jain, *Composite Fermions* (Cambridge University Press, Cambridge, England, 2007).
³B. I. Halperin, *Helv. Phys. Acta* **56**, 75 (1983).
⁴X.-G. Wen, *Phys. Rev. Lett.* **84**, 3950 (2000).
⁵N. Read and D. Green, *Phys. Rev. B* **61**, 10267 (2000).
⁶I. A. MacDonald and F. D. M. Haldane, *Phys. Rev. B* **53**, 15845 (1996).
⁷F. D. M. Haldane, *Phys. Rev. Lett.* **55**, 2095 (1985).
⁸X.-G. Wen and A. Zee, *Phys. Rev. B* **46**, 2290 (1992).
⁹X.-G. Wen, *Phys. Rev. B* **40**, 7387 (1989).
¹⁰X. G. Wen and A. Zee, *Phys. Rev. Lett.* **69**, 953 (1992).
¹¹F. D. M. Haldane, *Phys. Rev. Lett.* **51**, 605 (1983); See also *The Quantum Hall Effect*, 2nd ed., edited by R. E. Prange and S. M. Girvin (Springer-Verlag, New York, 1990).
¹²Steven H. Simon, E. H. Rezayi, N. R. Cooper, and I. Berdnikov, *Phys. Rev. B* **75**, 075317 (2007).
¹³R. B. Laughlin, *Phys. Rev. Lett.* **50**, 1395 (1983).
¹⁴D. Yoshioka, A. H. MacDonald, and S. M. Girvin, *Phys. Rev. B* **39**, 1932 (1989).
¹⁵D. Yoshioka, A. H. MacDonald, and S. M. Girvin, *Phys. Rev. B* **38**, 3636 (1988).
¹⁶N. Regnault, M. O. Goerbig, and Th. Jolicoeur, *Phys. Rev. Lett.* **101**, 066803 (2008).
¹⁷N. Read, *Phys. Rev. B* **79**, 045308 (2009).
¹⁸C. Tóke and J. K. Jain, *Phys. Rev. B* **80**, 205301 (2009).
¹⁹N. Regnault, B. A. Bernevig, and F. D. M. Haldane, *Phys. Rev. Lett.* **103**, 016801 (2009).
²⁰Z. Papić, M. O. Goerbig, N. Regnault, and M. V. Milovanović, [arXiv:0912.3103](https://arxiv.org/abs/0912.3103) (unpublished).
²¹N. Read and E. Rezayi, *Phys. Rev. B* **54**, 16864 (1996).
²²F. D. M. Haldane and E. H. Rezayi, *Phys. Rev. Lett.* **54**, 237 (1985).
²³E. Ardonne, *Phys. Rev. Lett.* **102**, 180401 (2009).
²⁴K. Nomura and D. Yoshioka, *Phys. Rev. B* **66**, 153310 (2002).
²⁵John Schliemann, S. M. Girvin, and A. H. MacDonald, *Phys. Rev. Lett.* **86**, 1849 (2001).
²⁶G. Möller, S. H. Simon, and E. H. Rezayi, *Phys. Rev. Lett.* **101**, 176803 (2008); *Phys. Rev. B* **79**, 125106 (2009).
²⁷E. J. Bergholtz, T. H. Hansson, M. Hermanns, A. Karlhede, and S. Viefers, *Phys. Rev. B* **77**, 165325 (2008).
²⁸S.-C. Zhang, T. H. Hansson, and S. Kivelson, *Phys. Rev. Lett.* **62**, 82 (1989); S. C. Zhang, *Int. J. Mod. Phys. B* **6**, 25 (1992).
²⁹Z. F. Ezawa and A. Iwazaki, *Phys. Rev. B* **48**, 15189 (1993).
³⁰D. Green, [arXiv:cond-mat/0202455](https://arxiv.org/abs/cond-mat/0202455).
³¹S. Sachdev, *Quantum Phase Transitions* (Cambridge University Press, Cambridge, England, 1999).
³²M. Grayson, D. C. Tsui, L. N. Pfeiffer, K. W. West, and A. M. Chang, *Phys. Rev. Lett.* **80**, 1062 (1998).
³³Subir Sachdev, T. Senthil, and R. Shankar, *Phys. Rev. B* **50**, 258 (1994).
³⁴D.-H. Lee and X.-G. Wen, [arXiv:cond-mat/9809160](https://arxiv.org/abs/cond-mat/9809160) (unpublished).
³⁵A. Lopez and E. Fradkin, *Phys. Rev. B* **59**, 15323 (1999).

Search Search History

All Databases

<< Return to Web of Science®

Citing Articles Title: Tunneling-driven breakdown of the 331 state and the emergent Pfaffian and composite Fermi liquid phases
Author(s): Papic, Z.; Goerbig, M. O.; Regnault, N.; et al.
Source: PHYSICAL REVIEW B Volume: 82 Issue: 7 Article Number: 075302 DOI: 10.1103/PhysRevB.82.075302 Published: AUG 3 2010

This item has been cited by items indexed in the databases listed below. [more information]

3 in All Databases

- 3 publication in Web of Science
0 publication in BIOSIS Citation Index
0 publication in SciELO Citation Index
0 publication in Chinese Science Citation Database
0 data sets in Data Citation Index
0 publication in Data Citation Index

Results: 3 Page 1 of 1 Go Sort by: Publication Date -- newest to oldest

Create Citation Report

Hide Refine

Refine Results

Search within results for

Search

Databases

Research Domains Refine

SCIENCE TECHNOLOGY

Research Areas Refine

PHYSICS

Document Types

Authors

Group/Corporate Authors

Editors

Funding Agencies

Source Titles

Conference/Meeting Titles

Publication Years

Languages

Countries/Territories

Select Page Add to Marked List (0) Send to: my.endnote.com

1. Title: Quasiparticles and excitons for the Pfaffian quantum Hall state
Author(s): Rodriguez, Ivan D.; Sterdyniak, A.; Hermanns, M.; et al.
Source: PHYSICAL REVIEW B Volume: 85 Issue: 3 Article Number: 035128 DOI: 10.1103/PhysRevB.85.035128 Published: JAN 30 2012
Times Cited: 6 (from All Databases)

Get it! Waterloo View abstract

2. Title: p-Wave Pairing in Quantum Hall Bilayers
Author(s): Papic, Z.; Milovanovic, M. V.
Source: ADVANCES IN CONDENSED MATTER PHYSICS Article Number: 614173 DOI: 10.1155/2011/614173 Published: 2011
Times Cited: 2 (from All Databases)

Get it! Waterloo View abstract

3. Title: Fractional quantum Hall effects in bilayers in the presence of interlayer tunneling and charge imbalance
Author(s): Peterson, Michael R.; Papic, Z.; Das Sarma, S.
Source: PHYSICAL REVIEW B Volume: 82 Issue: 23 Article Number: 235312 DOI: 10.1103/PhysRevB.82.235312 Published: DEC 9 2010
Times Cited: 4 (from All Databases)

Get it! Waterloo View abstract

Select Page Add to Marked List (0) Send to: my.endnote.com

Results: 3 Show 50 per page Page 1 of 1 Go Sort by: Publication Date -- newest to oldest

3 records matched your query of the 55,067,330 (contains duplicates) in the data limits you selected.

View in: 简体中文 繁體中文 English 日本語 한국어 Português Español

Tunneling-driven breakdown of the 331 state and the emergent Pfaffian and composite Fermi liquid phases

Z. Papić,^{1,2,3} M. O. Goerbig,² N. Regnault,³ and M. V. Milovanović¹¹Scientific Computing Laboratory, Institute of Physics, University of Belgrade, P. O. Box 68, 11 000 Belgrade, Serbia²Laboratoire de Physique des Solides, Univ. Paris-Sud, CNRS, UMR 8502, F-91405 Orsay Cedex, France³Laboratoire Pierre Aigrain, Ecole Normale Supérieure, CNRS, 24 rue Lhomond, F-75005 Paris, France

(Received 19 December 2009; revised manuscript received 11 July 2010; published 3 August 2010)

We examine the possibility of creating the Moore-Read Pfaffian in the lowest Landau level when the multicomponent Halperin 331 state (believed to describe quantum Hall bilayers and wide quantum wells at the filling factor $\nu=1/2$) is destroyed by the increase of tunneling. Using exact diagonalization of the bilayer Hamiltonian with short-range and long-range (Coulomb) interactions in spherical and periodic rectangular geometries, we establish that tunneling is a perturbation that drives the 331 state into a compressible composite Fermi liquid, with the possibility for an intermediate critical state that is reminiscent of the Moore-Read Pfaffian. These results are interpreted in the two-component BCS model for Cauchy pairing with a tunneling constraint. We comment on the conditions to be imposed on a system with fluctuating density in order to achieve the stable Pfaffian phase.

DOI: 10.1103/PhysRevB.82.075302

PACS number(s): 73.43.Cd, 73.21.Fg, 71.10.Pm

I. INTRODUCTION

When electrons are confined to a two-dimensional (2D) plane and subject to a strong perpendicular magnetic field, they organize themselves into fascinating strongly correlated quantum phases. The most prominent examples are the Laughlin states,¹ $|\Psi_L\rangle = \Phi_{2k+1}(\{z\})$, which may be written in terms of the Laughlin-Jastrow factor $\Phi_m(\{z\}) = \prod_{i<j} (z_i - z_j)^m$, where $z_j = x_j + iy_j$ denotes the complex coordinate of the j th electron, m, k are integers and we have neglected the Gaussian factor ubiquitous in the lowest Landau level (LLL). Laughlin states describe the fractional quantum Hall effect (FQHE) that occurs when the filling factor $\nu = N/N_\phi$, which is defined as the ratio between the number of electrons N and the number of flux quanta N_ϕ threading the 2D system, is a simple fraction with an odd denominator, $\nu = 1/(2k+1)$.² Laughlin's construction has been generalized, within the framework of the composite-fermion (CF) theory,³ to explain the rich phenomenology of a whole sequence of observed odd denominator fractions. According to the CF theory, one understands the FQHE as an integer quantum Hall effect in an effective magnetic field that vanishes at $\nu = 1/2$. As a consequence, CFs then form a compressible CF Fermi liquid (CFL),^{4,6} $|\Psi_{FL}\rangle = \mathcal{P}_{LLL} \det[\phi_i(z_j)] \Phi_2(\{z\})$, as seen in the absence of the Hall plateau in single thin layers at $\nu = 1/2$ in the LLL.⁵ Here, as before, the characteristic quantum Hall correlations are captured in the Jastrow factor $\Phi_2(\{z\})$ which we refer to as the *charge* part of the wave function (as it carries the flux through the system) and $\phi_i(z_j)$ are the single-particle states (an overall projection \mathcal{P}_{LLL} to the LLL may be needed to yield a proper trial wave function that is analytic in z_j).

However, some quantized *even* denominator states exist⁷ and are usually associated with the first excited Landau level, where the nature of the effective interaction is believed to facilitate the pairing between CFs.⁸ The paradigm of such paired states is the so-called "Pfaffian" state introduced by Moore and Read,⁹ $|\Psi_{Pf}\rangle = \text{Pf}[1/(z_i - z_j)] \Phi_2(\{z\})$, which explains the FQHE observed at $\nu = 5/2$.⁷ In addition to the

charge part $\Phi_2(\{z\})$, which fixes the filling factor, we have also a pairing in the *neutral* sector described by the object Pf.⁹ In contrast to the Laughlin and Jain states with anyonic excitations satisfying Abelian statistics, the Moore-Read state represents the simplest paired state of spin-polarized electrons which supports excitations with non-Abelian statistics¹⁰ of interest in topologically protected quantum computation.¹¹

If the spin of the electrons is not necessarily frozen out by the magnetic field, the electrons could find it more favorable to reorganize themselves into one of the competing Abelian phases called multicomponent Halperin states.¹² In these states the Hall quantization is a result of internal degrees of freedom of the electrons (provided by the spin or layer index). At half-filling, a two-component candidate is the 331 state, $|\Psi_{331}\rangle = \Phi_3^{\text{intra}}(\{z_\uparrow\}) \Phi_3^{\text{intra}}(\{z_\downarrow\}) \Phi_1^{\text{inter}}(\{z_\uparrow, z_\downarrow\})$, written as a straightforward generalization of the Laughlin state to two species of electrons \uparrow and \downarrow . In order to satisfy the constraint of the fixed filling factor $\nu = 1/2$, apart from the usual Laughlin-Jastrow factors between the electrons of the same species (Φ^{intra}), one also has to account for the interspecies correlations through the factor $\Phi_k^{\text{inter}}(\{z, w\}) = \prod_{i,j} (z_i - w_j)^k$. Alternatively, using the Cauchy identity¹³ we can cast the 331 state into the form $|\Psi_{331}\rangle = \det[1/(z_{i,\uparrow} - z_{j,\downarrow})] \Phi_2(\{Z\})$ which extracts the charge part Φ_2 (Z 's denote all particles regardless of their spin index) from the neutral part where the pairing is described in terms of a Cauchy determinant between \uparrow and \downarrow particles.¹⁴ Numerical calculations^{15–18} indicate that Halperin's 331 wave function is likely to be at the origin of the $\nu = 1/2$ FQHE in bilayer quantum Hall systems^{19,20} as well as in wide quantum wells.²¹

In this paper we investigate whether it is possible to create the Moore-Read Pfaffian in the LLL by converting the two-component 331 state into a single-component state. Mathematically, this is easily achieved by antisymmetrizing the neutral (Cauchy determinant) part of the $|\Psi_{331}\rangle$ between \uparrow and \downarrow .^{22,23} However, such a procedure is a very complex mathematical entity because it creates a state with different

physical properties (non-Abelian statistics out of the Abelian), while we are interested in a physical mechanism that mimics the antisymmetrization in an experimental situation. We restrict the discussion to the Coulomb bilayer system, which is a generic two-component system where the “spin” $\sigma = \uparrow, \downarrow$ denotes the two layers in which the electrons are localized. In such a system, it is commonly speculated that the antisymmetrization mechanism is provided by the tunneling term $\sim -\Delta_{SAS} S_x$, which combines the single-particle wave functions into symmetric (even) and antisymmetric (odd) superpositions, $\uparrow \pm \downarrow$. The tunneling term favors the even superposition (channel) where one expects to find a weakly paired (Moore-Read) phase. We establish that this route toward the Moore-Read state is complicated by the presence of the compressible CFL, which is the resulting phase for large tunneling. Along the way, one may arrive at a critical state that shares some properties with the Moore-Read Pfaffian, but we do not find evidence that this state represents a stable phase. Recent experiments^{24,25} found even denominator fractions in wide quantum wells in the LLL. The results obtained within the present bilayer model may be relevant also in the study of wide quantum wells insofar as the latter can, with moderate approximations, effectively be described by a bilayer Hamiltonian, where the tunneling term mimics the effective confinement gap between the lowest and the first excited electronic sublevel.¹⁷

The remainder of this paper is organized as follows. In Sec. II we introduce the BCS model for spinful fermions with tunneling, first proposed by Read and Green.²⁶ This model decouples into an even and odd channel, and the tunneling term increases the population of the even channel, where one expects to find the weak pairing (Pfaffian) phase. However, the increase of tunneling also leads to the effective weakening of the coupling, which eventually drives the system into a CFL phase when the total number of particles is held fixed. This is the situation we analyze in detail in our exact-diagonalization calculations in spherical and toroidal geometries (Sec. III). These results are discussed in the context of the phase diagram of Ref. 26 (see Sec. III C). We furthermore introduce a generalized tunneling constraint which, in the BCS description, leads to a stable weak pairing (Pfaffian) phase in the even channel when the density of the of the system is not fixed (Sec. IV). We present our conclusions in Sec. V.

II. BCS MODEL WITH TUNNELING

At $\nu = 1/2$, the CFs experience a zero net magnetic field,⁵ and if we limit ourselves to the neutral part of $|\Psi_{Pf}\rangle$, they may be described within the framework of the effective BCS model introduced in Ref. 26. We consider the system to be at zero temperature and neglect fluctuations in the Chern-Simons gauge field that are related to the charge part of $|\Psi_{Pf}\rangle$.²⁷ The Hamiltonian which describes the Cauchy pairing between \uparrow and \downarrow particles with tunneling Δ_{SAS} reads

$$H = \sum_{\mathbf{k}} \left[\tilde{\epsilon}_{\mathbf{k}} (c_{\mathbf{k}\uparrow}^\dagger c_{\mathbf{k}\uparrow} + c_{\mathbf{k}\downarrow}^\dagger c_{\mathbf{k}\downarrow}) + (\Delta_{\mathbf{k}} c_{\mathbf{k}\uparrow}^\dagger c_{-\mathbf{k}\downarrow}^\dagger + \text{H.c.}) - \frac{\Delta_{SAS}}{2} (c_{\mathbf{k}\uparrow}^\dagger c_{\mathbf{k}\downarrow} + c_{\mathbf{k}\downarrow}^\dagger c_{\mathbf{k}\uparrow}) \right], \quad (1)$$

where $\tilde{\epsilon}_{\mathbf{k}} = \epsilon_{\mathbf{k}} - \mu$, in terms of the putative CF dispersion re-

lation $\epsilon_{\mathbf{k}}$ and the chemical potential μ , which is assumed positive $\mu > 0$. Notice that because of the vanishing net magnetic field, the 2D wave vector $\mathbf{k} = (k_x, k_y)$ is again a good quantum number. The order parameter $\Delta_{\mathbf{k}} = \Delta_0(k_x - ik_y)$ is chosen to describe p -wave pairing, and we assume that $\Delta_{\mathbf{k}}$ and μ are not renormalized by the tunneling.

With the help of the even, $c_{\mathbf{k},e} = (c_{\mathbf{k},\uparrow} + c_{\mathbf{k},\downarrow})/\sqrt{2}$, and odd spin combinations $c_{\mathbf{k},o} = (c_{\mathbf{k},\uparrow} - c_{\mathbf{k},\downarrow})/\sqrt{2}$, the Hamiltonian (1) decouples into an even and odd channel,²⁶ $H = H^e + H^o$, where (the index τ denotes the even and odd channel, $\tau = e, o$)

$$H^\tau = \sum_{\mathbf{k}} [(\epsilon_{\mathbf{k}} - \mu^\tau) c_{\mathbf{k},\tau}^\dagger c_{\mathbf{k},\tau} + (\Delta_{\mathbf{k}}^\tau c_{\mathbf{k},\tau}^\dagger c_{-\mathbf{k},\tau}^\dagger + \text{H.c.})], \quad (2)$$

in terms of the chemical potentials $\mu^e = \mu + \Delta_{SAS}/2$ and $\mu^o = \mu - \Delta_{SAS}/2$ for the even and odd channels, respectively. Furthermore, the even/odd p -wave order parameters read $\Delta_{\mathbf{k}}^e = \Delta_{\mathbf{k}}/2 = (\Delta_0/2)(k_x - ik_y)$ and $\Delta_{\mathbf{k}}^o = -\Delta_{\mathbf{k}}/2 = -(\Delta_0/2)(k_x - ik_y)$.

For moderate tunnelings, the effective chemical potential μ^{eff} of the whole system may be viewed as the weighted sum of the two channels, $\mu^{\text{eff}} = P\mu^e + (1-P)\mu^o$, where P measures the population of the even channel ($1/2 \leq P \leq 1$) and may have a complicated dependence on Δ_{SAS} . In particular, for some values of Δ_{SAS} we may be below the critical line $\mu^{\text{eff}} = P\Delta_{SAS}$ and inside the non-Abelian (Pfaffian) phase. However, in the limit of large tunneling, the system is dominated by the even channel and the chemical potential of the whole system is $\mu^{\text{eff}} = \mu^e$ because $P = 1$. Remember that the associated BCS wave function in the even channel reads

$$|\psi_{BCS}\rangle = \prod_{\mathbf{k}} (1 + g_{\mathbf{k}} c_{\mathbf{k},e}^\dagger c_{-\mathbf{k},e}^\dagger) |\text{vacuum}\rangle, \quad (3)$$

in terms of the pairing function $g_{\mathbf{k}} \sim v_{\mathbf{k}}/u_{\mathbf{k}} \sim \mu^e/\Delta_0$. One notices then that an increase of the chemical potential μ^e controlled by the large value of the tunneling parameter Δ_{SAS} is equivalent to a reduction of the order parameter Δ_0 . Therefore the BCS system will eventually be transformed into the one of the Fermi liquid. We can see this more explicitly by examining the relevant excitations of the even channel,²⁶

$$E = \sqrt{(\epsilon_{\mathbf{k}} - \mu^e)^2 + \Delta_0^2 k^2}, \quad (4)$$

in the limit of large μ^e around $k = |\mathbf{k}| = 0$. They become unstable and $\mathbf{k} = 0$ becomes a point of local maximum. The minimum is expected to move to $|\mathbf{k}| = k_F$, the Fermi momentum.²⁶ Therefore if Δ_0 does not “renormalize” with increasing Δ_{SAS} , the net effect of the strong tunneling ($\mu^e \gg \mu$) on the Cauchy pairing is to drive the system into a Fermi liquid. This is not unexpected because one retrieves an effective one-component system in this limit, where all particles are “polarized” in the even channel. The Pfaffian physics may however play a role in the intermediate state before complete polarization. We revisit the BCS approach in Sec. IV, with a slightly different perspective in which the antisymmetrization is imposed, in a functional formalism, with the help of a Lagrangian multiplier which plays a similar role as the present tunneling term Δ_{SAS} .

As we pointed out earlier, the population of the even channel P may be a complicated function of tunneling. In the following section we use exact diagonalization of small finite systems in order to get a hint of the form of this dependence $P=P(\Delta_{SAS})$ and determine the nature of possible phases as P increases from $1/2$ to 1 .

III. EXACT DIAGONALIZATION

Here we study the full interacting quantum Hall bilayer Hamiltonian for small finite systems in the presence of tunneling,^{16,18}

$$H = -\Delta_{SAS}S_x + \sum_{i<j, \sigma \in \uparrow, \downarrow} V^{\text{intra}}(\mathbf{r}_{i\sigma} - \mathbf{r}_{j\sigma}) + \sum_{i,j} V^{\text{inter}}(\mathbf{r}_{i\uparrow} - \mathbf{r}_{j\downarrow}), \quad (5)$$

where in coordinate representation we have $2S_x = \int d\mathbf{r}[\Psi_{\uparrow}^{\dagger}(\mathbf{r})\Psi_{\downarrow}(\mathbf{r}) + \text{H.c.}]$, $\Psi_{\sigma}^{\dagger}(\mathbf{r})$ creates a particle at the position \mathbf{r} in the layer σ . We have decomposed the interaction into terms between electrons belonging to the same layer (V^{intra}) and those residing in opposite layers (V^{inter}). We consider a short-range interaction, defined as

$$V_{331}^{\text{intra}}(r) = V_1 \nabla^2 \delta(r), \quad V_{331}^{\text{inter}}(r) = V_0 \delta(r), \quad (6)$$

which produces the 331 state as the densest and unique zero energy state when V_0, V_1 are chosen positive.^{10,28} We also consider long-range Coulomb interaction,

$$V_{\text{Coul}}^{\text{intra}}(r) = e^2/\epsilon r, \quad V_{\text{Coul}}^{\text{inter}}(r) = e^2/\epsilon\sqrt{r^2 + d^2}, \quad (7)$$

where d is the distance between layers. We fix the total number of particles in our calculations to be an even integer and, unless stated otherwise, take $d=l_B$ (l_B is the magnetic length), which merely sets the range for the distance between the layers where the Coulomb ground state is supposed to be fairly well described by the 331 wave function. Confining the electrons to a compact surface such as the sphere²⁸ or torus,²⁹ the Hilbert space becomes finite and one may exactly diagonalize the interacting Hamiltonian (5).³⁰ The ground state obtained in this way can be numerically compared with the trial wave functions $|\Psi_{331}\rangle$ and $|\Psi_{\text{Pf}}\rangle$ as a simple scalar product between vectors in the Hilbert space. In these calculations $|\Psi_{\text{Pf}}\rangle$ is defined in the even basis, i.e., single-particle states are understood to be even combinations of the original \uparrow, \downarrow states.

A. Sphere

If we wrap the electron sheet into a sphere and place a magnetic monopole in the center which generates N_{ϕ} magnetic flux quanta perpendicular to the surface, we are left with a finite basis of single-particle states indexed by $0, \dots, N_{\phi}$. Translational symmetry in the plane is replaced by rotational symmetry, which leads to a classification of the many-body states by the eigenvalues of angular momentum L and its z -component L_z .²⁸ The two-body interaction such as Eqs. (6) and (7) is parametrized by Haldane pseudopotentials $V_L^{\sigma\sigma'}$ which represent the energy of a pair of particles located in layers σ, σ' with relative angular momentum L .²⁸ Incom-

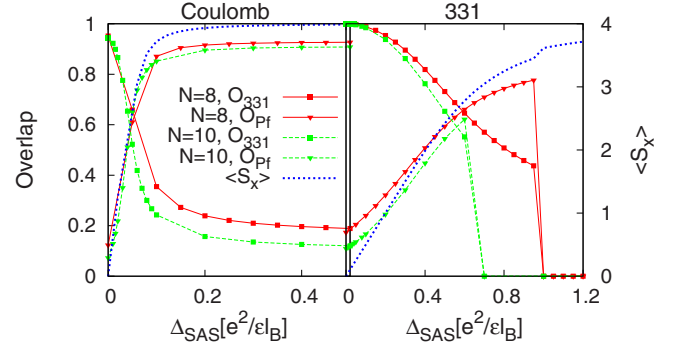


FIG. 1. (Color online) Overlaps between the exact ground state of the Coulomb bilayer (left panel) and short range 331 Hamiltonian (right panel) with the 331 state (O_{331}) and the Pfaffian (O_{Pf}), as a function of tunneling Δ_{SAS} . Also shown on the right axis is the expectation value of the S_x component of pseudospin (for $N=8$ system) which characterizes the two-component to one-component transition.

pressible quantum Hall states are invariably obtained in the $L=0$ sector of the Hilbert space. They are further characterized by a topological number called the *shift*²⁸ δ , defined through the relation $N_{\phi} = \frac{1}{\nu}N - \delta$. To specify uniquely the Hilbert space corresponding to the given trial state, one needs to know δ to get the correct value for the pair of (N, N_{ϕ}) . Sometimes it is possible to find different values of ν, δ that yield the same (N, N_{ϕ}) —this is called the aliasing problem because two different trial states get realized in the same Hilbert space. We disregard such cases in our calculations.

In Fig. 1 we present results of exact diagonalization on the sphere for the short-range (331) Hamiltonian (6) and long-range (Coulomb) Hamiltonian (7). 331 and Pfaffian trial states occur at the same value of the shift, thus we are able to track their evolution as a function of tunneling simultaneously. We also use $\langle S_x \rangle$, the expectation value of the S_x operator in the ground state, to monitor the two-component to one-component transition, whereas $\langle S_z \rangle$ remains zero throughout, which is due to the weaker interlayer as compared to the intralayer interaction. Starting from the long-range Hamiltonian (Fig. 1, left panel), we see that the 331 state gives way to a Pfaffian-like ground state, with the overlap quickly saturating to a value of around 0.92.^{16,18} The transition occurs for $\Delta_{SAS} \approx 0.1 e^2/\epsilon l_B$ which agrees well with the typical experimental value and shows little size dependence when the largest accessible system $N=10$ is considered (note that the subsequent $N=12$ system suffers from the aliasing problem). On the other hand, notice that for the short-range Hamiltonian (Fig. 1, right panel), the 331 state is much more robust to perturbation by Δ_{SAS} : before it reaches full polarization in the x direction (maximum $\langle S_x \rangle$), the overlap with both incompressible states drops precipitously beyond some critical Δ_{SAS} which is rather size-sensitive (it also depends on the values of the parameters one chooses in Eq. (6), but the qualitative features of the transition are reproduced for many different choices of V_0, V_1).

We see nonetheless that the breakdown of a two-component phase yields a one-component state manifested by $\langle S_x \rangle \rightarrow N/2$ (this is the limit $P \rightarrow 1$ from Sec. II). At the transition, $\langle S_x \rangle$ develops a small but visible kink. Focusing

on the large-tunneling limit, we find that the nature of the ground state is effectively that of the single-layer (polarized) ground state for the symmetric interaction $V^+(r)=[V^{\text{intra}}(r)+V^{\text{inter}}(r)]/2$. This intuitive result was directly verified for all the available system sizes, including very large $N=10$ system on both sphere and torus (see Sec. III B). In view of this, it is not surprising that the large-tunneling limit of the short-range Hamiltonian is the compressible CFL: V^+ in this case reduces to the repulsive hard core V_1 pseudopotential which has a tendency to produce the Jain CF state. This is also apparent in the fact that the ground states for large tunneling are obtained in the angular momentum sectors that agree with the predictions for the excitations of the CFL yielding overlap of 0.99 with the excited CF sea ground state.

Therefore, the results for the short-range Hamiltonian are suggestive that we may have a direct 331-CFL transition in the thermodynamic limit because the transition point seems to be shifting toward smaller tunnelings as we increase N . Notice, however, that in contrast to the incompressible 331 and Pfaffian states, which occur at a shift $\delta=3$, the CFL has a shift $\delta=4$. On the sphere, the two incompressible states can thus not be directly compared to the CFL, and the evidence for the 331-CFL transition is therefore indirect. This problem is circumvented in ED on the torus presented hereafter in Sec. III B. In the Coulomb case, on the other hand, we observe a curious saturation of the ground state overlap with the Pfaffian. We attribute this feature to the effect of the long range Coulomb potential on a finite system. One notices that by adding an asymptotic tail to the “intra” component of the short-range pseudopotentials $V_L^{\text{intra}}=V_{L,331}^{\text{intra}}+\alpha/2\sqrt{L}$ (α nonzero for $L\geq 3$), one progressively increases the critical value of Δ_{SAS} for the abrupt drop of the overlaps as $\alpha\rightarrow 1$ (pure Coulomb). In fact, for $N=8, 10$ it is sufficient to consider only V_3^{intra} to achieve the saturation and push the critical value of Δ_{SAS} to infinity.

Results for the Coulomb interaction in the large Δ_{SAS} limit (Fig. 1) are similar to those obtained in Ref. 31 where single-layer Zhang-Das Sarma interaction was used. As long as we are in the large Δ_{SAS} limit, $V^+(r)$ interaction produces numerically the same effect as the Zhang-Das Sarma interaction. In particular, transition to a Moore-Read Pfaffian will be induced if the layer separation d is sufficiently large.³¹ Of course, these two interactions are different from each other and the fact that they yield the same phenomenology (phase transitions as d is varied) only means we are probing a critical state where even the slightest perturbation away from pure Coulomb interaction (coupled with the bias of the shift) is sufficient to generate incompressibility. However, despite large overlap, the gap remains very small after the transition. The difference between the two interactions is obvious in the torus geometry (Sec. III B). The new result of the present paper is that we find the Pfaffian signature even in the region without full polarization ($P\leq 1$), as we elaborate in Sec. III C.

B. Torus

Another way to compactify an infinite plane is to impose periodic boundary conditions on a unit cell $a\times b$.^{28,29} This

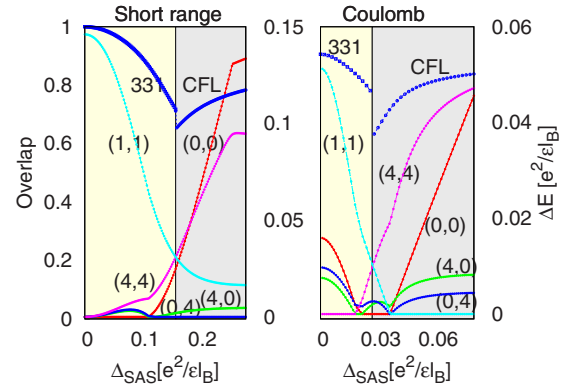


FIG. 2. (Color online) Low-energy part of the spectrum (relative to the ground state) of the short-range 331 (left panel) and the long-range Coulomb Hamiltonian (right panel) for $N=8$ electrons on the torus at $\nu=1/2$ and aspect ratio $a/b=0.97$ as a function of tunneling Δ_{SAS} (right axis). Also shown (left axis) is the overlap with the phases we identify as the 331 state and the CFL.

also produces a finite set of $N_\phi=ab/2\pi l_B^2$ single-particle states which are periodic functions under the transformation of coordinates $x\rightarrow x+a, y\rightarrow y+b$ (we assume that there are no additional phases generated by such a transformation). Because of the presence of magnetic field, the many-body Hamiltonian reduces in the invariant subspace of the magnetic translation group²⁹ and the eigenstates are labeled by the pseudomomentum \mathbf{k} , restricted to the Brillouin zone $(2\pi s/a, 2\pi t/b); s, t=0, \dots, \bar{N}-1$, where \bar{N} is the greatest common divisor of N, N_ϕ . Contrary to the sphere, trial states on the torus are uniquely specified by their filling factor and thus we can directly address transitions between the 331 state, the Pfaffian and the CFL. Moreover, states in this geometry are distinguished by their ground-state degeneracy. If the filling factor is $\nu=p/q$ (p, q having no common divisor), there is a generic degeneracy of q which comes from the center of mass motion²⁹ having no physical importance, so we implicitly assume it in what follows. Apart from this, there can be additional degeneracies occurring due to special point symmetry of the Brillouin zone (trivial) or those that arise from the multicomponent³² or the non-Abelian nature of the state.^{9,10} For the 331 state we expect a quadruplet of states (up to the center of mass degeneracy) one of which belongs to the $\mathbf{k}=0$ sector of the Hilbert space and the remaining three are located at the corners of the Brillouin zone, $\mathbf{k}=(0, \bar{N}/2), (\bar{N}/2, 0), (\bar{N}/2, \bar{N}/2)$. In contrast to the 331 state, the Moore-Read Pfaffian has only a threefold degeneracy²⁶ $\mathbf{k}=(0, \bar{N}/2), (\bar{N}/2, 0), (\bar{N}/2, \bar{N}/2)$, whereas compressible states in general do not possess clearly defined degeneracies (they may appear to have accidental degeneracies which are functions of the aspect ratio of the torus a/b , particle number and any other parameter). These are the expectations based on the analytic form of the trial wave functions and their parent conformal field theories,^{9,33} but they are also borne out exactly in the numerical diagonalization of the model Hamiltonians.^{8,34}

In Fig. 2 we show the relevant low energy part of the spectrum of the Hamiltonians (6) and (7) as a function of tunneling, measured relative to the ground state (right axis),

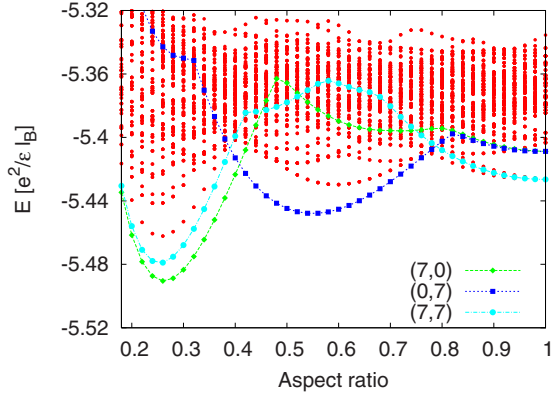


FIG. 3. (Color online) Spectrum of the $N=14$ electrons in a single layer at $\nu=1/2$ interacting with $V^+(r)$ ($d=l_B$), as a function of aspect ratio. We highlight the states with quantum numbers of the Moore-Read Pfaffian.

for $N=8$ electrons and the fixed aspect ratio 0.97 in the vicinity of the square unit cell. We identify the multiplet of four states that build up the 331 phase, whose exact degeneracy for the short-range Hamiltonian and small Δ_{SAS} (left panel) is partially lifted in case of the Coulomb interaction (right panel). 331 phase is destroyed for sufficiently large Δ_{SAS} when the $\mathbf{k}=(1,1)$ state (fourfold degenerate) comes down and eventually forms a gapless branch with $(0,4)$ and $(4,0)$ members of the 331 multiplet (other excited states not shown). We identify the large-tunneling phase as the CFL phase because exactly the same spectrum is seen in a single layer with Coulomb interaction and the same aspect ratio. This transition is quantitatively reflected also in the overlap with the trial 331 states and CFL as a function of tunneling (Fig. 2, left axis). In order to take into account the ground-state degeneracy, we define overlap on the torus in the following way:

$$|\langle \Psi_{\text{trial}} | \Psi \rangle|^2 \equiv \frac{1}{|\mathcal{S}_{\text{trial}}|} \sum_{\mathbf{k} \in \mathcal{S}_{\text{trial}}} |\langle \Psi_{\text{trial}}(\mathbf{k}) | \Psi(\mathbf{k}) \rangle|^2, \quad (8)$$

where $\mathcal{S}_{\text{trial}}$ stands for the degenerate subspace expected for $|\Psi_{\text{trial}}\rangle$. This amounts to adding together the overlap squared for each of the expected members in the ground-state multiplet (normalizing the sum by the expected ground-state degeneracy $|\mathcal{S}_{\text{trial}}|$ to be 1 at maximum) and the definition is obviously meaningful only in the case where we had previously established the correct level ordering in the spectrum.

Upon a closer look at Fig. 2, one notices that the torus spectra suggest little qualitative difference between the short-range and the Coulomb Hamiltonian. In particular, we do not see any indication of the Pfaffian threefold ground-state degeneracy for large Δ_{SAS} which could be expected from the large overlap on the sphere (Fig. 1). To reconcile these two results, we again focus on the large-tunneling limit and vary the aspect ratio of the torus to investigate the possibility of an emergent Pfaffian phase (Fig. 3). We assume that in the large-tunneling limit, we have effectively a single-layer (polarized) ground state for the symmetric interaction $V^+(r)$. In Fig. 3 we show the spectrum of the single-layer system of $N=14$ electrons interacting with $V^+(r)$ as a function of aspect

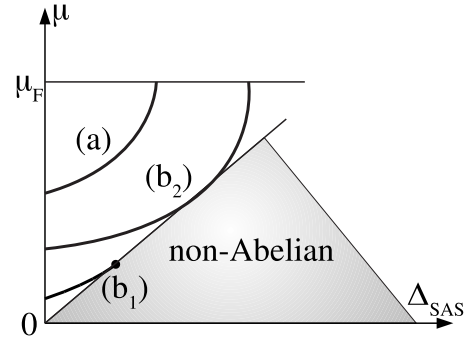


FIG. 4. Possible outcomes of tunneling on a two component system such as the transition to a Fermi liquid (a) or to a critical Moore-Read Pfaffian (b_1, b_2), in the context of phase diagram after Read and Green (Ref. 26). Note that the value for $\mu_F \sim 1/m^*$ is interaction-dependent due to the renormalized CF mass m^* and we may have different dividing lines $\mu = \mu_F$ depending on the kind of the interaction (Ref. 6).

ratio and connect the levels that have the quantum numbers of the Moore-Read Pfaffian. We also include the background charge correction.³⁵ One notices that, with the exception of a very narrow range of aspect ratios around 0.4, there is no evidence of a clear Moore-Read degeneracy. A narrow region where we see the threefold multiplet of states for $N=14$ also exists for $N=8$, but is obscured by the presence of higher energy levels in systems of $N=10$ and 12 electrons. Thus we conclude that it cannot represent a stable phase, but a possibility remains that it is a critical phase which becomes stronger as one approaches the thermodynamic limit or as one changes the interaction away from the pure Coulomb.

We note that varying d (at the fixed aspect ratio) does not lead to any qualitative change in the ground-state degeneracy as long as $V^+(r)$ interaction is used. This is clearly different from Zhang-Das Sarma interaction which induces level crossings in the spectrum in such a way that for large d (typically beyond $4l_B$), a Pfaffian degeneracy is seen for big enough systems,³⁶ with the exception of $N=10$. This is similar to the results in the second Landau level,³⁶ as well as the calculations on the sphere,³¹ but the prohibitively small gap suggests that such a state, if it exists, is very fragile.

C. Pfaffian signatures for intermediate tunneling and a proposal for the phase diagram

We conclude this section with a summary of our exact-diagonalization results in the two geometries in order to make a connection with the BCS analysis of Sec. II and sketch possible paths of the $\nu=1/2$ two component system with tunneling in the phase diagram of Read and Green,²⁶ see Fig. 4. In Fig. 4, μ has the meaning of the effective chemical potential μ^{eff} of the whole system as in Sec. II, renormalized by Δ_{SAS} , i.e., $\mu = \mu(\Delta_{SAS})$. It is assumed that it can be approximated by the value of the chemical potential of the dominant even channel, $\mu^{\text{eff}} \simeq \mu^e$ and the separation between the Abelian and non-Abelian phases in Fig. 4 is defined by setting then the value of the chemical potential of the odd channel to zero, i.e., $\mu^o \simeq \mu(\Delta_{SAS}) - \Delta_{SAS} = 0$. This approximation renders necessary taking into account the

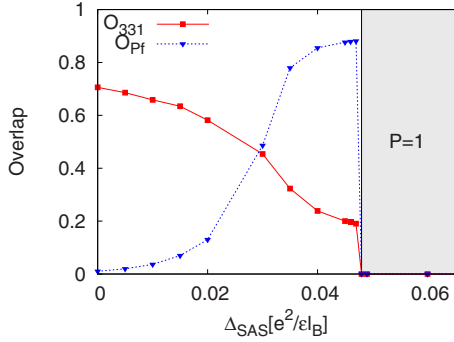


FIG. 5. (Color online) Overlaps between the exact ground state of $N=10$ electrons on the sphere with the 331 state (O_{331}) and the Pfaffian (O_{Pf}), as a function of tunneling Δ_{SAS} , for the Coulomb bilayer Hamiltonian and $d=0.4l_B$.

renormalization of the parameters in the BCS Hamiltonian (1) with tunneling, as in Ref. 26.

On the sphere, we first recall a very large difference in Δ_{SAS}^C , the critical value of tunneling required to fully polarize the system in the x direction, for the two interactions considered. A much larger value for the short-range 331 Hamiltonian suggests that the chemical potential for the even channel in this case is much more strongly renormalized than for the long-range Coulomb interaction and therefore such a system may assume a phase trajectory labeled (a) in Fig. 4, directly moving from 331 state through the Abelian phase and into a CFL.

A question we ask at this point is whether the CFL, a likely phase at $P=1$, leaves room for other one-component states to form as we increase the tunneling. In particular, is there a possibility for a system to evolve along the trajectory which terminates at (b_1) or touches (b_2) the critical line that separates the Abelian from the non-Abelian phase in Fig. 4? Such an intermediate phase could possess significant overlap with the Moore-Read Pfaffian, but it would necessarily have a small gap and we refer to it as “critical Pfaffian.”

On the sphere, a suitable system to detect the signature of the critical Pfaffian is the Coulomb $N=10$ system where the large-tunneling phase is compressible for $d \leq 0.5l_B$.³¹ We therefore fix $d=0.4l_B$ and vary Δ_{SAS} (Fig. 5). For $\Delta_{SAS}=0$, we are still largely in the 331 phase and for large Δ_{SAS} we are in the CFL; however, for intermediate tunnelings we see a developing Pfaffian that establishes in a narrow range around $\Delta_{SAS}=0.04e^2/\epsilon l_B$. Therefore, despite “weaker” incompressibility for small Δ_{SAS} and full compressibility for large Δ_{SAS} , for intermediate tunneling we find evidence for the Pfaffian, as suggested by the trajectory b_2 in Fig. 4). For larger values of d , as we remarked in Sec. III A, we observe saturation of the overlap for Coulomb interaction and the tentative trajectory in that case resembles b_1 .

The effects of CFL physics are rendered more transparent in the torus geometry, where we have identified the dominant phases as 331 and CFL (Fig. 2), with a direct transition between the two of them. We choose a value for $\Delta_{SAS}=0.03e^2/\epsilon l_B$ which places the system in the center of the transition region (compare also with Fig. 5) and examine the spectrum of an $N=8$ system as a function of aspect ratio for an emerging Pfaffian degeneracy, Fig. 6. In torus geometry

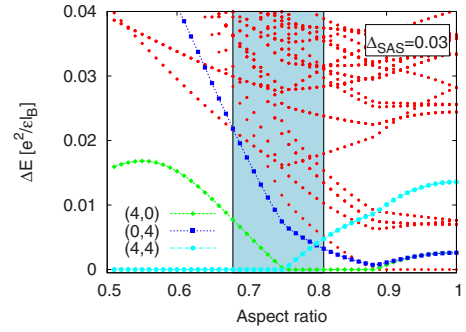


FIG. 6. (Color online) Low-energy part of the spectrum (relative to the ground state) of the Coulomb Hamiltonian (with $d=l_B$) for $N=8$ electrons on the torus at $\nu=1/2$ and $\Delta_{SAS}=0.03e^2/\epsilon l_B$, as a function of the aspect ratio. Shaded region represents the tentative phase with the Pfaffian degeneracy.

there is no subtle dependence on d , so we take as before $d=l_B$. In agreement with the results on sphere, we find a region of aspect ratios where the correct Pfaffian degeneracy is visible.

Previous results lend support to the scenario of an intermediate critical phase in a long-range Coulomb system, which has a small gap (Fig. 6) but possesses large overlap with the Moore-Read Pfaffian (Fig. 5). We would like to stress that all of our conclusions are based on the idealized bilayer Hamiltonian (5). As such, it is not clear at present to what extent they apply to the experiments^{24,25} where the electron density-profile differs significantly from an ideal bilayer. With respect to theoretical studies, stronger indication of topological degeneracy is likely to be found in a model that assumes nonzero thickness of each layer,³⁶ but that would lead also to a substantial decrease of the gap.³⁷

IV. GENERALIZED TUNNELING CONSTRAINT

In Sec. III we found that in a system with a fixed number of particles and the tunneling commonly expressed as $-\Delta_{SAS}S_x$, there is only circumstantial evidence for the clear Pfaffian phase in finite systems that can be studied by ED. This evidence appears most striking when Coulomb overlaps in the spherical geometry are considered (Fig. 1). However, these overlaps must be interpreted with caution: on the sphere we can indeed only study the competition between Pfaffian and an *excited* CFL state (containing a quasiparticle) because the ground-state candidates occur at different values for the shift δ as mentioned in Sec. III A. As we have explained there, the latter state is indeed favored by short-range interactions. Moreover, even when the ground state is described by the Pfaffian state, the energy spectrum is not that of a typical incompressible state with a gap to all excitations. Therefore, an explanation for the large Coulomb overlap with the Pfaffian may be the shift which artificially favors it over the CFL phase. This interpretation agrees with the results in the torus geometry, which treats both phases on the same footing and which suggests that the CFL is the likely outcome of tunneling on the 331 state. We can give two general arguments for this. First, strong tunneling has a tendency to polarize the spin in the x -direction, and one there-

fore crosses over to an effective one-component system that in the LLL favors the formation of a compressible CFL phase. Second, we have shown in the BCS approach for the charge-neutral sector (Sec. II) that tunneling does not only lower the chemical potential μ^o in the odd channel but also *increases* that in the even channel, μ^e . We argued that this leads to the insufficiency of the BCS model description, which then describes a local maximum and the system crosses over to a CFL.

It is clear that, in addition to tunneling, one also must find a way to prevent the effective even-channel chemical potential from becoming too large if the weakly paired phase is to be established in the system. In this section, we propose a way to implement this requirement formally via generalized tunneling constraint. On the level of the BCS model used in Sec. II, this constraint leads to a stable weak-pairing phase in the even channel. In the following Sec. IV A we describe a formal implementation of the constraint in a system of BCS paired fermions. On the basis of this model, we propose, in Sec. IV B a system in contact with a reservoir with which it can exchange particles so that, with the tunneling term included, a stable Pfaffian phase can be reached.

A. System with generalized tunneling constraint

Cauchy determinant pairing describes p -wave pairing of \uparrow and \downarrow particles, and in order to recover the spinless Pfaffian pairing, we need to “identify” \uparrow with \downarrow . Within a functional formalism, that amounts to adding a term of the form

$$\chi(\mathbf{r})[\Psi_{\uparrow}(\mathbf{r}) - \Psi_{\downarrow}(\mathbf{r})] \quad (9)$$

to the Lagrangian density via Grassmannian Lagrange multiplier $\chi(\mathbf{r})$. We will assume instead that we can alternatively express this via the constraint

$$\lambda(\mathbf{r})[\Psi_{\uparrow}^{\dagger}(\mathbf{r}) - \Psi_{\downarrow}^{\dagger}(\mathbf{r})][\Psi_{\uparrow}(\mathbf{r}) - \Psi_{\downarrow}(\mathbf{r})], \quad (10)$$

in terms of the bosonic multiplier $\lambda(\mathbf{r})$. By construction this constraint affects only the odd channel. Within the mean-field approximation of a spatially constant multiplier $\lambda(\mathbf{r}) = \lambda$, one may identify $\lambda = \Delta_{SAS}/2$, i.e., the effect of the multiplier is the same as the tunneling term in Sec. II, except for an overall decrease of the chemical potential, $\mu \rightarrow \mu - \lambda$, which eventually yields a λ -independent chemical potential in the even channel, $\mu^e = \mu$, as mentioned above. Integration over the Lagrange multiplier projects to $\Psi_o^{\dagger}\Psi_o = 0$, where $\Psi_o^{\dagger} = [\Psi_{\uparrow}^{\dagger}(\mathbf{r}) - \Psi_{\downarrow}^{\dagger}(\mathbf{r})]/\sqrt{2}$ is again the odd spin superposition written in terms of the fermion fields $\Psi_{\sigma}(\mathbf{r})$, i.e., it leaves us with no density in the odd channel.

The BCS Hamiltonian including the constraint [Eq. (10)] has the same form as Eq. (1) except that now $\tilde{\epsilon}_{\mathbf{k}} = \epsilon_{\mathbf{k}} - \mu + \lambda$, as a consequence of the above-mentioned shift in the chemical potential. We can diagonalize it by a Bogoliubov transformation,

$$\alpha_{\mathbf{k}} = u_{\uparrow}c_{\mathbf{k}\uparrow} + u_{\downarrow}c_{\mathbf{k}\downarrow} + v_{\uparrow}c_{-\mathbf{k}\uparrow}^{\dagger} + v_{\downarrow}c_{-\mathbf{k}\downarrow}^{\dagger}. \quad (11)$$

The equation $[\alpha_{\mathbf{k}}, H] = E\alpha_{\mathbf{k}}$ then defines the Bogoliubov–de Gennes equations and the Hamiltonian is transformed into the canonical form $H = \sum_{\mathbf{k}} E_{\alpha\mathbf{k}} \alpha_{\mathbf{k}}^{\dagger} \alpha_{\mathbf{k}} + \sum_{\mathbf{k}} E_{\beta\mathbf{k}} \beta_{\mathbf{k}}^{\dagger} \beta_{\mathbf{k}} + \tilde{E}_0$, where

the eigenvalues $\pm E_{\alpha\mathbf{k}}$ and $\pm E_{\beta\mathbf{k}}$ are given by

$$E_{\alpha\mathbf{k}} = \sqrt{\epsilon_{\mathbf{k},1}^2 + \Delta_0^2 k^2}, \quad \text{with } \epsilon_{\mathbf{k},1} = \epsilon_{\mathbf{k}} - \mu,$$

$$E_{\beta\mathbf{k}} = \sqrt{\epsilon_{\mathbf{k},2}^2 + \Delta_0^2 k^2}, \quad \text{with } \epsilon_{\mathbf{k},2} = \epsilon_{\mathbf{k}} - \mu + 2\lambda, \quad (12)$$

respectively. The eigenvectors corresponding to $E_{\alpha\mathbf{k}}$ and $E_{\beta\mathbf{k}}$ are, respectively,

$$\begin{aligned} \alpha_{\mathbf{k}} &= \frac{k}{2\sqrt{E_{\alpha\mathbf{k}}}} \frac{\sqrt{E_{\alpha\mathbf{k}} + \epsilon_{\mathbf{k},1}}}{k_x - ik_y} (c_{\mathbf{k}\uparrow} + c_{\mathbf{k}\downarrow}) \\ &\quad + \frac{\Delta_0 k}{2\sqrt{E_{\alpha\mathbf{k}}}} \frac{1}{\sqrt{E_{\alpha\mathbf{k}} + \epsilon_{\mathbf{k},1}}} (c_{-\mathbf{k}\uparrow}^{\dagger} + c_{-\mathbf{k}\downarrow}^{\dagger}), \\ \beta_{\mathbf{k}} &= \frac{k}{2\sqrt{E_{\beta\mathbf{k}}}} \frac{\sqrt{E_{\beta\mathbf{k}} + \epsilon_{\mathbf{k},2}}}{k_x - ik_y} (c_{\mathbf{k}\uparrow} - c_{\mathbf{k}\downarrow}) \\ &\quad - \frac{\Delta_0 k}{2\sqrt{E_{\beta\mathbf{k}}}} \frac{1}{\sqrt{E_{\beta\mathbf{k}} + \epsilon_{\mathbf{k},2}}} (c_{-\mathbf{k}\uparrow}^{\dagger} - c_{-\mathbf{k}\downarrow}^{\dagger}). \end{aligned} \quad (13)$$

To find the stationary point for the action defined by the diagonalized BCS Hamiltonian at zero temperature, it is useful to continue λ from the real axis to the complex plane \mathbb{C} (see Ref. 38 for details). The part \tilde{E}_0 , through its dependence on λ ,

$$\tilde{E}_0 = - \sum_{\mathbf{k}} \frac{\Delta_0^2 k^2}{2} \left(\frac{1}{E_{\alpha\mathbf{k}} + \epsilon_{\mathbf{k},1}} + \frac{1}{E_{\beta\mathbf{k}} + \epsilon_{\mathbf{k},2}} \right), \quad (14)$$

determines the stationary point: $\partial \tilde{E}_0 / \partial \lambda = 0$. Introducing the notation $\mu - 2\lambda \equiv \tilde{\mu} \in \mathbb{C}$ for the analytically continued chemical potential in the odd channel, we continue as $E_{\beta\mathbf{k}} + \epsilon_{\mathbf{k},2} = |\tilde{\mu}| - \tilde{\mu} + o(k^2)$, which gives us the stationary point $\text{Re } \tilde{\mu} \rightarrow -\infty$ or, equivalently, $\lambda \rightarrow +\infty$ and we have strong coupling in the odd channel. For our choice $\mu > 0$, we thus obtain weak coupling in the even channel that has a Pfaffian description²⁶ in $c_{\mathbf{k}\uparrow} + c_{\mathbf{k}\downarrow}$ (even) variables [see the expression for $\alpha_{\mathbf{k}}$ Eq. (13)]. Unlike the situation in Sec. II, with the same assumption that Δ_0 does not renormalize strongly with tunneling, the chemical potential of the even channel stays the same and the even channel can thus be weakly paired.

B. System with fluctuating density

The previous discussion was on the simplified model of the 331 physics in terms of neutral fermions with an additional constraint that leads to the Pfaffian, but seems artificial and hard to implement in an experimental setting. Nevertheless it suggests a possible way to achieve the stable Pfaffian phase. With respect to ordinary tunneling the generalized constraint can be modeled by strong tunneling and an additional term in the effective description, λN , where N is the total number of particles and λ tunneling strength as before.³⁹ The chemical potential (of the whole system) depends on the tunneling and changes as $\mu - \lambda$. Then we have the following physical picture in mind: as we take $\lambda > 0$ this decrease of the chemical potential with tunneling will imply the decrease of the density of the system. On the other hand,

from the solution of the BCS system with the generalized constraint, we see that the effective chemical potential of the even channel stays the same—equal to μ , Eq. (12). This means also that the number of particles in the even channel stays the same, so the effects of the tunneling and the additional term cancel, but the polarization P increases with tunneling. Thus we effectively maintain the same effective parameter μ with tunneling, its value will not increase, and we will be able to achieve the stable Pfaffian phase. To be more specific and quantitative about the role of fluctuating density in achieving the Pfaffian, we discuss in the remainder of this section the necessary dependence of density on tunneling. We will recover the demand for the decreasing density for the case of strong tunneling.

Our BCS Hamiltonian, which is also the thermodynamic potential Ω at zero temperature, is specific for the fact that the independent thermodynamic variable, along with volume and temperature, is the chemical potential μ^λ , given by $\mu^\lambda = \mu - \lambda$. Therefore, as we change λ (the parameter of the Hamiltonian), we also induce a change in the chemical potential $\delta\mu^\lambda = -\lambda$ and this implies

$$\frac{\partial\Omega}{\partial\lambda} = \frac{\partial\tilde{E}_0}{\partial\lambda} = N, \quad (15)$$

for the particular system. The effective chemical potential, on the other hand, is in this case

$$\mu^{\text{eff}} = \mu P + (\mu - 2\lambda)(1 - P) = \mu + (P - 1)2\lambda. \quad (16)$$

As before, this relation shows how the chemical potential renormalizes as a parameter λ of the BCS Hamiltonian is varied. We keep the volume constant and measure N with k_F in the usual ansatz,

$$N(k_F) = \sum_{\mathbf{k},\sigma} \rightarrow \frac{2 \times 2\pi}{(2\pi)^2} \int_0^{k_F} dk k = k_F^2/2\pi, \quad (17)$$

and Eq. (15) becomes

$$N(k_F) = \frac{\partial\tilde{E}_0(k_F, \lambda)}{\partial k_F} \frac{\partial k_F}{\partial\lambda} + \frac{\partial\tilde{E}_0(k_F, \lambda)}{\partial\lambda}. \quad (18)$$

Differentiating and converting the sum in \tilde{E}_0 into an integral over k , we obtain the partial differential equation,

$$k_F^2 = -\frac{\Delta_0^2 k_F^3}{2} \left(\frac{1}{E_{\alpha k_F} + \epsilon_{\mathbf{k}_F,1}} + \frac{1}{E_{\beta k_F} + \epsilon_{\mathbf{k}_F,2}} \right) \frac{\partial k_F}{\partial\lambda} + \int_0^{k_F} dk k^3 \frac{\Delta_0^2}{E_{\beta \mathbf{k}}(E_{\beta \mathbf{k}} + \epsilon_{\mathbf{k},2})}, \quad (19)$$

from which we can extract the limiting case $\lambda \gg \hbar^2 k_F^2 / 2m^*$ when

$$\frac{\partial N(k_F)}{\partial\lambda} = -cN(k_F), \quad (20)$$

with the constant factor $c > 0$, i.e., for large tunneling we should decrease the density of the system to stay at small μ^e and to stabilize the Pfaffian. We expect this limit to be pertinent to the experiments such as Ref. 25 where the com-

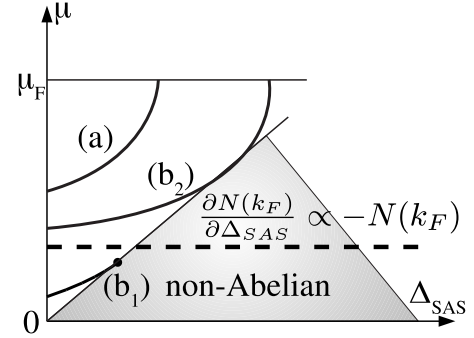


FIG. 7. Generalized tunneling constraint (dashed line) in the phase diagram of Fig. 4. Note that, as in Fig. 4, μ denotes the effective chemical potential equal to the chemical potential of the even channel in the strong tunneling limit.

pressible state starts to show signs of incompressibility upon density imbalance. Enforcing the condition (20) is then expected to lead to strengthening of the paired Pfaffian state, as summarized in Fig. 7 where the dashed line represents schematically a phase trajectory of the system that evolves under the generalized tunneling constraint (in the large Δ_{SAS} limit). As Eq. (20) shows, in this case the density of the system needs to be decreased simultaneously with the increase of tunneling Δ_{SAS} . This can be achieved conventionally via the application of a gate voltage to the evaporated top/bottom gates as, e.g., in Refs. 25 and 40 or by growing *in situ* a n^+ -GaAs layer that can serve as a gate.⁴¹

The main reason why we find it desirable to have an open system in the experiment is our inability to specify the parameters of the simplified, effective Read-Green model and pin-point the optimal density for which the Pfaffian state would be strong. With a better knowledge of the microscopic details of the system, one may as well fix a particular density (which we expect to be small) for a given, not too large, tunneling strength where the Pfaffian will be stable. However, an open system would allow a systematic study over a range of tunneling strengths in which the Pfaffian would show a characteristic strengthening that would distinguish it from any other incompressible candidates.

Therefore, in principle, by changing the density of the system we can achieve a stable Pfaffian phase. We would like to compare the present discussion which is based on the simplified model of neutral fermions (mean field in nature with the simplifying assumption $\Delta_o = -\Delta_e = \text{constant}$, i.e., independent of tunneling) with exact diagonalization in the LLL in the previous section. The arguments presented here call for an open system with adjustable density which demands also the adjustment of the magnetic field B to achieve the stable Pfaffian phase. Although doing so will preserve the filling factor, in general changing the total density may enhance the role of LL mixing and thus invalidate the LLL assumption in the exact diagonalizations. It will also lead to the renormalization of the parameters of the BCS effective model not taken into account in Sec. II. Indeed, when lowering the total chemical potential via the generalized constraint, the density is also decreased. On the other hand the ratio between interaction strength (e^2/l_B) and cyclotron frequency ($\omega_c \sim 1/l_B^2$) is proportional to $1/\sqrt{\rho}$, from which we

see that the LLL projection is invalidated if the density is significantly reduced. Therefore to reach and establish the Pfaffian phase it is likely that LL mixing has to be taken into account. This has been discussed in the recent literature^{42,43} as a way to stabilize the Pfaffian phase. Here we seek the Pfaffian in a two-component setting when a parameter of the system λ is varied, which makes the inclusion of higher LLs harder. If we remain in the LLL, changing of the density amounts to simple rescaling of spectra ($e^2/l_B \rightarrow ce^2/l_B$ with $c > 0$), which cannot induce any significant effect such as the change in the nature of (quasi)degeneracy of ground states on the torus. Even if the evidence for a Pfaffian phase is rather weak for the system sizes studied here, one may hope that the increase of these sizes will improve the case for such a state in the LLL as the odd channel may assume the role of the first excited Landau level before a complete polarization.

V. CONCLUSIONS

We investigated the possibility of creating the Moore-Read Pfaffian out of the paired two-component 331 state via tunneling. Exact diagonalization, performed under the constraint of LLL projection and fixed total number of particles, could not detect a stable Pfaffian phase, but a critical one between 331 and CFL phases. While the short-range interaction is likely to favor a direct transition from the 331 to the CFL phase, long-range Coulomb interactions leave the pos-

sibility for a Pfaffian-like phase if the parameters of the system are tuned in a special way. Based on the connection between our numerical results and the effective BCS Hamiltonian theory of paired states, we argue that one way to stabilize the Pfaffian state is to change the density (number of particles) of the system while increasing the tunneling.

Our analysis was restricted to the Coulomb bilayer system and the tunneling term of the form $-\Delta_{SAS}S_x$, which is small in magnitude and generally difficult to control. Similar considerations apply to the quantum well systems²⁵ where \uparrow, \downarrow stand for the two lowest electronic subbands and Δ_{SAS} acts like a Zeeman energy. In these systems, the analog of the tunneling term used in our paper can be deployed to create asymmetric charge distribution in the wide quantum well.²⁵ The interplay of these two kinds of terms, tunneling and Zeeman, will be addressed in future work.

ACKNOWLEDGMENTS

This work was supported by the Serbian Ministry of Science under Grant No. 141035, by the Agence Nationale de la Recherche under Grant No. ANR-JCJC-0003-01 and by grants from Région Ile-de-France. Illuminating discussions with H. Hansson, S. Das Sarma and M. Shayegan are gratefully acknowledged. Z.P. acknowledges discussions with D. Sheng, D. Yoshioka and especially Th. Jolicoeur and K. Vyborny.

-
- ¹R. B. Laughlin, *Phys. Rev. Lett.* **50**, 1395 (1983).
²D. C. Tsui, H. Stormer, and A. C. Gossard, *Phys. Rev. Lett.* **48**, 1559 (1982).
³J. Jain, *Composite Fermions* (Cambridge University Press, Cambridge, England, 2007).
⁴E. H. Rezayi and N. Read, *Phys. Rev. Lett.* **72**, 900 (1994).
⁵H. W. Jiang, H. L. Stormer, D. C. Tsui, L. N. Pfeiffer, and K. W. West, *Phys. Rev. B* **40**, 12013 (1989).
⁶B. I. Halperin, P. A. Lee, and N. Read, *Phys. Rev. B* **47**, 7312 (1993).
⁷R. Willett, J. P. Eisenstein, H. L. Störmer, D. C. Tsui, A. C. Gossard, and J. H. English, *Phys. Rev. Lett.* **59**, 1776 (1987).
⁸E. Rezayi and F. D. M. Haldane, *Phys. Rev. Lett.* **84**, 4685 (2000).
⁹G. Moore and N. Read, *Nucl. Phys. B* **360**, 362 (1991).
¹⁰N. Read and E. Rezayi, *Phys. Rev. B* **54**, 16864 (1996).
¹¹C. Nayak, S. H. Simon, A. Stern, M. Freedman, and S. Das Sarma, *Rev. Mod. Phys.* **80**, 1083 (2008).
¹²B. I. Halperin, *Helv. Phys. Acta* **56**, 75 (1983).
¹³F. D. Haldane and E. H. Rezayi, *Phys. Rev. Lett.* **60**, 956 (1988).
¹⁴D. Yoshioka, A. H. MacDonald, and S. M. Girvin, *Phys. Rev. B* **39**, 1932 (1989).
¹⁵S. He, S. Das Sarma, and X. C. Xie, *Phys. Rev. B* **47**, 4394 (1993).
¹⁶K. Nomura and D. Yoshioka, *J. Phys. Soc. Jpn.* **73**, 2612 (2004).
¹⁷Z. Papić, G. Möller, M. V. Milovanović, N. Regnault, and M. O. Goerbig, *Phys. Rev. B* **79**, 245325 (2009).
¹⁸Michael R. Peterson and S. Das Sarma, *Phys. Rev. B* **81**, 165304 (2010).
¹⁹J. Eisenstein, in *Perspectives in Quantum Hall Effects*, edited by S. Das Sarma and A. Pinczuk (Wiley, New York, 1997).
²⁰Y. W. Suen, L. W. Engel, M. B. Santos, M. Shayegan, and D. C. Tsui, *Phys. Rev. Lett.* **68**, 1379 (1992).
²¹Y. W. Suen, H. C. Manoharan, X. Ying, M. B. Santos, and M. Shayegan, *Phys. Rev. Lett.* **72**, 3405 (1994).
²²A. Cappelli, L. S. Georgiev, and I. T. Todorov, *Nucl. Phys. B* **599**, 499 (2001).
²³N. Regnault, M. O. Goerbig, and Th. Jolicoeur, *Phys. Rev. Lett.* **101**, 066803 (2008).
²⁴D. R. Luhman, W. Pan, D. C. Tsui, L. N. Pfeiffer, K. W. Baldwin, and K. W. West, *Phys. Rev. Lett.* **101**, 266804 (2008).
²⁵J. Shabani, T. Gokmen, and M. Shayegan, *Phys. Rev. Lett.* **103**, 046805 (2009); **103**, 256802 (2009).
²⁶N. Read and D. Green, *Phys. Rev. B* **61**, 10267 (2000).
²⁷N. E. Bonesteel, *Phys. Rev. Lett.* **82**, 984 (1999).
²⁸F. D. M. Haldane, *Phys. Rev. Lett.* **51**, 605 (1983); see also *The Quantum Hall Effect*, 2nd ed., edited by R. E. Prange and S. M. Girvin (Springer-Verlag, New York, 1990).
²⁹F. D. Haldane, *Phys. Rev. Lett.* **55**, 2095 (1985).
³⁰F. D. M. Haldane and E. H. Rezayi, *Phys. Rev. Lett.* **54**, 237 (1985).
³¹Z. Papić, N. Regnault, and S. Das Sarma, *Phys. Rev. B* **80**, 201303 (2009).
³²X.-G. Wen and A. Zee, *Phys. Rev. B* **58**, 15717 (1998).
³³M. Milovanović and N. Read, *Phys. Rev. B* **53**, 13559 (1996).
³⁴Hao Wang, D. N. Sheng, and F. D. M. Haldane, *Phys. Rev. B* **80**,

- 241311 (2009).
- ³⁵D. Yoshioka, B. I. Halperin, and P. A. Lee, *Phys. Rev. Lett.* **50**, 1219 (1983); D. Yoshioka, *Phys. Rev. B* **29**, 6833 (1984).
- ³⁶M. Peterson, Th. Jolicoeur, and S. Das Sarma, *Phys. Rev. B* **78**, 155308 (2008); *Phys. Rev. Lett.* **101**, 016807 (2008).
- ³⁷M. Storni, R. H. Morf, and S. Das Sarma, *Phys. Rev. Lett.* **104**, 076803 (2010).
- ³⁸A. Auerbach, *Interacting Electrons and Quantum Magnetism* (Springer-Verlag, 1994).
- ³⁹This is equivalent to imposing the following constraint for the BCS Hamiltonian (1) with only a tunneling term Δ_{SAS} : the increase of the tunneling Δ_{SAS} is followed by the decrease in the chemical potential μ by twice the same amount, $\delta\mu + \delta\Delta_{SAS}/2 = 0$, in our simplified model to maintain the chemical potential of the even channel, $\mu^e = \mu + \Delta_{SAS}/2$, stay constant.
- ⁴⁰G. A. Csáthy, Hwayong Noh, D. C. Tsui, L. N. Pfeiffer, and K. W. West, *Phys. Rev. Lett.* **94**, 226802 (2005).
- ⁴¹J. Nuebler, V. Umansky, R. Morf, M. Heiblum, K. von Klitzing, and J. Smet, *Phys. Rev. B* **81**, 035316 (2010).
- ⁴²Edward H. Rezayi and Steven H. Simon, [arXiv:0912.0109](https://arxiv.org/abs/0912.0109) (unpublished).
- ⁴³W. Bishara and C. Nayak, *Phys. Rev. B* **80**, 121302 (2009).

Search Search History

All Databases

<< Return to Web of Science®

Citing Articles Title: **Atypical Fractional Quantum Hall Effect in Graphene at Filling Factor 1/3**
 Author(s): Papic, Z.; Goerbig, M. O.; Regnault, N.
 Source: PHYSICAL REVIEW LETTERS Volume: 105 Issue: 17 Article Number: 176802 DOI: 10.1103/PhysRevLett.105.176802 Published: OCT 19 2010

This item has been cited by items indexed in the databases listed below. [more information]

- 17 in All Databases
- 17 publication in Web of Science
- 0 publication in BIOSIS Citation Index
- 0 publication in ScELO Citation Index
- 0 publication in Chinese Science Citation Database
- 0 data sets in Data Citation Index
- 0 publication in Data Citation Index

Results: 17 Page 1 of 1 Go Sort by: Publication Date -- newest to oldest

Create Citation Report

Hide Refine

Refine Results

Search within results for

Search

Databases

Research Domains Refine

SCIENCE TECHNOLOGY

Research Areas Refine

PHYSICS

SCIENCE TECHNOLOGY OTHER TOPICS

MATERIALS SCIENCE

more options / values...

Document Types

Authors

Group/Corporate Authors

Editors

Funding Agencies

Source Titles

Conference/Meeting Titles

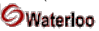

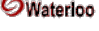
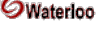







Publication Years

Languages

Countries/Territories

Select Page Add to Marked List (0) Send to: my.endnote.com

1. Title: **Fractional and integer quantum Hall effects in the zeroth Landau level in graphene**
 Author(s): Abanin, Dmitry A.; Feldman, Benjamin E.; Yacoby, Amir, et al.
 Source: PHYSICAL REVIEW B Volume: 88 Issue: 11 Article Number: 115407 DOI: 10.1103/PhysRevB.88.115407 Published: SEP 4 2013
 Times Cited: 0 (from All Databases)
 Get it! Waterloo [View abstract]
2. Title: **Fractional Quantum Hall Phase Transitions and Four-Flux States in Graphene**
 Author(s): Feldman, Benjamin E.; Levin, Andrei J.; Krauss, Benjamin, et al.
 Source: PHYSICAL REVIEW LETTERS Volume: 111 Issue: 7 Article Number: 076802 DOI: 10.1103/PhysRevLett.111.076802 Published: AUG 16 2013
 Times Cited: 2 (from All Databases)
 Get it! Waterloo [View abstract]
3. Title: **Fractional quantum Hall effect of topological surface states under a strong tilted magnetic field**
 Author(s): Zheng, Fawei; Wang, Zhigang; Fu, Zhen-Guo, et al.
 Source: EPL Volume: 103 Issue: 2 Article Number: 27001 DOI: 10.1209/0295-5075/103/27001 Published: JUL 2013
 Times Cited: 0 (from All Databases)
 Get it! Waterloo [View abstract]
4. Title: **Fractional quantum Hall effect in a tilted magnetic field**
 Author(s): Papic, Z.
 Source: PHYSICAL REVIEW B Volume: 87 Issue: 24 Article Number: 245315 DOI: 10.1103/PhysRevB.87.245315 Published: JUN 27 2013
 Times Cited: 2 (from All Databases)
 Get it! Waterloo [View abstract]
5. Title: **EXPLANATION OF COMPOSITE FERMION STRUCTURE IN FRACTIONAL QUANTUM HALL SYSTEMS**
 Author(s): Jacak, Janusz; Gonczarek, Ryszard; Jacak, Lucjan, et al.
 Source: INTERNATIONAL JOURNAL OF MODERN PHYSICS B Volume: 26 Issue: 23 Article Number: 1230011 DOI: 10.1142/S0217979212300113
 Published: SEP 20 2012
 Times Cited: 0 (from All Databases)
 Get it! Waterloo [View abstract]
6. Title: **Unconventional Sequence of Fractional Quantum Hall States in Suspended Graphene**
 Author(s): Feldman, Benjamin E.; Krauss, Benjamin; Smet, Jurgen H., et al.
 Source: SCIENCE Volume: 337 Issue: 6099 Pages: 1196-1199 DOI: 10.1126/science.1224784 Published: SEP 7 2012
 Times Cited: 13 (from All Databases)
 Get it! Waterloo [View abstract]
7. Title: **Spin and valley quantum Hall ferromagnetism in graphene**
 Author(s): Young, A. F.; Dean, C. R.; Wang, L., et al.
 Source: NATURE PHYSICS Volume: 8 Issue: 7 Pages: 550-556 DOI: 10.1038/nphys2307 Published: JUL 2012
 Times Cited: 24 (from All Databases)
 Get it! Waterloo [View abstract]
8. Title: **Multi-component fractional quantum Hall states in graphene: SU(4) versus SU(2)**
 Author(s): Toke, C.; Jain, J. K.
 Source: JOURNAL OF PHYSICS-CONDENSED MATTER Volume: 24 Issue: 23 Article Number: 235601 DOI: 10.1088/0953-8984/24/23/235601
 Published: JUN 13 2012
 Times Cited: 5 (from All Databases)
 Get it! Waterloo [View abstract]
9. Title: **Stability of the k=3 Read-Rezayi state in chiral two-dimensional systems with tunable interactions**
 Author(s): Abanin, D. A.; Papic, Z.; Barlas, Y., et al.
 Source: NEW JOURNAL OF PHYSICS Volume: 14 Article Number: 025009 DOI: 10.1088/1367-2630/14/2/025009 Published: FEB 28 2012
 Times Cited: 1 (from All Databases)
 Get it! Waterloo [View abstract]

10. Title: [Quantum Hall effects in graphene-based two-dimensional electron systems](#)
 Author(s): Barlas, Yafis; Yang, Kun; MacDonald, A. H.
 Source: NANOTECHNOLOGY Volume: 23 Issue: 5 Article Number: 052001 DOI: 10.1088/0957-4484/23/5/052001 Published: FEB 10 2012
 Times Cited: 17 (from All Databases)
 Get it!  [[View abstract](#)]
11. Title: [Numerical studies of the fractional quantum Hall effect in systems with tunable interactions](#)
 Author(s): Papic, Z.; Abanin, D. A.; Barlas, Y.; et al.
 Book Editor(s): Stocks, GM; Tropicovsky, MC
 Conference: 23rd IUPAP C20 Conference on Computational Physics (CCP) Location: Gatlinburg, TN Date: OCT 30-NOV 03, 2011
 Sponsor(s): Int Union Pure & Appl Phys (IUPAP); Int Union Pure & Appl Phys (IUPAP), Commiss Computat Phys (C20); Amer Phys Soc, Div Computat Phys (APS-DCOMP); Oak Ridge Natl Lab (ORNL); Ctr Defect Phys (CDP); Univ Tennessee (UT)ORNL, Joint Inst Computat Sci (JICS); Cray, Inc
 Source: IUPAP C20 CONFERENCE ON COMPUTATIONAL PHYSICS (CCP 2011) Book Series: Journal of Physics Conference Series Volume: 402 Article Number: 012020 DOI: 10.1088/1742-6596/402/1/012020 Published: 2012
 Times Cited: 1 (from All Databases)
 Get it!  [[View abstract](#)]
12. Title: [Theoretical aspects of the fractional quantum Hall effect in graphene](#)
 Author(s): Goerbig, M. O.; Regnault, N.
 Conference: Nobel Symposium on Graphene and Quantum Matter Location: Saltsjobaden, SWEDEN Date: MAY 27-31, 2010
 Source: PHYSICA SCRIPTA Volume: T146 Article Number: 014017 DOI: 10.1088/0031-8949/2012/T146/014017 Published: JAN 2012
 Times Cited: 4 (from All Databases)
 Get it!  [[View abstract](#)]
13. Title: [Tunable interactions and phase transitions in Dirac materials in a magnetic field](#)
 Author(s): Papic, Z.; Abanin, D. A.; Barlas, Y.; et al.
 Source: PHYSICAL REVIEW B Volume: 84 Issue: 24 Article Number: 241306 DOI: 10.1103/PhysRevB.84.241306 Published: DEC 19 2011
 Times Cited: 9 (from All Databases)
 Get it!  [[View abstract](#)]
14. Title: [Electronic properties of graphene in a strong magnetic field](#)
 Author(s): Goerbig, M. O.
 Source: REVIEWS OF MODERN PHYSICS Volume: 83 Issue: 4 Pages: 1193-1243 DOI: 10.1103/RevModPhys.83.1193 Published: NOV 3 2011
 Times Cited: 75 (from All Databases)
 Get it!  [[View abstract](#)]
15. Title: [Tunable Electron Interactions and Fractional Quantum Hall States in Graphene](#)
 Author(s): Papic, Z.; Thomale, R.; Abanin, D. A.
 Source: PHYSICAL REVIEW LETTERS Volume: 107 Issue: 17 Article Number: 176602 DOI: 10.1103/PhysRevLett.107.176602 Published: OCT 17 2011
 Times Cited: 17 (from All Databases)
 Get it!  [[View abstract](#)]
16. Title: [Multicomponent fractional quantum Hall effect in graphene](#)
 Author(s): Dean, C. R.; Young, A. F.; Cadden-Zimansky, P.; et al.
 Source: NATURE PHYSICS Volume: 7 Issue: 9 Pages: 693-696 DOI: 10.1038/NPHYS2007 Published: SEP 2011
 Times Cited: 83 (from All Databases)
 Get it!  [[View abstract](#)]
17. Title: [Quantum Hall effect in graphene: Status and prospects](#)
 Author(s): Sahoo, S.
 Source: INDIAN JOURNAL OF PURE & APPLIED PHYSICS Volume: 49 Issue: 6 Pages: 367-371 Published: JUN 2011
 Times Cited: 0 (from All Databases)
 Get it!  [[View abstract](#)]
- Select Page  Add to Marked List (0)   Send to:

Results: 17 Page 1 of 1 Sort by:

17 records matched your query of the 55,067,330 (contains duplicates) in the data limits you selected.

View in: [简体中文](#) | [繁體中文](#) | [English](#) | [日本語](#) | [한국어](#) | [Português](#) | [Español](#)© 2013 Thomson Reuters | [Terms of Use](#) | [Privacy Policy](#) | Please give us your feedback on using Web of Knowledge.

Atypical Fractional Quantum Hall Effect in Graphene at Filling Factor 1/3

Z. Papić,^{1,2,3} M. O. Goerbig,¹ and N. Regnault²

¹Laboratoire de Physique des Solides, CNRS UMR 8502, Univ. Paris-Sud, F-91405 Orsay cedex, France

²Laboratoire Pierre Aigrain, Département de Physique, ENS, CNRS, 24 Rue Lhomond, F-75005 Paris, France

³Institute of Physics, University of Belgrade, P.O. Box 68, 11 000 Belgrade, Serbia

(Received 2 June 2010; published 19 October 2010)

We study, with the help of exact-diagonalization calculations, a four-component trial wave function that may be relevant for the recently observed graphene fractional quantum Hall state at a filling factor $\nu_G = 1/3$. Although it is adiabatically connected to a 1/3 Laughlin state in the upper spin branch, with SU(2) valley-isospin ferromagnetic ordering and a completely filled lower spin branch, it reveals physical properties beyond such a state that is the natural ground state for a large Zeeman effect. Most saliently, it possesses at experimentally relevant values of the Zeeman gap low-energy spin-flip excitations that may be unveiled in inelastic light-scattering experiments.

DOI: 10.1103/PhysRevLett.105.176802

PACS numbers: 73.43.Nq, 71.10.Pm, 73.20.Qt

The recent observation of the fractional quantum Hall effect (FQHE) in graphene [1,2] has proven the relevance of Coulomb interactions in this novel two-dimensional (2D) electron system, in agreement with theoretical expectations [3–8]. The most pronounced state is the one found when the ratio $\nu_G = n_{\text{el}}/n_B$ between the electronic density n_{el} and that of the flux quanta $n_B = eB/h$ is $\nu_G = 1/3$. Although this state is reminiscent, at first sight, of the prominent 1/3 state observed in semiconductor heterostructures [9], which is described to great accuracy by the Laughlin state [10], several questions arise when taking fully into account the four-component structure of graphene, due to its fourfold spin-valley degeneracy. Whereas first numerical approaches [5] considered the physical spin to be frozen by the Zeeman effect and concentrated on the valley-isospin degree of freedom in a two-component system, a four-component approach [8] seems to be more appropriate in view of the rather small energy scale associated with the Zeeman effect Δ_Z , when compared to the leading energy scale of the Coulomb interaction, $e^2/\epsilon l_B$ at the magnetic length $l_B = \sqrt{\hbar c/eB}$. Indeed for a g factor of 2 [11], one obtains $\Delta_Z/(e^2/\epsilon l_B) \sim 0.002\sqrt{B[T]} \times \epsilon$, where ϵ is the relative dielectric constant.

A further complication arises in graphene, as compared to the 2D electron gas in semiconductor heterostructures, when one considers the definition of the filling factor ν_G , which is proportional to the carrier density n_{el} . In graphene, the carrier density vanishes at the Dirac point, where the spectrum is particle-hole symmetric. In the presence of a magnetic field, a fourfold degenerate zero-energy Landau level (LL) is formed that happens to be half filled when $n_{\text{el}} = 0$ and thus $\nu_G = 0$ —the situation at $\nu_G = 0$ is therefore more reminiscent of a filling factor of $\nu = 2$ in a usual four-component quantum Hall system [8], and the observed FQHE at $\nu_G = 1/3$ corresponds to a situation where two of the four spin-valley subbranches are completely filled and a third one 1/3 filled ($\nu = 2 + 1/3$).

As a consequence the observed FQHE is not a simple Laughlin state with an SU(4)-spin-valley ferromagnetic ordering, which would arise at $\nu_G = -2 + 1/3$ (or by particle-hole symmetry, at $\nu_G = 2 - 1/3$) [6,8]. A natural candidate for large values of the Zeeman gap would then be a valley-SU(2)-ferromagnetic Laughlin state $\Psi_{\downarrow L}^{\nu-\text{SU}(2)}$ in the spin- \downarrow branch of the zero-energy LL similar to the usual 1/3 physics. In this scenario, both states K and K' are completely filled in the spin- \uparrow branch. The small relative value of the Zeeman gap, however, casts doubt on such a scenario of complete spin polarization induced by an external field, without considering a cooperative effect mediated by the Coulomb interaction.

Here, we analyze the system in the zero-energy LL with the help of exact-diagonalization (ED) calculations for relativistic electrons in the spherical geometry with SU(4) symmetry that interact via the Coulomb interaction [4,5,8]. We show that already for a very small Zeeman effect, one may obtain a FQHE at $\nu_G = 1/3$ in graphene. This state may be described in terms of a four-component Halperin wave function $\Psi_{2+1/3}^{\text{SU}(4)}$ which is adiabatically connected to the valley-SU(2)-ferromagnetic state in the upper spin branch. The latter is the natural ground state for a large Zeeman splitting. Most saliently, in spite of this adiabatic connection, the low-energy excitations in an intermediate range of the Zeeman splitting are different from those of the simple SU(2) Laughlin state. In addition to the charge-density-wave mode with its characteristic magnetoroton minimum and the valley-isospin wave (ISW), which is the Goldstone mode associated with the spontaneous valley-isospin breaking in the spin- \downarrow branch, we find a low-energy spin-flip mode with a gap that depends linearly on the Zeeman coupling. These modes may be experimentally accessible in inelastic light-scattering measurements that have revealed similar modes in conventional quantum Hall systems in GaAs heterostructures [12,13]. That electrons in graphene reside at the sample

surface makes this novel 2D electron system even better adapted to optical measurements than the latter.

In order to describe the FQHE state at $\nu_G = 1/3$, which corresponds to a filling factor of $\nu = 2 + 1/3$ when counted from the bottom of the central $n = 0$ LL, we investigate the trial four-component wave function

$$\Psi_{2+1/3}^{\text{SU}(4)} = \prod_{\xi=K,K'} \prod_{i<j} (z_i^{\downarrow,\xi} - z_j^{\downarrow,\xi})^3 \times \prod_{i,j} (z_i^{\downarrow,K} - z_j^{\downarrow,K'})^3 \prod_{\xi=K,K'} \prod_{i<j} (z_i^{\uparrow,\xi} - z_j^{\uparrow,\xi}), \quad (1)$$

where $z_j^{\sigma,\xi}$ denotes the complex coordinate of the j th electron in the spin-valley subbranch σ , ξ ($\sigma = \uparrow$ or \downarrow and $\xi = K$ or K'). We have omitted a ubiquitous Gaussian factor in the expression. Notice that, in the absence of a symmetry-breaking field, the wave function (1) is not a good trial state because the Coulomb interaction potential respects the SU(4)-spin-valley symmetry [4,14], whereas the wave function (1) is not an eigenstate of the SU(4)-Casimir operators.

This is indeed corroborated by our ED calculations for $N = 17$ particles with $N_B = 6$ flux quanta threading the sphere, the relation between N and N_B being $N_B = (3/7)N - 9/7$ for the state (1) [15], which yields the required filling $\nu = 7/3$ in the thermodynamic limit. The ground state is then found in spin sectors different from that, $2S_z = 11$, expected for the state (1). A simple manner to stabilize the state (1) is to use appropriate pseudopotentials [16] that break the SU(4)-spin-valley symmetry in the interaction potential. However, surprisingly, this trial state becomes the ground state also when the SU(4) symmetry is broken by an external field—e.g., a very small value of the Zeeman effect turns out to be sufficient, $\Delta_Z^1 \approx 0.01 e^2/\epsilon l_B$, which is a tiny fraction of the leading Coulomb interaction energy scale $e^2/\epsilon l_B \sim 625(\sqrt{B[T]}/\epsilon)$ K. In a typical experimental situation, the $1/3$ state has been found at a magnetic field of roughly $B \sim 9, \dots, 12$ T [1,2], which corresponds to a ratio of $\Delta_Z/(e^2/\epsilon l_B) \sim 0.006, \dots, 0.008\epsilon$ if one uses $g \sim 2$ [11]. This value is slightly smaller than our theoretical estimate if one considers the smallest possible value of the dielectric constant ($\epsilon = 1$ for freestanding graphene). However, virtual interband excitations lower the dielectric constant that becomes $\epsilon_\infty \approx 4$ for freestanding graphene in the large-wave-vector limit [17], also in a strong magnetic field [18], and the precise value of the dielectric constant in graphene remains an open issue. Notice that it is even still under debate whether the Zeeman splitting is indeed the dominant SU(4)-symmetry-breaking perturbation or whether the valley splitting is more relevant. Our theory and the conclusions of this Letter, however, remain valid also in the latter case if one interchanges the role of spin and valley isospin and if one replaces Δ_Z by a “valley Zeeman effect” [19].

The energy spectrum, which we have obtained in ED calculations, is shown in Fig. 1 as a function of the Zeeman gap Δ_Z . Above the critical value Δ_Z^1 , the ground state is

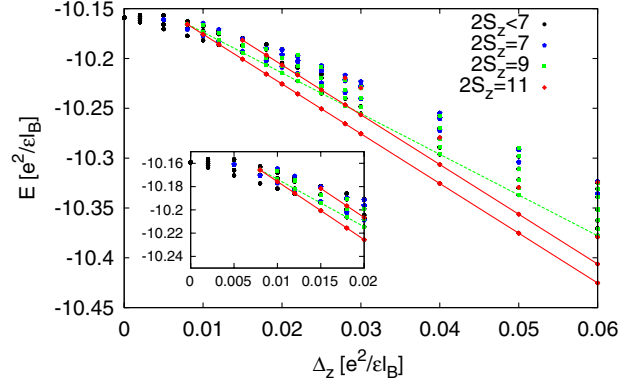


FIG. 1 (color online). Energy spectrum for $N = 17$ electrons at a filling factor $\nu_G = 1/3$ ($\nu = 2 + 1/3$), as a function of Δ_Z , obtained from ED calculations of the Coulomb interaction on the sphere ($N_B = 6$) with implemented SU(4) symmetry. Above $\Delta_Z^1 \approx 0.01 e^2/\epsilon l_B$ the ground state is found in the maximally spin-polarized sector ($2S_z = 11$, red diamonds). The inset shows a zoom on the region for small values of Δ_Z .

found in the maximally polarized spin sector that corresponds to the state (1), whereas the excited state with the lowest energy is in the same spin sector, $2S_z = 11$, only above a second value $\Delta_Z^2 \approx 0.03 e^2/\epsilon l_B$. For values of the Zeeman gap $\Delta_Z^1 \leq \Delta_Z \leq \Delta_Z^2$, the excited state with lowest energy is found in the spin sector $2S_z = 9$. Above Δ_Z^2 , however, the energy cost of this spin-flip excitation (SF, see Fig. 2) is larger than the lowest-lying excitation in the fully polarized sector $2S_z = 11$ (C in Fig. 2).

These results suggest that the state (1) may have physical properties beyond the simple $1/3$ Laughlin state in the spin- \downarrow branch, in the form of coherent spin-flip excitations in an intermediate range of Zeeman gaps. In order to test this scenario in more detail, we have investigated the two-component wave function

$$\Psi_{1+1/3}^{\text{SU}(2)} = \prod_{i<j} (z_i^{\downarrow} - z_j^{\downarrow})^3 \prod_{i<j} (z_i^{\uparrow} - z_j^{\uparrow}), \quad (2)$$

which would be a candidate in a two-component quantum Hall system, such as a conventional 2D electron gas in a GaAs heterostructure, at a filling factor $\nu = 1 + 1/3$. It is

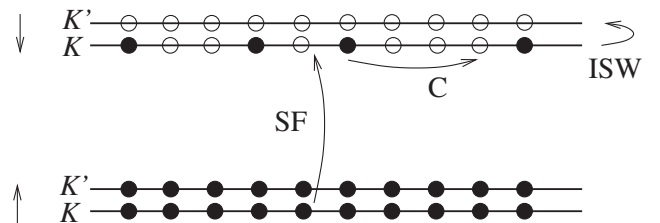


FIG. 2. Classification of the excitations of the $\Psi_{1/3}^{\text{SU}(4)}$ state. The excitations of a one-component Laughlin state are found in the same spin-valley sector (C), whereas the Goldstone mode due to the broken SU(2) valley-isospin symmetry in the spin- \downarrow branch is an isospin-wave mode (ISW). In addition to these conventional modes, the four-component state (1) possesses a spin-flip (SF) mode.

insofar related to the four-component wave function (1) as it describes the same physical situation if the valley-isospin degree of freedom for spin- \downarrow electrons is neglected. The novel wave function (2) therefore does not reveal any valley-ISW mode (see Fig. 2) that is the Goldstone mode of the spontaneously broken valley-SU(2) symmetry in the spin- \downarrow branch and that may eventually become gapped if one takes into account a possible valley splitting. In contrast to its four-component analogue (1), the two-component wave function (2) allows for a more detailed study of different system sizes in ED with an implemented SU(2) symmetry. Indeed, our ED calculations with an implemented SU(4) symmetry allowed only for one single system size ($N = 17$ particles, only $N_1 = 3$ populate the upper spin branch), in which case the subspace with maximal spin polarization ($2S_z = 11$) is of dimension one such that the overlap with the wave function (1) is trivially 1.

Figure 3(a) shows the energy spectrum for $N = 22$ particles and $N_B = 15$ flux quanta, in the different spin

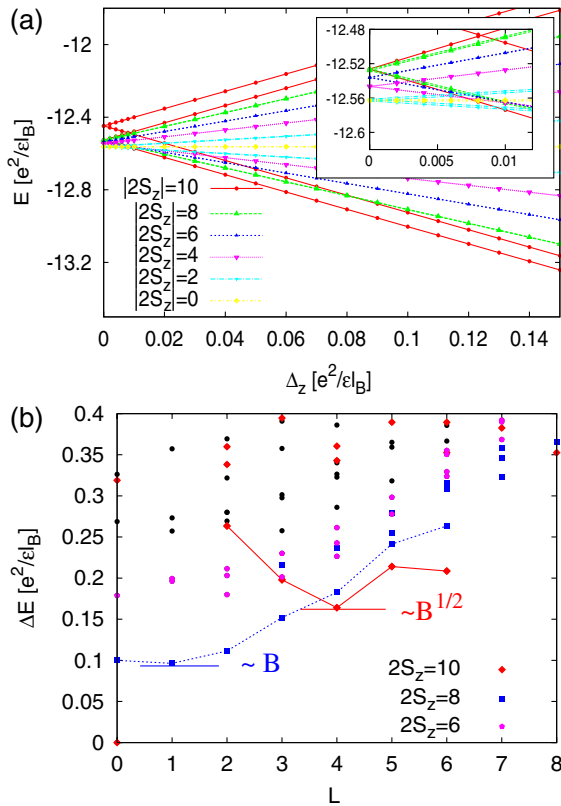


FIG. 3 (color online). (a) Energy spectrum for $N = 22$ electrons at a filling factor $\nu = 1 + 1/3$, as a function of Δ_Z in the different spin sectors $2S_z$, obtained from ED calculations of the Coulomb interaction on the sphere ($N_B = 15$) with implemented SU(2) symmetry. The inset shows a zoom on the region for small values of Δ_Z . (b) Excitation spectrum at $\Delta_Z = 0.05e^2/\epsilon l_B$, as a function of the angular momentum L . The energy is measured with respect to the ground state (at $L = 0$). The spin-flip mode is found in the $2S_z = 8$ sector (blue squares) and scales linearly in B , whereas the $2S_z = 10$ sector reveals the usual magnetoroton branch (red diamonds), which scales as \sqrt{B} with the B field.

sectors, obtained by ED of the SU(2) Coulomb interaction potential in the lowest LL. The spectrum is in qualitative agreement with that obtained for the four-component system at $\nu = 2 + 1/3$ (Fig. 1)—because the wave function (2) is not an eigenstate of the SU(2)-symmetric Coulomb potential, it does not describe the ground state at $\Delta_Z = 0$, where one obtains a threefold degenerate state (with $2S_z = 0, \pm 2$), but in a compressible sector ($L \neq 0$). As for the four-component case, a small symmetry-breaking Zeeman gap $\Delta_Z^1 \approx 0.01e^2/\epsilon l_B$ suffices to stabilize a state with maximal spin polarization ($2S_z = 10$ and $N_1 = 6$), which has an overlap of 99% with the wave function (2) [20], and the lowest-lying excited state in an intermediate range of the Zeeman gap, $\Delta_Z^1 \leq \Delta_Z \leq \Delta_Z^2 \approx 0.08e^2/\epsilon l_B$, involves a spin flip as it is found in the spin sector $2S_z = 8$.

It has been argued that, for vanishing Zeeman splitting, the state at $\nu = 1 + 1/3$ should be a spin-singlet composite-fermion (CF) state with reversed flux attachment [21]. Hund's rule, according to which the system chooses a maximally polarized spin inside each energy level, would then predict an unpolarized state because $\nu = 2/3$ corresponds to a completely filled lowest CF LL [21], but the same rule favors a completely polarized state if applied to the original electron coordinates. Our results indicate that already for a very small Zeeman splitting, a completely polarized state is favored that satisfies the electronic instead of the CF version of Hund's rule. Notice, however, that a direct numerical comparison between both states, CF spin singlet and state (2), is problematic in the spherical geometry because the spin-singlet state has a different flux-particle-number relation, $N_B = (3/4)N - 1$, than the polarized state (2), $N_B = (3/4)N - 3/2$. We find for $N = 20$ and $N_B = 14$ (results not shown) that the ground state is indeed a singlet at low Zeeman splittings, but it is maximally polarized above a value of $\Delta_Z/(e^2/\epsilon l_B) \sim 0.03$, which is on the same order of magnitude as Δ_Z^1 .

In order to gain further insight into the nature of the low-lying excitations, we have calculated the spectrum [Fig. 3(b)] at an intermediate value of the Zeeman gap, $\Delta_Z = 0.05e^2/\epsilon l_B$, where spin-flip excitations are expected to be relevant. The spectrum is now plotted as a function of the angular momentum in order to make apparent possible low-energy collective excitations of the incompressible state (2). Within the charge sector with no change in the spin polarization, one observes in Fig. 3(b) the usual magnetoroton branch (red diamonds) [22] which arises from gapped density-wave excitations [23] and which is a prominent feature of Laughlin-type physics. However, another mode is apparent in Fig. 3(b) that indicates the presence of collective excitations beyond the usual one-component Laughlin state and that is precisely a spin-flip excitation (blue squares). This mode, which is the lowest-energy excitation in the low- L regime, is well separated from the high-energy part of the excitation spectrum, such that it is likely to be a true collective mode. Notice that in the large- L

limit, the magnetoroton branch has a lower energy, and one may thus conjecture that the activation gap, i.e., the energy to create a well-separated quasi particle-quasihole pair at large values of L , does not involve a spin-flip excitation but is governed by one-component Laughlin physics.

The relevance of collective spin-flip excitations in an intermediate Zeeman-gap range may eventually be tested experimentally in inelastic light-scattering experiments that are capable of probing collective excitations at finite wave vectors [12,13]. Indeed, these experiments probe characteristic parts of the dispersion relation that show an enhanced density of states (such as at its minima and maxima). Because the spin-flip mode in Fig. 3(b) is almost flat at low angular momenta L that correspond to small wave vectors, one may expect an enhanced peak in such inelastic light-scattering measurements, at energies in the $0.1e^2/\epsilon l_B$ range (roughly half of the energy of the magnetoroton minimum, for the particular choice $\Delta_Z = 0.05e^2/\epsilon l_B$). As one may see in Fig. 3, the spin-flip excitation scales linearly with the Zeeman gap, such that the associated peak is expected to scale linearly with the magnetic field as well, whereas that of the usual magnetoroton would scale as \sqrt{B} [see Fig. 3(b)]. The observation of such a linear B -field dependence of the light-scattering peak would be clear evidence for the relevance of spin flip, beyond the properties of the Laughlin liquid, of the $\nu_G = 1/3$ state in graphene.

In conclusion, we have shown, within ED calculations for a four- and a two-component system on the sphere, how a FQHE can arise in graphene at $\nu_G = 1/3$ even at very small values of a spin-valley symmetry-breaking Zeeman field. Although the leading energy scale is given by the SU(4)-invariant Coulomb interaction, a small Zeeman gap $\Delta_Z/(e^2/\epsilon l_B) \sim 0.01$ is sufficient to fully polarize the electronic spin and thus to stabilize the state (1) which we have identified as being responsible for the observed graphene FQHE [1,2]. In spite of its reminiscence with the Laughlin state, novel collective excitations that are inherent to the four-component character of graphene determine the low-energy spectrum at intermediate values of the Zeeman gap, $\Delta_Z^1 \leq \Delta_Z \leq \Delta_Z^2$, that correspond to the experimental situation in which the FQHE has been observed. In order to gain further insight into the nature of these spin-flip excitations, which may be visible in inelastic light-scattering experiments, we have performed ED calculations in an analogous two-component quantum Hall system at a filling factor $\nu = 1 + 1/3$ that corresponds to a completely filled spin- \uparrow and a one-third filled spin- \downarrow branch. The spin-flip excitation is well separated from the high-energy part of the energy spectrum thus indicating its collective nature, in addition to the usual magnetoroton branch that determines the low-energy spectrum in the large angular-momentum regime.

This work was supported by Agence Nationale de la Recherche under Grant No. ANR-JCJC-0003-01 and by grants from Région Ile-de-France. Z.P. was furthermore supported by the Serbian Ministry of Science under Grant

No. 141035. We acknowledge fruitful discussions with Ch. Glattli and M. Milovanović.

-
- [1] X. Du, I. Skachko, F. Duerr, A. Luican, and E. Y. Andrei, *Nature (London)* **462**, 192 (2009).
 - [2] K. I. Bolotin, F. Ghahari, M. D. Shulman, H. L. Stormer, and P. Kim, *Nature (London)* **462**, 196 (2009).
 - [3] N. M. R. Peres, F. Guinea, and A. H. Castro Neto, *Phys. Rev. B* **73**, 125411 (2006).
 - [4] M. O. Goerbig, R. Moessner, and B. Douçot, *Phys. Rev. B* **74**, 161407 (2006).
 - [5] V. M. Apalkov and T. Chakraborty, *Phys. Rev. Lett.* **97**, 126801 (2006); C. Töke, P. E. Lammert, V. H. Crespi, and J. K. Jain, *Phys. Rev. B* **74**, 235417 (2006).
 - [6] K. Yang, S. Das Sarma, and A. H. MacDonald, *Phys. Rev. B* **74**, 075423 (2006).
 - [7] D. V. Khveshchenko, *Phys. Rev. B* **75**, 153405 (2007).
 - [8] C. Töke and J. K. Jain, *Phys. Rev. B* **75**, 245440 (2007); M. O. Goerbig and N. Regnault, *Phys. Rev. B* **75**, 241405 (2007); for a review on the theory of the FQHE in graphene, see Z. Papić, M. O. Goerbig, and N. Regnault, *Solid State Commun.* **149**, 1056 (2009).
 - [9] D. C. Tsui, H. L. Stormer, and A. C. Gossard, *Phys. Rev. Lett.* **48**, 1559 (1982).
 - [10] R. B. Laughlin, *Phys. Rev. Lett.* **50**, 1395 (1983).
 - [11] Y. Zhang, Z. Jiang, J. P. Small, M. S. Purewal, Y.-W. Tan, M. Fazlollahi, J. D. Chudow, J. A. Jaszczak, H. L. Stormer, and P. Kim, *Phys. Rev. Lett.* **96**, 136806 (2006).
 - [12] M. A. Eriksson, A. Pinczuk, B. S. Dennis, S. H. Simon, L. N. Pfeiffer, and K. W. West, *Phys. Rev. Lett.* **82**, 2163 (1999); Y. Gallais, T. H. Kirschenmann, I. Dujovne, C. F. Hirjibehedin, A. Pinczuk, B. S. Dennis, L. N. Pfeiffer, and K. W. West, *Phys. Rev. Lett.* **97**, 036804 (2006).
 - [13] For a review, see A. Pinczuk, in *Perspectives in Quantum Hall Effects*, edited by S. Das Sarma and A. Pinczuk (John Wiley, New York, 1997).
 - [14] J. Alicea and M. P. A. Fisher, *Phys. Rev. B* **74**, 075422 (2006).
 - [15] R. de Gail, N. Regnault, and M. O. Goerbig, *Phys. Rev. B* **77**, 165310 (2008).
 - [16] F. D. M. Haldane, *Phys. Rev. Lett.* **51**, 605 (1983).
 - [17] J. González, F. Guinea, and M. A. H. Vozmediano, *Phys. Rev. B* **59**, R2474 (1999).
 - [18] K. Shizuya, *Phys. Rev. B* **75**, 245417 (2007); R. Roldán, J.-N. Fuchs, and M. O. Goerbig, *Phys. Rev. B* **80**, 085408 (2009).
 - [19] For a recent review, see M. O. Goerbig, [arXiv:1004.3396](https://arxiv.org/abs/1004.3396), and references therein.
 - [20] Notice that the subspace $2S_z = 10$ is of dimension 6, instead of 1, for the subspace with maximal spin polarization in the SU(4) calculation with $N = 17$ electrons.
 - [21] X. G. Wu, G. Dev, and J. K. Jain, *Phys. Rev. Lett.* **71**, 153 (1993); J. K. Jain and X. G. Wu, *Phys. Rev. B* **49**, 5085 (1994).
 - [22] F. D. M. Haldane and E. H. Rezayi, *Phys. Rev. Lett.* **54**, 237 (1985); G. Fano, F. Ortolani, and E. Colombo, *Phys. Rev. B* **34**, 2670 (1986).
 - [23] S. M. Girvin, A. H. MacDonald, and P. M. Platzman, *Phys. Rev. B* **33**, 2481 (1986).

Search Search History

All Databases

<< Return to Web of Science®

Citing Articles Title: Fractional quantum Hall effects in bilayers in the presence of interlayer tunneling and charge imbalance
Author(s): Peterson, Michael R.; Papic, Z.; Das Sarma, S.
Source: PHYSICAL REVIEW B Volume: 82 Issue: 23 Article Number: 235312 DOI: 10.1103/PhysRevB.82.235312 Published: DEC 9 2010

This item has been cited by items indexed in the databases listed below. [more information]

4 in All Databases

- 4 publication in Web of Science
0 publication in BIOSIS Citation Index
0 publication in ScELO Citation Index
0 publication in Chinese Science Citation Database
0 data sets in Data Citation Index
0 publication in Data Citation Index

Results: 4 Page 1 of 1 Go Sort by: Publication Date -- newest to oldest

Create Citation Report

Hide Refine

Refine Results

Search within results for

Search

Databases

Research Domains

SCIENCE TECHNOLOGY

Research Areas

PHYSICS

Document Types

Authors

Group/Corporate Authors

Editors

Funding Agencies

Source Titles

Conference/Meeting Titles

Publication Years

Languages

Countries/Territories

Select Page Add to Marked List (0) Send to: my.endnote.com

1. Landau levels

Title: Variational Monte Carlo study of spin-polarization stability of fractional quantum Hall states against realistic effects in half-filled
Author(s): Biddle, J.; Peterson, Michael R.; Das Sarma, S.
Source: PHYSICAL REVIEW B Volume: 87 Issue: 23 Article Number: 235134 DOI: 10.1103/PhysRevB.87.235134 Published: JUN 25 2013
Times Cited: 1 (from All Databases)

Get it! Waterloo View abstract

2. Topological flat band models with arbitrary Chern numbers

Title: Topological flat band models with arbitrary Chern numbers
Author(s): Yang, Shuo; Gu, Zheng-Cheng; Sun, Kai; et al.
Source: PHYSICAL REVIEW B Volume: 86 Issue: 24 Article Number: 241112 DOI: 10.1103/PhysRevB.86.241112 Published: DEC 28 2012
Times Cited: 13 (from All Databases)

Get it! Waterloo View abstract

3. Quasi-Particle Localization by Disorder in nu=5/2 Fractional Quantum Hall State and Its Potential Application

Title: Quasi-Particle Localization by Disorder in nu=5/2 Fractional Quantum Hall State and Its Potential Application
Author(s): Goswami, P.
Source: ACTA PHYSICA POLONICA A Volume: 122 Issue: 4 Pages: 741-747 Published: OCT 2012
Times Cited: 0 (from All Databases)

Get it! Waterloo View abstract

4. The fractional quantum Hall effect at filling factor 5/2: numerically searching for non-abelian anyons

Title: The fractional quantum Hall effect at filling factor 5/2: numerically searching for non-abelian anyons
Author(s): Peterson, Michael R.
Book Editor(s): Stocks, GM; Tropicovsky, MC
Conference: 23rd IUPAP C20 Conference on Computational Physics (CCP) Location: Gatlinburg, TN Date: OCT 30-NOV 03, 2011
Sponsor(s): Int Union Pure & Appl Phys (IUPAP); Int Union Pure & Appl Phys (IUPAP), Commis Computat Phys (C20); Amer Phys Soc, Div Computat Phys (APS-DCOMP); Oak Ridge Natl Lab (ORNL); Ctr Defect Phys (CDP); Univ Tennessee (UT)/ORNL, Joint Inst Computat Sci (JICS); Cray, Inc
Source: IUPAP C20 CONFERENCE ON COMPUTATIONAL PHYSICS (CCP 2011) Book Series: Journal of Physics Conference Series Volume: 402 Article Number: 012021 DOI: 10.1088/1742-6596/402/1/012021 Published: 2012
Times Cited: 1 (from All Databases)

Get it! Waterloo View abstract

Select Page Add to Marked List (0) Send to: my.endnote.com

Results: 4 Show 50 per page Page 1 of 1 Go Sort by: Publication Date -- newest to oldest

4 records matched your query of the 55,067,330 (contains duplicates) in the data limits you selected.

View in: 简体中文 繁體中文 English 日本語 한국어 Português Español

Fractional quantum Hall effects in bilayers in the presence of interlayer tunneling and charge imbalance

Michael R. Peterson,¹ Z. Papić,^{2,3,4} and S. Das Sarma¹

¹*Condensed Matter Theory Center, Department of Physics, University of Maryland, College Park, Maryland 20742, USA*

²*Institute of Physics, University of Belgrade, Pregrevica 118, 11 000 Belgrade, Serbia*

³*Laboratoire Pierre Aigrain, Ecole Normale Supérieure, CNRS, 24 rue Lhomond, F-75005 Paris, France*

⁴*Laboratoire de Physique des Solides, Université Paris-Sud–CNRS, UMR 8502, F-91405 Orsay Cedex, France*

(Received 5 August 2010; published 9 December 2010)

Two-component fractional quantum Hall systems are providing a major motivation for a large section of the physics community. Here we study two-component fractional quantum Hall systems in spin-polarized half-filled lowest Landau level (filling factor $1/2$) and second Landau level (filling factor $5/2$) with exact diagonalization utilizing both the spherical and torus geometries. The two distinct two-component systems we consider are the true bilayer and effective bilayers (wide-quantum-well). In each model (bilayer and wide-quantum-well) we completely take into account interlayer tunneling and charge imbalancing terms. We find that in the half-filled lowest Landau level, the fractional quantum Hall effect (FQHE) is described by the two-component Abelian Halperin 331 state which is robust to charge imbalancing. In the half-filled second Landau, we find that the FQHE is likely described by the non-Abelian Moore-Read Pfaffian state which is also quite robust to charge imbalancing. Furthermore, we suggest the possibility of experimentally tuning from an Abelian to non-Abelian FQHE state in the second Landau level and comment on recent experimental studies of FQHE in wide-quantum-well structures.

DOI: [10.1103/PhysRevB.82.235312](https://doi.org/10.1103/PhysRevB.82.235312)

PACS number(s): 73.43.-f, 71.10.Pm

We theoretically investigate two-component spin-polarized fractional quantum Hall states in the bilayer half-filled first and second (first excited) Landau levels (LLs) considering the effects of both interlayer tunneling and charge imbalance tunneling using exact diagonalization. The aspect that is different in this work compared to previous studies^{1–5} is that we consider interlayer tunneling along with charge imbalance tunneling. The reason we consider this *extra* tunneling term (charge imbalance), along with the an interlayer tunneling term, is because recent experimental efforts^{6,7} have achieved bilayer fractional quantum Hall effect (FQHE) systems where both the interlayer and charge imbalance tunneling terms can be controlled by varying different system parameters (such as gate voltages) at a total filling factor of $1/2$ (Ref. 8) and a theoretical investigation of the physics of this system is both timely and important. Furthermore, the basic effects produced by a charge imbalance term in a theoretical exact diagonalization context is currently lacking. Before we delve into our results we provide an introduction, motivation, and historical perspective of this broad subject.

I. FRACTIONAL QUANTUM HALL EFFECT IN THE ONE- AND TWO-COMPONENT VARIETY

The FQHE (Refs. 9 and 10) has proved to be the paradigm for emergent quantum physics for the nearly 30 years of its existence. It occurs when electrons are confined to a (quasi-)two-dimensional plane (such as in semiconductor structures, e.g., GaAs/AlGaAs, with electron densities on the order of 10^{10} – 10^{11} cm⁻²) and a strong perpendicular magnetic field is applied (usually on the order of tens of tesla, sometimes up to ~ 40 T). Phenomenologically, the FQHE manifests as a quantized plateau in the Hall resistance R_{xy} (quantized to parts per billion) and a concomitant vanishing

(or deep minimum that displays activated behavior) of the longitudinal resistance R_{xx} . The FQHE is said to occur at rational fractional filling factor ν when the quantized value of the Hall resistance is $R_{xy} = h/(e^2\nu)$, where $\nu = \rho/\phi_0$ (here ρ is the electron density and $\phi_0 = hc/eB$ is the magnetic flux quantum and B is the magnetic field strength, hence, ν is the number of electrons per magnetic flux quanta). The perpendicular magnetic field quantizes the two-dimensional kinetic energy into Landau levels separated in energy by $\hbar\omega_c = \hbar eB/mc$ and when the filling factor ν is made to be fractional (like it is for the FQHE), by either adjusting the electron density and/or magnetic field strength, the kinetic energy is a constant and completely flat bands obtain. In the limit that $\hbar\omega_c \rightarrow \infty$ (or the extreme quantum limit) the electron-electron Coulomb interaction is the dominant term in the Hamiltonian for electrons fractionally filling a LL.

The one-component FQHE in the lowest orbital electronic Landau level is the most often discussed since it has been observed in the form of approximately 80 odd-denominator FQHE states and is well understood.^{10–14} Essentially, the FQHE occurs due to the nonperturbative and electron-electron interaction driven formation of an emergent topologically ordered¹⁵ incompressible quantum fluid at certain filling factors ν with nonzero energy gaps. This (bulk) energy gap, along with some sample disorder, explains the FQHE.¹¹

Recently, the FQHE in half-filled Landau levels has reinvented the community due to its possible connection to topological quantum computing, non-Abelian quasiparticles, and the requisite cutting edge material science advances that have produced much of this physics and continue to coax nature into revealing her secrets. In particular, the FQHE at filling factor $5/2$,¹⁶ which corresponds to filling factor $1/2$ in the second orbital electronic Landau level, has arguably produced most of the excitement.

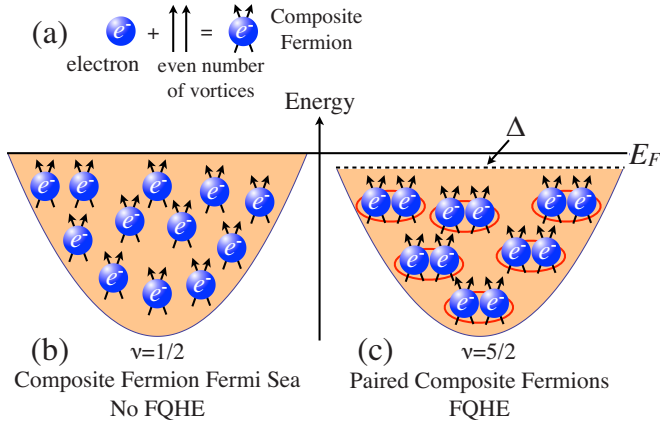


FIG. 1. (Color online) (a) A composite fermion is an electron bound (or attached) to an even number of quantum-mechanical vortices of the many-body wave function, see Refs. 13 and 14. (b) A compressible Fermi sea of composite fermions forms for a one-component system at filling factor $\nu=1/2$ in the lowest Landau level and produces *no FQHE* since a (composite fermion) Fermi sea has no energy gap. (c) In the half-filled second Landau level at $\nu=5/2$ the electron-electron interaction is modified compared to the electron-electron interaction in the lowest Landau level (see text) causing the weakly interacting composite fermions to pair into a spin-polarized *p*-wave BCS state described by the Moore-Read Pfaffian wave function. This state, due to the quasiparticle pairing, has an energy gap and thus exhibits the FQHE.

The denominator of ν for the “standard” fractional quantum Hall states is always odd and reflects the fermionic nature of the quasiparticles. At $\nu=1/(\text{even})$, naive, zeroth-order, theory asserts that no FQHE would be expected. This is because, at $\nu=1/(\text{even})$, the weakly interacting quasiparticles of the FQHE (composite fermions^{13,14}) experience a zero effective magnetic field and form a *gapless* exotic Fermi sea.^{17–19} In fact, no FQHE is experimentally observed in one-component systems at $\nu=1/2$ instead showing signatures of the exotic Fermi sea^{20–22} (see Fig. 1).

The FQHE at $\nu=2+1/2=5/2$ (the 2 comes from completely filling the spin-up and spin-down Landau levels) is particularly interesting and the only known and well-established violator of the “odd-denominator” rule for the one-component FQHE. A one-component FQH state with an even denominator suggests some kind of interaction driven pairing among the weakly interacting emergent (quasi-)fermions and does not find a description within the standard FQHE theory. All FQHE states observed in the second LL (SLL), such as $5/2$, $7/3=2+1/3$, $8/3=2+2/3$, $12/5=2+2/5$, etc. (there are about eight FQHE states observed in the SLL in all) are fragile when compared to the FQHE states in the lowest LL (LLL). The $5/2$ FQHE is one of the, if not the, strongest FQHE states in the SLL and yet has a measured activation gap only about 0.5 K or less. This is despite being measured in the world’s cleanest two-dimensional electron gas samples with mobilities over 30×10^6 cm²/V s at temperatures of less than 100 mK. Hence, there is a strong experimental drive to produce cleaner samples and apparatus capable of doing measurements at exceedingly low temperatures. Most early experimental observations of the

FQHE at $5/2$ indicated the state to be one component in nature.^{23–30} However, care needs to be taken when making broad absolute statements and there is some experimental evidence^{23,28,31} that puts the one-component interpretation of the $5/2$ FQHE into question, but, the interpretation of these results is notoriously difficult.³²

Recently, the FQHE was observed³³ at $\nu=5/2$ in a low magnetic field where the ratio of the cyclotron energy $\hbar\omega_c$ to the Coulomb energy $e^2/\epsilon l$ (where e is the electron charge, ϵ is the dielectric constant of the host semiconductor, and $l = \sqrt{\hbar/eB}$ is the characteristic length scale called the magnetic length) is near unity or less. In that situation, it is not clear how the system would be completely spin polarized and/or would not experience significant Landau-level mixing. Recent experiments^{34–36} have begun to seriously tackle these two issues. Not surprisingly, theoretical groups have enthusiastically taken up the (considerable) challenge of understanding the role of Landau-level mixing.^{37–40} That being said, the FQHE at $5/2$ has also been seen^{41,42} at magnetic field strengths of more than 10 T. A FQH state at fields that high is likely to be spin polarized and, hence, one component. Adding to the confusion is the fact that *all* theoretical work^{43,44} to date have established that, within a wide range of parameter space, the electrons are completely spin polarized at $\nu=5/2$. It is extremely difficult theoretically (computationally) to consider fully spin unpolarized FQHE and until there is definitive experimental evidence indicating the real system to be spin unpolarized we will theoretically consider the electron spin to be absolutely polarized throughout this work.

Arguably, the reason the FQHE at $5/2$ is so fascinating is its connection to topological quantum computing.^{45,46} An intriguing ansatz called the Moore-Read (MR) Pfaffian (Pf) (Ref. 47) is thought to describe the FQHE at $5/2$ and this ansatz has non-Abelian quasiparticle and quasihole excitations. It is proposed⁴⁸ that the world lines of these non-Abelian excitations can be braided around each other, thus changing the ground state in the degenerate manifold of ground states, and certain quantum computing gates can be achieved. This degenerate manifold of states is separated from the continuum by an energy gap that is topological in nature, since it is a FQHE state, thus, any sort of local disturbance to the system, like those caused from typical noise encountered in an experiment, will not be able to destroy the state due to its topological origin. Of course, if the disturbances are of an energy that is larger than the protective gap then the above does not hold. Using the non-Abelian quasiparticles and quasiholes of the MR Pf description of the $5/2$ state of the FQHE to achieve quantum computing gates that are topologically protected (called fault-tolerant topological quantum computation) is a major research goal.⁴⁶ (Note that the non-Abelian quasiparticles that might exist for the FQHE at $5/2$ are so-called Ising anyons and are unable to be used for *universal* quantum computation, see Ref. 46 for more details on this point and how Ising anyons can be augmented to achieve a version of universal fault-tolerant topological quantum computation.)

Intuitively, the existence of the Moore-Read Pfaffian can be understood (see Fig. 1). Any time a Landau level is half-filled (not just at $\nu=1/2$ as mentioned above but also at

$\nu=5/2=2+1/2$) naive zeroth-order theory tells us that a (composite fermion) Fermi sea^{17–19} can form. (Note that in this discussion we assume that the two completely filled Landau levels are inert which is the same as assuming that $\hbar\omega_c \rightarrow \infty$.) As is well known, any system of weakly interacting fermionic quasiparticles is unstable to pairing via the BCS (Refs. 49 and 50) pairing mechanism and, if the quasiparticles are spin polarized, the simplest pairing is chiral p -wave symmetry ($p_x + ip_y$) (see the work by Read and Green in Ref. 51 for a discussion of the BCS mean-field description of the FQHE in a half-filled Landau level.) The resulting paired state has an energy gap and the FQHE will occur as long as the system is clean enough and cold enough such and the Fermi energy lies within the FQHE gap. The Moore-Read Pfaffian wave function encapsulates this physics.

We briefly note that recently it has been pointed out^{52,53} that a competing state for the FQHE at $\nu=5/2$ is the so-called anti-Pfaffian which is the particle-hole conjugate of the Moore-Read Pfaffian. The anti-Pfaffian is topologically distinct from the Pfaffian due to the fact that the two have different edge state behavior which, in principle, makes it possible to tell the two apart experimentally. We emphasize that both the Moore-Read Pfaffian and anti-Pfaffian *both* support non-Abelian quasihole and quasiparticle excitations so both could perform as platforms for fault-tolerant topological quantum computation. Whichever one happens to be responsible (if either) for the FQHE at $\nu=5/2$ depends on how, and if, the particle-hole symmetry is broken⁵⁴ as well as experimental and material details such as disorder and Landau-level mixing.^{37–39} (All results in this work concerning the Pfaffian apply equivalently to the anti-Pfaffian within the constraints of our approximation scheme since the model we use does not distinguish between Pfaffian and anti-Pfaffian. The reason for this is that our Hamiltonian is particle-hole symmetric since we do not consider any particle-hole breaking terms such as those that might arise due to Landau-level mixing. Since the Pfaffian and anti-Pfaffian are particle-hole conjugates of one another, their (bulk) physics, the subject of our current work, is identical.)

A natural question is why the FQHE is observed at $\nu=5/2=(2+1/2)$ and not, so far, at $\nu=1/2$ for one-component systems. Theoretically, this is due to the physics of the lowest Landau level being different compared to the physics of the second Landau level,^{55–58} i.e., details matter. For the FQHE at filling factor $5/2$, the inert electrons in the lowest spin-up and spin-down Landau levels partially screen the electron-electron Coulomb interaction between the electrons half filling the second Landau level, in fact, the electrons in the lower Landau level *overscreen* the Coulomb interaction⁵⁷ which leads to a slight attraction among the quasiparticles causing them to form a BCS state, the Moore-Read Pfaffian state. The difference between the lowest Landau level and second Landau level can be seen in the form factor that modifies the Fourier transform of the interaction $V(q)$. For electrons in the n th Landau level the Fourier transform of the interaction is $[L_n(q^2/2)]^2 V(q)$, where $L_n(x)$ is the Laguerre polynomial with $L_0(x)=1$ and $L_1(x)=1-x$. Furthermore, the experimental details of a real quantum well, the single-electron wave function in the direction perpendicular to the two-dimensional surface has a finite extent [the so-called fi-

nite thickness of the quasi-two-dimensional electron system where typical experimental systems have widths ranging from approximately ~ 20 nm for the thinnest samples to ~ 60 nm for the wide-quantum-well (WQW) samples] which produces subtle effects that make the effective interaction felt by the electrons in the half-filled second Landau level even more amenable to forming a non-Abelian Moore-Read Pfaffian FQHE at $\nu=5/2$. Recently, it has been theoretically shown that (within certain approximate models) the effects of Landau-level mixing^{37–39} might produce nontrivial and subtle effects that drive the system to the Pfaffian³⁸ or the anti-Pfaffian³⁹ state.

We reiterate that experimentally the FQHE at $\nu=1/2$ has not been observed in *one-component systems* and theory^{4,59} suggests that it will not occur for a pure Coulomb interaction. However, one cannot rule out a Moore-Read Pfaffian FQHE at $\nu=1/2$ if the system parameters are tuned in the perfect way^{60–62} or, perhaps, at extremely low temperatures not currently experimentally accessible.

However, about the same time the experimental observation of the $5/2$ FQHE was realized, the FQHE was also observed by Suen *et al.*^{63–65} and Eisenstein *et al.*⁶⁶ in the lowest Landau level at filling factor $\nu=1/2$ in systems that were later determined by He *et al.*^{1–3} to be spin-polarized two-component systems. It turns out that the FQHE at $\nu=1/2$ in two-component systems is described by the (Abelian) Halperin 331 two-component wave function.⁶⁷ The system of Eisenstein⁶⁶ was an actual bilayer (two quasi-two-dimensional systems separated from one another by a tunneling barrier—typical parameters are quasi-two-dimensional electron systems of width ~ 20 nm separated from one another by a tunneling barrier of thickness ~ 3 – 10 nm with electron densities on the order of 10^{11} cm⁻²), thus, the two components are the two layers. The FQHE at $\nu=1/2$ in bilayers occurs by a two-part process where Laughlin¹⁰ states, at filling factor $1/3$, are formed in each layer and the fermions between layers form pairs. In the experiments by Suen *et al.*^{63–65} the electrons in the wide-quantum-well (a width of order ~ 70 nm and electron densities of $\sim 10^{11}$ cm⁻²) minimize their single-particle energy by reorganizing into effectively two “layers” and, again, the FQHE at $\nu=1/2$ occurs as described above. Recent observations^{6,7,68} of $\nu=1/2$ and $1/4$ in wide-quantum-wells have rekindled interest in this rich system.

The discovery and identification of the FQHE at $\nu=1/2$ was an exciting advance in the FQHE because it opened up the possibility of a fractional quantum Hall state outside those given in the “standard” theory.^{10,11,13,14} However, the Halperin 331 state is closely related to the standard theory being that it is essentially a pairing of Laughlin states. Scarola and Jain⁶⁹ further generalized the Halperin 331 state to pairings of FQHE states belonging to the Jain sequence producing states for bilayer systems at filling factors other than $\nu=1/2$ —they also produced *partially* pseudospin-polarized states at $\nu=1/2$ that are distinct from the Halperin 331 state.

Along with the recent observations^{6,7,68} of $\nu=1/2$ and $1/4$ in wide-quantum-wells are observations^{6,7} of bilayer FQHE at filling factor $1/2$ in the lowest Landau level with *asymmetric* charge distributions—so-called “tilted samples.” A tilted sample is created by an additional charge gate that produces

a charge asymmetry by “pushing” electrons from one side of the wide-quantum-well to the other. In the simplest approximation, this asymmetry produces a charge imbalance between one layer and the other while keeping the total filling factor ν fixed. That is, the individual filling factors in each layer, ν_1 and ν_2 , respectively (keeping $\nu_1 + \nu_2 = \nu$ fixed) can be varied between $(\nu_1, \nu_2) = (\nu, 0)$, to $(\nu_1, \nu_2) = (\nu/2, \nu/2)$, to $(\nu_1, \nu_2) = (0, \nu)$.

Of course, care should be taken when considering the effects of a charge gate that presumably causes charge asymmetry in a wide-quantum-well. Recently, Scarola *et al.*⁷⁰ have used the local-density approximation (LDA) to get a more realistic handle on exactly what tilting does to the charge distribution and relative single-electron energy levels in the quantum well. They went on to analyze the system with the use of variational wave functions finding that the recent experimental observation of the FQHE at $\nu = 1/2$ by Shabani *et al.*⁷ at intermediate charge imbalancing is likely described by a partially pseudospin-polarized bilayer state.^{69,70}

The purpose of the present work is to understand the general effects of charge imbalancing in the most minimal model one can consider to describe the bilayer FQHE in an exact context, that is, using exact diagonalization. Our work complements recent work⁷⁰ since we are solving the Hamiltonian exactly instead of using a combination of LDA and variational wave functions. As such, we are restricted to only certain ansatz, namely, the Moore-Read Pfaffian and the Halperin 331 state. We emphasize that our solution is general and exact.

In Sec. II we present our theoretical model in the form of a Hamiltonian that can describe either a true bilayer and effective (wide-quantum-well) bilayer where we consider both interlayer and charge imbalance tunneling terms. Four (two plus two) variational states are discussed in Sec. III that are thought to describe our bilayer and effective bilayer Hamiltonian. Sections IV and V present our results for the bilayer and wide-quantum-well model in both the lowest Landau level (in both the spherical and torus geometry) and second Landau level (in the spherical geometry). Finally, in Sec. VI, we present our conclusions.

II. THEORETICAL MODELS: TRUE BILAYER AND EFFECTIVE BILAYER

There are two experimental systems in which two-component FQHE systems can be produced. One of them is to manufacture a true bilayer system which consists of two parallel (quasi-)two-dimensional electron systems of width w separated from one another by a tunneling barrier of thickness d . This system is used extensively by the Eisenstein group at CalTech⁶⁶ and is what one generally thinks about when contemplating a bilayer system. The height of the barrier can be adjusted such that electrons are either localized in separate layers or delocalized between the two layers, i.e., large energetic barrier or small energetic barrier, respectively. In other words, the symmetric-antisymmetric energy gap, Δ_{SAS} , can be controlled independently of the individual well width w and the layer separation d . In this system, an elec-

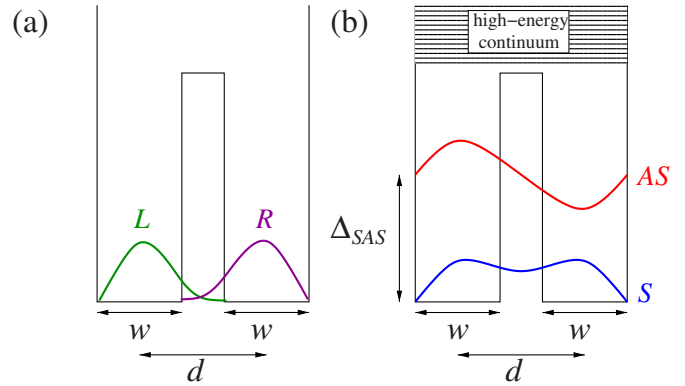


FIG. 2. (Color online) A bilayer system consisting of two (quasi-)two-dimensional quantum wells of width w separated from one another by d ($d \geq w/2$). (a) Typical density profile of an electron localized in either the right (R) or left (L) layer, respectively. (b) The ground-state single-particle wave function [the symmetric (S)] state and the next higher energy state [the antisymmetric (AS)] state separated in energy from one another by the so-called symmetric-antisymmetric energy gap Δ_{SAS} .

tron can be in the right (R) or left (L) state, written as $|R\rangle$ or $|L\rangle$, respectively. Figure 2 shows a schematic of a bilayer system consisting of two parallel two-dimensional electron systems where the electrons in each layer are confined to two dimensions by a quantum well of width w (both layers have the same width) and the quantum-well-center to quantum-well-center separation is d ($d \geq w/2$). A typical density profile of electrons in the right or left layer ($\langle R|R\rangle$ or $\langle L|L\rangle$) is also shown in Fig. 2(a). The ground state of the single-electron bilayer Hamiltonian is the symmetric state S given by

$$|S\rangle = \frac{|R\rangle + |L\rangle}{\sqrt{2}} \quad (1)$$

and the next higher energy state is the antisymmetric state given by

$$|AS\rangle = \frac{|R\rangle - |L\rangle}{\sqrt{2}} \quad (2)$$

(assuming no charge imbalance term in the Hamiltonian). The two states (S and AS) are separated by an energy difference Δ_{SAS} and their respective (typical) density profiles ($\langle S|S\rangle$ and $\langle AS|AS\rangle$) are shown in Fig. 2(b).

The other way to experimentally create a two-component FQHE system is to make a single (quasi-)two-dimensional electron gas of large width, a so-called WQW, as done by the Shayegan group at Princeton.^{6,7,63–65} In this case, the electrostatic interaction between the electrons (at the Hartree-Fock level) compels the system to behave as an effective bilayer. The electron density for the ground state is maximum (and symmetric) near the edges of the wide-quantum-well and depleted in the middle. The energy-level diagram and typical density profiles are similar to those shown in Fig. 3(a). Note that in this system, Δ_{SAS} is a strong function of the width W (and electron density) of the wide-quantum-well. This contrasts the bilayer system described above where, in principle,

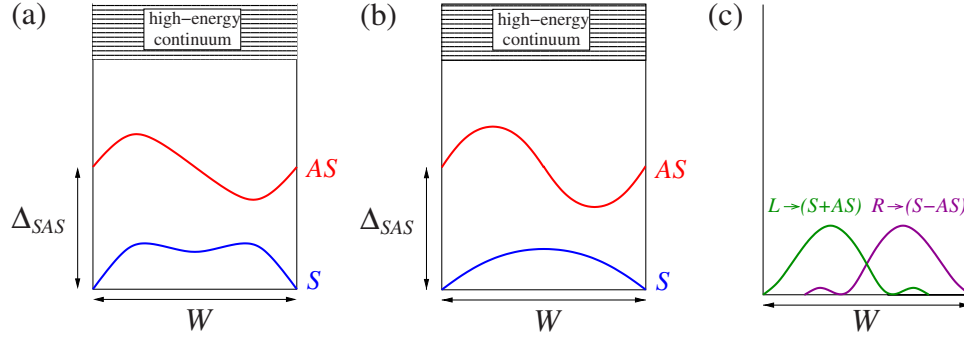


FIG. 3. (Color online) (a) A two-component system created by a wide-quantum-well (WQW). The electrostatic potential generated by the electrons self-consistently creates an effective bilayer system by pushing the electrons toward the walls of the WQW. Note that (a) is *not* identical to Fig. 2(b) even though they are very similar, specifically, Δ_{SAS} is a strong function of W and the electron density in WQW systems as opposed to bilayers. (b) The model of Papić *et al.* (Ref. 4) which can be transformed into the layer basis shown in (c).

Δ_{SAS} , the individual well width w , and the layer separation d can all be independently adjusted.

A simplified model for the WQW is due to Papić *et al.*⁴ where the ground state of a wide-quantum-well of width W is taken to be a symmetric state [for example, $\langle z|S\rangle \sim \sin(\pi z/W)$] and the next excited state an antisymmetric state [for example, $\langle z|AS\rangle \sim \sin(2\pi z/W)$], both the S and AS states are written on the interval $z \in [0, W]$. [The coordinates of the (quasi-)two-dimensional plane will always be denoted by x and y and the coordinates of the wide-quantum-well width, bilayer layer separation, or individual quantum-well thickness will be denoted by z .] The density profiles for the WQW model are shown in Fig. 3(b). In this model, one can transform to the layer basis (right and left layers) by taking $|L\rangle = (|S\rangle + |AS\rangle)/\sqrt{2}$ and $|R\rangle = (|S\rangle - |AS\rangle)/\sqrt{2}$, cf. Fig. 3.

The Hamiltonian for our two-component model systems can be written (in the SAS basis) as

$$\begin{aligned}
 H = & \frac{1}{2} \sum_{\{m_i, \sigma_i = S, AS\}} \langle m_1 \sigma_1, m_2 \sigma_2 | V | m_3 \sigma_3, m_4 \sigma_4 \rangle \\
 & \times c_{m_1 \sigma_1}^\dagger c_{m_2 \sigma_2}^\dagger c_{m_3 \sigma_3} c_{m_4 \sigma_4} \delta_{m_1 + m_2, m_3 + m_4} \\
 & - \frac{\Delta_{SAS}}{2} \sum_m (c_{mS}^\dagger c_{mS} - c_{mAS}^\dagger c_{mAS}) \\
 & + \frac{\Delta\rho}{2} \sum_m (c_{mS}^\dagger c_{mAS} + c_{mAS}^\dagger c_{mS}). \quad (3)
 \end{aligned}$$

The second to last term (the term with the prefactor $\Delta_{SAS}/2$) controls interlayer tunneling and, in the SAS basis is represented by the pseudospin operator \hat{S}_z , while the last term (prefactor $\Delta\rho/2$) controls charge imbalance and is represented by the pseudospin operator \hat{S}_x . In our convention, positive $\Delta\rho$ drives the electrons into the R layer. Notice that $\langle m_1 \sigma_1, m_2 \sigma_2 | V | m_3 \sigma_3, m_4 \sigma_4 \rangle$ is different in the bilayer case than it is in the WQW case, in general. Namely, in the bilayer case, the Coulomb matrix element is found by using the transformations given in Eqs. (1) and (2) and the fact that the potential energy between two electrons a distance r apart in a given layer (the right layer, say) of width w is given by the Zhang-Das Sarma⁷¹ potential $V_{\text{intra}}(r) = 1/\sqrt{r^2 + w^2}$ and the

potential between two electrons in two different layers separated by a distance d is given by $V_{\text{inter}}(r) = 1/\sqrt{r^2 + d^2}$. In the WQW system the Coulomb matrix element is calculated by considering the wave functions for the S and AS states ($\langle z|S\rangle$ and $\langle z|AS\rangle$) and doing the required integrals.

In the (left/right) layer basis we can write the bilayer Hamiltonian very simply as

$$\begin{aligned}
 \hat{H} = & \sum_{i < j} [V_{\text{intra}}(|\mathbf{r}_i - \mathbf{r}_j|) + V_{\text{intra}}(|\tilde{\mathbf{r}}_i - \tilde{\mathbf{r}}_j|) + V_{\text{inter}}(|\mathbf{r}_i - \tilde{\mathbf{r}}_j|)] \\
 & - \Delta_{SAS} \hat{S}_x + \Delta\rho \hat{S}_z, \quad (4)
 \end{aligned}$$

where operators \hat{O} with a tilde are written in the layer basis and coordinates \mathbf{r} and $\tilde{\mathbf{r}}$ belong to electrons in different layers. Switching from the layer to the SAS basis is a pseudospin rotation. Note that for $d=0$ the Hamiltonian is symmetric between Δ_{SAS} and $\Delta\rho$. Increasing d destroys this symmetry and it becomes harder to drive the system to be one component in the layer sense.

In all of our results we use the *natural* FQHE units: lengths are given in units of the magnetic length l and energies are given in units of the Coulomb energy $e^2/\epsilon l$. [Note that the system we are considering is a rather general two-component Hamiltonian and when the layer separation is zero any results we find are applicable to $SU(2)$ symmetric two-component systems where the constituents interact by a Coulomb-type interaction—exactly Coulombic for the lowest Landau level and a slightly modified Coulombic interaction for the second Landau level. For example, when $d=0$ the Hamiltonian [Eq. (3)] describes spinfull electrons interacting via a Coulomb interaction with both \hat{S}_z and \hat{S}_x terms.]

III. VARIATIONAL WAVE FUNCTIONS: MOORE-READ PFAFFIAN AND HALPERIN 331

We consider four variational wave functions to describe our FQH system for half-filled lowest and second Landau levels ($\nu=1/2$ and $\nu=5/2$, respectively) even though it will appear at first that we are only considering two. Namely, we consider the one-component Moore-Read Pf (Ref. 47) and two-component Halperin 331 (331) wave functions.⁶⁷ (Note

that work^{72–78} has been done on the FQHE at total filling factor of unity, i.e., $\nu=1/2+1/2=1$, however, that is not the case that we study in this work.)

The Moore-Read Pfaffian state is written as

$$\Psi_{\text{Pf}} = \text{Pf} \left\{ \frac{1}{z_{i,a} - z_{j,a}} \right\} \prod_{i < j}^N (z_{i,a} - z_{j,a})^2, \quad (5)$$

where $z_{i,a} = x_{i,a} - iy_{i,a}$ is the position of the i th electron in complex coordinates with a labeling its state, i.e., $a=S, AS, R$, or L . The origin of this wave function can be understood at an intuitive level. If one writes down an ansatz wave function to describe a BCS paired state of composite fermions in a half-filled Landau level then one arrives at a wave function of the Pfaffian form,⁷⁹ i.e.,

$$\text{Pf}\{g(r_{ij})\} \prod_{i < j} (z_i - z_j)^2 = \mathcal{A} \{g(r_{12})g(r_{34}) \cdots g(r_{N-1,N})\} \times \prod_{i < j} (z_i - z_j)^2, \quad (6)$$

where $g(|\mathbf{r}_i - \mathbf{r}_j|)$ is the real-space pairing amplitude for a pair of electrons located at position \mathbf{r}_i and \mathbf{r}_j , $\prod_{i < j} (z_i - z_j)^2$ binds two quantum-mechanical vortices of the many-body wave function to each electron (the composite fermion transformation and fixes the filling factor in a Landau level to $1/2$). \mathcal{A} is the antisymmetrization operator.

Despite the intuitive picture that goes along with the Moore-Read Pfaffian wave function it was originally derived using conformal field theory and, as such, the Pf has a low-energy effective conformal field theory description, cf. Refs. 47, 51, and 80. It is within this conformal field theory that the understanding of the non-Abelian nature of the quasiparticle excitations was first illuminated. However, whether or not the Pf has anything to do with the physics of the FQHE at $5/2$ has depended crucially on numerical calculations and comparisons with the results of exact diagonalization.^{43,44,59–62,81} As mentioned above, the details matter greatly in determining the physics of the FQHE at $5/2$, such as, finite thickness effects,^{60,61} the competition between FQHE states and non-FQHE striped phases⁸¹ and the compressible (composite fermion) Fermi sea^{17,18} (as mentioned, the latter occurs in the lowest Landau level at $\nu=1/2$ while the former occurs in the second Landau level at $\nu=5/2$), the effects of Landau-level mixing,^{37–39} etc. Note that most of the numerical studies mentioned above do not treat the $\nu=5/2$ problem in full complexity, i.e., with the lowest Landau level filled with two spin species and one Landau level half filled. Instead, because of computational simplicity, one considers a half-filled lowest Landau level (usually without spin) with an effective interaction that contains the form factors of the first excited Landau level, the appropriate Haldane pseudopotentials.⁸² This is what we mean by $\nu=5/2$ in an exact diagonalization context.

Thus, it should be clear that any effective conformal field theory (or effective BCS mean-field Hamiltonian⁵¹) written down to describe the physics at $5/2$ is only as good as its physical predictions and agreement with experiments *and* its agreement with numerical calculations. This is because the entire reason for the existence of the FQHE at all filling

factors is due to nonperturbative physics arising from the strongly interacting electrons interacting with a Coulomb interaction modified by the details of which Landau level is fractionally filled by electrons, the thickness the quantum well, the amount of Landau-level mixing that is taking place, etc. Hence, any mean-field theory that throws away all these details at the first step cannot explain, for example, why the FQHE occurs at $\nu=5/2$ and not $\nu=1/2$ (or for that matter, at $9/2$ or $13/2$) without the aid of both numerical calculations and, most importantly, experiments. In the end, whether a particular candidate wave function, e.g., Moore-Read Pfaffian or Laughlin or Halperin 331 or composite fermion states, etc., describes a real FQHE at some filling factor is an energetic question delicately depending on competing states where all the details of the microscopic Hamiltonian may eventually matter, and therefore, extreme caution is necessary in identifying experimental FQHE states with candidate incompressible wave functions, particularly in higher LLs and/or multicomponent systems where various competing states are, in general, more viable.

The Halperin (two-component) 331 wave function is written as

$$\Psi_{331} = \prod_{i < j}^{N/2} (z_{i,1} - z_{j,1})^3 \prod_{i < j}^{N/2} (z_{i,2} - z_{j,2})^3 \prod_{i,j}^N (z_{i,1} - z_{j,2}), \quad (7)$$

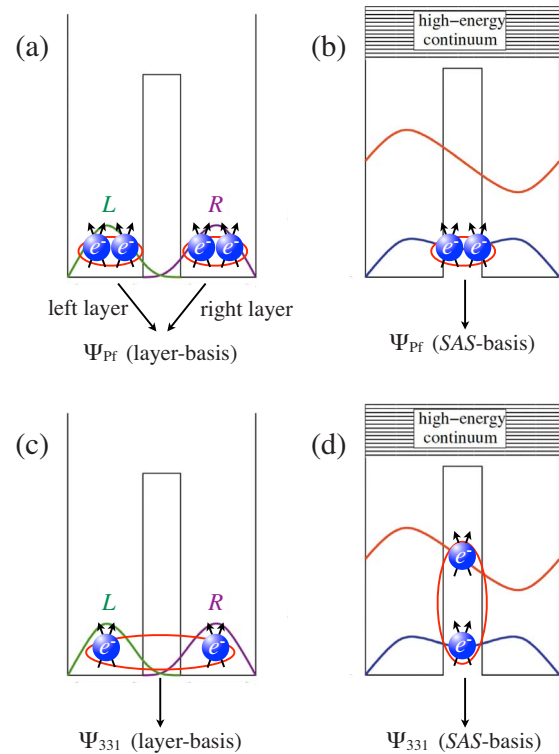


FIG. 4. (Color online) The Moore-Read Pfaffian wave function written in the (a) layer and (b) SAS basis where the p -wave pairing in the former is between Composite fermions in the right (or left) layer and the p -wave pairing in the SAS basis is between electrons in the S state. The Halperin 331 state is shown in (c) the layer basis and (d) the SAS basis where in the layer-basis the 331 state pairs composite fermions between layers and in the SAS basis it pairs composite fermions in the S and AS states.

where the subscript 1 (or 2) on $z_{i,1}$ labels the quantum number of the electron. This quantum number could describe spin (up or down), layer (R or L), subband (S or AS). Note that in our work, we consider the bilayer situation so the subscript will either denote the layer or the symmetric or antisymmetric state depending on in which basis we choose to work. Intuitively, the origin of this wave function is that, in a bilayer system in a half-filled Landau level, the electrons form $\nu=1/3$ Laughlin states¹⁰ [$\prod_{i<j}^N (z_i - z_j)^3$] among each electron component and then pair among different components [simple Jastrow factor $\prod_{i,j}^N (z_{i,1} - z_{j,2})$]. {Note that we always drop the Gaussian factors [$\sim \exp(-\sum_i |z_{i,a}|^2)$] that are always present when writing wave functions describing electrons entirely in (or projected into) the lowest Landau level, in fact, the Gaussian is often considered to be part of the measure so one is technically not “dropping” anything at all.}

It is important to realize that the Moore-Read Pfaffian is a one-component state that can be one component in both the SAS-basis sense or in the layer-basis sense, see Figs. 4(a) and 4(b). That is, the Pf wave function either describes pairing among one-component electrons in the R layer or L layer (the layer basis) or pairing among one-component electrons in the symmetric (S) state (the SAS basis). The former is the Pfaffian state that has its origin in the single-layer FQHE while the latter is the Pfaffian understood as the even (symmetric) channel of the BCS description by Read and Green.⁵¹ (We choose our charge imbalancing term to drive the electrons into the right layer, however, we could have equivalently chosen the charge imbalance term to drive the electrons into the left layer.) Thus, there are actually *two* Moore-Read Pfaffian states to consider when both tunneling terms (Δ_{SAS} and $\Delta\rho$) are nonzero (or three if we allow the sign of $\Delta\rho$ to change). When the system is $SU(2)$ symmetric, i.e., when the layer separation is zero, the two different states are simply related via a rotation in pseudospin space.

The Halperin 331 state can also be two component in two ways: it can describe pairing of electrons in the R and L layers (the layer basis) or it can describe pairing of electrons in the S and AS states (the SAS basis), see Figs. 4(c) and 4(d). Hence, there are two Halperin 331 states to consider when both tunneling terms are finite. Note, however, that the Halperin 331 state, as usually understood, is defined in the layer basis. Again, in the $SU(2)$ situation, these two 331 states are related via a pseudospin rotation.

Thus, instead of dealing with two variational wave functions (Pf and 331) we are dealing with four—two Pfs and two 331s. Even though the two pairs of wave functions are related via a pseudospin rotation, when the $SU(2)$ symmetry is broken this is no longer the case and the determination of which state describes the physics is nontrivial.

In our calculations we utilize the spherical geometry⁸² where the electrons are confined to the surface of a sphere of radius $\sqrt{N_\phi}/2$ and a radial magnetic field (perpendicular to the surface) is produced by a magnetic monopole of strength $N_\phi/2$ placed at the center. (We briefly consider the torus geometry below.) The total magnetic flux piercing the surface is N_ϕ and is either an integer or half integer according to Dirac.⁸³ The filling factor (in the partially filled Landau level) is given by $\lim_{N \rightarrow \infty} N/N_\phi$ for N electrons. In our case, we are considering the Moore-Read Pfaffian and Halperin

331 states which describe a half-filled Landau level, thus, the relationship between N and N_ϕ for a finite spherical system is $N_\phi = 2N - 3$, where “ -3 ” is known as the “shift” and is a consequence of the compact spherical geometry and, thus, of topological origin and used to identify the universality class of the topological order for which the particular ansatz belongs. Due to computational constraints we consider $N=8$ and $N_\phi=13$ (the $N=6$ particle system is aliased with a $2/3$ filled Landau level and, thus, produces ambiguous results and the $N=10$ electron system is too big to consider while adequately exploring the large parameter space inherent when tackling a two-component Hamiltonian with both interlayer and charge imbalancing tunneling). In the spherical geometry, possible FQHE states are uniform states with total angular momentum $L=0$. In this work we consider the overlap between the exact ground state of the model Hamiltonian and the four variational states: (1) Pf in the SAS basis, (2) Pf in the layer basis, (3) 331 in the SAS basis, and (4) 331 in the layer basis.

IV. RESULTS: LOWEST LANDAU LEVEL

We first present our results for the lowest Landau level where we consider (i) the wave-function overlap between the four variational states (Pf in the layer and SAS basis and the 331 in the layer and SAS basis) and the exact ground state of the Hamiltonian—note that since all the variational states describe the FQHE they have $L=0$ and so if the exact ground state of the Hamiltonian does not also have total angular momentum $L=0$ the overlaps will be trivially zero since they are then of different symmetry. (ii) The pseudospin expectation values of the exact ground state, which is more descriptively referred to as the expectation value of $(N_S - N_{AS})/2$ or $(N_R - N_L)/2$ where N_S , N_{AS} , N_R , and N_L are the expectation values of the number of electrons in the symmetric state, the antisymmetric state, the right layer, and the left layer, respectively. Alternatively, this is simply $\langle \hat{S}_z \rangle$ and $\langle \hat{S}_x \rangle$ in the SAS basis but we prefer to use the more physical $(N_S - N_{AS})/2$ and $(N_R - N_L)/2$ since this does not depend on the basis in which we choose to write the Hamiltonian. (iii) The FQHE energy gap which is *defined* here as the energy difference between the $L=0$ ground state and the first excited state (this is often times referred to as the “neutral gap” but we will call it the FQHE gap throughout this work) and, lastly, (iv) we investigate the energy spectra in the torus geometry. We show all of these quantities from a variety of vantage points to give the clearest picture of the physics since things can get complicated rather quickly with so many parameters in the Hamiltonian, namely, layer separation d or WQW width W , SAS energy gap Δ_{SAS} , and the charge imbalancing gap $\Delta\rho$.

A. Bilayer

We first present our results for the bilayer Hamiltonian. Figure 5(a) shows the overlap between the Moore-Read Pfaffian and the exact ground state in the layer basis (left column) and SAS basis (right column) as a function of Δ_{SAS} and $\Delta\rho$ for values of layer separation d ranging from $d=0.05$ to 6. For the layer basis (left column), it is clear that

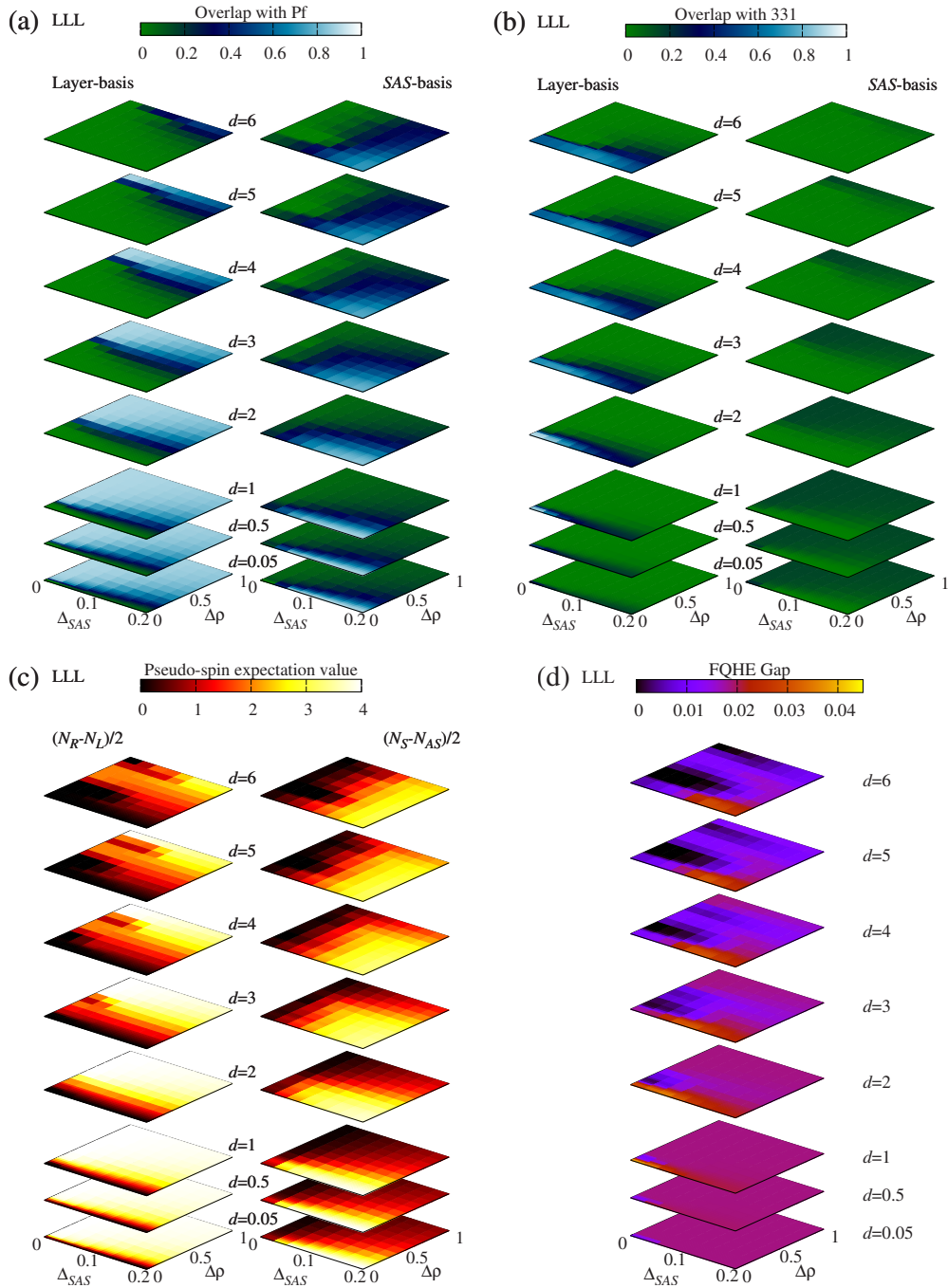


FIG. 5. (Color online) Lowest Landau level: (a) wave-function overlap between the exact ground state of the bilayer Hamiltonian and the Moore-Read Pfaffian written in the layer basis (left column) and the SAS basis (right column) shown as a function of interlayer tunneling Δ_{SAS} and charge imbalance $\Delta\rho$ for different values of layer separation d and zero individual layer thickness $w=0$. (b) Same as (a) but for the Halperin 331 wave function. (c) Pseudospin expectation value or, more physically, the expectation value of $(N_R - N_L)/2$ (left column) and $(N_S - N_{AS})/2$ (right column) as a function of Δ_{SAS} and $\Delta\rho$. (d) shows the FQHE (neutral) energy gap for the exact bilayer Hamiltonian.

increasing Δ_{SAS} does not drive the system into the Pf phase, i.e., it does not increase the overlap between the layer-basis Pf and the exact ground state. However, increasing the charge imbalance $\Delta\rho$ does drive the system into the Pf phase. For increasing values of d it takes a larger value of $\Delta\rho$ to produce a ground state with a high overlap with the layer-basis Pf. This behavior is easy to understand. Nonzero $\Delta\rho$ makes the system one component in the layer sense and thus a layer-basis Pf wave function (which is a one-component

wave function) has a large overlap. It is also understandable that finite layer separation d would make it harder to polarize the electrons in the layer sense, i.e., the electrons prefer to remain two component so they can take advantage of the reduction in potential energy between electrons in neighboring layers (the interaction is $1/\sqrt{r^2 + d^2}$ as opposed to $1/r$ for electrons in the same layer).

The overlap between the exact ground state and the Moore-Read Pfaffian in the SAS basis shows essentially the

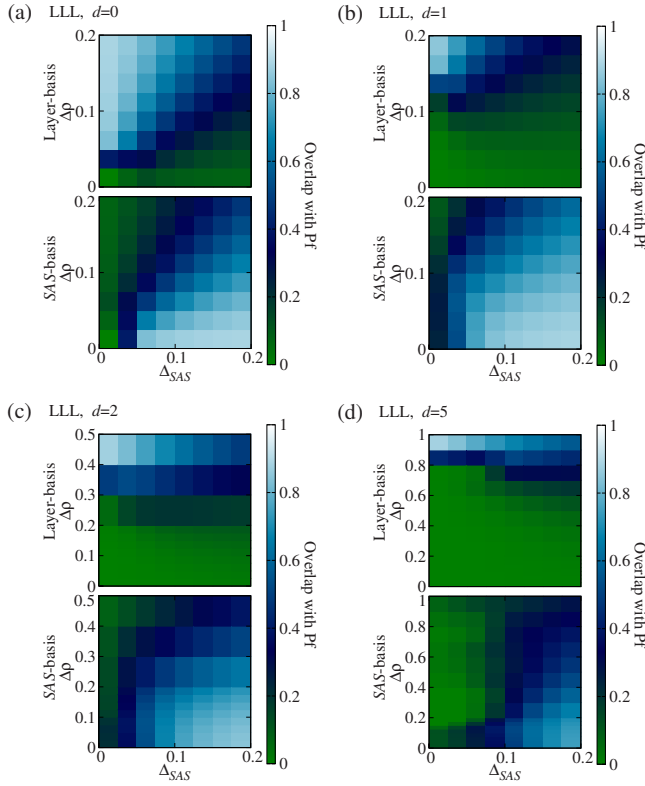


FIG. 6. (Color online) Lowest Landau level: wave-function overlap between the Moore-Read Pfaffian wave function in the layer basis (top panel) and the SAS basis (lower panel) and the exact ground state for (a) $d=0$, (b) $d=1$, (c) $d=2$, and (d) $d=5$.

opposite behavior. This time, nonzero Δ_{SAS} drives the system to be one component. Notice that for the smallest value of layer separation $d=0.05$ the system is nearly SU(2) symmetric and the two bases (layer and SAS) are (nearly) pseudospin rotations of each other. The figure is deceptive because the scale on the two axes is different but the two figures are essentially identical upon reflection across the $\Delta_{SAS}=\Delta\rho$ line. This symmetry is quite obviously destroyed upon increasing d .

A naive look at Fig. 5(a) would lead to a conclusion that we have found the Pfaffian state in some regions of $\Delta_{SAS}-\Delta\rho$ phase diagram. The reader may wonder how robust these conclusions are with increasing system size. Although we are unable to calculate the full phase diagram for $N=10$ electrons, we can gain insight into the limiting cases when either $\Delta\rho$ or Δ_{SAS} is very large. If we work in the layer basis and $\Delta\rho$ is very large, we recover the single-layer physics; for our system of $N=8$ electrons, it turns out⁶² that the ground state for the lowest Landau-level Coulomb interaction is already in the universality class of Moore-Read Pfaffian. However, this no longer holds for larger systems such as $N=10$ and $N=12$, leading to the conclusion that high overlaps with the Pfaffian in the layer basis in Fig. 5(a) are a finite-size effect for $\nu=1/2$. On the other hand, if we work in the SAS basis and increase Δ_{SAS} , all the electrons will occupy the symmetric subband. This is again a one-component system but with the interaction slightly softened with respect to pure Coulomb.⁸⁴ It is known⁶² that softening the Coulomb inter-

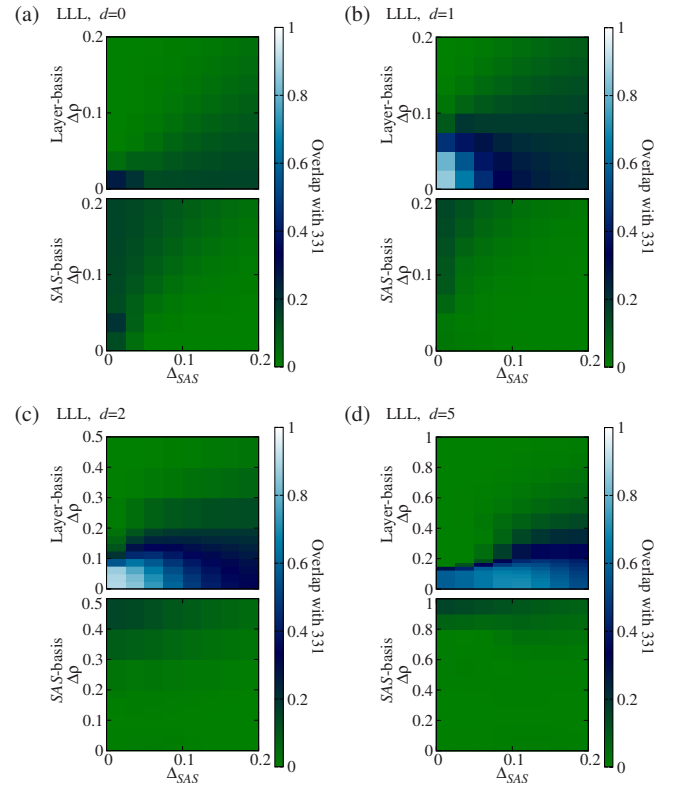


FIG. 7. (Color online) Lowest Landau level: wave-function overlap between the Halperin 331 wave function in the layer basis (top panel) and the SAS basis (lower panel) and the exact ground state for (a) $d=0$, (b) $d=1$, (c) $d=2$, and (d) $d=5$.

action via various finite-width corrections can lead to a phase transition between compressible and incompressible (non-Abelian) states but this also leads to a significant reduction in the gap (as we show below). Therefore, the Pfaffian which is seen in our data for SAS basis is also not a typical incompressible state but rather a “critical” state with some Pfaffian correlations and a small gap. In the remainder of this section, we will nonetheless, for the sake of brevity, refer to the one-component phase (fully polarized by either Δ_{SAS} or $\Delta\rho$) as described by the appropriate basis “Pfaffian” state, cautioning the reader that such a designation most likely does not survive in the thermodynamic limit.

Next we consider the overlap between the exact ground state and the Halperin 331 state in the layer basis (left column) and SAS basis (right column) in Fig. 5(b). For the SAS-basis 331 state the overlap is very small for all values of Δ_{SAS} , $\Delta\rho$, or layer separation d . On the other hand, the overlap with the layer-basis 331 state is nonzero for moderate values of Δ_{SAS} and for $1 \leq d \leq 4$ the overlap is large and, despite the fact that nonzero $\Delta\rho$ eventually destroys the 331, it is robust to charge imbalancing.

In Figs. 6 and 7 we show a clearer view of the overlaps. In particular, for $d=0$ when the system is SU(2) symmetric it is obvious in Figs. 6 and 7 that the layer basis and SAS basis are merely pseudospin rotations of one another. Furthermore, it is clear that for $d=0$ there is no region in phase space where the Halperin 331 wave function (in either basis) is a good description and only upon increasing d away from zero do

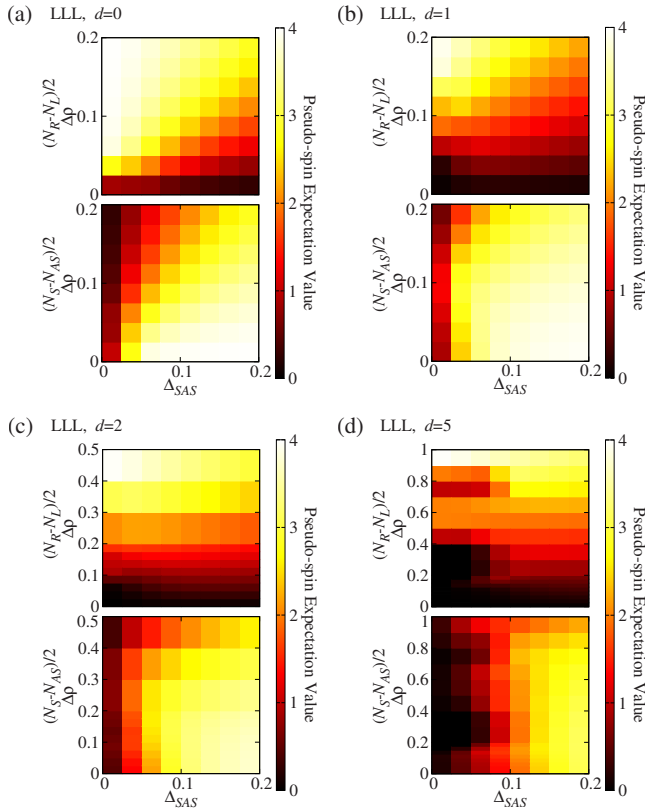


FIG. 8. (Color online) Lowest Landau level: (pseudospin) expectation value of the exact ground state of $(N_R - N_L)/2$ (top panel) and $(N_S - N_{AS})/2$ (lower panel) for (a) $d=0$, (b) $d=1$, (c) $d=2$, and (d) $d=5$. Note that these figures (especially for $d=0$) are qualitatively similar to our cartoon schematic in Fig. 9 since the pseudospin expectation value essentially describes the one- or two-component nature of the ground state. Also, finite d breaks the SU(2) symmetry of reflection across the $\Delta_{SAS} = \Delta\rho$ line assumed in Fig. 9.

we see any sort of reasonably sized overlaps when increasing Δ_{SAS} (though it should be noted that for $d=1$ and 2 the overlap with 331 is sizable for small values of both Δ_{SAS} and $\Delta\rho$). For the half-filled Landau level at $d=0$, theoretically, the system is known to be spin polarized,^{43,44} or one component, so it is not surprising that a two-component wave function such as the Halperin 331 state would not be a good description and, therefore, have a small overlap with the exact ground state. Note also that the one-component Moore-Read Pfaffian is also not a good description for the $d=0$ case since, in the lowest Landau level, the ground state is most likely a non-FQHE (composite fermion) Fermi sea.^{19,81}

Generally, on the example of our $N=8$ system we can conclude that (i) when the system is largely two component in nature then the overlap between the exact ground state and the Halperin 331 state is large, and (ii) when the system is largely one component in nature the overlap between the exact ground state and the Pf is large. This is more clearly shown in Fig. 5(c) where in the left and right columns we show the expectation value of $(N_R - N_L)/2$ and $(N_S - N_{AS})/2$, respectively. When the system is largely one component, either in the layer sense or SAS sense, the system concomitantly has a sizable overlap with the one-component Pf state

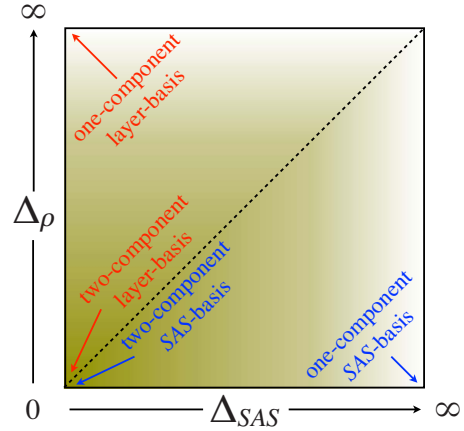


FIG. 9. (Color online) By varying either Δ_{SAS} or $\Delta\rho$ the system can be two component (in the SAS-basis or layer-basis sense) when Δ_{SAS} and $\Delta\rho$ are small and one component (again in either the SAS-basis or layer-basis sense) for large values of either Δ_{SAS} or $\Delta\rho$. The shading qualitatively indicates the one-component to two-component nature of the system with the darker shade indicating a two-component system and the lighter color a one-component system.

and when the system is largely two component the overlap with the Halperin 331 state is large. Again, Fig. 8 shows the pseudospin expectation values clearer for a few specific examples of layer separation d , note again how nonzero d destroys the symmetry between the layer and SAS basis obtained when $d=0$ and the system is SU(2) symmetric. We emphasize that the first conclusion (i) is not affected by finite-size effects whereas the conclusion (ii) likely holds only for a few special systems such as $N=8$ and it may be a finite-size artifact.

In Fig. 9 we show a schematic that encapsulates broad features of the bilayer model (and WQW model) for small layer separation d (small WQW width W). For large Δ_{SAS} and small $\Delta\rho$ the system is one component in the SAS basis and for large $\Delta\rho$ and small Δ_{SAS} the system is one component in the layer basis. When, both tunneling strengths approach

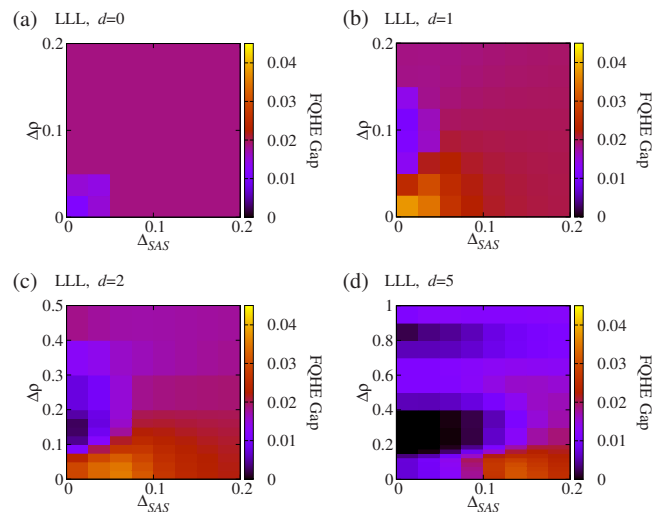


FIG. 10. (Color online) Lowest Landau level: FQHE energy gap for (a) $d=0$, (b) $d=1$, (c) $d=2$, and (d) $d=5$.

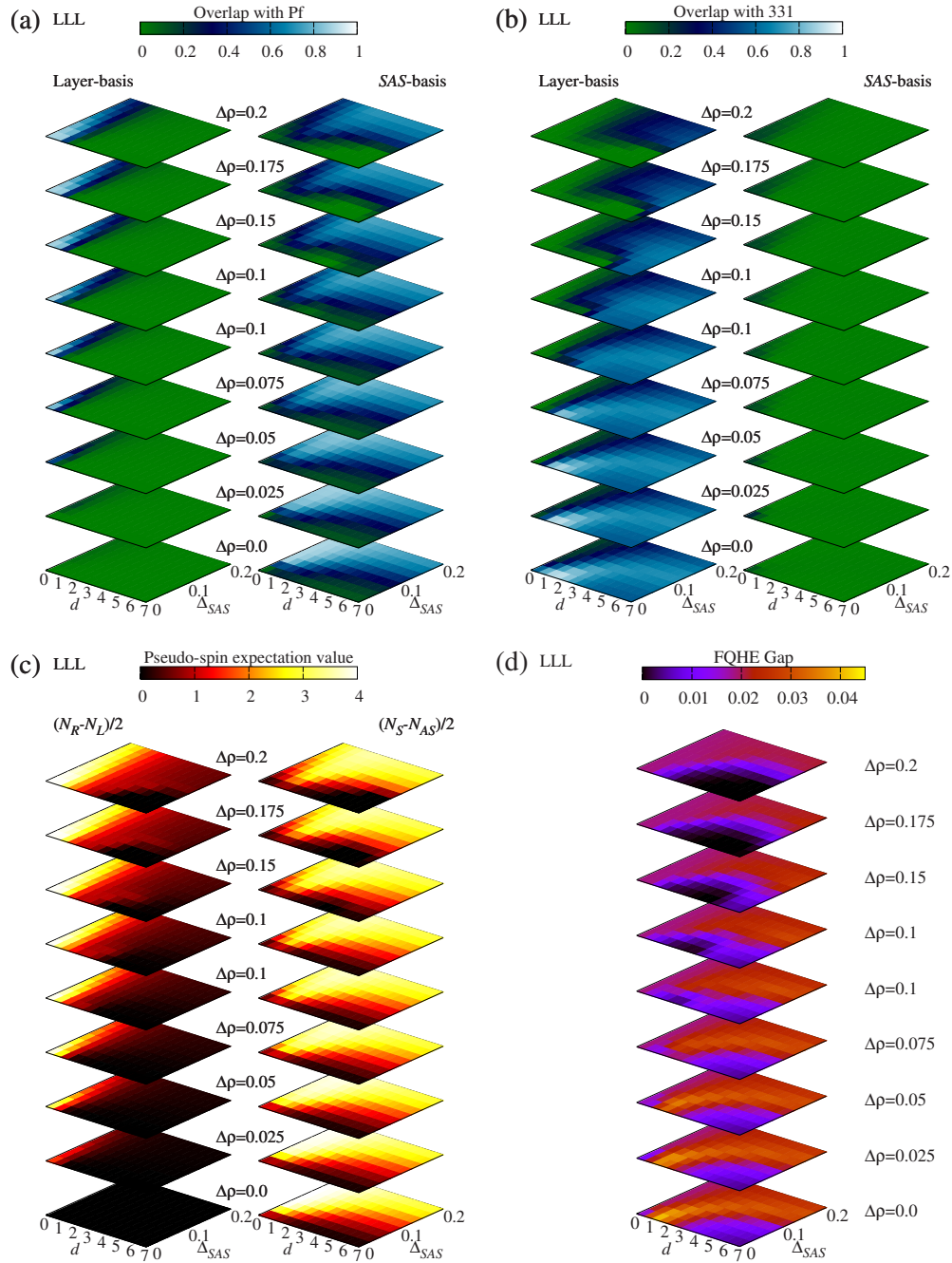


FIG. 11. (Color online) Lowest Landau level: same as Fig. 5 except that all plots are shown as a function of interlayer tunneling Δ_{SAS} and layer separation d for a number of different charge imbalances $\Delta\rho$ and zero individual layer thickness $w=0$.

zero, the system is two component in the layer basis, the SAS basis, or both. The diagram would be topologically similar for nonzero (and even large) values of layer separation d and WQW width W . The only difference is that the diagram would not be symmetric between Δ_{SAS} and $\Delta\rho$ since the system is not $SU(2)$ symmetric.

Lastly, in Fig. 5(d) we show the FQHE energy gap. For $d \lesssim 1$ the FQHE energy gap is relatively constant as Δ_{SAS} and $\Delta\rho$ vary. When d is increased past approximately $d \sim 2$ the FQHE gap shows interesting features as a function of the strength of the two tunneling terms. Somewhat surprisingly, the FQHE gap obtains a maximum for nonzero Δ_{SAS} and

finite d (this is related to similar results found recently in Ref. 5 where the FQHE gap is maximum on the “ridge” as a function of Δ_{SAS} and separation d for zero charge imbalance $\Delta\rho$). This ridge basically separates the regions in the quantum phase diagram where the system is either in the Pf or 331 phase. Figure 10 is a more detailed depiction of the FQHE energy gap.

Before moving on to results for the second Landau level we show essentially the same results as Figs. 5(a)–5(d) but as a function of Δ_{SAS} and layer separation d for several values of $\Delta\rho$ in Figs. 11(a)–11(d). This presentation is to more easily compare with previous bilayer works^{4,5} where the data

was presented this way. When considering the overlap between the exact ground state and the Pf we see that increasing imbalance (increasing $\Delta\rho$) eventually produces a high overlap for small values of d in the layer basis. In the SAS basis, charge imbalance pushes the maximum overlap to larger values of Δ_{SAS} and slightly larger values of d while generally decreasing the overlap along the way. For the overlap with the Halperin 331 wave function it is clear that there is no region in parameter space that produces a sizable overlap in the SAS basis. For the layer-basis 331, the overlap is large for moderate layer separation ($d \sim 1-2$) and Δ_{SAS} . The position of the maximum overlap is relatively constant as a function of $\Delta\rho$ until $\Delta\rho \sim 0.1$ when the maximum overlap shifts to higher values of d and decreases markedly in magnitude. The expectation values of the pseudospin operators [Fig. 11(c)] mirrors the results of the overlap calculations.

For the FQHE gap shown in Fig. 11(d) we see the familiar picture found in Ref. 5. We first reiterate that result. For $\Delta\rho=0$, the FQHE gap is largest along a ridge in Δ_{SAS} - d space and the overlap between the SAS-basis Halperin 331 state is largest in the region of phase space where the system is two component and the overlap between the SAS-basis Pf state is largest in the region of phase space where the system is largely one component. The FQHE gap ridge seems to function as the phase boundary between the two states in the quantum phase diagram, however, the maximum FQHE gap is slightly on the Halperin 331 side of the phase diagram and the experimentally observed⁶³⁻⁶⁶ FQHE at $\nu=1/2$ is of that nature. This is strongly thought to be the case because of recent work by Storni *et al.*⁵⁹ that showed that in the lowest Landau level the FQHE gap for one-component systems vanishes in the thermodynamic limit—even though it is nonzero in our finite-size calculation. Thus, our nonzero gap in the Pf region of the phase diagram for the lowest Landau level is most likely a finite-size effect.

For nonzero $\Delta\rho$ the above picture changes. The ridge is weakened and a maximum in the FQHE gap starts to appear for large Δ_{SAS} and large d until eventually weakening further. In the large $\Delta\rho$ limit we see a SAS-basis Pf state for large Δ_{SAS} and nonzero d and a layer-basis Pf for moderate Δ_{SAS} and very small d . However, we caution that the FQHE gap is globally weakened upon inclusion of $\Delta\rho$ and taking into account recent results,⁵⁹ an experimental system would most likely not exhibit the FQHE in that region of parameter space.

To summarize our results from the calculations on the sphere in the lowest Landau level, we find a robust layer-basis 331 state that has high overlap with the exact ground state and dominant gap in the phase diagram. Furthermore, we find a one-component state that has some properties of the Moore-Read Pfaffian but it is likely to show up as a compressible state in experiments. These conclusions are in agreement with the results of Ref. 84 (and consistent with Ref. 59) where transitions between 331 state, Pfaffian and composite fermion Fermi sea were studied in a bilayer model with tunneling Δ_{SAS} (in the layer basis) using exact diagonalization and effective mean-field BCS theory of Read-Green.⁵¹ There it was found that the increase of inter-layer tunneling converts the 331 state into a composite fermion Fermi sea because the effective chemical potential of

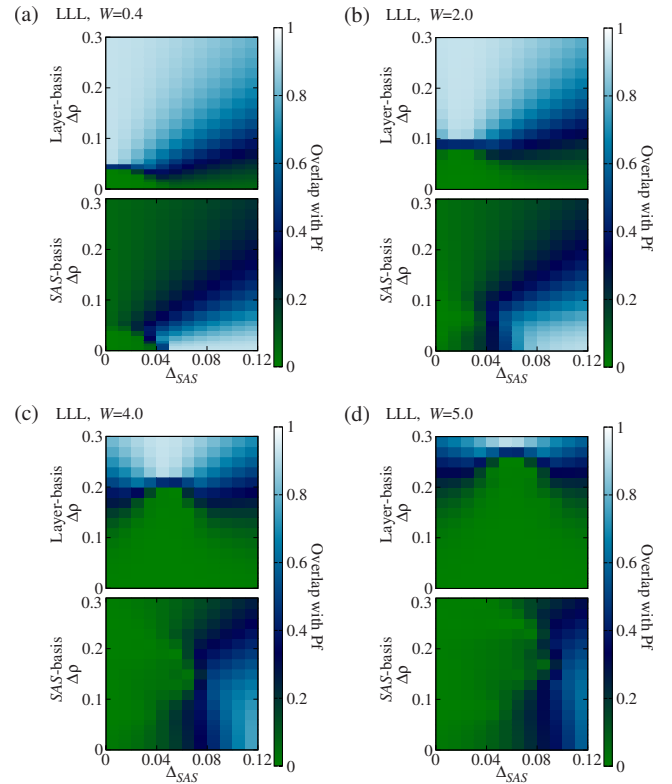


FIG. 12. (Color online) Lowest Landau level: wave-function overlap between the Moore-Read Pfaffian wave function in the layer basis (top panel) and the SAS basis (lower panel) and the exact ground state for the WQW for (a) $W=0.4$, (b) $W=2$, (c) $W=4$, and (d) $W=5$.

“even”-channel electrons becomes very large. Similar analysis is expected to apply when $\Delta\rho$ is large and the system is viewed in SAS basis.

B. Wide-quantum-well

We now turn to the WQW model which largely mirrors the results presented for the bilayer model. However, there are some differences between the two models which we point out below. An obvious difference between the bilayer and the WQW model is that the parameters W and Δ_{SAS} in the latter case are not independent. If we assume that the depth of the well constitutes the largest energy scale and the WQW can be considered an infinite well, we have $\Delta_{SAS}/(e^2/\epsilon l) = 3\pi^2\hbar^2\epsilon/(2me^2l) \times (l/W)^2$. For the typical experimental fields $B \sim 15$ T and $W/l \sim 4$, we obtain $\Delta_{SAS} \sim 0.1e^2/\epsilon l$. However, in each sample, Δ_{SAS} is expected to be renormalized and in what follows we regard it as a free parameter in exploring the phase diagram.

Figure 12 shows the overlap between the Moore-Read Pfaffian wave function (in both the SAS basis and the layer basis) and the exact ground state of the WQW model as a function of Δ_{SAS} and $\Delta\rho$ for a few values of the WQW width W . This figure should be compared with Fig. 6 for the bilayer model. *Qualitatively*, the two models produce very similar results. Of course, a layer separation of d in the bilayer model is not equivalent to the WQW width W and any similarities between the two at $d \sim W$ is coincidental. However,

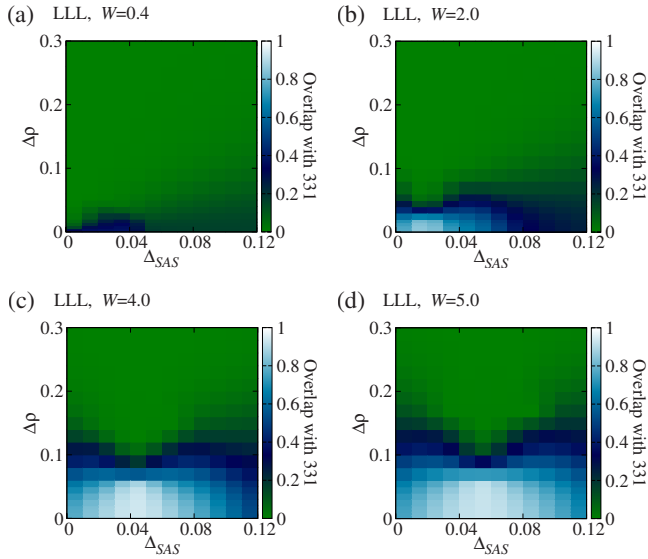


FIG. 13. (Color online) Lowest Landau level: wave-function overlap between the Halperin 331 wave function in the layer basis and the exact ground state for the WQW for (a) $W=0.4$, (b) $W=2$, (c) $W=4$, and (d) $W=5$.

the behavior for the bilayer model as d increases is the same as the behavior for the WQW model as W increases. That is, for small $W=0.4$, the overlap between the exact ground state and the one-component Pf in the layer basis becomes large when $\Delta\rho$ is increased since the system is being driven to be more one component in the layer sense. When Δ_{SAS} is increased, the overlap between the exact ground state and the Pf in the SAS basis becomes large since the system is being driven to be one component in the SAS basis.

Note, however, that for $W=0.4$ [Fig. 12(a)] the system is not as symmetric upon $\Delta_{SAS} \leftrightarrow \Delta\rho$ as it was for the $d=0$ bilayer model case where the model was actually $SU(2)$ symmetric. This is because the WQW model is not $SU(2)$ symmetric for small W because even as W becomes very small the Coulomb energy between electrons in the S and AS states is never equal, i.e., the AS state always has a node and therefore higher kinetic energy. That being said, the models produce very similar results.

In Fig. 13 we show the overlap between the exact ground state of the WQW model and the Halperin 331 state. This time, as opposed to Fig. 7 we only show the overlap with the 331 state written in the layer basis since, as we learned previously by studying the bilayer model results, and by confirming this with the WQW model, the overlap between the ground state of the WQW model and the SAS-basis 331 state is always nearly zero, hence, we do not bother to show these results explicitly. For the layer-basis 331, however, we again see qualitatively similar behavior compared to the bilayer model. For small W the overlap with the 331 state is very small and it can be increased by increasing W . One interesting difference between the results of the two models is that for $W=5$ the maximum overlap with 331 has a maximum for nonzero Δ_{SAS} for the WQW model. Furthermore, nonzero charge imbalance $\Delta\rho$ eventually destroys the Halperin 331 state by driving the system to be one component, however, the 331 state is robust to charge imbalancing.

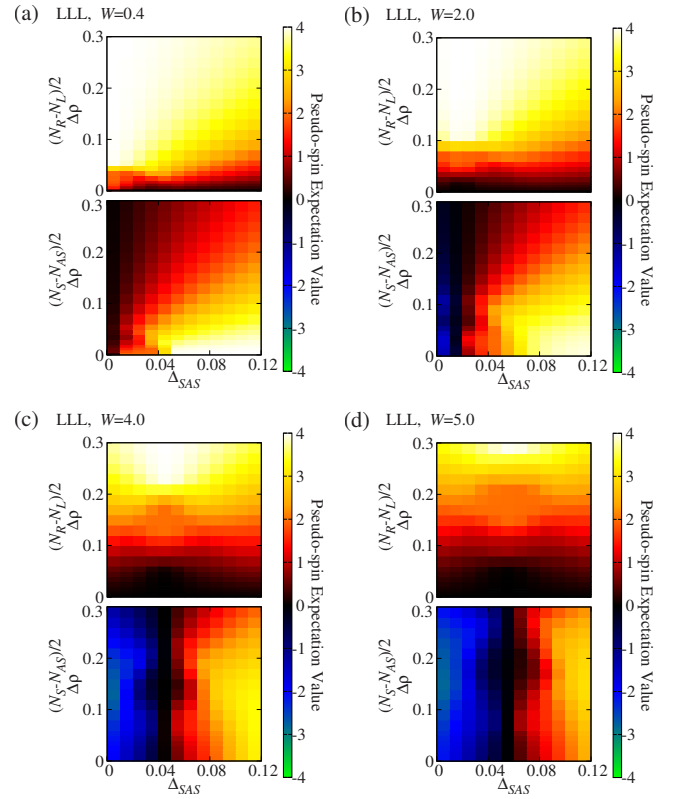


FIG. 14. (Color online) Lowest Landau level: (pseudospin) expectation value of the exact ground state (for the WQW model) of $(N_R - N_L)/2$ (top panel) and $(N_S - N_{AS})/2$ (lower panel) for (a) $W=0.4$, (b) $W=2$, (c) $W=4$, and (d) $W=5$. Note that the WQW model always breaks $SU(2)$ symmetry even for small W .

Similar to the bilayer model, the pseudospin expectation value for the WQW model in Fig. 14 mirrors the behavior of the overlaps. When the system is largely one component, either in the layer or SAS basis [large value of $(N_R - N_L)/2$ or $(N_S - N_{AS})/2$, respectively], the overlap with the appropriate basis Pf state is large. When the system is two component the overlap with the 331 is large. In investigating the pseudospin expectation value for the WQW model we see the most serious discrepancy between the two models, this effect was also seen previously in Ref. 4. For $W \geq 2$, and relatively small values of Δ_{SAS} , the ground has a negative value of $(N_S - N_{AS})/2$. This means that the electrons occupy the AS state compared to the S state. If we recall the overlap between the exact ground state and the Moore-Read Pfaffian in the SAS basis (lower panel of Fig. 12) the overlap is large for large Δ_{SAS} and this behavior mirrors the large value of $(N_S - N_{AS})/2$ shown in the lower panel of Fig. 14. However, the one-component Moore-Read Pfaffian we consider pairs electrons in the S state [shown schematically in Fig. 4(b)]. We have not checked the overlap with the one-component Pf written such that the pairing occurs between electrons in the AS state, thus, adding another version of the Pf. By examining the value of $(N_S - N_{AS})/2$ for $W \geq 2$ in the small Δ_{SAS} region of phase space we would expect a reasonable value of the overlap with a one-component Pf pairing electrons in the AS state.

The WQW model is more general than the usual bilayer model and the latter can be derived from it (see Sec. IVB of

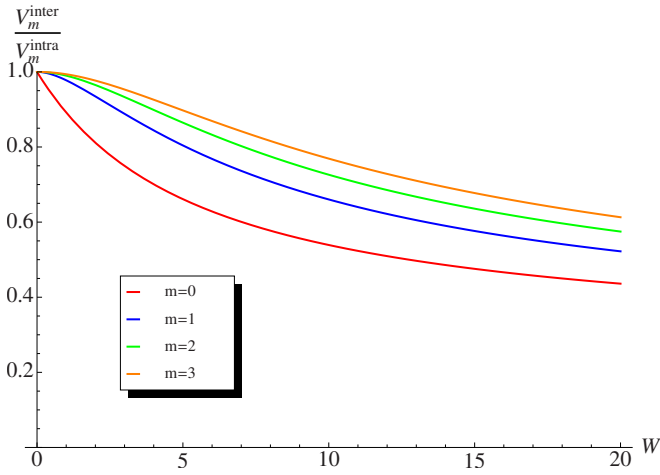


FIG. 15. (Color online) Ratio of the few strongest, interlayer and intralayer (bilayer) pseudopotentials $V_m^{\text{inter}}/V_m^{\text{intra}}$ derived using the WQW model (Ref. 4) as a function of width W . Note the saturation of the ratios for large widths W , illustrating the limit of validity of the WQW to describe bilayers.

Ref. 4 for a detailed discussion). However, if the well width W becomes very large, it is unjustified to restrict the model to only the lowest two subbands (and the inclusion of higher subbands cannot be treated exactly because of the computational complexity). On the other hand, as we map the WQW Hamiltonian to an effective bilayer, we find that the effective bilayer distance \tilde{d} saturates for large W . To see this, we can calculate the Haldane pseudopotentials $V_m^{\sigma_1\sigma_2\sigma_3\sigma_4}$, where m is the relative angular moment of the two electrons and $\sigma = S, AS$. If we denote by $\mathcal{F}^{\sigma_1\sigma_2\sigma_3\sigma_4}(\mathbf{r})$ the effective interaction in the plane, we have

$$\begin{aligned} \mathcal{F}^{\sigma_1\sigma_2\sigma_3\sigma_4}(\mathbf{r}) &= \int_0^W dz_1 \int_0^W dz_2 \langle \mathbf{r} | \sigma_1 \rangle(z_1) \langle \mathbf{r} | \sigma_2 \rangle(z_2) \\ &\quad \times \frac{1}{\sqrt{r^2 + |z_1 - z_2|^2}} \langle \mathbf{r} | \sigma_3 \rangle(z_1) \langle \mathbf{r} | \sigma_4 \rangle(z_2). \end{aligned} \quad (8)$$

The Haldane pseudopotentials for the effective interaction, written on the disk for simplicity (for the lowest Landau level), are

$$V_m^{\sigma_1\sigma_2\sigma_3\sigma_4} = \int \frac{d^2\mathbf{k}}{(2\pi)^2} e^{-k^2} \mathcal{L}_m(k^2) \mathcal{F}_{\mathbf{k}}^{\sigma_1\sigma_2\sigma_3\sigma_4},$$

where \mathcal{L}_m is the Laguerre polynomial and the Fourier transform $\mathcal{F}_{\mathbf{k}}^{\sigma_1\sigma_2\sigma_3\sigma_4}$ can be evaluated analytically. Furthermore, we can construct linear combinations⁴ of $V_m^{\sigma_1\sigma_2\sigma_3\sigma_4}$ to get the effective bilayer pseudopotentials, V_m^{intra} and V_m^{inter} . We plot the ratios of the few strongest V_m^{intra} and V_m^{inter} in Fig. 15 as a function of W . Notice that the limits saturate for large W , indicating that the interlayer repulsion decreases very slowly with respect to intrarepulsion for larger W , thus suggesting that the model becomes unrealistic in this regime. Also notice that the pseudopotentials involving a node in the z -wave function (the AS single-particle wave function has one node)

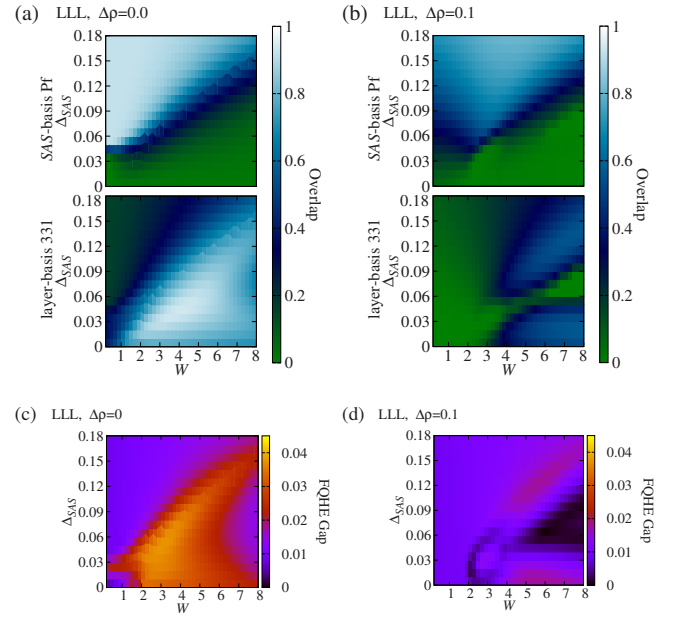


FIG. 16. (Color online) Lowest Landau level: FQHE energy gap for the WQW model as a function of W and Δ_{SAS} with (c) $\Delta\rho=0$ (left column) and (d) $\Delta\rho=0.1$ (right column). Also shown is the overlap between the SAS-basis Moore-Read Pfaffian (top panel) and the layer-basis Halperin 331 (bottom panel) wave functions and the exact ground state for (a) $\Delta\rho=0$ and (b) $\Delta\rho=0.1$.

can be smaller in absolute value than those without a node, indicating a possibility for some W to have a depopulation of the lowest subband and negative polarization ($N_S - N_{AS}$), as seen in the data.

Figure 16 shows the FQHE energy gap for the WQW model for $\Delta\rho=0$ and $\Delta\rho=0.1$, respectively. For $\Delta\rho=0$, we see similar behavior to the results of the bilayer model and shown previously,⁵ i.e., Fig. 11(d) for $\Delta\rho=0$. Of course, there are quantitative differences between the two models but the FQHE energy gap still shows a prominent ridge as a function of Δ_{SAS} and W . The ridge marks the transition line between the 331 and the Pfaffian or perhaps compressible states. Also, note that the maximum FQHE gap (the ridge) is slightly on the Halperin 331 side of the quantum phase diagram if the phase boundary is taken to be the place at which the 331 overlap is larger than the Pfaffian overlap, i.e., the 331 phase is the region where the Halperin 331 overlap is larger than the Pfaffian and vice versa, cf. Figs. 16(a) and 16(b). When the charge imbalancing term is increased to $\Delta\rho=0.1$ the FQHE gap is markedly reduced, as it was in the bilayer model. Again, as for $\Delta\rho=0$ the maximum gap is in the Halperin 331 part of the phase diagram. Interestingly, there appear to be two ridges forming for the $\Delta\rho=0.1$ situation in the FQHE gap and both ridge maxima are mirrored peaks in the 331 overlap, although, note that the overlaps (both 331 and Pf) for the $\Delta\rho=0.1$ situation are never very large and in a real experimental system the phase would most likely have been taken over by some other competing phase by the time the charge imbalancing strength reaches $\Delta\rho=0.1$, namely, a striped phase or, perhaps, a (composite fermion) Fermi sea.

Torus geometry

In this section we consider the wide-quantum-well model in the torus geometry^{85–87} which has one distinct advantage to the spherical geometry (of course, at the cost of other disadvantages). Recall in the spherical geometry, the filling factor is defined as $\lim_{N \rightarrow \infty} N/N_\phi$ and the relationship between N and N_ϕ for the Moore-Read Pfaffian and Halperin 331 is $N_\phi = 2N - 3$, where the “–3” is called the “shift” and is a consequence of the curvature of a spherical surface. Other competing phases for a half-filled Landau level, such as a (composite fermion) Fermi sea, have a different shift and comparing different states on an equal footing requires great care and extrapolation to the thermodynamic limit. However, on the torus, the filling factor is uniquely defined as simply N/N_ϕ and, therefore, different states can be directly compared for finite-size systems, of course, this does not mean a conclusion made for a finite-sized system will maintain as the thermodynamic limit is approached. (We note that it makes no sense to consider overlaps extrapolated to the thermodynamic limit since they trivially vanish.)

The torus geometry is generally defined using a domain with sides of length a and b with $a \neq b$. The aspect ratio of the toroidal system is $\tau = a/b$. The magnetic field does not allow the use of the usual translation operators but many-body states can be found⁸⁷ using the so-called magnetic translation operators with conserved pseudomomenta (K_x, K_y) . The pseudomomenta belong to a Brillouin zone with $(K_x = 2\pi s/a, K_y = 2\pi t/b)$ with $s, t = 0, \dots, N_0 - 1$ with N_0 being the greatest common divisor of N and N_ϕ .

Different FQHE states on the torus can be distinguished by their ground-state (topological) degeneracy. Generically, for a Landau-level filling factor of p/q there is always a center-of-mass degeneracy equal to q which is invariant to the form of the Hamiltonian and, thus, of no physical significance—we shall ignore it. Also there can be additional degeneracies that occur at special points in the Brillouin zone, such as at certain points in a hexagonal Brillouin zone, and we will consider these trivial. Finally, there can be degeneracies that are related to the specific topological nature of certain ground states and, therefore, nontrivial. For the two-component (Abelian) Halperin 331 state⁸⁸ we expect a quadruplet of states (up to the center-of-mass degeneracy, which in our case is 2) one of which belongs in the $(K_x, K_y) = (0, 0)$ sector and the remaining three are at the Brillouin-zone corners $(K_x, K_y) = (0, N_0/2)$, $(N_0/2, 0)$, and $(N_0/2, N_0/2)$. The non-Abelian Moore-Read Pfaffian^{47,89} (or equally the non-Abelian anti-Pfaffian^{52,53}) has only a *threefold* degeneracy⁵¹ of $(K_x, K_y) = (0, N_0/2)$, $(N_0/2, 0)$, and $(N_0/2, N_0/2)$, i.e., the $(K_x, K_y) = (0, 0)$ state is missing for even numbers of particles that we consider. Compressible states, such as the (composite fermion) Fermi sea, generally do not have clearly defined degeneracies, they may have accidental degeneracies that are strong functions of the aspect ratio τ , particle number N , or other Hamiltonian parameters. The *exact* degeneracies are expectations based on the (analytic) form of the variational ansatz wave functions and their respective conformal field theories.^{47,80} The ground state(s) of an actual Hamiltonian will not display exact degeneracies^{40,60,61,81} (perhaps they do in the thermodynamic

limit?) but the ground state(s) should qualitatively show the ground-state topological degeneracy corresponding to the variational ansatz if they are to be thought of as being in that “phase.” (We note that for a two-body Hamiltonian, such as the Coulomb interaction, in the absence of any particle-hole symmetry breaking terms the topological degeneracy of the ground state, if it were in the Moore-Read Pfaffian phase, would have a sixfold degeneracy ($3+3=6$) in the thermodynamic limit because, without particle-hole symmetry breaking terms, the Moore-Read Pfaffian and anti-Pfaffian are exactly degenerate. However, in a finite-sized system these two states are mixed leaving only a quasithreefold degeneracy.) Many states are sensitive to changes in τ while others are not. One should really investigate the properties of the system with regard to changes in τ , however, in the present case, a somewhat involved analytical calculation regarding the “background” charge is needed, and so we focus here on a fixed aspect ratio of $\tau = 0.97$.

All results on the torus correspond to a system of $N=8$ electrons in the half-filled lowest Landau level, $\nu = 1/2$. Figure 17(a) shows the energy spectrum of the low-lying states for the WQW model in the absence of any tunneling terms, i.e., $\Delta_{SAS} = \Delta\rho = 0$, as a function of the WQW width W . For each W , the lowest-lying energies are plotted relative to the ground state and shape and color coded to emphasize which states belong to which pseudomomenta sectors expected when considering the two-component Halperin 331 and one-component Moore-Read Pfaffian wave functions. Namely, we track the pseudomomenta sectors $(K_x, K_y) = (0, 4)$, $(4, 0)$, and $(4, 4)$ for the Pf with the addition of $(K_x, K_y) = (0, 0)$ for the 331 state. For large widths $W > 4.5$, the spectrum is characterized by a large energy gap separating a high-energy (quasi-)continuum of states from a low energy, nearly degenerate manifold of states at the pseudomomenta corresponding to the 331 state. As the width is decreased toward zero the $(K_x, K_y) = (0, 0)$ state that specifies the Halperin 331 state from the Moore-Read Pfaffian state goes up in energy joining the continuum. However, the $(K_x, K_y) = (0, 4)$ and $(4, 0)$ states of the Moore-Read Pfaffian also rise in energy into the continuum while at the same time a few states from the continuum drop down in energy mixing with states belonging to the 331 or Pf states. Finally, at very small $W < 1$ there is a single ground state of $(K_x, K_y) = (4, 4)$ and a large energy gap. However, there is no threefold degeneracy characteristic of the Moore-Read Pfaffian state present.

In Fig. 17(b) we fix $W = 6.5$ and $\Delta\rho = 0$ and vary the inter-layer tunneling strength Δ_{SAS} . For small $\Delta_{SAS} = 0$ we are clearly in the Halperin 331 part of the phase diagram since the spectra has a quasifourfold degeneracy characteristic of the 331 phase separated from the continuum by a large energy gap. Upon increasing Δ_{SAS} in an attempt to drive the system into the Moore-Read Pfaffian phase we see that while the $(K_x, K_y) = (0, 0)$ state of the 331 phase rise in energy and joins the continuum, the $(K_x, K_y) = (4, 4)$ state of the Pfaffian phase goes with it and a state from the high-energy continuum drops down into a quasithreefold degeneracy. However, this quasithreefold degeneracy does not contain the right pseudomomenta to describe the non-Abelian Moore-Read Pfaffian phase.

Lastly, in Fig. 17(c) we again set $W = 6.5$ but now fix $\Delta_{SAS} = 0$ and vary the charge imbalance $\Delta\rho$. As before, for

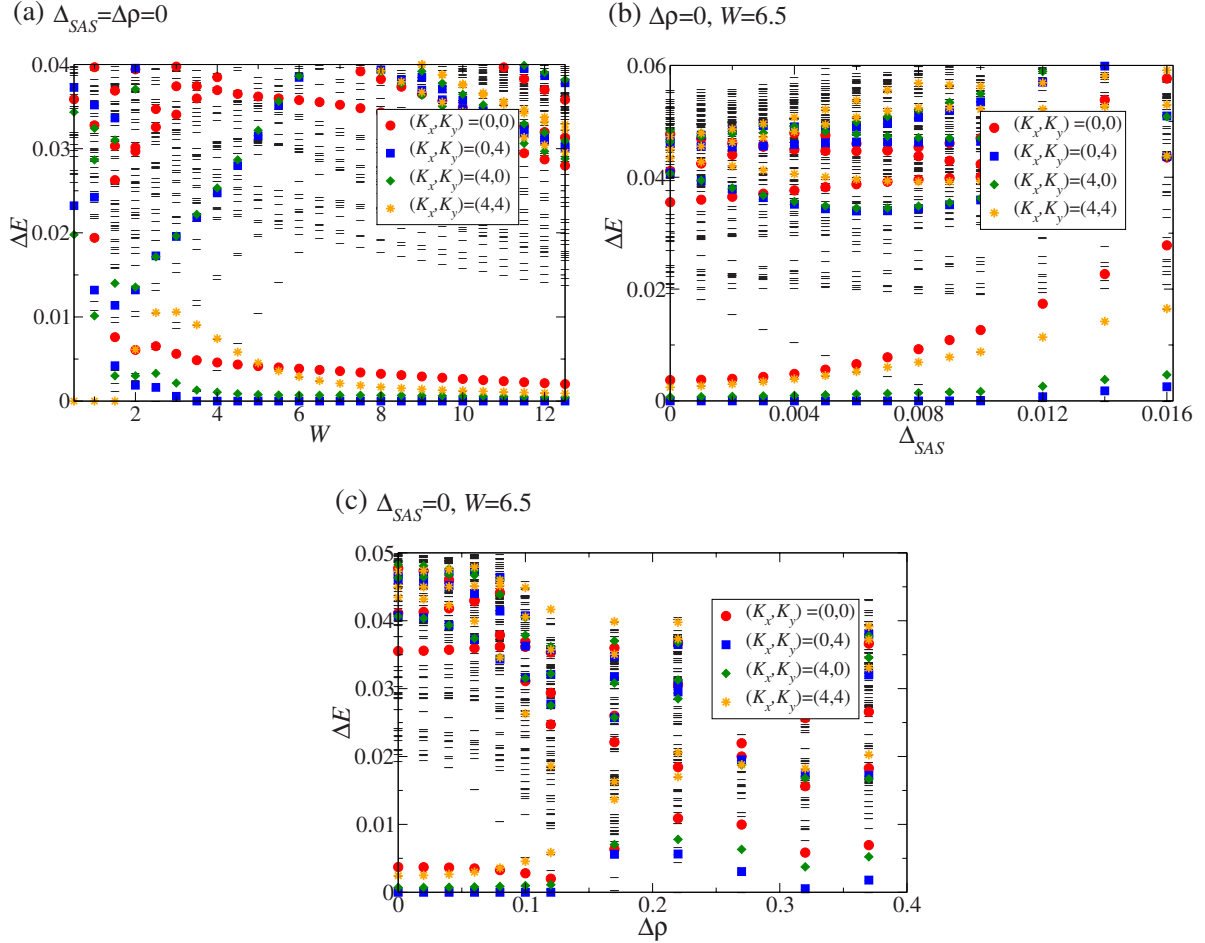


FIG. 17. (Color online) Lowest Landau level: energy spectra (given as the energy ΔE with respect to the ground state) for different pseudomomenta (the different levels) with (a) $\Delta_{SAS} = \Delta\rho = 0$ as a function of WQW width W , (b) $W = 6.5$ and $\Delta\rho = 0$ as a function of Δ_{SAS} , and (c) $W = 6.5$ and $\Delta_{SAS} = 0$ when the imbalance $\Delta\rho$ is increased from zero. The pseudomomenta corresponding to the Halperin 331 state and Moore-Read Pfaffian state ($(K_x, K_y) = (0,0)$ (solid red circle), $(0,4)$ (solid blue square), $(4,0)$ (solid green diamond), and $(4,4)$ (orange star) and $(K_x, K_y) = (0,4)$, $(4,0)$, and $(4,4)$, respectively. The black dashes correspond to states with pseudomomenta not belonging to either the 331 or Pf states.

small $\Delta\rho$ we see a clear signature of the Halperin 331 phase. However, as $\Delta\rho$ is increased the energy gap essentially collapses giving way to a phase that would most likely not exhibit the FQHE.

These conclusions corroborate our previous work using the spherical geometry and agree with the previous study⁸⁴ of bilayer model on the torus for $\nu = 1/2$. Namely, the Halperin 331 state is a good ansatz for the FQHE in the right parameter regions for bilayer and WQW systems. However, when the system is driven to be one component in the hopes of producing a FQHE described by the Moore-Read Pfaffian state the Hamiltonian details and Haldane pseudopotential⁸² values are such that the Moore-Read Pfaffian phase loses out to a different, most likely, non-FQHE state such as a striped phase or (composite fermion) Fermi sea.

V. RESULTS: SECOND LANDAU LEVEL

In this section we present results of our calculations for the second Landau level, that is, bilayer FQHE at $\nu = 5/2$.

(Work⁹⁰ has been done considering bilayer FQHE where the total filling factor is $\nu = 5/2 + 5/2 = 5$ but it is unrelated to our work.) We are neglecting Landau-level mixing and considering the electrons occupying the second Landau level to be spin polarized. Operationally, we have projected the half-filled electrons in the second Landau level into the lowest Landau level using the Haldane pseudopotentials.⁸² These effective pseudopotentials take into account the effective Coulomb interaction that occurs between the electrons in the SLL due to the different form of the single-particle wave functions compared to those in the LLL, the electrons in the LLL are taken to be inert, cf. discussion in Sec. I. We will not detail the procedure of using Haldane pseudopotentials in the FQHE as this procedure has been given in many places.^{13,82} Also, we (Peterson and Das Sarma⁵) have recently studied the FQHE in the SLL *without* the presence of a charge imbalancing term and will compare our results here extensively with the ones given previously.

Before we tackle the results for the second Landau level we briefly note that bilayer systems in higher Landau levels are quite subtle and nontrivial and actually provide some

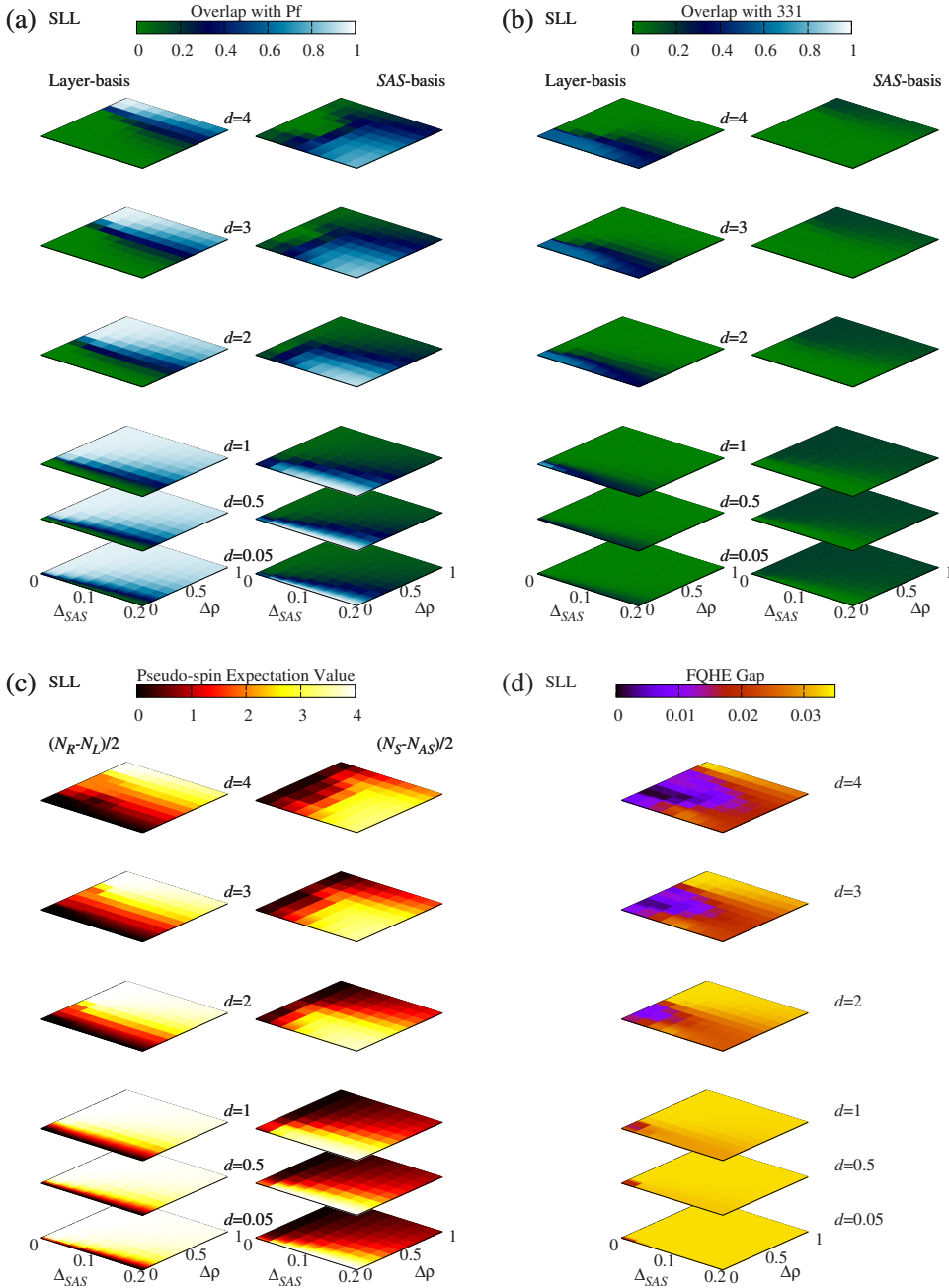


FIG. 18. (Color online) Second Landau level: (a) wavefunction overlap between the exact ground state of the bilayer Hamiltonian and the Moore-Read Pfaffian written in the layer basis (left column) and the SAS basis (right column) shown as a function of interlayer tunneling Δ_{SAS} and charge imbalance $\Delta\rho$ for different values of layer separation d and zero individual layer thickness $w=0$. (b) Same as (a) but for the Halperin 331 wave function. (c) Pseudospin expectation value or, more physically, the expectation value of $(N_R - N_L)/2$ (left column) and $(N_S - N_{AS})/2$ (right column) as a function of Δ_{SAS} and $\Delta\rho$. (d) The FQHE energy gap for the exact bilayer Hamiltonian.

conceptual difficulty. As recently discussed in Ref. 5, it is not obvious what happens to the electrons in the lowest spin-up and spin-down Landau levels when driving a one-component system at $\nu=5/2$ to a two-component (bilayer) system at total filling $\nu=5/2$. For this work, however, we take the conceptually well-defined and straightforward solution:⁵ we assume full spin polarization, hence the system is essentially spinless with each Landau level having only one spin index. Then the $\nu=5/2$ (balanced) two-component system is equivalent to one where each layer has $1+1/4$ filling with the lowest spin Landau level being completely full and the second Landau level being $1/4$ full. In this way, the incompressible FQHE states (Halperin 331 or Moore-Read Pfaffian) form completely in the second Landau level. This “solution” provides a completely well-defined mathematical problem. Of course, the real physical system, i.e., bilayer

FQHE systems in higher Landau levels, could be more complicated and produce rich physics. In fact, theoretically, the *full* solution is out of reach for any conceivable computer—the Hilbert space is too vast when including many (or at least three) Landau levels, spin up and spin down, and layer index. Thus, theoretical and experimental efforts in studying bilayer FQHE systems in higher Landau levels is likely a fertile ground for new discoveries.

A. Bilayer

In Fig. 18 we show overlaps between the exact ground state and the layer-basis and SAS-basis Pf and 331 wave functions, pseudospin expectation values, and the FQHE gap for the second Landau level. The difference between the LLL and the SLL are subtle but important.

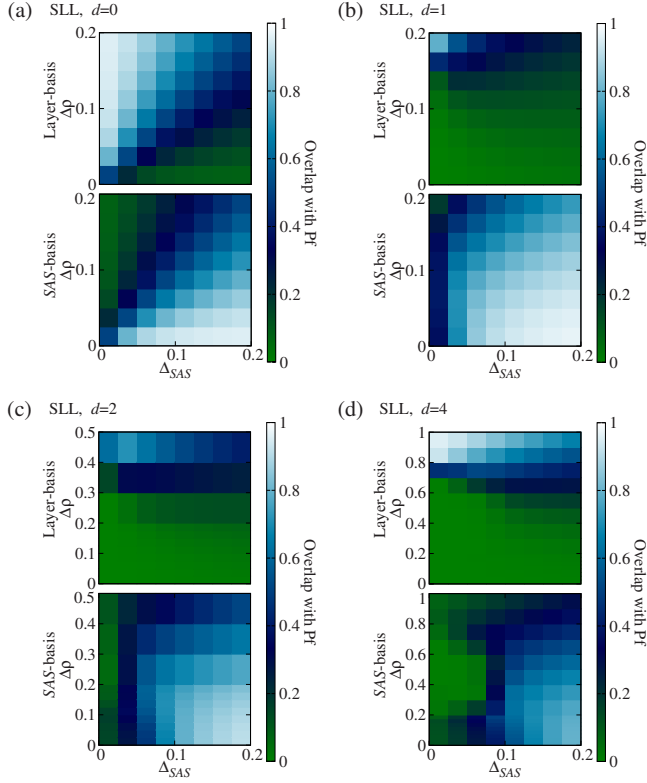


FIG. 19. (Color online) Second Landau level: wave-function overlap between the Moore-Read Pfaffian wave function in the layer basis (top panel) and the SAS basis (lower panel) and the exact ground state for (a) $d=0$, (b) $d=1$, (c) $d=2$, and (d) $d=4$.

First we focus on the overlaps between the Pf and 331 states and the exact ground state in both the layer and SAS bases, cf. Figs. 18(a) and 18(b). The main difference between the results in the LLL and the SLL is that, as has been shown previously^{5,60,61} for the case of zero charge imbalance $\Delta\rho = 0$, the overlap between the exact state and the Pf state(s) is higher in the SLL than it is in the LLL. In the SLL, the Pfaffian overlap is approximately ~ 0.97 at its largest while in the LLL it is approximately ~ 0.9 at its largest. This can be seen in Fig. 19 where, compared to the results of the LLL, in Fig. 19 where, compared to the results of the LLL, the overlap with the Pf state is higher in the SLL. [Again, for $d=0$ the system is SU(2) symmetric and the layer-basis and SAS-basis results are related via a pseudospin rotation.] We note that by increasing the width of the individual quantum well w , the Moore-Read Pfaffian overlap can be increased to nearly unity.^{5,60,61} This is a consequence of the differences between the Haldane pseudopotentials corresponding to the LLL versus those of the SLL with the SLL pseudopotentials being more amenable to pairing into a p -wave paired BCS state (of composite fermions), i.e., the Moore-Read Pfaffian.^{43,57,60,61,81,91}

There is another striking difference between the results in the LLL versus the SLL when considering the overlap between the Halperin 331 state. In the LLL, the 331 state provides a very good description of the FQHE for two-component systems when the separation d (or wide-well width W for the wide-quantum-well) and the tunneling

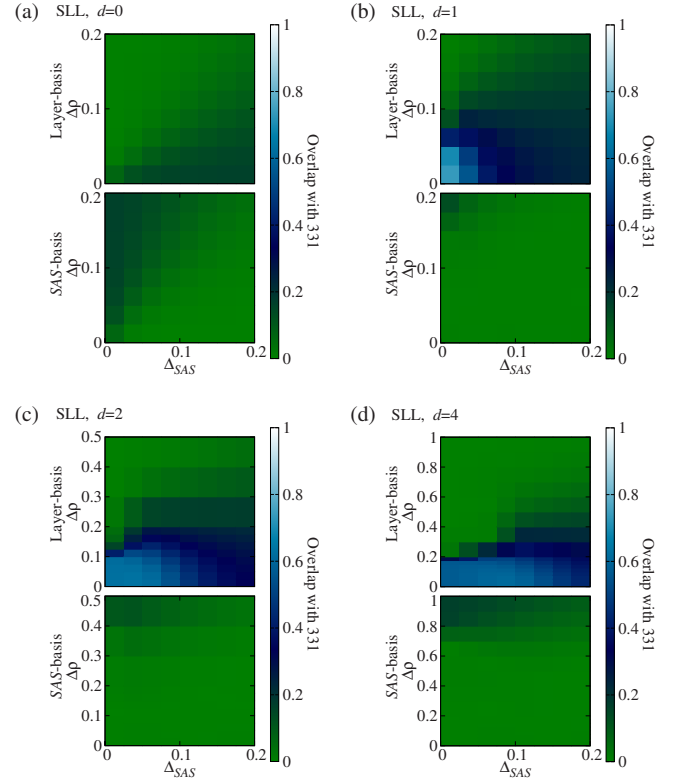


FIG. 20. (Color online) Second Landau level: wave-function overlap between the Halperin 331 wave function in the layer basis (top panel) and the SAS basis (lower panel) and the exact ground state for (a) $d=0$, (b) $d=1$, (c) $d=2$, and (d) $d=4$.

strengths are appropriate, this is evident by the value high value of the overlap that is obtained (~ 0.99). In the SLL, the qualitative behavior of the overlap as the system parameters are varied is similar to the LLL but the overlap does not obtain as high a value (only ~ 0.8 for $d \sim 1$ and $\Delta_{SAS} = \Delta\rho = 0$). This, again, can be seen in Fig. 20.

Looking at the pseudospin expectation value $(N_S - N_{AS})/2$ and $(N_R - N_L)/2$ in Fig. 18(c) (as well as Fig. 21) we see very little difference between the lowest and second Landau levels. In fact, visually it is difficult distinguishing the two.

Lastly, we consider the FQHE gap (Figs. 18(d) and 22), which does display some behavior that is qualitatively different from that of the LLL. This qualitatively different behavior manifests itself for values of layer separation $d > 2$. In this region of parameter space we see that for increasing values of $\Delta\rho$ the FQHE gap has a maximum for a wide range of Δ_{SAS} . This is in stark contrast to the FQHE gap in the LLL [cf. Fig. 5(d)] where the gap shows some indication of increasing for increasing $\Delta\rho$ but not to a *maximum*.

Figure 23 shows the overlaps, pseudospin expectation values, and FQHE gap as a function of layer separation d and tunneling strength Δ_{SAS} for several values of charge imbalance tunneling strength $\Delta\rho$. Qualitatively, the overlaps [Figs. 23(a) and 23(b)] are similar in the SLL and LLL. However, comparing them side by side, the overlap with the Halperin 331 state achieves a higher value in the LLL than it does in the SLL. The opposite is true for the overlap with the Moore-

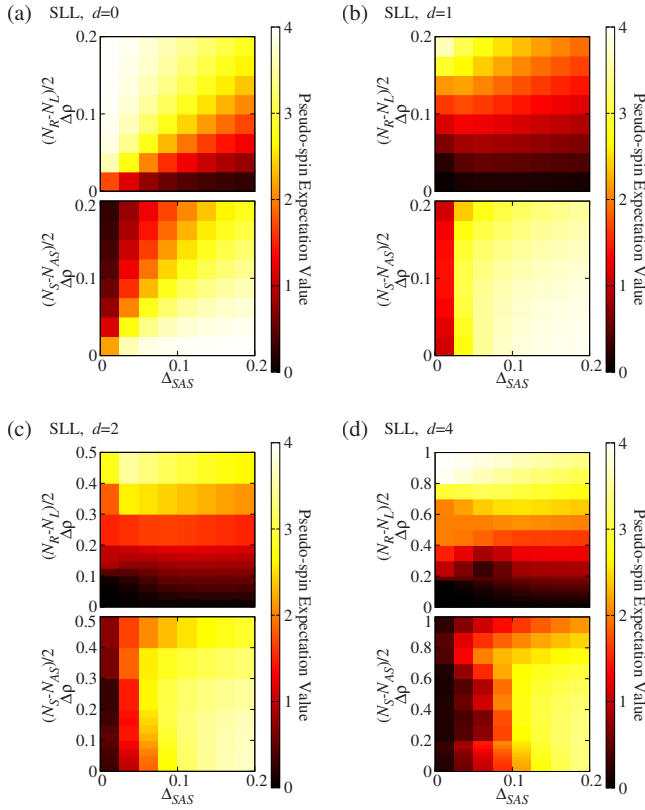


FIG. 21. (Color online) Second Landau level: (pseudospin) expectation value of the exact ground state of $(N_R - N_L)/2$ (top panel) and $(N_S - N_{AS})/2$ (lower panel) for (a) $d=0$, (b) $d=1$, (c) $d=2$, and (d) $d=4$.

Read Pfaffian state where the overlap achieves a higher value in the SLL than it does in the LLL. These differences are manifest even while the pseudospin expectation values [Fig. 23(c)] in the SLL, compared to the LLL, cannot visually be distinguished. Thus, while the values of the Haldane pseudopotentials in the SLL are not different enough from the LLL to change pseudospin expectation values, i.e., the system is

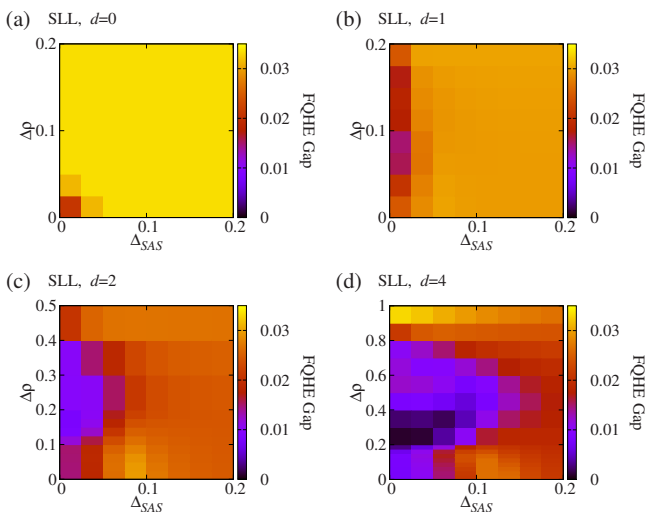


FIG. 22. (Color online) Second Landau level: FQHE energy gap for (a) $d=0$, (b) $d=1$, (c) $d=2$, and (d) $d=4$.

one component or two component at almost exactly the same place in parameter space in both the LLL and SLL, the differences are enough to change the character of the overlaps and the FQHE energy gap.

Figure 23(d) shows the FQHE energy gap, and again, there is a marked difference between the result in the LLL versus SLL. Similar to the higher overlap value between the exact ground state and the Moore-Read Pfaffian state in the SLL, the FQHE energy gap has a maximum in the Pf region of the approximate quantum phase diagram especially along the Δ_{SAS} axis for small d . (The opposite is true in the LLL—the FQHE energy gap is largest in the Halperin 331 region of the quantum phase diagram.) We see this behavior also in the wide-quantum-well results.

B. Wide-quantum-well

In Fig. 24 we plot the overlap between the exact ground state of the WQW model and the Moore-Read Pfaffian wave function written in the layer basis (top panel) and SAS basis (lower panel). This figure is, of course, similar to, and should be compared to, Fig. 19 showing the same thing for the bilayer model. Qualitatively, the same behavior is manifest in the two models. As the WQW width W is increased it takes a larger and larger tunneling strength to increase the overlap with the Pf.

The overlap between the ground state and the Halperin 331 state is shown in Fig. 25. Again, we only show the overlap with the Halperin 331 state written in the layer-basis since the overlap with the SAS-basis 331 state is almost zero throughout parameter space. The results are qualitatively similar to those of the bilayer model. However, for $W=2$ [Fig. 25(b)] there is a slight maximum in the overlap as Δ_{SAS} is increased from zero at $\Delta_{SAS} \sim 0.03$. This is an interesting result that is harder to understand, increasing Δ_{SAS} drives the system to be one component and one would surmise that increasing this parameter would lower the overlap with the 331 state monotonically. For $W=4$ we see that two peaks in the overlap appear; one for small values of Δ_{SAS} and another for a larger value with a strong minimum in between; behavior is particular to the WQW model. Similar to the lowest Landau level, the expectation value of $(N_S - N_{AS})/2$ for $W \geq 2$ is negative for small Δ_{SAS} and $\Delta\rho$. In fact, this negative value means that the system prefers to have more electrons in the AS state than the S state. However, the system is still more one component in those regions, such as the region in Fig. 26(b) along the $\Delta\rho=0$ axis near $\Delta_{SAS} \sim 0.3$, which correspond to a maximum in the overlap with the 331 state. At any rate, this behavior marks a qualitative difference between the bilayer and WQW models.

Lastly, we show the FQHE energy gap for $\Delta\rho=0$ in Fig. 27(b) along with the overlap between the SAS-basis Moore-Read Pfaffian state [top panel of Fig. 27(a)] and the layer-basis Halperin 331 state [bottom panel of Fig. 27(a)], respectively. When the FQHE energy gap is nonzero and the system therefore would be expected to exhibit the FQHE, the overlap with the Pfaffian state is large. On the other hand, in the region of parameter space where the FQHE energy gap is small, the Halperin 331 state has a larger overlap. Thus, in-

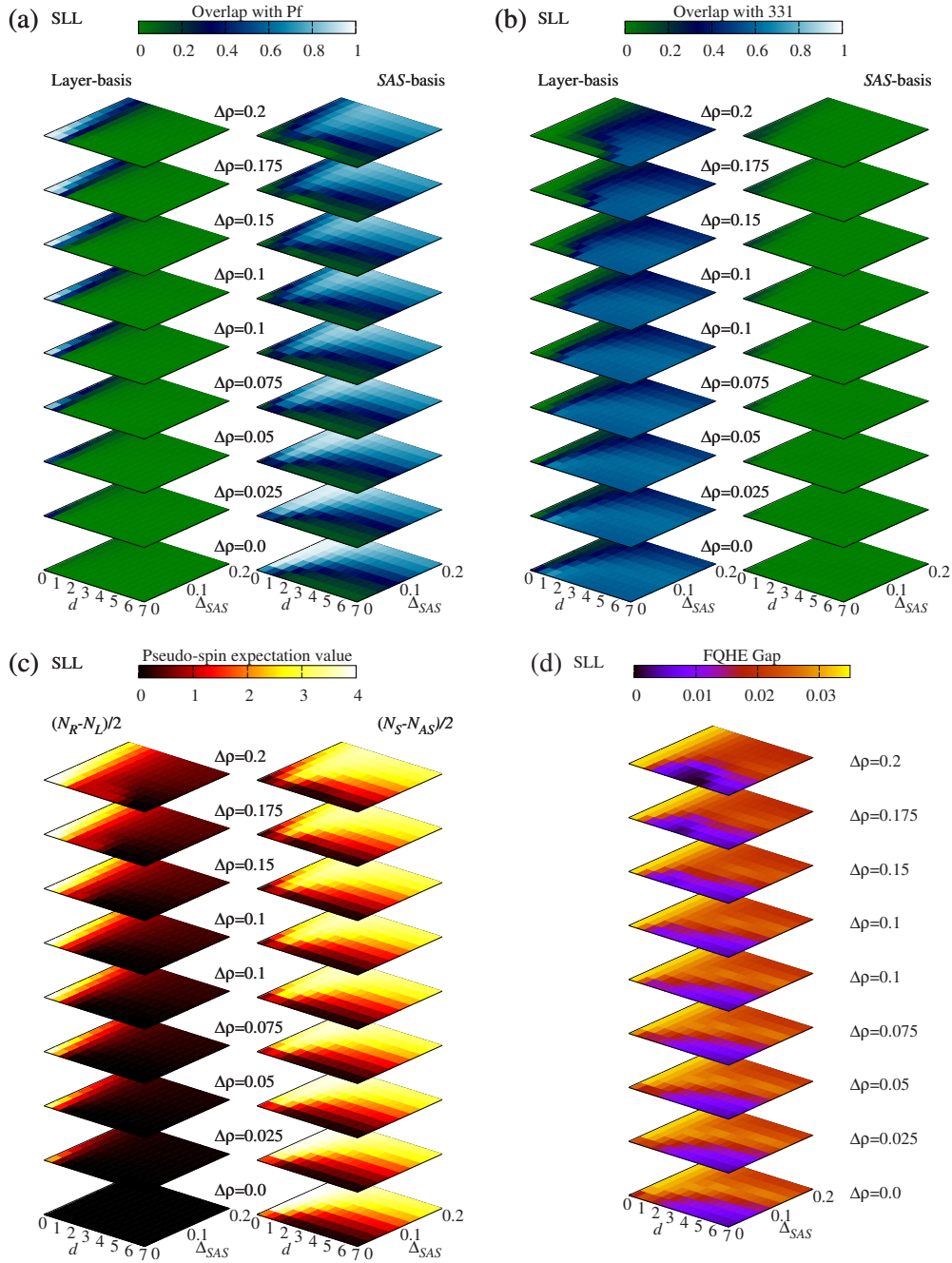


FIG. 23. (Color online) Second Landau level: same as Fig. 18 except that all plots are shown as a function of interlayer tunneling Δ_{SAS} and layer separation d for a number of different charge imbalances $\Delta\rho$ and zero individual layer thickness $w=0$.

dependent of our model of choice, the details of the electron-electron interaction in the second Landau level, compared to the lowest Landau level, make a profound difference. In the second Landau level the Pfaffian wave function is a good description of the physics when the system is largely one component. In the lowest Landau level, the Halperin 331 is a good description of the physics when the system is largely two component.

Note that there is a peak in the FQHE energy gap for $W \sim 2$ and $\Delta_{SAS} \approx 0$ which is well within the Halperin 331 part of the approximate quantum phase diagram. Even though the overlap with the 331 state is small in that region of parameter space it could correspond to a two-component Abelian

FQHE for bilayer systems in the second Landau level at total $\nu=5/2$ that is in the same universality class as the Halperin 331 state.

VI. CONCLUSIONS

In conclusion, we have investigated the FQHE in two-component systems for the half-filled lowest and second Landau levels ($\nu=1/2$ and $\nu=5/2$, respectively) as a function of both tunneling strengths; interlayer tunneling and charge imbalancing. This work was motivated by the recent experimental systems investigated in Refs. 6 and 7.

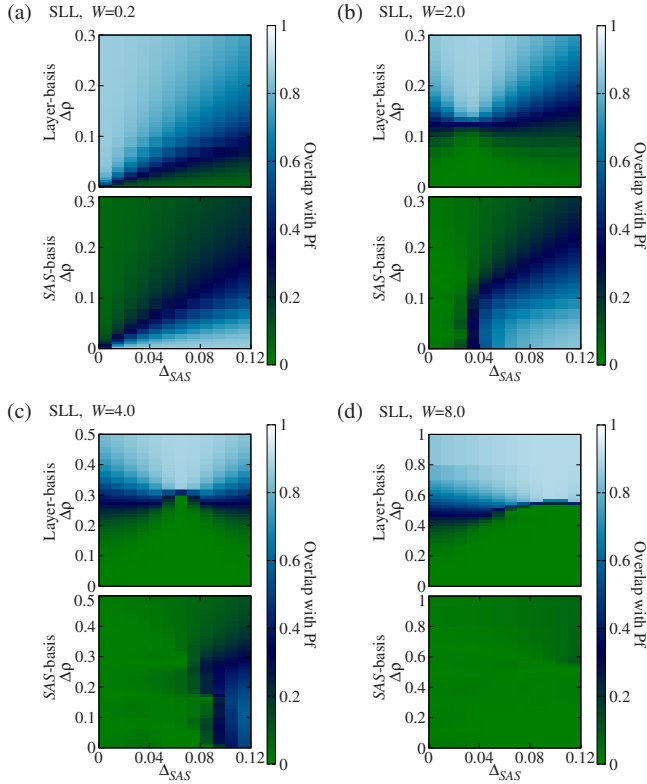


FIG. 24. (Color online) Second Landau level: wave-function overlap between the Moore-Read Pfaffian wave function in the layer basis (top panel) and the SAS basis (lower panel) and the exact ground state for the WQW for (a) $W=0.2$, (b) $W=2$, (c) $W=4$, and (d) $W=8$ as a function of Δ_{SAS} and $\Delta\rho$.

Our main results are as follows: (i) the FQHE at $\nu=1/2$ is described by the (Abelian) Halperin 331 two-component state which is robust to charge imbalance tunneling. When the system is driven into the one-component region of parameter space, we find that the (non-Abelian) Moore-Read Pfaffian state is most likely beaten out by other competing non-FQHE phases [cf. striped phase or (composite fermion) Fermi sea]. The reason we suspect this is because even though the overlap between the exact ground state and the Pf (in the SAS or layer basis, depending on the region of parameter space, i.e., whether Δ_{SAS} is large and $\Delta\rho$ is small or vice versa) is large, the FQHE energy gap has a peak that is (slightly) on the Halperin 331 side of the approximate quantum phase diagram, where the quantum phase diagram determination is described in Sec. IV. This result, along with recent numerical calculations by Storni *et al.*⁵⁹ (as well as Refs. 62 and 84), leads us to conclude that the one-component $\nu=1/2$ is likely to be a non-FQHE striped phase or (composite fermion) Fermi sea. In the effective BCS description, the increase in tunneling (in the layer basis) or charge imbalance (in the SAS basis) leads also to the increase in the effective chemical potential of the “even” channel which drives the system into a compressible phase.⁸⁴

We also find that our calculations are unable to explain the recent results of Shabani *et al.*,^{6,7} which consider *only* the

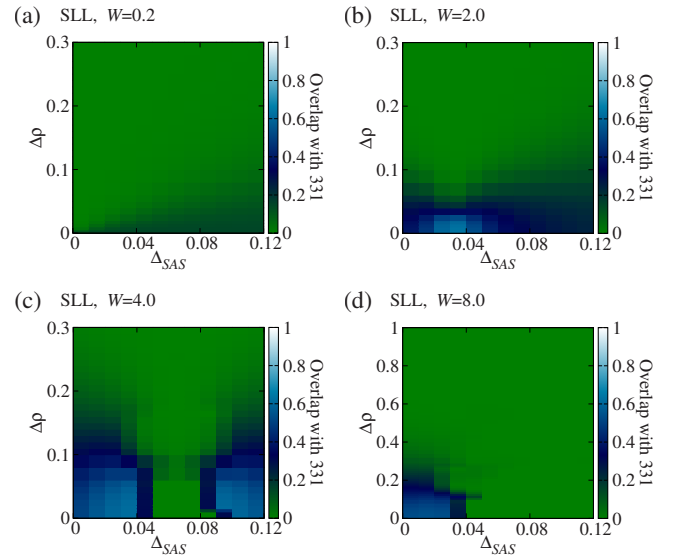


FIG. 25. (Color online) Second Landau level: wave-function overlap between the Halperin 331 wave function in the layer basis and the exact ground state for the WQW for (a) $W=0.2$, (b) $W=2$, (c) $W=4$, and (d) $W=8$ as a function of Δ_{SAS} and $\Delta\rho$. Note that the overlap with the layer-basis Halperin 331 state is not shown since it is always nearly zero.

competing Moore-Read Pfaffian and Halperin 331 states. In that work, they observe no FQHE at $\nu=1/2$ when the charge imbalance is zero, an emerging FQHE at $\nu=1/2$ for nonzero charge imbalance, and finally, that the FQHE is eventually destroyed upon increasing charge imbalance. While we find that the Halperin 331 FQHE is quite robust to a charge imbalance tunneling term, our results would suggest that the FQHE would monotonically decrease in strength with increasing charge imbalance (that is, the measured activation gap would decrease in strength, the minimum in R_{xx} would weaken, and/or the “quality” of the plateau in R_{xy} would deteriorate)—we would expect experiments to observe a FQHE at $\nu=1/2$ with zero charge imbalance that is eventually destroyed upon further imbalancing. The fact that this does not happen in the experiment indicates that the observed state at large imbalance must be something different from the 331 or the Pfaffian state, at least within our model calculations.

(ii) The FQHE in the second Landau level at $\nu=5/2$ is most likely the spin-polarized and one-component (non-Abelian) Moore-Read Pfaffian state. This state, similar to the Halperin 331 state in the lowest Landau level, is robust to charge imbalancing. We also find that in regions of parameter space when the system is largely two component, i.e., for small Δ_{SAS} and $\Delta\rho$, the system might display a FQHE described by the (Abelian) Halperin 331 state. This suggests⁵ the exciting possibility of experimentally tuning parameters to drive an Abelian FQHE state (331) at $\nu=5/2$ into a non-Abelian FQHE state (Pf) at $\nu=5/2$ by way of a quantum phase transition.

(iii) One of our surprising theoretical findings is that the Halperin 331 two-component bilayer Abelian paired FQHE

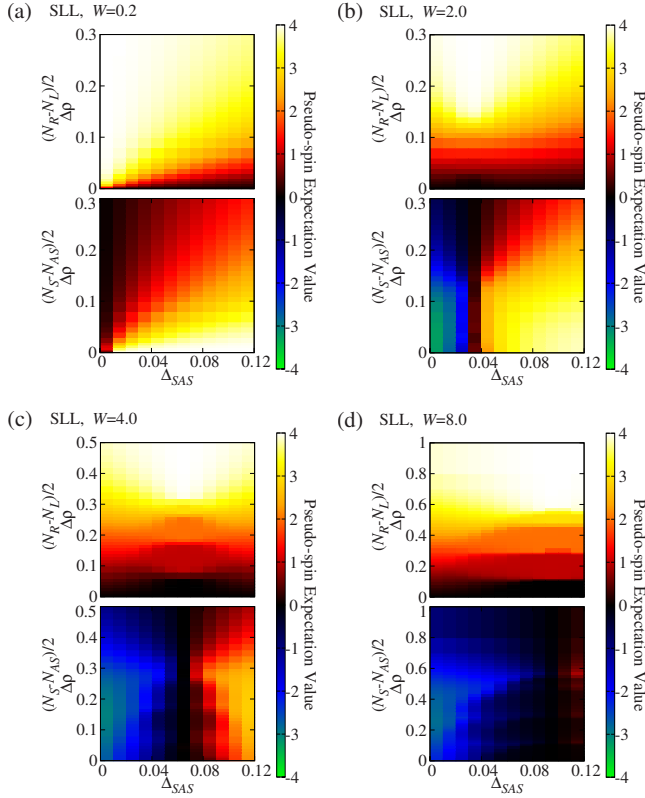


FIG. 26. (Color online) Second Landau level: pseudospin expectation value of the exact ground state (for the WQW model) of $(N_R - N_L)/2$ (top panel) and $(N_S - N_{AS})/2$ (lower panel) for (a) $W = 0.2$, (b) $W = 2$, (c) $W = 4$, and (d) $W = 8$. Note that the WQW model always breaks $SU(2)$ symmetry even for small W and that for $W \geq 2$ there are negative values of $(N_S - N_{AS})/2$ meaning the system prefers, in some regions of parameter space, to have more electrons in the AS state compared to the S state even for positive and nonzero Δ_{SAS} .

is robust, and survives, not only substantial interlayer tunneling, but also substantial charge imbalance. We suspect that this result is quite general and possibly also applies to other Abelian paired states⁶⁹ in the same universality class of the 331 state.

Finally, we address a possible criticism to our work. As mentioned previously, the Hilbert space of the bilayer problem is very large and, hence, we were only able to consider $N=8$ electrons while adequately exploring the large parameter space inherent in a problem with interlayer tunneling and charge imbalance. A central result of our work concerns the robustness of the Halperin 331 or Moore-Read Pfaffian state to interlayer tunneling and charge imbalance terms present in the Hamiltonian. Is it possible that this robustness is a finite-size effect? We strongly believe that our result is not a finite-size effect and the reason is as follows. We know that the Halperin 331 two-component state describes the FQHE at $\nu=1/2$ (LLL) in charged balanced bilayer systems with zero (or weak) interlayer tunneling and that the 331 state is robust to interlayer tunneling (measured as a fraction of the Coulomb energy)—this is known both

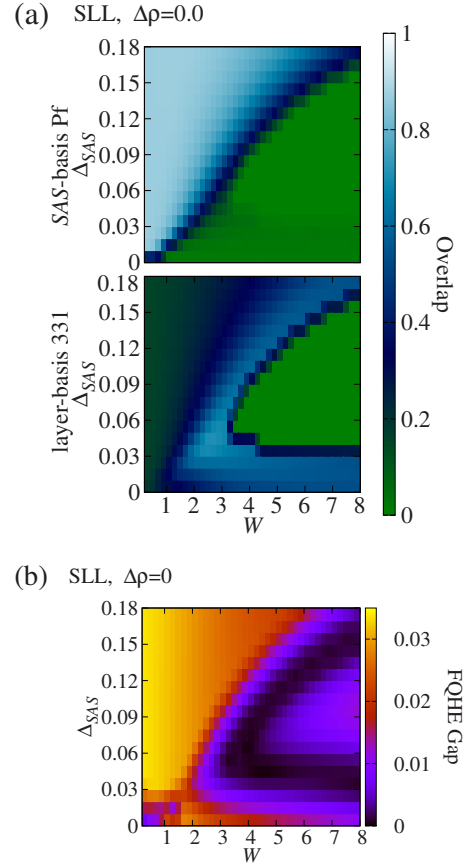


FIG. 27. (Color online) Second Landau level: (b) FQHE energy gap for the WQW model as a function of W and Δ_{SAS} with $\Delta\rho=0$. Also shown is the (a) overlap between the SAS -basis Moore-Read Pfaffian (top panel) and the layer-basis Halperin 331 (bottom panel) wave functions and the exact ground state for $\Delta\rho=0$.

theoretically,¹⁻⁵ and more importantly, experimentally.⁶³⁻⁶⁶ For zero layer separation, theoretically, the bilayer system with interlayer tunneling and zero charge imbalance is identical to the bilayer system with zero interlayer tunneling and finite charge imbalance via a pseudospin rotation. Further, for nonzero layer separation, nonzero charge imbalance, and zero interlayer tunneling, the theoretical results are qualitatively similar to the results for the charged balanced situation with nonzero layer separation and nonzero interlayer tunneling—finite layer separation breaks the $SU(2)$ invariance and thus the amount of interlayer tunneling needed to destroy the 331 state is not necessarily equal to the amount of charge imbalance needed to destroy the 331 state. However, the two “critical” values are qualitatively similar. Thus, we feel that our results concerning the robustness of the 331 state to charge imbalance is most likely *not* a finite-size effect but a real effect awaiting experimental verification. Finally, the physics of the bilayer FQHE at $\nu=5/2$ is extremely rich with many unanswered and fascination questions [not to mention the fact that the bilayer problem in higher Landau levels is conceptually difficult and nontrivial (see Sec. V)] that, in our opinion, are awaiting experimental answers.

ACKNOWLEDGMENTS

M.R.P. and S.D.S. are grateful to Microsoft Q for support. Z.P. was supported by the Serbian Ministry of Science under Grant No. 141035 and by the Agence Nationale de la

Recherche under Grant No. ANR-JCJC-0003-01. M.R.P. thanks Vito Scarola for helpful comments. Z.P. most gratefully acknowledges helpful discussions and former collaboration with M. Goerbig and N. Regnault on setting up the wide-quantum-well model.

- ¹S. He, S. Das Sarma, and X. C. Xie, *Phys. Rev. B* **47**, 4394 (1993).
- ²S. He, X. C. Xie, S. Das Sarma, and F. C. Zhang, *Phys. Rev. B* **43**, 9339 (1991).
- ³K. Nomura and D. Yoshioka, *J. Phys. Soc. Jpn.* **73**, 2612 (2004).
- ⁴Z. Papić, G. Möller, M. V. Milovanović, N. Regnault, and M. O. Goerbig, *Phys. Rev. B* **79**, 245325 (2009).
- ⁵M. R. Peterson and S. Das Sarma, *Phys. Rev. B* **81**, 165304 (2010).
- ⁶J. Shabani, T. Gokmen, and M. Shayegan, *Phys. Rev. Lett.* **103**, 046805 (2009).
- ⁷J. Shabani, T. Gokmen, Y. T. Chiu, and M. Shayegan, *Phys. Rev. Lett.* **103**, 256802 (2009).
- ⁸We note that charge imbalance has been considered before (Refs. 92–97) in bilayer systems for situations where the total filling factor was not equal to 1/2 and the physics for those systems is, in fact, very different from that studied in our current situation.
- ⁹D. C. Tsui, H. L. Stormer, and A. C. Gossard, *Phys. Rev. Lett.* **48**, 1559 (1982).
- ¹⁰R. B. Laughlin, *Phys. Rev. Lett.* **50**, 1395 (1983).
- ¹¹*Perspectives in Quantum Hall Effects*, edited by S. Das Sarma and A. Pinczuk (Wiley, New York, 1997).
- ¹²*Composite Fermions: A Unified View of the Quantum Hall Regime*, edited by O. Heinonen (World Scientific, New Jersey, 1998).
- ¹³J. K. Jain, *Composite Fermions* (Cambridge University Press, New York, 2007).
- ¹⁴J. K. Jain, *Phys. Rev. Lett.* **63**, 199 (1989).
- ¹⁵X. G. Wen and Q. Niu, *Phys. Rev. B* **41**, 9377 (1990).
- ¹⁶R. Willett, J. P. Eisenstein, H. L. Stormer, D. C. Tsui, A. C. Gossard, and J. H. English, *Phys. Rev. Lett.* **59**, 1776 (1987).
- ¹⁷B. I. Halperin, P. A. Lee, and N. Read, *Phys. Rev. B* **47**, 7312 (1993).
- ¹⁸V. Kalmeyer and S.-C. Zhang, *Phys. Rev. B* **46**, 9889 (1992).
- ¹⁹E. Rezayi and N. Read, *Phys. Rev. Lett.* **72**, 900 (1994).
- ²⁰R. L. Willett, R. R. Ruel, K. W. West, and L. N. Pfeiffer, *Phys. Rev. Lett.* **71**, 3846 (1993).
- ²¹R. R. Du, H. L. Stormer, D. C. Tsui, L. N. Pfeiffer, and K. W. West, *Phys. Rev. Lett.* **70**, 2944 (1993).
- ²²W. Kang, H. L. Stormer, L. N. Pfeiffer, K. W. Baldwin, and K. W. West, *Phys. Rev. Lett.* **71**, 3850 (1993).
- ²³J. P. Eisenstein, R. Willett, H. L. Stormer, D. C. Tsui, A. C. Gossard, and J. H. English, *Phys. Rev. Lett.* **61**, 997 (1988).
- ²⁴P. L. Gammel, D. J. Bishop, J. P. Eisenstein, J. H. English, A. C. Gossard, R. Ruel, and H. L. Stormer, *Phys. Rev. B* **38**, 10128 (1988).
- ²⁵W. Pan, J.-S. Xia, V. Shvarts, D. E. Adams, H. L. Stormer, D. C. Tsui, L. N. Pfeiffer, K. W. Baldwin, and K. W. West, *Phys. Rev. Lett.* **83**, 3530 (1999).
- ²⁶J. P. Eisenstein, K. B. Cooper, L. N. Pfeiffer, and K. W. West, *Phys. Rev. Lett.* **88**, 076801 (2002).
- ²⁷J. S. Xia, W. Pan, C. L. Vicente, E. D. Adams, N. S. Sullivan, H. L. Stormer, D. C. Tsui, L. N. Pfeiffer, K. W. Baldwin, and K. W. West, *Phys. Rev. Lett.* **93**, 176809 (2004).
- ²⁸G. A. Csáthy, J. S. Xia, C. L. Vicente, E. D. Adams, N. S. Sullivan, H. L. Stormer, D. C. Tsui, L. N. Pfeiffer, and K. W. West, *Phys. Rev. Lett.* **94**, 146801 (2005).
- ²⁹H. C. Choi, W. Kang, S. Das Sarma, L. N. Pfeiffer, and K. W. West, *Phys. Rev. B* **77**, 081301(R) (2008).
- ³⁰J. Nuebler, V. Umansky, R. Morf, M. Heiblum, K. von Klitzing, and J. Smet, *Phys. Rev. B* **81**, 035316 (2010).
- ³¹C. R. Dean, B. A. Piot, P. Hayden, S. Das Sarma, G. Gervais, L. N. Pfeiffer, and K. W. West, *Phys. Rev. Lett.* **101**, 186806 (2008).
- ³²S. Das Sarma, G. Gervais, and X. Zho, *Phys. Rev. B* **82**, 115330 (2010).
- ³³C. R. Dean, B. A. Piot, P. Hayden, S. Das Sarma, G. Gervais, L. N. Pfeiffer, and K. W. West, *Phys. Rev. Lett.* **100**, 146803 (2008).
- ³⁴C. R. Dean, B. A. Piot, G. Gervais, L. N. Pfeiffer, and K. W. West, *Phys. Rev. B* **80**, 153301 (2009).
- ³⁵T. D. Rhone, J. Yan, Y. Gallais, A. Pinczuk, L. Pfeiffer, and K. West, APS Meeting, Portland, OR, March 2010; e-print [arXiv:1011.3857](https://arxiv.org/abs/1011.3857) (unpublished).
- ³⁶M. Stern, P. Plochocka, V. Umansky, D. Maude, M. Potemski, and I. Bar-Joseph, *Phys. Rev. Lett.* **105**, 096801 (2010).
- ³⁷W. Bishara and C. Nayak, *Phys. Rev. B* **80**, 121302 (2009).
- ³⁸E. Rezayi and S. Simon, [arXiv:0912.0109](https://arxiv.org/abs/0912.0109) (unpublished).
- ³⁹A. Wojs, C. Töke, and J. Jain, *Phys. Rev. Lett.* **105**, 096802 (2010).
- ⁴⁰H. Wang, D. N. Sheng, and F. D. M. Haldane, *Phys. Rev. B* **80**, 241311 (2009).
- ⁴¹W. Pan, H. L. Stormer, D. C. Tsui, L. N. Pfeiffer, K. W. Baldwin, and K. W. West, *Solid State Commun.* **119**, 641 (2001).
- ⁴²C. Zhang, T. Knuutila, Y. Dai, R. R. Du, L. N. Pfeiffer, and K. W. West, *Phys. Rev. Lett.* **104**, 166801 (2010).
- ⁴³R. H. Morf, *Phys. Rev. Lett.* **80**, 1505 (1998).
- ⁴⁴A. E. Feiguin, E. Rezayi, C. Nayak, and S. Das Sarma, *Phys. Rev. Lett.* **100**, 166803 (2008).
- ⁴⁵A. Yu. Kitaev, *Ann. Phys.* **303**, 2 (2003).
- ⁴⁶C. Nayak, S. H. Simon, A. Stern, M. Freedman, and S. Das Sarma, *Rev. Mod. Phys.* **80**, 1083 (2008).
- ⁴⁷G. Moore and N. Read, *Nucl. Phys. B* **360**, 362 (1991).
- ⁴⁸S. Das Sarma, M. Freedman, and C. Nayak, *Phys. Rev. Lett.* **94**, 166802 (2005).
- ⁴⁹J. Bardeen, L. N. Cooper, and J. R. Schrieffer, *Phys. Rev.* **106**, 162 (1957).
- ⁵⁰J. Bardeen, L. N. Cooper, and J. R. Schrieffer, *Phys. Rev.* **108**, 1175 (1957).
- ⁵¹N. Read and D. Green, *Phys. Rev. B* **61**, 10267 (2000).

- ⁵²S.-S. Lee, S. Ryu, C. Nayak, and M. P. A. Fisher, *Phys. Rev. Lett.* **99**, 236807 (2007).
- ⁵³M. Levin, B. I. Halperin, and B. Rosenow, *Phys. Rev. Lett.* **99**, 236806 (2007).
- ⁵⁴M. R. Peterson, K. Park, and S. Das Sarma, *Phys. Rev. Lett.* **101**, 156803 (2008).
- ⁵⁵N. d'Ambrumenil and A. M. Reynolds, *J. Phys. C* **21**, 119 (1988).
- ⁵⁶A. H. MacDonald, *Phys. Rev. B* **30**, 3550 (1984).
- ⁵⁷V. W. Scarola, K. Park, and J. K. Jain, *Phys. Rev. B* **62**, R16259 (2000).
- ⁵⁸C. Töke, M. R. Peterson, G. S. Jeon, and J. K. Jain, *Phys. Rev. B* **72**, 125315 (2005).
- ⁵⁹M. Storni, R. H. Morf, and S. Das Sarma, *Phys. Rev. Lett.* **104**, 076803 (2010).
- ⁶⁰M. R. Peterson, T. Jolicœur, and S. Das Sarma, *Phys. Rev. Lett.* **101**, 016807 (2008).
- ⁶¹M. R. Peterson, T. Jolicœur, and S. Das Sarma, *Phys. Rev. B* **78**, 155308 (2008).
- ⁶²Z. Papić, N. Regnault, and S. Das Sarma, *Phys. Rev. B* **80**, 201303 (2009).
- ⁶³Y. W. Suen, L. W. Engel, M. B. Santos, M. Shayegan, and D. C. Tsui, *Phys. Rev. Lett.* **68**, 1379 (1992).
- ⁶⁴Y. W. Suen, M. B. Santos, and M. Shayegan, *Phys. Rev. Lett.* **69**, 3551 (1992).
- ⁶⁵Y. W. Suen, H. C. Manoharan, X. Ying, M. B. Santos, and M. Shayegan, *Phys. Rev. Lett.* **72**, 3405 (1994).
- ⁶⁶J. P. Eisenstein, G. S. Boebinger, L. N. Pfeiffer, K. W. West, and S. He, *Phys. Rev. Lett.* **68**, 1383 (1992).
- ⁶⁷B. I. Halperin, *Helv. Phys. Acta* **56**, 783 (1983).
- ⁶⁸D. R. Luhman, W. Pan, D. C. Tsui, L. N. Pfeiffer, K. W. Baldwin, and K. W. West, *Phys. Rev. Lett.* **101**, 266804 (2008).
- ⁶⁹V. W. Scarola and J. K. Jain, *Phys. Rev. B* **64**, 085313 (2001).
- ⁷⁰V. Scarola, C. May, M. Peterson, and M. Troyer, *Phys. Rev. B* **82**, 121304(R) (2010).
- ⁷¹F. C. Zhang and S. Das Sarma, *Phys. Rev. B* **33**, 2903 (1986).
- ⁷²A. H. MacDonald, P. M. Platzman, and G. S. Boebinger, *Phys. Rev. Lett.* **65**, 775 (1990).
- ⁷³J. Schliemann, S. M. Girvin, and A. H. MacDonald, *Phys. Rev. Lett.* **86**, 1849 (2001).
- ⁷⁴K. Nomura and D. Yoshioka, *Phys. Rev. B* **66**, 153310 (2002).
- ⁷⁵K. Park, *Phys. Rev. B* **69**, 045319 (2004).
- ⁷⁶S. H. Simon, E. H. Rezayi, and M. V. Milovanovic, *Phys. Rev. Lett.* **91**, 046803 (2003).
- ⁷⁷G. Möller, S. H. Simon, and E. H. Rezayi, *Phys. Rev. Lett.* **101**, 176803 (2008).
- ⁷⁸G. Möller, S. H. Simon, and E. H. Rezayi, *Phys. Rev. B* **79**, 125106 (2009).
- ⁷⁹See, J. R. Schrieffer, *Theory of Superconductivity* (Addison-Wesley, Reading, MA, 1964) and Ref. 51 for a discussion of the Pfaffian form of the real-space BCS pairing wave function.
- ⁸⁰M. Milovanović and N. Read, *Phys. Rev. B* **53**, 13559 (1996).
- ⁸¹E. H. Rezayi and F. D. M. Haldane, *Phys. Rev. Lett.* **84**, 4685 (2000).
- ⁸²F. D. M. Haldane, *Phys. Rev. Lett.* **51**, 605 (1983).
- ⁸³T. T. Wu and C. N. Yang, *Nucl. Phys. B* **107**, 365 (1976).
- ⁸⁴Z. Papić, M. Goerbig, N. Regnault, and M. Milovanović, *Phys. Rev. B* **82**, 075302 (2010).
- ⁸⁵D. Yoshioka, B. I. Halperin, and P. A. Lee, *Phys. Rev. Lett.* **50**, 1219 (1983).
- ⁸⁶D. Yoshioka, *Phys. Rev. B* **29**, 6833 (1984).
- ⁸⁷F. D. M. Haldane, *Phys. Rev. Lett.* **55**, 2095 (1985).
- ⁸⁸X.-G. Wen and A. Zee, *Phys. Rev. B* **58**, 15717 (1998).
- ⁸⁹N. Read and E. Rezayi, *Phys. Rev. B* **54**, 16864 (1996).
- ⁹⁰C. Shi, S. Jolad, N. Regnault, and J. K. Jain, *Phys. Rev. B* **77**, 155127 (2008).
- ⁹¹G. Möller and S. H. Simon, *Phys. Rev. B* **77**, 075319 (2008).
- ⁹²A. R. Champagne, J. P. Eisenstein, L. N. Pfeiffer, and K. W. West, *Phys. Rev. Lett.* **100**, 096801 (2008).
- ⁹³A. R. Champagne, A. D. K. Finck, J. P. Eisenstein, L. N. Pfeiffer, and K. W. West, *Phys. Rev. B* **78**, 205310 (2008).
- ⁹⁴A. Sawada, Z. F. Ezawa, H. Ohno, Y. Horikoshi, Y. Ohno, S. Kishimoto, F. Matsukura, M. Yasumoto, and A. Urayama, *Phys. Rev. Lett.* **80**, 4534 (1998).
- ⁹⁵V. T. Dolgoplov, A. A. Shashkin, E. V. Deviatov, F. Hastreiter, M. Hartung, A. Wixforth, K. L. Campman, and A. C. Gossard, *Phys. Rev. B* **59**, 13235 (1999).
- ⁹⁶E. Tutuc, S. Melinte, E. P. De Poortere, R. Pillarisetty, and M. Shayegan, *Phys. Rev. Lett.* **91**, 076802 (2003).
- ⁹⁷I. B. Spielman, M. Kellogg, J. P. Eisenstein, L. N. Pfeiffer, and K. W. West, *Phys. Rev. B* **70**, 081303 (2004).

Search Search History

All Databases

<< Return to Web of Science®

Citing Articles Title: **Topological Entanglement in Abelian and Non-Abelian Excitation Eigenstates**
 Author(s): Papic, Z. ; Bernevig, B. A. ; Regnault, N.
 Source: PHYSICAL REVIEW LETTERS Volume: 106 Issue: 5 Article Number: 056801 DOI: 10.1103/PhysRevLett.106.056801 Published: FEB 1 2011

This item has been cited by items indexed in the databases listed below. [more information]

- 13 in All Databases
- 13 publication in Web of Science
- 0 publication in BIOSIS Citation Index
- 0 publication in SciELO Citation Index
- 0 publication in Chinese Science Citation Database
- 0 data sets in Data Citation Index
- 0 publication in Data Citation Index

Results: 13 Page 1 of 1 Go Sort by: Publication Date -- newest to oldest

Create Citation Report

Hide Refine

Refine Results

Search within results for

Search

Databases

Research Domains Refine

SCIENCE TECHNOLOGY

Research Areas Refine

PHYSICS

MECHANICS

more options / values...

Document Types

Authors

Group/Corporate Authors

Editors

Funding Agencies

Source Titles

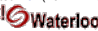
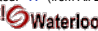
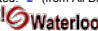

Conference/Meeting Titles

Publication Years

Languages

Countries/Territories

- Select Page Add to Marked List (0) Send to: my.endnote.com
1. Title: **Topological Characterization of Fractional Quantum Hall Ground States from Microscopic Hamiltonians**
 Author(s): Zaletel, Michael P.; Mong, Roger S. K.; Pollmann, Frank
 Source: PHYSICAL REVIEW LETTERS Volume: 110 Issue: 23 Article Number: 236801 DOI: 10.1103/PhysRevLett.110.236801 Published: JUN 4 2013
 Times Cited: 3 (from All Databases)
 Get it! Waterloo [View abstract]
 2. Title: **Exact matrix product states for quantum Hall wave functions**
 Author(s): Zaletel, Michael P.; Mong, Roger S. K.
 Source: PHYSICAL REVIEW B Volume: 86 Issue: 24 Article Number: 245305 DOI: 10.1103/PhysRevB.86.245305 Published: DEC 11 2012
 Times Cited: 8 (from All Databases)
 Get it! Waterloo [View abstract]
 3. Title: **Adiabatic continuity between Hofstadter and Chern insulator states**
 Author(s): Wu, Ying-Hai; Jain, J. K.; Sun, Kai
 Source: PHYSICAL REVIEW B Volume: 86 Issue: 16 Article Number: 165129 DOI: 10.1103/PhysRevB.86.165129 Published: OCT 22 2012
 Times Cited: 9 (from All Databases)
 Get it! Waterloo [View abstract]
 4. Title: **Entanglement spectrum of the Heisenberg XXZ chain near the ferromagnetic point**
 Author(s): Alba, Vincenzo; Haque, Masudul; Laeuuchi, Andreas M.
 Source: JOURNAL OF STATISTICAL MECHANICS-THEORY AND EXPERIMENT Article Number: P08011 DOI: 10.1088/1742-5468/2012/08/P08011
 Published: AUG 2012
 Times Cited: 2 (from All Databases)
 Get it! Waterloo [View abstract]
 5. Title: **Evaluation of Ranks of Real Space and Particle Entanglement Spectra for Large Systems**
 Author(s): Rodriguez, Ivan D.; Simon, Steven H.; Slingerland, J. K.
 Source: PHYSICAL REVIEW LETTERS Volume: 108 Issue: 25 Article Number: 256806 DOI: 10.1103/PhysRevLett.108.256806 Published: JUN 19 2012
 Times Cited: 9 (from All Databases)
 Get it! Waterloo [View abstract]
 6. Title: **Boundary-Locality and Perturbative Structure of Entanglement Spectra in Gapped Systems**
 Author(s): Alba, Vincenzo; Haque, Masudul; Laeuuchi, Andreas M.
 Source: PHYSICAL REVIEW LETTERS Volume: 108 Issue: 21 Article Number: 227201 DOI: 10.1103/PhysRevLett.108.227201 Published: MAY 29 2012
 Times Cited: 10 (from All Databases)
 Get it! Waterloo [View abstract]
 7. Title: **Real-space entanglement spectrum of quantum Hall states**
 Author(s): Sterdyniak, A.; Chandran, A.; Regnault, N.; et al.
 Source: PHYSICAL REVIEW B Volume: 85 Issue: 12 Article Number: 125308 DOI: 10.1103/PhysRevB.85.125308 Published: MAR 16 2012
 Times Cited: 13 (from All Databases)
 Get it! Waterloo [View abstract]
 8. Title: **Edge-mode combinations in the entanglement spectra of non-Abelian fractional quantum Hall states on the torus**
 Author(s): Liu, Zhao; Bergholtz, Emil J.; Fan, Heng; et al.
 Source: PHYSICAL REVIEW B Volume: 85 Issue: 4 Article Number: 045119 DOI: 10.1103/PhysRevB.85.045119 Published: JAN 19 2012
 Times Cited: 6 (from All Databases)
 Get it! Waterloo [View abstract]
 9. Title: **Bulk-edge correspondence in entanglement spectra**
 Author(s): Chandran, Anushya; Hermanns, M.; Regnault, N.; et al.
 Source: PHYSICAL REVIEW B Volume: 84 Issue: 20 Article Number: 205136 DOI: 10.1103/PhysRevB.84.205136 Published: NOV 22 2011
 Times Cited: 20 (from All Databases)
 Get it! Waterloo [View abstract]

- 10. Title: [Trace index and spectral flow in the entanglement spectrum of topological insulators](#)
 Author(s): Alexandradinata, A.; Hughes, Taylor L.; Bernevig, B. Andrei
 Source: PHYSICAL REVIEW B Volume: 84 Issue: 19 Article Number: 195103 DOI: 10.1103/PhysRevB.84.195103 Published: NOV 3 2011
 Times Cited: 3 (from All Databases)
 Get it!  [[View abstract](#)]
- 11. Title: [The hierarchical structure in the orbital entanglement spectrum of fractional quantum Hall systems](#)
 Author(s): Sterdyniak, A.; Bernevig, B. A.; Regnault, N.; et al.
 Source: NEW JOURNAL OF PHYSICS Volume: 13 Article Number: 105001 DOI: 10.1088/1367-2630/13/10/105001 Published: OCT 4 2011
 Times Cited: 11 (from All Databases)
 Get it!  [[View abstract](#)]
- 12. Title: [Entanglement measures for quasi-two-dimensional fractional quantum Hall states](#)
 Author(s): Biddle, J.; Peterson, Michael R.; Das Sarma, S.
 Source: PHYSICAL REVIEW B Volume: 84 Issue: 12 Article Number: 125141 DOI: 10.1103/PhysRevB.84.125141 Published: SEP 30 2011
 Times Cited: 2 (from All Databases)
 Get it!  [[View abstract](#)]
- 13. Title: [Decomposition of fractional quantum Hall model states: Product rule symmetries and approximations](#)
 Author(s): Thomale, Ronny; Estienne, Benoit; Regnault, Nicolas; et al.
 Source: PHYSICAL REVIEW B Volume: 84 Issue: 4 Article Number: 045127 DOI: 10.1103/PhysRevB.84.045127 Published: JUL 19 2011
 Times Cited: 15 (from All Databases)
 Get it!  [[View abstract](#)]

Select Page |  Add to Marked List (0) |  |  | Send to:

Results: 13 Page 1 of 1 Sort by:

13 records matched your query of the 55,067,330 (contains duplicates) in the data limits you selected.

View in: [简体中文](#) | [繁體中文](#) | [English](#) | [日本語](#) | [한국어](#) | [Português](#) | [Español](#)

© 2013 Thomson Reuters | [Terms of Use](#) | [Privacy Policy](#) | *Please give us your feedback on using Web of Knowledge.*

Topological Entanglement in Abelian and Non-Abelian Excitation Eigenstates

Z. Papić,^{1,2,3} B. A. Bernevig,⁴ and N. Regnault³

¹*Institute of Physics, University of Belgrade, Pregrevica 118, 11 000 Belgrade, Serbia*

²*Laboratoire de Physique des Solides, Univ. Paris-Sud, CNRS, UMR 8502, 91405 Orsay, France*

³*Laboratoire Pierre Aigrain, ENS and CNRS, 24 rue Lhomond, F-75005 Paris, France*

⁴*Department of Physics, Princeton University, Princeton, New Jersey 08544, USA*

(Received 12 September 2010; published 1 February 2011)

Entanglement in topological phases of matter has so far been investigated through the perspective of their ground-state wave functions. In contrast, we demonstrate that the excitations of fractional quantum Hall (FQH) systems also contain information to identify the system's topological order. Entanglement spectrum of the FQH quasihole (QH) excitations is shown to differentiate between the conformal field theory (CFT) sectors, based on the relative position of the QH with respect to the entanglement cut. For Read-Rezayi model states, as well as Coulomb interaction eigenstates, the counting of the QH entanglement levels in the thermodynamic limit matches exactly the CFT counting, and sector changes occur as non-Abelian quasiholes successively cross the entanglement cut.

DOI: 10.1103/PhysRevLett.106.056801

PACS numbers: 73.43.-f, 63.20.Pw, 63.22.-m

Topologically ordered systems are not characterized by local order parameters; nonlocal concepts, such as quantum entanglement [1], have been extensively used in recent years to describe such phases of matter. The favorite method of analyzing the entanglement—entanglement entropy (or its topological part for gapped systems [2])—does not result in a unique characterization of the system: different states of matter can have identical entanglement entropy. Complicated topological phases, such as fractional quantum Hall (FQH) states, are fully described by a multitude of universal parameters, notably braiding matrices [3], which are related to the properties of the FQH excitations under adiabatic exchanges in space-time. In finite systems, the braiding matrices are impossible to obtain and the question arises whether the universal properties of a topologically ordered state are obtainable via the entanglement of its excitations. Although scarcely addressed in the existing literature [4,5], the question is pertinent also in view of the phases of matter that can only be distinguished by their excitation spectra [6].

Recently, it was proposed [7] that the entanglement spectrum (ES), i.e., the (negative logarithm of the) full set of eigenvalues of the reduced density matrix ρ_A , is a rich source of information on the topological order in FQH ground states. Reduced density matrix ρ_A of the subsystem A of a pure FQH state $|\psi\rangle$ on the sphere [8] (Fig. 1) is given by the usual trace $\rho_A = \text{Tr}_B |\psi\rangle\langle\psi|$ over the complementary subsystem B . The levels of ρ_A can be classified according to the number of particles N_A and orbitals l_A in A , as well as the z -axis projection of the angular momentum L_z^A . The multiplicities and relative energy spectrum of ρ_A match that of the edge modes [7,9–11]. For ground states of Coulomb Hamiltonians in the same universality class with a FQH model state, the ES typically displays a branch of low-lying (high-probability) levels, very similar

to those of the model state, accompanied by spurious levels at high entanglement energy (low probability). The gap between the low and high levels, properly defined by taking the “conformal limit” [10], was conjectured and numerically substantiated to remain constant upon increasing the system size.

In this Letter we show that the ES of FQH excitation states contains information to identify the universal properties of topological phases of matter. We consider model wave functions, such as Laughlin [12], Moore-Read [13], and Read-Rezayi [14], whose ground and excited states with localized quasiholes (QHs) can be expressed as Jack polynomials [15,16]. Furthermore, we consider the eigenstates of Coulomb interaction potential with the impurities that pin the QHs at a circle of latitude [17,18]. The ES of a given FQH excitation is monitored as the QHs are moved across the cut (Fig. 1). This reveals that the ES of the excitations can probe different conformal field theory (CFT) fermion-number sectors, that it gives the correct counting of the edge states in the thermodynamic limit, and that it is extremely sensitive (within a single magnetic length) to whether non-Abelian QHs are on the same or opposite sides of the entanglement cut. The latter property

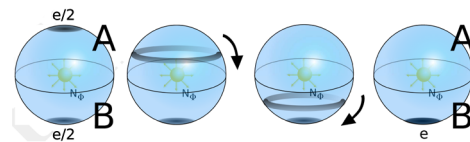


FIG. 1 (color online). FQH sphere with a monopole of N_ϕ magnetic flux quanta in the center, partitioned into hemispheres A and B , and containing the bosonic Moore-Read state with two QHs. We start with two separated QHs (left) and drag one QH from the north to the south hemisphere (middle). The moving QH is azimuthally delocalized. We end up with a QH twice the charge at the south pole (right).

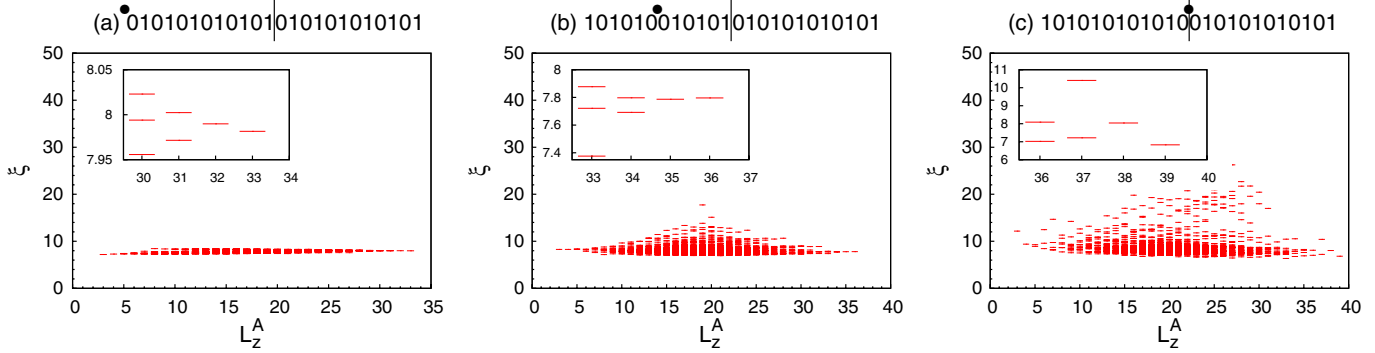


FIG. 2 (color online). Conformal-limit ES of the Laughlin model state of $N = 12$ bosons with a single QH, localized at one of the poles (a), the equator (c) and in between (b). The location of the QH is given by the dot above each root partition. Insets show high-probability ES levels.

can be taken as a simple manifestation of the non-Abelian nature of the phase. These findings are corroborated in studies of the realistic Coulomb interaction eigenstates. We also analyze the behavior of the quasielectron excitations, as well as the quasihole and quasielectron fluctuations when close to the entanglement cut.

The orbital of an electron confined to the lowest Landau level (LLL) moving on the Haldane sphere [8] (Fig. 1) can be written as $\phi_m(z) = \mathcal{N}_m z^m$, where $z = x + iy$ is the complex 2D electron coordinate, the quantum number m is the L_z eigenvalue, and \mathcal{N}_m is a geometrical normalization factor. Conformal limit [10] is defined as the geometry where the normalization factors \mathcal{N}_m are all equal to 1. General N -electron LLL states are analytic polynomials $\Psi_F(z_1, \dots, z_N) = \prod_{i < j} (z_i - z_j) \Psi_B$, which can be factorized into a Vandermonde determinant and a bosonic wave function Ψ_B . We may therefore focus on the systems of charged bosons in the LLL. Arbitrary Ψ_B is expandable in terms of symmetric monomials indexed by a partition λ represented by occupation numbers $n(\lambda) = \{n_m(\lambda), m = 0, 1, \dots\}$ of the orbitals ϕ_m . Certain FQH wave functions are, however, defined by a single *root* partition—all the remaining partitions in the expansion of Ψ_B are derived from it via “squeezing” operations [15]. This includes the Read-Rezayi [14] \mathbb{Z}_k series of trial states for bosons at filling factors $\nu \equiv N/N_\phi = k/2$ which can be identified with a family of Jack polynomials (Jacks) $J_{\lambda_k}^\alpha$, parametrized by $\alpha = -(k + 1)$ and indexed by a partition $n(\lambda_k) \equiv (k0k0k\dots)$, i.e., $\Psi_{RR}^k \propto J_{k0k0\dots}^{-(k+1)}(\{z_i\})$. Apart from FQH ground states, the Jacks also yield wave functions of the QH [15] and quasielectron [19] excitations, created by varying the magnetic flux through the sphere. If the flux is increased by one unit, k non-Abelian QHs of charge e/k each are nucleated and pinned at locations w_1, \dots, w_k . Let us consider such an arrangement of the QHs where the first n_1 QHs are fixed at one pole of the sphere, $n_2 = k - 1 - n_1$ are at the opposite pole, and the remaining mobile QH is at w_k in between the poles. The wave function for \mathbb{Z}_k states with a QH at w_k close to, e.g., the

north pole is given by a single Jack $J_{abab\dots ab}^{-(k+1)}(\{z_i\})$ with the root partition $abab\dots ab$, where $a = (k - 1 - \Delta n)/2$, $b = k - a$, and $\Delta n = n_2 - n_1$ [16]. As the QH at w_k is moved from the north to the south pole, the wave function mixes in several other Jacks [15,16], and we can track its progression. When the QH reaches the south pole, the wave function is again a single Jack, $J_{a+1b-1a+1b-1,\dots,a+1b-1}^{-(k+1)}(\{z_i\})$.

The Jack QH wave function for $k = 1$ describes a single Abelian QH, localized at one of the orbitals of the sphere. In Fig. 2 we show the numerically calculated ES in the conformal limit for the Laughlin state of $N = 12$ bosons and a single localized QH. The cut is fixed such that the subsystem A contains $l_A = 12$ orbitals and $N_A = 6$ particles. Above each plot in Figs. 2–4, we give the root configuration used to generate the wave function and draw the cut in orbital space (vertical line), showing the high-probability ES levels in the inset. When the QH is at one of the poles [Fig. 2(a)], the level counting matches that of the $U(1)$ chiral boson CFT. As we move the QH towards the equator [Fig. 2(b)], the levels spread upwards, but the CFT counting remains unaltered. The spreading reflects the quantum-mechanical oscillation of the QH around the cut but is expected to be confined within a magnetic

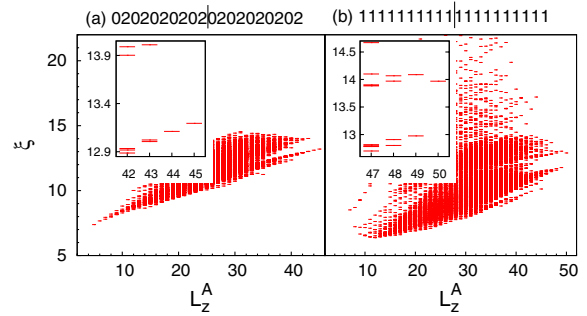


FIG. 3 (color online). Conformal-limit ES of the Moore-Read model state for $N = 20$ bosons with a unit flux added. (a) Abelian vortex 0202...02. (b) Two fractionalized $e/2$ non-Abelian QHs. Insets show high-probability ES levels.

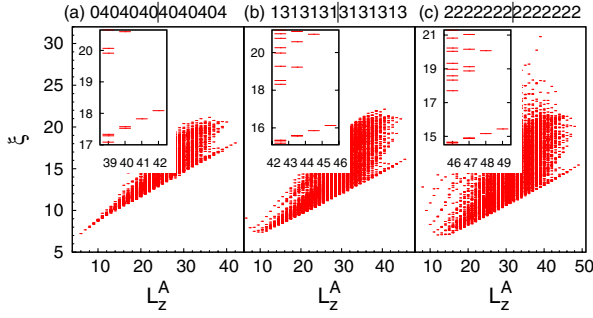


FIG. 4 (color online). Conformal-limit ES of the \mathbb{Z}_4 Read-Rezayi state of $N = 28$ bosons and a unit flux added. Abelian vortex (a) is fractionalized and the non-Abelian $e/4$ QHs are moved to the opposite pole one at a time [(b),(c)], causing the sector change. Insets show high-probability ES levels.

length around the equator; away from the equator, the counting of the QH entanglement levels remains a faithful representation of the FQH state. The CFT counting is lost *only* when the QH is situated *exactly* on the entanglement cut, which effectively splits the QH in two [Fig. 2(c)]. Using Jacks we obtained the ES of larger systems than those attainable by exact diagonalization, and $N = 12$ is presented only to facilitate comparison with the Coulomb case below.

For $k = 2$ Moore-Read state, two non-Abelian QHs are formed when a unit flux is added. When both QHs are at the same pole, the wave function is represented by the root 0202...02. When a single $e/2$ QH is fixed at one pole and the other is moved to the opposite pole, the Jack root is 1111...11. The ES for these two cases is shown in Fig. 3 and demonstrates that a *sector change* has taken place as the non-Abelian QH is moved across the cut: the counting 1, 1, 3, ... has changed into 1, 2, 4, ... The two different countings represent the two topological sectors of the theory, the even and odd fermion-number sectors, respectively. Sector change occurs immediately as the QH crosses the entanglement cut. The thermodynamic-limit counting of the two excitation wave functions is in one-to-one correspondence to that of the excitations above the ground

state for an even (20202000...) and odd (20201000...) number of particles.

An interesting question is what happens when more than two topological sectors are present in the theory. The simplest example is the \mathbb{Z}_4 Read-Rezayi state where the three sectors' counting is given by the excitations above the ground states with $N = 0, 1, 2 \pmod{4}$ number of particles: 4040404000..., the σ_1 sector 4040404010000... (equivalent to the σ_1' sector 404040403000000...), and the σ_2 sector 4040404020000... (σ_2 is its own conjugate). In Fig. 4 we show the ES for the \mathbb{Z}_4 state of $N = 28$ bosons with a single flux added. Starting from an Abelian vortex localized at one of the poles 0404...04 [Fig. 4(a)] with the counting 1, 1, 3, 5, ..., we transfer a single non-Abelian QH to the opposite pole. If we do this once [Fig. 4(b)], we obtain the state with the root 1313...13 and the counting 1, 2, 5, 8, ...; doing it once again results in a root 2222...22 and the counting 1, 2, 6, 9, ... [Fig. 4(c)].

Our main findings for the model states—the counting of the QH edge modes and the sector change upon crossing the cut—carry over to the realistic systems with LLL-projected Coulomb interaction. The problem of QH localization was solved generally in Ref. [17]. For the Laughlin filling $\nu = 1/2$, we simulate the probe by a delta-function impurity potential [18] of weight $0.005/\sqrt{N_\Phi/2}$, localized on the orbital m (Fig. 1). This potential is weak enough not to cause any level crossing in the spectrum, but only splits the degenerate multiplets of states. In Fig. 5 we show the ES of the Coulomb ground state in the presence of a localized QH by superimposing it on the model state from Fig. 2. A finite entanglement gap separates the CFT branch from the generic Coulomb continuum of higher entanglement-energy states. The CFT branch, however, displays the same counting as the model state. The Coulomb continuum largely remains fixed as we move the QH towards the equator, indicating that the scatter of energy levels in Fig. 5 is essentially similar to the QH oscillation across the cut and therefore due to the conformal levels spreading in the upward direction. The Coulomb QH therefore has the same behavior as the model one, at least sufficiently far from the cut.

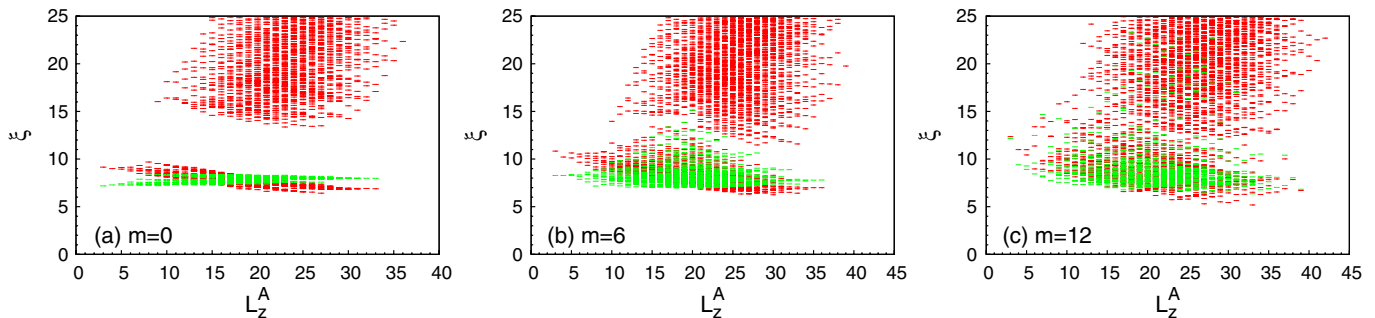


FIG. 5 (color online). Conformal-limit ES of the Coulomb $\nu = 1/2$ state of $N = 12$ bosons with a single QH, localized using delta impurity potential, at one of the poles $m = 0$ (a), the equator $m = 12$ (c), and in between $m = 6$ (b). The cut is the same as in Fig. 2.

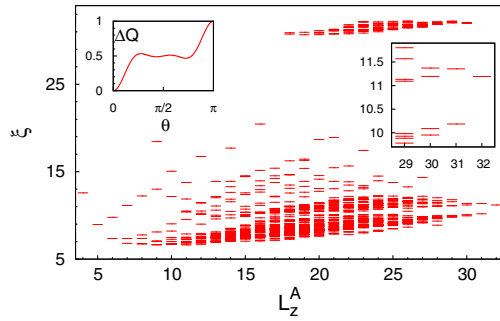


FIG. 6 (color online). Conformal-limit ES of the Coulomb $\nu = 1$ state for $N = 16$ bosons and a unit flux added. Delta impurity is located at each pole to pin the non-Abelian QH, as seen in the $e/2$ step in the plot of the excess charge (left-hand inset). The cut is defined by $N_A = 8$ and $l_A = 8$. Right-hand inset shows the zoom on the lowest ES levels.

We next study the $\nu = 1$ Coulomb state, expected to be in the universality class of Moore-Read. The Abelian vortex gives identical counting to the one derived from the root partition $0202 \dots 02$ in Fig. 3 [20]. To separate the two non-Abelian QHs, one on each pole, we use the method of Ref. [17] restricting the Hilbert space to the $L_z = 0$ sector of the Moore-Read zero modes. Within this subspace, we use a combination of two delta impurities, one on each pole, to trap the non-Abelian QHs [20]. To ensure that the QHs are indeed separated, we calculate the excess charge $\Delta Q(\theta)$ [20]. Note that for the fermionic Moore-Read state, a two-body potential is necessary in order to pin the QHs [17]. In Fig. 6 we recognize the same counting as the one that can be derived from the root configuration $1111 \dots 11$, which confirms that the sector change has occurred.

Finally, we have also analyzed the ES of the Laughlin model *quasielectron* states, Fig. 7, obtained as ground states of the pseudopotential Hamiltonian at one flux removed compared to the ground state and with a delta

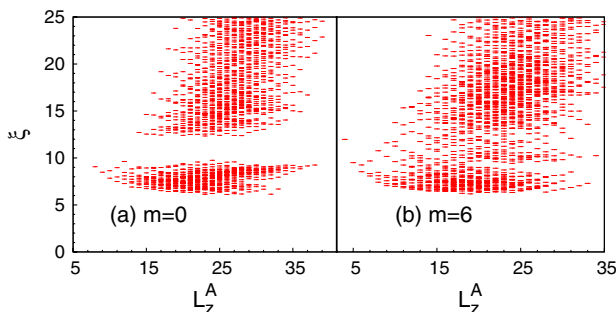


FIG. 7 (color online). Conformal-limit ES of the Laughlin model state of $N = 12$ bosons on the sphere with a unit flux removed. The quasielectron is locked to a delta impurity at one of the poles ($m = 0$) (a) and displaced halfway toward the equator ($m = 6$) (b).

impurity. Unlike the QH, quasielectron states show a finite entanglement gap. This is expected as they are not unique and densest zero modes of any local Hamiltonian [15]. Although the counting of the levels is again a faithful representation of the edge spectrum, the effect of oscillation across the cut is much more pronounced due to their larger size [21] compared to the corresponding QH excitation. This leads to a rapid closing of the entanglement gap as the quasielectron approaches the equator.

This work was supported by the Agence Nationale de la Recherche under Grant No. ANR-JCJC-0003-01. Z. P. acknowledges support by the Serbian Ministry of Science under Grants No. 141035 and No. ON171017, and by grants from Région Île-de-France. B. A. B. was supported by Princeton Startup Funds, Alfred P. Sloan Foundation, NSF DMR-095242, NSF China 11050110420, and MRSEC grant at Princeton University, NSF DMR-0819860. B. A. B. thanks the Ecole Normale Supérieure, Paris, for generous hosting.

- [1] L. Amico *et al.*, *Rev. Mod. Phys.* **80**, 517 (2008).
- [2] A. Kitaev and J. Preskill, *Phys. Rev. Lett.* **96**, 110404 (2006); M. Levin and X.G. Wen, *Phys. Rev. Lett.* **96**, 110405 (2006).
- [3] See, for example, P. Di Francesco, P. Mathieu, and D. Sénéchal, *Conformal Field Theory* (Springer-Verlag, Berlin, 1997).
- [4] A. Pal and D. A. Huse, *Phys. Rev. B* **82**, 174411 (2010).
- [5] S. Dong *et al.*, *J. High Energy Phys.* **05** (2008) 016.
- [6] M. Freedman, C. Nayak, and K. Shtengel, *Phys. Rev. B* **78**, 174411 (2008).
- [7] H. Li and F. D. M. Haldane, *Phys. Rev. Lett.* **101**, 010504 (2008).
- [8] F. D. M. Haldane, *Phys. Rev. Lett.* **51**, 605 (1983).
- [9] N. Regnault, B. A. Bernevig, and F. D. M. Haldane, *Phys. Rev. Lett.* **103**, 016801 (2009).
- [10] R. Thomale *et al.*, *Phys. Rev. Lett.* **104**, 180502 (2010).
- [11] A. Läuchli *et al.*, *Phys. Rev. Lett.* **104**, 156404 (2010); *New J. Phys.* **12**, 075004 (2010).
- [12] R. B. Laughlin, *Phys. Rev. Lett.* **50**, 1395 (1983).
- [13] G. Moore and N. Read, *Nucl. Phys.* **B360**, 362 (1991).
- [14] N. Read and E. Rezayi, *Phys. Rev. B* **59**, 8084 (1999).
- [15] B. A. Bernevig and F. D. M. Haldane, *Phys. Rev. Lett.* **100**, 246802 (2008); *Phys. Rev. B* **77**, 184502 (2008); *Phys. Rev. Lett.* **101**, 246806 (2008).
- [16] B. Estienne, B. A. Bernevig, and R. Santachiara, *arXiv:1005.3475*.
- [17] E. Prodan and F. D. M. Haldane, *Phys. Rev. B* **80**, 115121 (2009).
- [18] E. H. Rezayi and F. D. M. Haldane, *Phys. Rev. B* **32**, 6924 (1985).
- [19] B. A. Bernevig and F. D. M. Haldane, *Phys. Rev. Lett.* **102**, 066802 (2009).
- [20] C. Töke, N. Regnault, and J. K. Jain, *Phys. Rev. Lett.* **98**, 036806 (2007).
- [21] J. Nuebler *et al.*, *Phys. Rev. B* **81**, 035316 (2010).

All Databases **Select a Database** Web of Science **Additional Resources**

Search Search History

All Databases

<< Return to Web of Science®

Citing Articles Title: **Tunable Electron Interactions and Fractional Quantum Hall States in Graphene**
 Author(s): Papic, Z.; Thomale, R.; Abanin, D. A.
 Source: PHYSICAL REVIEW LETTERS Volume: 107 Issue: 17 Article Number: 176602 DOI: 10.1103/PhysRevLett.107.176602 Published: OCT 17 2011

This item has been cited by items indexed in the databases listed below. [more information]

17 in All Databases

- 17 publication in Web of Science
- 0 publication in BIOSIS Citation Index
- 0 publication in SciELO Citation Index
- 0 publication in Chinese Science Citation Database
- 0 data sets in Data Citation Index
- 0 publication in Data Citation Index

Results: 17

Page 1 of 1 Go

Sort by: Publication Date -- newest to oldest

Create Citation Report

Hide Refine

Refine Results

Search within results for

Search

Databases

Research Domains Refine

SCIENCE TECHNOLOGY

Research Areas Refine

PHYSICS

OPTICS

more options / values...

Document Types

Authors

Group/Corporate Authors

Editors

Funding Agencies

Source Titles

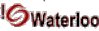
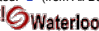
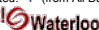

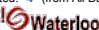

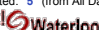



Conference/Meeting Titles

Publication Years

Languages

Countries/Territories

- Select Page Add to Marked List (0) Send to: my.endnote.com
1. Title: **Electron-hole pair condensation and Coulomb drag effect in a graphene double layer**
 Author(s): Zhang, Chuanyi; Jin, Guojun
 Source: JOURNAL OF PHYSICS-CONDENSED MATTER Volume: 25 Issue: 42 Article Number: 425604 DOI: 10.1088/0953-9984/25/42/425604 Published: OCT 23 2013
 Times Cited: 0 (from All Databases)
 Get it! Waterloo [View abstract]
 2. Title: **Fractional and integer quantum Hall effects in the zeroth Landau level in graphene**
 Author(s): Abanin, Dmitry A.; Feldman, Benjamin E.; Yacoby, Amir, et al.
 Source: PHYSICAL REVIEW B Volume: 88 Issue: 11 Article Number: 115407 DOI: 10.1103/PhysRevB.88.115407 Published: SEP 4 2013
 Times Cited: 0 (from All Databases)
 Get it! Waterloo [View abstract]
 3. Title: **Fractional Quantum Hall Phase Transitions and Four-Flux States in Graphene**
 Author(s): Feldman, Benjamin E.; Levin, Andrei J.; Krauss, Benjamin, et al.
 Source: PHYSICAL REVIEW LETTERS Volume: 111 Issue: 7 Article Number: 076802 DOI: 10.1103/PhysRevLett.111.076802 Published: AUG 16 2013
 Times Cited: 2 (from All Databases)
 Get it! Waterloo [View abstract]
 4. Title: **Fractional quantum Hall effect of topological surface states under a strong tilted magnetic field**
 Author(s): Zheng, Fawei; Wang, Zhigang; Fu, Zhen-Guo, et al.
 Source: EPL Volume: 103 Issue: 2 Article Number: 27001 DOI: 10.1209/0295-5075/103/27001 Published: JUL 2013
 Times Cited: 0 (from All Databases)
 Get it! Waterloo [View abstract]
 5. Title: **Effective theory of fractional topological insulators in two spatial dimensions**
 Author(s): Nikolic, Predrag
 Source: PHYSICAL REVIEW B Volume: 87 Issue: 24 Article Number: UNSP 245120 DOI: 10.1103/PhysRevB.87.245120 Published: JUN 20 2013
 Times Cited: 0 (from All Databases)
 Get it! Waterloo [View abstract]
 6. Title: **Tripartite entanglement of electron spins of noninteracting electron gases**
 Author(s): Ma, Xiao San; Qiao, Ying; Zhao, Guang Xing, et al.
 Source: QUANTUM INFORMATION PROCESSING Volume: 12 Issue: 4 Pages: 1807-1818 DOI: 10.1007/s11218-012-0495-3 Published: APR 2013
 Times Cited: 0 (from All Databases)
 Get it! Waterloo [View abstract]
 7. Title: **New Dirac points and multiple Landau level crossings in biased trilayer graphene**
 Author(s): Serbyn, Maksym; Abanin, Dmitry A.
 Source: PHYSICAL REVIEW B Volume: 87 Issue: 11 Article Number: 115422 DOI: 10.1103/PhysRevB.87.115422 Published: MAR 18 2013
 Times Cited: 0 (from All Databases)
 Get it! Waterloo [View abstract]
 8. Title: **Fractional Topological Phases and Broken Time-Reversal Symmetry in Strained Graphene**
 Author(s): Ghaemi, Pouyan; Cayssol, Jerome; Sheng, D. N., et al.
 Source: PHYSICAL REVIEW LETTERS Volume: 108 Issue: 26 Article Number: 266801 DOI: 10.1103/PhysRevLett.108.266801 Published: JUN 26 2012
 Times Cited: 20 (from All Databases)
 Get it! Waterloo [View abstract]
 9. Title: **Typology for quantum Hall liquids**
 Author(s): Parameswaran, S. A.; Kivelson, S. A.; Rezayi, E. H., et al.
 Source: PHYSICAL REVIEW B Volume: 85 Issue: 24 Article Number: 241307 DOI: 10.1103/PhysRevB.85.241307 Published: JUN 20 2012
 Times Cited: 3 (from All Databases)
 Get it! Waterloo [View abstract]

10. Title: [Importance of interband transitions for the fractional quantum Hall effect in bilayer graphene](#)
 Author(s): Snizhko, Kyrilo; Cheianov, Vadim; Simon, Steven H.
 Source: PHYSICAL REVIEW B Volume: **85** Issue: **20** Article Number: **201415** DOI: **10.1103/PhysRevB.85.201415** Published: **MAY 29 2012**
 Times Cited: **2** (from All Databases)
 Get it!  [[View abstract](#)]
11. Title: [Chirality effect in disordered graphene ribbon junctions](#)
 Author(s): Long, Wen
 Source: JOURNAL OF PHYSICS-CONDENSED MATTER Volume: **24** Issue: **17** Article Number: **175302** DOI: **10.1088/0953-8984/24/17/175302** Published: **MAY 2 2012**
 Times Cited: **2** (from All Databases)
 Get it!  [[View abstract](#)]
12. Title: [Stability of the \$k=3\$ Read-Rezayi state in chiral two-dimensional systems with tunable interactions](#)
 Author(s): Abanin, D. A.; Papic, Z.; Barlas, Y.; et al.
 Source: NEW JOURNAL OF PHYSICS Volume: **14** Article Number: **025009** DOI: **10.1088/1367-2630/14/2/025009** Published: **FEB 28 2012**
 Times Cited: **1** (from All Databases)
 Get it!  [[View abstract](#)]
13. Title: [Quantum discord of electron spins of noninteracting electron gases](#)
 Author(s): Ma, X. S.; Cheng, M. T.; Zhao, G. X.; et al.
 Source: EUROPEAN PHYSICAL JOURNAL D Volume: **66** Issue: **2** Article Number: **46** DOI: **10.1140/epjdd/2012-20704-6** Published: **FEB 2012**
 Times Cited: **1** (from All Databases)
 Get it!  [[View abstract](#)]
14. Title: [Numerical studies of the fractional quantum Hall effect in systems with tunable interactions](#)
 Author(s): Papic, Z.; Abanin, D. A.; Barlas, Y.; et al.
 Book Editor(s): Stocks, GM; Troparevsky, MC
 Conference: **23rd IUPAP C20 Conference on Computational Physics (CCP)** Location: **Gatlinburg, TN** Date: **OCT 30-NOV 03, 2011**
 Sponsor(s): **Int Union Pure & Appl Phys (IUPAP); Int Union Pure & Appl Phys (IUPAP), Commiss Computat Phys (C20); Amer Phys Soc, Div Computat Phys (APS-DCOMP); Oak Ridge Natl Lab (ORNL); Ctr Defect Phys (CDP); Univ Tennessee (UT)ORNL, Joint Inst Computat Sci (JICS); Cray, Inc**
 Source: **IUPAP C20 CONFERENCE ON COMPUTATIONAL PHYSICS (CCP 2011)** Book Series: **Journal of Physics Conference Series** Volume: **402** Article Number: **012020** DOI: **10.1088/1742-6596/402/1/012020** Published: **2012**
 Times Cited: **1** (from All Databases)
 Get it!  [[View abstract](#)]
15. Title: [Theoretical aspects of the fractional quantum Hall effect in graphene](#)
 Author(s): Goerbig, M. O.; Regnault, N.
 Conference: **Nobel Symposium on Graphene and Quantum Matter** Location: **Saltsjobaden, SWEDEN** Date: **MAY 27-31, 2010**
 Source: **PHYSICA SCRIPTA** Volume: **T146** Article Number: **014017** DOI: **10.1088/0031-8949/2012/T146/014017** Published: **JAN 2012**
 Times Cited: **4** (from All Databases)
 Get it!  [[View abstract](#)]
16. Title: [Tunable interactions and phase transitions in Dirac materials in a magnetic field](#)
 Author(s): Papic, Z.; Abanin, D. A.; Barlas, Y.; et al.
 Source: PHYSICAL REVIEW B Volume: **84** Issue: **24** Article Number: **241306** DOI: **10.1103/PhysRevB.84.241306** Published: **DEC 19 2011**
 Times Cited: **9** (from All Databases)
 Get it!  [[View abstract](#)]
17. Title: [Realizing Universal Edge Properties in Graphene Fractional Quantum Hall Liquids](#)
 Author(s): Hu, Zi-Xiang; Bhatt, R. N.; Wan, Xin; et al.
 Source: PHYSICAL REVIEW LETTERS Volume: **107** Issue: **23** Article Number: **236806** DOI: **10.1103/PhysRevLett.107.236806** Published: **DEC 1 2011**
 Times Cited: **5** (from All Databases)
 Get it!  [[View abstract](#)]
- Select Page  Add to Marked List (0) |  |  | Send to:

Results: **17** Page of 1 Sort by:

17 records matched your query of the 55,067,330 (contains duplicates) in the data limits you selected.

View in: [简体中文](#) | [繁體中文](#) | [English](#) | [日本語](#) | [한국어](#) | [Portugués](#) | [Español](#)© 2013 Thomson Reuters | [Terms of Use](#) | [Privacy Policy](#) | [Please give us your feedback on using Web of Knowledge.](#)

Tunable Electron Interactions and Fractional Quantum Hall States in Graphene

Z. Papić,¹ R. Thomale,² and D. A. Abanin^{2,3}

¹*Department of Electrical Engineering, Princeton University, Princeton, New Jersey 08544, USA*

²*Department of Physics, Princeton University, Princeton, New Jersey 08544, USA*

³*Princeton Center for Theoretical Science, Princeton University, Princeton, New Jersey 08544, USA*

(Received 22 February 2011; published 17 October 2011)

The recent discovery of fractional quantum Hall (FQH) states in graphene raises the question of whether the physics of graphene offers any advantages over GaAs-based materials in exploring strongly correlated states of two-dimensional electrons. Here we propose a method to continuously tune the effective electron interactions in graphene and its bilayer by the dielectric environment of the sample. Using this method, the charge gaps of prominent FQH states, including $\nu = 1/3$ or $\nu = 5/2$ states, can be increased several times, or reduced to zero. The tunability of the interactions can be used to realize and stabilize various strongly correlated phases and explore the transitions between them.

DOI: [10.1103/PhysRevLett.107.176602](https://doi.org/10.1103/PhysRevLett.107.176602)

PACS numbers: 72.80.Vp, 63.20.Pw, 63.22.-m, 87.10.-e

Introduction.—Two-dimensional electron systems (2DES) placed in a high magnetic field exhibit strongly correlated phases characterized by fractionally quantized Hall conductivity [1], quasiparticles that carry a fraction of electron charge [2], and fractional (Abelian or possibly non-Abelian) statistics [2,3]. These remarkable phenomena occur in the extreme quantum limit—the fractional quantum Hall (FQH) regime—when the number of electrons N_e is comparable to the number of magnetic flux quanta through the 2DES, N_Φ , corresponding to a partial filling $\nu = N_e/N_\Phi$ of one of the lower Landau levels (LLs). When ν is swept through the series of simple fractions in the lowest $n = 0$ Landau level (LLL) where $N_e < N_\Phi$, the electrons condense into Laughlin states which describe the strongest observed fractions ($\nu = 1/3, 1/5, \dots$) [2], or weaker states that belong to the so-called hierarchy [4,5] or composite fermion series [6]. Within the $n = 1$ LL, the effective interaction changes due to the nodal structure of LL orbitals, and some of the more exotic states, such as the Read-Rezayi states [7], are more likely to be favored. The experimentally most important member of the Read-Rezayi series is the Moore-Read (MR) “Pfaffian” state [3], believed to describe the FQH plateau at $\nu = 5/2$ [8,9]. Quasiparticles of the Read-Rezayi series obey the non-Abelian statistics [3] which is of interest for topological quantum computation [10].

Although many FQH states have been discovered in GaAs-based 2DES, these systems are plagued by the fact that their 2DES is buried inside a larger 3D structure. This fixes the effective interactions at values that are often not optimal for some of the most interesting FQH states, including the Read-Rezayi series. Theoretically, such states are known to be very sensitive to the form of the effective interactions [11,12]. Another problem stems from the strong dielectric screening and finite well-width [13] in GaAs, which weaken the electron-electron interactions, thereby making FQH states fragile. This has been a major

obstacle in the studies of the possibly non-Abelian states, which could only be observed in ultra-high-mobility samples [8] (see, however, [14]). Thus, it is desirable to find an alternative high-mobility 2DES with strong effective Coulomb interactions that are adjustable in a broad range.

A promising candidate for this kind of material is monolayer graphene (MG), a high-mobility atomically thick 2DES [15], where recently a $\nu = 1/3$ state [16], and several other states [17], have been discovered. Remarkably, due to graphene’s truly 2D nature, the short-range electron interactions greatly exceed those in GaAs, which leads to a significantly more robust FQH state at $\nu = 1/3$ [18]. A closely related material, bilayer graphene (BG) [15] has similarly high mobility, and exhibits interaction-induced quantum Hall states at integer filling factors at low magnetic fields [19]. This indicates that, similarly to MG, the underlying electron interactions are strong and one could expect robust FQH states in BG as well.

Main results.—Here we propose a way to continuously tune the interactions in graphene in a wide range, using the fact that 2DES in graphene is exposed and its properties can be controlled by the dielectric environment, as illustrated in Fig. 1. Using exact diagonalization calculations, we show that the tunability can be used to significantly increase the excitation gap of the $\nu = 1/3$ state in both MG and BG, as well as in the half-filled $n = 1$ LL in BG. The latter, similarly to the case of GaAs, resides in the gapped MR Pfaffian state [11,12]. As the gap is varied, the overlaps between the exact states and the model wave functions improve by a few percent, and their topological character becomes better protected. The reduction of the gap induces the transitions to compressible and crystalline phases [12].

Model.—A graphene sample is situated in a dielectric medium with permittivity ϵ_1 , and a semi-infinite dielectric plate with permittivity $\epsilon_2 \neq \epsilon_1$ is placed at a distance $d/2$

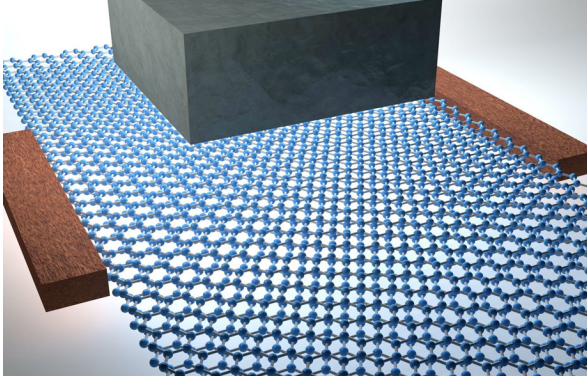


FIG. 1 (color online). Setup of a graphene system with tunable electron interactions. Electron states are affected by a dielectric plate placed in the vicinity of the surface. By varying the dielectric permittivity of the plate and its distance $d/2$ to the graphene layer, interactions of the desired form can be engineered.

away from the graphene sheet. The effective interactions between electrons in graphene change due to the surface charges induced at the boundary between dielectrics:

$$V(r) = \frac{e^2}{\epsilon_1 r} + \alpha \frac{e^2}{\epsilon_1 \sqrt{r^2 + d^2}}, \quad \alpha = \frac{\epsilon_1 - \epsilon_2}{\epsilon_1 + \epsilon_2}. \quad (1)$$

Below we measure the distance d in units of the magnetic length l_B and the energy in units of $e^2/\epsilon_1 l_B$. Ratio d/l_B controls the effective interactions within a partially filled LL (see below). All the gaps quoted here should be multiplied by a factor $\epsilon_{\text{GaAs}}/\epsilon_1$ if comparison is to be made with GaAs 2DES. An important advantage of this setup is that the interactions can be tuned *in situ* by varying the magnetic field B , which modifies the ratio d/l_B .

We project the interaction to a partially filled LL under consideration, following the standard procedure in FQH numerical studies [20]. Within a LL, $V(r)$ is parametrized by the Haldane pseudopotentials $\{V_m\}$ [20], which can be conveniently evaluated from the Fourier transform of the Coulomb interaction, $\tilde{V}(\mathbf{q})$, and the form factor $F(\mathbf{q})$ encoding the properties of LL orbitals. Because of the difference in band structure, the form factors in MG, BG are generally distinct from those of GaAs [21].

For what follows, it is useful to review the previous results on the relation between pseudopotential values and the stability of $\nu = 1/3$ and $\nu = 5/2$ states. At $\nu = 1/3$, the bare Coulomb interaction in $n = 0$ LL favors the Laughlin state. Reducing V_1 while keeping $V_{m \geq 3}$ constant eventually destroys the gap and a compressible state sets in [20]. At half filling of the LLL ($\nu = 1/2$), the Coulomb interaction gives rise to a gapless Fermi liquid of composite fermions [22]. However, in half-filled $n = 1$ LL there is a fully developed plateau in experiments [8], attributed to the MR state [3]. The MR state is an eigenstate of a particular three-body repulsive interaction [9]. Remarkably, in numerical studies, the ground state of the Coulomb interaction at $\nu = 5/2$ is seen to be adiabatically

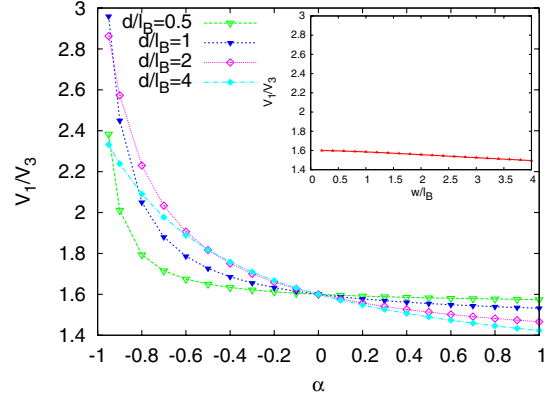


FIG. 2 (color online). Ratio V_1/V_3 as a function of α for several values of d/l_B in $n = 0$ LL of MG and BG. Inset: typical ratio V_1/V_3 for a GaAs infinite quantum well of width w/l_B , plotted on the same scale.

connected to the MR state [23,24]; the overlap of the ground state with the MR state is improved by the increase in V_1 pseudopotential (or, alternatively, by reducing V_3) [12]. Therefore, theory shows that varying the first few pseudopotentials provides a convenient way to assess stability and induce transitions between FQH states. However, so far it has been difficult to find a controlled way of tuning V_m 's experimentally in a sufficiently broad range.

In Fig. 2 we show an example of the ratio V_1/V_3 calculated for $n = 0$ LL of MG and BG using the setup illustrated in Fig. 1. Changing α and d/l_B leads to a large variation of V_1/V_3 with respect to its pristine value ($\alpha = 0$). For comparison, we also show a typical variation of V_1/V_3 achievable in GaAs wide quantum wells (inset). In what follows, we investigate the model defined by Eq. (1) using exact diagonalization studies [20]. We focus on the case of spin- and valley-polarized FQH states, such as the Laughlin or MR state, and consider the physics of a single nondegenerate Landau sublevel. For example, in case of the MR state, we expect the total filling factor $\nu = -4 + 2M + 3/2$ of the BG to be the most suitable for realizing the Pfaffian state. Note that the exchange interactions favor the following order of filling the eight $n = 0, 1$ Landau sublevels of the BG [25]: $|0\sigma_1s_1\rangle$, $|1\sigma_1s_1\rangle$, $|0\sigma_2s_2\rangle$, $|1\sigma_2s_2\rangle$, where $|\sigma_i s_i\rangle$, $1 \leq i \leq 4$ are the four orthogonal states in the space of internal indices, with s and σ denoting two spin and two valley species, respectively. At $\nu = -4 + 2M + 3/2$, where $M = 0, 1, 2, 3$, the M pairs of $n = 0, 1$ sublevels are expected to be filled, and in the topmost pair, $n = 0$ Landau sublevel is filled completely, as dictated by the exchange interactions, while $n = 1$ sublevel is half-filled. For brevity, below we refer to this $n = 1$ sublevel as “ $n = 1$ LL in BG.”

One important criterion of the stability of FQH states is their gap to excitations, which can be either neutral (quasiparticle-quasihole pair above the ground state) or charged (created by changing the magnetic flux by one

unit). These two gaps are generally different, but for the model defined by Eq. (1) we find that they show the same behavior as a function of parameters α and d/l_B . We therefore focus on the charge gap, defined by $\Delta_c \equiv E_{qh} + E_{qp} - 2E_0$, where E_0 is the ground-state energy and E_{qh}, E_{qp} are the energies at $N_\Phi + 1, N_\Phi - 1$, respectively (N_e is kept fixed). In evaluating Δ_c , it is convenient to place the FQH system on the surface of a sphere, where incompressible ground states are easily identified by their zero angular momentum. On a finite sphere, FQH states are further characterized by the shift \mathcal{S} [26], which relates N_e, N_Φ to the filling factor ν in the thermodynamic limit via $N_\Phi = N_e/\nu + \mathcal{S}$. In Fig. 3 we plot Δ_c for the case of $\nu = 1/3$ filling in the $n = 0$ LL (MG, BG) and $\nu = 1/2$ filling of $n = 1$ LL in BG. We do not show the results for the $n = 1$ LL of MG because they support significantly weaker pairing correlations than in BG [27]. In these plots, the system size is fixed at $N = 10$ ($\nu = 1/3$) and $N = 14$ ($\nu = 1/2$), and \mathcal{S} is chosen to be -3 . This shift corresponds to the case of bare Coulomb interaction where the states are known to be described by Laughlin and MR wave functions. We estimate that the gaps can be increased 2–3 times with respect to the vacuum value ($\alpha = 0$). The gaps in $n = 1$ LL of BG are overall significantly smaller than those in $n = 0$ LL, which is consistent with the experiments detecting fewer FQH states in $n = 1$ LL of GaAs. When $\alpha < 0$, the gaps become very small and our analysis would likely need to be extended to other shifts that may be preferred by these compressible states in minimizing their ground-state energy. This analysis will be provided elsewhere. We emphasize that all the systems smaller than those in Fig. 3 show qualitatively identical plots with the same relative variation of the gap (we use the rescaled magnetic length and background charge correction in Fig. 3 in order to minimize the finite-size effects [6]).

Comparing the gaps in Fig. 3 with the ratio V_1/V_3 , we note that the maximum value of V_1/V_3 does not coincide with the maximum of the gap. This is because the gaps are

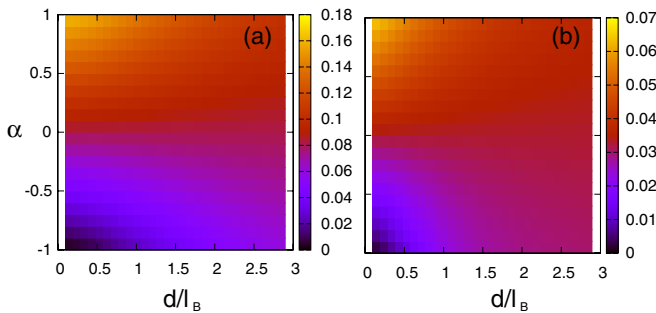


FIG. 3 (color online). Charge gaps for $N = 10$ particle $\nu = 1/3$ state in the $n = 0$ LL of MG and BG (a), and $N = 14$ particle $\nu = 1/2$ filled $n = 1$ LL of BG (b). By changing α and d/l_B , the gaps can be increased several times or brought down to zero, following similar trends in each of the LLs.

determined by the complete set of pseudopotentials—while negative α 's increase the ratio V_1/V_3 , they also reduce the magnitude of each individual V_m , thereby lowering the gap. However, the Laughlin states and higher order hierarchy states are excellent trial states for positive, as well as negative, α , i.e., for long-range Coulomb-like interaction as well as strong short-ranged repulsion. This is reflected in the high value of the overlap between an exact state and the Laughlin wave function which varies by as little as $\pm 1\%$ over the entire phase diagram in Fig. 3 (not shown).

The stability of the MR Pfaffian state is more subtle and we expect sharper variation of the overlap as a function of α and d/l_B . In Fig. 4 we show the overlap between the exact state of the dielectric model (for given α and d/l_B) and the MR Pfaffian state. The overlaps are remarkably consistent for the two choices of boundary conditions: on the sphere with $\mathcal{S} = -3$, Fig. 4(a), and on the torus with the hexagonal unit cell, Fig. 4(b). Although the MR state is threefold degenerate and characterized by different pseudomomenta \mathbf{k}_i , $i = 1, 2, 3$ on the torus [12], the sixfold symmetry of the Bravais lattice guarantees the degeneracy of these \mathbf{k}_i subspaces and makes it possible to calculate the overlap in the usual way. The maximum of the overlap occurs for d between l_B and $2l_B$, and is somewhat higher on the sphere, due to the bias of the shift which lifts the particle-hole symmetry (the anti-Pfaffian [28], having $\mathcal{S} = 1$, occurs in a different Hilbert space and does not “mix” with the Pfaffian, as on the torus).

We now present additional evidence in favor of the state being the MR Pfaffian (Fig. 5). First, we track the evolution of the state upon *further* variation of V_1 pseudopotential, Fig. 5(a). The increase of V_1 would partly mimic the effects of LL mixing [29] that we neglected so far (we do not investigate the effect of three-body interaction that also arises in this case). In Fig. 5(a) we show the overlaps between the exact state, $|\text{Diel}\rangle$, at $\alpha = 1$, $d = 1.5l_B$ [chosen from the high-overlap region in Fig. 4(b)], the bare Coulomb $n = 1$ LL state, $|C, n = 1\rangle$, with the MR Pfaffian $|\text{MR}\rangle$ and its particle-hole symmetrized version,

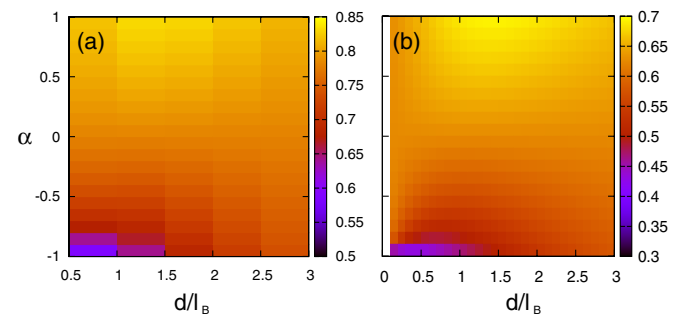


FIG. 4 (color online). Overlaps between the exact ground state, for each α and d/l_B , and the MR Pfaffian state, for $N = 16$ particles on the sphere (a), and $N = 14$ particles on the torus (b). Maximum overlap occurs for intermediate d/l_B .

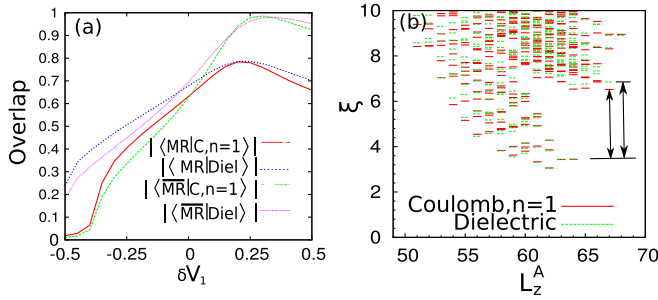


FIG. 5 (color online). (a) Overlaps between the (un)screened Coulomb interaction eigenstate and MR Pfaffian, as well as particle-hole symmetrized MR, for $N = 14$ particles on the torus. Screened Coulomb eigenstate is defined by $\alpha = 1$, $d = 1.5l_B$ [compare with Fig. 4(b)]. (b) Entanglement spectrum on the sphere for $N = 16$ electrons, for bare and screened Coulomb interaction. Entanglement cut is chosen as 0|1 in the notation of Ref. [30]; other cuts yield similar results.

$|\overline{\text{MR}}\rangle$. The bare Coulomb state and the dielectric state behave very similarly under the change of V_1 , the latter being slightly more robust. As noted in Ref. [12], the overlaps with $|\overline{\text{MR}}\rangle$ on the torus are large (97% and better), which is again the case for our dielectric state as well.

Another independent insight into the nature of the dielectric state is the entanglement spectrum [30]. The multiplicities of the low-lying levels of the entanglement spectrum contain topological information about a FQH state; this information is protected by an entanglement gap [24] whose magnitude measures the topological stability of a state. We calculate and compare the entanglement spectra on the sphere for the $\nu = 1/2$ Coulomb $n = 1$ LL state and the dielectric eigenstate tuned to a region of high overlap with the MR Pfaffian [Fig. 5(b)]. Not only do both spectra display the same counting as the MR state (up to some value of the subsystem A 's projection of the angular momentum L_z^A , set by the finite size of the sphere), but the entanglement gap [indicated by arrows in Fig. 5(b)] is also slightly enhanced with respect to the unscreened Coulomb interaction.

Conclusions.—In summary, we proposed a method to tune the electron interactions in graphene and its bilayer. In this approach, interaction pseudopotentials can be varied in a broad interval and FQH gaps can be enhanced several times or even reduced to zero, allowing for a more complete exploration of compressible and incompressible phases than can be attained in GaAs materials. The proposed method is expected to be very efficient in optimizing the Abelian FQH states that belong to the hierarchy series, where the variation of the charge gap is followed by a small change in the overlap that generally remains very close to unity. Non-Abelian states, although expected to be stabilized, may require a more subtle approach with several dielectric plates of different permittivities and thicknesses of the order of l_B placed in the vicinity of the surface. In such a system, interactions can be tuned in a broader range

and would admit a simultaneous change of several pseudopotentials that may be required for the realization of other non-Abelian and multicomponent FQH states [31]. Finally, we note that the experiments on the tunneling density of states [32] can directly measure the values of the tuned pseudopotentials [33].

We thank E. Andrei, C. Dean, P. Kim, C. Nayak, Y. Zhang, M. Goerbig, R. Bhatt, and especially S. Sondhi for insightful discussions. This work was supported by DOE Grant No. DE-SC0002140. D.A. thanks Aspen Center for Physics for hospitality. R.T. is supported by a Feodor Lynen fellowship of the Humboldt Foundation.

- [1] D. C. Tsui, H. L. Stormer, and A. C. Gossard, *Phys. Rev. Lett.* **48**, 1559 (1982).
- [2] R. B. Laughlin, *Phys. Rev. Lett.* **50**, 1395 (1983).
- [3] G. Moore and N. Read, *Nucl. Phys.* **B360**, 362 (1991).
- [4] *The Quantum Hall Effect*, edited by R. E. Prange and S. M. Girvin (Springer-Verlag, New York, 1990), 2nd ed.
- [5] B. I. Halperin, *Phys. Rev. Lett.* **52**, 1583 (1984); **52**, 2390 (E) (1984).
- [6] J. K. Jain, *Composite Fermions* (Cambridge University Press, Cambridge, U.K., 2007).
- [7] N. Read and E. Rezayi, *Phys. Rev. B* **59**, 8084 (1999).
- [8] R. Willett *et al.*, *Phys. Rev. Lett.* **59**, 1776 (1987).
- [9] M. Greiter, X.-G. Wen, and F. Wilczek, *Phys. Rev. Lett.* **66**, 3205 (1991); *Nucl. Phys.* **B374**, 567 (1992).
- [10] C. Nayak *et al.*, *Rev. Mod. Phys.* **80**, 1083 (2008).
- [11] R. H. Morf, *Phys. Rev. Lett.* **80**, 1505 (1998).
- [12] E. H. Rezayi and F. D. M. Haldane, *Phys. Rev. Lett.* **84**, 4685 (2000).
- [13] F. C. Zhang and S. Das Sarma, *Phys. Rev. B* **33**, 2903 (1986).
- [14] G. Gamez and K. Muraki, arXiv:1101.5856.
- [15] A. H. Castro Neto *et al.*, *Rev. Mod. Phys.* **81**, 109 (2009).
- [16] X. Du *et al.*, *Nature (London)* **462**, 192 (2009); K. I. Bolotin *et al.*, *Nature (London)* **462**, 196 (2009).
- [17] C. Dean *et al.*, *Nature Phys.* **7**, 693 (2011).
- [18] D. A. Abanin *et al.*, *Phys. Rev. B* **81**, 115410 (2010).
- [19] B. E. Feldman, J. Martin, and A. Yacoby, *Nature Phys.* **5**, 889 (2009).
- [20] F. D. M. Haldane and E. H. Rezayi, *Phys. Rev. Lett.* **54**, 237 (1985); F. D. M. Haldane in Ref. [4].
- [21] K. Nomura and A. H. MacDonald, *Phys. Rev. Lett.* **96**, 256602 (2006); M. O. Goerbig, R. Moessner, and B. Douçot, *Phys. Rev. B* **74**, 161407(R) (2006).
- [22] B. I. Halperin, P. A. Lee, and N. Read, *Phys. Rev. B* **47**, 7312 (1993).
- [23] M. Storni, R. H. Morf, and S. Das Sarma, *Phys. Rev. Lett.* **104**, 076803 (2010).
- [24] R. Thomale *et al.*, *Phys. Rev. Lett.* **104**, 180502 (2010).
- [25] Y. Barlas *et al.*, *Phys. Rev. Lett.* **101**, 097601 (2008); D. A. Abanin, S. A. Parameswaran, and S. L. Sondhi, *Phys. Rev. Lett.* **103**, 076802 (2009).
- [26] X. G. Wen and A. Zee, *Phys. Rev. Lett.* **69**, 953 (1992).

- [27] C. Tóke and J.K. Jain, *Phys. Rev. B* **76**, 081403(R) (2007).
- [28] M. Levin, B. I. Halperin, and B. Rosenow, *Phys. Rev. Lett.* **99**, 236806 (2007); S.-S. Lee *et al.*, *Phys. Rev. Lett.* **99**, 236807 (2007).
- [29] W. Bishara and C. Nayak, *Phys. Rev. B* **80**, 121302 (2009); E.H. Rezayi and S.H. Simon, *Phys. Rev. Lett.* **106**, 116801 (2011); A. Wojs, C. Tóke, and J.K. Jain, *Phys. Rev. Lett.* **105**, 096802 (2010).
- [30] H. Li and F.D.M. Haldane, *Phys. Rev. Lett.* **101**, 010504 (2008).
- [31] M. O. Goerbig and N. Regnault, *Phys. Rev. B* **75**, 241405 (2007); C. Tóke and J.K. Jain, *Phys. Rev. B* **75**, 245440 (2007); Z. Papić, M. O. Goerbig, and N. Regnault, *Phys. Rev. Lett.* **105**, 176802 (2010).
- [32] O. Dial *et al.*, *Nature (London)* **464**, 566 (2010).
- [33] A.H. MacDonald, *Phys. Rev. Lett.* **105**, 206801 (2010).

Search Search History

All Databases

<< Return to Web of Science®

Citing Articles Title: **Tunable interactions and phase transitions in Dirac materials in a magnetic field**
 Author(s): Papic, Z. ; Abanin, D. A. ; Barlas, Y. ; et al.
 Source: PHYSICAL REVIEW B Volume: 84 Issue: 24 Article Number: 241306 DOI: 10.1103/PhysRevB.84.241306 Published: DEC 19 2011

This item has been cited by items indexed in the databases listed below. [more information]

- 9 in All Databases
- 9 publication in Web of Science
 - 0 publication in BIOSIS Citation Index
 - 0 publication in ScELO Citation Index
 - 0 publication in Chinese Science Citation Database
 - 0 data sets in Data Citation Index
 - 0 publication in Data Citation Index

Results: 9 Page 1 of 1 Go Sort by: Publication Date -- newest to oldest

Create Citation Report

Hide Refine

Refine Results

Search within results for

Search

Databases

Research Domains Refine

SCIENCE TECHNOLOGY

Research Areas Refine

PHYSICS

SCIENCE TECHNOLOGY OTHER TOPICS

more options / values...

Document Types

Authors

Group/Corporate Authors

Editors

Funding Agencies

Source Titles

Conference/Meeting Titles

Publication Years

Languages

Countries/Territories

Select Page Add to Marked List (0) Send to: my.endnote.com

1. Title: **Fractional and integer quantum Hall effects in the zeroth Landau level in graphene**
 Author(s): Abanin, Dmitry A.; Feldman, Benjamin E.; Yacoby, Amir; et al.
 Source: PHYSICAL REVIEW B Volume: 88 Issue: 11 Article Number: 115407 DOI: 10.1103/PhysRevB.88.115407 Published: SEP 4 2013
 Times Cited: 0 (from All Databases)
 Get it! Waterloo [View abstract]
2. Title: **Fractional Quantum Hall Phase Transitions and Four-Flux States in Graphene**
 Author(s): Feldman, Benjamin E.; Levin, Andrei J.; Krauss, Benjamin; et al.
 Source: PHYSICAL REVIEW LETTERS Volume: 111 Issue: 7 Article Number: 076802 DOI: 10.1103/PhysRevLett.111.076802 Published: AUG 16 2013
 Times Cited: 2 (from All Databases)
 Get it! Waterloo [View abstract]
3. Title: **Fractional quantum Hall effect in a tilted magnetic field**
 Author(s): Papic, Z.
 Source: PHYSICAL REVIEW B Volume: 87 Issue: 24 Article Number: 245315 DOI: 10.1103/PhysRevB.87.245315 Published: JUN 27 2013
 Times Cited: 2 (from All Databases)
 Get it! Waterloo [View abstract]
4. Title: **The electronic properties of bilayer graphene**
 Author(s): McCann, Edward; Koshino, Mikiyo
 Source: REPORTS ON PROGRESS IN PHYSICS Volume: 76 Issue: 5 Article Number: 056503 DOI: 10.1088/0034-4885/76/5/056503 Published: MAY 2013
 Times Cited: 4 (from All Databases)
 Get it! Waterloo [View abstract]
5. Title: **New Dirac points and multiple Landau level crossings in biased trilayer graphene**
 Author(s): Serbyn, Maksym; Abanin, Dmitry A.
 Source: PHYSICAL REVIEW B Volume: 87 Issue: 11 Article Number: 115422 DOI: 10.1103/PhysRevB.87.115422 Published: MAR 18 2013
 Times Cited: 0 (from All Databases)
 Get it! Waterloo [View abstract]
6. Title: **Spin-helical transport in normal and superconducting topological insulators**
 Author(s): Tkachov, G.; Hankiewicz, E. M.
 Source: PHYSICA STATUS SOLIDI B-BASIC SOLID STATE PHYSICS Volume: 250 Issue: 2 Pages: 215-232 DOI: 10.1002/pssb.201248385 Published: FEB 2013
 Times Cited: 10 (from All Databases)
 Get it! Waterloo [View abstract]
7. Title: **Unconventional Sequence of Fractional Quantum Hall States in Suspended Graphene**
 Author(s): Feldman, Benjamin E.; Krauss, Benjamin; Smet, Jurgen H.; et al.
 Source: SCIENCE Volume: 337 Issue: 6099 Pages: 1196-1199 DOI: 10.1126/science.1224784 Published: SEP 7 2012
 Times Cited: 13 (from All Databases)
 Get it! Waterloo [View abstract]
8. Title: **Importance of interband transitions for the fractional quantum Hall effect in bilayer graphene**
 Author(s): Snizhko, Kyrylo; Cheianov, Vadim; Simon, Steven H.
 Source: PHYSICAL REVIEW B Volume: 85 Issue: 20 Article Number: 201415 DOI: 10.1103/PhysRevB.85.201415 Published: MAY 29 2012
 Times Cited: 2 (from All Databases)
 Get it! Waterloo [View abstract]
9. Title: **Stability of the k=3 Read-Rezayi state in chiral two-dimensional systems with tunable interactions**
 Author(s): Abanin, D. A.; Papic, Z.; Barlas, Y.; et al.
 Source: NEW JOURNAL OF PHYSICS Volume: 14 Article Number: 025009 DOI: 10.1088/1367-2630/14/2/025009 Published: FEB 28 2012
 Times Cited: 1 (from All Databases)
 Get it! Waterloo [View abstract]

Select Page Add to Marked List (0) Send to: my.endnote.com

Results: 9 Page of 1 Sort by:

9 records matched your query of the 55,067,330 (contains duplicates) in the data limits you selected.

View in: [简体中文](#) | [繁體中文](#) | [English](#) | [日本語](#) | [한국어](#) | [Portugués](#) | [Español](#)

© 2013 Thomson Reuters | [Terms of Use](#) | [Privacy Policy](#) | [Please give us your feedback on using Web of Knowledge.](#)

Tunable interactions and phase transitions in Dirac materials in a magnetic field

Z. Papić,¹ D. A. Abanin,^{2,3} Y. Barlas,⁴ and R. N. Bhatt^{1,2}

¹*Department of Electrical Engineering, Princeton University, Princeton, New Jersey 08544, USA*

²*Princeton Center for Theoretical Science, Princeton University, Princeton, New Jersey 08544, USA*

³*Department of Physics, Harvard University, Cambridge, Massachusetts 02138, USA*

⁴*National High Magnetic Field Laboratory and Department of Physics, Florida State University, Florida 32306, USA*

(Received 28 November 2011; published 19 December 2011)

A partially filled Landau level (LL) hosts a variety of correlated states of matter with unique properties. The ability to control these phases requires tuning the effective electron interactions within a LL, which has been difficult to achieve in GaAs-based structures. Here we consider a class of Dirac materials in which the chiral band structure, along with the mass term, gives rise to a wide tunability of the effective interactions by the magnetic field. This tunability is such that different phases can occur in a *single* LL, and phase transitions between them can be driven *in situ*. The incompressible, Abelian and non-Abelian, liquids are stabilized in interaction regimes different from GaAs. Our study points to a realistic method of controlling the correlated phases and studying the phase transitions between them in materials such as graphene, bilayer graphene, and topological insulators.

DOI: 10.1103/PhysRevB.84.241306

PACS number(s): 73.43.-f

In a magnetic field, the kinetic energy of electrons confined to move in two dimensions is quenched into a set of discrete Landau levels (LLs). The properties of a partially filled LL are therefore determined solely by the electron-electron interactions, which give rise to a number of fundamentally different many-body phases, including the incompressible fractional quantum Hall (FQH) states,¹⁻⁴ compressible Fermi-liquid-like states (CFL),⁵ as well as states with broken translational symmetry, such as charge-density waves (CDWs), stripes, and bubble phases.⁶

The competition between different phases at a given partial filling ν is sensitive to the form of the effective Coulomb interactions within a LL. To the best of our knowledge, experimentally, to date there is no reliable way of controlling the effective interactions within a LL.⁷ This is because in GaAs, the most common high-mobility two-dimensional (2D) electron system, the effective interactions depend only on the LL number, and not on the magnetic field. Thus, in order to control the FQH phases, it is advantageous to find alternative 2D electron systems with tunable interactions.⁸

Recently, a class of such materials clean enough to observe FQH phases has emerged. These so-called Dirac materials host chiral excitations with the nontrivial Berry phases. Examples include graphene, bilayer graphene,⁹ topological insulators,¹⁰ as well as certain quantum wells.¹¹ A natural question arises—could the Dirac materials offer any tunability in the FQH regime?

Here, we answer this question affirmatively, and provide a realistic model where the effective interactions can be widely tuned by varying an external magnetic field, giving rise to several phases within *each* LL, and quantum phase transitions (QPTs) between them. We map out the phase diagram of chiral materials at certain filling factors, identifying a different regime of the effective interactions where the non-Abelian Moore-Read (MR)¹² and other paired states¹³ are stable away from $n = 1$ LL of GaAs.¹³⁻¹⁵ Finally, we predict several types of phase transitions that occur in Dirac materials (from an incompressible FQH state to a compressible state, with or without breaking of translational symmetry, between an

Abelian and a non-Abelian FQH state), which, to the best of our knowledge, previously have only been considered in artificial theoretical models.

The control of the correlated phases proposed here is attractive for two reasons. First, it allows one to realize and stabilize the exotic states,¹³ or may lead to a discovery of alternate correlated states that are weak or absent in GaAs. Second, it provides a setting for studying the fundamental problem of phase transitions that involve topologically ordered states. Our study shows that both of these goals can be achieved by current experimental techniques of tuning the gap in the spectrum, e.g., in bilayer graphene,⁹ and topological insulators.¹⁰ In the former case, the gap is opened by a perpendicular electric field, and in the latter case by the deposition of magnetic adatoms. In graphene, it is more challenging to open the gap, although there exist several promising proposals (e.g., the mass can be generated either spontaneously, or as a result of sublattice symmetry breaking⁹).

We consider fermions with the Berry phase π and 2π , described by the 2×2 Hamiltonian,

$$H_{\lambda\pi} = \begin{bmatrix} \Delta & \mathcal{M}_\lambda(p_x + ip_y)^\lambda \\ \mathcal{M}_\lambda(p_x - ip_y)^\lambda & -\Delta \end{bmatrix}, \quad \lambda = 1, 2, \quad (1)$$

where $\mathcal{M}_1 \equiv v_0$ is the Fermi velocity, $\mathcal{M}_2 \equiv 1/2m$ (m is the effective mass), and 2Δ is the band gap. The case $\lambda = 1$ (Berry's phase π) is realized in graphene, topological insulators, and special quantum wells,¹¹ the case $\lambda = 2$ (Berry's phase 2π occurs in bilayer graphene).

A Landau-level spectrum for π carriers, obtained by solving the Schrödinger equation for H_π in a magnetic field, is given by $\varepsilon_n = \text{sgn}(n)\sqrt{\Delta^2 + \varepsilon_0^2|n|}$, $n = \pm 1, \pm 2, \dots$, $\varepsilon_0 = \sqrt{2\hbar}v_0/\ell_B$ is the characteristic energy scale, and $\ell_B = \sqrt{\hbar c/eB}$ is the magnetic length. The corresponding two-component wave functions are given by $\psi_n = (\cos \theta_n \varphi_{|n|-1}, \sin \theta_n \varphi_{|n|})$, where φ_n is the wave function of the n th nonrelativistic LL (standard magnetic oscillator wave function), and parameter θ can be expressed as $\tan \theta_n = [\text{sgn}(n)\sqrt{(\Delta/\varepsilon_0)^2 + |n|} - \Delta/\varepsilon_0]/\sqrt{|n|}$.

In the limit of zero mass (graphene case), $\tan \theta_n = \pm 1$, and the weights of $\varphi_{|n-1}$ and $\varphi_{|n|}$ in the wave function ψ_n become equal. In the opposite limit of very large mass $\Delta/\varepsilon_0 \gg 1$, the LLs become identical to the nonrelativistic ones: $\tan \theta_{|n|} \rightarrow 0$ [this corresponds to $\psi_{|n|} \approx (\varphi_{|n-1}, 0)$], and $\tan \theta_{-|n|} \rightarrow -\infty$ [$\psi_{-|n|} \approx (0, \varphi_{|n|})$]. Varying Δ/ε_0 between 0 and ∞ , which can be achieved by changing magnetic field, allows one to explore the whole range $\theta \in (0; \pi/2)$.

The two-component nature of the wave function modifies the effective interaction within a LL, which determines the many-body phases at a partial filling. We use the standard approximation and project the interaction onto a partially filled LL. In this case, the Fourier transform of the effective interaction is a product of bare Coulomb interaction $V(q) = 2\pi e^2/q$ and the form factor³ $|F_n(q)|^2$ which contains the information about the band structure. In case of the materials with the Berry phase π ,

$$F_n^\pi(q) = \cos^2 \theta L_{|n-1|}(q^2 \ell_B^2/2) + \sin^2 \theta L_{|n|}(q^2 \ell_B^2/2), \quad (2)$$

where L_k is the k th Laguerre polynomial, and for simplicity we omitted the index of θ . The form factor is a mixture of the $(|n| - 1)$ th and $|n|$ th LL form factors in a nonrelativistic two-dimensional electron system (2DES) with parabolic dispersion. At $\theta = \pi/4$, the above equation reduces to the form factor of pristine graphene.¹⁶

Similarly, for carriers with the Berry phase 2π , the LL spectrum is given by $\varepsilon_n = \text{sgn}(n)\sqrt{\Delta^2 + \varepsilon_c^2}|n|(|n| + 1)$, $n = \pm 1, \pm 2, \dots$, where $\varepsilon_c = eB/mc$ is the cyclotron energy. The corresponding wave functions are $\psi_n = (\cos \theta_n \varphi_{|n-1|}, \sin \theta_n \varphi_{|n+1|})$, with $\tan \theta_n = [\text{sgn}(n)\sqrt{(\Delta/\varepsilon_c)^2 + |n|(|n| + 1)} - \Delta/\varepsilon_c]/\sqrt{|n|(|n| + 1)}$. The form factor is a mixture of standard $(|n| - 1)$ th and $(|n| + 1)$ th form factors,

$$F_n^{2\pi}(q) = \cos^2 \theta L_{|n-1|}(q^2 \ell_B^2/2) + \sin^2 \theta L_{|n+1|}(q^2 \ell_B^2/2). \quad (3)$$

The tunable form of the effective interactions Eqs. (2) and (3) provides a way to realize the transitions between strongly correlated phases, as will be demonstrated below.

Much of the previous theoretical work on the quantum Hall effect in the Dirac materials has been limited to graphene, exploring the consequences of the fourfold LL degeneracy (valley and spin) that leads to unique SU(2)- and SU(4)-symmetric fractional states.¹⁷ Here we neglect the multicomponent degrees of freedom,¹⁸ and examine the effects originating from the interplay of the Coulomb interaction and band structure. The large variation of the effective interactions, due to the band structure, is assumed to be the dominant effect, even when corrections due to LL mixing¹⁹ are taken into account.

We proceed by studying the interacting states of Dirac materials using exact diagonalization in the spherical and torus geometry.^{20,21} The former is useful in studying the incompressible liquids, but is not suitable for states that break translational symmetry, when periodic boundary conditions are more natural.²¹ If the system has an underlying lattice structure, it is assumed that its lattice constant is much smaller than ℓ_B . We map out the phase diagram as a function of θ using the overlaps between an exact ground state and a trial

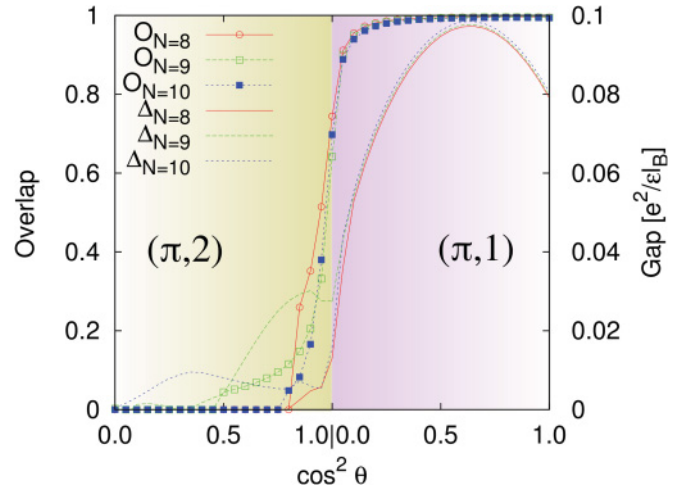


FIG. 1. (Color online) Transition between the Laughlin and the bubble state. Overlap with the Laughlin wave function O_N and charge gap Δ_N are plotted for an N -particle system at $\nu = 1/3$ filling of $(\pi, 1)$ and $(\pi, 2)$ LLs.

wave function. Moreover, we evaluate the energy gaps for creating charged excitations, $\Delta \equiv E_{\text{qp}} + E_{\text{qh}} - 2E_0$, where $E_{\text{qh}}(E_{\text{qp}})$ is the energy of the system in the presence of a quasihole (quasiparticle) and E_0 is the ground-state energy (all in units of $e^2/\varepsilon \ell_B$). For simplicity, when we use the spherical geometry, the form factors Eqs. (2) and (3) are calculated for a flat surface; the curvature is expected to produce only a small quantitative difference in larger systems and has a stronger impact on the energy gaps than the overlaps. Various choices of the single-particle Hamiltonian are denoted by $(\lambda\pi, n)$, where we restrict to $\lambda = 1, 2$ and $n = 1, 2$. Higher values of n are not considered because they do not support FQH states.

At partial filling $\nu = 1/3$, the Laughlin state is robust in $(\pi, 1)$, $(\pi, 2)$, and $(2\pi, 1)$ LLs. The overlaps between the exact ground state and the Laughlin wave function, as well as the charge gaps in $(\pi, 1)$ and $(\pi, 2)$ LLs, are illustrated in Fig. 1. The overlap remains very close to one for $\cos^2 \theta \in [0.2; 1]$ in the $(\pi, 1)$ LL. This is not surprising because the form factors of this LL are a mixture of 0 and 1 nonrelativistic form factors, both of which favor the Laughlin state. An interesting feature of Fig. 1 is that the energy gap shows a maximum at $\cos^2 \theta \approx 0.65$, rather than at $\cos^2 \theta = 1$ (pure $n = 0$ nonrelativistic LL). This special value of θ maximizes the ratio of V_1/V_3 Haldane pseudopotentials³ which controls the gap in this case. The overlap and the gap decrease drastically as $\cos^2 \theta \rightarrow 0$; furthermore, in $(\pi, 2)$ LL, the Laughlin state quickly undergoes a QPT to a bubble phase as the overlaps and gaps drop to zero. A signature of this transition is also detected in the projected structure factor,³ which develops a sharp peak in the bubble phase.²² The transition is more naturally captured in the torus geometry, where a large ground-state degeneracy,²³ characterized by a 2D array of crystal momenta, develops in $(\pi, 2)$ LL. Similar behavior is found in $(2\pi, 1)$ LL.²² One of the members of the multiplet belongs to the zero-momentum sector, which suggests that the transition is likely to be second order.

Next, we consider a half-filled LL, where we find evidence for the Moore-Read¹² correlations in half-filled chiral $(\pi, 1)$

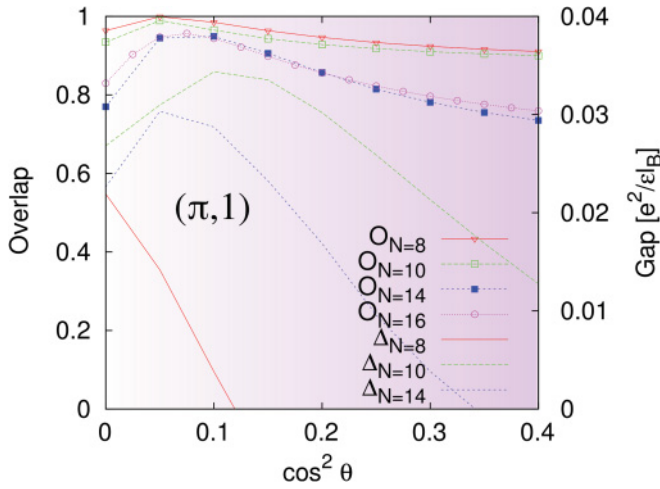


FIG. 2. (Color online) Transition between the Moore-Read and the CFL state. Overlap with the Pfaffian wave function O_N and charge gap Δ_N are plotted for an N -particle system at $\nu = 1/2$ filling of $(\pi, 1)$ LL.

and $(2\pi, 1)$ LLs. In the former case, the Pfaffian becomes more robust than its GaAs analog for $\cos^2 \theta \approx 0.1$ (Fig. 2). The point $\cos \theta = 0$ corresponds to a $n = 1$ nonrelativistic LL where the overlap is high (as expected). As $\cos \theta$ increases, the overlap reaches a maximum value at $\cos^2 \theta \approx 0.1$; this is followed by an enhancement of the gap, which peaks at approximately the same point (gaps show stronger finite-size effects than the overlaps). The increased stability of the Pfaffian was previously discussed in Ref. 24 in the context of biased bilayer graphene. On the other hand, away from the “optimal” point $\cos^2 \theta \approx 0.1$, the Pfaffian undergoes a QPT to the compressible CFL state.^{5,15} This transition is accompanied by a change in *shift*²⁵ of the ground state beyond $\cos^2 \theta = 0.4$, and is also manifested in the gaps dropping to zero (Fig. 2). A similar scenario is found in $(2\pi, 1)$ LL.²² At larger values of $\cos^2 \theta$, in both $(\pi, 1)$ and $(2\pi, 1)$, we expect a QPT into the CFL state; at very small $\cos^2 \theta$ in $(2\pi, 1)$ LL, the Pfaffian gives way to a stripe phase. Thus, chiral materials are suitable for studying phase transitions between the Pfaffian, stripe phase, and the CFL; these transitions are expected to be of a different nature, either first or second order.²⁶ This is a distinct advantage

over GaAs-based 2DES, where the effective interactions are significantly more difficult to tune in a controlled fashion.

Note that the enhancement of the overlaps and gaps might appear similar in nature to tweaking of the V_1 pseudopotential, known to have a favorable effect on the Pfaffian state.¹⁵ However, in the present case, the interaction that favors the MR state is a superposition of $n = 0$ and $n = 1$ form factors, including the long-range tail of the repulsive potential; thus it represents a different regime where the MR state is stable. This regime of stability does not crucially depend on the presence of the $n = 1$ LL form factor. Similar signatures of the paired states occur also in $(2\pi, 1)$ LL, where the interaction involves a superposition of $n = 0$ and $n = 2$ LL form factors, making the difference from GaAs even more striking.

We have also analyzed the filling $\nu = 3/5$ ²² (or $\nu = 2/5$), where the one expects to find the non-Abelian $k = 3$ Read-Rezayi state¹³ that supports universal topological quantum computation.²⁷ Similar to the MR state, in chiral materials we find non-Abelian correlations in both $(\pi, 1)$ and $(2\pi, 1)$ LLs, with a phase transition to the stripe phase and the Abelian hierarchy state²⁰ (see also Fig. 3).

Finally, we consider a model that generalizes the effective interaction given above and allows to map the phase diagram for a wider class of materials. Specifically, we study the form factors that are represented as a linear combination of $|n|$, $|n| + 1$, and $|n| + 2$ nonrelativistic form factors. Such form factors define a two-parameter family,

$$F_n(q) = \cos^2 \theta L_{|n|}(q^2 \ell_B^2 / 2) + \sin^2 \theta \cos^2 \varphi L_{|n|+1}(q^2 \ell_B^2 / 2) + \sin^2 \theta \sin^2 \varphi L_{|n|+2}(q^2 \ell_B^2 / 2). \quad (4)$$

The effective interactions of the above form arise in a number of materials, including trilayer graphene,²⁸ as well as bilayer graphene in the limit of large asymmetry between the two layers.^{24,29} The exact relation of the parameters (θ, φ) to the band structure of various materials will be discussed elsewhere.²² The phase diagram of the model in Eq. (4) for its $n = 0$ LL is illustrated in Fig. 3. Along certain axes (indicated by arrows), the generalized model reduces to one of the particular cases $(\lambda\pi, n)$ presented earlier. A salient feature of the generalized model is that non-Abelian states are found in a strip of θ, φ values where the effective interaction significantly deviates from the $n = 1$ nonrelativistic one. On

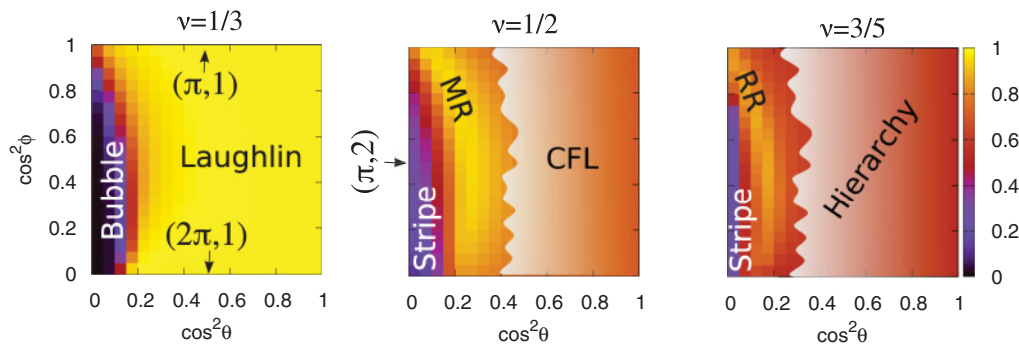


FIG. 3. (Color online) Phase diagram of a generic chiral material in a partially filled LL containing a mixture of $n = 0$, $n = 1$, and $n = 2$ nonrelativistic form factors. The color (grayscale) scheme on the right-hand side defines the magnitude of the overlaps with the Laughlin, Moore-Read, and the $k = 3$ Read-Rezayi (RR) wave function. The shaded regions represent the phases with different topological numbers (CFL, hierarchy state). The phase boundary between topological states is approximately drawn by a wiggly line.

the right-hand side of the strip, the states undergo a QPT to another FQH (or CFL) state with different topological numbers. These transitions are represented by wiggly lines in Fig. 3, where the shaded areas mark the resulting phases with a different shift. On the left-hand side, the system crosses over to compressible, CDW-like phases. The Abelian states dominate over a wide region of parameter space and are insensitive to variation in φ , unless $\cos\theta$ is close to zero. We note that the presented phase diagram is consistent with the one obtained by considering the charge gaps instead of the overlaps.²²

In summary, we showed that chiral materials sustain regimes of the effective interactions that are different from GaAs. This allows one to stabilize the desired phases (including non-Abelian ones) within a single LL, and provides a way to engineer QPTs between them. Our results apply to a number of available high-mobility 2DES,^{9,10,28} however, bilayer and trilayer graphene appear as most suitable

candidates because their band structure can be tuned by an external electric field. In fact, our proposal already can be realized in bilayer graphene with the existing experimental tools. It was demonstrated³⁰ that the gap can be controlled in the interval ± 125 meV. With the cyclotron energy of ~ 20 meV at $B = 10$ T, this translates into the ability to tune $\cos^2\theta$ in the interval (0.01; 0.99), sufficient for the realization of the non-Abelian states (see Fig. 3). We believe that experimental observation of the phases and QPTs predicted here should be feasible in the near future, as the fractional quantum Hall states in graphene have already been observed,³¹ and transport anomalies suggesting fractional states have been seen in topological insulators³² and bilayer graphene.³³

This work was supported by DOE Grant No. DE-SC0002140. Y.B. was supported by the State of Florida.

-
- ¹D. C. Tsui, H. L. Stormer, and A. C. Gossard, *Phys. Rev. Lett.* **48**, 1559 (1982).
- ²R. B. Laughlin, *Phys. Rev. Lett.* **50**, 1395 (1983).
- ³*The Quantum Hall Effect*, 2nd ed., edited by R. E. Prange and S. M. Girvin (Springer, New York, 1990).
- ⁴J. K. Jain, *Composite Fermions* (Cambridge University Press, Cambridge, UK, 2007).
- ⁵B. I. Halperin, P. A. Lee, and N. Read, *Phys. Rev. B* **47**, 7312 (1993).
- ⁶A. A. Koulakov, M. M. Fogler, and B. I. Shklovskii, *Phys. Rev. Lett.* **76**, 499 (1996); R. Moessner and J. T. Chalker, *Phys. Rev. B* **54**, 5006 (1996).
- ⁷J. Xia, V. Cvicek, J. P. Eisenstein, L. N. Pfeiffer, and K. W. West, *Phys. Rev. Lett.* **105**, 176807 (2010); J. Shabani, T. Gokmen, and M. Shayegan, *ibid.* **103**, 046805 (2009).
- ⁸Z. Papić, R. Thomale, and D. A. Abanin, *Phys. Rev. Lett.* **107**, 176602 (2011).
- ⁹A. H. Castro Neto *et al.*, *Rev. Mod. Phys.* **81**, 109 (2009).
- ¹⁰M. Z. Hasan and C. L. Kane, *Rev. Mod. Phys.* **82**, 3045 (2010).
- ¹¹B. A. Volkov and O. A. Pankratov, *Pi'sma Zh. Eksp. Teor. Fiz.* **42**, 145 (1985) [*JETP Lett.* **42**, 178 (1985)]; B. Buttner *et al.*, *Nat. Phys.* **7**, 418 (2011).
- ¹²G. Moore and N. Read, *Nucl. Phys. B* **360**, 362 (1991).
- ¹³N. Read and E. H. Rezayi, *Phys. Rev. B* **59**, 8084 (1999).
- ¹⁴R. H. Morf, *Phys. Rev. Lett.* **80**, 1505 (1998).
- ¹⁵E. H. Rezayi and F. D. M. Haldane, *Phys. Rev. Lett.* **84**, 4685 (2000).
- ¹⁶K. Nomura and A. H. MacDonald, *Phys. Rev. Lett.* **96**, 256602 (2006); M. O. Goerbig, R. Moessner, and B. Douçot, *Phys. Rev. B* **74**, 161407 (2006).
- ¹⁷V. M. Apalkov and T. Chakraborty, *Phys. Rev. Lett.* **97**, 126801 (2006); M. O. Goerbig and N. Regnault, *Phys. Rev. B* **75**, 241405 (2007); C. Töke and J. K. Jain, *ibid.* **75**, 245440 (2007); Z. Papić, M. O. Goerbig, and N. Regnault, *Phys. Rev. Lett.* **105**, 176802 (2010).
- ¹⁸The presence of a mass and spin Zeeman term will lead to valley and spin broken symmetry FQH states with exchange enhanced gaps.
- ¹⁹W. Bishara and C. Nayak, *Phys. Rev. B* **80**, 121302 (2009); A. Wojs, C. Töke, and J. K. Jain, *Phys. Rev. Lett.* **105**, 096802 (2010); E. H. Rezayi and S. H. Simon, *ibid.* **106**, 116801 (2011).
- ²⁰F. D. M. Haldane, *Phys. Rev. Lett.* **51**, 605 (1983).
- ²¹D. Yoshioka, B. I. Halperin, and P. A. Lee, *Phys. Rev. Lett.* **50**, 1219 (1983); F. D. M. Haldane, Ch. 8 in *The Quantum Hall Effect* (Ref. 3).
- ²²D. A. Abanin, Z. Papić, Y. Barlas, and R. N. Bhatt (unpublished).
- ²³E. H. Rezayi, F. D. M. Haldane, and K. Yang, *Phys. Rev. Lett.* **83**, 1219 (1999); F. D. M. Haldane, E. H. Rezayi, and K. Yang, *ibid.* **85**, 5396 (2000).
- ²⁴V. A. Apalkov and T. Chakraborty, *Phys. Rev. Lett.* **107**, 186803 (2011).
- ²⁵X. G. Wen and A. Zee, *Phys. Rev. Lett.* **69**, 953 (1992).
- ²⁶N. E. Bonesteel, *Phys. Rev. Lett.* **82**, 984 (1999).
- ²⁷C. Nayak *et al.*, *Rev. Mod. Phys.* **80**, 1083 (2008).
- ²⁸W. Bao *et al.*, *Nat. Phys.* **7**, 948 (2011); T. Taychatanapat *et al.*, *ibid.* **7**, 621 (2011); A. Kumar *et al.*, *Phys. Rev. Lett.* **107**, 126806 (2011); C. H. Lui *et al.*, *Nat. Phys.* **7**, 944 (2011).
- ²⁹E. McCann and V. I. Fal'ko, *Phys. Rev. Lett.* **96**, 086805 (2006).
- ³⁰Y. Zhang *et al.*, *Nature (London)* **459**, 820 (2009).
- ³¹X. Du *et al.*, *Nature (London)* **462**, 192 (2009); K. Bolotin *et al.*, *ibid.* **462**, 196 (2009); C. Dean *et al.*, *Nat. Phys.* **7**, 693 (2011).
- ³²Jum Xiong *et al.*, e-print arXiv:1101.1315v1.
- ³³W. Bao, Z. Zhao, H. Zhang, G. Liu, P. Kratz, L. Jing, J. Velasco, D. Smirnov, and C. N. Lau, *Phys. Rev. Lett.* **105**, 246601 (2010).

Search Search History

All Databases

<< Return to Web of Science®

Citing Articles Title: Stability of the k=3 Read-Rezayi state in chiral two-dimensional systems with tunable interactions
Author(s): Abanin, D. A. ; Papic, Z. ; Barlas, Y. ; et al.
Source: NEW JOURNAL OF PHYSICS Volume: 14 Article Number: 025009 DOI: 10.1088/1367-2630/14/2/025009 Published: FEB 28 2012

This item has been cited by items indexed in the databases listed below. [more information]

- 1 in All Databases
1 publication in Web of Science
0 publication in BIOSIS Citation Index
0 publication in SciELO Citation Index
0 publication in Chinese Science Citation Database
0 data sets in Data Citation Index
0 publication in Data Citation Index

Results: 1 Page 1 of 1 Go Sort by: Publication Date -- newest to oldest

Create Citation Report

Hide Refine

Refine Results

Search within results for

Search

Databases

Research Domains Refine

SCIENCE TECHNOLOGY

Research Areas Refine

PHYSICS

Document Types

Authors

Group/Corporate Authors

Editors

Funding Agencies

Source Titles

Conference/Meeting Titles

Publication Years

Languages

Countries/Territories

Select Page Add to Marked List (0) Send to: my.endnote.com

Title: Spin-helical transport in normal and superconducting topological insulators
Author(s): Tkachov, G.; Hankiewicz, E. M.
Source: PHYSICA STATUS SOLIDI B-BASIC SOLID STATE PHYSICS Volume: 250 Issue: 2 Pages: 215-232 DOI: 10.1002/pssb.201248385 Published: FEB 2013
Times Cited: 10 (from All Databases)
Get it! Waterloo View abstract

Select Page Add to Marked List (0) Send to: my.endnote.com

Results: 1 Show 50 per page Page 1 of 1 Go Sort by: Publication Date -- newest to oldest

1 records matched your query of the 55,067,330 (contains duplicates) in the data limits you selected.

View in: 简体中文 繁體中文 English 日本語 한국어 Português Español

Stability of the $k = 3$ Read–Rezayi state in chiral two-dimensional systems with tunable interactions

This article has been downloaded from IOPscience. Please scroll down to see the full text article.

2012 New J. Phys. 14 025009

(<http://iopscience.iop.org/1367-2630/14/2/025009>)

View [the table of contents for this issue](#), or go to the [journal homepage](#) for more

Download details:

IP Address: 128.112.48.129

The article was downloaded on 02/01/2013 at 14:19

Please note that [terms and conditions apply](#).

Stability of the $k = 3$ Read–Rezayi state in chiral two-dimensional systems with tunable interactions

D A Abanin^{1,2}, Z Papić^{3,5}, Y Barlas⁴ and R N Bhatt^{1,3}

¹ Princeton Center for Theoretical Science, Princeton University, Princeton, NJ 08544, USA

² Department of Physics, Harvard University, Cambridge, Massachusetts 02138, USA

³ Department of Electrical Engineering, Princeton University, Princeton, NJ 08544, USA

⁴ National High Magnetic Field Laboratory and Department of Physics, Florida State University, FL 32306, USA

E-mail: zpapic@princeton.edu

New Journal of Physics **14** (2012) 025009 (11pp)

Received 30 September 2011

Published 28 February 2012

Online at <http://www.njp.org/>

doi:10.1088/1367-2630/14/2/025009

Abstract. The $k = 3$ Read–Rezayi (RR) parafermion quantum Hall state hosts non-Abelian excitations which provide a platform for universal topological quantum computation. Although the RR state may be realized at the filling factor $\nu = 12/5$ in GaAs-based two-dimensional electron systems, the corresponding quantum Hall state is weak and at present nearly impossible to study experimentally. Here we argue that the RR state can alternatively be realized in a class of chiral materials with massless and massive Dirac-like band structure. This family of materials encompasses monolayer and bilayer graphene, as well as topological insulators. We show that, compared to GaAs, these systems provide several important advantages in realizing and studying the RR state. Most importantly, the effective interactions can be tuned *in situ* by varying the external magnetic field, and by designing the dielectric environment of the sample. This tunability enables the realization of RR state with controllable energy gaps in different Landau levels. It also allows one to probe the quantum phase transitions to other compressible and incompressible phases.

⁵ Author to whom any correspondence should be addressed.

Contents

1. Introduction	2
2. The model	3
3. The method and results	6
4. Conclusion	9
Acknowledgments	10
References	10

1. Introduction

Strongly correlated phases of electrons, confined to move in the plane and subjected to a perpendicular magnetic field, have attracted significant attention since the discovery of fractionally quantized Hall conductivity [1]. The profound role of topology in this extreme quantum limit leads to the presence of quasiparticles that carry a fraction of electron charge [2] and fractional (Abelian or possibly non-Abelian) statistics [2, 3]. The prospect of excitations possessing non-Abelian statistics has motivated different schemes for topological quantum computation [4] based on these systems.

These remarkable phenomena occur in the fractional quantum Hall (FQH) regime, when the number of electrons, N_e , is comparable to the number of magnetic flux quanta N_Φ through the two-dimensional electron system (2DES). Correlated FQH liquid states appear at certain partial filling $\nu = N_e/N_\Phi$ of the active Landau level (LL). In traditional semiconductor heterostructures, the physics of a partially filled $n = 1$ LL differs significantly from that of $n = 0$ LL, due to the node in the single-particle wavefunction [5]. As a consequence, the hierarchy/composite fermion states [6, 7], ubiquitous in the lowest Landau level (LLL), are significantly weakened in $n = 1$ LL, and some of the more exotic states, such as the Read–Rezayi (RR) parafermion states [8], are likely to be favored. A number of studies have focused on the simplest, $k = 2$ non-Abelian member of the RR sequence—the Moore–Read (MR) ‘Pfaffian’ state [3]. The Pfaffian or perhaps its particle–hole conjugate version—the anti-Pfaffian [9], with similar topological properties, is widely believed to describe the FQH plateau at $\nu = 5/2$ [10]. Quasiparticles of the MR and higher RR states obey the non-Abelian statistics [3] which is of interest for topological quantum computation [4]. However, for the purpose of *universal* topological quantum computation, the MR state is not sufficient, and one must go to a higher, $k = 3$ member of the RR sequence (see [4] and, for a general case, [11]). In GaAs systems, experiments [12, 13] have detected only a weak plateau at $\nu = 12/5$, which theoretical work [8] has tentatively identified with the particle–hole conjugate of the $k = 3$ RR state. This state, however, is very fragile and has been seen only in a small number of samples, triggering alternative theoretical proposals for its origin [14]. Numerical calculations suggest that the appearance of the RR $k = 3$ state is linked to the finite width of the 2DES in GaAs [15, 16], but little is known about the stability of the $k = 3$ RR state as the interaction is tuned away from the bare Coulomb point. For example, in the case of the $k = 2$ (Moore–Read) state, it is possible to construct a two-body interaction [17], resulting from particle–hole symmetrization of the hard-core three-body repulsion, which yields a ground state with high overlap with the exact ground state of the Coulomb interaction. This model interaction consists only of V_1 and V_3 Haldane pseudopotentials (to be defined below). In the case of the $k = 3$ RR state, such an

approximate two-body hard-core interaction has not been constructed, but one could expect that it requires higher order Haldane pseudopotentials (and perhaps some three-body terms as well).

One of the main disadvantages of the GaAs-based devices is that their 2DES is buried inside a larger, 3D structure. This unfortunate fact fixes the effective interactions at values that are often not optimal for some of the most interesting FQH states, including the RR series. For example, the MR state is found to lie very close to the boundary with a compressible phase [18, 19]. Another problem stems from the strong dielectric screening and finite well width [20] in GaAs, which weaken the electron–electron interactions and render FQH states fragile. This has been a major obstacle in the studies of the non-Abelian states, which could only be observed in ultra-high-mobility samples [10]. Thus, it is desirable to find an alternative high-mobility 2DES with strong effective Coulomb interactions that are adjustable in a broad range.

Recently, a new class of such high-mobility 2DESs that host chiral excitations with non-trivial Berry phases was discovered. These ‘chiral’ materials include graphene and bilayer graphene [21] and, more recently, topological insulators [22], as well as certain quantum wells [23]. The chiral nature of the quasiparticles gives rise to new electronic properties, including an unusual LL sequence, anomalous Hall effect and suppression of weak localization [21]. When these chiral materials are subjected to a perpendicular magnetic field, the kinetic energy quenches into discrete LLs, similar to the usual semiconductors with non-chiral carriers. However, due to the chiral band structure [24] and the fact that the surface of these materials is exposed [25], they offer new possibilities to tune the effective interactions and explore strongly correlated phases.

In this paper, we analyze two practical ways of tuning the effective interactions in the chiral 2DES, and the effect this has on the non-Abelian FQH states. As a case study, we choose to focus on the $k = 3$ RR state. In stark contrast to GaAs, we find that the chiral 2DESs allow for a more robust RR state along with the possibility of its realization in *several* LLs. Additional insights can be obtained by driving transitions between the RR state and the Abelian hierarchy state, or the compressible stripe phase [26]. Such transitions can be implemented in chiral and *massive* 2DES by varying the external field. Overall, the tunability of the chiral 2DES allows one to explore new interesting regimes of the effective Coulomb interactions, not achievable in GaAs.

2. The model

We consider a family of 2D materials that are characterized by non-trivial Berry phases. One such material is monolayer graphene, a high-mobility atomically thick 2DES [21], where recently several FQH states of the type $\nu = m/3$ have been discovered [27]. A closely related material, bilayer graphene [21], has similarly high mobility and exhibits interaction-induced quantum Hall states at integer filling factors at low magnetic fields [34]. Graphene and its bilayer are characterized by the Berry phase π [28] (graphene-like) and 2π [29] (bilayer-graphene-like with an energy gap), respectively.

Many of the previous theoretical works on chiral materials have been restricted to graphene, exploring the consequences of the fourfold LL degeneracy (valley and spin) that leads to new SU(2) and SU(4)-symmetric fractional states [30]. Instead, we focus on the high-field limit, neglecting the multicomponent degrees of freedom, and examine the effects from the interplay between the Coulomb interaction and band structure. We consider a family of band structures introduced in [24], which describe a number of high-mobility materials,

including graphene with *massive* carriers (mass is generated either spontaneously or as a result of sublattice symmetry breaking [21]), topological insulators [22], bilayer graphene [21], trilayer graphene [31], and similar materials. Pristine graphene, which hosts massless Dirac-like fermions, is contained in this model as a particular case. More explicitly, we consider a family of 2×2 Hamiltonians with the Berry phase π and 2π [24]. The case of π -carriers is realized in graphene, topological insulators and special quantum wells [23]; the case of 2π -carriers occurs in bilayer graphene, where the energy gap can be controlled in a wide range by a perpendicular electric field [21]. These 2×2 effective Hamiltonians can be derived perturbatively starting from a tight-binding model for each of the materials with a given chirality σ ; however, the effective model will be applicable in a narrower energy range for larger σ [32]. As is well known for the case of graphene, the one-body eigenstates of such Hamiltonians possess a spinor structure. Consequently, the harmonic oscillator raising/lowering operators will mix the different components to produce an effective form factor that has a richer structure than in the case of a simple parabolic band such as in GaAs, making it possible to tune the effective interaction.

For π carriers, the single-particle wavefunctions are given by [24] $\psi_n = (\cos \theta_n \phi_{|n|-1}, \sin \theta_n \phi_{|n|})$, where ϕ_n is the wave function of the n th non-relativistic LL ($n = \pm 1, \pm 2, \dots$), and the parameter θ depends on the ratio $\Delta / (\hbar v_0 / \ell_B)$, where Δ is the mass gap, v_0 the Fermi velocity and $\ell_B = \sqrt{\hbar c / e B}$ the magnetic length. We use the notation $(\sigma\pi, n)$ to denote the n th LL for $\sigma\pi$ carriers ($\sigma = 1, 2$). As a consequence of the spinor wavefunction, the effective form factor [5] $F_n^\pi(q)$ that describes the interaction projected to a (π, n) LL is given by

$$F_n^\pi(q) = \cos^2 \theta L_{|n|-1} \left(\frac{q^2 \ell_B^2}{2} \right) + \sin^2 \theta L_{|n|} \left(\frac{q^2 \ell_B^2}{2} \right), \quad (1)$$

where L_k is the k th Laguerre polynomial, and for simplicity we omitted the index of θ . The form factor is a mixture of the $(|n| - 1)$ th and $|n|$ th LL form-factors in a non-relativistic 2DES with parabolic dispersion. At $\theta = \pi/4$, the above equation reduces to the form factor of graphene [33]; however, quite generally by varying $\Delta / (\hbar v_0 / \ell_B)$, one can realize any value of $\theta \in (0; \pi/2)$.

Similarly, for carriers with the Berry phase 2π , the single-particle wavefunctions are $\psi_n = (\cos \theta_n \phi_{|n|-1}, \sin \theta_n \phi_{|n|+1})$, and the form factor is a mixture of standard $(|n| - 1)$ th and $(|n| + 1)$ th form factors,

$$F_n^{2\pi}(q) = \cos^2 \theta L_{|n|-1} \left(\frac{q^2 \ell_B^2}{2} \right) + \sin^2 \theta L_{|n|+1} \left(\frac{q^2 \ell_B^2}{2} \right). \quad (2)$$

The tunable form of the effective interaction equations (1,2) provides a way of engineering transitions between strongly correlated phases *in situ* by changing the field. As pointed out by Haldane [5], an interacting many-body system of electrons, confined to a partially filled LL, is defined by a finite set of numbers—the Haldane pseudopotentials. For rotationally invariant systems, these numbers V_m represent the amplitudes of a state of two electrons with the relative angular momentum m . The physics of the FQHE is determined by small- m pseudopotentials, i.e. V_1, V_3, V_5, \dots . The role of higher V_m 's is to enforce charge neutrality, but they do not affect the incompressibility. Therefore, the ratio of the two strongest pseudopotentials, V_1 / V_3 , can be a rough indicator of the expected many-body phases. In figure 1(b) we show this ratio for several types of charge carriers and LLs. The variation of V_1 / V_3 as a function of θ is to be contrasted with figure 1(a) where the same quantity is plotted for an infinite GaAs quantum well of width

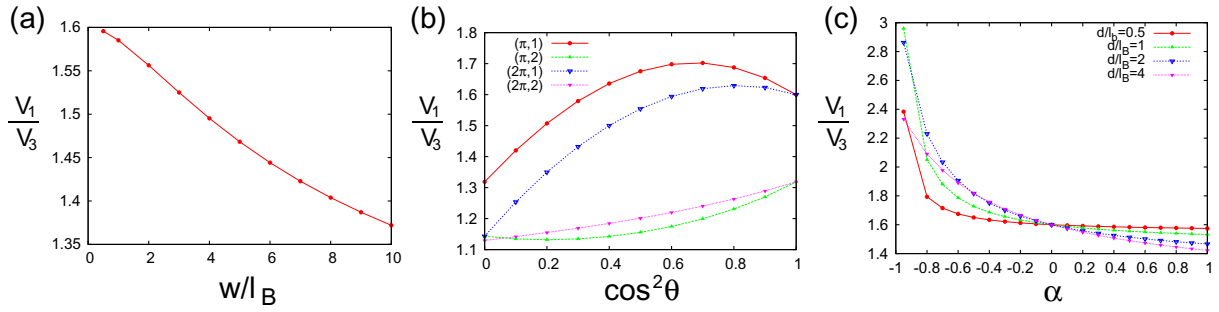


Figure 1. The variability of the ratio V_1/V_3 of the Haldane pseudopotentials for GaAs and chiral 2DES. (a) V_1/V_3 as a function of the width w in the case of an infinite quantum well model, appropriate for GaAs. (b, c) V_1/V_3 in chiral materials, shown as a function of the band structure parameter θ , introduced in Eq. (1, 2) (b), and as a function of the screening parameter α and the distance of the dielectric plate d (c). Chiral 2DESs offer a possibility of tuning V_1/V_3 in a much broader range than is possible within a quantum well model.

w . In GaAs the width of the well can be tuned by electrostatic gates; however, it invariably reduces V_1/V_3 , whereas the chiral 2DESs allow for both an increase *and* decrease of V_1/V_3 and in a wider range.

Up to this point, we have discussed the change in the effective interaction $V(q)|F(q)|^2$ that resulted from a modification of the single-particle wavefunctions and therefore $F(q)$. The second method, proposed in [25], allows one to directly change $V(q)$. Chiral materials, such as graphene, are often exposed to the environment, which allows for dielectric material to be deposited on top of them. We consider a setup where the graphene sample is situated in a dielectric medium with permittivity ϵ_1 , and a semi-infinite dielectric plate with permittivity $\epsilon_2 \neq \epsilon_1$ is placed at a distance $d/2$ away from the graphene sheet. The effective interactions between electrons in graphene change due to the surface charges induced at the boundary between dielectrics [25]:

$$V(r) = \frac{e^2}{\epsilon_1 r} + \alpha \frac{e^2}{\epsilon_1 \sqrt{r^2 + d^2}}, \quad \text{where } \alpha = \frac{\epsilon_1 - \epsilon_2}{\epsilon_1 + \epsilon_2}. \quad (3)$$

The ratio d/l_B controls the effective interactions within a partially filled LL. However, the overall energy scale is also modified and this has an impact on the magnitude of the excitation gap. The gap should be multiplied by a factor $\epsilon_{\text{GaAs}}/\epsilon_1$ if comparison is to be made with the GaAs 2DES. Again, an important advantage of this setup is that the interactions can be tuned *in situ* by varying the magnetic field B , which modifies the ratio d/l_B . The consequences for the many-body system are illustrated in figure 1(c). In the dielectric case, V_1/V_3 is found to have a substantially larger variation as a function of α than the quantum well model or the tuning of the band structure through θ . In particular, for intermediate $d \sim l_B$ and negative α , V_1/V_3 can be readily increased by 50% compared to its bare value ($\alpha = 0$).

Therefore, based on the behavior of V_1/V_3 , we expect that chiral 2DESs offer many possibilities of tuning the interactions. By increasing V_1/V_3 , we expect to stabilize the incompressible phases; on the other hand, by reducing it, one can drive a transition to compressible phases, such as stripes and bubbles. In the following, we will explicitly verify these statements in exact diagonalization calculations and determine the stability of the $k = 3$

RR state. In the operational sense, one can define several criteria for the ‘stability’ of a state; the more those criteria are met, the more ‘stable’ the state is. For example, one can compare the overlap (scalar product) between an exact many-body ground state and the RR wavefunction; if the overlap, defined below, is consistently close to unity for a number of system sizes, we consider it as one of the indicators that the state is in the RR phase. However, there are known examples of different phases of matter which possess ground states of high overlap with each other in finite systems [35]; conversely, a relatively poor overlap cannot be taken as a definitive proof that a phase is not realized. Additional indicators to identify the phase of matter are, for example, the ground-state degeneracy on the torus and the shift on the sphere (selected to minimize the total ground-state energy). Finally, the robustness of a phase is also determined by the magnitude of the gap for creating neutral and charged excitations. All of these indicators should be assessed together in determining the nature of a phase being studied.

3. The method and results

We consider an interacting, N -electron problem with an LL spectrum given above, on a compact surface threaded by N_ϕ magnetic flux quanta using exact diagonalization. In the study of FQHE, two kinds of surfaces are available that preserve the translational invariance of an infinite 2DEG: sphere [6] and torus ([36], see also chapter by F D M Haldane in [5]). The two choices of boundary conditions illustrate the specific features of an FQH state under investigation: on a sphere, the FQH state couples to the curvature of the manifold, which is characterized by the topological number called shift [37]. The shift produces a small offset between N_ϕ and the magnetic monopole, whose strength is denoted by $2S$, placed in the center of a sphere. As a consequence, different FQH states ‘live’ in different Hilbert spaces and, in principle, can be directly compared only after extrapolation to the thermodynamic limit. On the other hand, the flat surface of a torus leads to a unique definition of N_ϕ for given N and ν , so that different candidate states describing the same filling ν are all realized in the same Hilbert space. The caveats of this geometry are the additional geometric parameters, the angle and aspect ratio of the torus; the Hamiltonian of a finite-size system depends on these parameters and their specific values favor one FQH phase over the others. Thus, an analysis is slightly more involved but the advantage is that a ground-state degeneracy can be used to identify the phase. For example, in order to detect a stripe phase, we use a rectangular geometry with a specific aspect ratio that best accommodates the stripe in one direction. In contrast, on the sphere FQH states always appear as non-degenerate, zero angular momentum ground states.

We will mostly present data for the spherical geometry because this allows for a number of simple diagnostic quantities to be evaluated in a straightforward manner. The spherical representation of broken-symmetry states, however, necessarily contains defects, and periodic boundary conditions have to be used in this case. A number of useful insights can be inferred from the study of the energy spectrum; in addition, we will use overlap calculations to compare an exact, many-body ground state Ψ_{exact} , with a numerical representation of a trial wavefunction, Ψ_{trial} . The overlap is defined as a scalar product between two normalized vectors, $\mathcal{O} = |\langle \Psi_{\text{trial}} | \Psi_{\text{exact}} \rangle|$. If \mathcal{O} is consistently close to unity for a number of system sizes considered, we consider the trial wavefunction to be a faithful description of an FQH phase. From the knowledge of a ground-state wavefunction Ψ_0 , we also evaluate the (projected) static structure factor [39]. Sharp peaks in the structure factor indicate the onset of compressible phases [40].

In figure 2 we show the overlap between the $k = 3$ RR wavefunction and the exact ground state of a system in $(\pi, 1)$ and $(\pi, 2)$ LLs, as a function of θ . We set the shift to

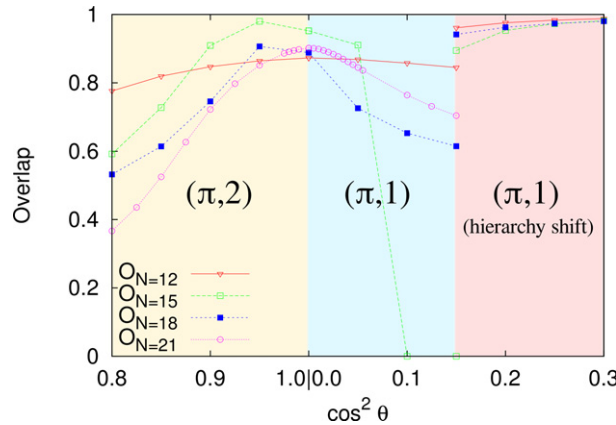


Figure 2. Overlap between the $k = 3$ RR state and the exact ground state in $(\pi, 1)$ and $(\pi, 2)$ LLs as a function of θ , for systems of different sizes N . High overlap is found close to the bare Coulomb interaction in $n = 1$ non-relativistic LL. At $\cos^2 \theta \approx 0.15$, the ground state undergoes a change in shift, and a hierarchy state sets in (right). For $\cos^2 \theta \leq 0.8$ in $(\pi, 2)$ LL, the system undergoes an incompressible–compressible transition to a stripe phase.

–3, corresponding to that of the RR state, and do not consider other candidate states with different values of the shift [38]. The RR model wavefunction can be obtained by diagonalizing a four-body short-range interaction [8], which quickly becomes numerically prohibitive as the number of particles grows, or recursively via Jack polynomials [41]. The filling factor is fixed at $\nu = 3/5$, but in the absence of LL mixing, our results directly apply to $\nu = 2/5$ via particle–hole symmetry. The highest overlap is found for the effective interaction that is in the vicinity of the pure $n = 1$ non-relativistic Coulomb potential. Smaller systems (under $N = 21$ particles) indicate that the RR state might be enhanced for $\cos^2 \theta$ slightly less than 1 in $(\pi, 2)$ LL, which corresponds to a small relative *decrease* of V_1 pseudopotential [8]. However, the largest system one can obtain by exact diagonalization, $N = 21$, suggests that the maximum overlap is practically at the bare Coulomb point. It cannot be determined with certainty whether this is an intrinsic feature of the RR state or a finite-size effect that plagues $N = 21$ system. Finite-size effects are generally very strong at this filling factor and further theoretical studies, possibly employing density-matrix renormalization group techniques, are needed. On either side of the bare Coulomb point, the RR state is quickly destroyed. On the left, for $\cos^2 \theta \leq 0.8$ in $(\pi, 2)$ LL, there is an incompressible–compressible transition to a stripe phase. As mentioned earlier, states with broken translational symmetry are not adequately represented in the spherical geometry; however, we can still detect the stripe by the presence of a sharp peak in the structure factor. One arrives at the same conclusion (but more transparently) in the torus geometry, where it is found that the system develops a manifold of nearly degenerate ground states for $\cos^2 \theta \leq 0.8$ that are characterized by a linear (uni-directional) array of pseudomomenta that defines the preferred direction of a stripe. As we move away from the pure Coulomb point in $(\pi, 1)$ LL, the ground state undergoes a change in shift for $\cos^2 \theta \geq 0.15$ in order to minimize the energy. The new value of the shift is that of a hierarchy state. Therefore, in chiral 2DES, one can, in principle, study a subtle phase transition between two topological phases with Abelian and non-Abelian excitations.

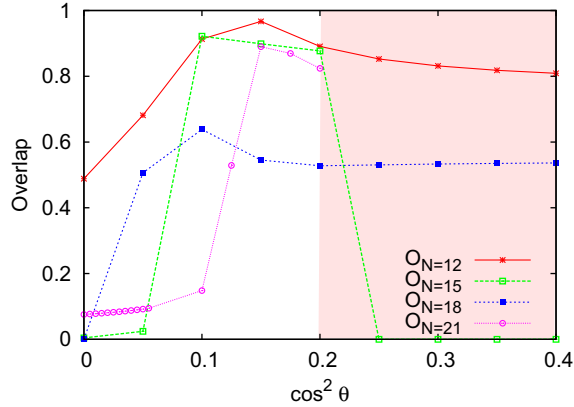


Figure 3. Overlap between the $k = 3$ RR state and the exact ground state in $(2\pi, 1)$ LL as a function of θ , for various system sizes N . The region of high overlap is found in the window between the stripe phase and the hierarchy phase.

An interesting feature, shown in figure 3, is the presence of $k = 3$ RR correlations in a $(2\pi, 1)$ LL. Note that the effective interaction in this case interpolates between pure $n = 0$ and $n = 2$ (non-relativistic) LL Coulomb repulsion; therefore it is quite different from the $n = 1$ LL form factor (figure 2). In this case, the RR state appears in a narrow window, between the stripe phase (for $\cos^2 \theta \leq 0.5$) and the hierarchy state (shaded region in figure 3, for $\cos^2 \theta \geq 0.2$). We note that the $N = 18$ system has a significantly poorer overlap than all the other systems considered, including a larger $N = 21$ system, which leads us to conclude that the poor overlap might be a finite-size effect⁶. More importantly, the excitation gap in the window where the ground state is well described by the RR wavefunction is very small (and also smaller than in $(\pi, 1)$, $(\pi, 2)$ LLs). This, together with the presence of a strong incompressible hierarchy phase, would make it difficult to observe experimentally.

In the remainder of this paper, we investigate the dependence of the excitation gap as we tune the parameters of the system. As mentioned above, the experimental gap at $\nu = 12/5$ in GaAs is tiny. It is therefore essential to find ways of enhancing this gap in order to manipulate the state, e.g. via surface probes. To this end, we consider a generalized model for the material that involves a superposition of $n = 0$, $n = 1$ and $n = 2$ LL non-relativistic form factors [24]:

$$F_n(q) = \cos^2 \theta L_{|n|} \left(\frac{q^2 \ell_B^2}{2} \right) + \sin^2 \theta \cos^2 \phi L_{|n|+1} \left(\frac{q^2 \ell_B^2}{2} \right) + \sin^2 \theta \sin^2 \phi L_{|n|+2} \left(\frac{q^2 \ell_B^2}{2} \right). \quad (4)$$

In figure 4 we plot the charge gap at $\nu = 3/5$ for $N = 18$ particles. The ground state of this particular system has a somewhat poorer overlap with the RR state than other system sizes; however, the charge gap shows no such difference from other cases. Along certain lines, indicated by arrows, the phase diagram reduces to one of the cases studied above. Note that proper finite-size scaling needs to be performed in order to get the correct values for the gap; however, it was previously found for filling factors $\nu = 1/3$ and $\nu = 1/2$ [24, 25] that this rigorous analysis produces values that are roughly in agreement with those shown in figure 4.

⁶ Such effects on the sphere often originate from the aliasing problem, but in this case it is not clear what the competing state is. The aliasing problem on the sphere was introduced by N d'Ambrumenil and R Morf (1989 *Phys. Rev. B* **40** 6108).

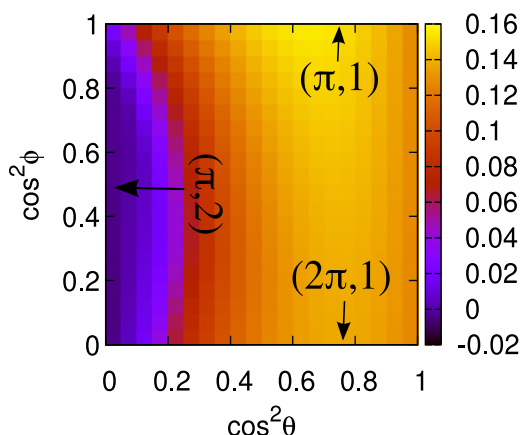


Figure 4. Charge gap (in units of $e^2/\epsilon\ell_B$) at $\nu = 3/5$ for the generalized material described by equation (4). The gap smoothly decreases from the hierarchy phase down to zero (stripe phase). The RR state appears in the transition region. The gaps are calculated for $N = 18$ particles at the shift -3 .

At $\nu = 3/5$ the number of available system sizes is too small to perform such an extrapolation reliably, and the plot in figure 4 should only be viewed qualitatively. We find a smooth transition between the hierarchy state and a stripe, with the gaps gradually dropping to zero for small $\cos^2 \theta$. In the curved, narrow region around the transition, we previously found large overlaps with the RR state [24]. The excitation gaps in the transition region are much smaller than in the hierarchy phase, but they are nonetheless higher than at the pure $n = 1$ non-relativistic LL point ($\cos^2 \theta = 0$, $\cos^2 \phi = 1$). Therefore, tuning the band structure does allow for a modest enhancement of the gap in the RR phase. Qualitatively similar results are obtained for the neutral, instead of charge, gap.

A larger variation of the gap can be achieved in the setup that utilizes the dielectric screening (equation (3)). In figure 5 we show the charge gap as a function of the screening parameter α and the distance of the dielectric plate, d/ℓ_B . Unless α is close to unity, the gap does not vary significantly with d/ℓ_B , which hints at the strong finite-size effects present even in this, fairly large, system of $N = 18$ particles. However, as α becomes close to unity, the gap displays a clear maximum for $d \sim \ell_B$, which is roughly twice as large as that for the bare interaction. The overlap with the RR wavefunction is zero for $\alpha < -0.5$, but fairly large otherwise. Therefore, at least for positive α , the gap can be tuned without reducing the good overlap with the model wavefunction.

4. Conclusion

In this paper we have explored the stability of the $k = 3$ RR state, the prime candidate for topological quantum computation, in the phase diagram as we tune the effective interaction via band structure parameters (that depend on the chirality of the material), or via dielectric screening. Numerical calculations suggest that the RR state is most stable in the vicinity of the bare $n = 1$ non-relativistic LL Coulomb potential, the same one that describes GaAs materials. Nevertheless, the chiral 2DEs offer several advantages over GaAs. Firstly, we find that the RR state can be realized in various (as opposed to a single) LLs, where the interactions have

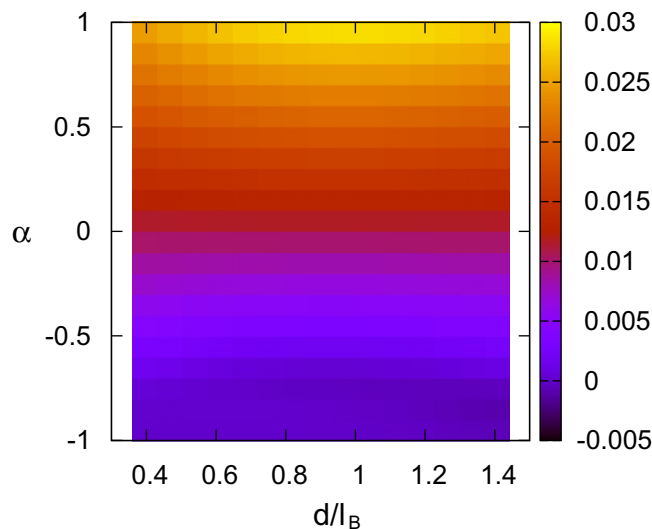


Figure 5. Charge gap (in units of $e^2/\epsilon_1 \ell_B$) at $\nu = 3/5$ as a function of the screening parameter α and the distance of the dielectric, d/ℓ_B . The gap is largest for α close to unity and intermediate $d \sim \ell_B$. For negative α , the gap vanishes and the system is in the stripe phase. Data are shown for $N = 18$ particles on the sphere at the shift -3 .

a different form than that in GaAs. More importantly, the excitation gaps can be enhanced and the nature of the RR state can be further probed by driving *in situ* quantum phase transitions, either to compressible states with stripe ordering or to an incompressible (hierarchy/composite fermion) state.

Acknowledgments

This work was supported by DOE grant number DE-SC0002140. YB was supported by the State of Florida. We acknowledge previous collaboration with R Thomale.

References

- [1] Tsui D C, Stormer H L and Gossard A C 1982 *Phys. Rev. Lett.* **48** 1559
- [2] Laughlin R B 1983 *Phys. Rev. Lett.* **50** 1395
- [3] Moore G and Read N 1991 *Nucl. Phys. B* **360** 362
- [4] Kitaev Yu A 2003 *Ann. Phys.* **303** 2
 Kitaev Yu A 2006 *Ann. Phys.* **321** 2
 Freedman M *et al* 2002 *Commun. Math. Phys.* **227** 605
 Freedman M *et al* 2002 *Commun. Math. Phys.* **228** 177
 Nayak C *et al* 2008 *Rev. Mod. Phys.* **80** 1083
- [5] Prange R E and Girvin S M (ed) 1990 *The Quantum Hall Effect* 2nd edn (New York: Springer)
- [6] Haldane F D M 1983 *Phys. Rev. Lett.* **51** 605
- [7] Jain J K 2007 *Composite Fermions* (Cambridge: Cambridge University Press)
- [8] Read N and Rezayi E 1999 *Phys. Rev. B* **59** 8084
- [9] Levin M, Halperin B I and Rosenow B 2007 *Phys. Rev. Lett.* **99** 236806
 Lee S-S, Ryu S, Nayak C and Fisher M P A 2007 *Phys. Rev. Lett.* **99** 236807

- [10] Willett R *et al* 1987 *Phys. Rev. Lett.* **59** 1776
- [11] Hormozi L, Bonesteel N E and Simon S H 2009 *Phys. Rev. Lett.* **103** 160501
- [12] Xia J S *et al* 2004 *Phys. Rev. Lett.* **93** 176809
- [13] Kumar A, Csathy G A, Manfra M J, Pfeiffer L N and West K W 2010 *Phys. Rev. Lett.* **105** 246808
- [14] Bonderson P and Slingerland J K 2008 *Phys. Rev. B* **78** 125323
Bonderson P, Feiguin A E, Möller G and Slingerland J K 2012 *Phys. Rev. Lett.* **108** 036806
Wojs A 2009 *Phys. Rev. B* **80** 041104
- [15] Rezaei E H and Read N 2009 *Phys. Rev. B* **79** 075306
- [16] Papić Z, Regnault N and Das Sarma S 2009 *Phys. Rev. B* **80** 201303
- [17] Peterson M R, Park K and Das Sarma S 2008 *Phys. Rev. Lett.* **101** 156803
- [18] Morf R H 1998 *Phys. Rev. Lett.* **80** 1505
- [19] Rezaei E H and Haldane F D M 2000 *Phys. Rev. Lett.* **84** 4685
- [20] Zhang F C and Das Sarma S 1986 *Phys. Rev. B* **33** 2903
- [21] Castro Neto A H *et al* 2009 *Rev. Mod. Phys.* **81** 109
- [22] Hasan M Z and Kane C L 2010 *Rev. Mod. Phys.* **82** 3045
- [23] Volkov B A and Pankratov O A 1985 *Pisma Zh. Eksp. Teor. Fiz.* **42** 145
Volkov B A and Pankratov O A 1985 *JETP Lett.* **42** 178
Buttner B *et al* 2011 *Nat. Phys.* **7** 418
- [24] Papić Z, Abanin D A, Barlas Y and Bhatt R N 2011 *Phys. Rev. B* **84** 241306(R)
- [25] Papić Z, Thomale R and Abanin D A 2011 *Phys. Rev. Lett.* **107** 176602
- [26] Koulakov A A, Fogler M M and Shklovskii B I 1996 *Phys. Rev. Lett.* **76** 499
Moessner R and Chalker J T 1996 *Phys. Rev. B* **54** 5006
- [27] Du X *et al* 2009 *Nature* **462** 192
Bolotin K *et al* 2009 *Nature* **462** 196
Dean C R *et al* 2011 *Nature Phys.* **7** 693
- [28] Novoselov K S *et al* 2005 *Nature* **438** 197–200
Zhang Y *et al* 2005 *Nature* **438** 201–4
- [29] Novoselov K *et al* 2006 *Nat. Phys.* **2** 177–80
- [30] Apalkov V M and Chakraborty T 2006 *Phys. Rev. Lett.* **97** 126801
Töke C and Jain J 2007 *Phys. Rev. B* **75** 245440
Papić Z, Goerbig M O and Regnault N 2010 *Phys. Rev. Lett.* **105** 176802
- [31] Bao W *et al* 2011 *Nature Phys.* **7** 948
Taychatanapat T *et al* 2011 *Nature Phys.* **7** 621
Kumar A *et al* 2011 *Phys. Rev. Lett.* **107** 126806
Lui C H *et al* 2011 *Nature Phys.* **7** 944
- [32] Barlas Y, Yang K and MacDonald A H 2011 arXiv:1110.1069
- [33] Nomura K and MacDonald A H 2006 *Phys. Rev. Lett.* **96** 256602
Goerbig M O, Moessner R and Douçot B 2006 *Phys. Rev. B* **74** 161407
- [34] Feldman B E, Martin J and Yacoby A 2009 *Nat. Phys.* **5** 889
- [35] Steven Simon H, Rezaei E H, Cooper N R and Berdnikov I 2007 *Phys. Rev. B* **75** 075317
- [36] Yoshioka D, Halperin B I and Lee P A 1983 *Phys. Rev. Lett.* **50** 1219
- [37] Wen X G and Zee A 1992 *Phys. Rev. Lett.* **69** 953
- [38] Hermanns M 2010 *Phys. Rev. Lett.* **104** 056803
Sreejith G J, Töke C, Wojs A and Jain J K 2011 *Phys. Rev. Lett.* **107** 086806
- [39] He S, Simon S H and Halperin B I 1994 *Phys. Rev. B* **50** 1823
- [40] Rezaei E H, Haldane F D M and Yang K 1999 *Phys. Rev. Lett.* **83** 1219
Haldane F D M, Rezaei E H and Yang K 2000 *Phys. Rev. Lett.* **85** 5396
- [41] Andrei B and Bernevig Haldane F D M 2008 *Phys. Rev. Lett.* **100** 246802

All Databases **Select a Database** Web of Science **Additional Resources**

Search Search History

All Databases

<< Return to Web of Science®

Citing Articles Title: **Band mass anisotropy and the intrinsic metric of fractional quantum Hall systems**
 Author(s): Yang, Bo ; Papic, Z. ; Rezayi, E. H. ; et al.
 Source: PHYSICAL REVIEW B Volume: 85 Issue: 16 Article Number: 165318 DOI: 10.1103/PhysRevB.85.165318 Published: APR 24 2012

This item has been cited by items indexed in the databases listed below. [more information]

8 in All Databases

- 8 publication in Web of Science
- 0 publication in BIOSIS Citation Index
- 0 publication in ScELO Citation Index
- 0 publication in Chinese Science Citation Database
- 0 data sets in Data Citation Index
- 0 publication in Data Citation Index

Results: 8 Page 1 of 1 Go Sort by: Publication Date -- newest to oldest

Create Citation Report

Hide Refine

Refine Results

Search within results for

Search

Databases

Research Domains Refine

SCIENCE TECHNOLOGY

Research Areas Refine

PHYSICS

Document Types

Authors

Group/Corporate Authors

Editors

Funding Agencies

Source Titles

Conference/Meeting Titles

Publication Years

Languages

Countries/Territories

Select Page Add to Marked List (0) Send to: my.endnote.com

1. Title: **Field theory of the quantum Hall nematic transition**
 Author(s): Maciejko, J.; Hsu, B.; Kivelson, S. A.; et al.
 Source: PHYSICAL REVIEW B Volume: 88 Issue: 12 Article Number: 125137 DOI: 10.1103/PhysRevB.88.125137 Published: SEP 27 2013
 Times Cited: 0 (from All Databases)

Get it! Waterloo View abstract

2. Title: **Geometrical description of fractional Chern insulators based on static structure factor calculations**
 Author(s): Dobardzic, E.; Milovanovic, M. V.; Regnault, N.
 Source: PHYSICAL REVIEW B Volume: 88 Issue: 11 Article Number: 115117 DOI: 10.1103/PhysRevB.88.115117 Published: SEP 10 2013
 Times Cited: 0 (from All Databases)

Get it! Waterloo View abstract

3. Title: **Minimal entangled states and modular matrix for fractional quantum Hall effect in topological flat bands**
 Author(s): Zhu, W.; Sheng, D. N.; Haldane, F. D. M.
 Source: PHYSICAL REVIEW B Volume: 88 Issue: 3 Article Number: 035122 DOI: 10.1103/PhysRevB.88.035122 Published: JUL 17 2013
 Times Cited: 1 (from All Databases)

Get it! Waterloo View abstract

4. Title: **Evidence for nu=5/2 fractional quantum Hall nematic state in parallel magnetic fields**
 Author(s): Liu, Yang; Hasdemir, S.; Shayegan, M.; et al.
 Source: PHYSICAL REVIEW B Volume: 88 Issue: 3 Article Number: 035307 DOI: 10.1103/PhysRevB.88.035307 Published: JUL 15 2013
 Times Cited: 0 (from All Databases)

Get it! Waterloo View abstract

5. Title: **Fractional quantum Hall effect in a tilted magnetic field**
 Author(s): Papic, Z.
 Source: PHYSICAL REVIEW B Volume: 87 Issue: 24 Article Number: 245315 DOI: 10.1103/PhysRevB.87.245315 Published: JUN 27 2013
 Times Cited: 2 (from All Databases)

Get it! Waterloo View abstract

6. Title: **Analytic wave functions for neutral bulk excitations in fractional quantum Hall fluids**
 Author(s): Yang, Bo
 Source: PHYSICAL REVIEW B Volume: 87 Issue: 24 Article Number: 245132 DOI: 10.1103/PhysRevB.87.245132 Published: JUN 27 2013
 Times Cited: 0 (from All Databases)

Get it! Waterloo View abstract

7. Title: **Composite Fermions with Tunable Fermi Contour Anisotropy**
 Author(s): Kamburov, D.; Liu, Yang; Shayegan, M.; et al.
 Source: PHYSICAL REVIEW LETTERS Volume: 110 Issue: 20 Article Number: 206801 DOI: 10.1103/PhysRevLett.110.206801 Published: MAY 13 2013
 Times Cited: 2 (from All Databases)

Get it! Waterloo View abstract

8. Title: **Fractional quantum Hall states in two-dimensional electron systems with anisotropic interactions**
 Author(s): Wang, Hao; Narayanan, Rajesh; Wan, Xin; et al.
 Source: PHYSICAL REVIEW B Volume: 86 Issue: 3 Article Number: 035122 DOI: 10.1103/PhysRevB.86.035122 Published: JUL 16 2012
 Times Cited: 4 (from All Databases)

Get it! Waterloo View abstract

Select Page Add to Marked List (0) Send to: my.endnote.com

Results: 8 Show 50 per page Page 1 of 1 Go Sort by: Publication Date -- newest to oldest

8 records matched your query of the 55,067,330 (contains duplicates) in the data limits you selected.

View in: | [简体中文](#) | [繁體中文](#) | [English](#) | [日本語](#) | [한국어](#) | [Português](#) | [Español](#)

© 2013 Thomson Reuters | [Terms of Use](#) | [Privacy Policy](#) | *Please give us your feedback on using Web of Knowledge.*

Band mass anisotropy and the intrinsic metric of fractional quantum Hall systemsBo Yang,¹ Z. Papić,² E. H. Rezayi,³ R. N. Bhatt,² and F. D. M. Haldane¹¹*Department of Physics, Princeton University, Princeton, New Jersey 08544, USA*²*Department of Electrical Engineering, Princeton University, Princeton, New Jersey 08544, USA*³*Department of Physics, California State University, Los Angeles, California 90032, USA*

(Received 13 March 2012; published 24 April 2012)

It was recently pointed out that topological liquid phases arising in the fractional quantum Hall effect (FQHE) are not required to be rotationally invariant, as most variational wave functions proposed to date have been. Instead, they possess a geometric degree of freedom corresponding to a shear deformation that acts like an intrinsic metric. We apply this idea to a system with an anisotropic band mass, as is intrinsically the case in many-valley semiconductors such as AlAs and Si or in isotropic systems like GaAs in the presence of a tilted magnetic field, which breaks the rotational invariance. We perform exact diagonalization calculations with periodic boundary conditions (torus geometry) for various filling fractions in the lowest, first, and second Landau levels. In the lowest Landau level, we demonstrate that FQHE states generally survive the breakdown of rotational invariance by moderate values of the band mass anisotropy. At $1/3$ filling, we generate a variational family of Laughlin wave functions parametrized by the metric degree of freedom. We show that the intrinsic metric of the Laughlin state adjusts as the band mass anisotropy or the dielectric tensor is varied, while the phase remains robust. In the $n = 1$ Landau level, mass anisotropy drives transitions between incompressible liquids and compressible states with charge density wave ordering. In $n \geq 2$ Landau levels, mass anisotropy selects and enhances stripe ordering with compatible wave vectors at partial $1/3$ and $1/2$ fillings.

DOI: [10.1103/PhysRevB.85.165318](https://doi.org/10.1103/PhysRevB.85.165318)

PACS number(s): 73.43.Cd, 73.21.Fg, 71.10.Pm

I. INTRODUCTION

Two-dimensional electron systems (2DES) placed in a high magnetic field exhibit a wide variety of strongly correlated phases, which have been the subject of numerous theoretical and experimental investigations since the first observation of fractionally quantized Hall conductivity.¹ Examples of such phases of matter are the Laughlin states,² describing partial fillings $\nu = 1/3$ and $1/5$ of the lowest ($n = 0$) Landau level (LL) as well as their generalizations to other odd-denominator fillings in the framework of hierarchy³ and composite fermion theory.⁴ These phases are topologically ordered and possess quasiparticle excitations with fractional statistics. At half-filling of the first excited, $n = 1$ LL, an even more exotic paired state, the Moore-Read Pfaffian,⁵ might be realized, which possesses non-Abelian excitations—the Majorana fermions.^{5,6}

Besides the incompressible liquids, some fillings ν also lead to compressible phases without quantized conductance. This is the case with the simplest of all fractions— $\nu = 1/2$ in $n = 0$ LL, which is a Fermi liquid of composite fermions⁷ that only supports an anomalous Hall effect.⁸ Generically for any ν , apart from the incompressible liquids, the natural candidates are compressible phases that break translational symmetry, such as charge density waves (CDWs).⁹ Those were in fact proposed to describe the ground state of 2DES before FQHE was observed.¹⁰ When ν is very small (under $1/7$), a correlated Wigner crystal indeed becomes energetically superior to a Laughlin-type state.^{11,12} Furthermore, when $\nu > 2$, several varieties of states with broken translational symmetry become energetically favorable. Around half-filling of $n \geq 2$ LL, the ground state becomes a charge density wave in one spatial direction or a “stripe”;^{13–16} away from half-filling, two-dimensional crystalline order sets in, resulting in a “bubble” phase.^{13–15,17} Some of these phases also occur in $n < 2$ LLs when the hard-core component of the effective interaction is

significantly softer than Coulomb interaction.¹⁸ More recently, experiments on AlAs (see Ref. 19 for an overview) have suggested interesting physics may arise from the interplay between quantum Hall ordering and spontaneously broken internal symmetries.²⁰ Furthermore, transport experiments on GaAs under tilted field have shown²¹ that it is possible to have, at the same time, the quantization of resistance and anisotropic transport, suggesting a possible coexistence of an incompressible liquid with a compressible (“nematic”) phase.²²

Theoretical understanding of the FQHE was pioneered by Laughlin’s method of many-body trial wave functions.² Model wave functions can be formulated using the conformal field theory⁵ and conveniently evaluated in finite-size systems via exact diagonalization of the parent Hamiltonians.²³ In addition, excitation spectra containing quasiparticles/quasiholes above the ground state can be studied. Such analytical and numerical studies are made much easier by exploiting symmetry and the corresponding quantum numbers to characterize the ground state and excitations. To this end, rotational symmetry has been very useful;²⁴ occasionally, periodic boundary conditions have also been used.^{25,26}

However, as it was recently pointed out,³⁴ rotational symmetry is not fundamental to the appearance of FQHE. In a theoretical treatment of the FQHE, it is important to distinguish several “metrics” that naturally arise in the problem. The band mass tensor yields a metric that defines the shape of the LL orbitals. A second metric derives from the dielectric tensor of the semiconducting material and defines the shape of the equipotential contours around an electron. Rotational invariance means that these two metrics are congruent, however, in a real sample they might be different from one another, thus lifting the rotational invariance.

It turns out, however, that a given FQH state also possesses an intrinsic metric that is derived from the two types

introduced above. FQH fluids can be described as condensates of composite bosons,²⁸ which are topological objects that explain the quantization of the Hall conductance and the emergence of fractionally charged quasiparticles. However, apart from topology, composite bosons also have a geometrical degree of freedom—the intrinsic metric that controls their *shape*. In a rotationally invariant case, the intrinsic metric is equal to the metric in the Hamiltonian; more generally, as we explicitly demonstrate below, the shape of composite bosons can be defined even in systems without rotational invariance. The fluctuation of the intrinsic metric plays an important role for the geometrical field theory of the FQHE²⁷ and determines the energetics of quasiparticles, collective modes, etc. Generalizations of the Laughlin wave function to the broken-rotational-symmetry case have been proposed for liquid crystal and nematic Hall phases,²⁹ and very recently Laughlin and Moore-Read wave functions (as well as their parent Hamiltonians) have been formulated for the anisotropic case.³⁰

The motivation for studying the effect of anisotropy in FQHE is twofold. On the one hand, anisotropy probes the variations of the intrinsic metric of FQH fluids, a fundamental physical quantity that relates to the geometric description of FQHE. Secondly, we explore the possible effects resulting from tuning the rotational-symmetry breaking by an external parameter. Note that the rotational invariance is explicitly broken in real samples due to the presence of impurities, which are essential for the emergence of FQH plateaus. Furthermore, it is possible to induce the breaking of rotational invariance by tilting the magnetic field,³¹ or by using systems with anisotropic bands, e.g., many-valley semiconductors like AlAs or Si in the presence of uniaxial stress. The former method is performed routinely and belongs to the most popular techniques for studying the FQHE; the latter method is relevant to AlAs³² and some new classes of materials where FQHE might be studied. We provide brief arguments how the tilting of the field can be mapped to an effective variation of the metric and then focus on the second method.

This paper is organized as follows. In Sec. II, we introduce and motivate the model for a FQH system with band mass anisotropy. In Sec. III, we discuss the intrinsic metric of the Laughlin state. We define a family of the Laughlin wave functions characterized by the varying shape of their elementary droplets. Intrinsic metric is determined variationally by optimizing the overlap between this family of wave functions and the exact Coulomb ground state. In Sec. IV, we perform exact diagonalization of finite systems at several filling factors to explore quantum phase transitions that occur as a function of the anisotropy. Our conclusions are presented in Sec. V.

II. MODEL

Consider an electron moving in the plane with the perpendicular magnetic field $B\hat{z} = \nabla \times \mathbf{A}(\mathbf{r})$. The Hamiltonian can be written in the following, manifestly covariant form:

$$K^{\alpha,\phi} = \frac{1}{2m} g^{ab} \pi_a \pi_b. \quad (1)$$

Here, $\pi_a = p_a - \frac{e}{c} A_a(\mathbf{r})$, $a = x, y$ represents the dynamical momentum and g is the 2×2 mass tensor parametrized

by the anisotropy α and the angle of the principal axis ϕ . Note that the Hamiltonian is covariant with respect to spatial transformations, but does not couple time and space coordinates. The mass tensor is unimodular $\det g = 1$. In the isotropic case when g is the unit matrix, we can obtain the single-particle energies (Landau levels) by choosing, for example, a symmetric gauge $A_x = By/2, A_y = -Bx/2$. In this case, the dynamical momenta become $\pi_x = -i\hbar \frac{\partial}{\partial x} + \frac{\hbar}{2\ell_B^2} y$ and $\pi_y = -i\hbar \frac{\partial}{\partial y} - \frac{\hbar}{2\ell_B^2} x$, in terms of the magnetic length $\ell_B = \sqrt{\hbar/eB}$. The Hamiltonian can be transformed into diagonal form $K = \frac{\hbar\omega_c}{2} (a^\dagger a + \frac{1}{2})$ with the help of ladder operators $a \propto \pi_x + i\pi_y$ and $a^\dagger \propto \pi_x - i\pi_y$. However, for each value of $a^\dagger a$, there is residual degeneracy equal to the number of the magnetic flux quanta N_ϕ . This degeneracy is resolved by a second pair of operators b, b^\dagger that commute with a, a^\dagger and depend on the *guiding center* coordinates of the electron, $R^a = r^a - \frac{e^{ab}}{\hbar} \pi_b \ell_B^2$. Operators b^\dagger create the (unnormalized) single-particle eigenstates of the lowest LL,

$$\phi_l^{\alpha=1, \phi=0}(z) = z^l e^{-z^* z / 4\ell_B^2}, \quad (2)$$

with $z = x + iy$ being the complex coordinate of an electron in the plane (and z^* denoting its complex conjugate). The quantum number l is an eigenvalue of the angular momentum L_z and the single-particle states ϕ_l are localized on concentric rings around the origin.

To illustrate the effect of mass anisotropy, we take the principal axes of the mass tensor to be along the x and y directions ($\phi = 0$), with different masses along the two directions ($\alpha \neq 1$). Via simple rescaling $x \rightarrow x/\sqrt{\alpha}, y \rightarrow y\sqrt{\alpha}$, and therefore introducing $\tilde{a} \propto \sqrt{\alpha}\pi_x + \frac{i}{\sqrt{\alpha}}\pi_y$ and $\tilde{a}^\dagger \propto \sqrt{\alpha}\pi_x - \frac{i}{\sqrt{\alpha}}\pi_y$, we can immediately write down the single-particle orbitals for this case:

$$\phi_l^\alpha(x, y) = \left(\frac{x}{\sqrt{\alpha}} + iy\sqrt{\alpha} \right)^l e^{-\frac{1}{4\ell_B^2} \left(\frac{x^2}{\alpha} + \alpha y^2 \right)}. \quad (3)$$

Notice that the probability density $|\phi_l|^2$ is no longer localized on a circle, but rather an ellipse for $\alpha \neq 1$. Therefore, on a single-particle level, the effect of mass anisotropy is to stretch or squeeze the one-body orbitals along certain directions, possibly rotating the principal axis (for $\phi \neq 0$).

As we mentioned in Sec. I, certain semiconductor materials are likely to have nontrivial metric defined by the anisotropy. Alternatively, the effective mass tensor can be experimentally tuned by tilting the magnetic field.²¹ Tilting is known to produce complicated effects because it induces the coupling between electronic subbands and LL mixing, and a detailed analysis will be presented elsewhere. To express formally the connection between tilt and mass anisotropy, let us add a parallel field component to the system $B_{||}$ and pick the gauge $\mathbf{A} = (0, B_{\perp}x - B_{||}z, 0)$. The one-body Hamiltonian is then given by

$$H = \frac{1}{2m} \left[p_x^2 + \left(p_y + \frac{e}{c} B_{\perp}x - \frac{e}{c} B_{||}z \right)^2 + p_z^2 \right] + \frac{1}{2} m \omega_0 z^2,$$

where it is assumed that normal confinement (perpendicular to the Hall surface) is given by a harmonic well. This Hamiltonian can be mapped to two harmonic oscillators, with characteristic

oscillator frequencies:³³

$$\omega_{1,2}^2 = \frac{1}{2}[(\omega_z^2 + \omega_c^2) \pm (\omega_z^2 - \omega_c^2) \sec(2\bar{\theta})], \quad (4)$$

where $\omega_z = \sqrt{\omega_0^2 + \omega_{\parallel}^2}$ is the harmonic frequency of the normal confinement and $\omega_{\parallel} = eB_{\parallel}/m$. The mixing of the cyclotron frequency and the confinement frequency is parametrized by $\tan 2\bar{\theta} = 2\omega_c\omega_{\parallel}/(\omega_c^2 - \omega_z^2)$. Defining $\ell_0 = \sqrt{1/eB_{\perp}}$ and $\ell_i = 1/\sqrt{m\omega_i}$, $i = 1, 2$, the eigenstates of the Hamiltonian are given by

$$\begin{aligned} \psi_{n_1, n_2}(\mathbf{r}) \propto e^{iky} \psi_{n_1}^{(1)}[\cos \bar{\theta}(x + \ell_0^2 k) - \sin \bar{\theta} z] \\ \times \psi_{n_2}^{(2)}[\sin \bar{\theta}(x + \ell_0^2 k) + \cos \bar{\theta} z], \end{aligned} \quad (5)$$

where $\psi_{n_i}^i$ is the usual harmonic oscillator wave function for level n_i . If we focus on the ground state ($n_1 = n_2 = 0$) and define $\lambda_{i=1,2} = \omega_i/\omega_c$, we can express its in-plane wave function as

$$\psi_{00}^{x-y}(\mathbf{r}) \propto e^{iky} \exp\left[-\frac{1}{2\ell_0^2} \alpha_1 (x + \ell_0^2 k^2)^2\right],$$

where

$$\alpha_1 = \frac{\lambda_1 \lambda_2}{\lambda_1 \sin^2 \bar{\theta} + \lambda_2 \cos^2 \bar{\theta}}.$$

Therefore the metric can be immediately read off as

$$g = \begin{pmatrix} 1/\alpha_1 & 0 \\ 0 & \alpha_1 \end{pmatrix}.$$

More generally, parametrizing the in-plane magnetic field by $\mathbf{B}_{\parallel} = (B_{\parallel} \cos \phi, B_{\parallel} \sin \phi)$, the effective metric associated with the tilt can be shown to be given by

$$g = \begin{pmatrix} \cosh 2\theta + \sinh 2\theta \cos 2\phi & \sinh 2\theta \sin 2\phi \\ \sinh 2\theta \sin 2\phi & \cosh 2\theta - \sinh 2\theta \cos 2\phi \end{pmatrix}, \quad (6)$$

where $\cosh 2\theta = \frac{1}{2}(\alpha + \frac{1}{\alpha})$. Therefore the effect of tilting on the LLL single-particle levels can be captured by the variation of the mass tensor.

In order to study a finite, interacting system of N_e electrons, it is convenient to choose a compact surface to represent the 2DES. As we emphasized in Sec. I, the presence of mass anisotropy destroys rotational invariance, and one must use periodic boundary conditions,^{25,26} i.e., put the 2DES on the surface of a torus. The unit cell can generally be chosen as a parallelogram with sides \mathbf{a} and \mathbf{b} whose area \mathcal{S} is quantized because of the magnetic translations algebra: $\mathcal{S} \equiv |\mathbf{a} \times \mathbf{b}| = 2\pi \ell_B^2 N_{\phi}$. The single-particle states compatible with periodic boundary conditions are given in the Landau gauge by

$$\begin{aligned} \phi_{j,n}^{\alpha}(\mathbf{r}) = \frac{1}{\sqrt{\mathcal{N}}} \sum_k e^{i(X_j + ka)y - \frac{1}{2\alpha}(X_j + ka + x)^2} \\ \times H_n\left(\frac{X_j + ka + x}{\sqrt{\alpha}}\right), \end{aligned} \quad (7)$$

where $j = 0, \dots, N_{\phi} - 1$, $X_j \equiv 2\pi j/b$, normalization factor is $\mathcal{N} = b\sqrt{\pi}\sqrt{\alpha}2^n n!$, and the sum over k extends over all integers. We have set $\ell_B = 1$. The wave function for the n th LL involves a Hermite polynomial H_n . For simplicity, we assumed the case of a rectangular torus and $g = \text{diag}[\alpha, 1/\alpha]$,

but Eq. (7) can be generalized to an arbitrary shape/anisotropy using Jacobi theta functions.

Many-body states, like in the isotropic case, can be classified using a crystal quasimomentum \mathbf{K} defined in a Brillouin zone.²⁶ With a suitable definition of the Brillouin zone, incompressible states always occur at $\mathbf{K} = 0$, and are characterized by the gap in their excitation spectrum. The Hamiltonian for N_e electrons is given by the sum of the kinetic term and the Coulomb interaction,

$$H^{\alpha,\phi} = \sum_i K_i^{\alpha,\phi} + \sum_{i<j} \frac{1}{|\mathbf{r}_i - \mathbf{r}_j|_{\epsilon}}. \quad (8)$$

Note the explicit appearance of two distinct metrics in the above equation. As discussed above, one of these metrics parametrizes the shape of the cyclotron orbits (α, ϕ). However, because 2DES is embedded in a three-dimensional dielectric host material, which is characterized by its own dielectric tensor ϵ , there is a second metric that defines the shape of equipotential lines around an electron, denoted by $|\mathbf{r}_i - \mathbf{r}_j|_{\epsilon}$. These two metrics are physically distinct, however, the properties of the system are determined only by the relative difference between the mass and the dielectric tensors, and for simplicity, we can set the latter to unity. In other words, we assume that Coulomb interaction is isotropic in space, hence its Fourier transform is $V(\mathbf{q}) = 1/q \equiv 1/\sqrt{q_x^2 + q_y^2}$ [to model finite-width effects, we use the softened form of $V(\mathbf{q})$, following the Fang-Howard prescription]. Projected to a single n th LL, the interaction part of the Hamiltonian becomes $H = \sum_{\{j_i\}} V_{j_1 j_2 j_3 j_4} c_{j_1}^{\dagger} c_{j_2}^{\dagger} c_{j_3} c_{j_4}$, where

$$\begin{aligned} V_{j_1 j_2 j_3 j_4} = \frac{1}{2\mathcal{S}} \sum_{\mathbf{q}} V(\mathbf{q}) \mathcal{L}_n\left(\frac{1}{2}q_g^2\right) \\ \times e^{-\frac{1}{2}q_g^2} e^{iq_x(X_{j_1} - X_{j_3})} \delta'_{l, j_1 - j_4} \delta'_{j_1 + j_2, j_3 + j_4}, \end{aligned} \quad (9)$$

where $q_g^2 \equiv g^{ab} q_a q_b$ (e.g., in case of a diagonal mass tensor, $q_g^2 = \alpha q_x^2 + q_y^2/\alpha$) and \mathcal{L}_n is the Laguerre polynomial. The primed δ functions are to be taken (mod N_{ϕ}), and the sum over \mathbf{q} extends over the reciprocal space (the prime on the sum indicates that the diverging $\mathbf{q} = 0$ term is canceled by the positive background charge).

Apart from the many-body translational symmetry, discrete symmetries can be used to further reduce the Hilbert space. Several types of Bravais lattices are possible, depending on the angle θ between the sides of the torus, \mathbf{a} and \mathbf{b} , and the aspect ratio, $|\mathbf{a}|/|\mathbf{b}|$. Both of these can be tuned as free parameters. In the presence of anisotropy, however, the highest symmetry is only given by the rectangular lattice, even when $|\mathbf{a}| = |\mathbf{b}|$. Tuning the angle θ enables to perform the area-preserving deformations of the torus, which is useful in resolving the collective modes of FQH states in finite systems, and probing quantities such as Hall viscosity.³⁴

In this paper, we only consider spin-polarized electrons and neglect the so-called multicomponent degrees of freedom, which can be the usual spin or bilayer/valley degree of freedom. This means that the filling factors we refer to as $n + \nu$ correspond to $kn + \nu$ in experiments, where integer k denotes the additional degeneracy that comes from several ‘‘flavors’’ of electrons.

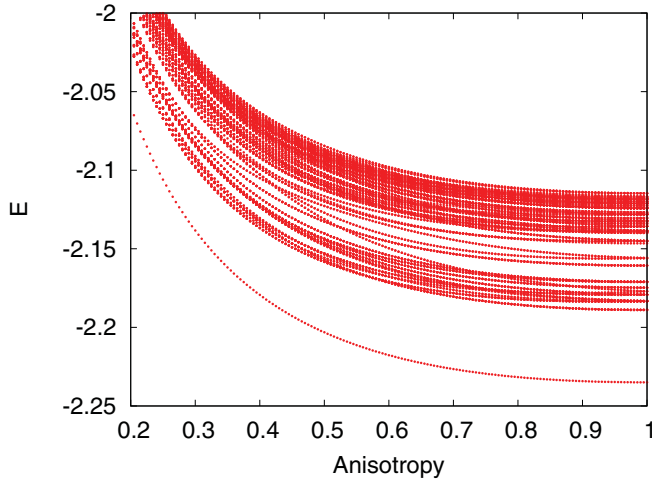


FIG. 1. (Color online) Energy spectrum in units of $e^2/\epsilon\ell_B$ as a function of anisotropy α for the square unit cell and $n = 0$ LL Coulomb interaction at $\nu = 1/3$. The system is $N_e = 7$ electrons and $\phi = 0$. Due to the square unit cell, the spectrum is symmetric under $\alpha \rightarrow 1/\alpha$.

III. ANISOTROPY IN THE LOWEST LANDAU LEVEL: ROBUSTNESS AND THE INTRINSIC METRIC OF THE LAUGHLIN STATE

In Fig. 1, we present the energy spectrum of the Coulomb interaction at $\nu = 1/3$ as a function of anisotropy (we assume $\phi = 0$). The system is placed on the torus with a square unit cell, and energies are expressed in units of $e^2/\epsilon\ell_B$. A very flat minimum around isotropy point and the existence of a robust gap suggest that the ground state of the Coulomb interaction at $\nu = 1/3$ is remarkably stable to variation in anisotropy. As we show below, in this range of α , the ground state is described by a generalized Laughlin wave function. Moreover, the set of lowest neutral excitations, forming a magnetoroton branch, are also stable and separated from the rest of the spectrum. Within this manifold, some level crossings occur as α is changed, but this only corresponds to the redistribution of the levels within a roton branch. Beyond $\alpha \approx 0.5$, the ground-state energy rises, indicating an instability and the eventual destruction of the Laughlin phase.

In rotationally-invariant situations, the incompressible liquids at fillings $\nu = 1/m$ of $n = 0$ LL (m being an odd integer) are described by the Laughlin wave function.² In the geometry of an infinite plane, the Laughlin state is given by

$$\Psi_L^{\nu=1/m} = \prod_{i<j} (z_i - z_j)^m e^{-\sum_k z_k^* z_k / 4\ell_B^2}. \quad (10)$$

Here, $z = x + iy$ stands for the usual complex representation of the coordinates in the plane and can also be expressed in terms of spinor coordinates providing a mapping to the spherical geometry.²⁴ However, the Laughlin state can also be extended to the torus geometry,³⁵ where the continuous rotation symmetry is broken down and survives at most in form of a discrete subgroup. In this case, $\Psi_L^{\nu=1/m}$ is defined by its short-distance correlations that assume the form of the (odd) Jacobi ϑ_1 theta function of $z_i - z_j$.³⁵

As a trial wave function, $\Psi_L^{\nu=1/3}$ provides an excellent description of the physical system at $\nu = 1/3$ in the limit of strong cyclotron energy with respect to the Coulomb repulsion in the 2DES plane, $\hbar\omega_c \gg e^2/\epsilon\ell_B$, when excitations to higher LLs are prohibited. In this limit, the operators a, \tilde{a} act trivially and the only dynamical degrees of freedom are the (noncommuting) guiding centers. Up to the normalization, we can then view the wave function (10) as follows:

$$\Psi_L^{\nu=1/m}(g) \propto \prod_{i<j} [b_i^\dagger(g) - b_j^\dagger(g)]^m |0\rangle, \quad (11)$$

where $b_i^\dagger(g)$ explicitly depend on the metric g .³⁴ For general g , $b_i^\dagger(g)$ is obtained by a Bogoliubov transformation from the b_i, b_i^\dagger in the rotationally invariant case. Equivalently, the wave function can be expressed by a unitary transformation $\Psi_L(g) = \exp(-i\xi_{\alpha\beta}\Lambda^{\alpha\beta})\Psi_L(0)$, where $\xi_{\alpha\beta}$ is a real symmetric tensor and $\Lambda^{\alpha\beta} = \frac{1}{4}\sum_i \{R_i^a, R_i^b\}$ is the generator of area-preserving diffeomorphisms.³⁴ The expression for the transformation matrix and the first-quantized expression for the wave function in Eq. (11) is given in Ref. 30.

The freedom in choosing g implies that the usual rotationally symmetric Laughlin wave function is a representative of a class of wave functions. However, being a topological phase, the physics of the Laughlin state does not depend on any given metric or length scales. Various wave functions $\Psi_L^{\nu=1/m}(g)$ differ from one another microscopically in terms of the shapes of their elementary droplets. For a FQH state at filling $\nu = p/q$ (p, q are not necessarily co-prime), an elementary droplet is a unit of fluid containing p particles in an area that encloses q flux quanta. The incompressible state is a condensate of such elementary droplets. For example, at $\nu = 1/3$, we have a single particle occupying each three consecutive orbitals and preventing more particles from populating this region. In the language of root partitions and the Jack polynomials,³⁶ the Laughlin $\nu = 1/3$ state is defined by a root pattern 100100100100..., and therefore its elementary droplet is 100. Note that these simple patterns only serve as labels for correlated wave functions that cannot be thought of as a simple crystal of electrons pinned at each third orbital and repelling each other via electrostatic forces.

For a model wave function, the ‘‘gauge’’ freedom in b, b^\dagger implies that the shape of elementary droplets changes with varying g , but the basic physical properties remain invariant unless the anisotropy magnitude α becomes too large or too small. If α is such that the maximum effective separation between electrons along some direction is of the order of ℓ_B or smaller, the FQH liquid correlations are expected to break down and CDW states might be favored (we will present some examples of this in Sec. IV). On the other hand, a generic state involves a competition of two different metrics—the cyclotron g_m and the Coulomb g_C metrics—therefore it is best approximated by the Laughlin state with an intrinsic metric g that is generally different from both g_m and g_C . Intrinsic metric g is the one that minimizes the variational energy E_g ,

$$E_g = \frac{\langle \Psi_L(g) | H(g_m, g_C) | \Psi_L(g) \rangle}{\langle \Psi_L(g) | \Psi_L(g) \rangle}. \quad (12)$$

To find the intrinsic metric in the microscopic calculation, we use a slightly different criterion that g should maximize the overlap with the exact ground state of $H(g_m, g_C)$. In the rotationally invariant case, the ground state of the Coulomb interaction at $\nu = 1/3$ is known to have a remarkably high overlap with the Laughlin wave function. The overlap is defined as a scalar product between two normalized vectors, and in this particular case it is typically greater than 97%. Therefore we expect the intrinsic metric chosen to maximize the overlap also to minimize the correlation energy (12). To obtain the anisotropic Laughlin states, we perform exact diagonalization of the “ V_1 Hamiltonian” on the torus. This Hamiltonian gives $\Psi_L^{\nu=1/3}$ as a unique and densest zero-energy ground state.²³ Note that any translationally invariant interaction can be expanded in terms of the Laguerre polynomials, $V(\mathbf{q}) = \sum_m V_m \mathcal{L}_m(\mathbf{q}^2)$, where the coefficients V_m are the Haldane pseudopotentials.²³ Truncating this expansion at the first term, $V_1 \mathcal{L}_1(\mathbf{q}^2)$, singles out the strongest (“hard-core”) component, which defines the Laughlin state at filling $\nu = 1/3$. As the pseudopotential Hamiltonian is just a projection operator in the relative angular momentum space, the metric in $V_1 \mathcal{L}_1(\mathbf{q}^2)$ is the same as that originating from the cyclotron orbits.

In Fig. 2, we pick the ground state of the Coulomb interaction with fixed mass anisotropy $\alpha_0 = 2, \phi_0 = 0$ (the metric of the dielectric tensor is implicitly assumed to be $\alpha = 1, \phi = 0$), and we evaluate the overlap with a family of Laughlin states generated by varying α, ϕ . The overlap $|\langle \Psi_L^{\alpha, \phi} | \Psi_C^{\alpha_0=2, \phi_0=0} \rangle|$ is plotted as a function of α and ϕ . We observe that the principal axis of the Laughlin state is aligned with that of the Coulomb state (maximum overlap occurs for $\phi = \phi_0 = 0$). Interestingly, the maximum overlap does *not* occur for $\alpha = \alpha_0$, but for some value of the anisotropy that is a “compromise” between the dielectric $\alpha = 1$ and a cyclotron one $\alpha = 2$. The value of the anisotropy that defines the intrinsic metric depends linearly on the band mass anisotropy (see Fig. 3). This result illustrates the ability of the Laughlin state to optimize the shape of its fundamental droplets and maximize

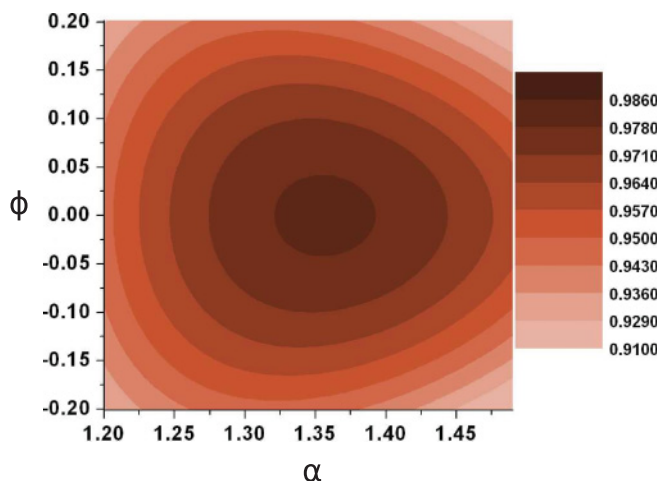


FIG. 2. (Color online) Overlap between the Coulomb ground state at $\nu = 1/3$ for fixed anisotropy $\alpha_0 = 2, \phi_0 = 0$, and the family of Laughlin states parametrized by varying α, ϕ . The system is $N_e = 9$ electrons on a hexagonal torus.

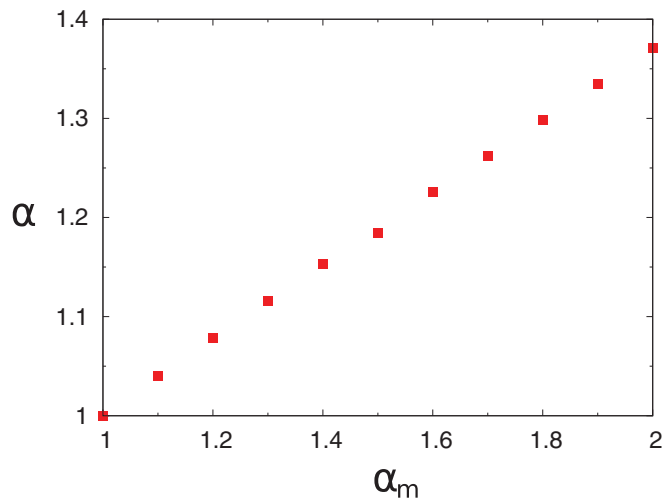


FIG. 3. (Color online) Dependence of the intrinsic metric α on the mass metric α_m (Coulomb metric is set to identity).

the overlap with a given anisotropic ground state of a finite system.

An alternative way to obtain the intrinsic metric is to analyze the shape of the lowest excitation, the magnetoroton mode, which was successfully described by the single-mode approximation.³⁷ In a rotationally invariant case, this mode has a minimum at $k \sim \ell_B^{-1}$. In the presence of anisotropy, the minimum occurs at different $|k|$ in the different directions (see Fig. 4). This leads to an alternative definition of the intrinsic metric based on the shape of the roton minimum in the 2D momentum plane. We numerically establish that this definition agrees well with our previous definition of the intrinsic metric. In Fig. 4, we plot the energy spectrum of an anisotropic Coulomb interaction at $\nu = 1/3$ as a function of the rescaled momentum $\sqrt{g^{ab} k_a k_b}$, where g is the guiding center metric that maximizes the overlap with the family of Laughlin wave functions (see Fig. 3). With the usual definition

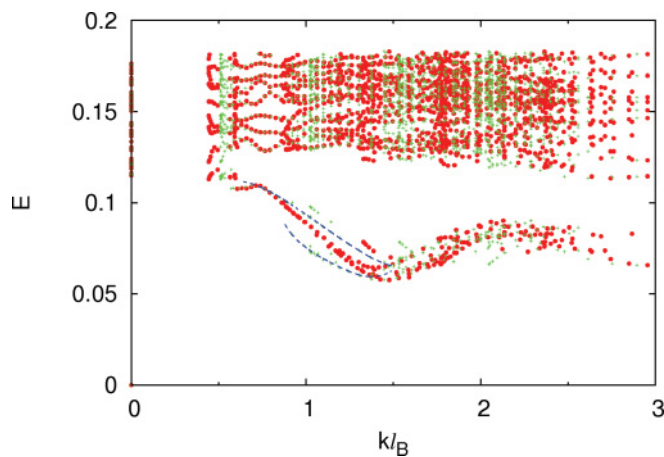


FIG. 4. (Color online) Energy spectrum of $N_e = 9$ electrons at $\nu = 1/3$ with the effective mass anisotropy $\alpha_m = 2$ along the x axis. When plotted as a function of $\sqrt{k_x^2 + k_y^2}$ (green crosses), two branches of the magnetoroton mode are present (blue dotted lines are guide to the eye). If the spectrum is plotted as a function of $\sqrt{g^{ab} k_a k_b}$, the two branches collapse onto the same curve.

of the momentum $|k|$, several roton minima appear. Different magnetoroton branches collapse onto the same curve if we plot them as a function of $\sqrt{g^{ab}k_a k_b}$. This is reasonable, because the magnetoroton mode is well approximated by single-mode approximation up to the roton minimum,³⁸ which is defined entirely in terms of the properties of the ground state. The anisotropy of the ground state structure factor (determined by the shape of elementary droplets) dictates the position of the roton minimum.

The analysis of this section, in principle, applies to other LLL states at fillings $\nu = p/(2p + 1), p = 2, 3, \dots$, though it is more involved because of the “multicomponent nature” of these states and typically a smaller excitation gap.

IV. HIGHER LANDAU LEVELS: QUANTUM PHASE TRANSITIONS DRIVEN BY ANISOTROPY

We have found that $\nu = 1/3$ in the LLL is particularly robust with respect to anisotropy, and this is the case also with other prominent FQH states. In higher LLs, due to a number of nodes in the single-particle wave function, the region of the phase diagram where incompressible states occur becomes increasingly narrower, and compressible phases such as stripes and bubbles take over. In this section, we discuss the effects of anisotropy on FQH states in higher LLs, focusing on fillings $\nu = 1/3$ and $1/2$. Because of closer energy scales, we find that moderate changes in the anisotropy induce phase transitions between compressible and incompressible phases.

A. $n \geq 2$ Landau levels: stripes and bubbles

In $n = 2$ LL and higher, isotropic FQH states are energetically less favorable than stripe and bubble phases at filling $\nu = n + 1/2$ and $\nu = n + 1/3$, respectively. In Fig. 5, we show the energy spectrum (in units of $e^2/\epsilon\ell_B$) as a function of anisotropy α (we set the angle ϕ to zero). Energies are plotted relative to the ground state at each α , and we chose the relatively modest system sizes ($N_e = 8$ and 10 electrons) to facilitate comparison with the existing isotropic data in the

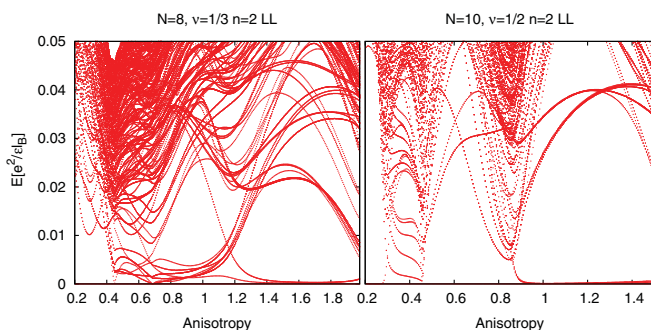


FIG. 5. (Color online) Energy spectrum of $\nu = 1/3$ (left) and $\nu = 1/2$ filled $n = 2$ LL (right): mass anisotropy establishes and reinforces the stripe order. At $\nu = 1/3$, a large set of quasidegenerate levels around $\alpha = 1$ belongs to the bubble phase;¹⁷ for $\alpha > 1.2$, a smaller subset of these levels, together with some excited levels, form another quasidegenerate multiplet that belongs to a stripe phase. At $\nu = 1/2$, the ground state is a stripe already for $\alpha = 1$,¹⁶ and its gap and splitting within the multiplet change as α is increased.

literature.^{16,17} The aspect ratio is set to the optimal values for the appearance of stripes or bubbles (see Refs. 16 and 17).

As we see on the right panel of Fig. 5, at $\nu = 1/2$, the presence of mass anisotropy reinforces the stripe when α is increased. This leads to a more pronounced quasidegeneracy of the ground-state multiplet and an increase of the gap between this multiplet and the excited states. For yet larger values of α , it appears that some of these excited states may become the ground state, however, this occurs for very large α when this finite system effectively becomes one-dimensional under anisotropy deformations.

In case of $\nu = 2 + 1/3$ state, it has been argued that the isotropy point is described by a two-dimensional CDW order known as the bubble phase.¹⁷ A bubble differs from a stripe in having a larger degeneracy and a two-dimensional mesh of (quasi)degenerate ground-state wave vectors (as opposed to the one-dimensional array in case of a stripe). The spread of the quasidegenerate levels was also found to be somewhat larger than in case of stripes. All of these features are obvious in Fig. 5 (left) for $\alpha = 1$. The bubble phase remains stable to some extent when α is reduced; for very small α , it is eventually destroyed and replaced by a simple CDW. On the other hand, when α is increased, a smaller subset of momenta becomes very closely degenerate with some of the excited levels. This second-order (or weakly first order) transition results in a stripe phase. As for the $\nu = 1/2$ case, this stripe becomes enhanced as α is further increased. Therefore, in $n \geq 2$ LLs mass anisotropy generally produces stripes, even when isotropic ground states have a tendency to forming a bubble phase.

B. $n = 1$ Landau level: incompressible to compressible transitions driven by anisotropy

In $n = 1$ LL, $\nu = 1/3$ state is significantly weaker than its $n = 0$ LL counterpart, having an experimental gap an order of magnitude smaller and roughly the same as the gap of $\nu = 1/2$ state. This has been anticipated in early numerical calculations that found the ground state of the Coulomb interaction projected to $n = 1$ LL to be at the transition point between compressible and incompressible phases.²³

Although idealized numerical calculations with pure (projected) Coulomb interaction work exceedingly well in $n = 0$ LL, more realistic models are required to describe phases in $n = 1$ LL. In particular, the inclusion of finite-width effects⁴³ and varying a few strongest Haldane pseudopotentials is necessary to determine the phase diagram. We find that varying the V_1 pseudopotential leads to the following outcomes: (i) generically, for $\delta V_1 < 0$, the system is pushed deeper into a compressible phase, and (ii) for $\delta V_1 > 0$, finite-size calculations on systems up to $N_e = 9$ electrons permit the existence of two regimes: for $0 < \delta V_1^a < \delta V_1^b$, the ground state is in the Laughlin universality class, but the lowest excitation is not the magnetoroton, and for $\delta V_1 > \delta V_1^b$, the ground state and the excitation spectrum is the same as in $n = 0$ LL. For smaller systems, δV_1^b is estimated to be around $0.1e^2/\epsilon\ell_B$, while δV_1^a is around $0.04e^2/\epsilon\ell_B$. Larger systems suggest that these two points might merge in the thermodynamic limit, when only a small modification of the interaction might be needed for the Laughlin physics to

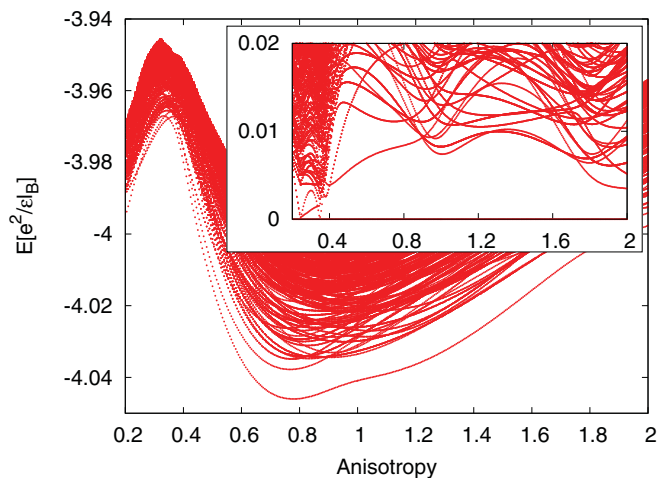


FIG. 6. (Color online) Spectrum of $N_e = 8$ electrons at $\nu = 1 + 1/3$ with thickness $w = 2\ell_B$. Inset: same spectrum plotted relative to the ground state at each α . Unit cell has a rectangular shape with aspect ratio $3/4$.

appear at $\nu = 1/3$ in $n = 1$ LL. Alternatively, we can consider the Fang-Howard ansatz that mimicks the finite-width effects. In this case, the width of ℓ_B or smaller is sufficient to drive a phase transition between the compressible state and the Laughlin-like state, in agreement with results on the sphere and using an alternative finite-width ansatz.³⁹

In summary, the ground state at $\nu = 1 + 1/3$ very likely belongs to the Laughlin universality class. We note that the collective mode in this case displays significantly more wiggles than in the LLL (some wiggles exist in case of $n = 0$ LL Coulomb state, but they are less pronounced). For large momenta, the magnetoroton mode also appears to merge with the continuum of quasiparticle-quasihole excitations. This is likely a finite-size artefact, although we cannot rule out that it represents an intrinsic feature of $\nu = 1 + 1/3$ state, in which case, it might have an observable signature in optical experiments that distinguishes it from the $\nu = 1/3$ state.

Because of the fragility of $\nu = 1 + 1/3$ state, we expect that mass anisotropy might have more dramatic consequences than in the LLL. In Fig. 6, we plot the energy spectrum as a function of anisotropy. One notices that the isotropy point ($\alpha = 1$) does not bear any special importance; indeed, the system appears more stable in the vicinity of it where it can lower its ground-state energy or increase the neutral gap. On either side of the isotropy point, however, the system remains in the Laughlin universality class; e.g., at $\alpha = 0.8$ and 1.3 , the maximum overlap with the Laughlin state is 75% and 80%, respectively (these overlaps, although modest compared to the standards of $n = 0$ LL, can be adiabatically further increased by tuning the V_1 pseudopotential). Note that the quoted maximum overlaps are achieved by the Laughlin state with α' somewhat different from α of the Coulomb state, analogous to Fig. 2.

The new aspect of Fig. 6 is the transition to a compressible state with CDW ordering for $\alpha \lesssim 0.4$. In that region of parameter space, the system is very sensitive to changes in the boundary condition—the sharp degeneracies seen in rectangular geometry in Fig. 6 are not obvious in case of higher

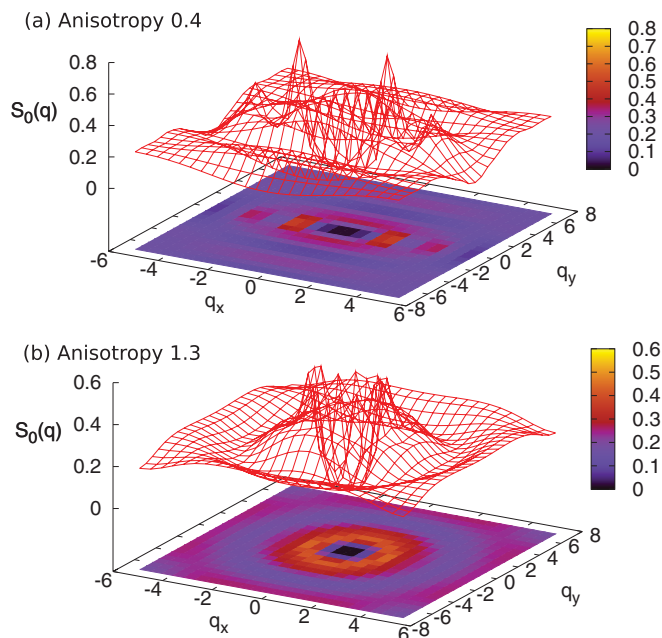


FIG. 7. (Color online) Guiding-center structure factor $S_0(\mathbf{q})$ for $\nu = 1/3$ state in $n = 1$ LL with thickness $w = 2\ell_B$ and anisotropy $\alpha = 0.4$ (a). For comparison, we also show $S_0(\mathbf{q})$ for the state with $\alpha = 1.3$ which is in the Laughlin universality class (b). Two peaks in the response function (a) represent the onset of compressibility and CDW ordering.

symmetry, square or hexagonal, unit cell. As an additional diagnostic tool for the compressible states, it is useful to consider a guiding-center structure factor,

$$S_0(\mathbf{q}) = \frac{1}{N_\phi} \sum_{i,j} \langle e^{i\mathbf{q}\cdot\mathbf{R}_i} e^{-i\mathbf{q}\cdot\mathbf{R}_j} \rangle - \langle e^{i\mathbf{q}\cdot\mathbf{R}_i} \rangle \langle e^{-i\mathbf{q}\cdot\mathbf{R}_j} \rangle, \quad (13)$$

where the expression for the Fourier components of the guiding-center density, $\rho(\mathbf{q}) = \sum_i e^{i\mathbf{q}\cdot\mathbf{R}_i}$, has been used. Note that $S_0(\mathbf{q})$ is normalized per flux quantum rather than (conventional) per particle.³⁴ In Fig. 7(a), we show the plot of $S_0(\mathbf{q})$ evaluated for the state with $\alpha = 0.4$ in Fig. 6. Two sharp peaks in the response, similar to those previously identified in $n \geq 2$ LL states,¹⁶ are the hallmark of CDW order. They are to be contrasted with the smooth response in case of an anisotropic state in the Laughlin universality class for $\alpha = 1.3$, Fig. 7(b).

As a second example in $n = 1$ LL, we consider half-filling where the Moore-Read Pfaffian state⁵ is believed to be realized in some regions of the phase diagram. This state has a non-Abelian nature, which is reflected in the nontrivial ground-state degeneracy⁶ when subjected to periodic boundary conditions. For $\nu = 1/2$, the eigenstates of any translationally invariant interaction possess a twofold center-of-mass degeneracy.²⁶ On top of this, Moore-Read state has an additional threefold degeneracy. Conventionally, the many-body Brillouin zone is defined for $p = 1$, $q = 2$ and has a size N^2 (N being the GCD of N_e and N_ϕ), which forces the degenerate ground states to belong to a Brillouin zone corner $\mathbf{K} = (N/2, N/2)$ and centers of the sides, $\mathbf{K} = (0, N/2); (N/2, 0)$. It is also possible to define a “quartered” Brillouin zone such that the three degenerate states are all mapped to zero momentum.⁴⁰

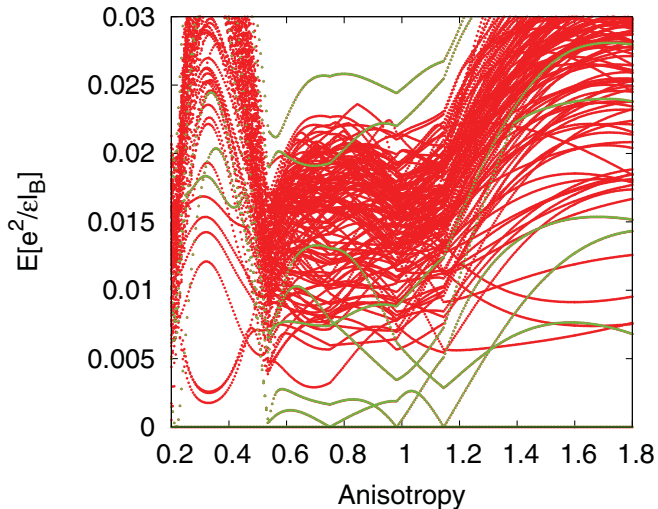


FIG. 8. (Color online) Spectrum of $N_e = 14$ electrons at $\nu = 1 + 1/2$ with thickness $w = 2l_B$ as a function of anisotropy α . Energies are plotted relative to the ground state at each α , and the unit cell has a rectangular shape with aspect ratio $3/4$.

The three \mathbf{K} sectors are equivalent for a hexagonal unit cell, however, in an anisotropic system, the degeneracy is always lifted.

In Fig. 8, we plot the spectrum of the Coulomb interaction as a function of anisotropy (states belonging to \mathbf{K} sectors where the Moore-Read state is realized, are indicated). As earlier, we assume finite width of $w = 2l_B$ in order to instate the Pfaffian correlations.¹⁸ Note that our calculation only uses two-body (Coulomb) interaction, therefore in each finite system, the Moore-Read state will mix with its particle-hole conjugate pair, the anti-Pfaffian.⁴¹ The mixing between the two states can be controlled by including higher LLs.⁴² For $0.5 \leq \alpha \leq 1.3$, we find a threefold quasidegenerate multiplet, suggesting the presence of Moore-Read state at the isotropy point and in the neighborhood of it. In finite systems, there is some splitting of the degeneracy that might be reduced upon tuning the V_1 and V_3 pseudopotentials. Also, upon tuning the anisotropy around $\alpha = 1$, there are crossings within the multiplet of degenerate ground states without apparent closing of the gap. The region of the Moore-Read state is defined by sharp transitions toward crystal phases. These transitions are likely second order because they do not appear to involve any

level crossing, but rather lifting of the degeneracy within a ground-state multiplet.

V. CONCLUSION

We have presented a method to study the effects of anisotropy on FQH phases in finite-size systems. We found that the prominent FQH states (as in the lowest Landau level) are robust to variations of anisotropy due to the adjustment of the intrinsic metric describing the shape of their elementary droplets. As we demonstrated using the example of the Laughlin $\nu = 1/3$ state, this metric is usually a compromise between the metric dictated by the cyclotron motion and the metric originating in the dielectric environment of the 2DES. In this sense, it is unlike the noninteracting Landau level problem, or the problem of weak localization,⁴⁴ where the anisotropy can be completely “gauged away” (i.e., removed) by length rescaling. Instead, it is more akin to the problem of shallow donors in many-valley semiconductors.⁴⁵ Indeed, such compromise picture leads to a quantitatively accurate description of the variation of the critical density of the metal-insulator transition (an intrinsically many-body phenomenon) in three-dimensional doped many-valley semiconductors,⁴⁶ so one may wish to ascertain to what extent this can lead to quantitative predictions in the FQHE case. In higher LLs, anisotropy induces quantum phase transitions, likely of second order, to compressible phases with broken symmetry.

Anisotropy is an important aspect of FQHE as it represents a mechanism that probes the intrinsic metric of incompressible fluids in the geometrical picture of the FQHE. In addition, because our calculations show the possibility of phase transitions in the $n > 0$ Landau levels as a function of mass anisotropy, it motivates experimental studies on systems with both moderate mass anisotropy (e.g., AlAs and Si, $\alpha \sim 3-5$) as well as systems with large mass anisotropy (e.g., Ge, $\alpha \sim 20$), where behavior may be different in the upper Landau levels from the anisotropic GaAs. In these systems, as in GaAs, anisotropy could be further tuned using tilted fields, thereby adding to the richness of the FQHE phenomena.

Note added. Following the completion of this work, a related manuscript has appeared⁴⁷ that studies in more detail the anisotropy effects at $\nu = 1/3$ filling.

ACKNOWLEDGMENT

This work was supported by DOE Grant DE-SC0002140.

¹D. C. Tsui, H. L. Stormer, and A. C. Gossard, *Phys. Rev. Lett.* **48**, 1559 (1982).

²R. B. Laughlin, *Phys. Rev. Lett.* **50**, 1395 (1983).

³*The Quantum Hall Effect*, edited by R. E. Prange and S. M. Girvin, 2nd ed. (Springer-Verlag, New York, 1990).

⁴J. K. Jain, *Composite Fermions* (Cambridge University Press, 2007).

⁵G. Moore and N. Read, *Nucl. Phys. B* **360**, 362 (1991).

⁶N. Read and D. Green, *Phys. Rev. B* **61**, 10267 (2000).

⁷B. I. Halperin, P. A. Lee, and N. Read, *Phys. Rev. B* **47**, 7312 (1993).

⁸F. D. M. Haldane, *Phys. Rev. Lett.* **93**, 206602 (2004).

⁹M. P. Lilly, K. B. Cooper, J. P. Eisenstein, L. N. Pfeiffer, and K. W. West, *Phys. Rev. Lett.* **82**, 394 (1999); R. R. Du, D. C. Tsui, H. L. Stormer, L. N. Pfeiffer, K. W. Baldwin, and K. W. West, *Solid State Commun.* **109**, 389 (1999); K. B. Cooper, M. P. Lilly, J. P. Eisenstein, L. N. Pfeiffer, and K. W. West, *Phys. Rev. B* **60**, R11285 (1999).

¹⁰H. Fukuyama, P. M. Platzman, and P. W. Anderson, *Phys. Rev. B* **19**, 5211 (1979).

¹¹P. K. Lam and S. M. Girvin, *Phys. Rev. B* **30**, 473 (1984).

- ¹²K. Yang, F. D. M. Haldane, and E. H. Rezayi, *Phys. Rev. B* **64**, 081301(R) (2001).
- ¹³A. A. Koulakov, M. M. Fogler, and B. I. Shklovskii, *Phys. Rev. Lett.* **76**, 499 (1996).
- ¹⁴M. M. Fogler, A. A. Koulakov, and B. I. Shklovskii, *Phys. Rev. B* **54**, 1853 (1996).
- ¹⁵R. Moessner and J. T. Chalker, *Phys. Rev. B* **54**, 5006 (1996).
- ¹⁶E. H. Rezayi, F. D. M. Haldane, and K. Yang, *Phys. Rev. Lett.* **83**, 1219 (1999).
- ¹⁷F. D. M. Haldane, E. H. Rezayi, and K. Yang, *Phys. Rev. Lett.* **85**, 5396 (2000).
- ¹⁸E. H. Rezayi and F. D. M. Haldane, *Phys. Rev. Lett.* **84**, 4685 (2000).
- ¹⁹M. Shayegan, E. P. De Poortere, O. Gunawan, Y. P. Shkolnikov, E. Tutuc, and K. Vakili, *Int. J. Mod. Phys. B* **21**, 1388 (2007).
- ²⁰D. A. Abanin, S. A. Parameswaran, S. A. Kivelson, and S. L. Sondhi, *Phys. Rev. B* **82**, 035428 (2010).
- ²¹J. Xia, J. P. Eisenstein, L. N. Pfeiffer, and K. W. West, *Nat. Phys.* **7**, 845 (2011).
- ²²M. Mulligan, C. Nayak, and S. Kachru, *Phys. Rev. B* **82**, 085102 (2010).
- ²³F. D. M. Haldane in Ref. 3.
- ²⁴F. D. M. Haldane, *Phys. Rev. Lett.* **51**, 605 (1983).
- ²⁵D. Yoshioka, B. I. Halperin, and P. A. Lee, *Phys. Rev. Lett.* **50**, 1219 (1983).
- ²⁶F. D. M. Haldane, *Phys. Rev. Lett.* **55**, 2095 (1985).
- ²⁷F. D. M. Haldane, *Phys. Rev. Lett.* **107**, 116801 (2011).
- ²⁸S. C. Zhang, T. H. Hansson, and S. Kivelson, *Phys. Rev. Lett.* **62**, 82 (1989).
- ²⁹K. Musaelian and R. Joynt, *J. Phys.: Condens. Matter* **8**, L105 (1996); O. Ciftja and C. Wexler, *Phys. Rev. B* **65**, 045306 (2001); **65**, 205307 (2002).
- ³⁰R.-Z. Qiu, F. D. M. Haldane, Xin Wan, Kun Yang, and Su Yi, *Phys. Rev. B* **85**, 115308 (2012).
- ³¹J. Xia, V. Cvicek, J. P. Eisenstein, L. N. Pfeiffer, and K. W. West, *Phys. Rev. Lett.* **105**, 176807 (2010).
- ³²Y. P. Shkolnikov, K. Vakili, E. P. De Poortere, and M. Shayegan, *Phys. Rev. Lett.* **92**, 246804 (2004); O. Gunawan, Y. P. Shkolnikov, E. P. De Poortere, E. Tutuc, and M. Shayegan, *ibid.* **93**, 246603 (2004); Y. P. Shkolnikov, S. Misra, N. C. Bishop, E. P. De Poortere, and M. Shayegan, *ibid.* **95**, 066809 (2005); T. Gokmen, Medini Padmanabhan, E. Tutuc, M. Shayegan, S. De Palo, S. Moroni, and Gaetano Senatore, *Phys. Rev. B* **76**, 233301 (2007); T. Gokmen, Medini Padmanabhan, and M. Shayegan, *Phys. Rev. Lett.* **101**, 146405 (2008); *Phys. Rev. B* **81**, 235305 (2010).
- ³³Daw-Wei Wang, Eugene Demler, and S. Das Sarma, *Phys. Rev. B* **68**, 165303 (2003).
- ³⁴F. D. M. Haldane, e-print [arXiv:0906.1854](https://arxiv.org/abs/0906.1854); N. Read and E. H. Rezayi, *Phys. Rev. B* **84**, 085316 (2011).
- ³⁵F. D. M. Haldane and E. H. Rezayi, *Phys. Rev. B* **31**, 2529 (1985).
- ³⁶B. A. Bernevig and F. D. M. Haldane, *Phys. Rev. Lett.* **100**, 246802 (2008).
- ³⁷S. M. Girvin, A. H. MacDonald, and P. M. Platzman, *Phys. Rev. Lett.* **54**, 581 (1985); *Phys. Rev. B* **33**, 2481 (1986).
- ³⁸B. Yang, Z. Hu, Z. Papić, and F. D. M. Haldane, e-print [arXiv:1201.4165](https://arxiv.org/abs/1201.4165).
- ³⁹Z. Papić, N. Regnault, and S. Das Sarma, *Phys. Rev. B* **80**, 201303 (2009).
- ⁴⁰Z. Papić, F. D. M. Haldane, and E. Rezayi (unpublished).
- ⁴¹M. Levin, B. I. Halperin, and B. Rosenow, *Phys. Rev. Lett.* **99**, 236806 (2007); S.-S. Lee, S. Ryu, C. Nayak, and M. P. A. Fisher, *ibid.* **99**, 236807 (2007).
- ⁴²Waheb Bishara and Chetan Nayak, *Phys. Rev. B* **80**, 121302 (2009); Arkadiusz Wójs, Csaba Tóke, and Jainendra K. Jain, *Phys. Rev. Lett.* **105**, 096802 (2010); Edward H. Rezayi and Steven H. Simon, *ibid.* **106**, 116801 (2011).
- ⁴³M. R. Peterson, T. Jolicœur, and S. DasSarma, *Phys. Rev. Lett.* **101**, 016807 (2008); *Phys. Rev. B* **78**, 155308 (2008).
- ⁴⁴P. Wolfle and R. N. Bhatt, *Phys. Rev. B* **30**, 3542(R) (1984).
- ⁴⁵W. Kohn, in *Solid State Physics*, edited by F. Seitz and D. Turnbull, Vol. 5 (Academic, New York, 1957), p. 257; see also G. A. Thomas, M. Capizzi, F. DeRosa, R. N. Bhatt, and T. M. Rice, *Phys. Rev. B* **23**, 5472 (1981).
- ⁴⁶R. N. Bhatt, *Phys. Rev. B* **24**, 3630(R) (1981).
- ⁴⁷Hao Wang, Rajesh Narayanan, Xin Wan, and Fuchun Zhang, e-print [arXiv:1203.1982](https://arxiv.org/abs/1203.1982).

Search Search History

All Databases

<< Return to Web of Science®

Citing Articles Title: Model Wave Functions for the Collective Modes and the Magnetoroton Theory of the Fractional Quantum Hall Effect
Author(s): Yang, Bo ; Hu, Zi-Xiang ; Papic, Z. ; et al.
Source: PHYSICAL REVIEW LETTERS Volume: 108 Issue: 25 Article Number: 256807 DOI: 10.1103/PhysRevLett.108.256807 Published: JUN 19 2012

This item has been cited by items indexed in the databases listed below. [more information]

3 in All Databases

- 3 publication in Web of Science
0 publication in BIOSIS Citation Index
0 publication in ScELO Citation Index
0 publication in Chinese Science Citation Database
0 data sets in Data Citation Index
0 publication in Data Citation Index

Results: 3 Page 1 of 1 Go Sort by: Publication Date -- newest to oldest

Create Citation Report

Hide Refine

Refine Results

Search within results for

Search

Databases

Research Domains

SCIENCE TECHNOLOGY

Research Areas

PHYSICS

Document Types

Authors

Group/Corporate Authors

Editors

Funding Agencies

Source Titles

Conference/Meeting Titles

Publication Years

Languages

Countries/Territories

Select Page Add to Marked List (0) Send to: my.endnote.com

Title: Field theory of the quantum Hall nematic transition
Author(s): Maciejko, J.; Hsu, B.; Kivelson, S. A.; et al.
Source: PHYSICAL REVIEW B Volume: 88 Issue: 12 Article Number: 125137 DOI: 10.1103/PhysRevB.88.125137 Published: SEP 27 2013
Times Cited: 0 (from All Databases)

Get it! Waterloo -View abstract

Title: Analytic wave functions for neutral bulk excitations in fractional quantum Hall fluids
Author(s): Yang, Bo
Source: PHYSICAL REVIEW B Volume: 87 Issue: 24 Article Number: 245132 DOI: 10.1103/PhysRevB.87.245132 Published: JUN 27 2013
Times Cited: 0 (from All Databases)

Get it! Waterloo -View abstract

Title: Exactly Solvable Fermion Chain Describing a v=1/3 Fractional Quantum Hall State
Author(s): Nakamura, Masaaki; Wang, Zheng-Yuan; Bergholtz, Emil J.
Source: PHYSICAL REVIEW LETTERS Volume: 109 Issue: 1 Article Number: 016401 DOI: 10.1103/PhysRevLett.109.016401 Published: JUL 2 2012
Times Cited: 12 (from All Databases)

Get it! Waterloo -View abstract

Select Page Add to Marked List (0) Send to: my.endnote.com

Results: 3 Show 50 per page Page 1 of 1 Go Sort by: Publication Date -- newest to oldest

3 records matched your query of the 55,067,330 (contains duplicates) in the data limits you selected.

View in: 简体中文 繁體中文 English 日本語 한국어 Português Español

Model Wave Functions for the Collective Modes and the Magnetoroton Theory of the Fractional Quantum Hall Effect

Bo Yang,¹ Zi-Xiang Hu,^{2,3} Z. Papić,² and F. D. M. Haldane¹

¹*Department of Physics, Princeton University, Princeton, New Jersey 08544, USA*

²*Department of Electrical Engineering, Princeton University, Princeton, New Jersey 08544, USA*

³*Department of Physics, ChongQing University, ChongQing, 440004, China*

(Received 26 January 2012; published 19 June 2012)

We construct model wave functions for the collective modes of fractional quantum Hall systems. The wave functions are expressed in terms of symmetric polynomials characterized by a root partition that defines a “squeezed” basis, and show excellent agreement with exact diagonalization results for finite systems. In the long wavelength limit, we prove that the model wave functions are identical to those predicted by the single-mode approximation, leading to intriguing interpretations of the collective modes from the perspective of the ground-state guiding-center metric.

DOI: [10.1103/PhysRevLett.108.256807](https://doi.org/10.1103/PhysRevLett.108.256807)

PACS numbers: 73.43.Cd, 73.43.Lp

One of the main driving forces in characterizing the topological phases arising in the context of the fractional quantum Hall (FQH) effect [1] has been the construction of the model wave functions and their parent Hamiltonians [2–5]. Depending on the nature of the effective interaction within a partially filled Landau level, numerous phases appear, ranging from crystals to incompressible liquids with fractional [2] and possibly non-Abelian [4] quasiparticle statistics. Within the lowest Landau level (LLL), the kinetic energy of the electrons is a constant, and all dynamics come from the Coulomb repulsion [3]. Thus, the essential features of the many-body ground states and the low-lying excitations are solely determined by the particle statistics and quantum fluctuations that minimize the repulsion. Laughlin’s wave function [2] is a prominent example: the statistics are taken care of by the odd power in the Jastrow factor and, for rotationally invariant systems, the energy is minimized by placing all zeros of the wave function on the electrons. Subsequently, an intuitive picture of “composite fermions” was put forward by Jain [6], which lead to a classification of the numerous fractional states observed experimentally, and also provided a numerical procedure for constructing various model wave functions [6]. While much effort has been devoted to formulating FQH ground-state wave functions and those of charged excitations (quasihole and quasielectron), relatively little progress has been made in understanding the *neutral* excitations since the seminal work of Girvin, MacDonald, and Platzman introduced the single-mode approximation (SMA) to describe the lowest excitation in terms of a neutral density wave, or the “magnetoroton” [7]. Very recently, this question was revisited and explicit wave functions for the neutral collective excitations were proposed for the Abelian, as well as non-Abelian, FQH states utilizing a multicomponent composite fermion approach [8,9].

In this Letter, we construct model wave functions for the collective modes of FQH states by extending the Jack polynomial description [10,11]. We model the lowest neutral excitation as a dipole formed by a single quasielectron and a single quasihole. At the Laughlin $\nu = 1/3$ filling, we obtain a single bosonic mode that corresponds to the magnetoroton; in the Moore-Read $\nu = 5/2$ case, we obtain in addition a neutral fermionic mode [12,13] that stems from the non-Abelian statistics. We identify the long wavelength limit of the bosonic modes as a “spin-2” excitation (analogous to the graviton), and that of the fermionic mode as a “spin-3/2” (with a possible analogy to the gravitino). Our model wave functions show excellent agreement with exact diagonalization results at all wavelengths. In the limit of long wavelengths, we present a proof that the model wave functions become equivalent to the SMA result, which thus remains an accurate description even at energies lying above the threshold of the roton-pair continuum.

We first review some basic properties of the Jack polynomials. The Jacks are symmetric multivariable polynomials $J_\lambda^\alpha(z_1, z_2, \dots, z_{N_e})$, parametrized by a number α and a root partition λ with length $l_\lambda \leq N_e$, where N_e is the number of electrons. For bosonic FQH states, the statistics of the system restrict us to only symmetric monomials with a fixed total degree, which corresponds to a fixed angular momentum on a disk or a sphere [14]. Fermionic FQH states are obtained by multiplying the bosonic counterpart with a Vandermonde determinant. The root partitions encode the clustering properties that effectively “keep electrons apart” from each other; a “ (k, r, N_e) -admissible” partition is such that no more than k electrons are found in r consecutive orbitals. The root partition tells us how the wave function vanishes when particles are brought together. For example, the root partition of the ground state and the quasihole states at $\nu = 1/m$ Laughlin filling contains no more than one electron in m consecutive orbitals.

The corresponding Jack vanishes at least with a power of m when two electrons approach each other.

From a practical point of view, the Hilbert space we are interested in, after reduction by particle statistics and symmetry, only needs to include polynomials with appropriate clustering properties (whereby Jacks are special cases). In fact, for the ground state and single quasihole states of the Read-Rezayi series (including the Laughlin and Moore-Read states), such Hilbert space is one-dimensional and spanned by a *single* Jack polynomial with $\alpha = -\frac{k+1}{r-1}$ that can be obtained directly via recursive relations [15]. Quasielectron states, on the other hand, are more complicated [16] because they contain local defects where electrons are forced to get closer to each other than allowed in the ground state. The same difficulty arises in collective modes that consist of quasielectron-quasihole pairs. In these cases, the reduced Hilbert space is no longer one-dimensional with a single Jack polynomial.

We now proceed to construct explicit model wave functions for the magnetoroton mode in the Laughlin state at $\nu = 1/3$ filling. We work in the spherical geometry with a monopole of strength $2S$ placed at the center [14]. The root partition for the Laughlin ground state is well known: $\lambda = \{100100100100 \cdots 1001\}$ [10]. The clustering property in this case means that no more than a single electron can exist in three consecutive orbitals [17]. The collective mode in the limit of momentum $\mathbf{k} \rightarrow 0$ consists of two quasielectron-quasihole pairs, forming a quadrupole. As the momentum increases, a dipole moment develops with the separation of one quasielectron-quasihole pair. This is summarized in the explicit set of root partitions, as follows:

$$\begin{aligned} \ddot{1}100001001001001001 \cdots L = 2, \\ \ddot{1}100010001001001001 \cdots L = 3, \\ \ddot{1}100010010001001001 \cdots L = 4, \\ \ddot{1}100010010010001001 \cdots L = 5, \\ \ddot{1}100010010010010001 \cdots L = 6. \end{aligned} \quad (1)$$

⋮

We label the states by their total angular momentum L on the sphere. Note the ground state with the root partition $\{1001001 \cdots 1001\}$ has $L = 0$, and the excitation with the smallest momentum that can be created is $L = 2$. In Eq. (1), the black dot schematically indicates the position of a quasielectron, while the white dot that of a quasihole. To determine the position of a quasiparticle, we look at any three consecutive orbitals in the root partitions above, and count the number of electrons to see if it violates the ground-state clustering property. In this particular case, if there is more (less) than one electron, we then have a quasielectron (quasihole), which is located right below the middle of the three consecutive orbitals. Due to rotational invariance on the sphere, we next impose the highest weight condition on the wave functions $|\psi_\lambda^L\rangle$ to single out the state with quasiparticles piled up at the north pole:

$$L^+ |\psi_\lambda^L\rangle = 0, \quad |\psi_\lambda^L\rangle = \sum_{\mu \leq \lambda} a_\mu m_\mu, \quad (2)$$

where m_μ are monomials with partition μ [10]. The summation is over all partitions μ that can be squeezed from the root partition λ . For example, $m_{\{1001\}} \sim z_1^3 - z_2^3$, $m_{\{0110\}} \sim z_1^2 z_2 - z_1 z_2^2$, and $\{0110\}$ is squeezed from $\{1001\}$. The constraints in Eq. (2) substantially reduce the Hilbert space dimension (e.g., the basis dimension is less than 20 for 10 particles). The resulting lowest-energy eigenstates of the Hamiltonian, restricted to this Hilbert space, are very good approximations to the exact magnetoroton mode.

The innovation we implement here is to impose an additional constraint that can be formally expressed as

$$\hat{V}_1 c_1 c_2 |\psi_\lambda^L\rangle = 0. \quad (3)$$

Here, \hat{V}_1 is the operator corresponding to the first Haldane pseudopotential [3], and c_i annihilates an electron at the i th orbital. This additional constraint renders $|\psi_\lambda^L\rangle$ unique by enforcing the following clustering property: the wave function is vanishing only when two or more clusters of two particles coincide in real space.

The resulting implementation is numerically much less expensive, with variational energies only slightly above the ones obtained in the Hilbert space defined by constraints (2), and improving with the increase in system size. We note that the model wave functions $|\psi_\lambda^L\rangle$ inherit rich algebraic structures from the underlying Jacks. When the geometric normalization factors on the sphere are removed, the coefficients of the decomposition in Fock space are integers, with the coefficient of the root configuration normalized to 1. Furthermore, they satisfy a ‘‘product rule’’ [15,18] if the first five orbitals are treated as one ‘‘big’’ orbital, which allows us to generate a large subset of coefficients recursively. This suggests the product rule is not restricted to pure Jacks and is robust against local defects of the wave function. An approximation to $|\psi_\lambda^L\rangle$ can be built from the product rules; the overlap between the approximate and exact model wave functions is high and increases with system size (see Table I). These properties reduce the computational cost for generating these model wave functions compared to direct diagonalization.

We now proceed to evaluate the variational energies of the model wave functions obtained via constraints Eqs. (2) and (3). In Fig. 1, the variational energies are plotted versus

TABLE I. The overlap of the approximate model wave functions constructed from product rules and the true model wave functions.

Number of electrons	9	10	11	12
$L = 2$	89.83%	90.13%	90.31%	90.42%
$L = 3$	86.42%	86.99%	87.37%	87.63%
$L = 4$	83.63%	84.59%	85.23%	85.69%

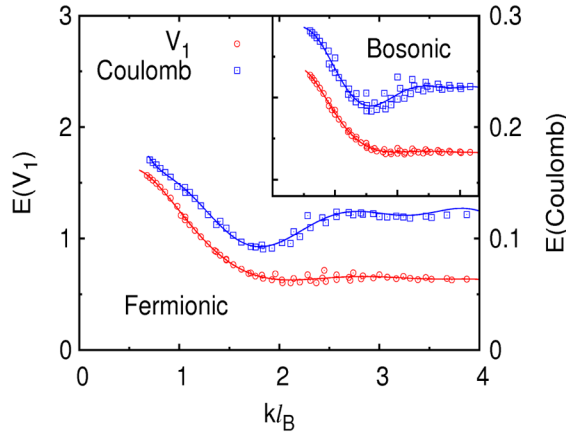


FIG. 1 (color online). The variational energy of the model wave functions defined by Eqs. (2) and (3), against \hat{V}_1 (left axis, arbitrary units) and Coulomb Hamiltonians (right axis, in units of $e^2/\epsilon\ell_B$), plotted as a function of momentum. The data are generated from system sizes ranging from 6 to 12 electrons (the inset shows the same plot for the bosonic Laughlin state).

momentum $k = L/\sqrt{S}$, where $N_{\text{orb}} = 2S + 1$ is the number of orbitals in the LLL. We include the data for a number of system sizes and rescale the magnetic length ℓ_B by a factor $\sqrt{S/N_{\text{orb}}}$ to minimize the finite size effects. For the model \hat{V}_1 Hamiltonian and Coulomb Hamiltonian, the dispersion obtained using the model wave function is in excellent agreement with the results from exact diagonalization, both in small k and large k regime. Our model wave functions compare favorably with the exact diagonalization eigenstates, with 99% overlap for 10 electrons.

Using the same approach, we can construct the collective-mode wave functions for the entire Read-Rezayi series. As an example, we consider an interesting case of the Moore-Read state, where in addition to the bosonic mode, we also obtain a mode that corresponds to the unpaired electron—the neutral fermion (NF) mode [13]. On the sphere, the root configurations of the two modes are given by

$$\begin{aligned}
 11100100110011 \cdots L = 2, \\
 111000110011 \cdots L = 3/2, \\
 11100101010011 \cdots L = 3, \\
 111001010011 \cdots L = 5/2, \\
 11100101010101 \cdots L = 4, \\
 111001010101 \cdots L = 7/2, \quad \vdots
 \end{aligned} \tag{4}$$

The Moore-Read ground-state root partition is given by 2 electrons in 4 consecutive orbitals [10]. Similarly to the Laughlin state, any deviation from the uniform background density yields the position of the quasihole or quasielectron [not labeled in Eq. (4)]. In Eq. (4), the left column with an integer angular momentum is the magnetoroton mode. The

NF mode with a half-integer angular momentum is given in the right column. Unique model wave functions can be constructed by imposing the constraint Eq. (2) and, in addition, a modified constraint Eq. (3) that reads $H_{3b}c_1c_2c_3|\psi_\lambda^{\text{MR}}\rangle = 0$, where H_{3b} is the Moore-Read three-body Hamiltonian. Their variational energies are plotted in Fig. 2.

We would like to emphasize for both the Laughlin and Moore-Read case that the collective modes enter the multi-roton continuum in the long wavelength limit. The continuum starts at energy that is double the energy gap of the roton minimum. While this makes exact diagonalization ambiguous, the root partitions give clear physical interpretation for the modes for the entire momentum range. Interestingly, the $L = 1$ state (and $L = 1/2$ state for the neutral fermion mode) vanishes with the set of constraints we impose. Thus, in the long wavelength limit, the collective mode is given by a quadrupole excitation. In light of the geometrical picture [19] of the FQH effect, we identify the magnetoroton mode as a spin-2 “graviton” and the NF mode as a spin- $3/2$ “gravitino,” or the “supersymmetric partner” of the magnetoroton mode.

Recently, model wave functions for the excitations at $\nu = 1/2$ filling for bosons were also obtained in a multi-component composite fermion picture [8,9]. We have confirmed that the wave functions of Ref. [9] are numerically identical to ours in finite size systems. The approach of Ref. [9], though completely different at the outset, arrives at the wave functions that satisfy the same clustering properties as ours, which fixes them to be unique. The uniqueness property motivates us to investigate the SMA wave functions obtained from the ground state $|\psi_0\rangle$ by the guiding-center density modulation, $|\psi_{\mathbf{k}}\rangle = \hat{\rho}_{\mathbf{k}}|\psi_0\rangle$, where

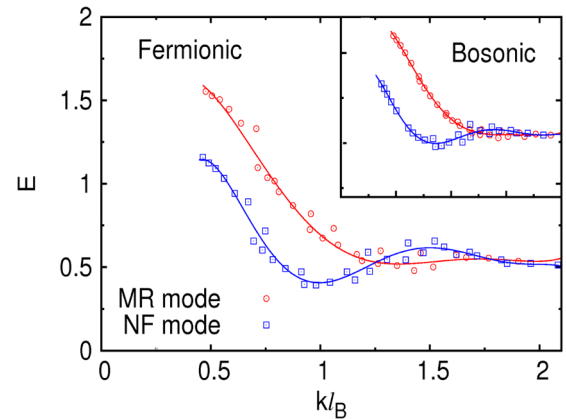


FIG. 2 (color online). The variational energy of the model wave functions for the magnetoroton (MR) mode and the neutral fermion (NF) mode, evaluated against the three-body Hamiltonian. The data are generated from system sizes ranging from 5 to 17 electrons, where the odd number of electrons contribute to the NF mode, and the even number of electrons contribute to the magnetoroton mode. (The inset shows the same plot for the bosonic Moore-Read state.)

$\hat{\rho}_{\mathbf{k}} = \sum_i e^{i\mathbf{k}\cdot\mathbf{R}_i}$ is the guiding-center density operator. The SMA yields excitation energies manifestly as a property of the ground state. Though it successfully predicts the magnetoroton minimum of the collective mode of FQH states at $\nu = 1/m$, there is some ambiguity in the limit of $\mathbf{k} \rightarrow 0$ when the SMA variational energy enters the roton-pair continuum, eluding comparisons with exact diagonalization. It is thus useful to compare the SMA prediction with our model wave functions in the small \mathbf{k} limit, since the latter are valid in that regime and have transparent physical properties given by the root partitions.

The SMA construction can be adapted to the sphere as follows. The ground state on a sphere has the total angular momentum $L = 0$, and the SMA wave function with total angular momentum L is obtained by boosting one electron with orbital angular momentum L . The projection into the LLL is equivalent to the projection of the boosted single-particle state into the sub-Hilbert space of the total spin S . Formally, we have

$$|\psi_{LM}^{\text{SMA}}\rangle = \sum_i \hat{C}_{m_i+M, M, m_i}^{S, L, S} |\psi_0\rangle, \quad (5)$$

where i is the electron index, and $\hat{C}_{m', M, m}^{S, L, S}$ is defined by its action on the single electron state $\hat{C}_{m', M, m}^{S, L, S} |m\rangle = C_{m' M m}^{S L S} |m'\rangle$, where $C_{m' M m}^{S L S} = \langle m' | \hat{Y}^{LM} | m \rangle$ are the Clebsch-Gordan coefficients, and \hat{Y}^{LM} are the spherical harmonics. This is a result of the Wigner-Eckart theorem, and due to rotational invariance we can set $M = L$ in Eq. (5). The dispersion of the SMA wave functions is plotted in Fig. 3 along with that of our model wave functions.

For small momenta, the variational energies of the two classes of wave functions agree very well, while the SMA mode evidently becomes invalid for momenta larger than the magnetoroton minimum. Note that at $L = 2, 3$ the SMA wave functions only involve the elements of the basis

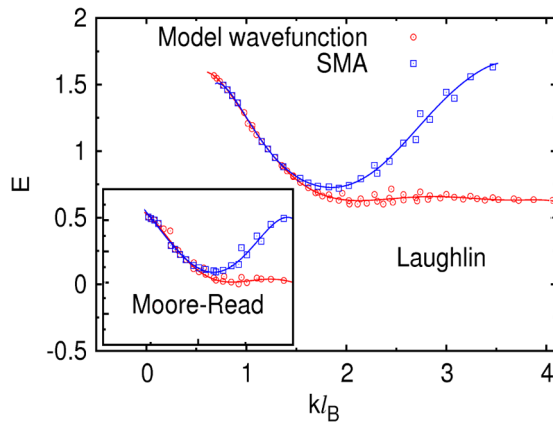


FIG. 3 (color online). The variational energies for the SMA model wave functions compared to our model wave functions for the Laughlin state at $\nu = 1/3$ filling. (The inset shows the same comparison for the magnetoroton mode of the Moore-Read state.)

squeezed from the same root partition that defines our model wave functions. Taking the Laughlin $1/3$ as an example, we now prove the SMA wave functions are actually identical to ours at $L = 2, 3$. By the product rule of the Jack polynomial, we can write

$$|\psi_0\rangle \sim J_{\lambda_1}^\alpha \otimes J_{\lambda_2}^\alpha + J_{\lambda_3}^\alpha \otimes J_{\lambda_4}^\alpha + |\bar{\psi}_0\rangle, \quad (6)$$

where we suppressed the relative coefficients because they are unimportant for the proof. The partitions $\lambda_1 = \{10010\}$, $\lambda_2 = \{01001001 \dots\}$, $\lambda_3 = \{10001\}$, $\lambda_4 = \{10001001 \dots\}$, and $|\bar{\psi}_0\rangle$ involve the rest of the squeezed basis. It is easy to check that $c_1 c_2 \sum_i \hat{C}_{m_i+L, L, m_i}^{S, L, S} |\bar{\psi}_0\rangle = 0$. We thus have

$$\hat{V}_1 c_1 c_2 |\psi_{LL}^{\text{SMA}}\rangle \sim \hat{V}_1 \{0000\} \otimes (J_{\lambda_2}^\alpha + t J_{\lambda_4}^\alpha) = 0. \quad (7)$$

Again, the coefficients are suppressed in Eq. (7), and $t = 0$ for $L = 2$. Thus, the SMA wave functions satisfy exactly the same constraints as our model wave functions, which makes them identical. Note that for $L > 3$ the SMA wave functions contain unsqueezed basis components with respect to the root partitions used in our model wave function, and the proof breaks down.

In conclusion, we demonstrated a numerically efficient method of constructing accurate model wave functions for the collective modes in FQH systems. The wave functions are identified with the SMA wave functions in the long wavelength limit. This result reveals a crucial link between the “graviton” mode and the SMA mode at long wavelengths, which plays an important role in the geometrical theory of the FQH effect [19]. For realistic Coulomb or pseudopotential interactions, the “graviton” mode decays into multiroton pairs and appears experimentally inaccessible. It would be interesting to see if the interaction can be tuned in such a way as to expose the “graviton” mode at $\mathbf{k} \rightarrow 0$ below the roton-pair continuum.

We thank B. A. Bernevig for useful discussions. This work was supported by DOE Grant No. DE-SC0002140.

-
- [1] D. C. Tsui, H. L. Stormer, and A. C. Gossard, *Phys. Rev. Lett.* **48**, 1559 (1982).
 - [2] R. B. Laughlin, *Phys. Rev. Lett.* **50**, 1395 (1983).
 - [3] *The Quantum Hall Effect*, edited by R. E. Prange and S. M. Girvin (Springer-Verlag, New York, 1990), 2nd ed.
 - [4] G. Moore and N. Read, *Nucl. Phys.* **B360**, 362 (1991).
 - [5] N. Read and E. Rezayi, *Phys. Rev. B* **59**, 8084 (1999).
 - [6] J. K. Jain, *Phys. Rev. Lett.* **63**, 199 (1989).
 - [7] S. M. Girvin, A. H. MacDonald, and P. M. Platzman, *Phys. Rev. Lett.* **54**, 581 (1985); *Phys. Rev. B* **33**, 2481 (1986).
 - [8] G. J. Sreejith, C. Töke, A. Wójs, and J. K. Jain, *Phys. Rev. Lett.* **107**, 086806 (2011).
 - [9] I. D. Rodriguez, A. Serdyniak, M. Hermanns, J. K. Slingerland, and N. Regnault, *Phys. Rev. B* **85**, 035128 (2012).

- [10] B. A. Bernevig and F. D. M. Haldane, *Phys. Rev. Lett.* **100**, 246802 (2008).
- [11] B. A. Bernevig and F. D. M. Haldane, *Phys. Rev. B* **77**, 184502 (2008).
- [12] N. Read and D. Green, *Phys. Rev. B* **61**, 10267 (2000).
- [13] G. Möller, A. Wójs, and N. R. Cooper, *Phys. Rev. Lett.* **107**, 036803 (2011); P. Bonderson, A. E. Feiguin, and C. Nayak, *ibid.* **106**, 186802 (2011).
- [14] F. D. M. Haldane, *Phys. Rev. Lett.* **51**, 605 (1983).
- [15] B. A. Bernevig and N. Regnault, *Phys. Rev. Lett.* **103**, 206801 (2009).
- [16] B. A. Bernevig and F. D. M. Haldane, *Phys. Rev. Lett.* **102**, 066802 (2009).
- [17] The bosonic counterpart has no more than a single particle in two consecutive orbitals, yielding a Jack given by J_{λ}^{-2} , which is a function that vanishes as a power of 2 when two particles approach each other, i.e., the Laughlin wave function.
- [18] R. Thomale, B. Estienne, N. Regnault, and B. A. Bernevig, *Phys. Rev. B* **84**, 045127 (2011).
- [19] F. D. M. Haldane, *Phys. Rev. Lett.* **107**, 116801 (2011).

Search Search History

All Databases

<< Return to Web of Science®

Citing Articles Title: Comparison of the density-matrix renormalization group method applied to fractional quantum Hall systems in different geometries
Author(s): Hu, Zi-Xiang ; Papic, Z. ; Johri, S. ; et al.
Source: PHYSICS LETTERS A Volume: 376 Issue: 30-31 Pages: 2157-2161 DOI: 10.1016/j.physleta.2012.05.031 Published: JUN 18 2012

This item has been cited by items indexed in the databases listed below. [more information]

3 in All Databases

- 3 publication in Web of Science
0 publication in BIOSIS Citation Index
0 publication in SciELO Citation Index
0 publication in Chinese Science Citation Database
0 data sets in Data Citation Index
0 publication in Data Citation Index

Results: 3 Page 1 of 1 Go Sort by: Publication Date -- newest to oldest

Create Citation Report

Hide Refine

Refine Results

Search within results for

Search

Databases

Research Domains

SCIENCE TECHNOLOGY

Research Areas

PHYSICS

Document Types

Authors

Group/Corporate Authors

Editors

Funding Agencies

Source Titles

Conference/Meeting Titles

Publication Years

Languages

Countries/Territories

Select Page Add to Marked List (0) Send to: my.endnote.com

1. Title: Bulk-edge correspondence in fractional Chern insulators
Author(s): Liu, Zhao; Kovrizhin, D. L.; Bergholtz, Emil J.
Source: PHYSICAL REVIEW B Volume: 88 Issue: 8 Article Number: 081106 DOI: 10.1103/PhysRevB.88.081106 Published: AUG 26 2013
Times Cited: 1 (from All Databases)

Get it! Waterloo -View abstract

2. Title: Topological Characterization of Fractional Quantum Hall Ground States from Microscopic Hamiltonians
Author(s): Zaletel, Michael P.; Mong, Roger S. K.; Polmann, Frank
Source: PHYSICAL REVIEW LETTERS Volume: 110 Issue: 23 Article Number: 236801 DOI: 10.1103/PhysRevLett.110.236801 Published: JUN 4 2013
Times Cited: 3 (from All Databases)

Get it! Waterloo -View abstract

3. Title: Matrix product states for trial quantum Hall states
Author(s): Estienne, B.; Papic, Z.; Regnault, N.; et al.
Source: PHYSICAL REVIEW B Volume: 87 Issue: 16 Article Number: 161112 DOI: 10.1103/PhysRevB.87.161112 Published: APR 15 2013
Times Cited: 4 (from All Databases)

Get it! Waterloo -View abstract

Select Page Add to Marked List (0) Send to: my.endnote.com

Results: 3 Show 50 per page Page 1 of 1 Go Sort by: Publication Date -- newest to oldest

3 records matched your query of the 55,067,330 (contains duplicates) in the data limits you selected.

View in: 简体中文 繁體中文 English 日本語 한국어 Português Español



Comparison of the density-matrix renormalization group method applied to fractional quantum Hall systems in different geometries

Zi-Xiang Hu^{a,b,*}, Z. Papić^a, S. Johri^a, R.N. Bhatt^a, Peter Schmitteckert^c

^a Department of Electrical Engineering, Princeton University, Princeton, NJ 08544, USA

^b Department of Physics, ChongQing University, ChongQing 400044, China

^c Institut für Nanotechnologie, Forschungszentrum Karlsruhe, D-76021 Karlsruhe, Germany

ARTICLE INFO

Article history:

Received 30 March 2012

Accepted 14 May 2012

Available online 17 May 2012

Communicated by R. Wu

ABSTRACT

We report a systematic study of the fractional quantum Hall effect (FQHE) using the density-matrix renormalization group (DMRG) method on two different geometries: the sphere and the cylinder. We provide convergence benchmarks based on model Hamiltonians known to possess exact zero-energy ground states, as well as an analysis of the number of sweeps and basis elements that need to be kept in order to achieve the desired accuracy. The ground state energies of the Coulomb Hamiltonian at $\nu = 1/3$ and $\nu = 5/2$ filling are extracted and compared with the results obtained by previous DMRG implementations in the literature. A remarkably rapid convergence in the cylinder geometry is noted and suggests that this boundary condition is particularly suited for the application of the DMRG method to the FQHE.

© 2012 Elsevier B.V. All rights reserved.

1. Introduction

Strongly correlated systems in low dimensions are among the most active areas in the condensed matter physics. These systems contain a large number of particles that interact strongly with each other and cannot be understood in a single-particle picture. A paradigm of strongly correlated systems is the fractional quantum Hall effect [1] (FQHE) that occurs when a system of two-dimensional electrons partially fills one of the Landau levels in a strong perpendicular magnetic field. Since the kinetic energy is frozen in a partially-filled Landau level, the electron–electron interaction is the only relevant term in the Hamiltonian and leads to the emergence of non-perturbative ground-states with fractionalized charge [2] and anyonic, Abelian and non-Abelian [3], statistics.

Due to the non-perturbative nature of the FQHE, numerical methods have played a crucial role since the original work of Laughlin [2]. In particular, exact diagonalization (ED) presented itself as a versatile and extremely powerful tool that unraveled many of the complexities of FQH systems [4,5]. The popularity and quick success of ED was due to the specific correlations of FQH systems that rapidly minimize the finite-size effects with increasing the number of particles in the simulation. Highly accurate predictions of the system's properties in the thermodynamic limit could be obtained by considering systems as small as 10 particles [5].

As it is well known, the main bottleneck of ED calculations lies in the exponential explosion of the size of the many-body Hilbert space as the number of particles grows. While for the simplest FQH fractions, such as the Laughlin $\nu = 1/3$ state [2], admittedly all essential physical properties can be obtained in the systems attainable by ED, in the majority of other cases ED is not sufficient. This is particularly striking in case of spin degree of freedom, or SU(4) internal symmetry if we consider FQHE in graphene [6]. However, similar constraints arise even in the spin-polarized case of the non-Abelian Read–Rezayi sequence [7], where electrons are believed to pair into $k \geq 2$ -body clusters. Therefore, a non-Abelian N_e -particle state at level k is likely to have finite-size effects comparable to the Laughlin-like state of N_e/k particles. Hence, to address the properties of the non-Abelian ground-state it is desirable to consider systems at least k times as large. It is therefore of essential importance to develop new numerical methods that can reach larger system sizes than ED.

One such method is the density matrix renormalization group (DMRG), invented by White [8] in 1992. DMRG has been quite successful over the last decade when it was applied to one-dimensional systems such as the Heisenberg spin chains and the one-dimensional Hubbard model. In essence, it is a variational method to get the ground state and the low-lying energy states of the system. The algorithm contains two main parts. One is called the infinite size algorithm which grows the system to a big size, and the other one is referred to as the finite-size algorithm, which makes the ground state converge. The only approximation in the DMRG method is the truncation of the Hilbert space according to the eigenvalues of the reduced density matrix for the

* Corresponding author at: Department of Electrical Engineering, Princeton University, Princeton, NJ 08544, USA.

E-mail address: zihu@princeton.edu (Z.-X. Hu).

subblock which is used to construct the large system. The more states are kept in the reduced density matrix, the higher the accuracy one can achieve in principle. It is generally believed that the entanglement entropy of a subregion often grows like the boundary area of the subregion [9]. A larger entanglement entropy, or larger correlation, means that one needs to keep more states to achieve a sufficient accuracy. The success of DMRG in the one-dimensional systems was ensured by the low entanglement between the two subregions which only have a point surface between two blocks.

On the other hand, a FQH system is two-dimensional and thus the success of the DMRG method in FQHE is by no means obvious. However, in a Landau gauge, the one-body orbitals are Gaussian-localized and provide a mapping to an effective “one-dimensional” chain with the long-range Coulomb interaction. This motivates an attempt to apply the DMRG to the FQHE system. The first such attempt was done for the periodic boundary conditions (torus geometry) by Shibata and Yoshioka [10], mostly considering compressible, stripe and bubble, phases in higher Landau levels. Feiguin et al. [11] developed a DMRG scheme for the ground state and excited states in the spherical geometry for larger systems at filling factors $\nu = 1/3$ and $\nu = 5/2$. Hard-core interactions were also studied on thin cylinders in an unpublished work [12], and for bosonic systems in Ref. [13]. Most recently, Zhao et al. [14] developed an independent DMRG implementation that by far exceeds the previous attempts. In this study, the maximal system size was $N_e = 24$ for $\nu = 1/3$ and $N_e = 34$ for $\nu = 5/2$. The independent implementations [10–14] appear to differ significantly from each other in various aspects, in particular in the number of basis states that are kept, ranging from a few hundred in the torus geometry, up to $N_{\text{keep}} = 20000$ states in Ref. [14].

In this Letter, we report on the systematic study of the FQHE system in the spherical and cylinder geometry based on our independent implementation of the DMRG method. We address the well-studied FQH systems at fillings $\nu = 1/3$ and $\nu = 5/2$ with the goal of providing a detailed benchmark of the DMRG algorithm and comparing it with the previous implementations. New physical results obtained with the current DMRG implementation will be presented elsewhere [15].

The remainder of this Letter is organized as follows. In Section 2 we analyze the convergence of the V_1 Haldane pseudopotential [4, 5] Hamiltonian on the sphere that is analytically known to yield the Laughlin wavefunction as an exact zero-energy ground state. In the case of Coulomb interaction, we evaluate the ground state energy for $\nu = 1/3$ and $\nu = 5/2$ fillings corresponding to the Laughlin [2] and Moore–Read [3] states. The ground-state energies per particle are extrapolated to the thermodynamic limit using finite-size scaling techniques. In Section 3, we draw some comparisons with the cylinder geometry, which is an alternative geometry for studying the FQHE that so far has scarcely been used [16]. The convergence for the V_1 Hamiltonian is found to be significantly faster on the cylinder than on the sphere, suggesting that this boundary condition might be promising for further studies of the FQHE. Discussion and conclusions are given in Section 4.

2. Sphere geometry

We study a model for spin-polarized electrons moving on the surface of a sphere, with a magnetic monopole $2S$ placed in the center to generate a radially-symmetric magnetic field perpendicular to the surface [4]. In strong magnetic fields, electrons in general completely fill $(n - 1)$ single particle Landau levels which are considered to be “inert”, and all dynamics comes from a partially-filled n th Landau level. Any two-body Hamiltonian, projected to this n th Landau level (neglecting the excitations to higher Landau levels),

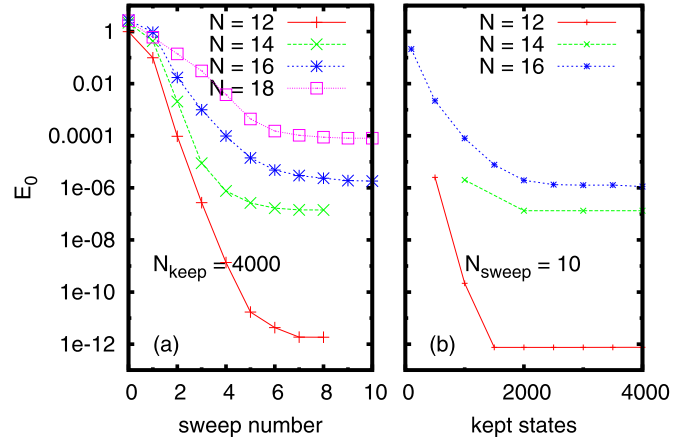


Fig. 1. (a) The convergence of the ground-state energies for the hard-core V_1 Hamiltonian at $\nu = 1/3$ as a function of the finite size sweeping number when keeping 4000 states in the subsystem. (b) The ground-state energy as a function of the number of kept states. We perform 10 finite-size sweeps for each point. The energies are on a logarithmic scale.

can be written in the usual second-quantized form,

$$H = \frac{1}{2} \sum_{m_1, m_2, m_3, m_4} \langle m_1 m_2 | V | m_3 m_4 \rangle a_{m_1}^+ a_{m_2}^+ a_{m_3} a_{m_4}. \quad (1)$$

In the spherical geometry, quantum numbers m_i 's label the z -component of the angular momentum for particle i which takes values: $-S, -(S - 1), \dots, S$. The one-body orbitals are the monopole harmonics [4] Y_{Slm} which generalize the usual spherical harmonics obtained for $S = 0$. When we target a specific many-body state, we also need to adjust the flux $2S$ to take into account the so-called shift that determines the total number of the available orbitals. This means that $2S = \frac{1}{\nu} N_e + S$, where S is a universal number that characterizes each many-body state, e.g. $S = -3$ for the Laughlin and Moore–Read state.

Because of rotational and translational invariance, any two-body interaction matrix element $\langle m_1 m_2 | V | m_3 m_4 \rangle$ can be decomposed as [18]

$$\begin{aligned} & \langle m_1 m_2 | V | m_3 m_4 \rangle \\ &= \sum_{J=0}^{2S} \sum_{M=-J}^J \langle S m_1, S m_2 | J M \rangle \langle S m_3, S m_4 | J M \rangle V_J^{(S)} / R, \end{aligned} \quad (2)$$

where V_J are the Haldane pseudopotentials [4] and $R = \sqrt{S} \ell_B$ is the radius of the sphere in terms of the magnetic length $\ell_B = \sqrt{\hbar/eB}$. The first two terms in the above equation are the Clebsch–Gordan coefficients on the sphere. When symmetry is taken into account, at filling $\nu = 1/3$ the Lanczos method can diagonalize the sparse Hamiltonian matrix for up to 14 electrons, corresponding to the Hilbert space dimension of $\sim 10^8$.

As shown by Haldane [5], the advantage of the pseudopotential formulation is that model wavefunctions can be defined as ground states of the truncated Hamiltonians. For example, the Laughlin wavefunction is obtained as an exact zero-energy ground state for the hard-core interaction with $V_1 > 0$, $V_{m>1} = 0$, with an excitation gap controlled by the magnitude of V_1 . From the computational point of view, V_1 Hamiltonian is nearly as sparse as the full Coulomb Hamiltonian, but it serves as a universal reference to test the accuracy of the DMRG code for large systems because the ground-state energy is known to be exactly zero for any system size.

In Fig. 1 we show the ground-state energy convergence for different system sizes as a function of the finite-size sweep number

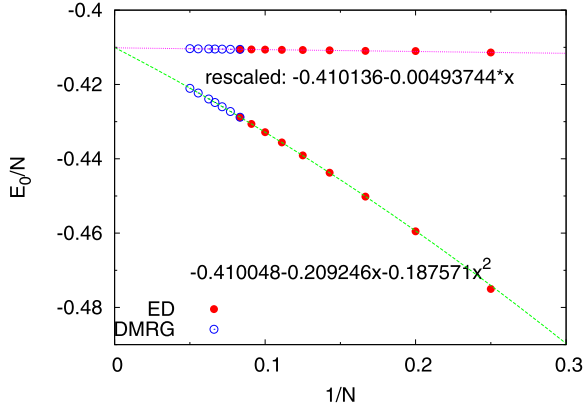


Fig. 2. Ground-state energy per particle for the $\nu = 1/3$ state up to 20 electrons as a function of size of the system. Solid points are the results of exact diagonalization and the blank circles represent DMRG results. The two fitting curves are with (upper) and without (lower) rescaling the magnetic length as described in Refs. [19, 20]. The energy in the thermodynamic limit is $\approx -0.4101e^2/\ell_B$ which is consistent with previous studies [11,14].

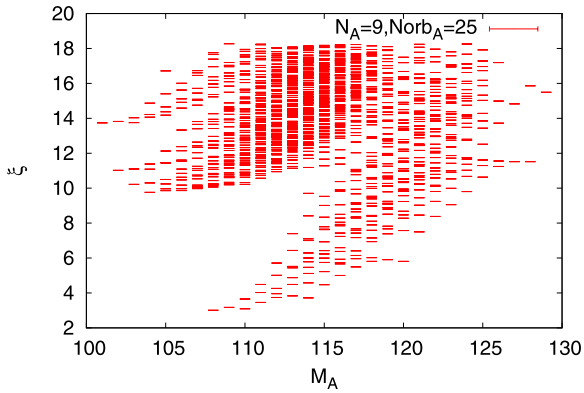


Fig. 3. The entanglement spectrum for 18 electrons at $\nu = 1/3$ with the Coulomb interaction. The subsystem contains 9 electrons in 25 orbitals.

with the fixed number of states kept ($N_{\text{keep}} = 4000$), or as a function of the number of kept states in the subsystem with a fixed sweep number. For a fixed number of kept states, the accuracy of the ground state energy decreases when we increase the system size. It means that more states for the larger systems need to be kept if the same accuracy is demanded. As shown in Fig. 1(b), increasing the number of kept states obviously helps the convergence although the energy drops very slowly when N_{keep} is large. However, for the largest system size with $N_e = 18$ we tested in Fig. 1, the ground-state energy drops to 10^{-4} when just keeping 4000 states and after finishing 10 finite size sweeps. This energy is far below the gap between the ground state and the first excited state. We assume the ground state is close enough to the Laughlin state in this case. To improve the accuracy, one needs more finite-size sweeps and keeping more states in the truncation.

Having established the convergence scaling for the hard-core Hamiltonian, we move to the full Coulomb interaction. At $\nu = 1/3$ we calculate the ground-state energy for systems up to 20 electrons. All the results are obtained by keeping up to 5000 states in the subsystem. With keeping the same number of states, we find the efficiency of our code is the same as that shown in Fig. 1 of Ref. [14]. The results for different system sizes at $\nu = 1/3$ are summarized in Fig. 2, which includes the data both from the ED and the DMRG. It shows they match with each other very well. We do the finite-size scaling for the ground-state energy per electron with a quadratic polynomial, and extrapolate the thermo-

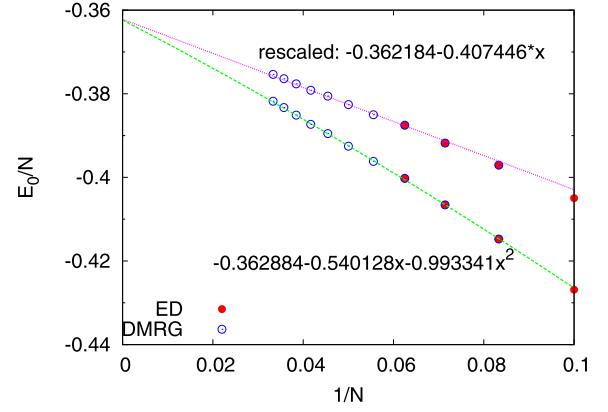


Fig. 4. Finite size scaling of the ground-state energy per particle for $\nu = 5/2$ FQH state up to $N_e = 30$ electrons. The results are obtained by keeping up to 5000 states in the truncation and after completing 10 finite size sweeps. The energy in the thermodynamic limit is consistent before and after rescaling the magnetic length ℓ_B , which means that the large system sizes have automatically eliminated the curvature effects.

dynamic limit energy to be $-0.410048e^2/\ell_B$. On finite spheres, it has been suggested [19,20] that the curvature effects can be substantially minimized by rescaling the magnetic length ℓ_B . We also plot the rescaled energies in Fig. 2 and do the finite-size scaling with a linear function. The energy in the thermodynamic limit $-0.410136e^2/\ell_B$ is almost the same as that without rescaling the magnetic length. This means the large-scale study by the DMRG method has already removed the finite-size effects coming from the curvature. Our results are also consistent with the previous DMRG study [11,14]. Besides the ground-state energy, we also plot the entanglement spectrum [21] in Fig. 3 for 18 electrons at $\nu = 1/3$, for which we cut the system into two equal parts. The splitting between the conformal part [21] and the non-conformal part, and the counting of the conformal states in the entanglement spectrum, demonstrate that DMRG has captured the correct topological properties of the ground state.

As a second case, we consider the filling $\nu = 5/2$, believed to be described by the Moore–Read Pfaffian state [3]. This state is more fragile than the Laughlin state and has a smaller gap by nearly an order of magnitude. To study the convergence, it is in principle possible to use the exact interaction that produces the Moore–Read state as a zero-energy ground state, but this is much more costly because it is a three-body interaction. The results for the Coulomb interaction projected to $n = 1$ Landau level are shown in Fig. 4. The ground-state energies are obtained for up to 30 electrons by keeping at most 5000 states. The result for the largest system size presented in this plot was obtained within one week on a computer cluster with 12 cores and 144G memory. With the same scaling techniques as in the $\nu = 1/3$ case, we extract the ground-state energy per electron in the thermodynamic limit $\approx -0.3622e^2/\ell_B$, consistent with Refs. [11,14].

3. Cylinder geometry

To complement the results obtained in the spherical geometry, in this section we consider the cylinder geometry [16]. Cylinder geometry is interesting because it shares some features with the compact geometries, such as sphere or torus, but also possesses two open boundaries, which makes it convenient for the study of the edge effects, like the disk geometry [22–24]. Compared to the sphere, the attractive feature of the cylinder is the flat surface and lack of curvature effects.

Cylinder boundary condition is compatible with the Landau gauge where periodic boundary condition is assumed along one

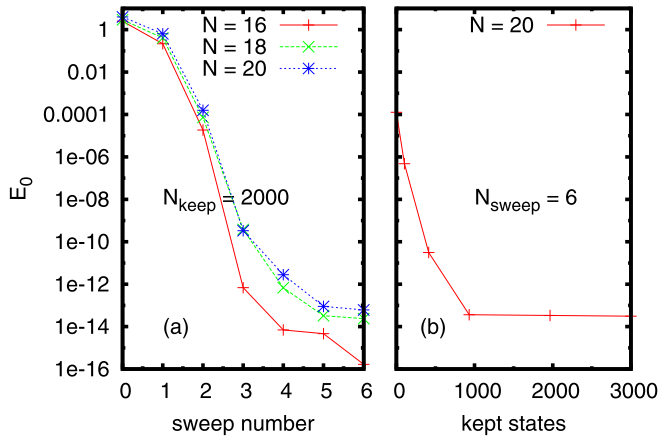


Fig. 5. The convergence of the ground-state energy for electrons with hard-core interaction on the cylinder. (a) We keep 2000 states in the truncation procedure for all the system sizes. The ground-state energy drops very fast in the finite-size sweeping procedure. (b) The dependence of the ground-state energy on the number of kept states for 20 electrons.

direction (say y -axis) with a repeat distance L , and open boundary condition in the other direction (x -axis). The single-body wavefunction in the lowest Landau level is given by

$$\psi_m(x, y) = \frac{1}{\sqrt{\pi^{1/2} L \ell_B}} e^{ik_m y} e^{-(x+k_m \ell_B)^2 / 2\ell_B^2}, \quad (3)$$

where $k_m = 2\pi m/L$ is the momentum for the m th orbital. The orbital index m takes values $0, 1, \dots, N_{orb} - 1$, and the distance in x -direction between two nearest orbitals is $2\pi/L$.

For a finite size system with N_e particles at filling $\nu = 1/3$ for example, the number of orbitals is $N_{orb} = 3N_e - 2$, and thus the area of the cylinder is quantized to be $2\pi N_{orb} \ell_B^2$. To accommodate the finite number of the orbitals N_{orb} , we fix the extent in the x -direction to be $X = 2\pi N_{orb} \ell_B^2 / L$. Similar to the torus geometry, the properties of many-body states depend on the aspect ratio $\lambda = X/L = 2\pi N_{orb} \ell_B^2 / L^2$. In the following we concentrate on the FQH states that are realized in the vicinity of $\lambda = 1$.

For the V_1 hard-core interaction, the Hamiltonian (in units $\ell_B = 1$) can be written in a simple form [16]:

$$H = \frac{1}{2} \sum_{m,n,l} (m^2 - n^2) e^{-(m^2+n^2)/2} a_{n+l}^+ a_{m+l}^+ a_{m+n+l} a_l. \quad (4)$$

Exact diagonalization studies [16,17] show that H has a zero-energy ground state, but the nature of the ground state changes from the incompressible liquid to the charge-density wave upon varying the aspect ratio. Here we focus on the liquid state and obtain it by DMRG method for large systems up to 20 electrons with the hard-core interaction.

The convergence of the ground state energy as a function of the sweep number and the number of kept states is shown in Fig. 5. For the system with 20 electrons, we obtain the ground state energy 10^{-13} when keeping only 2000 states and after completing 6 finite-size sweeps. On the other hand, if we look at the final ground state energy as a function of the number of the kept states, we observe that the same accuracy can be reached even by keeping only 1000 states.

To verify that the ground state is indeed the Laughlin state, we plot the average occupation number $\langle c_m^+ c_m \rangle$ for the system with 20 electrons in 58 orbitals in Fig. 6. For an incompressible liquid, the average occupation number is roughly constant in the bulk and equal to ν , with some deviations close to the two edges. This is indeed what we observe in Fig. 6.

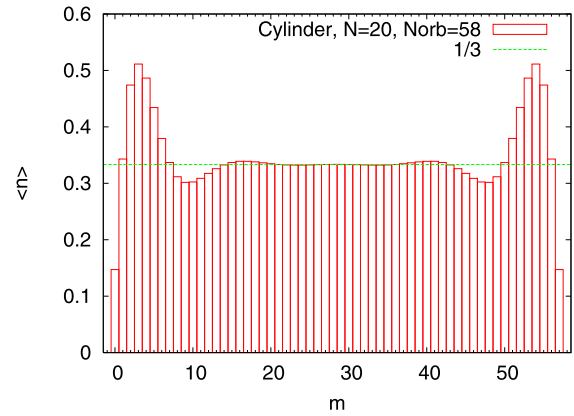


Fig. 6. The mean orbital occupation number for 20 electrons with hard-core interaction at $\nu = 1/3$ on the cylinder. DMRG calculation is performed by keeping 3000 states and finishing 6 finite size sweeps.

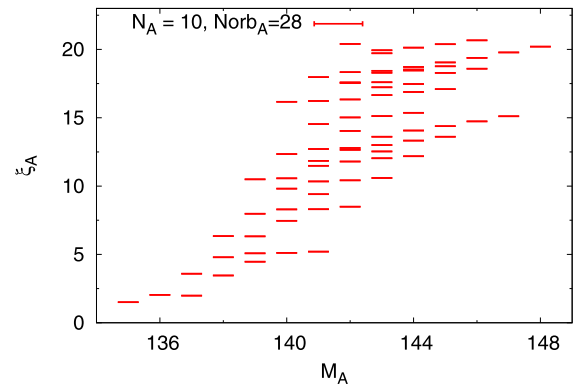


Fig. 7. The entanglement spectrum of the Laughlin state for 20 electrons on the cylinder. Because of the hard-core interaction, the entanglement spectrum only contains the conformal branch, with the same counting as in Fig. 3.

We also plot the entanglement spectrum on the cylinder, Fig. 7. Because we use the ground-state of the V_1 pseudopotential Hamiltonian, the entanglement spectrum only contains a conformal branch, but is otherwise similar to the spectrum obtained on the sphere, Fig. 3. In particular, the counting of the conformal levels is identical in the two cases (up to the limit set by the size of the sphere). Note that although the true energy spectrum reflects the presence of two edges on the cylinder, the entanglement spectrum involves only a single cut and thus probes only a single edge, in complete analogy with the sphere.

4. Conclusions and discussion

We presented a systematic study of the FQHE at two well-known and important filling factors, $\nu = 1/3$ and $\nu = 5/2$, for boundary conditions using our independent implementation of the DMRG method. In the spherical geometry, the DMRG results for the ground state energies at filling $\nu = 1/3$ and $\nu = 5/2$ are consistent with the exact diagonalization study for small system sizes, and the previous DMRG studies [11,14] for large system sizes. For the largest system size we have reached, the error of the ground state energy is about 10^{-4} which is roughly two–three orders of magnitude below the energy gap to the excited states. The consistency in the extrapolation of the ground-state energy shows that these system sizes have negligible curvature effects.

The application of the DMRG method to the cylinder geometry shows much higher efficiency compared to the sphere. Based on the convergence for the V_1 interaction, we expect the cylinder to

be the more promising venue for the future applications of DMRG. Due to the presence of two open edges, the treatment of the full Coulomb interaction is not as straightforward as in the compact spherical geometry, and requires special care in defining the confining potential to contain the fluid. One may furthermore expect various phase transitions as a function of the aspect ratio and the magnitude of the confining potential relative to $e^2\epsilon\ell_B$. Details of these studies will be presented elsewhere [15].

Acknowledgements

We would like to thank E.H. Rezayi, F.D.M. Haldane for simulating discussions. Z.-X. Hu also thanks Jize Zhao for comparing the results on the sphere. This work is supported by DOE grant No. DE-SC0002140.

References

- [1] D.C. Tsui, H.L. Stormer, A.C. Gossard, Phys. Rev. Lett. 48 (1982) 1559.
- [2] R.B. Laughlin, Phys. Rev. Lett. 50 (1983) 1395.
- [3] G. Moore, N. Read, Nucl. Phys. B 360 (1991) 362.
- [4] F.D.M. Haldane, Phys. Rev. Lett. 51 (1983) 605.
- [5] R.E. Prange, S.M. Girvin (Eds.), The Quantum Hall Effect, 2nd ed., Springer-Verlag, New York, 1990.
- [6] X. Du, et al., Nature 462 (2009) 192;
K. Bolotin, et al., Nature 462 (2009) 196;
C.R. Dean, et al., Nat. Phys. 7 (2011) 693.
- [7] N. Read, E. Rezayi, Phys. Rev. B 59 (1999) 8084.
- [8] S.R. White, Phys. Rev. Lett. 69 (1992) 2863.
- [9] J. Eisert, M. Cramer, M.B. Plenio, Rev. Mod. Phys. 82 (2010) 277.
- [10] N. Shibata, D. Yoshioka, Phys. Rev. Lett. 86 (2001) 5755.
- [11] A.E. Feiguin, E. Rezayi, C. Nayak, S. Das Sarma, Phys. Rev. Lett. 100 (2008) 166803.
- [12] E.J. Bergholtz, A. Karlhede, arXiv:cond-mat/0304517.
- [13] D.L. Kovrizhin, Phys. Rev. B 81 (2010) 125130.
- [14] Jize Zhao, D.N. Sheng, F.D.M. Haldane, Phys. Rev. B 83 (2011) 195135.
- [15] S. Johri, Z.-X. Hu, Z. Papić, R.N. Bhatt, F.D.M. Haldane, in preparation.
- [16] E.H. Rezayi, F.D.M. Haldane, Phys. Rev. B 50 (1994) 17199.
- [17] P. Soulé, T. Jolicoeur, arXiv:1111.2519.
- [18] G. Fano, F. Ortolani, E. Colombo, Phys. Rev. B 34 (1986) 2670.
- [19] R.H. Morf, Phys. Rev. Lett. 80 (1998) 1505.
- [20] R.H. Morf, N. d'Ambrumenil, S. Das Sarma, Phys. Rev. B 66 (2002) 075408.
- [21] H. Li, F.D.M. Haldane, Phys. Rev. Lett. 101 (2008) 010504.
- [22] X.-G. Wen, Int. J. Mod. Phys. B 6 (1992) 1711.
- [23] X. Wan, K. Yang, E.H. Rezayi, Phys. Rev. Lett. 88 (2002) 056802.
- [24] X. Wan, Z.-X. Hu, E.H. Rezayi, K. Yang, Phys. Rev. B 77 (2008) 165316.

Search Search History

All Databases

<< Return to Web of Science®

Citing Articles Title: Quantum Phase Transitions and the $\nu=5/2$ Fractional Hall State in Wide Quantum Wells
Author(s): Papic, Z.; Haldane, F. D. M.; Rezayi, E. H.
Source: PHYSICAL REVIEW LETTERS Volume: 109 Issue: 26 Article Number: 266806 DOI: 10.1103/PhysRevLett.109.266806 Published: DEC 27 2012

This item has been cited by items indexed in the databases listed below. [more information]

2 in All Databases

- 2 publication in Web of Science
0 publication in BIOSIS Citation Index
0 publication in SciELO Citation Index
0 publication in Chinese Science Citation Database
0 data sets in Data Citation Index
0 publication in Data Citation Index

Results: 2 Page 1 of 1 Go Sort by: Publication Date -- newest to oldest

Create Citation Report

Hide Refine

Refine Results

Search within results for

Search

Databases

Research Domains

SCIENCE TECHNOLOGY

Research Areas

PHYSICS

Document Types

Authors

Group/Corporate Authors

Editors

Funding Agencies

Source Titles

Conference/Meeting Titles

Publication Years

Languages

Countries/Territories

Select Page Add to Marked List (0) Send to: my.endnote.com

1. Title: Fractional quantum Hall effect in a tilted magnetic field
Author(s): Papic, Z.
Source: PHYSICAL REVIEW B Volume: 87 Issue: 24 Article Number: 245315 DOI: 10.1103/PhysRevB.87.245315 Published: JUN 27 2013
Times Cited: 2 (from All Databases)

Get it! Waterloo View abstract

2. Title: Landau level mixing and the fractional quantum Hall effect
Author(s): Sodemann, I.; MacDonald, A. H.
Source: PHYSICAL REVIEW B Volume: 87 Issue: 24 Article Number: 245425 DOI: 10.1103/PhysRevB.87.245425 Published: JUN 21 2013
Times Cited: 3 (from All Databases)

Get it! Waterloo View abstract

Select Page Add to Marked List (0) Send to: my.endnote.com

Results: 2 Show 50 per page Page 1 of 1 Go Sort by: Publication Date -- newest to oldest

2 records matched your query of the 55,067,330 (contains duplicates) in the data limits you selected.

View in: 简体中文 繁體中文 English 日本語 한국어 Português Español

Quantum Phase Transitions and the $\nu = 5/2$ Fractional Hall State in Wide Quantum Wells

Z. Papić,¹ F. D. M. Haldane,¹ and E. H. Rezayi²

¹*Department of Physics, Princeton University, Princeton, New Jersey 08544, USA*

²*Department of Physics, California State University, Los Angeles, California 90032, USA*

(Received 2 October 2012; published 27 December 2012)

We study the nature of the $\nu = 5/2$ quantum Hall state in wide quantum wells under the mixing of electronic subbands and Landau levels. A general method is introduced to analyze the Moore-Read Pfaffian state and its particle-hole conjugate, the anti-Pfaffian state, under periodic boundary conditions in a “quartered” Brillouin zone scheme containing both even and odd numbers of electrons. By examining the rotational quantum numbers on the torus, we show spontaneous breaking of the particle-hole symmetry can be observed in finite-size systems. In the presence of electronic-subband and Landau-level mixing, the particle-hole symmetry is broken in such a way that the anti-Pfaffian state is unambiguously favored, and becomes more robust in the vicinity of a transition to the compressible phase, in agreement with recent experiments.

DOI: [10.1103/PhysRevLett.109.266806](https://doi.org/10.1103/PhysRevLett.109.266806)

PACS numbers: 73.43.Cd, 63.20.Pw, 63.22.-m

The quantized Hall state at the $\nu = 5/2$ Landau level (LL) filling factor [1] has been the subject of significant recent interest due to a strong suspicion, with considerable support from the numerical calculations [2–5], that it is described by the Moore-Read “Pfaffian” (Pf) state [6]. This incompressible quantum fluid, which is a prototype state for non-Abelian exchange statistics [6,7], is found in the vicinity of the phase boundary with compressible phases characterized by stripe order and Fermi-liquid-like behavior [3]. Generally, the incompressible fluids of the fractional quantized Hall effect [8–10] possess protected gapless edge modes, and gapped bulk excitations which carry fractional charge and obey fractional statistics [6,11,12]. These attributes—quantization, fractionalization, and protection—represent the hallmark of topological phases [13]. In the case of non-Abelian states, the degeneracy of the quasiparticle states may be suitable to implement a “fault-tolerant” quantum computation [14].

The Moore-Read state, though defined in a half-filled LL, is not invariant under the particle-hole (p - h) transformation, and therefore its p - h conjugate partner—the “anti-Pfaffian” (APf) state [15]—emerged as a competing candidate to describe the ground state of $\nu = 5/2$. In experiment, either the Pf or APf state is realized, depending on the explicit form of the p - h symmetry-breaking fields (e.g., 3-body interaction [16] or more generally LL mixing [17–19]). In the absence of those, the true ground state is selected by spontaneous p - h symmetry breaking. A similar outcome should be reproducible in finite-size calculations, which have been known to capture remarkably well the fundamental aspects of fractional quantized Hall effect physics [10]. However, for technical reasons (see below), this never occurs for an even number of electrons, which has been the assumption of most studies to date [20,21].

Although the Pf and APf states have identical non-Abelian braiding properties in the bulk, they represent

distinct phases of matter as reflected, e.g., in their edge physics [22,23]—a signature of the underlying topological order [13]. A number of recent experiments have focused on measuring the quasiparticle charge at $\nu = 5/2$ [24–26], and on detecting the non-Abelian statistics using edge-tunneling interferometry [27,28]. These probes, while not definitive in all regards, are consistent with the non-Abelian statistics, and have provided additional insights into the nature of the ground state. In particular, the discovery of the counterpropagating mode [29] is consistent only with the APf state.

At the same time, other experiments have probed the stability of $\nu = 5/2$ by driving the transitions from the incompressible to the compressible phases such as the Fermi liquid-like state [30,31], and the anisotropic, stripe, and nematic phases [3,32]. This was accomplished by tilting the magnetic field [32], and by tuning the density in wide quantum well (WQW) samples [33,34]. In the latter case, it was recently noticed [34] that the quantized $\nu = 5/2$ state becomes stronger in the vicinity of a transition to the Fermi liquid-like phase.

In this Letter we introduce a new method to study the physics of the Moore-Read state and its p - h conjugate. We consider a compact torus geometry [35,36] with a quartered many-body Brillouin zone (BZ) for both even and odd numbers of electrons N_e . Regardless of the parity of N_e , for the Moore-Read 3-body Hamiltonian we obtain a zero-energy and zero-momentum ground state, with bosonic (“magneton”) and fermionic (“neutral fermion” [37]) collective modes at fixed N_e . This is in stark contrast, e.g., to the spherical geometry [38], where the zero-energy ground state only exists for even N_e , and the fermionic mode can only be obtained for odd N_e [37]. The essential physical similarity of the even and odd N_e cases on the torus enables us to restrict to the latter case when Pf and APf states can be further classified by their

invariance under discrete rotations in high symmetry Bravais lattices. For special odd values of N_e we recover spontaneous p - h symmetry breaking in finite systems as Pf and APf states acquire different angular momenta compatible with periodic boundary conditions (PBCs). This formalism is then applied to a realistic model of a wide quantum well with two subbands, $S1$ (symmetric subband with the $n = 1$ LL form factor) and $A0$ (antisymmetric subband with the $n = 0$ LL form factor), where p - h symmetry is broken explicitly by the mixing of electronic subbands and LLs as a result of tuning the density [34]. We identify the APf state as the one describing the ground state in these circumstances, and show that its gap increases prior to the transition to the compressible phase, in agreement with experiments [34].

We consider N_e electrons in a fundamental domain $\mathbf{L}_1 \times \mathbf{L}_2$ subject to magnetic field $B\hat{z}$. An operator that translates a single electron and commutes with the Hamiltonian is the magnetic translation operator which obeys a noncommutative algebra, leading to the quantization of the flux N_Φ threading the system, $\hat{z} \cdot (\mathbf{L}_1 \times \mathbf{L}_2) = 2\pi\ell_B^2 N_\Phi$, where $\ell_B = \sqrt{\hbar/eB}$ is the magnetic length. In a many-body system, symmetry classification is achieved by the help of the emergent many-body translation operators [36], which can be factorized into a center of mass and a relative part. The action of the former produces a characteristic degeneracy equal to q , where $N_e = pN$, $N_\Phi = qN$, and N is canonically assumed to be the greatest common divisor of N_e and N_Φ such that p and q are coprime. The eigenvalue of the relative translation operator is a many-body momentum \mathbf{k} [36] that fully classifies the spectrum in the BZ $N \times N$ zone, with the exception of high symmetry points where discrete symmetries may produce additional degeneracies, as we explain below.

For the outlined algebraic derivation it is not essential that p , q be coprime numbers. In fact, enforcing this condition might hide the important physical features of a fractional quantum Hall (FQH) state. This occurs for the Moore-Read state which possesses a pairing structure revealed in its fundamental root pattern 110011001100... that defines the clustering properties on genus-0 surfaces [39]. The corresponding filling factor $\nu = 1/2$ should be viewed as $\nu = 2/4$ because the root pattern admits two particles in each four consecutive orbitals. To incorporate this clustering condition, we need to map the wave vectors onto a quartered BZ $\tilde{N} \times \tilde{N}$ zone [40], which can be viewed as a result of “folding” the original $N \times N$ zone [see Fig. 1(a)]. For N even, the zone corner and midpoints of the zone sides all map to a $\mathbf{k} = 0$ point [red points in Fig. 1(a)]. These wave vectors also define the sectors of the Hilbert space where a threefold degenerate Moore-Read ground state is obtained [6]. The Moore-Read parent Hamiltonian also possesses a zero-energy ground state for an odd number of electrons, which corresponds to a single unpaired electron with $\mathbf{k} = 0$ [7]. In this case, the folding

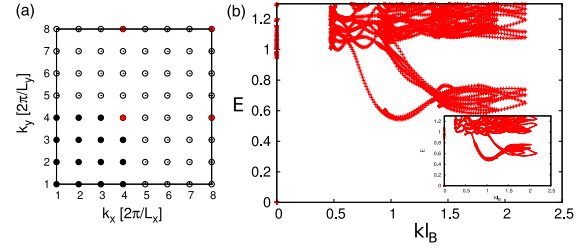


FIG. 1 (color online). (a) An example of a squared many-body BZ (open circles), and the folding to a quartered BZ (black circles) for even N_e . Red circles denote sectors that map to the zero momentum $\mathbf{k} = 0$ sector. (b) Energy spectrum of the Moore-Read 3-body Hamiltonian in a quartered BZ for $N_e = 14$ and $N_e = 13$ (inset) particles.

still “compactifies” the original BZ, but the $\mathbf{k} = 0$ sector remains invariant under the folding. Thus, in the quartered BZ, the ground states of the Moore-Read Hamiltonian are invariably obtained in the $\mathbf{k} = 0$ sector of the Hilbert space, as they should be for an incompressible liquid, and the threefold degenerate states are allowed to mix.

Advantages of the quartered BZ become obvious when the full energy spectrum of the Moore-Read 3-body Hamiltonian $H_{3b} = -\sum_{i<j<k} \mathcal{S}_{ijk} [\nabla_i^4 \nabla_j^2 \delta(\mathbf{r}_i - \mathbf{r}_j) \delta(\mathbf{r}_j - \mathbf{r}_k)]$ is studied as a function of momentum [see Fig. 1(b)]. Using the conventional definition of the BZ, there is no obvious structure in the low-lying excitation spectrum of the Moore-Read 3-body Hamiltonian. However, if the same spectrum is replotted in a quartered zone, it reveals a bosonic mode (the magnetoroton) and a fermionic mode (neutral fermion) [37]. Because of the BZ folding, in the even case ($N_e = 14$) we obtain three copies of the bosonic mode and a single copy of the fermionic one. In the odd case ($N_e = 13$), the multiplicities are interchanged [40]. Contrary to spherical geometry where spectra for different particle numbers have to be superimposed on the same plot to resolve the two modes, on the torus both modes are obtained for a fixed system size N_e . An additional advantage of PBCs is that one can access a quasicontinuum of the momenta \mathbf{k} , as opposed to a much smaller subset of angular momenta on the sphere. This is achieved by adiabatic variation of the shape of the unit cell in terms of its aspect ratio $|\mathbf{L}_1|/|\mathbf{L}_2|$ or the angle between vectors \mathbf{L}_1 and \mathbf{L}_2 , subject to a constraint that the area $|\mathbf{L}_1 \times \mathbf{L}_2|$ remains fixed and equal to $2\pi\ell_B^2 N_\Phi$. In Fig. 1 we set the ratio equal to unity, and vary the angle between the square and the hexagon.

Using the quartered BZ we can also directly address the phase transition between the Moore-Read state and the composite Fermi liquid (CFL). Spherical geometry is inadequate for this purpose because the two states have different “shifts” [41]. To capture the transition, we study the energy spectrum of a Hamiltonian that interpolates between the model 3-body Hamiltonian and the $n = 0$ LL Coulomb interaction, $\lambda H_{3b} + (1 - \lambda) H_C$. In a quartered

BZ, the spectra for even and odd N_e are strikingly similar, and the data in Fig. 2 correspond to $N_e = 11$ which is also studied in a different model below. The neutral fermion and the magnetoroton modes become significantly distorted and difficult to identify for $\lambda < 1$; nevertheless, one can track their evolution until the eventual collapse of the gap for $\lambda \rightarrow 0$. At this point the ground state moves from $k = 0$ to some $k \sim \ell_B^{-1}$, and the system undergoes a second-order transition to the compressible phase. In contrast, for the $n = 1$ LL Coulomb interaction, a similar calculation does not lead to the gap closing for any λ . Adiabatic variation of PBCs also enables one to calculate, e.g., the Hall viscosity, which is expected to diverge at the $\lambda = 0$ point. The regime of small λ might display an interesting crossover between type-I and type-II superconducting behavior [42].

In order to address the competition between the Pf and APf states for the generic (2-body) interactions, it is essential to consider all possible symmetries of the Hamiltonian at half filling. In particular, the two symmetries of interest here are the p - h conjugation τ_{ph} , and discrete rotations compatible with PBCs [43,44]. The first is represented by an antiunitary operator formally similar to the well-known case of the time-reversal operator [45]. In the presence of both symmetries, extra (isolated) degeneracies may occur which belong to conjugate or corepresentations of discrete rotations [36,45]. In the case of even N_e , rotational symmetry does not lead to any additional quantum numbers for the ground state at $\nu = 5/2$. For some $\mathbf{k} = 0$ excited states, $\tau_{ph}^2 = -1$ and these, following Kramer's theorem, are all doubly degenerate. On the other hand, for odd N_e and $\mathbf{k} = 0$, $\tau_{ph}^2 = 1$ and only isolated degeneracies are possible. The ground state in this case is either unique or a doublet. For any geometry other than hexagonal, the ground state is a singlet. For hexagonal geometry, the ground state is also a singlet if the number of electrons is given by $N_e = 6m + 1$, where $m \in \mathbb{Z}$. For other N_e , the ground state is a doublet [46].

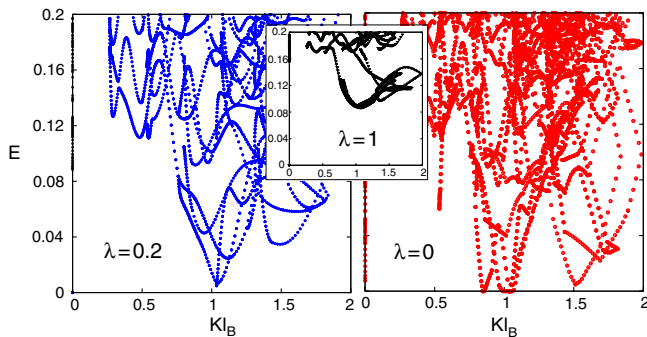


FIG. 2 (color online). Transition between the Moore-Read and the composite Fermi liquid state. Energy spectrum of $\lambda H_{3b} + (1 - \lambda)H_C$ is plotted as a function of momentum for $\lambda = 0.2$ (left) and $\lambda = 0$ (right), illustrating the collapse of the neutral mode around $k \sim \ell_B^{-1}$. Inset shows the spectrum for pure H_{3b} .

To understand these trends for generic Hamiltonians it is helpful to consider the rotational properties of Pf and APf model states. On the torus with n -fold point symmetry, the angular momentum of the APf state, measured relative to the Pf state, is given by $\Delta M = 2N_{\text{pair}} \pmod{n}$, where N_{pair} is the number of paired electrons. For $n = 2$ or $n = 4$ (square or lower symmetry), $\Delta M = 0$ since N_{pair} is always even. Thus there is no symmetry reason for the Pf and APf states (being the eigenstates of different Hamiltonians) to be orthogonal. On the other hand, for $n = 6$, $\Delta M \neq 0$ if $N_e \neq 6m + 1$, and the two states are necessarily orthogonal. It is under precisely these conditions that the doublet ground states are observed. These seemingly unrelated events are another confirmation that in the case of the Coulomb interactions the system is in the Moore-Read phase. There are always doublets present in the spectrum, but they describe the ground state only in cases where the Pf and APf states have $\Delta M \neq 0$. Evidently, the rotational quantum numbers of the doublet match those of the Pf and APf states. There will be no spontaneous breaking of the p - h symmetry in the absence of such degeneracies until the thermodynamic limit is reached. Achieving this property for finite sizes makes the comparison of the exact ground state with the Pf or APf state much cleaner than the case of even N_e , for example. As we show below, LL mixing splits the doublets in such a way that each member has a finite overlap with either the Pf or APf state, while having zero overlap with the other.

We illustrate the ideas above on a model of the WQW in which electrons can populate two “active” subbands with LL indices $n = 0$ and $n = 1$ [47]. We refer to these levels as A0 and S1, where S, A stands for the wave function in the perpendicular $z \in [0, w]$ direction, w being the width of the well. For simplicity, we assume reflection symmetry around $z = w/2$, and the two subbands are given by symmetric or antisymmetric infinite square well wave functions $\varphi_S = \sqrt{2/w} \sin(\pi z/w)$, $\varphi_A = \sqrt{2/w} \sin(2\pi z/w)$. The remaining subbands are either completely filled or completely empty, and excitations to them are forbidden. The energy splitting between the subbands, Δ_{SAS} , can be realistically tuned by electrostatic gates [34], but in our calculation it is assumed to be an independent parameter. This model is expected to provide a realistic description of a number of recent experiments on the WQWs where FQH states were probed by tuning the effective interaction via subband and LL mixing. In particular, we focus on $\nu = 5/2$ considering a half-filled S1 level mixing with an A0 level. It is assumed that the electron spin is fully polarized [2,48–51].

In Fig. 3(a) we plot the neutral gap and mean value of the pseudospin operator $S_z = \frac{1}{2} \sum_i (c_{S,i}^\dagger c_{S,i} - c_{A,i}^\dagger c_{A,i})$ in the ground state for $N_e = 10$ particles. We set $w/\ell_B = 2.7$, which roughly agrees with the experimental width [32,34]. When Δ_{SAS} is large, excitations to the A0 level are costly, and the ground state is fully polarized in the S1 level and it

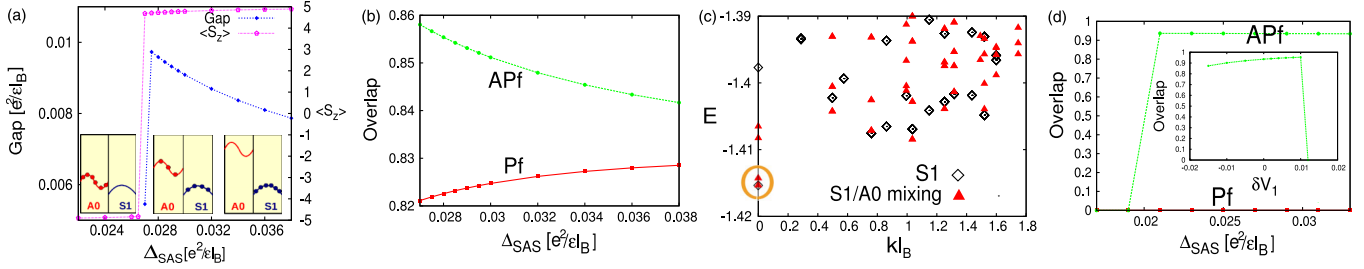


FIG. 3 (color online). (a) Neutral gap and mean value of the pseudospin S_z for $N_e = 10$ particles at half filling in a WQW ($w/\ell_B = 2.7$). Transition is driven by changing Δ_{SAS} , and relative position of the electronic subbands is schematically shown in the inset. (b) Overlap between the exact $N_e = 10$ ground state (projected onto $S1$ subband) and the Pf and APf wave functions. In the transition region ($\Delta_{SAS} \approx 0.028$) APf becomes favored. (c) Energy spectrum for infinite Δ_{SAS} (black diamonds) with an exact doublet at $k = 0$, and the splitting of the doublet when Δ_{SAS} is reduced (red triangles). (d) Same as in (b) but for $N_e = 11$, when Pf and APf are mutually orthogonal. Δ_{SAS} breaks PH symmetry and unambiguously selects APf (95% overlap) over Pf (zero overlap). Inset shows the effect of varying the V_1 pseudopotential.

is of the same nature as the one that is usually observed in wide samples. As Δ_{SAS} becomes smaller, the difference of $n = 0$ and $n = 1$ LL form factors makes it increasingly favorable to promote particles into the A0 level and reduce the correlation energy. Eventually, all particles migrate to the A0 subband, where they form a composite Fermi liquid; as shown in Fig. 3(a), this happens slightly before the actual coincidence of the two subbands. The steplike behavior of $\langle S_z \rangle$ suggests the transition to be very sharp, and we find it to be more affected by the difference in LL (rather than the subband) form factors. Right before the transition, excitations from $S1$ to A0 lead to an increase of the neutral gap of the system [34]. We believe the increase of the gap to be an intrinsic feature of the system, but limitations on the system sizes attainable by exact diagonalization prevent us from performing a proper finite-size scaling of the gap.

Finally, we investigate the nature of the ground state before the transition to the compressible phase. In Fig. 3(b) we compare the $N_e = 10$ electron ground state (projected to the $S1$ level) with the Pf and APf wave functions defined on a hexagonal unit cell. At large Δ_{SAS} , the p - h symmetry is preserved, and the Pf and APf states have identical overlaps with the exact state. In the transition region, p - h symmetry is lifted, and the APf overlap is growing while that of the Pf state is decreasing. However, the Pf and APf states have a significant overlap with each other for $N_e = 10$ particles [19]. To avoid this problem, we instead consider the $N_e = 11$ case, when discrete symmetry forces the Pf and APf states to be orthogonal. At the same time, the Coulomb ground state, which is exactly twofold degenerate for infinite Δ_{SAS} , splits when Δ_{SAS} is reduced [see Fig. 3(c)]. The size of the full Hilbert space for $N_e = 11$ is very large to be directly diagonalized, so we limit the number of excitations to the higher subband [19]. The convergence is found to be rapid, and the essential properties of the ground state and the transition point can be captured accurately by allowing for not more than three electrons in a higher subband. The effect of a small amount

of symmetry-breaking by Δ_{SAS} is sufficient to select the APf state with 95% overlap with the ground state, while the Pf overlap drops to zero [see Fig. 3(d)]. The APf overlap can be increased further by varying the V_1 pseudopotential in a “SU(2)-invariant” manner [19] [see Fig. 3(d), inset]. These results provide unambiguous evidence that the ground state of the WQW is described by the APf state.

In summary, we have demonstrated that PBCs for special finite systems with an appropriately defined BZ are essential for the study of the non-Abelian FQH states, their collective excitation spectra, and the effects of particle-hole symmetry breaking in WQWs under LL and subband mixing. Although we have presented results for the case of $S1$ and A0 mixing, the more common case of $S1$ and $S2$ mixing (applicable to narrower quantum well samples) similarly selects the APf state to describe the ground state. This conclusion is not affected by mixing in even higher LLs ($S3$ and beyond). The sharpness of the transition and the “population inversion” illustrated in Fig. 3 might be relevant for the emergence of lowest LL physics under extreme tilting of the magnetic field [32].

We thank J. Eisenstein, M. Levin, N. Read, S. H. Simon, and in particular Y. Liu and M. Shayegan for valuable discussions. Z.P. would like to thank A. Sterdyniak, N. Regnault, and B. A. Bernevig for useful comments. We acknowledge support by DOE Grant No. DE-SC0002140, and the Keck Foundation.

- [1] R. Willett, D. C. Tsui, A. C. Gossard, and J. H. English, *Phys. Rev. Lett.* **59**, 1776 (1987).
- [2] R. H. Morf, *Phys. Rev. Lett.* **80**, 1505 (1998).
- [3] E. H. Rezayi and F. D. M. Haldane, *Phys. Rev. Lett.* **84**, 4685 (2000).
- [4] M. Storni, R. H. Morf, and S. D. Sarma, *Phys. Rev. Lett.* **104**, 076803 (2010).
- [5] H. Lu, S. D. Sarma, and K. Park, *Phys. Rev. B* **82**, 201303 (2010).
- [6] G. Moore and N. Read, *Nucl. Phys.* **B360**, 362 (1991).

- [7] N. Read and D. Green, *Phys. Rev. B* **61**, 10267 (2000).
- [8] D.C. Tsui, H.L. Stormer, and A.C. Gossard, *Phys. Rev. Lett.* **48**, 1559 (1982).
- [9] R.B. Laughlin, *Phys. Rev. Lett.* **50**, 1395 (1983).
- [10] *The Quantum Hall Effect*, edited by R.E. Prange and S.M. Girvin (Springer-Verlag, Berlin, 1990), 2nd ed.
- [11] N. Read and E. Rezayi, *Phys. Rev. B* **54**, 16864 (1996).
- [12] D. Arovas, J.R. Schrieffer, and F. Wilczek, *Phys. Rev. Lett.* **53**, 722 (1984); P. Bonderson, V. Gurarie, and C. Nayak, *Phys. Rev. B* **83**, 075303 (2011).
- [13] X.-G. Wen, *Int. J. Mod. Phys. B* **06**, 1711 (1992).
- [14] A. Y. Kitaev, *Ann. Phys. (Amsterdam)* **303**, 2 (2003); C. Nayak, A. Stern, M. Freedman, and S.D. Sarma, *Rev. Mod. Phys.* **80**, 1083 (2008).
- [15] M. Levin, B. I. Halperin, and B. Rosenow, *Phys. Rev. Lett.* **99**, 236806 (2007); S.-S. Lee, S. Ryu, C. Nayak, and M.P.A. Fisher, *Phys. Rev. Lett.* **99**, 236807 (2007).
- [16] H. Wang, D. N. Sheng, and F. D. M. Haldane, *Phys. Rev. B* **80**, 241311(R) (2009).
- [17] W. Bishara and C. Nayak, *Phys. Rev. B* **80**, 121302 (2009).
- [18] A. Wójs, C. Tóke, and J.K. Jain, *Phys. Rev. Lett.* **105**, 096802 (2010).
- [19] E.H. Rezayi and S.H. Simon, *Phys. Rev. Lett.* **106**, 116801 (2011).
- [20] M. R. Peterson, K. Park, and S. D. Sarma, *Phys. Rev. Lett.* **101**, 156803 (2008).
- [21] M. R. Peterson, T. Jolicoeur, and S. D. Sarma, *Phys. Rev. B* **78**, 155308 (2008); M. R. Peterson, T. Jolicoeur, and S. D. Sarma, *Phys. Rev. Lett.* **101**, 016807 (2008).
- [22] M. Milovanović and N. Read, *Phys. Rev. B* **53**, 13559 (1996).
- [23] X. Wan, Z.-X. Hu, E. H. Rezayi, and K. Yang, *Phys. Rev. B* **77**, 165316 (2008).
- [24] I. Radu, J.B. Miller, C.M. Marcus, M.A. Kastner, L.N. Pfeiffer, and K.W. West, *Science* **320**, 899 (2008).
- [25] M. Dolev, M. Heiblum, V. Umansky, A. Stern, and D. Mahalu, *Nature (London)* **452**, 829 (2008).
- [26] V. Venkatachalam, A. Yacoby, L. Pfeiffer, and K. West, *Nature (London)* **469**, 185 (2011).
- [27] R.L. Willett, L. N. Pfeiffer, and K. W. West, *Phys. Rev. B* **82**, 205301 (2010).
- [28] S. An, P. Jiang, H. Choi, W. Kang, S.H. Simon, L.N. Pfeiffer, K. W. West, and K. W. Baldwin, [arXiv:1112.3400](https://arxiv.org/abs/1112.3400).
- [29] A. Bid, N. Ofek, H. Inoue, M. Heiblum, C.L. Kane, V. Umansky, and D. Mahalu, *Nature (London)* **466**, 585 (2010).
- [30] E. Rezayi and N. Read, *Phys. Rev. Lett.* **72**, 900 (1994).
- [31] B.I. Halperin, P.A. Lee, and N. Read, *Phys. Rev. B* **47**, 7312 (1993).
- [32] J. Xia, V. Cvicek, J. Eisenstein, L. Pfeiffer, and K. West, *Phys. Rev. Lett.* **105**, 176807 (2010).
- [33] J. Nuebler, B. Friess, V. Umansky, B. Rosenow, M. Heiblum, K. von Klitzing, and J. Smet, *Phys. Rev. Lett.* **108**, 046804 (2012).
- [34] Y. Liu, D. Kamburov, M. Shayegan, L. Pfeiffer, K. West, and K. Baldwin, *Phys. Rev. Lett.* **107**, 176805 (2011).
- [35] D. Yoshioka, B. I. Halperin, and P. A. Lee, *Phys. Rev. Lett.* **50**, 1219 (1983).
- [36] F.D.M. Haldane, *Phys. Rev. Lett.* **55**, 2095 (1985).
- [37] G. Möller, A. Wójs, and N.R. Cooper, *Phys. Rev. Lett.* **107**, 036803 (2011); P. Bonderson, A.E. Feiguin, and C. Nayak, *Phys. Rev. Lett.* **106**, 186802 (2011).
- [38] F.D.M. Haldane, *Phys. Rev. Lett.* **51**, 605 (1983).
- [39] B. A. Bernevig and F. D. M Haldane, *Phys. Rev. Lett.* **100**, 246802 (2008).
- [40] F. D. M. Haldane (unpublished).
- [41] X. G. Wen and A. Zee, *Phys. Rev. Lett.* **69**, 953 (1992).
- [42] S. A. Parameswaran, S. A. Kivelson, S. L. Sondhi, and B. Z. Spivak, *Phys. Rev. Lett.* **106**, 236801 (2011).
- [43] Z. Papić *et al.* (unpublished).
- [44] Y.-L. Wu, N. Regnault, and B. A. Bernevig, *Phys. Rev. B* **86**, 085129 (2012).
- [45] M. Tinkham, *Group Theory and Quantum Mechanics* (McGraw Hill, New York, 1964).
- [46] In some cases the doublet is not the ground state but very near it. Tweaking the interaction by varying the thickness of the two-dimensional layer or varying the pseudopotentials makes it the ground state.
- [47] Z. Papić, G. Möller, M. V. Milovanović, N. Regnault, and M. O. Goerbig, *Phys. Rev. B* **79**, 245325 (2009).
- [48] A.E. Feiguin, E. Rezayi, K. Yang, C. Nayak, and S.D. Sarma, *Phys. Rev. B* **79**, 115322 (2009).
- [49] M. Stern *et al.*, [arXiv:1201.3488](https://arxiv.org/abs/1201.3488).
- [50] L. Tiemann *et al.*, [arXiv:1201.3737](https://arxiv.org/abs/1201.3737).
- [51] X. Lin, C. Dillard, M. Kastner, L. Pfeiffer, and K. West, *Phys. Rev. B* **85**, 165321 (2012).

All Databases | Select a Database | Web of Science | Additional Resources

Search Search History

All Databases

<< Return to Web of Science®

Citing Articles Title: Matrix product states for trial quantum Hall states
Author(s): Estienne, B. ; Papic, Z. ; Regnault, N. ; et al.
Source: PHYSICAL REVIEW B Volume: 87 Issue: 16 Article Number: 161112 DOI: 10.1103/PhysRevB.87.161112 Published: APR 15 2013

This item has been cited by items indexed in the databases listed below. [more information]

4 in All Databases

- 4 publication in Web of Science
0 publication in BIOSIS Citation Index
0 publication in ScELO Citation Index
0 publication in Chinese Science Citation Database
0 data sets in Data Citation Index
0 publication in Data Citation Index

Results: 4 Page 1 of 1 Go Sort by: Publication Date -- newest to oldest

Create Citation Report

Refine Results

Search within results for

Search

Databases

Research Domains Refine

SCIENCE TECHNOLOGY

Research Areas Refine

PHYSICS

Document Types

Authors

Group/Corporate Authors

Editors

Funding Agencies

Source Titles

Conference/Meeting Titles

Publication Years

Languages

Countries/Territories

Select Page Add to Marked List (0) Send to: my.endnote.com

1. Author(s): Bergholtz, Emil J.; Liu, Zhao
Source: INTERNATIONAL JOURNAL OF MODERN PHYSICS B Volume: 27 Issue: 24 Article Number: 1330017 DOI: 10.1142/S021797921330017X
Published: SEP 30 2013
Times Cited: 0 (from All Databases)
Get it! Waterloo View abstract

2. Author(s): Jackson, T. S.; Read, N.; Simon, S. H.
Source: PHYSICAL REVIEW B Volume: 88 Issue: 7 Article Number: 075313 DOI: 10.1103/PhysRevB.88.075313 Published: AUG 26 2013
Times Cited: 0 (from All Databases)
Get it! Waterloo View abstract

3. Author(s): Liu, Zhao; Kovrizhin, D. L.; Bergholtz, Emil J.
Source: PHYSICAL REVIEW B Volume: 88 Issue: 8 Article Number: 081106 DOI: 10.1103/PhysRevB.88.081106 Published: AUG 26 2013
Times Cited: 1 (from All Databases)
Get it! Waterloo View abstract

4. Author(s): Zaletel, Michael P.; Mong, Roger S. K.; Pollmann, Frank
Source: PHYSICAL REVIEW LETTERS Volume: 110 Issue: 23 Article Number: 236801 DOI: 10.1103/PhysRevLett.110.236801 Published: JUN 4 2013
Times Cited: 3 (from All Databases)
Get it! Waterloo View abstract

Select Page Add to Marked List (0) Send to: my.endnote.com

Results: 4 Show 50 per page Page 1 of 1 Go Sort by: Publication Date -- newest to oldest

4 records matched your query of the 55,067,330 (contains duplicates) in the data limits you selected.

View in: 简体中文 繁體中文 English 日本語 한국어 Português Español

Matrix product states for trial quantum Hall states

B. Estienne,¹ Z. Papić,² N. Regnault,^{2,3} and B. A. Bernevig²

¹*LPTHE, CNRS, UPMC, Université Paris 06, Boîte 126, 4 Place Jussieu, F-75252 Paris CEDEX 05, France*

²*Department of Physics, Princeton University, Princeton, New Jersey 08544, USA*

³*Laboratoire Pierre Aigrain, ENS and CNRS, 24 Rue Lhomond, 75005 Paris, France*

(Received 20 November 2012; revised manuscript received 8 April 2013; published 15 April 2013)

We obtain an exact matrix-product-state (MPS) representation of a large series of fractional quantum Hall (FQH) states in various geometries of genus 0. The states in question include all paired $k = 2$ Jack polynomials, such as the Moore-Read and Gaffnian states, as well as the Read-Rezayi $k = 3$ state. We also outline the procedures through which the MPSs of other model FQH states can be obtained, provided their wave function can be written as a correlator in a $1 + 1$ conformal field theory (CFT). The auxiliary Hilbert space of the MPS, which gives the counting of the entanglement spectrum, is then simply the Hilbert space of the underlying CFT. This formalism enlightens the link between entanglement spectrum and edge modes. Properties of model wave functions such as the thin-torus root partitions and squeezing are recast in the MPS form, and numerical benchmarks for the accuracy of the new MPS prescription in various geometries are provided.

DOI: [10.1103/PhysRevB.87.161112](https://doi.org/10.1103/PhysRevB.87.161112)

PACS number(s): 73.43.-f, 05.10.Cc, 11.25.Hf, 71.27.+a

The understanding and simulation of quantum many-body states in one space dimension has experienced revolutionary progress with the advent of the density matrix renormalization group.¹ In modern language, this method can be viewed as a variational optimization over the set of matrix product states (MPSs).^{2,3} Indeed, gapped one-dimensional systems (which generally have low entanglement) can be very efficiently simulated by expressing the weights of many-body noninteracting states in an interacting wave function as products of finite-dimensional matrices $B[i]^{m_i}$ associated with each occupied ($m_i = 1$) or unoccupied ($m_i = 0$) site i (or spin): $|\psi\rangle = \sum_{\{m_i\}} P_L B[1]^{m_1} B[2]^{m_2} \dots B[N_s]^{m_{N_s}} P_R |m_1, m_2, \dots, m_{N_s}\rangle$. P_L , P_R are projectors into the state at the end of the chain (absent for periodic boundary conditions or the infinite chain). As long as the “bond dimension” χ of the matrix $B[i]$ is less than 2^i , this provides a more economical representation of the state. Generic 1D gapped systems can be approximated by finite χ .⁴ Critical systems however require an MPS with an infinite bond dimension.^{5,6}

Due to their perimeter law entanglement, 2D systems (such as the fractional quantum Hall effect) are harder to simulate by MPSs.^{7–10} In a recent paper¹¹ exploiting the fact that fractional quantum Hall (FQH) model states can be written as correlators of primary fields in conformal field theories (CFTs), an MPS expression was obtained for continuum Laughlin¹² and Moore-Read¹³ states on infinite cylinders. The bond dimension χ grows with the number of particles but scales with the circumference L of the cylinder rather than its area. Approximate expressions can be obtained by truncating χ of the exact MPS. A key ingredient of Ref. 11 is the expansion of operators in a free basis (boson for Laughlin and Majorana plus boson for Moore-Read), which cannot be easily implemented in the more complicated, interacting bases of other FQH states such as the Read-Rezayi series.¹⁴ The exciting possibility is that if all model FQH states could be written in MPS form, current numerical barriers could be broken and properties such as correlation functions would be computable for large sizes. This is supported by the continuous MPS proposed in Ref. 15.

In this Rapid Communication we provide a generic prescription that enables us to obtain the unnormalized (thin annulus) MPS form of a model FQH state which is the correlator of a primary field in a CFT. We explicitly construct the MPS for the $(k, r) = (2, r)$ paired Jack polynomial states^{16,17} ($r = 2, 3$ being the Moore-Read and Gaffnian¹⁸ wave functions), as well as for $(k, r) = (3, 2)$ corresponding to the Read-Rezayi Z_3 wave function.¹⁴ Several key ingredients and subtleties, such as the presence of non-orthonormal bases, null vectors, and intricate operator commutation relations, are discussed. We then show how to extend the MPS description to different manifolds such as the cylinder, sphere, and plane, and how several known properties of the CFT wave functions such as squeezing arise naturally in this description. We then generate several [($k, r) = (2, 2), (2, 3), (2, 6), (3, 2)$] of these states numerically to verify our MPS, and provide numerical benchmarks to attest to the accuracy of the MPS on the cylinder¹⁹ and sphere.²⁰

A large class of FQH ground states are described by the many-point correlation function of an electron operator field $V(z)$ in a chiral $1 + 1$ CFT:¹³

$$\langle N_e \sqrt{q} | V(z_{N_e}) \dots V(z_1) | 0 \rangle = \sum_{\lambda} c_{\lambda} m_{\lambda}(z_1, \dots, z_{N_e}) \quad (1)$$

where m_{λ} are monomials (or Slater determinants for fermions) of angular momentum $\lambda = (\lambda_1, \dots, \lambda_{N_e})$. N_e is the number of electrons, and the filling fraction is $\nu = 1/q$ (note that q will not always be integer). The state $\langle N_e \sqrt{q} |$ describes the background charge at infinity. The coefficient c_{λ} can be obtained by contour integrals. Upon inserting a complete basis of states on the left-hand side of (1) we get

$$c_{\lambda} = \sum_{\{\alpha_j\}} \prod_{j=1}^{N_e} \frac{1}{2\pi i} \oint \frac{dz_j}{z_j^{\lambda_j+1}} \langle \alpha_j | V(z_j) | \alpha_{j-1} \rangle. \quad (2)$$

The $U(1)$ charge of $|\alpha_0\rangle, |\alpha_{N_e}\rangle$ is $0, N_e \sqrt{q}$, respectively. This is an infinite, site (Landau level orbital momentum) dependent MPS $|\Psi\rangle = \sum_{\{m_i\}} (\tilde{B}^{m_1}[1] \dots \tilde{B}^{m_{N_e}}[N_{\Phi}])_{N_e \sqrt{q}, 0} |m_1 \dots m_{N_e}\rangle$, with the matrices for an orbital j being, in the limit of an annulus with a very large radius (the so-called “conformal limit”) $\langle \alpha' | \tilde{B}^0[j] | \alpha \rangle = \delta_{\alpha', \alpha}$ and $\langle \alpha' | \tilde{B}^1[j] | \alpha \rangle =$

$\delta_{\Delta_{\alpha'}, \Delta_{\alpha+h+j}} \langle \alpha' | V(1) | \alpha \rangle$. h is the conformal dimension of $V(z)$, and higher occupation number (of occupation m) matrices are simply $\tilde{B}^m[j] = (\tilde{B}^1[j])^m / \sqrt{m!}$.

To obtain a site-independent MPS, we need to spread the background charge uniformly over the droplet. We make explicit the dependence on the $U(1)$ charge by writing states $|\alpha\rangle = |Q\rangle \otimes |\tilde{\alpha}\rangle$, where Q is the $U(1)$ charge and $\tilde{\alpha}$ encodes the rest (descendant, neutral sector). As the matrix element $\langle \tilde{\alpha}' | V(1) | \tilde{\alpha} \rangle$ does not depend on charge Q , we are free to modify the distribution of the background charge. Spreading uniformly the background charge amounts to an insertion of a $U(1)$ background charge $-1/\sqrt{q}$ between each orbital. This yields a site-independent MPS with $B^m = e^{-i/2\sqrt{q}\varphi_0} V_0^m e^{-i/2\sqrt{q}\varphi_0} / \sqrt{m!}$, where φ_0 is the $U(1)$ boson zero mode.

$$\langle \alpha' | V_0 | \alpha \rangle = \frac{1}{2\pi i} \oint \frac{dz}{z} \langle \alpha' | V(z) | \alpha \rangle, \quad (3)$$

where α and α' are the basis of descendants in the CFT (not free fermions as in Ref. 11). Our expression further differs from the one in Ref. 11 by time-evolution terms $U(\delta\tau) = \exp(-\delta\tau L_0)$, which give the cylinder normalization. Conformal invariance yields

$$\langle \alpha' | V(z) | \alpha \rangle = z^{\Delta_{\alpha'} - \Delta_{\alpha} - h} \langle \alpha' | V(1) | \alpha \rangle, \quad (4)$$

where h, Δ_{α} are the conformal dimensions of the primary field $V(z)$ and of the descendent $|\alpha\rangle$. The matrix elements of V_0 are then related to the CFT 3-point function $\langle \alpha' | V_0 | \alpha \rangle = \delta_{\Delta_{\alpha'}, \Delta_{\alpha+h}} \langle \alpha' | V(1) | \alpha \rangle$. The ‘‘electron operator’’ is a primary field of the tensor product form $V(z) = \Phi(z) \otimes : e^{i\sqrt{q}\varphi(z)} :$, where $\Phi(z)$ lives in the so-called neutral $|a\rangle$ conformal field theory CFT_n factorized from the $U(1)$ sector $|b\rangle$. In this basis $|\alpha\rangle = |a\rangle \otimes |b\rangle$ the 3-point function factorizes as $\langle a'; b' | V(1) | a; b \rangle = \delta_{\Delta_{a'}, \Delta_{b'}, \Delta_a + \Delta_b + h} \langle a' | \Phi(1) | a \rangle \langle b' | : e^{i\beta\varphi(1)} : | b \rangle$ where $h = q^2/2 + h_{\Phi}$ is the conformal dimension of $V(z)$. Note the delta function in the total conformal dimension of the field and not separately in the neutral and $U(1)$ parts. In the following we explain how to obtain the neutral, interacting CFT matrix elements for the case of (k, r) Jacks for $k = 2$ and $k = 3$.

First, we reevaluate the $U(1)$ matrix elements in a way easily generalizable to non-free-field CFT and in a basis where they are real:

$$\varphi(w) = \varphi_0 - i a_0 \ln(w) + i \sum_{n \neq 0} \frac{1}{n} a_n w^{-n}, \quad (5)$$

where a_n are the bosonic modes obeying the Heisenberg algebra $[a_n, a_m] = n \delta_{n+m, 0}$. a_0 is the zero mode of the conserved current and measures the $U(1)$ charge, while φ_0 is its canonical conjugate ($[\varphi_0, a_0] = i$). Primary fields are the vertex operators $\mathcal{V}_{\beta}(z) = : e^{i\beta\varphi(z)} :$ with conformal dimension $\beta^2/2$. The corresponding highest weight state $|\beta\rangle = \mathcal{V}_{\beta}(0)|0\rangle$, which is annihilated by all $a_{n>0}$, has $U(1)$ charge β . Since we defined the $U(1)$ charge to be a_0 , the electric charge is $\frac{1}{\sqrt{q}} a_0$. Descendants are obtained by acting on $|\beta\rangle$ with the lowering operators $a_n^{\dagger} = a_{-n}$, $n > 0$. They are labeled by a partition $\mu = \{\mu_j\}$, with $\mu_1 \geq \mu_2 \geq \dots \geq \mu_n > 0$:

$$|Q, \mu\rangle = \prod_j a_{-\mu_j} |Q\rangle, \quad a_0 |Q, \mu\rangle = Q |Q, \mu\rangle. \quad (6)$$

For multiplicities of element j , $m_j = m_j(\mu)$ the norm is

$$\langle Q, \mu | Q', \mu' \rangle = z_{\mu} \delta_{Q, Q'} \delta_{\mu, \mu'}, \quad z_{\mu} = \prod_j j^{m_j} m_j!. \quad (7)$$

The matrix elements of the primary field between the *normalized* basis of descendants can be computed easily using the recurrence $[a_m, : e^{i\beta\varphi(z)} :] = : e^{i\beta\varphi(z)} : \beta z^m$. They are of the form

$$\langle Q', \mu' | : e^{i\beta\varphi(z)} : | Q, \mu \rangle = z^{|\mu'| - |\mu| + \beta Q} A_{\mu', \mu} \delta_{Q', Q + \beta}, \quad (8)$$

which is consistent with Eq. (4) and with charge conservation; βQ comes from the difference in conformal dimensions $(Q'^2 - Q^2)/2$. With $m_j = m_j(\mu)$ and $m'_j = m'_j(\mu')$ being the multiplicities of j in μ and μ' , one finds

$$A_{\mu', \mu} = \prod_{j \geq 1} \sum_{r=0}^{m'_j} \sum_{s=0}^{m_j} \frac{(-1)^s}{r! s!} \left(\frac{\beta}{\sqrt{j}} \right)^{r+s} \delta_{m'_j + s, m_j + r} \frac{\sqrt{m'_j! m_j!}}{(m_j - s)!}. \quad (9)$$

These matrix elements are real (useful for numerics) with the symmetry $A_{\mu, \mu'}(\beta) = A_{\mu', \mu}(-\beta)$.

We now move to the neutral part, starting with the case of $(k, r) = (2, r)$ Jacks. The CFT can be factorized as a $U(1)$ free boson times a neutral minimal model $M(3, 2+r)$.²¹ The underlying symmetry of this minimal model is the Virasoro algebra

$$[L_n, L_m] = (n - m) L_{n+m} + \frac{c}{12} n(n^2 - 1) \delta_{n+m, 0} \quad (10)$$

with central charge $c = 1 - 6(g - 1)^2/g$, $g = \frac{2+r}{3}$. The electron operator is $V(z) = \Psi(z) : e^{i\sqrt{2h_{\Psi} + m\varphi(z)}} :$. $\Psi(z) = \Phi_{(1|2)}(z)$ is a primary field in the neutral CFT, with conformal dimension h_{Ψ} kept generic. Like in the $U(1)$ case, the Hilbert space of the neutral CFT is made of the primary fields $|\Delta\rangle$, eigenstates (with eigenvalue Δ) of L_0 and annihilated by lowering operators $L_n, n > 0$, and their descendants, indexed by a partition $\lambda = (\lambda_1, \lambda_2, \dots, \lambda_n)$:

$$|\Delta, \lambda\rangle = L_{-\lambda_1} L_{-\lambda_2} \dots L_{-\lambda_n} |\Delta\rangle, \quad (11)$$

also eigenstates of L_0 with eigenvalues $\Delta + |\lambda|$, where $|\lambda| = \sum_i \lambda_i$. Using the Virasoro algebra (10) and $L_n^{\dagger} = L_{-n}$, we can compute any overlap between descendants. While descendants with different $|\lambda|$ are clearly orthogonal (having different L_0 eigenvalues), a major difference from the $U(1)$ case is that the descendants (11) are generically independent but not orthogonal. Hence, at each level $|\lambda|$, we have to *numerically* build an orthonormal basis.

Another issue is that for nonunitary CFTs (such as the one underlying the Gaffnian) some descendants have a negative norm. These states have to be included, and the sign of their norm can be handled by an extra diagonal matrix D acting on the right of the MPS matrices: $B^m \rightarrow B^m D$.

A final major difference from the $U(1)$ case is the presence of null vectors, states of vanishing norm under the scalar product defined by $L_n^{\dagger} = L_{-n}$. This is a reflection of the fact that for special values of Δ (which include all the interesting cases), some states in (11) are not independent. CFT characters count the number of independent descendants at each level, from which one can deduce the number of null vectors. Our

numerical procedure for computing overlaps reproduces this counting. At each level we need to detect and drop all null vectors before performing the Gram-Schmidt process.

To compute matrix elements $\langle \Delta', \lambda' | \Psi(1) | \Delta, \lambda \rangle$ between descendants, it is convenient to work in the overcomplete (due to null vectors) “basis” (11) and then transform back to the orthonormal basis. The level-0 matrix element $\langle \Delta' | \Psi(1) | \Delta \rangle$ is simply the OPE structure constant $D_{\Delta', h_\psi, \Delta}$, known in the closed form for minimal models, and gives an overall prefactor which can be ignored. Others can be computed using a method similar to that for the $U(1)$ CFT; for all $m \in \mathbb{Z}$,

$$[L_m - L_0, \Phi^{(h)}(1)] = m h \Phi^{(h)}(1), \quad (12)$$

where $\Phi^{(h)}$ is any primary field with a generic conformal dimension h . Any matrix element can in principle be computed exactly using this method but to the best of our knowledge there is no analytical closed formula.

We are now in the position to write down the MPS matrices for $(k=2, r)$ Jack states. The state $|\Delta, \lambda; Q, \mu\rangle = |\Delta, \lambda\rangle \otimes |Q, \mu\rangle$ of an *overcomplete* “basis” of states in the CFT for $k=2$ Jack states has level (“momentum”) $P = |\lambda| + |\mu|$, which serves as the truncation parameter for the MPS. The matrix elements $\langle \Delta', \lambda'; Q', \mu' | B^m | \Delta, \lambda; Q, \mu \rangle$ for $m = 0, 1$ are given by

$$B^0 : \delta_{\mu, \mu'} \delta_{Q', Q - \frac{1}{\sqrt{q}}} \delta_{\Delta, \Delta'} \langle \Delta', \lambda' | \Delta, \lambda \rangle, \quad (13)$$

$$B^1 : \delta_{\Delta' + |\lambda'| + |\mu'| + \sqrt{q}Q, \Delta + |\lambda| + |\mu| + h_\psi + 1/2} \times \langle \Delta', \lambda' | \Psi(1) | \Delta, \lambda \rangle \delta_{Q', Q + \sqrt{q} - 1/\sqrt{q}} A_{\mu', \mu}. \quad (14)$$

$\langle \Delta', \lambda' | \Psi(1) | \Delta, \lambda \rangle$ can be computed using the neutral CFT, then changed to an orthonormal basis. $A_{\mu', \mu}$ is given in (9) for $\beta = \sqrt{q}$. The values of Δ, Δ' are fixed by the fusion rules of the electron operator in the neutral sector. For the $(k, r) = (2, r)$ Jacks, these are $\Psi \times \Psi = 1, \Psi \times 1 = \Psi$, which gives rise to two neutral sectors $|x\rangle$ $x = 0, 1$ with conformal dimension $\Delta = x h_\psi$ and

$$\langle x', \lambda' | \Psi(1) | x, \lambda \rangle = \delta_{x+x', 1} \langle x', \lambda' | \Psi(1) | x, \lambda \rangle. \quad (15)$$

We have implemented the above MPS numerically and verified that it exactly reproduces all $(k, r) = (2, 2), (2, 3), (2, 6)$ Jack states. The $P = 0$ MPS recovers the thin torus limit²² (root partition) of these Jacks. The topological sector (responsible for the ground-state degeneracy) can be fixed by choosing matrix elements of the product $B^{m_1} \dots B^{m_{N_\psi}}$ between different primary fields. One can describe quasihole states by inserting quasihole matrices in the MPS, as was done for Laughlin and Moore-Read states in Ref. 11. Or alternatively, edge states are obtained by choosing matrix elements involving descendant states instead of primaries. This means that the MPS formalism establishes a mapping between edge states and the auxiliary space, which in turns controls the entanglement spectrum. In particular the MPS makes transparent the counting of the orbital entanglement spectrum for such states.²³

We now move to the Read-Rezayi Z_3 state, exemplified by the $k=3$ Jack polynomial. For $k > 2$ Jack states, the only known approach is to deal with a CFT with an enlarged algebra, the so-called \mathcal{W}_k algebra [see Eqs. (44), (45), and (46) of Ref. 24], which includes a W current of spin 3. This generic approach, which applies to all $(k, r) = (3, r)$ Jack states,

becomes inefficient for the Z_3 Read-Rezayi (RR) state due to the appearance of an extremely large number of null vectors (at each level of truncation). The underlying CFT for the $k=3$ RR state is known to be equivalent to the minimal model $M(5, 6)$, the field $\Psi_1(z)$ becoming the primary field $\Phi_{(3|1)}(z)$. This alternative approach provides a basis in which matrix elements involve only Virasoro modes L_n . The electron operator is $V(z) =: e^{i\sqrt{q}\varphi(z)} : \otimes \Psi_1(z)$ with $q = 2/3 + m$. The neutral CFT field $\Phi_{(3|1)}$ can be split into two chiral fields $\Psi_1(z), \Psi_{-1}(z)$ with conformal dimension $h_\psi = 2/3$. Their fusion rules in the \mathcal{W}_3 framework are $\Psi_1 \times \Psi_1 = \Psi_{-1}, \Psi_1 \times \Psi_{-1} = 1$. While in the \mathcal{W}_3 algebra language $|W\rangle = \sqrt{3/c} W_{-3} |0\rangle$ is a descendant of the identity, it is primary (with conformal dimension 3) with respect to the Virasoro algebra: $L_n |W\rangle = 0, n > 0$. Accordingly, in the minimal model $M(5, 6)$ framework one has to work with the fusion rule $\Psi_1 \times \Psi_{-1} = 1 + W$.

The Z_3 parafermions have three sectors corresponding to the Z_3 charge of the field $x = 0, \pm 1$. Working in the Virasoro algebra, the $x = 0$ sector contains two primaries $|0\rangle, |W\rangle$ as well as their descendants obtained just like above by the action of the Virasoro generators L_{-n} , whereas $x = \pm 1$ are made of $|\psi_{\pm 1}\rangle$ and their descendants. The matrix element between descendants $\langle \Delta', \lambda' | \Psi_1(1) | \Delta, \lambda \rangle$ vanishes unless $x' = x + 1 \pmod{3}$. The matrix elements we need are $\langle \Psi_1, \lambda' | \Psi_1(1) | 0, \lambda \rangle, \langle \Psi_1, \lambda' | \Psi_1(1) | W, \lambda \rangle, \langle \Psi_{-1}, \lambda' | \Psi_1(1) | \Psi_1, \lambda \rangle$, all others being obtained from the above by charge conjugation $\langle \alpha' | \Psi_1(1) | \alpha \rangle = \langle C(\alpha) | \Psi_1(1) | C(\alpha') \rangle$, where charge conjugation interchanges $|\Psi_{\pm 1}\rangle$, leaves $|0\rangle$ invariant, and flips the sign of $|W\rangle$. Using Eq. (12), we can compute these matrix elements up to one coefficient, namely $\langle \Psi_1 | \Psi_1(1) | W \rangle / \langle \Psi_1 | \Psi_1(1) | 0 \rangle$. But this is simply an OPE structure constant, which is found to be $\sqrt{26/9}$.

Once the matrix elements (real, with this normalization) between descendants are known, it is easy to find the explicit form of the MPS B matrices for the RR state, $\langle \Delta', \lambda'; Q', \mu' | B^0 | \Delta, \lambda; Q, \mu \rangle$ and $\langle \Delta', \lambda'; Q', \mu' | B^1 | \Delta, \lambda; Q, \mu \rangle$:

$$B^0 : \delta_{\mu, \mu'} \delta_{Q', Q - 1/\sqrt{q}} \langle \Delta', \lambda' | \Delta, \lambda \rangle, \quad (16)$$

$$B^1 : \delta_{\Delta' + |\lambda'| + |\mu'| + \sqrt{q}Q, \Delta + |\lambda| + |\mu| + h_\psi + 1/2} \times \langle \Delta', \lambda' | \Psi_1(1) | \Delta, \lambda \rangle \delta_{Q', Q + \sqrt{q} - 1/\sqrt{q}} A_{\mu', \mu}, \quad (17)$$

with $h_\psi = 2/3$. $A_{\mu', \mu}$ is given in (9) for $\beta = \sqrt{q}$. $\lambda = \{\lambda_i\}$ is a partition of descendants of all four primary fields (W included) in the theory. As before, $P = |\lambda| + |\mu|$ is the truncation parameter for the MPS. As before the $P = 0$ MPS recovers the root partition $\dots 10^{m-1} 10^{m-1} 10^{m+1} 10^{m-1} 10^{m-1} 1$, which is the thin-torus limit of the RR state multiplied by m Jastrow factors.

The obtained MPS description of the Jacks (un-normalized wave functions on the annulus) is trivially transmuted to other geometries: For the sphere and the infinite plane, we obtain a site-dependent MPS with $B^{m_i}[i] = B^{m_i}/N_i(i)$, where N_i is the norm of the single particle orbital z^i in the respective geometries. For the cylinder, a site-independent MPS is possible by introducing a time evolution $e^{-2\pi L_0/L}$, with L denoting the circumference of the cylinder. The well-known squeezing properties of FQH states easily follow from the MPS description.

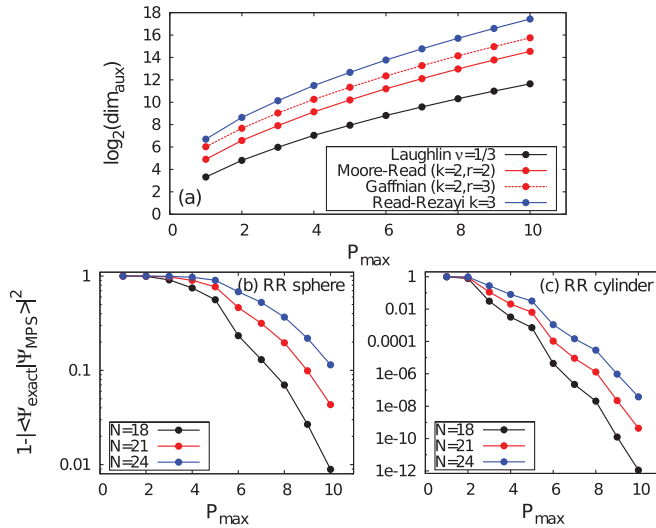


FIG. 1. (Color online) Growth of the auxiliary Hilbert space and convergence criteria for different types of boundary conditions. Upper panel: Dimension of the auxiliary space for the Laughlin, Moore-Read, Gaffnian, and Read-Rezayi Z_3 state as a function of P_{max} . Lower panel: Quantum distance between the exact Read-Rezayi Z_3 and the truncated MPS state on the sphere (b) and on the cylinder with aspect ratio 1 (c) as a function of P_{max} . Note that for $N = 24$ and $P_{\text{max}} = 10$, the MPS only gives 40% of the 6.2×10^7 components. Smaller quantum distances are obtained for Laughlin, Moore-Read, and Gaffnian (not shown).

So far the MPS description we have provided is exact. For numerical purposes of approximating a given state, we introduce the truncation level P_{max} , which is the maximum allowed value of $P = |\lambda| + |\mu|$. $P_{\text{max}} = 0$ gives the root partition (thin-torus limit) of the Jack polynomials and amounts to dropping all descendants in the CFT Hilbert space. $P_{\text{max}} = 1$ gives the correct weights for all configurations obtained through a *single* squeezing of the root partition. Generically, the truncation at P_{max} amounts to restricting the number of any squeezing steps from the root partition to P_{max} . This is also the momentum quantum number labeling the entanglement spectrum levels.²⁵ Due to the shape of the orbital spectrum, the truncation to a certain P_{max} is expected to be equivalent to keeping the states

with the highest Schmidt weight in the ground state. This is also related (though not equivalent) to expansions around the thin cylinder limit,^{26,27} where the weights of configurations decrease with the amount of squeezings from the root partition (equivalent to the exponential decay of correlation functions in the associated CFT).

In Fig. 1 we provide numerical benchmarks for the accuracy of approximating the full Jack states by the MPS truncated at level P_{max} . The approximate Laughlin, Moore-Read, Gaffnian, and Read-Rezayi states have been constructed by MPS B matrices whose auxiliary Hilbert space dimension grows as shown in Fig. 1(a). The accuracy of the approximation is quantified by the overlap of an MPS state with a full Jack polynomial, and an example of the Read-Rezayi Z_3 state is given in Figs. 1(b) and 1(c). We observe that the approximate MPS state becomes an excellent approximation of the exact FQH state for relatively low values of $P_{\text{max}} = 10$. Note that the convergence to the exact state on the sphere [Fig. 1(b)] is strikingly slower than on the cylinder [Fig. 1(c)], making this a preferred type of boundary condition for DMRG implementations.^{28–31}

In conclusion, we have provided a method to obtain the MPS description of FQH model states given by correlators of the primary fields in a CFT. We have furthermore obtained the exact MPS form of the $(k, r) = (2, r), (3, 2)$ Jack states (including Moore-Read, Gaffnian, and Read-Rezayi $k = 3$ state), and compared the approximate MPS (truncated to a certain P_{max}) with the exact states. Comparatively small values of P_{max} were found to be sufficient for obtaining extremely accurate approximations of these states on the cylinder, which might have consequences for the improved DMRG implementations of realistic (Coulomb) Hamiltonians.

We wish to thank F. D. M. Haldane, A. Sterdyniak, R. Santachiara, and J. Dubail for inspiring discussions. B.A.B. and N.R. were supported by NSF CAREER DMR-095242, ONR-N00014-11-1-0635, ARMY-245-6778, MURI-130-6082, the Packard Foundation, and a Keck grant. Z.P. acknowledges support by DOE Grant No. DE-SC0002140 and thanks KITP for hospitality (supported in part by NSF PHY11-25915).

¹S. R. White, *Phys. Rev. Lett.* **69**, 2863 (1992).

²M. Fannes, B. Nachtergaele, and R. Werner, *Commun. Math. Phys.* **144**, 443 (1992).

³D. Perez-Garcia, F. Verstraete, M. Wolf, and J. Cirac, *Quantum Inf. Comput.* **7**, 401 (2007).

⁴F. Verstraete, J. I. Cirac, J. I. Latorre, E. Rico, and M. M. Wolf, *Phys. Rev. Lett.* **94**, 140601 (2005).

⁵J. I. Cirac and G. Sierra, *Phys. Rev. B* **81**, 104431 (2010).

⁶A. E. B. Nielsen, J. I. Cirac, and G. Sierra, *J. Stat. Mech.: Theory Exp.* (2011) P11014.

⁷Y. Zhang, T. Grover, and A. Vishwanath, *Phys. Rev. B* **84**, 075128 (2011).

⁸H.-C. Jiang, Z. Wang, and L. Balents, *Nat. Phys.* **8**, 902 (2012).

⁹A. E. B. Nielsen, J. I. Cirac, and G. Sierra, *Phys. Rev. Lett.* **108**, 257206 (2012).

¹⁰L. Cincio and G. Vidal, *Phys. Rev. Lett.* **110**, 067208 (2013).

¹¹M. P. Zaletel and R. S. K. Mong, *Phys. Rev. B* **86**, 245305 (2012).

¹²R. B. Laughlin, *Phys. Rev. Lett.* **50**, 1395 (1983).

¹³G. Moore and N. Read, *Nucl. Phys. B* **360**, 362 (1991).

¹⁴N. Read and E. Rezayi, *Phys. Rev. B* **59**, 8084 (1999).

¹⁵J. Dubail, N. Read, and E. H. Rezayi, *Phys. Rev. B* **86**, 245310 (2012).

¹⁶B. A. Bernevig and F. D. M. Haldane, *Phys. Rev. Lett.* **100**, 246802 (2008).

¹⁷B. A. Bernevig and F. D. M. Haldane, *Phys. Rev. Lett.* **101**, 246806 (2008).

- ¹⁸S. H. Simon, E. H. Rezayi, N. R. Cooper, and I. Berdnikov, *Phys. Rev. B* **75**, 075317 (2007).
- ¹⁹E. H. Rezayi and F. D. M. Haldane, *Phys. Rev. B* **50**, 17199 (1994).
- ²⁰F. D. M. Haldane, *Phys. Rev. Lett.* **51**, 605 (1983).
- ²¹P. Di Francesco, P. Mathieu, and D. Sénéchal, *Conformal Field Theory* (Springer, New York, 1997).
- ²²E. J. Bergholtz and A. Karlhede, *Phys. Rev. B* **77**, 155308 (2008).
- ²³A. Chandran, M. Hermanns, N. Regnault, and B. A. Bernevig, *Phys. Rev. B* **84**, 205136 (2011).
- ²⁴B. Estienne and R. Santachiara, *J. Phys. A* **42**, 445209 (2009).
- ²⁵H. Li and F. D. M. Haldane, *Phys. Rev. Lett.* **101**, 010504 (2008).
- ²⁶M. Nakamura, Z.-Y. Wang, and E. J. Bergholtz, *Phys. Rev. Lett.* **109**, 016401 (2012).
- ²⁷P. Soulé and T. Jolicoeur, *Phys. Rev. B* **85**, 155116 (2012).
- ²⁸N. Shibata and D. Yoshioka, *Phys. Rev. Lett.* **86**, 5755 (2001).
- ²⁹A. E. Feiguin, E. Rezayi, C. Nayak, and S. Das Sarma, *Phys. Rev. Lett.* **100**, 166803 (2008).
- ³⁰J. Zhao, D. N. Sheng, and F. D. M. Haldane, *Phys. Rev. B* **83**, 195135 (2011).
- ³¹Z. Hu, Z. Papić, S. Johri, R. N. Bhatt, and P. Schmitteckert, *Phys. Lett. A* **376**, 2157 (2012).

Search Search History

All Databases

<< Return to Web of Science®

Citing Articles Title: Fractional quantum Hall effect in a tilted magnetic field
Author(s): Papic, Z.
Source: PHYSICAL REVIEW B Volume: 87 Issue: 24 Article Number: 245315 DOI: 10.1103/PhysRevB.87.245315 Published: JUN 27 2013

This item has been cited by items indexed in the databases listed below. [more information]

2 in All Databases

- 2 publication in Web of Science
0 publication in BIOSIS Citation Index
0 publication in ScELO Citation Index
0 publication in Chinese Science Citation Database
0 data sets in Data Citation Index
0 publication in Data Citation Index

Results: 2 Page 1 of 1 Go Sort by: Publication Date -- newest to oldest

Create Citation Report

Hide Refine

Refine Results

Search within results for

Search

Databases

Research Domains

SCIENCE TECHNOLOGY

Research Areas

PHYSICS

Document Types

Authors

Group/Corporate Authors

Editors

Funding Agencies

Source Titles

Conference/Meeting Titles

Publication Years

Languages

Countries/Territories

Select Page Add to Marked List (0) Send to: my.endnote.com

1. Title: Field theory of the quantum Hall nematic transition
Author(s): Maciejko, J.; Hsu, B.; Kivelson, S. A.; et al.
Source: PHYSICAL REVIEW B Volume: 88 Issue: 12 Article Number: 125137 DOI: 10.1103/PhysRevB.88.125137 Published: SEP 27 2013
Times Cited: 0 (from All Databases)

Get it! Waterloo View abstract

2. Title: Geometrical description of fractional Chern insulators based on static structure factor calculations
Author(s): Dobardzic, E.; Milovanovic, M. V.; Regnault, N.
Source: PHYSICAL REVIEW B Volume: 88 Issue: 11 Article Number: 115117 DOI: 10.1103/PhysRevB.88.115117 Published: SEP 10 2013
Times Cited: 0 (from All Databases)

Get it! Waterloo View abstract

Select Page Add to Marked List (0) Send to: my.endnote.com

Results: 2 Show 50 per page Page 1 of 1 Go Sort by: Publication Date -- newest to oldest

2 records matched your query of the 55,067,330 (contains duplicates) in the data limits you selected.

View in: 简体中文 繁體中文 English 日本語 한국어 Português Español

Fractional quantum Hall effect in a tilted magnetic field

Z. Papić

Department of Electrical Engineering, Princeton University, Princeton, New Jersey 08544, USA

(Received 12 May 2013; published 27 June 2013)

We discuss the orbital effect of a tilted magnetic field on the quantum Hall effect in parabolic quantum wells. Many-body states realized at the fractional $\frac{1}{3}$ and $\frac{1}{2}$ filling of the second electronic subband are studied using finite-size exact diagonalization. In both cases, we obtain the phase diagram consisting of a fractional quantum Hall fluid phase that persists for moderate tilts, and eventually undergoes a direct transition to the stripe phase. It is shown that tilting of the field probes the geometrical degree of freedom of fractional quantum Hall fluids, and can be partly related to the effect of band-mass anisotropy.

DOI: [10.1103/PhysRevB.87.245315](https://doi.org/10.1103/PhysRevB.87.245315)

PACS number(s): 73.43.Cd, 73.21.Fg, 71.10.Pm

I. INTRODUCTION

When a thin two-dimensional (2D) layer of highly mobile charge carriers is placed in a perpendicular magnetic field, it gives rise to a fascinating variety of phases¹ that have been the subject of intensive study over the last three decades.² Among the most remarkable of these phases are those that display an excitation gap, and therefore quantized Hall conductivity in transport, even when their valence Landau level is only partially filled.¹ This phenomenon, the fractional quantum Hall effect (FQHE), was soon realized to be a direct manifestation of the many-body nature of these phases, and a variety of elaborate theoretical concepts have been put forward to understand it. These techniques have included, *inter alia*, the method of writing down “inspired” first-quantized wave functions à la Laughlin³ which have been shown to possess intricate analytical structure,⁴ the Chern-Simons topological field theory⁵ and the conformal field theory,⁶ composite fermion theory,⁷ and of course the explicit microscopic calculations based on exact diagonalization.⁸ Perhaps somewhat surprisingly, the last method has been particularly successful due to the specific nature of the correlations in FQHE that rapidly quench the finite-size effects as the number of particles is increased. A most striking example of this occurs for the fractionally filled $\nu = \frac{1}{3}$ Laughlin state, where the essential physical properties (the quantum numbers of the ground states, the type of collective excitation mode and its gap) can be identified in systems as small as four particles. Similarly, composite fermion theory⁷ in many cases achieves an astonishing quantitative accuracy in calculations of the overlaps between the composite-fermion trial wave functions and the exact ground states of the realistic Coulomb Hamiltonians.

Because of the synergy of the theoretical approaches mentioned above, a fairly good agreement between experiment and theory has been established in a number of cases. The level of agreement appears to be the best in the lowest Landau level (LL) defined by the filling factors $0 < \nu < 2$. In this range of ν 's, the “hierarchy” theory^{9–11} and composite-fermion theory⁷ account for nearly all of the observed experimental phenomenology. Because of the high magnetic field, in typical samples the role of multicomponent degrees of freedom, such as spin, is not crucial. However, recently FQHE also been observed in graphene¹² where multicomponent degrees of freedom are known to play a much more subtle role,¹³ and

agreement between theory and experiment is generally poorer at this stage.

Another effect that is potentially important is the so-called “Landau-level mixing.”^{14,21} In most theoretical descriptions of a partially filled Landau level, excitations to other Landau levels are disregarded. This approximation is particularly desirable in numerics, where the inclusion of multiple Landau levels leads to an extremely rapid increase of the size of the Hilbert space. While physically the neglect of LL mixing appears to be reasonable in the lowest $n = 0$ LL, recent work¹⁴ shows that this approximation is somewhat poor for $n = 1$ LL. This is unfortunate because some of the most exciting FQH states are realized in $n = 1$ LL, such as the celebrated $\nu = \frac{5}{2}$ (Ref. 15) and $\nu = \frac{12}{5}$ (Ref. 16) states that are believed to possess non-Abelian quasiparticles in the bulk.^{6,17} In the case of half filling, LL mixing is the mechanism that breaks the particle-hole symmetry, and selects one of the two candidate wave functions proposed for it.^{6,18–20} More accurate treatment of LL mixing has inspired some recent work,^{14,21} but in general its effects on various filling factors are still poorly understood.

In this paper, we discuss another mechanism that is also ubiquitous to many FQHE experiments, yet has not been fully understood theoretically. We consider the so-called “tilted field” setup²² where, in addition to the perpendicular component of the magnetic field along the z axis, a parallel component of the field is introduced along the x axis. The total magnetic field in that case points along an angle θ with respect to the vertical axis, which we refer to as the tilt angle. This technique has been immensely popular in experiment,^{22–31} e.g., as a probe for spin polarization: to the lowest order, the only effect of parallel field is to increase the Zeeman coupling, therefore it distinguishes a polarized ground state from an unpolarized one. However, this is true only in the limit of a sample with zero thickness. Since the real samples are typically a few tens of nanometers thick, and the experiments are often performed at very large tilt angles reaching 70° – 80° , one expects a strong coupling between the tilt and the orbital motion of electrons. Therefore, the consequences of tilting could be far more dramatic for the many-body states than it naively appears. This was vividly illustrated in several recent experiments.^{25–31}

The remainder of this paper is organized as follows. In Sec. II, we review the solution of the one-body problem in a parabolic quantum well subject to a combination of

perpendicular and parallel fields. In Sec. III, we derive the matrix elements of the interaction Hamiltonian adapted for finite-size studies. In the main Sec. IV, we present the results of numerical simulations for the fractional fillings $\frac{1}{3}$ and $\frac{1}{2}$ of one of the excited subbands that was the subject of recent experiments.^{28,31} We conclude with the discussion of these results (Sec. V), pointing out their limitations, connection to related recent work in the literature, and future directions.

II. ONE-BODY PROBLEM

In this section we review the quantum-mechanical solution for a single particle inside a parabolic quantum well confined in a potential $U = \frac{1}{2}m^*\omega_0^2z^2$, with a perpendicular component of the magnetic field $B_z\hat{z}$ and a parallel (x) component B_{\parallel} . This solution was first given in Maan *et al.*³² (see also Refs. 33 and 34). We consider parabolic confinement for simplicity since an analytic solution is not possible for square quantum wells. However, the two models, square and parabolic, are expected to show the same qualitative features up to some rescaling of the effective width of the well (see Ref. 35 for details).

The input parameters are the tilting angle θ , defined by $\tan\theta = B_{\parallel}/B_z$, and ω_0/ω_z , where ω_0 is the confinement frequency. We also have $\omega_c^2 = \omega_x^2 + \omega_z^2$, i.e., $\omega_z = \omega_c \cos\theta$, $\omega_x = \omega_c \sin\theta$. We are interested in preserving the filling factor as the field is tilted, i.e., we assume ω_z is constant (perpendicular field determines the filling factor), and hence we can work in units $\ell_0^2 = \hbar/m\omega_z = 1$.

The one-body problem is conveniently solved in the Landau gauge $(0, B_zx - B_{\parallel}z, 0)$, and maps to a sum of two harmonic oscillators by the rotation in the x' - z plane, where $x' \equiv x + ck_y/eB_z$ and k_y is the momentum along the y axis. The rotation angle ϕ is given by

$$\tan 2\phi = \frac{-2\omega_x\omega_z}{\omega_0^2 + \omega_x^2 - \omega_z^2},$$

and the frequencies of the two oscillators are given by

$$\begin{aligned}\omega_1^2 &= (\omega_0^2 + \omega_x^2) \sin^2\phi + \omega_z^2 \cos^2\phi + 2\omega_x\omega_z \sin\phi \cos\phi, \\ \omega_2^2 &= (\omega_0^2 + \omega_x^2) \cos^2\phi + \omega_z^2 \sin^2\phi - 2\omega_x\omega_z \sin\phi \cos\phi.\end{aligned}$$

These frequencies define two effective magnetic lengths

$$\ell_1^2 = \omega_z/\omega_1, \quad \ell_2^2 = \omega_z/\omega_2.$$

Note that ω_1 denotes the frequency of the oscillator with the coordinate $x' \cos\phi - z \sin\phi$. Therefore, when the tilt angle is zero, $\omega_1 \rightarrow \omega_z$ and $\ell_1 \rightarrow 1$, which ensures that the problem correctly reduces to the situation without the parallel field. For $\phi = 0$, the parabolic confinement has an effect only on the z coordinate that couples to the magnetic length ℓ_2 which may be different from ℓ_0 .

Energy levels of a single particle are thus labeled by (n_1, n_2) corresponding to the quantum numbers of the two oscillators. It is instructive to analyze the first few low-lying levels as a function of the tilt, as shown in Fig. 1. Energies are quoted in units of ω_z , which is assumed to be constant. In general, the subbands display a number of crossings as the parallel field is increased. However, we will focus on the two lowest subbands $(0, 0)$ and $(1, 0)$, which are experimentally relevant and do not

cross any other subband or each other. In Fig. 1 we show energy levels for three choices of confinement $\omega_0/\omega_z \geq 1$. These values correspond to higher mobility quantum wells, which are relevant for FQHE that we study below (in principle, $\omega_0/\omega_z < 1$ is also possible but those quantum wells typically have lower mobilities). Note that for very large tilts (60° and higher), the levels organize into subbands $(n_1, 0)$, $(n_1, 1)$, $(n_1, 2)$, etc. In this interesting regime, each of the new emergent bands represents a continuum of LLs that have collapsed on top of each other. This strong-mixing regime is difficult to study theoretically, and the results of this paper are not expected to hold there. We will further comment on this in Sec. V.

In the Landau gauge with an open boundary condition along x (cylinder geometry), the single-particle wave functions are given by

$$\begin{aligned}\phi_j^{00}(x, y, z) &= \frac{1}{\sqrt{b\pi\ell_1\ell_2}} e^{iX_jy} \chi_{\ell_1}(\mathcal{X}) \chi_{\ell_2}(\mathcal{Z}), \\ \phi_j^{10}(x, y, z) &= \frac{1}{\sqrt{2b\pi\ell_1\ell_2}} H_1\left(\frac{\mathcal{X}}{\ell_1}\right) e^{iX_jy} \chi_{\ell_1}(\mathcal{X}) \chi_{\ell_2}(\mathcal{Z}),\end{aligned}$$

where $\chi_{\ell}(x) = \exp(-x^2/2\ell^2)$, $\mathcal{X} \equiv (X_j + x) \cos\phi - z \sin\phi$, $\mathcal{Z} \equiv (X_j + x) \sin\phi + z \cos\phi$, and H_1 is the first Hermite polynomial. The repeat distance along y is denoted by b and $X_j \equiv 2\pi j/b$, where j is an integer labeling the orbitals. In order to eliminate edge effects, it is useful to consider a fully periodic boundary condition, i.e., wrap the cylinder along x onto a torus. The wave functions in that case are given by

$$\Phi_j^{\sigma\sigma'}(x, y, z) = \sum_{k \in \mathbb{Z}} \phi_{j+kN_\phi}^{\sigma\sigma'}(x, y, z), \quad (1)$$

where a is the dimension of torus along x , and the quantization of flux leads to the constraint $ab = 2\pi N_\phi$ (σ, σ' label the subbands). The index j runs from 0 to $N_\phi - 1$. The wave functions above are written for a rectangular torus; at the cost of a few extra complications, they can be straightforwardly generalized to an arbitrary twisted torus, which is needed if one wishes to study, e.g., a unit cell with highest (hexagonal) symmetry in the two-dimensional plane.³⁵

III. MANY-BODY HAMILTONIAN

Using the one-body wave functions in Eq. (1), we can construct the interacting Hamiltonian by computing the matrix elements³⁶

$$\begin{aligned}\int d^2\mathbf{r}_1 d^2\mathbf{r}_2 \int dz_1 dz_2 \Phi_{j_1}^{\sigma_1\sigma_1'}(\mathbf{r}_1, z_1) \Phi_{j_2}^{\sigma_2\sigma_2'}(\mathbf{r}_2, z_2) \\ \times V(\mathbf{r}_1 - \mathbf{r}_2, z_1 - z_2) \Phi_{j_3}^{\sigma_3\sigma_3'}(\mathbf{r}_2, z_2) \Phi_{j_4}^{\sigma_4\sigma_4'}(\mathbf{r}_1, z_1),\end{aligned} \quad (2)$$

where \mathbf{r} denotes the vector in the x - y plane. As it stands, Coulomb interaction in Eq. (2) admits all types of scattering processes from subbands $(\sigma_1\sigma_1'), (\sigma_2\sigma_2')$ into subbands $(\sigma_3\sigma_3'), (\sigma_4\sigma_4')$, subject to the momentum conservation [see Eq. (3) below]. However, as we are mainly interested in partially filled $(0, 0)$ and $(1, 0)$ subbands, which become well separated from other subbands for large values of the confinement (see Fig. 1), we will neglect all scattering processes between different subbands, i.e., retain only $\sigma_1 = \dots = \sigma_4$ and $\sigma_1' = \dots = \sigma_4'$. This method is analogous to the ‘‘lowest Landau-level projection’’ commonly used in FQH finite-size

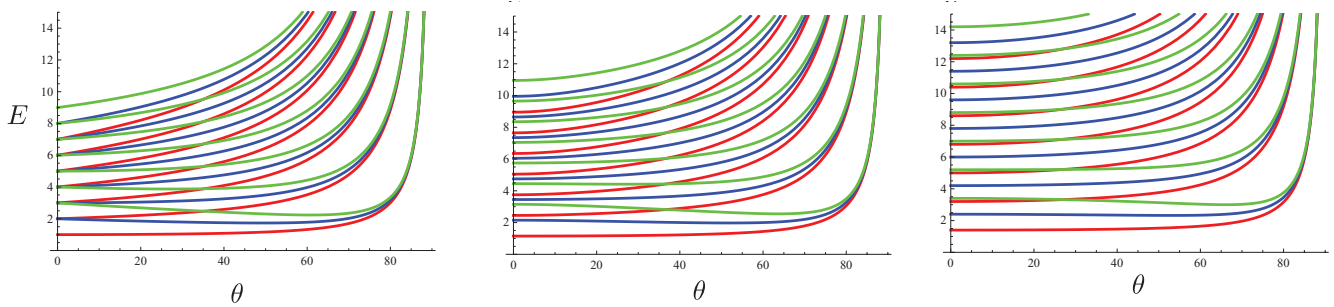


FIG. 1. (Color online) Energy levels $E = (n_1 + 1/2)\omega_1 + (n_2 + 1/2)\omega_2$ in units of ω_z as a function of tilt angle θ , for several low-lying subbands (n_1, n_2) and three choices of the confining potential $\omega_0/\omega_z = 1, 1.3, 1.8$ (from left to right). Red lines correspond to the subbands $(0, n_2)$, blue lines correspond to $(1, n_2)$, green lines correspond to $(2, n_2)$. If the confinement is equal to 1, subbands $(0, 1)$ and $(1, 0)$ are degenerate, as expected.

studies.² We expect this approximation to become increasingly better as the confinement is increased.

To evaluate the matrix element, it is convenient to use the Fourier transform

$$V(\mathbf{r}_1 - \mathbf{r}_2, z_1 - z_2) = \sum_{\mathbf{q}} \int dq_z \frac{1}{\mathbf{q}^2 + q_z^2} e^{i\mathbf{q}(\mathbf{r}_1 - \mathbf{r}_2)} e^{iq_z(z_1 - z_2)}.$$

Note that this is a Fourier transform of the three-dimensional (3D) Coulomb potential, but at end we will integrate out q_z . Finally, the torus matrix element for subband $(0, 0)$ reads as

$$\begin{aligned} V_{j_1 \dots j_4} &= \frac{\delta'_{j_1 + j_2, j_3 + j_4}}{N_\phi} \sum'_{q_x = \frac{2\pi s}{a}, q_y = \frac{2\pi t}{b}} \delta'_{q_y, X_{j_1} - X_{j_4}} e^{-iq_x(X_{j_1} - X_{j_3})} \\ &\times e^{-\frac{q_x^2}{2}(\ell_2^2 \cos^2 \phi + \ell_2^2 \sin^2 \phi) - \frac{q_y^2}{2}(\frac{\cos^2 \phi}{\ell_1^2} + \frac{\sin^2 \phi}{\ell_2^2})} \\ &\times \int dq_z \frac{1}{q_x^2 + q_y^2 + q_z^2} e^{-\frac{1}{2}q_z^2(\ell_2^2 \cos^2 \phi + \ell_1^2 \sin^2 \phi)} \\ &\times e^{q_x q_z \sin \phi \cos \phi (\ell_1^2 - \ell_2^2)}. \end{aligned} \quad (3)$$

The prime on the delta functions stands for “modulo N_ϕ ” and the prime on the summation indicates that the $\mathbf{q} = 0$ component has been canceled out by the neutralizing (positive) background charge. In the case of the $(0, 0)$ subband, the above matrix element can be analytically further simplified to some extent, but this is no longer the case when higher subbands are considered, and one is left with the general expression quoted in Eq. (3).

The effective matrix element projected to one of the higher subbands is obtained by multiplying the integrand in Eq. (3) by an extra form factor $|F(\mathbf{q}, q_z)|^2$. The computation of this form factor is straightforward and involves the standard algebra of Landau-level raising/lowering operators,² but it quickly becomes tedious for very high subbands. Here, we quote the result for the excited subband $(0, 1)$ where $F(\mathbf{q}, q_z)$ is given by

$$F^{01}(\mathbf{q}, q_z) = 1 - \frac{1}{2\ell_2^2} q_y^2 \sin^2 \phi - \frac{1}{2} \ell_2^2 (q_x \sin \phi + q_z \cos \phi)^2,$$

and for the $(1, 0)$ subband

$$\begin{aligned} F^{10}(\mathbf{q}, q_z) &= 1 - \frac{1}{2}(\ell_1^2 q_x^2 + q_y^2 / \ell_1^2) \cos^2 \phi \\ &- \frac{1}{2} \ell_1^2 q_z \sin \phi (-2q_x \cos \phi + q_z \sin \phi). \end{aligned}$$

Altogether, the matrix elements have a somewhat complicated form, but all the intermediate integrals/sums converge rapidly, hence can be straightforwardly evaluated in practice. Therefore, one can follow the standard approach of diagonalizing the many-body Hamiltonian in a basis of periodic orbitals on the surface of the torus.³⁷ To reduce the computational cost, it is desirable to use invariance under magnetic translations to block-reduce the Hamiltonian. This formalism was first given in Ref. 37 (see Refs. 38 and 39 for pedagogical reviews).

Note that the form of the Hamiltonian (3) it is clear that the parallel field explicitly builds in anisotropy in the problem: the components q_x and q_y in the Gaussian factor are coupled to different effective magnetic lengths. This can be understood semiclassically: in a purely perpendicular field, the cyclotron orbits of an electron are circles. When the field is tilted, electrons orbit around the tilted axis. Due to the confinement of electrons to the 2D layer, the true shape of their orbits is a projection of these circles to the 2D plane, i.e., their shape becomes elliptical.

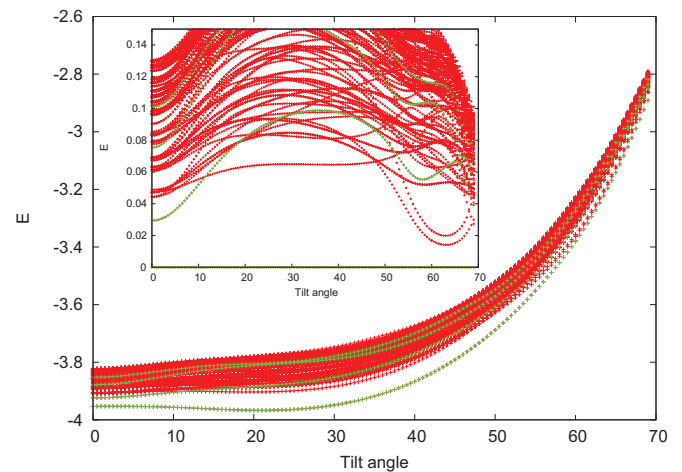


FIG. 2. (Color online) Energy spectrum for $N = 10$ particles at filling $\frac{1}{3}$ of the subband $(1, 0)$ as a function of tilt angle (measured in degrees). Inset shows the same spectrum but plotted relative to the ground state at each tilt angle, which represents the neutral gap of the system as a function of tilt. Energy levels belonging to $\mathbf{k} = 0$ momentum sectors are shown in green color.

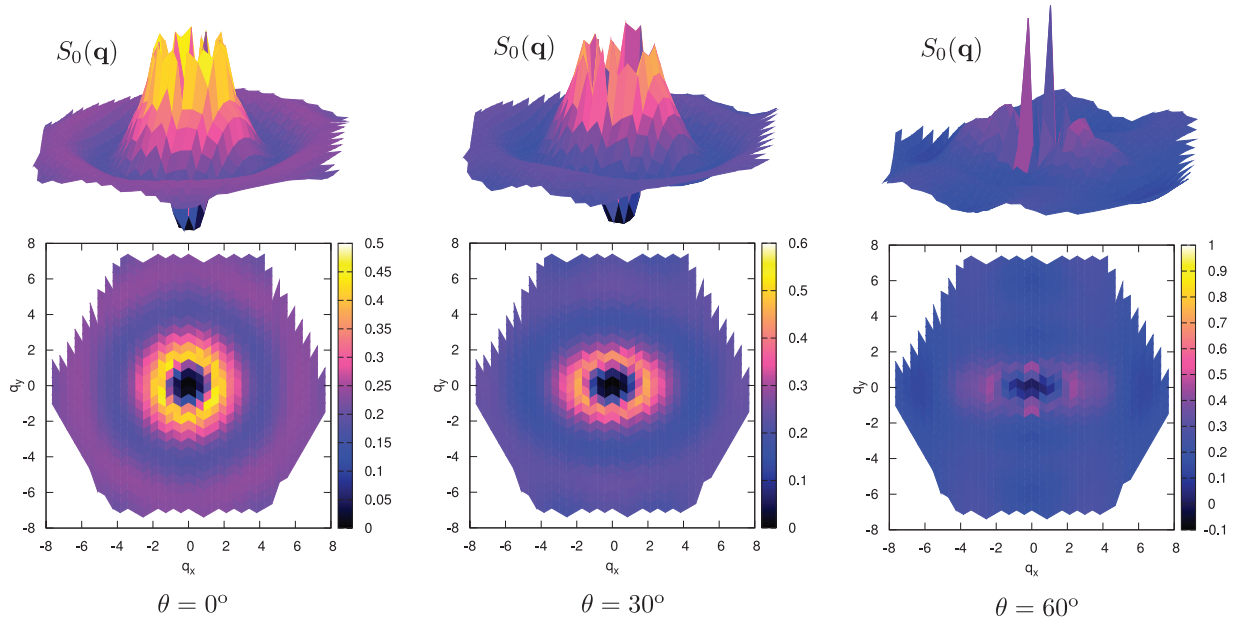


FIG. 3. (Color online) Guiding-center structure factor for $N = 10$ particles at $\nu = \frac{1}{3}$ filling and tilt angle zero, 30° and 60° (left to right). The state at the largest tilt angle has charge-density order reflected in two sharp peaks, while for two smaller tilt angles the ground state is a liquid.

IV. RESULTS

In this section, we present the results of exact diagonalization of the Hamiltonian (3) for a finite number of electrons in a toroidal geometry. This choice of boundary condition is dictated by two requirements: (i) compatibility of the Landau gauge with the presence of a parallel field, and (ii) the absence of open boundaries which avoids the complications due to the edge physics. The presence of parallel field does not affect the standard symmetry classification, as we mentioned in Sec. III, and Haldane’s many-body momentum³⁷ can be used to label the states. We will consider hexagonal unit cells, and focus on partial fillings $\frac{1}{3}$ and $\frac{1}{2}$ of the subband (1,0). This corresponds to filling factors $\nu = \frac{7}{3}$ and $\nu = \frac{5}{2}$ which have been the subject of recent experimental studies.^{28,29,31} Also, for simplicity we fix $\omega_0/\omega_z = 1.3$, which roughly corresponds to the sample design in Ref. 31. (The main conclusions do not depend on the precise value of this ratio.) Note that in the simulations presented here we neglect the spin of the electrons, and only concentrate on the orbital effects of the tilt because the ground states at $\nu = \frac{7}{3}$ and $\nu = \frac{5}{2}$ are believed to be polarized.^{40,41}

In Fig. 2, we show the energy spectrum of $N = 10$ particles at filling $\frac{1}{3}$ of the subband (1,0) as a function of tilt angle (measured in degrees). Inset shows the same spectrum but plotted relative to the ground state at each tilt angle. In other words, the inset illustrates the behavior of the neutral gap of the system as a function of tilt (in units of $e^2/\epsilon\ell_0$). Note that the experimentally measured gaps in transport correspond to the so-called “charge” gaps, which are significantly harder to compute in the periodic geometry (for the purpose of computing charge gaps, sphere geometry has been used, almost universally, in the literature⁷).

The evolution depicted in Fig. 2 suggests that $\nu = \frac{7}{3}$ is fairly robust for small tilt angles (up to 30° – 40°). The neutral

gap even appears to increase for small tilt angles up to 10° , however, a careful extrapolation of the gap as a function of $1/N$ would be needed to firmly conclude whether the state becomes enhanced for small tilt as some of the experiments seemed to indicate.²⁹ Beyond 40° , the ground-state energy sharply rises, and states from different \mathbf{k} sectors join to form a quasidegenerate ground-state manifold. Upon closer examination, we find that the momenta of the quasidegenerate states are of the form $(k_x, 0)$, indicating linear order along the x direction. This is known to be one of the signatures of the stripe phase.^{42–46}

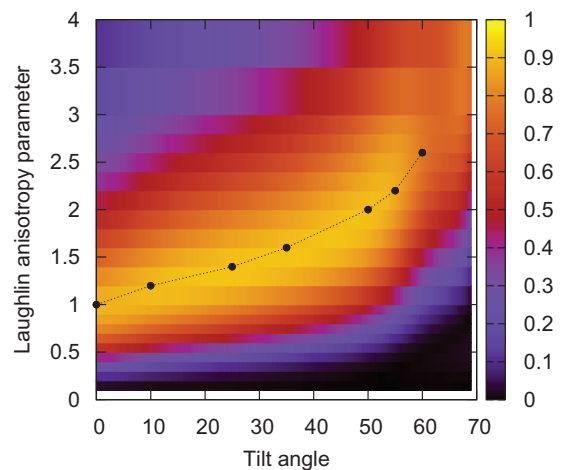


FIG. 4. (Color online) Overlap between the exact ground state at each tilt angle θ , $\Psi_0(\theta)$, and a family of Laughlin states parametrized by the metric of their fundamental droplet Ψ_L^α . Color scale represents the value of the overlap as a function of tilt angle and parameter α that defines the metric. Black points indicate the maximal overlap for the given tilt angle.

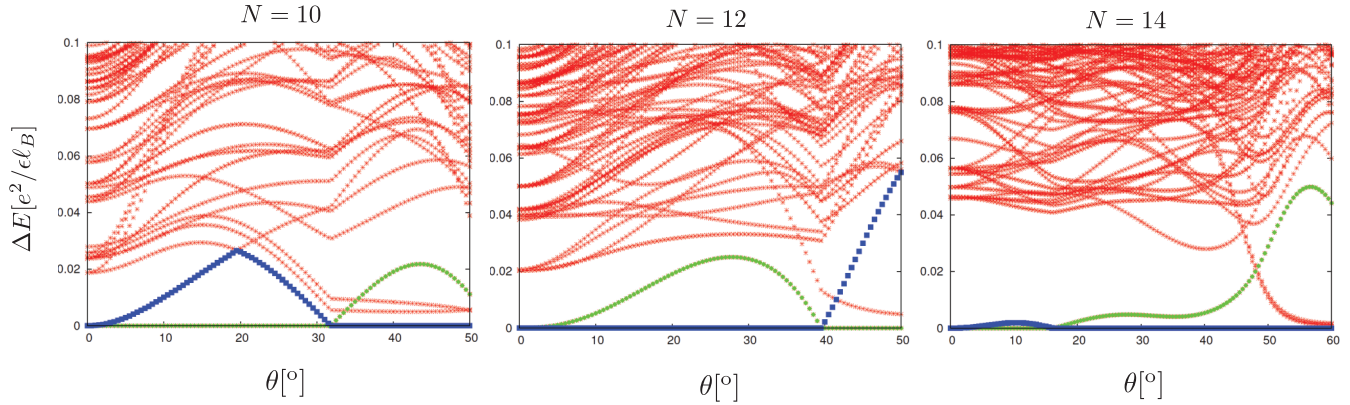


FIG. 5. (Color online) Energy spectrum for $N = 10, 12$, and 14 particles at filling $\frac{1}{2}$ in the subband $(1,0)$ as a function of tilt angle (measured in degrees). Spectrum is plotted relative to the ground state at each tilt angle, illustrating the behavior of the neutral gap of the system. Levels tentatively belonging to the topologically degenerate Moore-Read ground states are denoted by blue and green colors.

Further evidence for the stripe phase is found in the shape of the guiding-center structure factor¹⁰

$$S_0(\mathbf{q}) = \frac{1}{N_\phi} \sum_{i,j} \langle e^{i\mathbf{q}\cdot\mathbf{R}_i} e^{-i\mathbf{q}\cdot\mathbf{R}_j} \rangle - \langle e^{i\mathbf{q}\cdot\mathbf{R}_i} \rangle \langle e^{-i\mathbf{q}\cdot\mathbf{R}_j} \rangle, \quad (4)$$

as a function of tilt, as shown in Fig. 3. In the definition of $S_0(\mathbf{q})$, the brackets $\langle \dots \rangle$ denote the ground-state expectation value of the operator representing the Fourier component of the guiding-center density

$$\rho(\mathbf{q}) = \sum_i^N e^{i\mathbf{q}\cdot\mathbf{R}_i}. \quad (5)$$

Here, \mathbf{R}_i denotes the guiding-center coordinate² of the particle i . Compared to the standard definition,⁴⁷ S_0 has the single-particle form factors stripped off, and it is normalized per flux quantum instead of per particle. For zero tilt, S_0 has a characteristic circular maximum, and tends to a constant value $\nu - \nu^2$ (for the normalization chosen above) as $q \rightarrow \infty$.¹⁰ For a tilt angle of 30° , the structure factor has a similar behavior as a function of q_x, q_y , but the locus of its maxima has become an ellipse stretched along the x direction. Finally, for a tilt of 60° , S_0 displays a qualitatively different shape with two sharp peaks, indicating broken-symmetry ordering in the x direction. This is another evidence⁴⁶ for the formation of the stripe phase in the regime of tilt beyond 40° .

In the regime between zero and 30° tilt, we identify the ground state as a FQH liquid corresponding to the family of Laughlin wave functions with the internal metric fluctuating to optimize itself with respect to the external perturbation (tilt). The existence of this internal degree of freedom was recently pointed out in Ref. 48. A convenient way of formally defining the family of FQH liquid states with a varying internal metric is through the pseudopotential formalism.¹⁰ In the case of the Laughlin $\frac{1}{3}$ filling, this family of states $\{\Psi_L^g\}$ is defined by the zero-mode condition

$$\hat{V}_1(g)\Psi_L^g = 0, \quad (6)$$

where $\hat{V}_1(g)$ is the generalized Haldane pseudopotential Hamiltonian with a given metric g (Ref. 48):

$$\hat{V}_1(g) = \sum_{\mathbf{q}} L_1(q_g^2 \ell_0^2) \exp\left(-\frac{q_g^2 \ell_0^2}{2}\right) \rho(\mathbf{q}) \rho(-\mathbf{q}). \quad (7)$$

Here, the operator ρ is defined in Eq. (5), and L_1 is the first Laguerre polynomial. Two-dimensional metric g defines the norm of $q_g^2 \equiv g^{ab} q_a q_b$ and is taken to be unimodular $\det g = 1$. The first-quantized expressions for Ψ_L^g are given in Ref. 49.

Previously, generalized Laughlin wave functions have been studied in the context of anisotropic systems,^{50,51} where it was assumed that the band-mass tensor or the Coulomb dielectric tensor is explicitly anisotropic. These works have established that FQHE physics survives some amount of anisotropy, while the phase corresponding to large anisotropy was identified with a stripe. In Ref. 51, some evidence for a quantum Hall nematic phase⁵² was provided for the intermediate regime

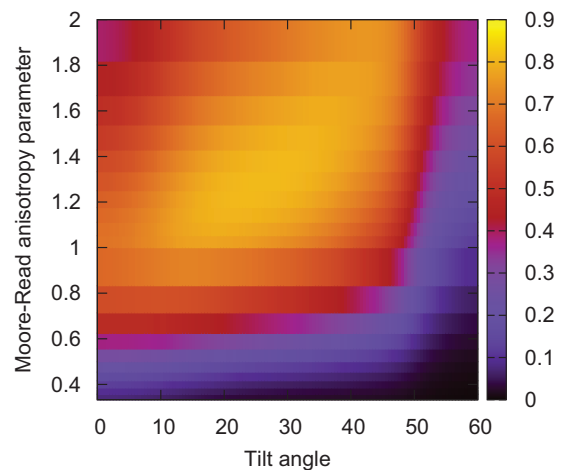


FIG. 6. (Color online) Overlap between the exact ground state at each tilt angle θ , $\Psi_0(\theta)$, and a family of Moore-Read states parametrized by the metric of their fundamental droplet Ψ_{MR}^g . Color scale represents the value of the overlap as a function of the tilt angle and the parameter α that defines the metric. System size is $N = 14$ particles on a hexagonal torus in $(0,7)$ momentum sector.

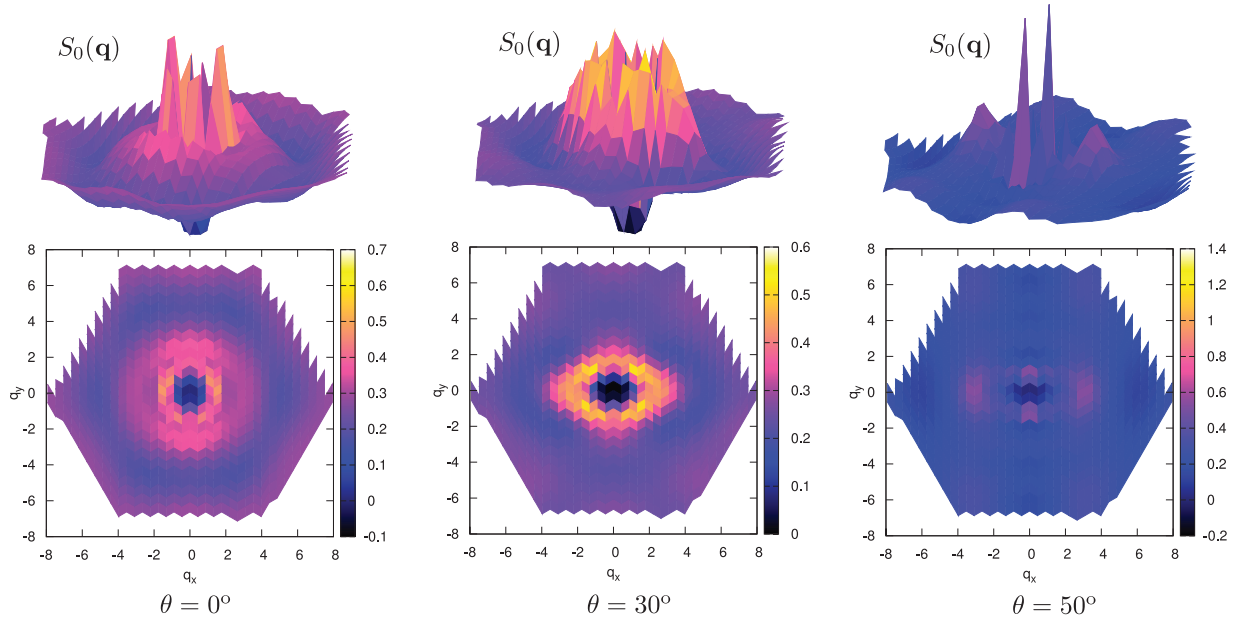


FIG. 7. (Color online) Guiding-center structure factor for a particular member of the ground-state manifold [labeled (0,7) in Fig. 5] for $N = 14$ particles at $\nu = \frac{1}{2}$ in (1,0) subband, for tilt angles 0° , 30° , and 50° degrees. The state at the largest tilt angle has charge-density order reflected in two sharp peaks, whereas for smaller tilt angles the ground state is a liquid.

of anisotropies. As we mentioned in Sec. III, the dominant Gaussian term in the tilted Hamiltonian has the same form as in mass-anisotropic systems, therefore, we might expect some similarity with the results obtained in Refs. 50 and 51. However, the presence of extra terms in Eq. (3) prevents a complete mapping of the tilted field onto a mass-anisotropic problem.

To further motivate the identification of the small-tilt phase with the FQH liquid, we compute the overlap between the exact ground state at a given tilt, and the family of Laughlin states Ψ_L^g parametrized the anisotropy parameter α (Fig. 4). We assume g is unimodular, and does not contain any off-diagonal terms. Therefore, the metric g is parametrized by $\alpha, 1/\alpha$ on the diagonal. By varying α , for each tilt angle we find it is possible to achieve a high overlap (in excess of 97%), typical of the Laughlin state. The maximum overlap can be used as a criterion for determining the internal metric of the Laughlin state at a given tilt. As seen in Fig. 4, the maximum overlap varies approximately linearly with tilt for tilt angles smaller than 40° , in agreement with the result found in systems with band anisotropy.⁵⁰

Another fractional state of interest in the (1,0) subband is the $\nu = \frac{1}{2}$, corresponding to the total filling $\nu = \frac{5}{2}$ in experiment. In GaAs heterostructure samples without tilt, this state is roughly of the same strength as $\nu = \frac{7}{3}$.¹⁶ A great deal of theoretical evidence^{40,53} points to the fact that the $\nu = \frac{5}{2}$ state is described by the Moore-Read Pfaffian wave function, and might have non-Abelian quasiparticles in the bulk, which makes it more exotic than the states of the Laughlin type. A necessary requirement for the non-Abelian statistics in this case is the full spin polarization of the ground state, which is consistent with theoretical predictions⁴⁰ as well as experimental findings.⁴¹

In Fig. 5, we show the energy spectrum at filling $\frac{1}{2}$ of the subband (1,0) as a function of tilting angle (in degrees).

This state is more fragile than the $\frac{1}{3}$ state, therefore we show three different system sizes ($N = 10, 12, 14$) to illustrate the convergence to the thermodynamic limit. As before, the data in the upper panel in Fig. 5 correspond to the raw energy spectrum, and the lower panel shows the neutral gap.

The difficulty in establishing convergence to the thermodynamic limit in this case is partly related to the fact that the Moore-Read state has a sixfold topological degeneracy on the torus. Using the conventional symmetry classification, this degeneracy can be factored into a trivial twofold degeneracy,³⁷ and the residual threefold degeneracy resulting from the non-Abelian statistics.⁵⁴ The threefold degenerate states belong to the same momentum sector only in case of the hexagonal symmetry. The tilted field, however, reduces the symmetry down to centered rectangular, and only two of the states remain in the same sector. In finite systems, there will be some amount of splitting between the sectors, as can be seen in Fig. 5. As the $N = 14$ system shows, the splitting gets suppressed as larger sizes are approached and is consistent with eventually becoming zero in the thermodynamic limit. The fact that there is a well-defined threefold ground state multiplet even for the small systems that can be accessed by exact diagonalization is an important piece of evidence in favor of the Moore-Read state.

Apart from topological degeneracy, it is also possible to compute the overlap between the exact ground state and the Moore-Read wave function. Similar to the Laughlin case discussed above, in a situation where tilt is present, one must consider a family of Moore-Read states parametrized by the internal metric. The overlaps between this family of states and the exact ground state are given in Fig. 6. The behavior of the maximum overlap as a function of tilt is qualitatively consistent with Fig. 4. The value of the maximum overlap with the Moore-Read state is smaller than in case of the

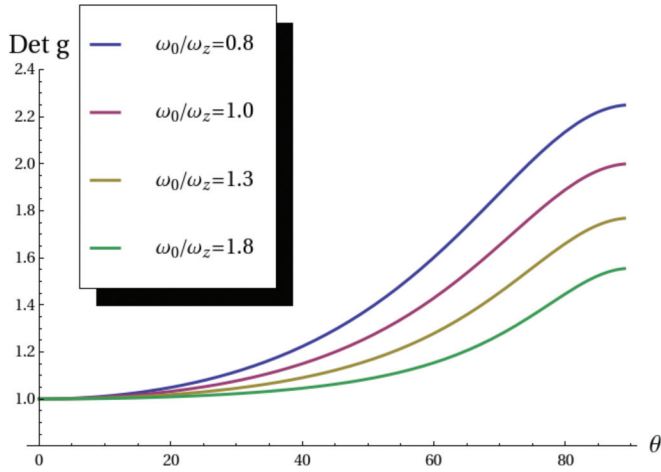


FIG. 8. (Color online) Determinant of the metric in the Gaussian form factor of Eq. (3) as a function of tilt, for several values of the confining potential.

Laughlin state, but it can be improved by varying some of the short-range Haldane pseudopotentials, as it has been done in the literature.⁵³

Apart from some amount of splitting within the ground-state manifold, the evolution of the energy spectrum in Fig. 5 is also reminiscent of the $\frac{1}{3}$ case (Fig. 2). The quantum Hall state remains stable up to 30° – 40° tilt, at which point it gives rise to a stripe phase. This transition is again captured in the behavior of the structure factor displayed in Fig. 7.

V. DISCUSSION AND CONCLUSIONS

In this paper, we have studied the effect of coupling between a parallel component of the magnetic field and the electronic motion restricted to the 2D plane of a parabolic quantum well. We have demonstrated that this coupling probes the geometrical degree of freedom of fractional quantum Hall liquid states.⁴⁸ For filling factors $\frac{1}{3}$ and $\frac{1}{2}$ of the excited (1,0) subband, the ground states are incompressible fluids when the parallel field is zero. As the tilt angle is increased from zero to 30° , the internal geometry of these states adjusts itself to accommodate the variation of the external metric imposed by the tilt. Up to this distortion of the elementary droplets from circular to elliptical, the FQHE physics is maintained in this regime. Beyond 40° tilt, the states undergo a transition to the broken-symmetry phase with stripe order.

Previously, FQHE was studied in systems with explicit anisotropy introduced through the band-mass tensor⁵⁰ or the dielectric tensor defining the Coulomb interaction⁵¹ (see also experimental results for the anisotropic “composite Fermi-liquid” state in Ref. 55). For small tilt angles, our results are in qualitative agreement because the Gaussian factor (3) contains a metric g that is nearly unimodular, and hence (neglecting the complicated prefactors) the tilted problem can be rewritten as an effective mass anisotropy. The “volume” is given by

$\det g = (\ell_1^2 \cos^2 \phi + \ell_2^2 \sin^2 \phi)(\cos^2 \phi / \ell_1^2 + \sin^2 \phi / \ell_2^2)$, and $\det g$ is plotted as a function of tilt in Fig. 8. The volume remains fairly close to unity for tilts smaller than 40° , supporting the similarity between tilt and mass anisotropy. Note that lower values of the confinement ω_0/ω_z lead to a faster deviation of the volume away from unity, and therefore the intrinsic tilt effects are effectively stronger in this regime. Furthermore, it would be interesting to explore connections between a spatially nonuniform tilt and the so-called Fubini-Study metric in lattice analogs of FQHE.⁵⁶

In principle, the tilted-field phase diagram might also admit the existence of the so-called nematic quantum Hall phases.⁵² These phases are believed to spontaneously break rotational symmetry, whereas the tilted field breaks such a symmetry explicitly. Although we do not find direct evidence for such phases in the case of generic (Coulomb) interaction studied here, it would be important to understand better the connection between nematic phases^{57,58} and quantum Hall phases with elliptical elementary droplets, and how one could tune between them by modifying the interaction.

Finally, we mention several limitations of this work. Apart from the “obvious” assumptions of zero temperature and clean (translationally invariant) systems, the main limitations of this work are the neglect of the electron spin, and the mixing between various subbands. Incorporating spin would be useful for other fractions, notably $\nu = \frac{2}{5}$ (corresponding to $\nu = \frac{12}{5}$ in experiment) where a spin transition was detected as a function of tilt.³⁰ However, this fraction has a much smaller gap in comparison to $\frac{1}{3}$ or $\frac{1}{2}$, and numerical techniques beyond exact diagonalization are required to access sufficiently large systems that are not plagued by the finite-size effects. Similarly, the mixing between different subbands is another effect that is difficult to treat reliably within exact-diagonalization schemes. While we do not expect our results to be strongly affected by the mixing when tilt is less than 40° – 50° , in the regime of large tilts ($\geq 70^\circ$) they will undoubtedly be important, as we can see from the Landau-level structure (Fig. 1). With respect to the results presented here, mixing effects are furthermore important for two specific reasons. First, the mixing lifts the particle-hole symmetry between the Pfaffian and anti-Pfaffian¹⁴ and selects only one of them to describe the ground state at $\nu = \frac{5}{2}$. Second, experiments performed in the regime of extremely large tilts ($\sim 70^\circ$) have found a puzzling reemergence of *isotropic* transport²⁸ in that limit. It would be interesting to understand the connection between isotropic transport and extreme LL mixing in future work.

ACKNOWLEDGMENTS

This work was supported by DOE Grant No. DE-SC0002140. I would like to thank S. Johri, R. Bhatt, J. Maciejko, E. Rezayi, and M. Milovanović for useful comments, and Y. Liu and M. Shayegan for discussing experimental data.

¹D. C. Tsui, H. L. Stormer, and A. C. Gossard, *Phys. Rev. Lett.* **48**, 1559 (1982).

²*The Quantum Hall Effect*, 2nd ed., edited by R. E. Prange and S. M. Girvin (Springer, New York, 1990).

³R. B. Laughlin, *Phys. Rev. Lett.* **50**, 1395 (1983).

⁴B. A. Bernevig and F. D. M. Haldane, *Phys. Rev. Lett.* **100**, 246802 (2008).

- ⁵S. C. Zhang, T. H. Hansson, and S. Kivelson, *Phys. Rev. Lett.* **62**, 82 (1989).
- ⁶G. Moore and N. Read, *Nucl. Phys. B* **360**, 362 (1991).
- ⁷J. K. Jain, *Composite Fermions* (Cambridge University Press, Cambridge, UK, 2007).
- ⁸F. D. M. Haldane and E. H. Rezayi, *Phys. Rev. Lett.* **54**, 237 (1985).
- ⁹F. D. M. Haldane, *Phys. Rev. Lett.* **51**, 605 (1983).
- ¹⁰F. D. M. Haldane, in Ref. 2.
- ¹¹B. I. Halperin, *Phys. Rev. Lett.* **52**, 2390(E) (1984).
- ¹²X. Du *et al.*, *Nature (London)* **462**, 192 (2009); K. Bolotin *et al.*, *ibid.* **462**, 196 (2009); C. R. Dean *et al.*, *Nat. Phys.* **7**, 693 (2011); F. Ghahari, Y. Zhao, P. Cadden-Zimansky, K. Bolotin, and P. Kim, *Phys. Rev. Lett.* **106**, 046801 (2011); B. E. Feldman *et al.*, *Science* **337**, 1196 (2012).
- ¹³Kun Yang, S. Das Sarma, and A. H. MacDonald, *Phys. Rev. B* **74**, 075423 (2006); C. Töke and J. K. Jain, *ibid.* **75**, 245440 (2007); Z. Papić, M. O. Goerbig, and N. Regnault, *Phys. Rev. Lett.* **105**, 176802 (2010); Z. Papić, D. A. Abanin, Y. Barlas, and R. N. Bhatt, *Phys. Rev. B* **84**, 241306 (2011).
- ¹⁴Waheb Bishara and Chetan Nayak, *Phys. Rev. B* **80**, 121302 (2009); Arkadiusz Wójs, Csaba Töke, and Jainendra K. Jain, *Phys. Rev. Lett.* **105**, 096802 (2010); Edward H. Rezayi and Steven H. Simon, *ibid.* **106**, 116801 (2011); I. Sodemann and A. H. MacDonald, *Phys. Rev. B* **87**, 245425 (2013); M. Peterson and C. Nayak, [arXiv:1303.1541](https://arxiv.org/abs/1303.1541); S. H. Simon and E. H. Rezayi, *Phys. Rev. B* **87**, 155426 (2013).
- ¹⁵R. Willett, J. P. Eisenstein, H. L. Stormer, D. C. Tsui, A. C. Gossard, and J. H. English, *Phys. Rev. Lett.* **59**, 1776 (1987).
- ¹⁶J. S. Xia, W. Pan, C. L. Vicente, E. D. Adams, N. S. Sullivan, H. L. Stormer, D. C. Tsui, L. N. Pfeiffer, K. W. Baldwin, and K. W. West, *Phys. Rev. Lett.* **93**, 176809 (2004); W. Pan, J. S. Xia, H. L. Stormer, D. C. Tsui, C. Vicente, E. D. Adams, N. S. Sullivan, L. N. Pfeiffer, K. W. Baldwin, and K. W. West, *Phys. Rev. B* **77**, 075307 (2008); A. Kumar, G. A. Csathy, M. J. Manfra, L. N. Pfeiffer, and K. W. West, *Phys. Rev. Lett.* **105**, 246808 (2010).
- ¹⁷N. Read and E. Rezayi, *Phys. Rev. B* **59**, 8084 (1999).
- ¹⁸Yang Liu, D. Kamburov, M. Shayegan, L. N. Pfeiffer, K. W. West, and K. W. Baldwin, *Phys. Rev. Lett.* **107**, 176805 (2011).
- ¹⁹N. Samkharadze, L. N. Pfeiffer, K. W. West, and G. A. Csáthy, [arXiv:1302.1444](https://arxiv.org/abs/1302.1444).
- ²⁰M. Levin, B. I. Halperin, and B. Rosenow, *Phys. Rev. Lett.* **99**, 236806 (2007); S.-S. Lee, S. Ryu, C. Nayak, and M. P. A. Fisher, *ibid.* **99**, 236807 (2007).
- ²¹Z. Papić, F. D. M. Haldane, and E. H. Rezayi, *Phys. Rev. Lett.* **109**, 266806 (2012).
- ²²J. P. Eisenstein, R. Willett, H. L. Stormer, D. C. Tsui, A. C. Gossard, and J. H. English, *Phys. Rev. Lett.* **61**, 997 (1988).
- ²³L. W. Engel, S. W. Hwang, T. Sajoto, D. C. Tsui, and M. Shayegan, *Phys. Rev. B* **45**, 3418 (1992).
- ²⁴G. A. Csáthy, J. S. Xia, C. L. Vicente, E. D. Adams, N. S. Sullivan, H. L. Stormer, D. C. Tsui, L. N. Pfeiffer, and K. W. West, *Phys. Rev. Lett.* **94**, 146801 (2005).
- ²⁵C. R. Dean, B. A. Piot, P. Hayden, S. Das Sarma, G. Gervais, L. N. Pfeiffer, and K. W. West, *Phys. Rev. Lett.* **101**, 186806 (2008).
- ²⁶Chi Zhang, T. Knuutila, Yanhua Dai, R. R. Du, L. N. Pfeiffer, and K. W. West, *Phys. Rev. Lett.* **104**, 166801 (2010).
- ²⁷J. Xia, V. Cvicek, J. P. Eisenstein, L. N. Pfeiffer, and K. W. West, *Phys. Rev. Lett.* **105**, 176807 (2010).
- ²⁸J. Xia, J. P. Eisenstein, L. N. Pfeiffer, and K. W. West, *Nat. Phys.* **7**, 845 (2011).
- ²⁹Guangtong Liu, Chi Zhang, D. C. Tsui, Ivan Knez, Aaron Levine, R. R. Du, L. N. Pfeiffer, and K. W. West, *Phys. Rev. Lett.* **108**, 196805 (2012).
- ³⁰Chi Zhang, Chao Huan, J. S. Xia, N. S. Sullivan, W. Pan, K. W. Baldwin, K. W. West, L. N. Pfeiffer, and D. C. Tsui, *Phys. Rev. B* **85**, 241302 (2012).
- ³¹Yang Liu, S. Hasdemir, M. Shayegan, L. N. Pfeiffer, K. W. West, and K. W. Baldwin, [arXiv:1302.6304](https://arxiv.org/abs/1302.6304).
- ³²J. C. Maan, in *Two Dimensional Systems, Heterostructures and Superlattices*, edited by G. Bauer, F. Kucher, and H. Heinrich (Springer, Heidelberg, 1984).
- ³³V. Halonen, P. Pietilainen, and T. Chakraborty, *Phys. Rev. B* **41**, 10202 (1990).
- ³⁴Daw-Wei Wang, Eugene Demler, and S. Das Sarma, *Phys. Rev. B* **68**, 165303 (2003).
- ³⁵Michael R. Peterson, Th. Jolicœur, and S. Das Sarma, *Phys. Rev. B* **78**, 155308 (2008).
- ³⁶E. H. Rezayi, F. D. M. Haldane, and K. Yang, *Phys. Rev. Lett.* **50**, 1219 (1983).
- ³⁷F. D. M. Haldane, *Phys. Rev. Lett.* **55**, 2095 (1985).
- ³⁸T. Chakraborty and P. Pietilainen, *The Quantum Hall Effects* (Springer, New York, 1995).
- ³⁹B. A. Bernevig and N. Regnault, *Phys. Rev. B* **85**, 075128 (2012).
- ⁴⁰R. H. Morf, *Phys. Rev. Lett.* **80**, 1505 (1998).
- ⁴¹M. Stern *et al.*, [arXiv:1201.3488](https://arxiv.org/abs/1201.3488); L. Tiemann *et al.*, [arXiv:1201.3737](https://arxiv.org/abs/1201.3737); X. Lin *et al.*, *Phys. Rev. B* **85**, 165321 (2012).
- ⁴²M. P. Lilly, K. B. Cooper, J. P. Eisenstein, L. N. Pfeiffer, and K. W. West, *Phys. Rev. Lett.* **82**, 394 (1999); R. R. Du, D. C. Tsui, H. L. Stormer, L. N. Pfeiffer, K. W. Baldwin, and K. W. West, *Solid State Commun.* **109**, 389 (1999); K. B. Cooper, M. P. Lilly, J. P. Eisenstein, L. N. Pfeiffer, and K. W. West, *Phys. Rev. B* **60**, R11285 (1999).
- ⁴³A. A. Koulakov, M. M. Fogler, and B. I. Shklovskii, *Phys. Rev. Lett.* **76**, 499 (1996).
- ⁴⁴M. M. Fogler, A. A. Koulakov, and B. I. Shklovskii, *Phys. Rev. B* **54**, 1853 (1996).
- ⁴⁵R. Moessner and J. T. Chalker, *Phys. Rev. B* **54**, 5006 (1996).
- ⁴⁶E. H. Rezayi, F. D. M. Haldane, and K. Yang, *Phys. Rev. Lett.* **83**, 1219 (1999).
- ⁴⁷S. M. Girvin, A. H. MacDonald, and P. M. Platzman, *Phys. Rev. Lett.* **54**, 581 (1985); *Phys. Rev. B* **33**, 2481 (1986).
- ⁴⁸F. D. M. Haldane, *Phys. Rev. Lett.* **107**, 116801 (2011).
- ⁴⁹R.-Z. Qiu, F. D. M. Haldane, Xin Wan, Kun Yang, and Su Yi, *Phys. Rev. B* **85**, 115308 (2012).
- ⁵⁰Bo Yang, Z. Papić, E. H. Rezayi, R. N. Bhatt, and F. D. M. Haldane, *Phys. Rev. B* **85**, 165318 (2012).
- ⁵¹Hao Wang, Rajesh Narayanan, Xin Wan, and Fuchun Zhang, *Phys. Rev. B* **86**, 035122 (2012).
- ⁵²L. Balents, *Europhys. Lett.* **33**, 291 (1996); K. Musaelian and R. Joynt, *J. Phys.: Condens. Matter* **8**, L105 (1996); E. Fradkin and S. A. Kivelson, *Phys. Rev. B* **59**, 8065 (1999); M. M. Fogler, *Europhys. Lett.* **66**, 572 (2004).
- ⁵³E. H. Rezayi and F. D. M. Haldane, *Phys. Rev. Lett.* **84**, 4685 (2000).

- ⁵⁴N. Read and D. Green, *Phys. Rev. B* **61**, 10267 (2000).
- ⁵⁵Dobromir Kamburov, Yang Liu, Mansour Shayegan, Loren N. Pfeiffer, Kenneth W. West, and Kirk W. Baldwin, *Phys. Rev. Lett.* **110**, 206801 (2013).
- ⁵⁶R. Roy, [arXiv:1208.2055](https://arxiv.org/abs/1208.2055); E. Dobardzic, M. V. Milovanovic, and N. Regnault, [arXiv:1303.7131](https://arxiv.org/abs/1303.7131).
- ⁵⁷M. Mulligan, C. Nayak, and S. Kachru, *Phys. Rev. B* **82**, 085102 (2010).
- ⁵⁸J. Maciejko, B. Hsu, S. A. Kivelson, YeJe Park, and S. L. Sondhi, [arXiv:1303.3041](https://arxiv.org/abs/1303.3041).

Search Search History

All Databases

<< Return to Web of Science®

Citing Articles Title: Universal Slow Growth of Entanglement in Interacting Strongly Disordered Systems
Author(s): Serbyn, Maksym ; Papic, Z. ; Abanin, Dmitry A.
Source: PHYSICAL REVIEW LETTERS Volume: 110 Issue: 26 Article Number: 260601 DOI: 10.1103/PhysRevLett.110.260601 Published: JUN 28 2013

This item has been cited by items indexed in the databases listed below. [more information]

5 in All Databases

- 5 publication in Web of Science
0 publication in BIOSIS Citation Index
0 publication in ScELO Citation Index
0 publication in Chinese Science Citation Database
0 data sets in Data Citation Index
0 publication in Data Citation Index

Results: 5 Page 1 of 1 Go Sort by: Publication Date -- newest to oldest

Create Citation Report

Hide Refine

Refine Results

Search within results for

Search

Databases

Research Domains Refine

SCIENCE TECHNOLOGY

Research Areas Refine

PHYSICS

MECHANICS

more options / values...

Document Types

Authors

Group/Corporate Authors

Editors

Funding Agencies

Source Titles

Conference/Meeting Titles

Publication Years

Languages

Countries/Territories

Select Page Add to Marked List (0) Send to: my.endnote.com

1. Title: QUANTUM DYNAMICS WITH AN ENSEMBLE OF HAMILTONIANS
Author(s): Rahmani, Armin
Source: MODERN PHYSICS LETTERS B Volume: 27 Issue: 26 Article Number: 1330019 DOI: 10.1142/S0217984913300196 Published: OCT 20 2013
Times Cited: 0 (from All Databases)

Get it! Waterloo View abstract

2. Title: Probing Real-Space and Time-Resolved Correlation Functions with Many-Body Ramsey Interferometry
Author(s): Knap, Michael; Kantian, Adrian; Giamarchi, Thierry; et al.
Source: PHYSICAL REVIEW LETTERS Volume: 111 Issue: 14 Article Number: 147205 DOI: 10.1103/PhysRevLett.111.147205 Published: OCT 4 2013
Times Cited: 0 (from All Databases)

Get it! Waterloo View abstract

3. Title: Ballistic Spreading of Entanglement in a Diffusive Nonintegrable System
Author(s): Kim, Hyungwon; Huse, David A.
Source: PHYSICAL REVIEW LETTERS Volume: 111 Issue: 12 Article Number: 127205 DOI: 10.1103/PhysRevLett.111.127205 Published: SEP 20 2013
Times Cited: 1 (from All Databases)

Get it! Waterloo View abstract

4. Title: Local Conservation Laws and the Structure of the Many-Body Localized States
Author(s): Serbyn, Maksym; Papic, Z.; Abanin, Dmitry A.
Source: PHYSICAL REVIEW LETTERS Volume: 111 Issue: 12 Article Number: 127201 DOI: 10.1103/PhysRevLett.111.127201 Published: SEP 17 2013
Times Cited: 1 (from All Databases)

Get it! Waterloo View abstract

5. Title: Area laws in a many-body localized state and its implications for topological order
Author(s): Bauer, Bela; Nayak, Chetan
Source: JOURNAL OF STATISTICAL MECHANICS-THEORY AND EXPERIMENT Article Number: P09005 DOI: 10.1088/1742-5468/2013/09/P09005
Published: SEP 2013
Times Cited: 0 (from All Databases)

Get it! Waterloo View abstract

Select Page Add to Marked List (0) Send to: my.endnote.com

Results: 5 Show 50 per page Page 1 of 1 Go Sort by: Publication Date -- newest to oldest

5 records matched your query of the 55,067,330 (contains duplicates) in the data limits you selected.

View in: 简体中文 繁體中文 English 日本語 한국어 Português Español

Universal Slow Growth of Entanglement in Interacting Strongly Disordered Systems

Maksym Serbyn,¹ Z. Papić,² and Dmitry A. Abanin^{3,4}

¹*Department of Physics, Massachusetts Institute of Technology, Cambridge, Massachusetts 02138, USA*

²*Department of Electrical Engineering, Princeton University, Princeton, New Jersey 08544, USA*

³*Perimeter Institute for Theoretical Physics, Waterloo, Ontario N2L 2Y5, Canada*

⁴*Institute for Quantum Computing, Waterloo, Ontario N2L 3G1, Canada*

(Received 24 April 2013; revised manuscript received 7 June 2013; published 28 June 2013)

Recent numerical work by Bardarson, Pollmann, and Moore revealed a slow, logarithmic in time, growth of the entanglement entropy for initial product states in a putative many-body localized phase. We show that this surprising phenomenon results from the dephasing due to exponentially small interaction-induced corrections to the eigenenergies of different states. For weak interactions, we find that the entanglement entropy grows as $\xi \ln(Vt/\hbar)$, where V is the interaction strength, and ξ is the single-particle localization length. The saturated value of the entanglement entropy at long times is determined by the participation ratios of the initial state over the eigenstates of the subsystem. Our work shows that the logarithmic entanglement growth is a universal phenomenon characteristic of the many-body localized phase in any number of spatial dimensions, and reveals a broad hierarchy of dephasing time scales present in such a phase.

DOI: [10.1103/PhysRevLett.110.260601](https://doi.org/10.1103/PhysRevLett.110.260601)

PACS numbers: 05.60.Gg, 05.30.Rt, 37.10.Jk, 72.15.Rn

Introduction.—While it is well known that arbitrarily weak disorder localizes all single-particle quantum-mechanical states in one and two dimensions, the effect of a disorder potential on the states of interacting systems largely remains an open problem. References [1,2] conjectured that localization in a many-body system survives in the presence of weak interactions. When the strength of the interactions is increased, at some critical value a transition to the delocalized phase—a “many-body localization” transition—takes place, as observed in the numerical simulations [3–13].

An important challenge is to understand the physical properties of the many-body localized (MBL) phase. Recent work [14] (see also Ref. [4]) revealed that even very weak interactions dramatically change the growth of entanglement of nonequilibrium many-body states. The authors of Ref. [14] studied the time evolution of product states in a 1D disordered XXZ spin chain. In the absence of interactions, such states maintain a low degree of entanglement upon evolution, and the entanglement entropy S_{ent} obeys an area law. In contrast, in the presence of interactions the states showed a slow, logarithmic in time, growth of S_{ent} (here and below we use “entanglement” and “entanglement entropy” interchangeably). The saturated value of S_{ent} was found to vary approximately linearly with system size, and remained well below the maximum possible value [14–16].

In this Letter, we identify a mechanism that underlies the logarithmic growth of entanglement in interacting MBL states. The key observation is that although very weak interactions have a small effect on the MBL eigenstates, they nevertheless induce small corrections to their energies, which ultimately lead to the dephasing between

different eigenstates at long time scales. We argue that this gives rise to a logarithmic growth of S_{ent} with time for a broad class of initial states that are a product of states in the two subsystems, a special example of which was considered in Ref. [14].

For weak interactions, our mechanism leads to the following predictions regarding entanglement growth as a function of the system’s parameters: (i) entropy grows as $S_{\text{ent}}(t) \propto \xi \log(Vt/\hbar)$, where V is the interaction strength and ξ is the single-particle localization length; (ii) the saturation value of S_{ent} is of the order of the “diagonal entropy” S_{diag} [17] of the given initial state. Diagonal entropy is determined by the participation ratios of the initial state in the basis of eigenstates of the system for $V = 0$. We also illustrate these predictions with numerical simulations of finite systems, in particular by constructing examples of initial states for which the saturated S_{ent} is equal to S_{diag} .

Model.—Without loss of generality, we consider a 1D lattice model of fermions with on-site disorder and nearest-neighbor interactions

$$H = J \sum_{\langle ij \rangle} c_i^\dagger c_j + \sum_i W_i \hat{n}_i + V \sum_{\langle ij \rangle} \hat{n}_i \hat{n}_j, \quad \hat{n}_i = c_i^\dagger c_i, \quad (1)$$

where $i, j = 1, \dots, N$, and $\langle ij \rangle$ denotes nearest neighbors. This model is equivalent to the random-field XXZ spin chain [14]. From our discussion below, it will become apparent that the logarithmic growth of entanglement in MBL systems is a robust phenomenon which does not depend on the dimensionality or the microscopic details of the system.

We will focus mostly on the regime of weak interactions for which the logarithmic growth of S_{ent} found in Ref. [14]

is perhaps the most striking. In the absence of interactions, $V = 0$, disorder localizes the single-particle states, with localization length ξ , and the many-body eigenstates are simply states in which a certain number of single-particle orbitals is occupied. Interactions that are much weaker compared to the typical level spacing $\sim 1/\xi$ do not significantly modify the many-body eigenstates. We have explicitly verified this statement for small systems, and assume it holds in general. However, even though the eigenstates are not strongly affected by the interactions, their energies are modified. If we fix the positions of all particles, except for a pair of particles situated at a distance $x \gg \xi$ away from each other, the interaction energy of this pair is $\sim Ve^{-x/\xi}$, and the corresponding dephasing time is $t_{\text{deph}} \sim \hbar e^{x/\xi}/V$. This gives rise to a hierarchy of dephasing time scales present in the problem, ranging from the fastest $t_{\text{min}} = \hbar/V$ to the slowest $t_{\text{max}} = t_{\text{min}} e^{L/\xi}$, where L is the system size.

Generally, the product initial states considered in Ref. [14], as well as the initial states of other kinds considered below, are a superposition of many eigenstates. The interactions introduce a slow dephasing between different states, and effectively generate entanglement between different remote parts of the system. A subsystem of size x becomes nearly maximally entangled with the rest of the system after an exponentially long time $t_{\text{deph}}(x) \sim \hbar e^{x/\xi}/V$; thus, the bipartite S_{ent} will increase logarithmically in time.

Two particles.—Let us start with a simple example which demonstrates that the slow growth of entanglement occurs for just two particles. Consider two distant particles prepared in an equal-weight superposition of two neighboring localized orbitals $|\Psi_0\rangle = 1/2(c_1^\dagger + c_2^\dagger)(c_3^\dagger + c_4^\dagger)|0\rangle$, where c_i^\dagger creates an eigenstate localized near site i . We assume that the distance between the support of the wave functions 1, 2 and 3, 4 is large ($x \gg \xi$) (see Fig. 1).

In the absence of interactions, no entanglement is generated during time evolution. Interactions, however, introduce a correction to the energy of the state $|\alpha\beta\rangle = c_\alpha^\dagger c_\beta^\dagger|0\rangle$, where $\alpha = 1, 2, \beta = 3, 4$. In the leading order of perturbation theory, the energy of this state is given by $E_{\alpha\beta} = \varepsilon_\alpha + \varepsilon_\beta + \delta E_{\alpha\beta}$, where $\varepsilon_\alpha, \varepsilon_\beta$ are the single-particle energies, and the last term $\delta E_{\alpha\beta} = C_{\alpha\beta} V e^{-x/\xi}$ is due to the interactions, $C_{\alpha\beta}$ being a constant which depends only algebraically on x .

The time-evolved state is given by $|\Psi(t)\rangle = 1/2 \sum_{\alpha,\beta} \exp(-iE_{\alpha\beta}t) |\alpha\beta\rangle$, and the reduced density matrix for the first particle reads

$$\hat{\rho}_L = \frac{1}{2} \begin{pmatrix} 1 & F(t)/2 \\ F^*(t)/2 & 1 \end{pmatrix}, \quad (2)$$

where $F(t) = e^{-i\Omega t}(1 + e^{-i\delta\Omega t})$, $\delta\Omega = \delta E_{14} - \delta E_{24} - \delta E_{13} + \delta E_{23}$, and $\Omega = \varepsilon_1 - \varepsilon_2 + \delta E_{13} - \delta E_{23}$. The eigenstates of $\hat{\rho}_L$ therefore oscillate with a very long period

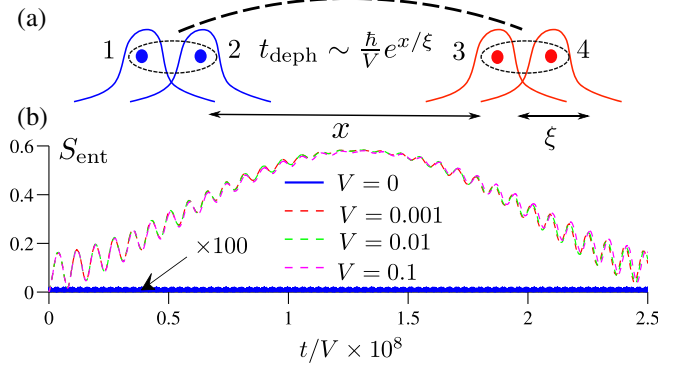


FIG. 1 (color online). (a) Generation of entanglement between two remote particles, each prepared in an equal superposition of two eigenstates. Exponentially small overlap of the orbitals leads to the dephasing time growing exponentially with distance. (b) S_{ent} as a function of time for a given realization of disorder and different interaction strengths. When $V = 0$, $S_{\text{ent}} \sim 10^{-4}$ and remains small at all times. For $V \neq 0$, values of $S_{\text{ent}}(t)$ collapse on a single curve when time is scaled by $1/V$. System size is $L = 10$ sites, and disorder strength is $W = 6$.

$T = 2\pi/\delta\Omega \sim (\hbar/V)e^{x/\xi}$. At times $t = (2n + 1)\pi/\delta\Omega$, the off-diagonal elements vanish, and the eigenvalues become equal to $1/2$. At these times, the particles become maximally entangled with $S_{\text{ent}} = \ln 2$. Figure 1 demonstrates that even weak interactions lead to the entanglement of the order of $S_{\text{ent}} \approx \ln 2$, and the rate of entanglement change is inversely proportional to the interaction strength. In Fig. 1, particles are in a superposition of states which are not the exact eigenstates; hence, the maximum value of S_{ent} is slightly below $\ln 2 \approx 0.69$. Note that no disorder or time averaging is used.

General case.—Turning to the general many-body case, let us divide the system into two parts \mathcal{L} and \mathcal{R} , labeling the single-particle orbitals that are localized dominantly in \mathcal{L} by index α_n , and those residing in \mathcal{R} by β_n . There may be some ambiguity for the state residing near the boundary between \mathcal{L} and \mathcal{R} , but we will be interested in systems of size $L \gg \xi$, for which the boundary effects are not very important.

We consider initial states that are products of some superposition of states with definite numbers of particles in \mathcal{L} and \mathcal{R} :

$$|\Psi(t=0)\rangle = \sum_{\{\alpha\} \in \mathcal{L}} A_{\{\alpha\}} |\alpha_1 \dots \alpha_K\rangle \times \sum_{\{\beta\} \in \mathcal{R}} B_{\{\beta\}} |\beta_1 \dots \beta_M\rangle. \quad (3)$$

Coefficients A, B are chosen such that Ψ is normalized.

Neglecting the change to the eigenstate due to interactions, the reduced density matrix for \mathcal{L} after time evolution reads $\hat{\rho}_L = \sum_{\alpha,\alpha'} \rho_{\alpha\alpha'} |\alpha\rangle\langle\alpha'|$, where $\rho_{\alpha\alpha'} = A_\alpha A_{\alpha'}^* \sum_{\beta} |B_\beta|^2 e^{i(E_{\alpha'\beta} - E_{\alpha\beta})t}$, and we have used a shorthand notation $\alpha \equiv \{\alpha\}$, $\beta \equiv \{\beta\}$. It is convenient to define

$A_\alpha(t) = A_\alpha e^{-iE_\alpha t}$, where E_α is the energy of the $|\alpha\rangle$ state for the isolated \mathcal{L} subsystem. Assuming that $|\alpha\rangle \times |\beta\rangle$ remains an eigenstate (this may not be true near the boundary, but the boundary effect is not important for entanglement growth, at least in large systems), the above equation, written in terms of coefficients $A_\alpha(t)$, preserves the same form, except the energies $E_{\alpha\beta}$ should be substituted by the interaction energy $\delta E_{\alpha\beta}$ between particles in the \mathcal{L} and \mathcal{R} subsystems. For particles that reside far away from the boundary, this correction can be calculated in perturbation theory.

The energy difference $\delta E_{\alpha'\beta} - \delta E_{\alpha\beta}$ that enters the off-diagonal elements of $\hat{\rho}_\mathcal{L}$, to the leading order, is proportional to $Ve^{-x/\xi}$. Here x is the minimum distance between a particle in \mathcal{L} , the position of which is different in states α and α' , and the particles in \mathcal{R} . However, it also contains many smaller contributions, which arise due to the interaction between more distant pairs of particles. Thus, the off-diagonal elements oscillate at a number of very different, incommensurate frequencies.

The interaction energy leads to dephasing, which decreases the off-diagonal elements of $\hat{\rho}_\mathcal{L}$, thus generating entanglement. Effectively, at times $t(x) \sim t_{\min} e^{x/\xi}$ the degrees of freedom within a distance $x(t) \sim \ln(t/t_{\min})$ from the boundary between \mathcal{L} and \mathcal{R} are affected by dephasing, while states that differ only in the positions of particles further away from the boundary are still phase coherent. This generates the entropy

$$S_{\text{ent}}(t) = CS_{\text{diag}}, \quad S_{\text{diag}} = -\sum P_i(x) \ln P_i(x), \quad (4)$$

where $P_i(x)$ are the probabilities of different states $|\alpha\rangle$ in a segment of size x , calculated from the wave function of the initial state. Quantity S_{diag} is the diagonal entropy—a maximum achievable entropy for a given initial state, assuming that interactions do not change the eigenstates. S_{ent} is expected to be smaller than S_{diag} by a factor $C \leq 1$; the precise value of this prefactor is nonuniversal, and depends on the preparation of the initial state. In the long-time limit, assuming that $\mathcal{R} \gg \mathcal{L}$ and the initial state is a superposition of many different states, we expect the off-diagonal elements to become very small such that the entanglement entropy approaches its maximum value with $C \rightarrow 1$.

Since for initial product states S_{diag} is proportional to the subsystem size, entanglement grows logarithmically:

$$S_{\text{ent}}(t) \propto \xi \log(Vt/\hbar). \quad (5)$$

We emphasize that our argument does not rely on averaging, and therefore entanglement grows according to Eq. (5) even for a single disorder realization, and even for relatively small systems.

Numerical simulations.—In order to illustrate the above mechanism, and to explore the growth of entanglement for different initial states, we performed numerical simulations

of the model (1) with a finite number of particles in a random potential uniformly distributed in the interval $[-W, W]$. Hopping is set to $J = 1/2$ and we consider chains with an even number of sites and open boundary conditions at half filling. The number of different disorder realizations ranged from 30 000 ($L = 8$) to 800 ($L = 14$); the number of initial states was $2^{L/2}$ for each disorder realization. In the figures below, error bars (if not shown) are approximately equal to the size of the symbols in each plot.

Using exact diagonalization for systems up to 14 sites, we compute the time evolution of various initial states, which allows us to obtain $S_{\text{ent}}(t)$ for half partition. We study its average $\bar{S}_{\text{ent}}(t)$ over different initial states belonging to the same class, and over different realizations of disorder. Similar to Ref. [14], we first consider a class of localized product states (LPS) where each fermion is initially located at a given site. Results for $\bar{S}_{\text{ent}}(t)$ for a system of $L = 12$ sites and disorder $W = 5$ are shown in Fig. 2(a). After a rapid increase of entropy on time scales of the inverse hopping, due to diffusive transport on a scale smaller than the localization length, $\bar{S}_{\text{ent}}(t)$ saturates for a noninteracting system. In the presence of even weak interactions, $\bar{S}_{\text{ent}}(t)$ continues to grow further. In full agreement with our analysis above, values of $\delta\bar{S}_{\text{ent}} \equiv \bar{S}_{\text{ent}} - \bar{S}_0$ collapse onto a single curve as a function of $\ln(Vt/\hbar)$ [see the inset of Fig. 2(a)], where \bar{S}_0 is the saturation entropy of a noninteracting system.

The saturation value $\bar{S}_{\text{ent}}(\infty)$ does not vary appreciably with interaction strength when interactions are weak. This further supports the conclusion that weak interactions only weakly alter the eigenstates of the system. For fixed $V = 0.01$, $\bar{S}_{\text{ent}}(\infty)$ and S_{diag} decrease with disorder [see Fig. 2(b)] approximately as $1/W$ (scaling not shown). Such

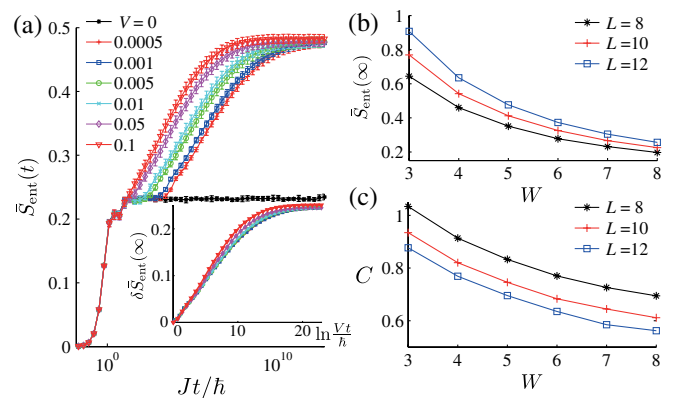


FIG. 2 (color online). (a) Averaged entanglement entropy of initial product states, in which all fermions are localized at some sites, shows a characteristic logarithmic growth on long time scales (system size is $L = 12$, $W = 5$). Growth rate is found to be proportional to $\ln(Vt/\hbar)$ (inset). Saturated entanglement (b) and the ratio $C = \bar{S}_{\text{ent}}(\infty)/S_{\text{diag}}$ (c) decrease with W (for fixed $V = 0.01$).

scaling stems from the fact that when ξ is of the order of one lattice spacing, the leading contribution to the entanglement comes from rare resonant pairs of neighboring sites (rather than typical off-resonant sites), which occur with probability J/W . Each pair contributes a number of the order $\sim \ln 2$ to the entanglement as well as diagonal entropy.

We compare the saturated entanglement to S_{diag} , calculated using the values of $P_i(L/2)$ for the initial state of the \mathcal{L} subsystem. The $P_i(L/2)$ are obtained from the density matrix, using the eigenstates of the interacting Hamiltonian restricted to \mathcal{L} . In this sense, while $\bar{S}_{\text{ent}}(\infty)$ is determined from the time evolution of the system, S_{diag} is solely the property of the initial state.

To interpret the dependence of the ratio $C = \bar{S}_{\text{ent}}(\infty)/\bar{S}_{\text{diag}}$ on system size and disorder [see Fig. 2(c)], we must take into account two additional effects important for small systems: (i) the diffusion of particles across the entanglement cut; and (ii) the inefficiency of decoherence when the number of terms in Eq. (3) is small or when \mathcal{L} and \mathcal{R} are of equal size. These effects counteract each other, as diffusion leads to an additional contribution to S_{ent} not captured by Eq. (4). On the other hand, inefficient decoherence leads to incomplete dephasing, and decreases $\bar{S}_{\text{ent}}(\infty)$ compared to S_{diag} . The positive contribution from (i) is suppressed for larger systems or smaller localization lengths. The effect of (ii) depends on the initial state. For LPS in the localized phase, the participation ratio is of order unity, and the effect (ii) is very pronounced. Thus, C is smaller than 1, and it decreases with increasing disorder or system size [see Fig. 2(c)].

Next, we consider a different kind of initial states with larger participation ratios. The initial state of the \mathcal{R} and \mathcal{L} subsystem is chosen as a projection to the half-filled sector of the state $\prod_i 1/\sqrt{2}(1 \pm c_i^\dagger)|0\rangle$, with \pm signs chosen at random. Particles within each subsystem are therefore strongly entangled, but there is no entanglement between the subsystems at $t = 0$. In this case, we find the same logarithmic entanglement growth, but $\bar{S}_{\text{ent}}(\infty)$ [see the solid lines in Fig. 3(a)] is larger compared to the previous case, and varies weakly with disorder. The ratio C [see the upper panel of Fig. 3(b)] now scales to 1 when system size is increased, contrary to the LPS. For this type of initial state, due to larger values of $\bar{S}_{\text{ent}}(\infty)$, the boundary diffusion contribution is less important; also, the superposition of a large number of eigenstates in each half of the system makes decoherence more efficient; thus, C is closer to 1.

Finally, we construct an example where S_{ent} reaches S_{diag} . We take a product of the LPS in \mathcal{L} , and the strongly entangled state in \mathcal{R} . To further suppress the diffusion, we require the two sites adjacent to the entanglement cut to be always empty. $\bar{S}_{\text{ent}}(\infty)$ displays the behavior similar to the LPS case [see the dashed lines in Fig. 3(a)], but is larger due to the more effective dephasing. Remarkably, Fig. 3(b)

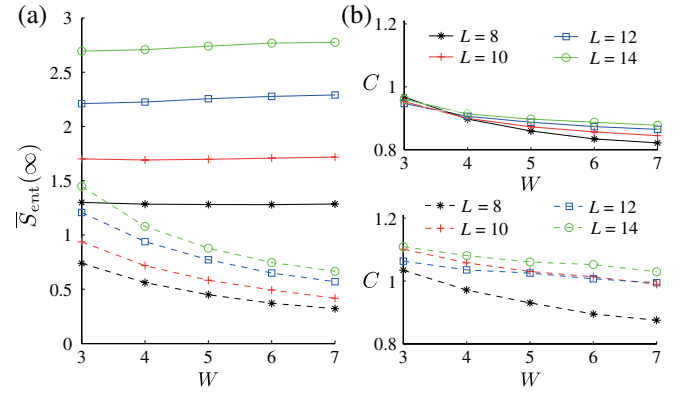


FIG. 3 (color online). (a) Saturated entanglement entropy as a function of disorder W for a strongly entangled state (solid lines), and a product of a strongly entangled state and an LPS state (dashed lines). (b) Ratio of saturated and diagonal entropy as a function of disorder W for the same two states. For the product of a strongly entangled state and an LPS state (lower panel), C tends to 1 for larger system sizes as W is increased (interaction is set to $V = 0.01$).

demonstrates that for larger system sizes, saturation and diagonal entropies become equal, in agreement with the above analysis.

Discussion.—To summarize, we presented a mechanism of the logarithmic growth of entanglement in the MBL phase. We also established the laws governing the entanglement growth, and tested them in numerical simulations for different initial states. We note that in the delocalized phase the entanglement is expected to grow much faster (as a power-law function of time), suggesting that the scaling of S_{ent} can be used as a potential tool for studying the localization-delocalization critical point and its properties.

Although we focused on the limit of weak interactions, in which the eigenstates are similar to those of a non-interacting model, we expect our conclusions to hold also for stronger interactions which do modify the eigenstates. In this case, $\bar{S}_{\text{ent}}(\infty)$ is expected to be determined by the participation ratios of the initial state in the basis of the interacting subsystem’s eigenstates. Furthermore, our conclusions are expected to apply to localized interacting systems in any number of spatial dimensions.

Our work indicates an exponentially broad distribution of dephasing time scales present in a MBL system. It gives support to the “strong-localization” scenario of the many-body localization transition, and shows that the entanglement growth arises due to interaction-induced dephasing, rather than due to the effect of interactions on the eigenstates, as was hypothesized in Ref. [14].

We note that recently Vosk and Altman [18] considered an XXZ model with random exchange interactions, but without a random field. For a special initial state, they developed a strong-disorder renormalization group procedure, and found that S_{ent} grows as a power of $\ln t$. The difference from our result stems from the fact that the state

considered in Ref. [18] was critical; however, the basic underlying mechanism—dephasing due to exponentially weak interactions between remote spins—is qualitatively similar. After this Letter was submitted, we became aware of a related independent work [19] where the logarithmic growth of entanglement was established from phenomenological considerations.

We would like to thank E. Altman and J. Moore for useful comments on the manuscript. This research was supported in part by Perimeter Institute for Theoretical Physics. Research at Perimeter Institute is supported by the Government of Canada through Industry Canada and by the Province of Ontario through the Ministry of Economic Development & Innovation. Z. P. was supported by DOE Grant No. DE-SC0002140. The simulations presented in this article were performed on computational resources supported by the High Performance Computing Center (PICSciE) at Princeton University.

-
- [1] D. Basko, I. Aleiner, and B. Altshuler, *Ann. Phys. (Amsterdam)* **321**, 1126 (2006).
 - [2] I. V. Gornyi, A. D. Mirlin, and D. G. Polyakov, *Phys. Rev. Lett.* **95**, 206603 (2005).
 - [3] V. Oganesyan and D. A. Huse, *Phys. Rev. B* **75**, 155111 (2007).

- [4] M. Znidaric, T. Prosen, and P. Prelovšek, *Phys. Rev. B* **77**, 064426 (2008).
- [5] C. Monthus and T. Garel, *Phys. Rev. B* **81**, 134202 (2010).
- [6] T. C. Berkelbach and D. R. Reichman, *Phys. Rev. B* **81**, 224429 (2010).
- [7] A. Pal and D. A. Huse, *Phys. Rev. B* **82**, 174411 (2010).
- [8] C. Gogolin, M. P. Müller, and J. Eisert, *Phys. Rev. Lett.* **106**, 040401 (2011).
- [9] E. Canovi, D. Rossini, R. Fazio, G. E. Santoro, and A. Silva, *Phys. Rev. B* **83**, 094431 (2011).
- [10] M. Rigol, V. Dunjko, V. Yurovsky, and M. Olshanii, *Phys. Rev. Lett.* **98**, 050405 (2007).
- [11] F. Buccheri, A. De Luca, and A. Scardicchio, *Phys. Rev. B* **84**, 094203 (2011).
- [12] E. Cuevas, M. Feigel'man, L. Ioffe, and M. Mezard, *Nat. Commun.* **3**, 1128 (2012).
- [13] A. De Luca and A. Scardicchio, *Europhys. Lett.* **101**, 37003 (2013).
- [14] J. H. Bardarson, F. Pollmann, and J. E. Moore, *Phys. Rev. Lett.* **109**, 017202 (2012).
- [15] G. D. Chiara, S. Montangero, P. Calabrese, and R. Fazio, *J. Stat. Mech.* **2006**, P03001 (2006).
- [16] F. Iglói, Z. Szatmári, and Y.-C. Lin, *Phys. Rev. B* **85**, 094417 (2012).
- [17] A. Polkovnikov, *Ann. Phys. (Amsterdam)* **326**, 486 (2011).
- [18] R. Vosk and E. Altman, *Phys. Rev. Lett.* **110**, 067204 (2013).
- [19] D. A. Huse and V. Oganesyan, [arXiv:1305.4915](https://arxiv.org/abs/1305.4915).

All Databases | Select a Database | Web of Science | Additional Resources

Search Search History

All Databases

<< Return to Web of Science®

Citing Articles Title: Local Conservation Laws and the Structure of the Many-Body Localized States
Author(s): Serbyn, Maksym ; Papic, Z. ; Abanin, Dmitry A.
Source: PHYSICAL REVIEW LETTERS Volume: 111 Issue: 12 Article Number: 127201 DOI: 10.1103/PhysRevLett.111.127201 Published: SEP 17 2013

This item has been cited by items indexed in the databases listed below. [more information]

1 in All Databases

- 1 publication in Web of Science
0 publication in BIOSIS Citation Index
0 publication in ScELO Citation Index
0 publication in Chinese Science Citation Database
0 data sets in Data Citation Index
0 publication in Data Citation Index

Results: 1 Page 1 of 1 Go Sort by: Publication Date -- newest to oldest

Create Citation Report

Hide Refine

Refine Results

Search within results for

Search

Databases

Research Domains

SCIENCE TECHNOLOGY

Research Areas

PHYSICS

Document Types

Authors

Group/Corporate Authors

Editors

Funding Agencies

Source Titles

Conference/Meeting Titles

Publication Years

Languages

Countries/Territories

Select Page Add to Marked List (0) Send to: my.endnote.com

Title: Probing Real-Space and Time-Resolved Correlation Functions with Many-Body Ramsey Interferometry
Author(s): Knap, Michael; Kantian, Adrian; Giamarchi, Thierry; et al.
Source: PHYSICAL REVIEW LETTERS Volume: 111 Issue: 14 Article Number: 147205 DOI: 10.1103/PhysRevLett.111.147205 Published: OCT 4 2013
Times Cited: 0 (from All Databases)

Get it! Waterloo View abstract

Select Page Add to Marked List (0) Send to: my.endnote.com

Results: 1 Show 50 per page Page 1 of 1 Go Sort by: Publication Date -- newest to oldest

1 records matched your query of the 55,067,330 (contains duplicates) in the data limits you selected.

View in: 简体中文 繁體中文 English 日本語 한국어 Português Español

Local Conservation Laws and the Structure of the Many-Body Localized States

Maksym Serbyn,¹ Z. Papić,² and Dmitry A. Abanin^{3,4}

¹*Department of Physics, Massachusetts Institute of Technology, Cambridge, Massachusetts 02138, USA*

²*Department of Electrical Engineering, Princeton University, Princeton, New Jersey 08544, USA*

³*Perimeter Institute for Theoretical Physics, Waterloo, Ontario N2L 2Y5, Canada*

⁴*Institute for Quantum Computing, Waterloo, Ontario N2L 3G1, Canada*

(Received 5 June 2013; revised manuscript received 10 July 2013; published 17 September 2013)

We construct a complete set of local integrals of motion that characterize the many-body localized (MBL) phase. Our approach relies on the assumption that local perturbations act locally on the eigenstates in the MBL phase, which is supported by numerical simulations of the random-field XXZ spin chain. We describe the structure of the eigenstates in the MBL phase and discuss the implications of local conservation laws for its nonequilibrium quantum dynamics. We argue that the many-body localization can be used to protect coherence in the system by suppressing relaxation between eigenstates with different local integrals of motion.

DOI: [10.1103/PhysRevLett.111.127201](https://doi.org/10.1103/PhysRevLett.111.127201)

PACS numbers: 75.10.Pq, 05.30.Rt, 64.70.Tg, 72.15.Rn

Introduction.—Localization of eigenstates of a single particle in the presence of disorder is among the most remarkable consequences of quantum mechanics. Although the single-particle localization and localization-delocalization transition are well understood [1,2], much less is known about the nature of the eigenstates in interacting many-body disordered systems. The interest in the problem of the many-body localization was rekindled when recent works [3,4] suggested that the localized phase is stable with respect to weak interactions. This conjecture was also corroborated by numerical studies [5–16].

In the noninteracting localized phase, dynamics is simple because any initial wave function can be decomposed into a superposition of localized single-particle eigenstates. However, when interactions are introduced, the dynamics becomes notably richer [7,16–18]. Although particle transport is still expected to be blocked, the time evolution of initial product states in the interacting localized phase generates a universal slow growth of entanglement entropy [17]. Saturated entropy was established to be proportional to system size [7,16–18], and such growth of the entanglement was argued to reflect “partial thermalization” of the system. However, the type of the ensemble describing the many-body localized (MBL) phase is unknown.

On the experimental side, probing the dynamics of interacting disordered systems has become feasible due to the advances in the field of ultracold atomic gases [19,20]. In particular, nearly isolated quantum systems of cold atoms can now be engineered, prepared in a variety of initial states (including product states [21]), and studied during their subsequent time evolution. These opportunities call for developing a better understanding of the laws that govern the dynamics in the MBL phase.

Here we consider a many-body system whose eigenstates at all energies are localized, and show that they

can be characterized by a large number of emergent local integrals of motion corresponding to multiple local conservation laws. These integrals of motion form a complete set, in the sense that their values completely determine the eigenstates. Local conservation laws strongly constrain the quantum dynamics in the MBL phase, preventing a complete thermalization of any given subsystem. Any initial state can be decomposed in terms of the eigenstates possessing definite values of the integrals of motion. During time evolution, the weights of different states cannot change. However, because of the exponentially weak interaction between distant degrees of freedom, the relative phases between the states with different values of local integrals of motion become randomized. Any local observable at long times is therefore determined only by the set of probabilities of local integrals of motion that affect the degrees of freedom in the region where the observable is measured. We refer to this as the local diagonal ensemble. The dephasing due to the interactions between distant subsystems is a distinct feature of the MBL phase compared to the noninteracting one, and underlies the slow growth of entanglement [16,17,22,23].

Integrals of motion.—First, we note that for the noninteracting case the local integrals of motion are simply given by $\hat{I}_i = c_i^\dagger c_i$, where c_i^\dagger creates a localized single-particle state. For fermions, the possible eigenvalues of this integral of motion are $I_i \in \{0, 1\}$. In a system with K orbitals, there are 2^K eigenstates, which are uniquely labeled by the eigenvalues of K integrals of motion.

In order to explicitly construct local integrals of motion for an interacting system, we assume the following property of the localized phase: local perturbations lead only to local modifications of the eigenstates in the MBL phase. That is, if we act on a MBL eigenstate with a local perturbation, introduced either adiabatically or instantaneously, the degrees of freedom situated at a distance $L \gg \xi$

(here ξ is the localization length [24]) away from the support of the perturbation operator, are generally affected exponentially weakly. We will support this statement below by the numerical study of the random-field XXZ chain, also considered in Refs. [7,10,12,15,16].

Let us consider a MBL system described by a local Hamiltonian, and let us divide it into subsystems of size $l \gg \xi$. Without loss of generality, we consider a 1D system, although our conclusions apply to localized phases in any number of spatial dimensions. We number the subsystems by $i = 1, \dots, N$ from left to right, assuming the number of degrees of freedom \mathcal{M} in each subsystem is the same (e.g., for K spins, $\mathcal{M} = 2^K$). For the fixed subsystem i , we denote parts of the full system to the left and to the right of i by \mathcal{L}_i and \mathcal{R}_i , respectively. The Hamiltonian can be written as

$$H = H_{\mathcal{L}} + H_i + H_{\mathcal{R}} + H_{\mathcal{L}_i} + H_{\mathcal{R}_i}, \quad (1)$$

where $H_{\mathcal{L}}$, $H_{\mathcal{R}}$, H_i act only on the degrees of freedom in \mathcal{L} , \mathcal{R} , i , while $H_{\mathcal{L}_i}$, $H_{\mathcal{R}_i}$ couple \mathcal{L} , i and \mathcal{R} , i .

If the subsystems \mathcal{L} , i , \mathcal{R} are disconnected from each other (i.e., $H_{\mathcal{L}_i}$, $H_{\mathcal{R}_i}$ are set to zero), the eigenstates are simple products: $|\alpha\beta\gamma\rangle_0 = |\alpha\rangle_{\mathcal{L}} \otimes |\beta\rangle_i \otimes |\gamma\rangle_{\mathcal{R}}$, where $\alpha \in \{1, \dots, \mathcal{M}^{i-1}\}$, $\beta = \{1, \dots, \mathcal{M}\}$, $\gamma = \{1, \dots, \mathcal{M}^{N-i}\}$. Once the subsystems are connected, the eigenstates of the full Hamiltonian (1) are obtained from the product states $|\alpha\beta\gamma\rangle_0$ by nearly local rotations. We label the resulting eigenstates by their ‘‘ancestors,’’ omitting the ‘‘0’’ subscript,

$$|\alpha\beta\gamma\rangle = \hat{O}_{\mathcal{L}_i} \hat{O}_{\mathcal{R}_i} |\alpha\rangle_{\mathcal{L}} \otimes |\beta\rangle_i \otimes |\gamma\rangle_{\mathcal{R}}. \quad (2)$$

Operator $\hat{O}_{\mathcal{L}_i}$ is a unitary many-body rotation which strongly transforms only the degrees of freedom within a distance $\sim \xi$ away from the boundary between \mathcal{L} and i (similarly for $\hat{O}_{\mathcal{R}_i}$). The commutator of $\hat{O}_{\mathcal{L}_i}$ and $\hat{O}_{\mathcal{R}_i}$, as well as the action on the degrees of freedom far away, decays exponentially. We note that the assignment (2), which links the eigenstates of the system to the eigenstates of subsystems, is not unique, and assume that a certain one-to-one correspondence is chosen.

We now define the integral of motion for subsystem i

$$\hat{I}_i = \sum_{\beta=1}^{\mathcal{M}} \beta \sum_{\alpha=1}^{\mathcal{M}^{i-1}} \sum_{\gamma=1}^{\mathcal{M}^{N-i}} |\alpha\beta\gamma\rangle \langle \alpha\beta\gamma|. \quad (3)$$

Being a linear combination of projectors onto the exact eigenstates, \hat{I}_i necessarily commutes with the Hamiltonian and assumes eigenvalues $1, \dots, \mathcal{M}$. Intuitively, states with the same eigenvalue of \hat{I}_i look nearly identical within the subsystem i at distances larger than ξ away from the boundaries with subsystems \mathcal{L} , \mathcal{R} .

Sums of projectors onto the eigenstates are integrals of motion by construction; however, generally such operators are nonlocal and affect all degrees of freedom of the system. The operator in Eq. (3) is special in that it is local;

i.e., it weakly affects the degrees of freedom in \mathcal{L} or \mathcal{R} at a distance $x \gg \xi$ away from the boundaries with the i th subsystem. The locality of \hat{I}_i follows directly from the locality of operators $\hat{O}_{\mathcal{L}_i}$, $\hat{O}_{\mathcal{R}_i}$, which implies that the sum of projectors becomes very close to the identity operator far away from the boundaries. Below, we will test the locality of the operator in Eq. (3) in a specific model.

Having defined the integral of motion for the subsystem i , we can similarly define $N - 1$ integrals of motion for the remaining $N - 1$ subsystems, such that in total we have N integrals \hat{I}_i , $i = 1, \dots, N$. Different \hat{I}_i commute with each other $[\hat{I}_i, \hat{I}_j] = 0$ since they are sums of projectors onto the exact eigenstates of the full system. Each \hat{I}_i has \mathcal{M} possible eigenvalues; thus, the full description of the system via integrals of motion requires \mathcal{M}^N parameters, which coincides with the dimensionality of the Hilbert space. An operator \hat{I}_i can also be viewed as the z component $\hat{I}_i = \hat{S}_{iz}$ of a ‘‘spin’’ $S = (\mathcal{M} - 1)/2$. Raising and lowering operators can then be used to construct the entire set of eigenstates, starting from any given eigenstate $|I_1 I_2 \dots I_N\rangle$ characterized by the integrals of motion I_1, I_2, \dots, I_N . Therefore, specifying the eigenvalues of all integrals of motion defined above completely determines the eigenstates of the system.

Hamiltonian and its relation to integrals of motion.—The Hamiltonian takes an especially simple form when written in terms of the integrals of motion:

$$H = \sum_i^N \sum_{I_i=1}^{\mathcal{M}} E_{I_i} \hat{\mathcal{P}}_{I_i}^i + \sum_{i \neq j}^N \sum_{I_i, I_j=1}^{\mathcal{M}} E_{I_i I_j} \hat{\mathcal{P}}_{I_i}^i \hat{\mathcal{P}}_{I_j}^j + \sum_{i < j < k}^N \sum_{I_i, I_j, I_k=1}^{\mathcal{M}} E_{I_i I_j I_k} \hat{\mathcal{P}}_{I_i}^i \hat{\mathcal{P}}_{I_j}^j \hat{\mathcal{P}}_{I_k}^k + \dots, \quad (4)$$

where $\hat{\mathcal{P}}_{I_i}^i$ is the projector onto the subspace for which the eigenvalue of the i th integral of motion is equal to I_i . In the above equation, E_{I_i} can be roughly viewed as the energy of the i th subsystem for the sector I_i , $E_{I_i I_j}$ is the interaction energy between i and j subsystems, etc. There are interactions between any given n subsystems; however, they are exponentially small. Generally, we expect that energies E_{I_i} are proportional to l , the size of the subsystems. $E_{I_i I_j}$ are proportional to ξ when $i = j \pm 1$, and are suppressed as $\xi e^{-l(|i-j|-1)/\xi}$ otherwise (the interactions between the neighboring subsystems are limited to the boundary and are therefore proportional to ξ). The above representation of the Hamiltonian gives us a way to describe the dynamics in the MBL phase for various kinds of initial states [7,10–12,16,17].

Dynamics.—As a first step, we consider the dynamics of an eigenstate which is perturbed locally. We assume a sudden action of the local unitary operator \hat{U} on the eigenstate $|\Psi_0\rangle = |I_1 I_2 \dots I_N\rangle$. Operator \hat{U} acts only on the degrees of freedom in subsystem 1, and its support is

situated far from the boundary between subsystems 1 and 2. The initial wave function $|\Psi(t=0)\rangle$ can be decomposed in terms of the eigenstates:

$$|\Psi(t=0)\rangle = \hat{U}|\Psi_0\rangle = \sum_{I'_1} U_{I_1 I'_1} |I'_1 I_2 \dots I_N\rangle + \dots \quad (5)$$

This form of the decomposition is dictated by the fact that the values of the integrals of motion I_2, \dots, I_N can be changed only with an exponentially small probability; hence, the terms with other values of I_2, I_3, \dots in Eq. (5) are represented by ellipses. Neglecting these terms, the subsequent dynamics becomes trivial:

$$|\Psi(t)\rangle = \sum_{I'_1} U_{I_1 I'_1} e^{-iE_{I'_1 I_2 \dots I_N} t} |I'_1 I_2 \dots I_N\rangle, \quad (6)$$

where $E_{I'_1 I_2 \dots I_N}$ is the energy of the state $|I'_1 I_2 \dots I_N\rangle$. Generally, we expect a finite number of different I'_1 which have significant matrix elements $U_{I_1 I'_1}$, typically comparable to the dimensionality of a subsystem of size $\sim \xi$. Therefore, the time evolution (6) describes coherent oscillations that involve a finite number of states. Any local observable in region 1 would therefore oscillate at a number of frequencies, showing revivals but no dephasing. This situation changes if the state $|\Psi_0\rangle$ is not an eigenstate, but a superposition of several eigenstates which involve different values of I_2, I_3, \dots, I_k . In this case, exponentially slow dephasing arises, suppressing the revivals and oscillations of local observables in the long-time limit. The values of observables at long times are determined by the probabilities $|U_{I_1 I'_1}|^2$.

Second, we describe the global evolution of states which differ from the eigenstates everywhere, not just locally. For definiteness, consider an initial product state of subsystems 1, 2, \dots , N :

$$|\Psi\rangle = \otimes_{i=1}^N \left(\sum_{\alpha_i} A_{\alpha_i} |\alpha_i\rangle \right), \quad (7)$$

where $|\alpha_i\rangle$ is an eigenstate of the Hamiltonian H_i . Modern experimental techniques allow for the preparation and manipulation of such states in optical lattices [21].

Each component $\otimes_{i=1}^N |\alpha_i\rangle$ of the product state (7) can be related to the eigenstate of the whole system, $|I_1 I_2 \dots I_N\rangle$, by the set of local rotations acting near the boundaries between different subsystems. The dynamics corresponding to this effect will be limited to the boundaries between pairs of subsystems. However, for each wave function, degrees of freedom at a distance $x \gg \xi$ away from the boundary will remain undisturbed. Such dynamics therefore does not generate long-range entanglement.

More importantly, since we are dealing with a superposition of different product states $\otimes_{i=1}^N |\alpha_i\rangle$, the degrees of freedom in the subsystem i will be in a superposition of states with different values of the integral of motion I_i . Different states entering this superposition are eigenstates;

therefore, their relative weights cannot change under time evolution. However, their phases will become random due to the interactions with distant subsystems, as is evident from the Hamiltonian (4). Such dephasing, though exponentially slow, will produce long-range entanglement, and thus give rise to the entanglement entropy that is extensive in the system size and determined by the participation ratios of different eigenstates [25], as discussed in detail in Ref. [16].

Numerical simulations.—Although our construction is general, we now test the validity of our basic assumption using exact diagonalization of a particular model—the random-field XXZ spin chain. We consider a chain of L spins with open boundary conditions, exchange $J_{\perp} = 1$, and interaction strength $J_z = V$, while the random onsite magnetic field is uniformly distributed in the interval $\pm W$. The total z component of the spin is conserved, and calculations are restricted to the $S_z = 0$ sector. For $V = 0$ the model is equivalent to free fermions with disorder, and all states are localized. Because of the limits on the accessible system sizes in exact diagonalization, we restrict ourselves to the case of the symmetric bipartite division of the full system \mathcal{LR} into the left (\mathcal{L}) and right (\mathcal{R}) half.

First, we study the averaged entanglement entropy S_{ent} of the \mathcal{L} subsystem in the eigenstates of \mathcal{LR} , illustrated in Fig. 1(a). For strong disorder, S_{ent} saturates to a value of the order 1 with increasing system size, indicating short-range entanglement in the MBL eigenstates, which is consistent with our basic assumption.

Next, we use the inverse participation ratio (IPR) as an intuitive, albeit somewhat indirect, test of the locality of operators $\hat{O}_{\mathcal{L}i}$ from Eq. (2), which, when acting on products of eigenstates of systems \mathcal{L} , \mathcal{R} , give eigenstates of \mathcal{LR} . The IPR for some state $|\Psi\rangle$ over a complete basis $|\alpha_i\rangle$ is defined as $\text{IPR}(|\Psi\rangle) = (\sum p_i^2)^{-1}$, where $p_i = |\langle \Psi | \alpha_i \rangle|^2$ represents the probability of finding a state $|\alpha_i\rangle$. Defined in such a way, the IPR takes values between 1 and the Hilbert space dimension, and effectively tells us how many

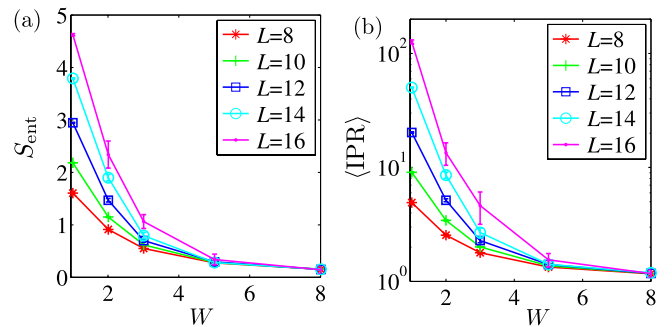


FIG. 1 (color online). (a) Averaged entanglement entropy is of the order 1 and varies weakly with L for strong disorder, indicating that eigenstates are short-range entangled. Interaction strength is $V = 1$. (b) Inverse participation ratios for the product of two eigenstates of the \mathcal{L} and \mathcal{R} subsystems are close to 1 and do not depend on L for strong disorder.

components have nonzero weight in the decomposition of the given state over the chosen complete basis. Figure 1(b) shows the average IPR for the product $|\alpha\rangle \otimes |\beta\rangle$ of two random eigenstates of the \mathcal{L} and \mathcal{R} subsystems over the eigenstates $|\lambda\rangle$ of \mathcal{LR} . The value of the IPR at strong disorder is very close to 1, indicating that the product of eigenstates of \mathcal{L} and \mathcal{R} is “close” to the eigenstate of the full system \mathcal{LR} . Furthermore, the IPR does not grow with L for strong disorder, suggesting that the product of eigenstates of \mathcal{L} and \mathcal{R} differs from the eigenstate of the full system only near the boundary.

To provide further support for our construction of the integrals of motion, we numerically implemented the projector operator similar to the one defined in Eq. (3). Every eigenstate $|\lambda\rangle$ of \mathcal{LR} is labeled by its “ancestor” in \mathcal{L} as in Eq. (2). To find the ancestor, we calculate the density matrix $\hat{\rho}_\lambda$ for the \mathcal{L} subsystem from $|\lambda\rangle$. Using $\hat{\rho}_\lambda$, we extract the probabilities of all eigenstates of \mathcal{L} as $p_\alpha = |\langle\alpha|\hat{\rho}_\lambda|\alpha\rangle|^2$. In the limit of very strong disorder the typical value of the largest p_α is close to 1 [26]. Thus, the “ancestor” for $|\lambda\rangle$ is defined to be an eigenstate of \mathcal{L} with the largest probability p_α .

Although we do not assign labels for the right subsystem, such labeling is sufficient to implement the operator $\hat{P}_\alpha = \sum_\beta \hat{P}_{\alpha\beta}$ as a projector onto the subspace of all eigenstates with the same label α for the \mathcal{L} . As a simple test, we study the locality of the projector \hat{P}_α : by construction it must have trivial action in the right subsystem. To test this property, we perturb some eigenstate with label α , $|\lambda^\alpha\rangle$, at the right boundary $|\psi^\alpha\rangle = (1/2 + 2\mathbf{S}_L \cdot \mathbf{S}_{L-1})|\lambda^\alpha\rangle$. Because we are interested in the weight of $|\psi^\alpha\rangle$ in the subspace with the same label α , we plot the averaged $\langle\psi^\alpha|\hat{P}_\alpha|\psi^\alpha\rangle$ as a function of disorder in Fig. 2. For strong disorder, even when the interaction strength is $V = 1$, the perturbed state $|\psi^\alpha\rangle$ has almost all of its weight in the subspace with index α , indicating that the degrees of

freedom in the subsystem \mathcal{L} are not affected by the perturbation acting on the subsystem \mathcal{R} . It is evident from Fig. 2(b) that the weight within the subspace α grows as a function of system size at $W > W_*$, and decreases at $W < W_*$, where $W_* \approx 3$. Thus, W_* gives an estimate of the MBL transition location in agreement with Ref. [10]. We note that the construction described above allows for more explicit tests to be done, which will be presented in future work [27]. Additional numerical verifications of our central assumption can be found in Ref. [26].

Discussion.—We established that the MBL phase is characterized by a number of local integrals of motion, supporting the hypothesis put forward in Ref. [18]. This implies that the MBL phase does not thermalize, and only partial thermalization of initial product states, constrained by the local conservation laws, is possible.

It should be noted that there are many ways to define local integrals of motion. For example, in certain problems [28] it might be helpful to label the integrals of motion by a set of $1/2$ pseudospins. Then, $\mathcal{M} = 2^K$ possible values of a given integral of motion \hat{I}_i can be viewed as states of K pseudospins σ_i^η , $\eta = 1, \dots, K$. The z projections of these pseudospins form a complete set of integrals of motion, and the Hamiltonian only involves σ_{iz}^η operators and their products. Operators σ_i^η can be viewed as effective degrees of freedom, in terms of which the dynamics becomes trivial: up-down states of spins are eigenstates, so time evolution can only lead to the dephasing between them.

Another implication of our work concerns the structure of the MBL eigenstates: they are short-range entangled, obey the area law, and can be generally represented as a product of eigenstates of the subsystems of size $\gg \xi$ which have been locally “corrected” near the boundaries with neighboring subsystems. This suggests an efficient numerical procedure for describing the MBL eigenstates in terms of matrix-product states. Starting from the product of eigenstates of decoupled blocks of size $\gg \xi$, entanglement between the blocks is introduced by the repeated action of the boundary terms in the Hamiltonian. The boundary terms generate only a finite-dimensional space; thus, diagonalizing the boundary Hamiltonian for each finite-dimensional subspace, it should be possible to find the eigenstates of two coupled blocks, etc.

Finally, our picture suggests a realistic route to extending coherence times in nearly isolated quantum systems, where decoherence is induced by interactions. Examples of such systems, in addition to systems of ultracold atoms, include nuclear spins and NV centers in diamond [29]. Assuming that one could induce strong static disorder leading to the many-body localization, the coherence time of a subsystem can be made very long. To achieve this, one needs to prepare a subsystem of size $\gg \xi$ (e.g., subsystem 1 in the above example), as well as its immediate neighborhood (e.g., subsystem 2) in some eigenstate. Then, local operations on the subsystem’s degrees of

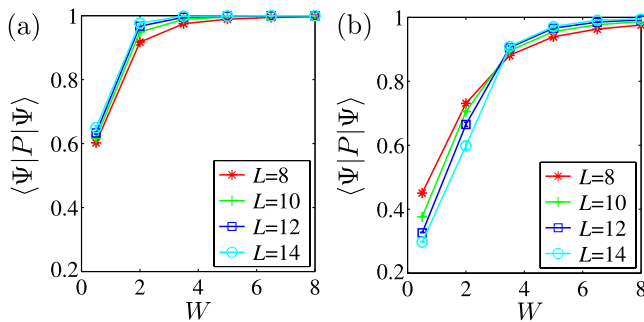


FIG. 2 (color online). The weight of the perturbed eigenstate $|\lambda^\alpha\rangle$ in the subspace with index α . For strong disorder, the action of the projector is contained within the subspace α , irrespective of the interaction: the case of no interaction $V = 0$ is shown in (a), and $V = 1$ in (b). The weight increases with system size. For weak disorder ($W < 3$), the presence of interactions causes the weight to decrease with the system size, suggesting the onset of the delocalized phase.

freedom would couple states with different integrals of motion I_1 , but with fixed values of I_2 . Therefore, even though the rest of the system is in some complicated superposition state, it will only give rise to an exponentially weak dephasing, with the rate proportional to $\exp(-l/\xi)$.

We thank J. Moore for useful discussions. Research at Perimeter Institute is supported by the Government of Canada through Industry Canada and by the Province of Ontario through the Ministry of Economic Development & Innovation. Z.P. was supported by DOE Grant No. DE-SC0002140. M.S. was supported by the National Science Foundation under Grant No. DMR-1104498. The simulations presented in this article were performed on computational resources supported by the High Performance Computing Center (PICSciE) at Princeton University.

Note added.—During the completion of this manuscript, we became aware of a related work [28] discussing the existence of local integrals of motion in the MBL phase.

-
- [1] P. Anderson, *Phys. Rev.* **109**, 1492 (1958).
 [2] P. Lee and T. V. Ramakrishnan, *Rev. Mod. Phys.* **57**, 287 (1985).
 [3] D. Basko, I. Aleiner, and B. Altshuler, *Ann. Phys. (Amsterdam)* **321**, 1126 (2006).
 [4] I. V. Gornyi, A. D. Mirlin, and D. G. Polyakov, *Phys. Rev. Lett.* **95**, 206603 (2005).
 [5] M. Rigol, V. Dunjko, V. Yurovsky, and M. Olshanii, *Phys. Rev. Lett.* **98**, 050405 (2007).
 [6] V. Oganesyan and D. A. Huse, *Phys. Rev. B* **75**, 155111 (2007).
 [7] M. Žnidarič, T. Prosen, and P. Prelovšek, *Phys. Rev. B* **77**, 064426 (2008).
 [8] C. Monthus and T. Garel, *Phys. Rev. B* **81**, 134202 (2010).
 [9] T. C. Berkelbach and D. R. Reichman, *Phys. Rev. B* **81**, 224429 (2010).
 [10] A. Pal and D. A. Huse, *Phys. Rev. B* **82**, 174411 (2010).
 [11] C. Gogolin, M. P. Müller, and J. Eisert, *Phys. Rev. Lett.* **106**, 040401 (2011).
 [12] E. Canovi, D. Rossini, R. Fazio, G. E. Santoro, and A. Silva, *Phys. Rev. B* **83**, 094431 (2011).
 [13] F. Buccheri, A. De Luca, and A. Scardicchio, *Phys. Rev. B* **84**, 094203 (2011).
 [14] E. Cuevas, M. Feigel'man, L. Ioffe, and M. Mezard, *Nat. Commun.* **3**, 1128 (2012).
 [15] A. De Luca and A. Scardicchio, *Europhys. Lett.* **101**, 37003 (2013).
 [16] M. Serbyn, Z. Papić, and D. A. Abanin, *Phys. Rev. Lett.* **110**, 260601 (2013).
 [17] J. H. Bardarson, F. Pollmann, and J. E. Moore, *Phys. Rev. Lett.* **109**, 017202 (2012).
 [18] R. Vosk and E. Altman, *Phys. Rev. Lett.* **110**, 067204 (2013).
 [19] I. Bloch, J. Dalibard, and W. Zwerger, *Rev. Mod. Phys.* **80**, 885 (2008).
 [20] A. Polkovnikov, K. Sengupta, A. Silva, and M. Vengalattore, *Rev. Mod. Phys.* **83**, 863 (2011).
 [21] S. Trotzky, Y.-A. Chen, A. Flesch, I. P. McCulloch, U. Schollwöck, J. Eisert, and I. Bloch, *Nat. Phys.* **8**, 325 (2012).
 [22] F. Iglói, Z. Szatmári, and Y.-C. Lin, *Phys. Rev. B* **85**, 094417 (2012).
 [23] G. D. Chiara, S. Montangero, P. Calabrese, and R. Fazio, *J. Stat. Mech.: Theory Exp.* **2006**, P03001.
 [24] Localization length depends on the energy density, and ξ should be viewed as the largest localization length. One may envision models where different excitations are characterized by different localization lengths. In this case as well, ξ should be chosen as the largest localization length.
 [25] A. Polkovnikov, *Ann. Phys. (Amsterdam)* **326**, 486 (2011).
 [26] See Supplemental Material at <http://link.aps.org/supplemental/10.1103/PhysRevLett.111.127201> for additional numerical tests and more details on the construction of the projector operator.
 [27] M. Serbyn, Z. Papić, and D. A. Abanin (to be published).
 [28] D. A. Huse and V. Oganesyan, [arXiv:1305.4915](https://arxiv.org/abs/1305.4915).
 [29] L. Childress, M. V. G. Dutt, J. M. Taylor, A. S. Zibrov, F. Jelezko, J. Wrachtrup, P. R. Hemmer, and M. D. Lukin, *Science* **314**, 281 (2006).

Search | Search History

All Databases

[<< Return to Web of Science®](#)

Citing Articles Title: **Theoretical expectations for a fractional quantum Hall effect in graphene**
 Author(s): Papic, Z.; Goerbig, M. O.; Regnault, N.
 Source: SOLID STATE COMMUNICATIONS Volume: 149 Issue: 27-28 Pages: 1056-1060 DOI: 10.1016/j.ssc.2009.02.050 Published: JUL 2009

This item has been cited by items indexed in the databases listed below. [\[more information\]](#)

13 in All Databases

- 13 publication in Web of Science
- 0 publication in BIOSIS Citation Index
- 0 publication in ScELO Citation Index
- 0 publication in Chinese Science Citation Database
- 0 data sets in Data Citation Index
- 0 publication in Data Citation Index [i](#)

Results: 13

Page 1 of 1

Sort by: Publication Date -- newest to oldest

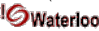
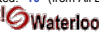

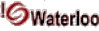


Create Citation Report

Refine Results

Search within results for

Databases

 SCIENCE TECHNOLOGY PHYSICS SCIENCE TECHNOLOGY OTHER TOPICS[more options / values...](#) Select Page Add to Marked List (0) Send to: Title: **More realistic Hamiltonians for the fractional quantum Hall regime in GaAs and graphene**Author(s): Peterson, Michael R.; Nayak, Chetan
Source: PHYSICAL REVIEW B Volume: 87 Issue: 24 Article Number: 245129 DOI: 10.1103/PhysRevB.87.245129 Published: JUN 27 2013
Times Cited: 2 (from All Databases) Title: **EXPLANATION OF COMPOSITE FERMION STRUCTURE IN FRACTIONAL QUANTUM HALL SYSTEMS**Author(s): Jacak, Janusz; Gonczarek, Ryszard; Jacak, Lucjan; et al.
Source: INTERNATIONAL JOURNAL OF MODERN PHYSICS B Volume: 26 Issue: 23 Article Number: 1230011 DOI: 10.1142/S0217979212300113
Published: SEP 20 2012
Times Cited: 0 (from All Databases) Title: **Unconventional Sequence of Fractional Quantum Hall States in Suspended Graphene**Author(s): Feldman, Benjamin E.; Krauss, Benjamin; Smet, Jurgen H.; et al.
Source: SCIENCE Volume: 337 Issue: 6099 Pages: 1196-1199 DOI: 10.1126/science.1224784 Published: SEP 7 2012
Times Cited: 13 (from All Databases) Title: **Transconductance Fluctuations as a Probe for Interaction-Induced Quantum Hall States in Graphene**Author(s): Lee, Dong Su; Skakalova, Viera; Weitz, R. Thomas; et al.
Source: PHYSICAL REVIEW LETTERS Volume: 109 Issue: 5 Article Number: 056602 DOI: 10.1103/PhysRevLett.109.056602 Published: AUG 2 2012
Times Cited: 4 (from All Databases) Title: **Theoretical aspects of the fractional quantum Hall effect in graphene**Author(s): Goerbig, M. O.; Regnault, N.
Conference: Nobel Symposium on Graphene and Quantum Matter Location: Saltsjobaden, SWEDEN Date: MAY 27-31, 2010
Source: PHYSICA SCRIPTA Volume: T146 Article Number: 014017 DOI: 10.1088/0031-8949/2012/T146/014017 Published: JAN 2012
Times Cited: 4 (from All Databases) Title: **Electronic properties of graphene in a strong magnetic field**Author(s): Goerbig, M. O.
Source: REVIEWS OF MODERN PHYSICS Volume: 83 Issue: 4 Pages: 1193-1243 DOI: 10.1103/RevModPhys.83.1193 Published: NOV 3 2011
Times Cited: 75 (from All Databases) Title: **Quantum Hall effect in graphene: Status and prospects**Author(s): Sahoo, S.
Source: INDIAN JOURNAL OF PURE & APPLIED PHYSICS Volume: 49 Issue: 6 Pages: 367-371 Published: JUN 2011
Times Cited: 0 (from All Databases) Title: **Search for non-Abelian statistics in half-filled Landau levels of graphene**Author(s): Wojs, A.; Moeller, G.; Cooper, N. R.
Book Editor(s): Muraki, K; Takeyama, S
Conference: Horiba International Conference/19th International Conference on the Application of High Magnetic Fields in Semiconductor Physics and Nanotechnology (HMF) Location: Tokyo Univ, Fukuoka, JAPAN Date: AUG 01-06, 2010
Sponsor(s): Inst Solid State Phys, Tokyo Univ; Global Ctr Excellence Phys Sci Frontier, Tokyo Univ
Source: HORBIA INTERNATIONAL CONFERENCE: THE 19TH INTERNATIONAL CONFERENCE ON THE APPLICATION OF HIGH MAGNETIC FIELDS IN SEMICONDUCTOR PHYSICS AND NANOTECHNOLOGY Book Series: Journal of Physics Conference Series Volume: 334 Article Number: 012048 DOI: 10.1088/1742-6596/334/1/012048 Published: 2011
Times Cited: 0 (from All Databases)

- 9. Title: [Atypical Fractional Quantum Hall Effect in Graphene at Filling Factor 1/3](#)
 Author(s): Papić, Z.; Goerbig, M. O.; Regnault, N.
 Source: PHYSICAL REVIEW LETTERS Volume: 105 Issue: 17 Article Number: 176802 DOI: 10.1103/PhysRevLett.105.176802 Published: OCT 19 2010
 Times Cited: 17 (from All Databases)
Get it!  [[View abstract](#)]
 - 10. Title: [Properties of graphene: a theoretical perspective](#)
 Author(s): Abergel, D. S. L.; Apalkov, V.; Berashevich, J.; et al.
 Source: ADVANCES IN PHYSICS Volume: 59 Issue: 4 Pages: 261-482 DOI: 10.1080/00018732.2010.487978 Published: 2010
 Times Cited: 267 (from All Databases)
Get it!  [[View abstract](#)]
 - 11. Title: [Local density of states of electron-crystal phases in graphene in the quantum Hall regime](#)
 Author(s): Poplavskyy, O.; Goerbig, M. O.; Smith, C. Morais
 Source: PHYSICAL REVIEW B Volume: 80 Issue: 19 Article Number: 195414 DOI: 10.1103/PhysRevB.80.195414 Published: NOV 2009
 Times Cited: 10 (from All Databases)
Get it!  [[View abstract](#)]
 - 12. Title: [Fractional Quantum Hall Effects in Graphene and Its Bilayer](#)
 Author(s): Shibata, Naokazu; Nomura, Kentaro
 Source: JOURNAL OF THE PHYSICAL SOCIETY OF JAPAN Volume: 78 Issue: 10 Article Number: 104708 DOI: 10.1143/JPSJ.78.104708 Published: OCT 2009
 Times Cited: 15 (from All Databases)
Get it!  [[View abstract](#)]
 - 13. Title: [Special Issue Recent Progress in Graphene Studies Preface](#)
 Author(s): Fal'ko, Vladimir; Geim, Andre; Das Sarma, Sankar; et al.
 Source: SOLID STATE COMMUNICATIONS Volume: 149 Issue: 27-28 Pages: 1039-1040 DOI: 10.1016/j.ssc.2009.04.009 Published: JUL 2009
 Times Cited: 1 (from All Databases)
Get it! 
- Select Page | Add to Marked List (0) |  |  | Send to:

Results: 13

 Page 1 of 1

Sort by:

13 records matched your query of the 55,067,330 (contains duplicates) in the data limits you selected.

View in: [简体中文](#) | [繁體中文](#) | [English](#) | [日本語](#) | [한국어](#) | [Português](#) | [Español](#)



Theoretical expectations for a fractional quantum Hall effect in graphene

Z. Papić^{a,b}, M.O. Goerbig^{a,*}, N. Regnault^c

^a Laboratoire de Physique des Solides, Univ. Paris-Sud, CNRS, UMR 8502, F-91405 Orsay Cedex, France

^b Institute of Physics, P.O. Box 68, 11080 Belgrade, Serbia

^c Laboratoire Pierre Aigrain, Ecole Normale Supérieure, CNRS, 24 rue Lhomond, F-75005 Paris, France

ARTICLE INFO

Article history:

Received 6 November 2008

Accepted 2 February 2009 by the Guest

Editors

Available online 20 March 2009

PACS:

73.43.-f

71.10.-w

81.05.Uw

Keywords:

A. Graphene

D. Fractional quantum Hall effect

D. Strongly correlated electrons

ABSTRACT

Due to its fourfold spin-valley degeneracy, graphene in a strong magnetic field may be viewed as a four-component quantum Hall system. We investigate the consequences of this particular structure on a possible, yet unobserved, fractional quantum Hall effect in graphene within a trial-wavefunction approach and exact-diagonalisation calculations. This trial-wavefunction approach generalises an original idea by Halperin to account for the SU(2) spin in semiconductor heterostructures with a relatively weak Zeeman effect. Whereas the four-component structure at a filling factor $\nu = 1/3$ adds simply a SU(4)-ferromagnetic spinor ordering to the otherwise unaltered Laughlin state, the system favours a valley-unpolarised state at $\nu = 2/5$ and a completely unpolarised state at $\nu = 4/9$. Due to the similar behaviour of the interaction potential in the zero-energy graphene Landau level and the first excited one, we expect these states to be present in both levels.

© 2009 Elsevier Ltd. All rights reserved.

1. Introduction

Electrons in graphene may be viewed as a particular form of the two-dimensional electron gas (2DEG), with the fundamental difference that, due to the particular band structure, their low-energy properties are described in terms of a zero-mass Dirac equation rather than the usual effective-mass Schrödinger equation [1]. One of the most salient features of the 2DEG, when submitted to a strong magnetic field, is the quantum Hall effect which occurs in an integer (IQHE) as well as in a fractional (FQHE) form. The former is also manifest in graphene [2,3], and its observation is a spectacular proof of relativistic electrons (and holes) in graphene, due to an unusual quantisation of the Hall conductivity, $\sigma_H = 2(e^2/h)(2n + 1)$, in terms of the integer n , as expected on theoretical grounds [4–6].

Experimental evidence for the FQHE, which is due to electron–electron interactions in a partially filled Landau level (LL), is yet lacking in graphene. In the usual 2DEG in GaAs/AlGaAs heterostructures, the FQHE is, indeed, seen in samples with high mobilities yet unaccessed in graphene on a SiO₂ substrate ($\mu \sim 50\,000\text{ cm}^2/\text{V s}$ for typical samples). Higher mobilities ($\mu \sim 200\,000\text{ cm}^2/\text{V s}$) have been achieved in current-annealed

suspended graphene [7], but unexpectedly the IQHE happens to break down above 1T, probably due to extrinsic effects that are not related to the intrinsic electronic properties of these graphene samples [8]. In spite of the missing FQHE, interaction physics is likely to be at the origin of additional plateaus in the Hall conductivity at LL filling factors $\nu_G = \pm 1$ (and 0) [9], where $\nu_G = n_C/n_B$ is the ratio between the carrier density ($n_C > 0$ for electron and $n_C < 0$ for hole transport) and that, $n_B = B/(h/e)$, of the flux quanta threading the graphene sheet.

From a theoretical point of view, interactions in graphene LLs are expected to be relevant. Indeed, one needs to compare the typical energy for exchange interaction $V_C = e^2/\epsilon R_C \simeq 25\sqrt{B[\text{T}]/\epsilon}\sqrt{2n+1}\text{ meV}$, in terms of the dielectric constant ϵ and the cyclotron radius $R_C = l_B\sqrt{2n+1}$, with the magnetic length $l_B = \sqrt{\hbar/eB} = 25/\sqrt{B[\text{T}]}\text{ nm}$, to the LL separation $\Delta_n = \sqrt{2\hbar}(v_F/l_B)(\sqrt{n+1} - \sqrt{n})$, where v_F is the Fermi velocity. In spite of the decreasing LL separation in the large- n limit, the ratio between both energy scales remains constant and reproduces the fine-structure constant of graphene, $\alpha_G = V_C/\Delta_n = e^2/\hbar v_F \epsilon \simeq 2.2/\epsilon$. Notice that the Coulomb interaction respects the fourfold spin-valley degeneracy to lowest order in $a/l_B \simeq 0.005\sqrt{B[\text{T}]}$, where $a = 0.14\text{ nm}$ is the distance between nearest-neighbour carbon atoms in graphene. This fourfold spin-valley symmetry is described in the framework of the SU(4) group which covers the two copies of the SU(2) spin and the SU(2) valley isospin. Lattice effects break this SU(4) symmetry at an energy scale $V_C(a/l_B) \simeq 0.1B[\text{T}]/\epsilon\text{ meV}$ [10–13], which is roughly on the

* Corresponding author.

E-mail address: goerbig@lps.u-psud.fr (M.O. Goerbig).

same order of magnitude as the expected Zeeman effect in graphene [9]. Other symmetry-breaking mechanisms have been proposed [14–16] but happen to be equally suppressed with respect to the leading interaction energy scale V_C . An exception may be graphene on a graphite substrate, where the natural lattice commensurability of the substrate and the sample may lead to a stronger coupling than for graphene on a SiO_2 substrate [17]. This yields a mass term in the Dirac Hamiltonian which lifts the valley degeneracy of the zero-energy LL [14].

Based on these considerations, graphene in a strong magnetic field may thus be viewed as a four-component quantum Hall system, and we neglect $\text{SU}(4)$ -symmetry breaking terms in the remainder of the paper. An interesting theoretical expectation resulting from this feature is the formation of a quantum Hall ferromagnet at $\nu = \pm 1$ [18,10,11,19] with $\text{SU}(4)$ -skyrmion excitations, which may have peculiar magnetic properties [19,20]. Also for the FQHE, the $\text{SU}(4)$ spin-valley symmetry is expected to play a relevant role and has been considered within a composite-fermion approach [21] as well as one based on $\text{SU}(4)$ Halperin wavefunctions [22,23].

In this paper, we review how the four-component structure of graphene may have particular signatures in a possible FQHE. In a first step, we discuss the structure of the interaction model for electrons restricted to a single graphene LL. We concentrate on the spin-valley $\text{SU}(4)$ symmetric part of the interaction model, which constitutes the leading energy scale, and discuss, based on the behaviour of the pseudopotentials, theoretical expectations for the FQHE in graphene in the LLs $n = 0$ and 1. In the second part of this paper, we corroborate these qualitative expectations with the help of the $\text{SU}(4)$ wavefunction approach [22,23] and exact-diagonalisation calculations.

2. Interaction model

In the case of a partially filled LL, one may separate the “low-energy” degrees of freedom, which consist of intra-LL excitations, from the “high-energy” inter-LL excitations. In the absence of disorder, all states within the partially filled LL have the same kinetic energy such that intra-LL excitations may be described by considering only electron–electron interactions,

$$H_{\lambda n} = \frac{1}{2} \sum_{\mathbf{q}} v(q) \rho_{\lambda n}(-\mathbf{q}) \rho_{\lambda n}(\mathbf{q}), \quad (1)$$

where $v(q) = 2\pi e^2/\epsilon q$ is the 2D Fourier-transformed Coulomb interaction potential. The Fourier components $\rho_{\lambda n}(\mathbf{q})$ of the density operator are constructed solely from states within the n -th LL in the band λ ($\lambda = +$ for the conduction and $\lambda = -$ for the valence band). This construction is analogous to that used in the conventional 2DEG, but the density operators $\rho_n(\mathbf{q})$ are now built up from spinor states of the 2D Dirac equation,

$$\psi_{\lambda n, m}^{\xi} = \frac{1}{\sqrt{2}} \begin{pmatrix} |n-1, m\rangle \\ \lambda |n, m\rangle \end{pmatrix} \quad (2)$$

for $n \neq 0$ and

$$\psi_{n=0, m}^{\xi} = \begin{pmatrix} 0 \\ |n=0, m\rangle \end{pmatrix} \quad (3)$$

for the zero-energy LL $n = 0$, in terms of the harmonic oscillator states $|n, m\rangle$ and the guiding-centre quantum number $m = 0$. Here, we have chosen the first component of the spinor to represent at the K point ($\xi = +$) the amplitude on the A sublattice and that on the B sublattice at the K' point ($\xi = -$). Notice that the valley and the sublattice indices happen to be the same in the zero-energy LL $n = 0$ and that, thus, a perturbation that breaks

the inversion symmetry (the equivalence of the two sublattices) automatically lifts the valley degeneracy [14–16]. In terms of the spinor states (2) and (3), the density operator may be written

$$\rho_{\lambda n}(\mathbf{q}) = \sum_{\xi, m} \left(\psi_{\lambda n, m}^{\xi} \right)^{\dagger} e^{-i\mathbf{q}\cdot\mathbf{r}} \psi_{\lambda n, m'}^{\xi} c_{\lambda n, m; \xi}^{\dagger} c_{\lambda n, m'; \xi}, \quad (4)$$

where $c_{\lambda n, m; \xi}^{\dagger}$ annihilates (creates) an electron in the state $\psi_{\lambda n, m}^{\xi}$. In Eq. (4), we have neglected the contributions that are off-diagonal in the valley index. Indeed, these contributions give rise to a rapidly oscillating phase $\exp(\pm i\mathbf{K}\cdot\mathbf{r})$ in the matrix elements, where $\pm\mathbf{K} = \pm(4\pi/3\sqrt{3}a)\mathbf{e}_x$ is the location of the K and K' points, respectively, and yield terms in the Hamiltonian (1), which break the valley- $\text{SU}(2)$ symmetry of the interaction. They are suppressed by a factor a/l_B with respect to the leading interaction energy scale $e^2/\epsilon l_B$ [10], as mentioned in the introduction. For the sake of simplicity and because of their smallness, we neglect these terms here.

Within the symmetric gauge, $\mathbf{A} = (B/2)(-y, x, 0)$, the position operator \mathbf{r} in Eq. (4) may be decomposed into the guiding-centre position \mathbf{R} and the cyclotron variable $\boldsymbol{\eta}$. Whereas the latter only affects the quantum number n , \mathbf{R} acts on m , and we may therefore rewrite the density operator (4), $\rho_{\lambda n}(\mathbf{q}) = \mathcal{F}_n(\mathbf{q}) \bar{\rho}(\mathbf{q})$, as a product of the *projected* density operator

$$\bar{\rho}(\mathbf{q}) = \sum_{\xi; m, m'} \langle m | e^{-i\mathbf{q}\cdot\mathbf{R}} | m' \rangle c_{\lambda n, m; \xi}^{\dagger} c_{\lambda n, m'; \xi} \quad (5)$$

and the *graphene form factor*

$$\begin{aligned} \mathcal{F}_n(q) &= \frac{1}{2} \left((n-1) \langle e^{-i\mathbf{q}\cdot\boldsymbol{\eta}} | n-1 \rangle + \langle n | e^{-i\mathbf{q}\cdot\boldsymbol{\eta}} | n \rangle \right) \\ &= \frac{1}{2} \left[L_{n-1} \left(\frac{q^2 l_B^2}{2} \right) + L_n \left(\frac{q^2 l_B^2}{2} \right) \right] e^{-q^2 l_B^2 / 4} \end{aligned} \quad (6)$$

for $n \neq 0$, in terms of Laguerre polynomials, and

$$\mathcal{F}_{n=0}(q) = \langle 0 | e^{-i\mathbf{q}\cdot\boldsymbol{\eta}} | 0 \rangle = e^{-q^2 l_B^2 / 4} \quad (7)$$

for $n = 0$. With the help of the projected density operators, the interaction Hamiltonian (1) reads

$$H_{\lambda n} = \frac{1}{2} \sum_{\mathbf{q}} v_n^G(q) \bar{\rho}(-\mathbf{q}) \bar{\rho}(\mathbf{q}), \quad (8)$$

where we have defined the effective interaction potential for graphene LLs,

$$v_n^G(q) = \frac{2\pi e^2}{\epsilon q} [\mathcal{F}_n(q)]^2. \quad (9)$$

Notice that the structure of the Hamiltonian (8) is that of electrons in a conventional 2DEG restricted to a single LL if one takes into account that the projected density operators satisfy the magnetic translation algebra [24]

$$[\bar{\rho}(\mathbf{q}), \bar{\rho}(\mathbf{q}')] = 2i \sin \left(\frac{\mathbf{q}' \wedge \mathbf{q}}{2} \right) \bar{\rho}(\mathbf{q} + \mathbf{q}'), \quad (10)$$

where $\mathbf{q}' \wedge \mathbf{q} \equiv q'_x q_y - q_x q'_y$ is the 2D vector product. This is a remarkable result in view of the different translation symmetries of the zero-field Hamiltonian; whereas the electrons in the 2DEG are non-relativistic and therefore satisfy Galilean invariance, the relativistic electrons in graphene are Lorentz-invariant. However, once submitted to a strong magnetic field and restricted to a single LL, the translation symmetry of the electrons is described by the magnetic translation group in *both* cases.

2.1. SU(4) symmetry

The most salient difference between the conventional 2DEG and graphene arises from the larger internal symmetry of the latter, due to its valley degeneracy. This valley degeneracy may be accounted for by an SU(2) valley *isospin* in addition to the physical SU(2) spin, which we have omitted so far and the symmetry of which is respected by the interaction Hamiltonian. Similarly to the projected charge density operator (5), we may introduce spin and isospin density operators, $\bar{S}^\mu(\mathbf{q})$ and $\bar{I}^\mu(\mathbf{q})$, respectively, with the help of the tensor products [20]

$$\begin{aligned}\bar{S}^\mu(\mathbf{q}) &= (S^\mu \otimes \mathbb{1}) \otimes \bar{\rho}(\mathbf{q}), \\ \bar{I}^\mu(\mathbf{q}) &= (\mathbb{1} \otimes I^\mu) \otimes \bar{\rho}(\mathbf{q}).\end{aligned}\quad (11)$$

Here, the operators S^μ and I^μ are (up to a factor 1/2) Pauli matrices, which act on the spin and valley isospin indices, respectively. The operators $(S^\mu \otimes \mathbb{1})$ and $(\mathbb{1} \otimes I^\mu)$ may also be viewed as the generators of the SU(2)×SU(2) symmetry group, which is smaller than the abovementioned SU(4) group. However, once combined in a tensor product with the projected density operators $\bar{\rho}(\mathbf{q})$, the SU(2)×SU(2)-extended magnetic translation group is no longer closed due to the non-commutativity of the Fourier components of the projected density operators. By commuting $[\bar{S}^\mu(\mathbf{q}), \bar{I}^\nu(\mathbf{q})]$, one obtains the remaining generators of the SU(4)-extended magnetic translation group [20], which is, thus, the relevant symmetry that describes the physical properties of electrons in graphene restricted to a single LL.

2.2. Effective interaction potential and pseudopotentials

Another difference, apart from the abovementioned larger internal symmetry, between the 2DEG and graphene in a strong magnetic field arises from the slightly different effective interaction potentials in the n -th LL. The effective interaction for graphene is given by Eq. (9) whereas that in the conventional 2DEG reads

$$v_n^{2DEG}(q) = \frac{2\pi e^2}{\epsilon q} \left[L_n \left(\frac{q^2 l_B^2}{2} \right) e^{-q^2 l_B^2/4} \right]^2. \quad (12)$$

The difference between the two of them vanishes for $n = 0$, as well as in the large- n limit [10], but leads to quite important physical differences in the first excited LL ($n = 1$) when comparing graphene to the 2DEG.

For the discussion of the FQHE, it is more appropriate to use Haldane's pseudopotential construction [25], which is an expansion of the effective interaction potential in the basis of two-particle states with a fixed relative angular momentum ℓ . In the Laughlin state at filling factor $\nu = 1/m$ [26],

$$\phi_m^L(\{z_j, z_j^*\}) = \prod_{k<l} (z_k - z_l)^m e^{-\sum_j |z_j|^2/4}, \quad (13)$$

in terms of the complex position $z_j = (x_j + iy_j)/l_B$ of the j -th particle, e.g., no particle pair has a relative angular momentum less than $\ell = m$. Therefore, all pseudopotentials $V_{\ell < m}$ are completely screened, and the Laughlin state (13) is the exact N -particle ground state with zero energy of a model interaction potential with $V_{\ell < m} > 0$ and $V_{\ell \geq m} = 0$ [25]. Although this model interaction potential is quite different from the pseudopotentials of the effective interaction potentials (9) and (12), it allows one to generate numerically the Laughlin state, which may be then compared to those obtained within exact-diagonalisation calculations of the realistic interaction potential.

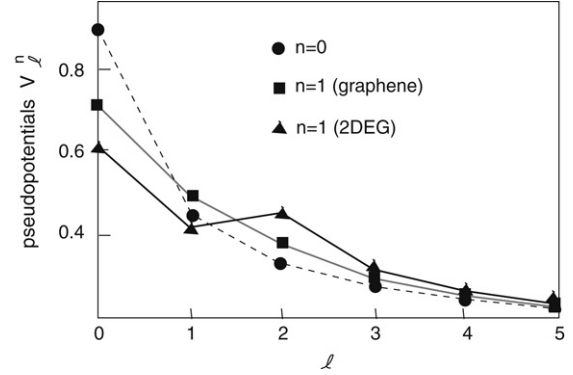


Fig. 1. Pseudopotentials for graphene and the 2DEG in $n = 0$ (graphene and 2DEG, circles), $n = 1$ (graphene, squares), and $n = 1$ (2DEG, triangles). The energy is measured in units of $e^2/\epsilon l_B$. The lines are a guide to the eye.

Notice that one may easily obtain the pseudopotentials of a given interaction potential $v_n(q)$ in Fourier space, such as (12) or (9), with the help of

$$V_\ell^n = \sum_{\mathbf{q}} v_n(q) L_\ell(q^2 l_B^2) e^{-q^2 l_B^2/2}. \quad (14)$$

The pseudopotentials for $n = 0$ and $n = 1$ in graphene and the 2DEG are shown in Fig. 1, which allows us to make some qualitative statements about a potential FQHE in graphene as compared to that of the 2DEG. First, apart from the internal symmetry, the polarised FQHE states in the zero-energy LL are expected to be the same in graphene as in the 2DEG because there is no difference in the effective interaction potential. The only difference stems from the larger internal symmetry in graphene, which affects the unpolarised FQHE states in $n = 0$. Second, the $n = 1$ LL in graphene is much more reminiscent of the $n = 0$ LL than of the $n = 1$ LL in the 2DEG. From an interaction point of view, one would therefore expect that the quantum phases encountered in the $n = 1$ graphene LL are merely a copy of those in $n = 0$. Furthermore, if one considers spin-polarised FQHE states, only pseudopotentials with *odd* angular momentum are relevant due to the fermionic nature of the electrons. It is apparent from Fig. 1 that odd- ℓ pseudopotentials are systematically larger in $n = 1$ than in $n = 0$. Therefore, the overall energy scale of FQHE states in $n = 1$ is slightly larger (by $\sim 10\%$) than in $n = 0$, and one would expect, somewhat counterintuitively, that the $n = 1$ FQHE states are more stable than those in $n = 0$, for the same B -field value. These qualitative predictions [10] have been corroborated within exact-diagonalisation studies, where only the valley isospin degree of freedom was considered and the physical spin was taken as completely polarised [27,28].

3. Trial wavefunctions

In order to account for the internal SU(4) symmetry in graphene LLs, two of us have proposed a trial-wavefunction approach [22] based on an original idea by Halperin [29] for the description of two-component FQHE states. These states,

$$\psi_{m_1, \dots, m_K; n_{ij}}^{SU(4)} = \phi_{m_1, \dots, m_4}^L \phi_{n_{ij}}^{inter} e^{-\sum_{j=1}^K \sum_{k_j=1}^{N_j} |z_{k_j}^{(j)}|^2/4}, \quad (15)$$

consist of a product of four Laughlin wavefunctions (13) (one per spin-valley component)

$$\phi_{m_1, \dots, m_K}^L = \prod_{j=1}^4 \prod_{k_j < l_j} (z_{k_j}^{(j)} - z_{l_j}^{(j)})^{m_j}$$

and a term

$$\phi_{n_{ij}}^{inter} = \prod_{i < j}^4 \prod_{k_i}^{N_i} \prod_{k_j}^{N_j} (z_{k_i}^{(i)} - z_{k_j}^{(j)})^{n_{ij}}$$

that takes into account correlations between the different components, labeled by the indices $i, j = 1, \dots, 4$. Whereas the exponents m_j must be odd integers to account for the fermionic statistics of the electrons, the exponents n_{ij} , which describe inter-component correlations, may also be even. Notice further that not all wavefunctions are good candidates for a possible FQHE in graphene; it has indeed been shown, within the plasma analogy [26], that some wavefunctions correspond to a liquid in which the components undergo a spontaneous phase separation [23].

The exponents n_{ij} and $n_{jj} \equiv m_j$ define a symmetric 4×4 matrix $M = (n_{ij})$, which determines the component densities ρ_j – or else the component filling factors $\nu_j = \rho_j/n_B$,¹

$$\begin{pmatrix} \nu_1 \\ \nu_2 \\ \nu_3 \\ \nu_4 \end{pmatrix} = M^{-1} \begin{pmatrix} 1 \\ 1 \\ 1 \\ 1 \end{pmatrix}. \quad (16)$$

Eq. (16) is only well-defined if the matrix M is invertible. If M is not invertible, some of the component filling factors, e.g. ν_1 and ν_2 , remain unfixed, but not necessarily the sum of the two ($\nu_1 + \nu_2$). This is a particular feature of possible underlying ferromagnetic properties of the wavefunction [22], as is discussed below for some special cases.

In the following, we consider some particular subclasses of the trial wavefunctions (15), which are natural candidates for a FQHE in graphene. Explicitly, we attribute the four spin-valley components as $1 = (\uparrow, K)$, $2 = (\uparrow, K')$, $3 = (\downarrow, K)$, and $4 = (\downarrow, K')$, where the first component denotes the spin orientation (\uparrow or \downarrow) and the second the valley (K or K'). We investigate wavefunctions, where all intracomponent exponents are identical $m_i = m$, i.e. we consider the same interaction potential for any of the components, as it is the case in graphene. Furthermore, we consider $n_{13} = n_{24} \equiv n_a$ and $n_{12} = n_{14} = n_{23} = n_{34} \equiv n_e$, which makes an explicit distinction between inter-component correlations in the same valley (n_a) and those in different valleys (n_e). This distinction may seem somewhat arbitrary – indeed, it does no longer treat the spin on the same footing as the valley isospin – but it happens to be useful in some cases if one intends to describe states with intermediate polarisation, such as for a moderate Zeeman field. The equivalence between spin and valley isospin is naturally restored for $n_e = n_a$. We use the notation $[m; n_e, n_a]$ to describe these subclasses of trial wavefunctions (15), the validity of which we check by exact diagonalisation of N particles on a sphere [25].

3.1. $[m; m, m]$ wavefunctions

If all exponents are identical odd integers m , we obtain a completely antisymmetric orbital wavefunction, which is nothing other than the Laughlin wavefunction (13). In this case, the distinction between the components vanishes, and the component filling factors are not fixed – one may, without changing the orbital wavefunction, fill only one particular component as well as another one or distribute the particles over all components. Only the total filling factor is fixed at $\nu = 1/m$. The corresponding exponent

Table 1

Overlap \mathcal{O} between the (3, 3, 2) wavefunction and the state obtained from exact diagonalisation of the effective interaction potential in $n = 0$ and $n = 1$.

Number of particles N	4	6	8	10
Overlap \mathcal{O} in $n = 0$	0.990	0.985	0.979	0.970
Overlap \mathcal{O} in $n = 1$	0.965	0.882	0.896	0.876

matrix M is indeed not invertible (of rank 1), and the residual freedom of distributing the electrons over the four components may be viewed as the arbitrary orientation of a four-spinor in $SU(4)$ space. The Laughlin wavefunction in graphene is therefore associated with an $SU(4)$ ferromagnetism, similar to that of the state at $\nu_G = \pm 1$ [18, 10, 11, 19, 20], where a graphene quantum Hall effect has been observed at high magnetic fields [9].

As already mentioned above, the Laughlin wavefunction has the good property of screening all pseudopotentials with angular momentum $\ell < m$ and has, for $m = 3$, the usual large overlap with the Coulomb ground state [21].

3.2. $[m; m - 1, m]$ wavefunctions

A similarly good wavefunction is $[m; m - 1, m]$, where the intervalley-component exponents are decreased by one. It also screens all pseudopotentials $V_{\ell < m}$ in any pair of electrons within the same valley, but an electron pair in two different valleys is affected by the pseudopotential $V_{\ell = m - 1}$. The filling factor, where this wavefunction may occur, is

$$\nu = \frac{2}{2m - 1},$$

i.e. at slightly larger densities as the Laughlin wavefunction with the same m . The exponent matrix M is still not invertible but of rank 2, and indeed only the filling factors in the two valleys, $\nu_K = \nu_1 + \nu_3$ and $\nu_{K'} = \nu_2 + \nu_4$, respectively, are fixed, $\nu_K = \nu_{K'} = 1/(2m - 1)$. The wavefunction, thus, describes a state with ferromagnetic spin ordering, but which is valley-isospin unpolarised. One may alternatively view this $[m; m - 1, m]$ wavefunction as a tensor product of an $SU(2)$ Halperin ($m, m, m - 1$) isospin-singlet wavefunction [29] and a completely symmetric (ferromagnetic) two-spinor that describes the physical spin.

We have checked within exact diagonalisation calculations that the $[3; 2, 3]$ wavefunction ($m = 3$) describes indeed, to great accuracy, the ground state in graphene at $\nu = 2/5$. It was shown by exact diagonalisation in Ref. [21] that, for $N = 4$ and 6 particles, the physical properties are indeed governed by an $SU(2)$ symmetry, as suggested by the $[m; m - 1, m]$ wavefunction. The overlap between this trial state and the one obtained by exact diagonalisation with implemented $SU(2)$ symmetry of the Coulomb interaction in $n = 0$ and 1 is shown in Table 1 for up to 10 particles. It is above 97% for all studied system sizes in the zero-energy LL $n = 0$, but slightly smaller ($\sim 88\%$) in $n = 1$. We have used the planar pseudopotentials (14) in the calculation of the $n = 1$ LL and checked that the difference is less than 1% in $n = 0$ when compared to using the more accurate spherical ones, even for the smallest system sizes $N = 4$ and 6.

It has been shown that the ground state at $\nu = 2/5$ in the conventional 2DEG is well described by an unpolarised (3, 3, 2) $SU(2)$ Halperin wavefunction once the spin degree of freedom is taken into account [30]. This wavefunction is identical to the composite-fermion wavefunction when including the $SU(2)$ spin. The energy difference between the polarised and the unpolarised $2/5$ states is, however, relatively small as compared to the Zeeman effect at the corresponding magnetic fields, such that a polarised state is usually favoured. Intriguing spin transitions have furthermore been observed experimentally at $\nu = 2/5$ and hint to even more complex physical properties of the $2/5$

¹ The filling factors used here are those that arise naturally in FQHE studies, i.e. they are defined with respect to the *bottom* of the partially filled LL, in contrast to ν_G defined with respect to the *center* of $n = 0$. In order to make the connection between the two filling factors, one needs to choose $\nu = \nu_1 + \nu_2 + \nu_3 + \nu_4 = \nu_G + 2$.

FQHE [31]. Notice that the situation of the $[3; 2, 3]$ state in graphene is remarkably different from that in the 2DEG: even in the presence of a strong Zeeman effect, only the ferromagnetically ordered physical spin is polarised, while the state remains a valley-isospin singlet. Whether such a valley-isospin singlet state is indeed encountered in graphene depends sensitively on the valley-symmetry breaking terms; whereas a possible easy-axis ferromagnetism, as has been proposed for the zero-energy LL $n = 0$ [11], may destroy the $[3; 2, 3]$ state, it is favoured in the case of an easy-plane valley-isospin anisotropy, which may occur in the $n = 1$ graphene LL due to intervalley coupling terms of the order $V_C(a/l_B)$ [10].

We have furthermore studied the $(5, 5, 4)$ wavefunction ($m = 5$) at $\nu = 2/9$. Its overlap with the state obtained by exact diagonalisation is lower than for the $(3, 3, 2)$ case (with $\mathcal{O} = 0.941$ for $N = 4$ and $\mathcal{O} = 0.892$ for $N = 6$), but remains relatively high.

3.3. $[m; m - 1, m - 1]$ wavefunctions

Another candidate is the $[m; m - 1, m - 1]$ wavefunction [23] which may describe FQHE states at

$$\nu = \frac{4}{4m - 3}.$$

The corresponding exponent matrix M is now invertible, and the filling factor of each spin-valley component is $\nu = 1/(4m - 3)$, i.e. the state is an $SU(4)$ singlet. As for the $[m; m, m]$ and $[m; m - 1, m]$ wavefunctions, all intracomponent correlations are such that the pseudopotentials $V_{\ell < m}$ are screened, but $V_{\ell = m - 1}$ is relevant for all intercomponent interactions.

As an example, we consider the $[3; 2, 2]$ wavefunction ($m = 3$), which is a candidate for a possible graphene FQHE at $\nu = 4/9$. Our exact-diagonalisation calculations with implemented $SU(4)$ symmetry, for $N = 4$ and 8 particles, indicate that this trial wavefunction describes indeed to great accuracy the ground state for the Coulomb interaction potential in the $n = 0$ LL, with an overlap of $\mathcal{O} = 0.999$ for $N = 4$ and $\mathcal{O} = 0.992$ for $N = 8$. In $n = 1$, it is $\mathcal{O} = 0.944$ for $N = 8$, for the case where one uses the planar pseudopotentials (14). These results indicate that a possible $4/9$ FQHE state in graphene is, remarkably, of a completely different nature than the composite-fermion state at $\nu = 4/9$ in a one-component system, such as the conventional 2DEG with complete spin polarisation. It is, nevertheless, an open issue to what extent the $SU(4)$ singlet state survives if one takes into account the Zeeman effect at high magnetic fields, which favours a polarisation in the spin channel. A complementary composite-fermion calculation with $SU(4)$ symmetry has revealed that, at $\nu = 4/9$, states with intermediate $SU(4)$ isospin polarisation – such as a valley-isospin singlet with full spin polarisation – may exist, with a slightly higher energy than the composite-fermion $SU(4)$ singlet [21], which is indeed identical to the $[3; 2, 2]$ wavefunction. One may, therefore, expect a transition between two $4/9$ states with different polarisation when the Zeeman energy outcasts the energy difference between the two states. This is similar to the abovementioned $2/5$ state in a conventional 2DEG [30].

4. Conclusions

In conclusion, we have investigated theoretically some particular features of the FQHE in graphene as compared to the 2DEG. The electrons in graphene lose their relativistic character associated with the Lorentz invariance once they are restricted to a single LL, in which case the translations are governed by the magnetic translation group, as in the 2DEG case. The main difference

between the 2DEG and graphene arises from the approximate $SU(4)$ spin-valley symmetry, which is respected in a wide energy range. Another difference arises from the spinor character of the wavefunctions, which yields a different effective electron–electron interaction in graphene as compared to the 2DEG. The graphene interaction potential in the first excited LL $n = 1$ (in both the valence and the conduction band) is shown to be similar to that in the central zero-energy LL $n = 0$, yet with a slightly larger overall energy scale (roughly 10% larger).

The FQHE at $\nu = 1/3$ is described as a Laughlin state [26] with $SU(4)$ -ferromagnetic spin-valley ordering, similar to the state at $\nu = 1$ [18,10,11,19,20]. In contrast to this state, the system profits from its internal degrees of freedom by choosing a state with partial and full $SU(4)$ -isospin depolarisation at $\nu = 2/5$ and $\nu = 4/9$, respectively. The $[3; 2, 3]$ state at $\nu = 2/5$ is a valley-isospin singlet, but its physical spin is ferromagnetically ordered and may eventually be oriented by the Zeeman effect. The state at $\nu = 4/9$ is described in terms of a $[3; 2, 2]$ Halperin wavefunction, which is an $SU(4)$ singlet with necessarily zero spin and valley isospin polarisation. A possible FQHE at $\nu = 4/9$ in graphene may therefore be sensitive to the Zeeman effect at high magnetic fields, and one may expect transitions between states with different polarisation, similar to the 2DEG at $\nu = 2/5$ and $2/3$ [31].

Acknowledgments

This work was funded by the Agence Nationale de la Recherche under Grant Nos. ANR-06-NANO-019-03 and ANR-JCJC-0003-01. ZP was supported by the European Commission, through a Marie Curie Foundation contract MEST CT 2004-51-4307 and Center of Excellence Grant CX-CMCS, as well as by the Serbian Ministry of Science under Grant No. 141035. We acknowledge further material support from the Basque “Les Bugnes” Foundation.

References

- [1] For a recent review, see A.H. Castro Neto, N.M.R. Peres, K.S. Novoselov, A.K. Geim, Rev. Mod. Phys. 81 (2009) 109.
- [2] K.S. Novoselov, A.K. Geim, S.V. Morosov, D. Jiang, M.I. Katsnelson, I.V. Grigorieva, S.V. Dubonos, A.A. Firsov, Nature 438 (2005) 197.
- [3] Y. Zhang, Y.-W. Tan, H.L. Stormer, P. Kim, Nature 438 (2005) 201.
- [4] T. Ando, Zheng, Phys. Rev. B 65 (2002) 245420.
- [5] V.P. Gusynin, S.G. Sharapov, Phys. Rev. Lett. 93 (2005) 146801.
- [6] N.M.R. Peres, F. Guinea, A.H. Castro Neto, Phys. Rev. B 73 (2006) 125411.
- [7] K.I. Bolotin, K.J. Sikes, Z. Jiang, M. Klima, G. Fudenberg, J. Hone, P. Kim, H.L. Stormer, Solid State Commun. 146 (2008) 351.
- [8] P. Kim, talk at the ICTP conference “Graphene Week 2008”.
- [9] Y. Zhang, Z. Jiang, J.P. Small, M.S. Purewal, Y.-W. Tan, M. Fazlollahi, J.D. Chudow, J.A. Jaszczak, H.L. Stormer, P. Kim, Phys. Rev. Lett. 96 (2006) 136806.
- [10] M.O. Goerbig, R. Moessner, B. Douçot, Phys. Rev. B 74 (2006) 161407.
- [11] J. Alicea, M.P.A. Fisher, Phys. Rev. B 74 (2006) 075422.
- [12] D.A. Abanin, P.A. Lee, L.S. Levitov, Phys. Rev. Lett. 98 (2007) 156801.
- [13] R.L. Doretto, C. Morais smith, Phys. Rev. B 76 (2007) 195431.
- [14] F.D.M. Haldane, Phys. Rev. Lett. 61 (1988) 2015.
- [15] J.-N. Fuchs, P. Lederer, Phys. Rev. Lett. 98 (2007) 016803.
- [16] I. Herbut, Phys. Rev. B 75 (2007) 165411; Phys. Rev. B 76 (2007) 085432.
- [17] G. Li, A. Luican, E.Y. Andrei, 2008. arXiv:0803.4016.
- [18] K. Nomura, A.H. MacDonald, Phys. Rev. Lett. 96 (2006) 256602.
- [19] K. Yang, S. Das Sarma, A.H. MacDonald, Phys. Rev. B 74 (2006) 075423.
- [20] B. Douçot, M.O. Goerbig, P. Lederer, R. Moessner, Phys. Rev. B 78 (2008) 195327.
- [21] C. Töke, J.K. Jain, Phys. Rev. B 75 (2007) 245440.
- [22] M.O. Goerbig, N. Regnault, Phys. Rev. B 75 (2007) 241405.
- [23] R. de Gail, N. Regnault, M.O. Goerbig, Phys. Rev. B 77 (2008) 165310.
- [24] S.M. Girvin, A.H. MacDonald, P.M. Platzman, Phys. Rev. B 33 (1986) 2481.
- [25] F.D.M. Haldane, Phys. Rev. Lett. 61 (1988) 2015.
- [26] R.B. Laughlin, Phys. Rev. Lett. 50 (1983) 1395.
- [27] V.M. Apalkov, T. Chakraborty, Phys. Rev. Lett. 97 (2006) 126801.
- [28] C. Töke, P.E. Lammert, V.H. Crespi, J.K. Jain, Phys. Rev. B 74 (2006) 235417.
- [29] B.I. Halperin, Helv. Phys. Acta 56 (1983) 75.
- [30] T. Chakraborty, F.C. Zhang, Phys. Rev. B 29 (1984) 7032.
- [31] W. Kang, J.B. Young, S.T. Hannahs, E. Palm, K.L. Campman, A.C. Gossard, Phys. Rev. B 56 (1997) R12776; I.K. Kukushkin, K.v. Klitzing, K. Eberl, Phys. Rev. Lett. 82 (1999) 3665.

DISORDERING OF THE CORRELATED STATE OF THE QUANTUM HALL BILAYER AT FILLING FACTOR $\nu = 1$

Z. PAPIĆ^{*,†,‡} and M. V. MILOVANOVIĆ^{*}

^{*}*Scientific Computing Laboratory, Institute of Physics,
University of Belgrade, P. O. Box 68, 11 000 Belgrade, Serbia*

[†]*Laboratoire de Physique des Solides, University Paris-Sud,
CNRS, UMR 8502, F-91405 Orsay Cedex, France*

[‡]*zpanic@ipb.ac.rs*

Received 13 April 2012

Revised 13 May 2012

Accepted 16 May 2012

Published 13 July 2012

The phase diagram of a quantum Hall bilayer at total filling $\nu = 1$ contains an incompressible superfluid for small distances d between the layers, as well as the compressible phase corresponding to two uncoupled Fermi liquids for large d . Using exact diagonalization on the sphere and torus geometry, we investigate a long-standing question of the nature of the transition between the two regimes, and the possibility for the existence of a paired phase in the transition region. We find considerable evidence for a direct transition between the superfluid and the Fermi liquid phase, based in particular on the behavior of the ground state energy on the sphere (including appropriate finite-size corrections) as a function of d . At the critical distance $d_C \approx 1.6\ell_B$ the topological number (“shift”) of the ground state changes, suggesting that tuning the layer separation d in experiment likely leads to a direct transition between the superfluid and the Fermi liquid phase.

Keywords: Fraction quantum Hall effect; quantum Hall bilayer; Chern–Simons theory; exact diagonalization; superfluid disordering.

PACS Number(s): 63.22.-m, 87.10.-e, 63.20.Pw

Quantum Hall bilayer (QHB) is a semiconductor structure that consists of two quantum wells spatially separated by an insulating barrier that is of the same order of magnitude as the width of each of the wells. When QHB is placed in the perpendicular magnetic field, adjusted in such a way that the ratio of the number of electrons in the system (N) and the magnetic flux quanta (N_ϕ) is exactly $\nu = N/N_\phi = 1$, remarkable manifestations of quantum-mechanical coherence take place on the macroscopic scale.¹ These interesting effects occur upon varying a single parameter, d/ℓ_B , the ratio of the center-to-center distance between the wells

d to the magnetic length $\ell_B = \sqrt{\hbar c/eB}$. Much of the QHB physics has been well established in the extreme cases when d is (1) much smaller, or (2) much larger than ℓ_B .

When $d \ll \ell_B$, i.e. the Coulomb interaction between electrons in the same layer and in the opposite layers is of about the same magnitude, a good starting point for the physical description is the Halperin state Ψ_{111} ,² explicitly defined below in Eq. (1). The physics contained in Ψ_{111} is that of exciton binding:^{1,3} an electron in one layer and a correlation hole directly opposite to it in the other layer, are in a coherent quantum-mechanical superposition dictated by the form of the Ψ_{111} wave function. This exciton description can be a viewpoint of the phenomenon of superfluidity found in these systems,⁴ and is closely connected to the concept of composite bosons (CBs)⁵⁻⁷ that can be used as natural quantum Hall quasiparticles in the small d/ℓ_B regime.

On the other hand, when $d \gg \ell_B$ we have the case of the decoupled layers and the ground state (GS) is a product of two Fermi seas, each described by the Rezayi–Read wave function Ψ_{RR} ,⁸ defined below in Eq. (3). The underlying quasiparticles in this case are composite fermions (CFs), the usual quasiparticles of the single-layer quantum Hall physics.⁹

To address the range of intermediate d , when the system is a disordered superfluid, one may try to capture the basic physics by interpolating between the two limits described above. In other words, one may describe the physics by using mixed states of CBs and CFs.¹⁰ This is a phenomenological approach in which we start from the identical underlying electrons, split them into a group of those that correlate as CBs, and a group of those that correlate as CFs. The wave function for the superfluid state at small d will involve mainly CBs; the disordering of the CB superfluid can be viewed as caused by “nucleation” of CF quasiparticles as d is increased.

In the remainder of this paper, we first introduce and systematically review the construction of mixed states of CBs and CFs,^{11,12} paying special emphasis on the kind of pairing between CFs that might be relevant for the bilayer system to produce a paired state. After presenting the analytic arguments that motivate the existence of a paired state in the transition region between superfluid and Fermi liquid phases, we present the results of exact diagonalization calculations on the torus and sphere, and conclude by discussing some of their implications.

The basic ingredients for the construction of mixed CB/CF states are the Halperin 111 state, describing the bilayer ground state for very small distances d , and the Rezayi–Read wave function that describes the Fermi liquid state in a single-layer quantum Hall system at $\nu = 1/2$. The 111 state is given by

$$\Psi_{111}(\{z^\uparrow, z^\downarrow\}) = \prod_{i < j}^{N_\uparrow} (z_i^\uparrow - z_j^\uparrow) \prod_{k < l}^{N_\downarrow} (z_k^\downarrow - z_l^\downarrow) \prod_{m=1}^{N_\uparrow} \prod_{n=1}^{N_\downarrow} (z_m^\uparrow - z_n^\downarrow). \quad (1)$$

Here $z_\sigma = x_\sigma + iy_\sigma$ is the complex 2D coordinate of an electron in the layer $\sigma \in \{\uparrow, \downarrow\}$ (containing N_σ particles), and we have set the magnetic length ℓ_B equal to 1, suppressing the spinor part of the wave function and the ubiquitous lowest Landau level (LLL) Gaussian factors. Because it describes identical electrons, this wave function is subject to the constraint that there is the same number of magnetic flux quanta per particle. This translates into the following flux-counting relation

$$N_\phi = N_\uparrow - 1 + N_\downarrow = N_\downarrow - 1 + N_\uparrow, \quad (2)$$

which necessitates $N_\uparrow = N_\downarrow = N/2$.

On the other hand, the Rezayi–Read CF-sea state⁸ at $\nu = 1/2$ is given by

$$\Psi_{\text{RR}}(z) = \mathcal{P}_{\text{LLL}} \mathcal{F}(z, \bar{z}) \prod_{i < j} (z_i - z_j)^2, \quad (3)$$

where \mathcal{F} stands for the Slater determinant of free waves. Because \mathcal{F} contains the terms involving \bar{z} , we need to project those by \mathcal{P}_{LLL} to obtain a holomorphic LLL wave function. The wave function for two decoupled layers is then simply given by the product $\Psi_{\text{RR}}(z_\uparrow) \times \Psi_{\text{RR}}(z_\downarrow)$.

Possible corrections to the 111 state, resulting from increasing the distance d that leads to superfluid disordering, have been the subject of numerous previous works in the literature. For example, an approach based on the traditional Chern–Simons theory⁷ of CBs in the RPA approximation finds the following correction to Ψ_{111} :¹³

$$\Psi_{\text{ph}} = \exp \left\{ -\frac{1}{2} \sum_{\mathbf{k}} \frac{\sqrt{\frac{V_S(\mathbf{k})}{\bar{\rho}/m}}}{|\mathbf{k}|} \rho_{\mathbf{k}}^S \rho_{-\mathbf{k}}^S \right\} \Psi_{111}, \quad (4)$$

where $\rho_{\mathbf{k}}^S \equiv \rho_{\mathbf{k}}^\uparrow - \rho_{\mathbf{k}}^\downarrow$ is the difference of the densities of two layers, $V_S(\mathbf{k}) = \frac{V_{\uparrow\uparrow}(\mathbf{k}) - V_{\uparrow\downarrow}(\mathbf{k})}{2}$ is the interaction in the neutral channel, m is the electron mass and $\bar{\rho}$ is the uniform total density. As usual, the bilayer problem at $\nu = 1$ has been decomposed into the charge and neutral channel, and the latter reduces to the problem of an ordinary superfluid with the phonon contribution, hence our notation for the correction Ψ_{ph} . In the small d limit $V_S(\mathbf{k}) = \pi d$, and we can expand the expression Ψ_{ph} as

$$\Psi_{\text{ph}} = \Psi_{111} - \left(\sum_{\mathbf{k}} \frac{c\sqrt{d}}{|\mathbf{k}|} \rho_{-\mathbf{k}}^S \rho_{\mathbf{k}}^S \right) \Psi_{111} + \dots, \quad (5)$$

where c is a positive constant. The terms after the first one represent corrections, in the order of importance, to the Ψ_{111} ansatz as d increases. The form of the correction is fixed by the basic phenomenology and sum rules for a superfluid in two dimensions.¹⁴

The previous correction can be recovered as a special case of the mixed CB-CF ansatz, as we now show. For small distances d , it was argued in Refs. 10–12 that the low-energy physics of the bilayer should be captured by the following mixed state

of CBs and CFs:

$$\Psi_1 = \mathcal{A}_\uparrow \mathcal{A}_\downarrow \left\{ \Psi_{111}(z_\uparrow, z_\downarrow) \Psi_{\text{RR}}(w_\uparrow) \Psi_{\text{RR}}(w_\downarrow) \prod_{i,j} (z_{i\uparrow} - w_{j\uparrow}) \prod_{k,l} (z_{k\uparrow} - w_{l\downarrow}) \right. \\ \left. \times \prod_{p,q} (z_{i\downarrow} - w_{q\uparrow}) \prod_{m,n} (z_{m\downarrow} - w_{n\downarrow}) \right\}, \quad (6)$$

where \mathcal{A}_σ stands for the anti-symmetrization in the layer σ , and we omitted the projection to the LLL. By using the expressions for the densities of electrons in each layer, $\rho^\sigma(\eta) = \sum_i \delta^2(\eta - z_i^\sigma) + \sum_i \delta^2(\eta - w_i^\sigma)$, we can further rewrite the wave function in the following way:¹²

$$\Psi_1 = \int \prod_{n \in \text{CF}} d^2 \eta_{n\sigma} \left\{ \frac{\prod_{k < l} (\eta_{k\uparrow} - \eta_{l\uparrow}) \prod_{p < q} (\eta_{p\downarrow} - \eta_{q\downarrow})}{\prod_{i,j} (\eta_{i\uparrow} - \eta_{j\downarrow})} \mathcal{F}(\eta_\uparrow) \right. \\ \left. \times \mathcal{F}(\eta_\downarrow) \times \rho^\uparrow(\eta_{1\uparrow}) \cdots \rho^\downarrow(\eta_{n\downarrow}) \Psi_{111}(z_\uparrow, z_\downarrow) \right\}, \quad (7)$$

where n is the total number of electrons that correlate as CFs. This expression is exactly equivalent to Eq. (6) (up to an unimportant numerical factor).

Let us compare the first phonon corrections in both approaches to find out which possibilities for the pairing are allowed amongst the most simple choices for the (weak) pairing function. Based on the usual Chern–Simons approach, the first phonon correction is $\sim \sum_{\mathbf{k}} \frac{1}{|\mathbf{k}|} \rho_{\mathbf{k}}^\uparrow \rho_{-\mathbf{k}}^\downarrow$. On the other hand, the mixed wave function including pairing suggests the following simplest correction when there are two CFs:

$$\int d^2 \eta_{1\uparrow} \int d^2 \eta_{2\downarrow} \frac{1}{(\eta_{1\uparrow} - \eta_{2\downarrow})} g(\eta_{1\uparrow} - \eta_{2\downarrow}) \rho^\uparrow(\eta_{1\uparrow}) \rho^\downarrow(\eta_{2\downarrow}), \quad (8)$$

where g is the pairing function. If we choose $g(z) = 1/z$, we obtain *no correction whatsoever* to the 111 state. Among other simple choices, the next candidate for the pairing function could be $g(z) = \sqrt{z/\bar{z}}$ (\bar{z} is the complex conjugate of z). When substituted in Eq. (8), this reduces to the form of the first phonon contribution in the long-distance limit with the $\frac{1}{|\mathbf{k}|}$ singularity, Eq. (5). Thus $g(z) = \sqrt{z/\bar{z}}$ accommodates the usual (on the level of RPA) superfluid description given in Eq. (5). It can be shown that $g(z) = \text{const.}$ i.e. no pairing, also produces a trivial correction; see Table 1 caption. We can continue exploring the simple choices for pairing, e.g. the next possibility in the order of weakness of the pairing that retains the same angular momentum for the pairing as $g(z) = \sqrt{z/\bar{z}}$ is $g(z) = 1/\bar{z}$. The phonon contribution in this case turns out to be $\sim \sum_{\mathbf{k}} \ln(|\mathbf{k}| \ell_B) \rho_{\mathbf{k}}^\uparrow \rho_{-\mathbf{k}}^\downarrow$.¹² Our results can be summarized as in Table 1.

Having identified some simple pairing functions allowed in the bilayer system starting from Ψ_1 and at small d/ℓ_B , we can ask whether any of those may lead to a paired phase in the intermediate range of d/ℓ_B and can we find a simple wave function to describe this phase. If the translation symmetry remains unbroken as we

Table 1. Phonon corrections for different choices of the pairing function. The functions f_1 , f_2 and f_3 define the weight of each correction in terms of the bilayer distance d . In the first case (no pairing) the correction is proportional to $\sum_{\mathbf{k}} \frac{1}{(k_x + ik_y)} \rho_{\mathbf{k}}^\uparrow \rho_{-\mathbf{k}}^\downarrow$, but we expect that with no constraint on the number of CFs [as in Eqs. (4) and (5)], this will correspond to $\sum_{\mathbf{k}} \frac{1}{(k_x + ik_y)} \rho_{\mathbf{k}}^S \rho_{-\mathbf{k}}^S$ i.e. zero (no correction) due to the anti-symmetry under $\mathbf{k} \rightarrow -\mathbf{k}$ exchange.

$g(z) = \text{const. (no pairing)}$	$\sum_{\mathbf{k}} f_1(d) \frac{1}{(k_x + ik_y)} \rho_{\mathbf{k}}^\uparrow \rho_{-\mathbf{k}}^\downarrow$
$g(z) = 1/z$	no correction when multiplies Ψ_{111}
$g(z) = \sqrt{z/\bar{z}}$	$\sum_{\mathbf{k}} f_2(d) \frac{1}{ \mathbf{k} } \rho_{\mathbf{k}}^\uparrow \rho_{-\mathbf{k}}^\downarrow$
$g(z) = 1/\bar{z}$	$\sum_{\mathbf{k}} f_3(d) \ln(\mathbf{k} \ell_B) \rho_{\mathbf{k}}^\uparrow \rho_{-\mathbf{k}}^\downarrow$

increase d , one of the viable candidates is the mixed CB/CF wave function with the pairing $g(z) = 1/\bar{z}$. This pairing has the same angular momentum as $g(z) = \sqrt{z/\bar{z}}$, but it also has an additional amplitude factor to it. If we take the choice $g(z) = 1/\bar{z}$ and examine the final form of the mixed state when there are no CBs, we are lead to its following forms (see Ref. 12 for details),

$$\begin{aligned} \Psi_2 &= \det \left(\frac{1}{\bar{z}_{i\uparrow} - \bar{z}_{j\downarrow}} \right) \prod_{i < j} (z_{i\uparrow} - z_{j\uparrow})^2 \prod_{k < l} (z_{k\downarrow} - z_{l\downarrow})^2 \\ &= \det \left(\frac{1}{\bar{z}_{i\uparrow} - \bar{z}_{j\downarrow}} \right) \det \left(\frac{1}{z_{k\uparrow} - z_{l\downarrow}} \right) \Psi_{111}, \end{aligned} \quad (9)$$

where we used the Cauchy determinant identity in going from the first to the second line. The neutral part of Ψ_2 (i.e. the two determinants which do not carry a net flux through the system as Ψ_{111} does) can be viewed as a correlator of vertex operators of a single *nonchiral* bosonic field. According to Ref. 15, CFT correlators not only describe quantum Hall ground state wave functions, but can also be used to find out about the excitation spectrum and connect its edge and bulk theories. Using CFT analogy, one can construct the neutral excitations for Ψ_2 in terms of the vertex operators that multiply the ground state wave function (see Ref. 12 for the precise form of these operators). These vertex operators are parametrized by the exponents β_1 and β_2 ; if the low-lying spectrum were consisting only of $\beta_1 = \frac{1}{2}$ and $\beta_2 = \frac{1}{2}$ quasiparticle excitations, our system would be described by the so-called BF Chern–Simons theory or the theory of the 2D superconductor.¹⁶ Combining the analysis with the charge part (Ψ_{111}) in which only charge-1 excitations are allowed (half-flux quantum excitations are strongly confined¹⁷), we arrive at the conclusion that the degeneracy of the system’s ground state on the torus must be four.^{16,18} However, the vertex operators yield a single-valued expression acting on the ground state also for any real β_1 , including $\beta_1 = 0$ (no excitation), and therefore one can expect a gapless branch of excitations parametrized by a continuum of β_1 ,

and compressible (gapless) behavior of the system in the neutral sector (the charge channel, being described by Ψ_{111} , is incompressible).

In the following, we explore the prospects for the paired phase in finite-size systems using exact diagonalization for different choices of boundary conditions. There have been many numerical studies of the quantum Hall bilayer at $\nu = 1$.^{10,19–27} In particular, elaborate studies in Refs. 10 and 20 demonstrated the relevance of CB/CF constructions for the clean systems (no impurities). Trial wave functions of this kind describe a continuous crossover between the CB superfluid and the two decoupled CF liquids via a possible intermediate p -wave paired phase that in our analysis corresponds to Ψ_2 , Eq. (9). Here we would like to focus on addressing the question whether such a phase has a clear signature in small finite systems that can be studied numerically. This question is relevant in light of the new experimental results which indicate that the CF liquid phase in the usual samples is partially spin-polarized.²⁸ Since the 111 state is a QH ferromagnet, the experiments appear to preclude the possibility of a smooth crossover and instead suggest a first-order transition.²⁹ For larger Zeeman fields, the transition becomes smooth and the critical point drifts to larger values of d .^{28,30}

The topological content of Ψ_2 is the four-fold ground state degeneracy on the torus. In Ref. 20 this degeneracy was analyzed as a function of d , and different shapes of the torus unit cell, but no definite conclusion was drawn due to the strong finite-size effects. We corroborate this finding by diagonalizing a larger system of $N = 16$ particles, Fig. 1. N electrons are placed on the surface of a torus i.e. we impose periodic boundary conditions in the presence of $N_\phi = N/\nu = N$ quanta of

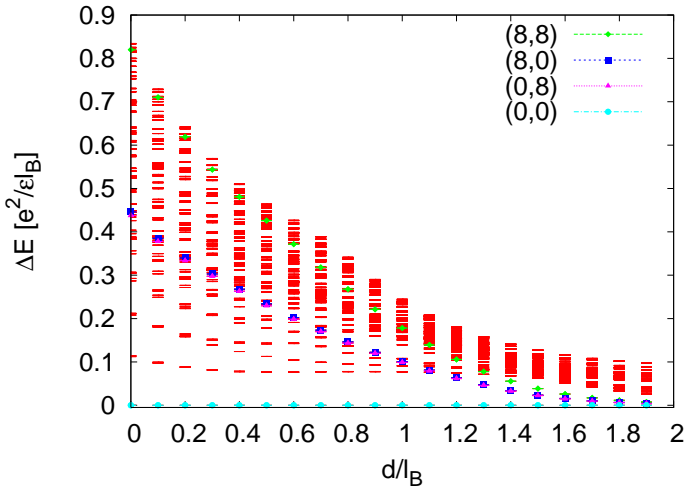


Fig. 1. (Color online) Energy spectrum of the quantum Hall bilayer at total filling $\nu = 1$ on the torus. The system contains $N = 16$ electrons in a rectangular domain $a \times b$ with the aspect ratio $a/b = 0.99$. Spectrum is plotted relative to the ground state at each d/l_B , and special symbols denote the momentum sectors where the paired phase is expected to be degenerate.

the perpendicular magnetic field. The interaction between the electrons in the same layer is given by $V_c^{\uparrow\uparrow}(r) = e^2/\epsilon r$ and between those in opposite layers $V_c^{\uparrow\downarrow}(r) = e^2/\epsilon\sqrt{r^2 + d^2}$. Note that, for simplicity, in numerical calculations we consider a fixed number of electrons in each layer (negligible interlayer tunneling). However, the CF/CB construction in Eq. (6) can easily accommodate the charge imbalance by a redistribution of CBs, which was also revealed in experiments. On the other hand, it can be shown¹² that compressible states cannot easily accommodate such a redistribution.

The bilayer Hamiltonian is numerically diagonalized for each d/ℓ_B , and eigen-energies are plotted in Fig. 1. Four seemingly degenerate states can be identified in the lowest-lying spectrum starting from $d = 1.4\ell_B$, but the gap decreases smoothly with the increase of d , which suggests that these states belong to the compressible CF liquid. Two decoupled CF liquids are allowed to display a four-fold degeneracy due to their center-of-mass motion.³¹ This degeneracy, contrary to the one of Ψ_2 , has no topological content, but in a finite system it may nonetheless persist for some variation of the aspect ratio or other parameters i.e. it may appear quasi-robust. However, since the gap of the system smoothly decreases as a function of d , it is unlikely that there is a third phase, distinct from the 111 state and the decoupled CF liquids.

We can also change the boundary condition and place N electrons on the surface of a sphere³² with a magnetic monopole in the center. In order to probe a given many-body state ψ at the filling factor ν , the number of flux quanta generated by the monopole has to be adjusted in such a way that $N_\phi = N/\nu - \mathcal{S}$, where \mathcal{S} is the *shift*, a topological number that characterizes each ψ . Since the Hilbert space is defined by (N, N_ϕ) , two different states ψ_1 and ψ_2 , which describe the same filling factor $\nu_1 = \nu_2 = \nu$, may be realized in different Hilbert spaces if $\mathcal{S}_1 \neq \mathcal{S}_2$. As an example, take $\tilde{\Psi}_2$ which is characterized by the shift $\mathcal{S} = 1$, like the 111 state, whereas CF liquid state occurs at $\mathcal{S} = 2$. Therefore, one cannot directly compare e.g. the overlaps of the exact ground state with the 111 state and CF liquids for a fixed N . Instead, one must perform an extrapolation to the thermodynamic limit to discriminate between phases. Overlaps are not useful from this point of view because they would extrapolate to zero in the thermodynamic limit, however ground state energy is an example of a quantity that is meaningful in this sense. It defines the transition point d_C between the 111 state and CF liquids as the value of d above which the ground state energy is lower at the shift $\mathcal{S} = 2$ than at $\mathcal{S} = 1$. We estimate d_C from the crossing point of the ground state energies for the two shifts, $\mathcal{S} = 1$ and 2, for various system sizes $N = 6 - 16$, Fig. 2. In doing so, it is essential to include the background charge correction and rescale the magnetic length in order to carefully compare the energies of the systems living on two slightly different FQH spheres.³³ It can be shown³³ that beyond $d \sim 1.5\ell_B$, which we identified as the critical value for the appearance of the four-fold degeneracy on the torus, one should no longer describe the system at the shift of $\mathcal{S} = 1$. Therefore, it is likely that the 111 phase goes directly into the CF liquids even at this finite value of d ,

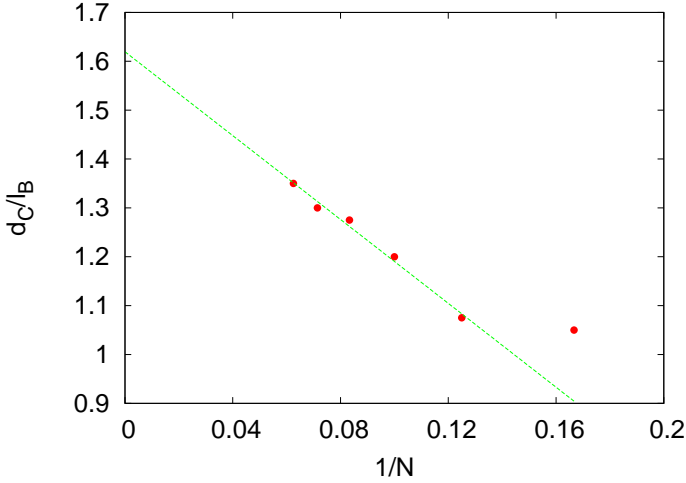


Fig. 2. Critical bilayer distance d_C defined as the crossing point of the ground state energies at shifts $\mathcal{S} = 1$ and $\mathcal{S} = 2$ on the sphere. Linear extrapolation for $N \rightarrow \infty$ yields $d_C \sim 1.6\ell_B$ and does not involve the smallest system $N = 6$ which shows strong finite-size effects.

and not via the p -wave paired state. Nevertheless, the two energies remain very close to each other and the paired wave function such as $\tilde{\Psi}_2$ is not conclusively ruled out as a candidate for the description of the system. It may either describe an excited state of the CF liquid or a phase with a tiny gap that would be hard to discern from an ordinary compressible state in the experiment.

Our estimate of critical $d_C \sim 1.6\ell_B$ roughly agrees with that obtained by complementary methods in the literature, e.g. in Ref. 21 where d_C was estimated by measuring the change in the pseudospin expectation value at a fixed shift $\mathcal{S} = 1$ and zero tunneling. Although the obtained d_C is in reasonable agreement with the experiments, it does not imply that we have proved a direct transition between the two shifts for the ground state ($\mathcal{S} = 1$ versus $\mathcal{S} = 2$). In order to do that, one would want, for each fixed d , to diagonalize the Hamiltonian for all the available system sizes and make the thermodynamic extrapolation of the energies (with the appropriate corrections) as a function of $1/N$. While this works nicely for the shift of $\mathcal{S} = 1$, in the case of CF shift $\mathcal{S} = 2$ the ground state energy has a nontrivial dependence on $1/N$ which reflects the shell-filling effect³³ The dependence of energy on $1/N$ is somewhat similar to that reported in Ref. 34 for the single layer at $\mathcal{S} = 2$, except that the energy minima occur for $N/2 = n^2, n = 2, 3, \dots$. In between the minima, the energy has a local maximum. Therefore, in order to perform a reliable extrapolation, a few minima/maxima would be required, but since we are only able to diagonalize up to $N = 16$, that gives us a single minimum $n = 2$. However, the fact that for all the available systems we consistently obtain lower ground state energy at $\mathcal{S} = 2$ for sufficiently large d strongly suggests that the transition involves a change in shift at finite d .

In conclusion, we discussed how the ground state of the quantum Hall bilayer at $\nu = 1$ evolves with the changing distance between the layers in the light of trial wave functions describing the mixed states of CBs and CFs, as well as using numerical diagonalization on the sphere and torus. The study of the ground state energy on the sphere gives considerable support for the direct transition between superfluid and Fermi liquid phases. Paired state may only exist in the regions of the phase diagram where the interaction is significantly different from the pure Coulomb repulsion studied in this work.

Acknowledgments

We thank Steven Simon for his comments. This work was supported by the Serbian Ministry of Education and Science under project No. ON171017.

References

1. J. P. Eisenstein and A. H. MacDonald, *Nature* **432** (2004) 691.
2. B. I. Halperin, *Helv. Phys. Acta* **56** (1983) 75.
3. H. A. Fertig, *Phys. Rev. B* **40** (1989) 1087.
4. I. B. Spielman, J. P. Eisenstein, L. N. Pfeiffer and K. W. West, *Phys. Rev. Lett.* **84** (2000) 5808.
5. N. Read, *Phys. Rev. Lett.* **62** (1989) 86.
6. S. C. Zhang, H. Hansson and S. Kivelson, *Phys. Rev. Lett.* **62** (1989) 82.
7. S. C. Zhang, *Int. J. Mod. Phys. B* **6** (1992) 25.
8. E. H. Rezayi and N. Read, *Phys. Rev. Lett.* **72** (1994) 900.
9. J. Jain, *Composite Fermions* (Cambridge University Press, 2007).
10. S. H. Simon, E. H. Rezayi and M. V. Milovanovic, *Phys. Rev. Lett.* **91** (2003) 046803.
11. Z. Papić and M. V. Milovanović, *Phys. Rev. B* **75** (2007) 195304.
12. M. V. Milovanović and Z. Papić, *Phys. Rev. B* **79** (2009) 115319.
13. L. Jiang and J. Ye, *Phys. Rev. B* **74** (2006) 245311.
14. A. Lopez and E. Fradkin, *Phys. Rev. B* **51** (1995) 4347.
15. G. Moore and N. Read, *Nucl. Phys. B* **360** (1991) 362.
16. T. H. Hansson, V. Oganesyan and S. L. Sondhi, *Ann. Phys.* **313** (2004) 497.
17. G. S. Jeon and J. Ye, *Phys. Rev. B* **71** (2005) 125314.
18. E. Demler, C. Nayak and S. Das Sarma, *Phys. Rev. Lett.* **86** (2001) 1853.
19. G. Möller, S. H. Simon and E. H. Rezayi, *Phys. Rev. Lett.* **101** (2008) 176803.
20. G. Möller, S. H. Simon and E. H. Rezayi, *Phys. Rev. B* **79** (2009) 125106.
21. J. Schliemann, S. M. Girvin and A. H. MacDonald, *Phys. Rev. Lett.* **86** (2001) 1849.
22. A. Burkov, J. Schliemann, A. H. MacDonald and S. M. Girvin, *Physica E* **12** (2002) 28.
23. J. Schliemann, *Phys. Rev. B* **67** (2003) 035328.
24. J. Schliemann, *Phys. Rev. B* **83** (2011) 115322.
25. K. Nomura and D. Yoshioka, *Phys. Rev. B* **66** (2002) 153310.
26. N. Shibata and D. Yoshioka, *J. Phys. Soc. Jpn.* **75** (2006) 043712.
27. D. Yoshioka and N. Shibata, *J. Phys. Soc. Jpn.* **79** (2010) 064717.
28. P. Giudici, K. Muraki, N. Kumada, Y. Hirayama and T. Fujisawa, *Phys. Rev. Lett.* **100** (2008) 106803.
29. P. Giudici, K. Muraki, N. Kumada and T. Fujisawa, *Phys. Rev. Lett.* **104** (2010) 056802.

30. A. D. K. Finck, J. P. Eisenstein, L. N. Pfeiffer and K. W. West, *Phys. Rev. Lett.* **104** (2010) 016801.
31. F. D. M. Haldane, *Phys. Rev. Lett.* **55** (1985) 2095.
32. F. D. M. Haldane, *Phys. Rev. Lett.* **51** (1983) 605.
33. Z. Papić and M. V. Milovanović, *p-Wave Pairing in Quantum Hall Bilayers*, Advances in Condensed Matter Physics, Vol. 2011, Article ID 614173, 2011, doi:10.1155/2011/614173.
34. R. Morf and N. d'Ambrumenil, *Phys. Rev. Lett.* **74** (1995) 5116.

DOKAZNI MATERIJAL ZA PREDAVANJA PO POZIVU

(pozivna pisma za konferencije, najava predavanja i sl.)



Bulletin of the American Physical Society

APS March Meeting 2013 Volume 58, Number 1

Monday–Friday, March 18–22, 2013; Baltimore, Maryland

[Session Y3: Invited Session: New Directions in Fractional Quantum Hall Phenomena](#)

8:00 AM–11:00 AM, Friday, March 22, 2013
Room: Ballroom III

Sponsoring Units: DCMP DCOMP
Chair: Mansour Shayegan, Princeton University

Abstract ID: BAPS.2013.MAR.Y3.4

Abstract: Y3.00004 : Tunable interactions and the fractional quantum Hall effect

9:48 AM–10:24 AM

[Preview Abstract](#) [View Presentation](#) 

MathJax **On** | [Off](#) ← Abstract →

Author:

Zlatko Papic
(Princeton University)

We explore several realistic methods of tuning the interactions in two-dimensional electronic systems in high magnetic fields. We argue that these experimental probes can be useful in studying the interplay of topology, quantum geometry and symmetry breaking in the fractional quantum Hall effect (FQHE). In particular, we show that the mixing of subbands and Landau levels in GaAs wide quantum wells breaks the particle-hole symmetry between the Moore-Read Pfaffian state and its particle-hole conjugate, the anti-Pfaffian, in such a way that the latter is unambiguously favored and generically describes the ground state at $5/2$ filling [1]. Furthermore, the tilting of the magnetic field, or more generally variation of the band mass tensor, probes the fluctuation of the intrinsic metric degree of freedom of the incompressible fluids, and ultimately induces the crossover to the broken-symmetry and nematic phases in higher Landau levels [2]. Some of these mechanisms also lead to an enhancement of the excitation gap of the non-Abelian states, as observed in recent experiments. Finally, we compare the tuning capabilities in conventional systems with that in multilayer graphene and related materials with Dirac-type carriers where tuning the band structure and dielectric environment provides a simple and direct method to engineer more robust FQHE states and to study quantum transitions between them [3]. [\[1\]](#) Z. Papic, F. D. M. Haldane, and E. H. Rezayi, arXiv:1209.6606 (2012). [\[2\]](#) Bo Yang, Z. Papic, E. H. Rezayi, R. N. Bhatt, F. D. M. Haldane, Phys. Rev. B 85, 165318 (2012). [\[3\]](#) Z. Papic, R. Thomale, D. A. Abanin, Phys. Rev. Lett. 107, 176602 (2011); Z. Papic, D. A. Abanin, Y. Barlas, and R. N. Bhatt,

[Phys. Rev. B 84, 241306\(R\) \(2011\)](#); [D. A. Abanin, Z. Papic, Y. Barlas, and R. N. Bhatt, New J. Phys. 14, 025009 \(2012\)](#).

To cite this abstract, use the following reference: <http://meetings.aps.org/link/BAPS.2013.MAR.Y3.4>

[APS Home](#) | [APS Meetings](#) | [Join APS](#) | [Help](#) | [Contact APS Meetings](#)

© 2013 American Physical Society

CPM seminars

Talks: [Colloquia \(past\)](#) [ASTRO \(past\)](#) [Astroparticle \(past\)](#)
[CHEP \(past\)](#) [CPM \(past\)](#) [MPU \(past\)](#)
 (un)subscribe [Calendar 2013/14](#) [Online PSC presentations](#)
[Events \(past\)](#) [PhD Defences \(past\)](#)

[Home](#)
[People »](#)
[News](#)
[Alumni news](#)
[Talks etc. »](#)
[Outreach](#)

Research

[Areas »](#)
[Centres »](#)

Studies

[Graduate »](#)
[Undergrad »](#)

Collections

[Rutherford](#)
[McPherson](#)

External

[McGill](#)
[Faculty of Science](#)

Topological phases in graphene

Zlatko Papic*Perimeter Institute/Waterloo Institute for Quantum Computing*

As realized for the first time in 1980s, quantum systems in reduced spatial dimensions can sometimes undergo a special type of ordering which does not break any symmetry but introduces long-range entanglement and emergent excitations that have radically different properties from their original constituents. Most of our experimental knowledge of such “*topological*” phases of matter comes from studies of two-dimensional electron gases in GaAs semiconductors in high magnetic fields and at low temperatures. In the first part of this talk, I will give an introduction to these systems and review some latest theoretical developments related to the physics of the non-Abelian states and the interplay of symmetry breaking with quantum geometry. In the second part, I will discuss new directions for experimental realization and study of the topological phases, focusing in particular on bilayer graphene. I will present evidence that this material supports the “*even-denominator*” fractional state, whose observation has recently been reported, which is related to the Moore-Read state. Finally, I will outline several proposals for the tunability of the effective electron-electron interactions in graphene systems, which might enable further experimental progress beyond GaAs.

Thursday, December 5th 2013, 15:30

Ernest Rutherford Physics Building, R.E. Bell Conference Room (room 103)

Ernest Rutherford Physics Building [MAP]
 McGill University
 3600 rue University
 Montréal, QC
 Canada H3A 2T8

General inquiries: +1 514 398 6490
 Undergraduate affairs: +1 514 398 6477
 Graduate affairs: +1 514 398 6485
 Fax: +1 514 398 8434
 Email: secretariat@physics.mcgill.ca

Comments and suggestions: webmaster@physics.mcgill.ca
 © 1994-2013 Department of Physics, McGill University
 Last modified 2013/11/11



Department of Physics

[Home](#) » [Calendar](#) » [Condensed Matter Seminar](#)

Zlatko Papic

Princeton University

"Fractional quantum Hall effect in wide quantum wells at half filling"



Zlatko Papic

Friday February 01, 2013

3:30pm PHYS 203

Refreshments are served at 3:00 p.m. in Physics room 242.

<http://www.princeton.edu/~zpapic/>

In this talk I will discuss several aspects of fractional quantum Hall physics relevant to the even-denominator states in wide quantum wells.

In these systems, the interactions can be tuned in a complex way by varying the sample thickness, tunnelling between subbands, and density imbalance, such that one can explore transitions between a non-Abelian incompressible state, the multicomponent 331 Halperin state, and the compressible Fermi-liquid-like state.

Furthermore, I will show that in the incompressible phase, the mixing between Landau levels and electronic subbands breaks the particle-hole symmetry in such a way that the ground state at $\nu=5/2$ filling is generically described by the "anti-Pfaffian" state [1]. The interplay between subbands also leads to an enhancement of the excitation gap of the non-Abelian state, as observed in recent experiments.

[1] Z. Papic, F. D. M. Haldane, E. H. Rezayi, Phys. Rev. Lett. 109, 266806 (2012).

Purdue University, West Lafayette, Indiana 47907 USA, Phone: (765) 494-4600

Copyright © 2013, Purdue University, all rights reserved. Purdue University is [an equal](#)

[access/equal opportunity university](#). If you have trouble accessing this page because of a disability, please contact the Physics Webmaster at www@physics.purdue.edu.

Laboratoire de Physique Théorique Toulouse - UMR 5152

Mardi 17 décembre 2013-14:00

Entanglement in topological phases and interacting quantum disordered systems

Zlatko Papić (Perimeter Institute, Waterloo, Canada)

par Gabriel LeMarié - 17 décembre

Though it has been recognized early on as one of the fundamental aspects of quantum mechanics, entanglement has played an increasingly important role in condensed matter physics as well, in particular due to the fact that it underlies the recent "tensor network" description of many-body systems, and through its practical uses as a resource for quantum computing. In this talk I will illustrate the profound role of the entanglement in two, rather different, types of physical systems : the topological phases arising in the context of the fractional quantum Hall effect, and the quantum disordered systems in a "many-body localized" phase. I will show that the entanglement provides a way to understand the structure of the topologically-ordered ground states via a direct link between conformal field theory, solvable models, and the "matrix-product state" formalism. Furthermore, I will demonstrate that the entanglement also provides specific signatures for the non-equilibrium dynamics of disordered systems and for the nature of the eigenstates in the "many-body localized phase", which may have important consequences for controlling the coherence of isolated quantum systems in experiment.

Post-scriptum :

contact : D. Poilblanc

KAVLI INSTITUTE FOR THEORETICAL PHYSICS

UNIVERSITY OF CALIFORNIA
SANTA BARBARA, CALIFORNIA 93106-4030
<http://www.kitp.ucsb.edu>

TELEPHONE:(805) 893-7337
(805) 893-4111
FAX: (805) 893-2431
INTERNET: gross@kitp.ucsb.edu

February 10, 2012

Dr. Zlatko Papic
Department of Electrical Engineering
Princeton University
Olden Street
Princeton, NJ 08544

Dear Dr. Papic:

As you know, the Kavli Institute for Theoretical Physics in Santa Barbara is organizing a research program entitled *Frustrated Magnetism and Quantum Spin Liquids: From Theory and Models to Experiments* that will take place during the period August 13 – November 9, 2012. Where magnetic order is suppressed all the way to zero temperature, an unusual class of phases, quantum spin liquids, may be realized in principle. Recently, a growing number of experimental spin liquid candidates have emerged. A central goal of this program is bring together scientists involved in numerical simulation, formal theory, and experiments to assess the subject and its prospects for the future. It is being coordinated by Kazushi Kanoda, Patrick Lee, Ashvin Vishwanath, and Steven White, assisted by Leon Balents and Radu Coldea as scientific advisors. An associated conference *Exotic Phases of Frustrated Magnets* will be held from October 8—12, 2012. Further details on both activities may be found on our web site: <http://www.kitp.ucsb.edu/activities/dbdetails?acro=chirps12>.

After consultation with the coordinators, I would like to invite you to participate in the program for the period October 1, 2012 to November 9, 2012. While you are here, we will reimburse you for living expenses up to a maximum \$85/day.* We understand that you are able to provide for your travel expenses from other resources.

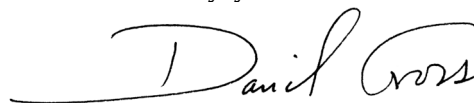
If, however, at some point you find that you are having difficulty accepting because of financial strictures, for example because you will be accompanied by family members, please contact the Deputy Director to see whether KITP may be able to provide further assistance. We attempt to facilitate long-term visits within the limitations of our budget and regulations.

For your reference, I enclose important information about visiting KITP plus a page listing some of our administrative staff who assist in arranging visits and supporting visitors. If you will not have medical insurance coverage applicable to your stay here, please contact Timber Kelley for further information.

* U.S. tax laws and University of California regulations require that reimbursements for meals not exceed \$60.00/day, and that lodging and all other expenses beyond \$60.00/day be documented by original receipts. If you are not a U.S. citizen or permanent resident, it is imperative that you bring your passport and have either the proper status (W-B, W-1) or proper visa (usually a B-1 or a J-1) in order to be reimbursed by the KITP. If you will have a visa (J or H) issued by another institution, please contact Timber Kelley at myvisit@kitp.ucsb.edu for instructions.

I would greatly appreciate learning from you promptly (no later than Sunday, March 4) if you will be able to participate. In your response, by e-mail to myvisit@kitp.ucsb.edu, please let us know explicitly whether the proposed dates are acceptable. Because of space and financial limitations, any significant change in the duration or time of your visit requires consultation with the coordinators and with us. This includes changes that would result in your participation for less than the whole period for which you are invited.[†] We look forward to an exciting and productive research program. Please do not hesitate to contact the Deputy Director Marty Einhorn (meinhorn@kitp.ucsb.edu; 805-893-6309) or me if you have any questions.

Sincerely yours,

A handwritten signature in black ink that reads "David Gross". The signature is written in a cursive style with a large, sweeping "D" and "G".

David Gross
Director

DG: tk
Encl: staff list, ipp

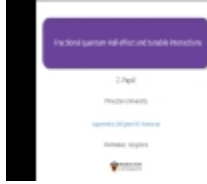
[†] If you have questions about alternative dates or financial arrangements, you should contact directly the Deputy Director, Martin Einhorn, meinhorn@kitp.ucsb.edu.

[Home](#) | [Help](#) | [Advanced search](#) | [Send Feedback](#)

PERIMETER INSTITUTE RECORDED SEMINAR ARCHIVE

Speaker

Go



PIRSA: 12110081 ([Flash Presentation](#) , [MP4 Low Res](#) , [MP3](#) , [PDF](#)) Which Format?

Fractional quantum Hall effect and tunable interactions

Speaker(s): [Zlatko Papić](#)

Abstract: In this talk I will review some existing experimental methods, as well as a few recent theoretical proposals, to tune the interactions in a number of low-dimensional systems exhibiting the fractional quantum Hall effect (FQHE). The materials in question include GaAs wide quantum wells and multilayer graphene, where the tunability of the electron-electron interactions can be achieved via modifying the band structure, dielectric environment of the sample, by tilting the magnetic field

or varying the mass tensor, and by mixing of electronic subbands and Landau levels. Because the interesting topological (and in particular, non-Abelian) states arise solely due to strong interactions, the ability to tune them is essential for “designing” more robust FQHE states.

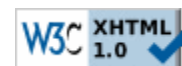
Furthermore, I will argue that some of these mechanisms can also be used to probe the subtle aspects of FQHE physics, such as the breaking of particle-hole symmetry between the Moore-Read Pfaffian and anti-Pfaffian states, and the transition between FQHE fluids and broken-symmetry states due to the fluctuation of the intrinsic geometric degree of freedom.

Date: 29/11/2012 - 2:00 pm

Series: [Condensed Matter](#)

URL:

<http://pirsa.org/12110081/> Share:



Microsoft Research

Our research Connections Careers [About us](#)

[Labs](#) Research areas Community Media resources Contact us



Station Q Seminars and Events

Our seminar takes place on Tuesdays at **2:30pm** in our seminar room (Elings Hall 2250), unless otherwise noted below.

Spring 2014 schedule

- 01/07: **David Clarke**, Caltech
tba
- 01/14: **Dong Liu**, Michigan State
tba

Fall 2013 schedule

- 08/13 and 08/14 (9-11m and 1-3pm): **Cirprian Manolescu**, UCLA
The triangulation conjecture
- 10/01: **Mike Zaletel**, UC Berkeley
Exact matrix product states for the quantum Hall effect - from conformal block wave functions to tensor networks
- 10/03: **Matthew Gilbert**, UIUC
Interplay between Topology and Superconductivity in 2D Time-Reversal Invariant Insulators
- 10/04 (**11:00 am**): **Ravin Bhatt**, Princeton
Anderson model of localization: Has the fat lady sung yet?
- 10/08: **Titus Neupert**, Princeton
Fractional Chern insulators in doped irradiated grapheme
- 10/22: **Curt von Keyserlingk**, Oxford
Exactly solvable models of topological matter in 3D
- 10/30 (**2:00 pm**): **Mike Freedman**, Station Q
Ginzburg-Landau superconductivity with exotic covariant derivatives
- 10/31: **Shivaji Sondhi**, Princeton
Non-equilibrium topological matter
- 11/05: **Pavel Ioselevich**, Landau Institute
Tunneling into a Majorana fermion
- 11/12: **Jeffrey Teo**, UIUC
Twist Defects in Topological Systems with Anyonic Symmetries
- 11/13 (**11am**): **Gideon Wachtel**, Hebrew University, Jerusalem
Critical temperature enhancement in a composite superconductor
- 11/19: **Yang-Le Wu**, Princeton
Quantum Hall Wave Functions: Lattice Models and Non-Abelian Quasiholes

Spring 2013 schedule

- 01/07 - 03/28: **KITP Workshop Control of Complex Quantum Systems**
For the current schedule, refer to the [KITP weekly schedule](#)
- 02/19: **Joe Polchinski**, KITP
Black Holes: Complementarity of Firewalls
- 04/02 (**2:00pm**): **Alexey Soluyanov**, ETH Zurich
Wannier functions and topological invariants
- 05/02: **Ali Yazdani**, Princeton
Majorana Fermions in Chains of Magnetic Atoms on a Superconductor
- 06/04: **Taylor Hughes**, UIUC

[Station Q Home Page](#)

[Research At Station Q](#)

[Meet the Researchers](#)

[Seminars & Events](#)

[Publications](#)

[Postdoctoral Positions](#)

[Graduate Fellowships](#)

Geometric response and topological defects in topological insulators and superconductors

- 06/11: **Anton Akhmerov**, Harvard
Macroscopic manipulation of Majorana fermions with superconducting circuits

Fall 2012 schedule

- 09/18: **Zhengcheng Gu**, Caltech
Duality between symmetry protected topological order and intrinsic topological order
- 09/25: **Guifre Vidal**, Perimeter Institute
Characterizing topological order by studying the ground states of an infinite cylinder
- 10/04: **Jonathan Ruhman**, Weizmann
Tunable magnetism and strong correlations in the STO/LAO interface
- 10/16: **Xiao-Gang Wen**, Perimeter Institute
Symmetry protected topological/"trivial" (SPT) phases
- 10/19: **Andrew Potter**, MIT
Coexistence of Ferromagnetism and Superconductivity at LaAlO₃/SrTiO₃ Interfaces
- 10/30 (**10:30am**): **Paul Bruillard**, Texas A&M
Topological Quantum Computation – Classification of Pre-modular Categories and Wang's Conjecture
- 10/31: **Liza Huijse**, Harvard
A multi-critical point of strongly interacting itinerant fermions with supersymmetry
- 11/01: **Zlatko Papić**, Princeton
Aspects of tunability of the interactions in the quantum Hall effect: probing the interplay of topology, quantum geometry and symmetry breaking
- 11/05: **Maissam Barkeshli**, Stanford
Synthetic Topological Qubits in Conventional Bilayer Quantum Hall Systems
- 11/06 (**10:30am**): **Miles Stoudenmire**, UC Irvine
Exact Calculations in the 1D Continuum for DFT and Beyond
- 11/06: **Wei Pan**, Sandia National Lab
Spin transition in the $\nu=8/3$ fractional quantum Hall effect
- 11/27 (**2:00pm**): **Jeongwan Haah**, Caltech
An exotic spin model and topological phase in 3D
- 11/28: **Adam Nahum**, Oxford
Loop models, vortex lines, and SU(n) magnets

Share



[Contact us](#) [Privacy & cookies](#) [Terms of use](#) [Trademarks](#) [Code of conduct](#) [Feedback](#) [Mobile](#)

©2013 Microsoft 

OAK RIDGE NATIONAL LABORATORY

MANAGED BY UT-BATTELLE FOR THE DEPARTMENT OF ENERGY

Dr. G. Malcolm Stocks
Bldg. 4100, MS-6114
P.O. Box 2008
Oak Ridge, TN 37831-6114
Phone: (865) 574-5163
Fax: (865) 576-4944
E-mail: stocksgm@ornl.gov
August 25, 2011

Dr. Zlatko Papic
Department of Electrical Engineering
Princeton University
Via email to: zpapic@Princeton.EDU

Dear Dr. Papic,

On behalf of the organizers of CCP 2011, I am inviting you to present a talk at the *Conference on Computational Physics 2011 (CCP 2011)* to be held in Gatlinburg, Tennessee, USA, during the period 30th October – 3rd November 2011. The Conference on Computational Physics (CCP) series is an annual international conference that is dedicated to presenting an overview of the most recent developments and opportunities in computational physics across a broad range of topical areas.

Scientifically, CCP 2011 is being organized around cross-cutting themes that bring together researchers from different scientific domains with the intent to stimulate cross fertilization within the overall context of computational physics. While you are invited to present a talk of your choosing, we would hope that you address current issues in the field of Fractional Quantum Hall Effect. Ideally, your talk should aim to provide an overview of recent progress in the field that would be accessible to a wide scientific audience and bring out links to other areas covered in the conference. A full description of the thematic structure and domain science sub-structure of the conference can be seen at the CCP 2011 website: <http://ccp2011.ornl.gov> and in the attached conference announcement.

The CCP series is sponsored by the International Union of Pure and Applied Physics (IUPAP; <http://www.iupap.org/index.html>) and has been in existence more than 20 years. The series alternates amongst the nations of the world divided (roughly) into Eastern, Central and Western zones with the most recent ones having been held in Ouro Preto, Brazil in 2008, Taiwan in 2009 and Trondheim, Norway in 2010. As a major international conference, the CCP series aims to draw computational scientists from around the world, both as invited speakers and as conference participants. Your participation as an invited speaker will contribute greatly to the quality of the program and help ensure a high level of participation from fellow scientists, post-doctoral fellows, and students from all parts of the globe.

If you choose to accept our invitation we will be happy to waive the registration fee and, in case of extraordinary hardship, make a contribution to your travel expenses.

Sincerely,



G. Malcolm Stocks
For the Local Organizing Committee and International Advisory Committee

Conference email address: ccp2011@ornl.gov
Conference website: <http://ccp2011.ornl.gov>



Search for Topological Phases of Matter

New Frontiers in Low-Dimensional Systems Program

21-22 April 2011

**Jadwin Hall
Fourth Floor, Room 407**

Topological order is a new kind of order in quantum systems which can arise in the absence of any symmetry breaking. Topologically ordered states, or topological phases, have fundamentally new physical properties, including fractionally charged quasiparticles which obey anyonic or non-abelian statistics and quantized edge states. Apart from fundamental importance, topological states may be of practical importance because they provide a platform for new kind of quantum computation. Currently, one of the main challenges in this field is to find condensed matter systems which exhibit robust and tunable topological phases.

In this short workshop, we will bring together a small number of leading researchers working on topological states in various systems, from frustrated magnets and fractional quantum Hall systems to cold atoms and Josephson junction arrays. We are hoping to cover some of the most exciting recent breakthroughs in this field. Our primary goal will be to identify the most promising future directions in the search for topological phases, as well as to formulate outstanding theoretical and experimental challenges.

Please register on line at pcts.princeton.edu/pcts

Organizers:

Dmitry Abanin, Andrei Bernevig, M. Zahid Hasan, Shivaji Sondhi

Speakers

Fakher Assaad, University Wurzburg
Bryan Clark, Princeton University
Markus Greiner, Harvard University
Zenji Hiroi, University Tokyo
Andrew Houck, Princeton University
Andreas Lauchli, Max Planck Institute
Lindsay LeBlanc, NIST

Benjamin Lev, University of Illinois at Urbana-Champaign
Roderich Moessner, MPI-PKS Dresden
Zlatko Papan, Princeton University
Mansour Shayegan, Princeton University
Steven White, University California, Irvine
Minoru Yamashita, Kyoto University